BEILSTEIN JOURNAL OF ORGANIC CHEMISTRY

Multivalent glycosystems for nanoscience

Edited by Thisbe K. Lindhorst

Imprint

Beilstein Journal of Organic Chemistry
www.bjoc.org
ISSN 1860-5397
Email: journals-support@beilstein-institut.de

The *Beilstein Journal of Organic Chemistry* is published by the Beilstein-Institut zur Förderung der Chemischen Wissenschaften.

Beilstein-Institut zur Förderung der Chemischen Wissenschaften
Trakehner Straße 7–9
60487 Frankfurt am Main
Germany
www.beilstein-institut.de

BEILSTEIN JOURNAL OF ORGANIC CHEMISTRY

Multivalent glycosystems for nanoscience

Thisbe K. Lindhorst

Editorial

Open Access

Address:
Otto Diels Institute of Organic Chemistry, Christiana Albertina University of Kiel, Otto-Hahn-Platz 3/4, 24098 Kiel, Germany

Email:
Thisbe K. Lindhorst - tklind@oc.uni-kiel.de

Keywords:
multivalent glycosystems

Beilstein J. Org. Chem. **2014,** *10,* 2345–2347.
doi:10.3762/bjoc.10.244

Received: 08 September 2014
Accepted: 24 September 2014
Published: 08 October 2014

This article is part of the Thematic Series "Multivalent glycosystems for nanoscience"

Guest Editor: T. K. Lindhorst

Carbohydrates constitute the most abundant class of biomolecules on Earth. They are "global players" and indeed play many roles. They store energy and water. They serve as metabolic intermediates. They function as stable, raw materials or as intelligent, bioengineered products. They are even active in "social media", that is, they mediate communication between cells and they store information by molecular shaping. They adopt more forms and shapes than one can conceive in 24 hours. They exist as small mono- or oligo-saccharides, as large and highly complex polysaccharides, and in conjugation with, for example, proteins and lipids, forming a kingdom of glycoconjugates that are found on every cell surface.

Hence, carbohydrates are like Alice's Wonderland—they can assume any role. They can be big or small, sweet or sour, silent or explicit, crucial or, less often, irrelevant. What we do understand, however, is that carbohydrates are essential to life, both in a state of health and in the case of disease. Consequently, the glycosciences have gained great respect in chemistry and biology. It is now generally considered important to be able to synthesize carbohydrates and glycoconjugates, to purify and analyze their structures, and to advance our understanding of the biology of carbohydrates in living systems. The two Thematic Series "Synthesis in the glycosciences" I [1] and II [2-35] that precede this Thematic Series have impressively documented the state of the art in this field of research.

Now, a third "sweet" Thematic Series is presented in which the borderline between Alice's Wonderland and real-life applications of carbohydrates has been deliberately crossed. The structural world of natural sugars has been extended towards artificial carbohydrate architectures to achieve potential innovations offered by glycoconjugates. Since 2011, approximately 70 group leaders from 21 countries have gathered in an international COST (European Cooperation in Science and Technology) Action, funded by the European Union (EU) to address the challenges and opportunities in the field of glycosciences. This enterprise has focused its research on the potential applications and social benefits that lie in the field. For instance, multivalent glycoconjugates can be used as anti-adhesive drugs against microbial infections. They could be developed into bioimaging agents that can target specific tissues. Indeed, they will certainly find applications in materials science and in medicine, for example, in drug delivery or diagnostics [36]. Consequently, this COST Action (CM1102) [37] was called "MultiGlycoNano" to illustrate that multivalent glycostructures

now enter the era of nanoscience. Some of the achievements of this team of researchers are collected within the presented volume.

I am very grateful to the five colleagues of our international network who have dealt with the manuscripts submitted for this Thematic Series entitled, "Multivalent glycosystems for nanoscience". Bruce Turnbull (United Kingdom) has amassed contributions dedicated to "Synthetic methods to make multivalent glycosystems", Alessandro Casnati (Italy) has delivered manuscripts regarding "Glycoconjugates for the delivery of drugs and diagnostic probes" for review, Roland Pieters (The Netherlands) has taken care of manuscripts related to "Glycoconjugates as anti-pathogenic agents", Vladimir Křen (Czech Republic) has supervised the area of "Glycoconjugates as modulators of the immune system", and finally, Jean-Louis Reymond (Switzerland) has received contributions regarding "Glycosystems in nanotechnology". As a result, 27 excellent publications are presented in this fine collection. I would like to sincerely congratulate all contributors for their research and results. We can be proud of what has been achieved. We should be inspired by what has been suggested. And we have definitely been encouraged by the delightful experiences we shared in an international network of colleagues and friends. In our community, we have been obliged to diversity and equality, to liberty and freedom, and to truth and reason. Therefore, in the name of all glycoscientists who have contributed to this Thematic Series, I finally express the hope that the ethical standards that we have applied in our work will provide guidance and confidence, if our healthy world will once have to face the challenges of distrust, fanaticism and hate, as it is currently the case in many areas of this planet.

Thisbe K. Lindhorst

Kiel, October 2014

References

1. Lindhorst, T. K. *Beilstein J. Org. Chem.* **2010,** *6,* No. 16. doi:10.3762/bjoc.6.16
2. Lindhorst, T. K. *Beilstein J. Org. Chem.* **2012,** *8,* 411–412. doi:10.3762/bjoc.8.45
3. Boettcher, S.; Matwiejuk, M.; Thiem, J. *Beilstein J. Org. Chem.* **2012,** *8,* 413–420. doi:10.3762/bjoc.8.46
4. Thomas, B.; Fiore, M.; Bossu, I.; Dumy, P.; Renaudet, O. *Beilstein J. Org. Chem.* **2012,** *8,* 421–427. doi:10.3762/bjoc.8.47
5. Křenek, K.; Šimon, P.; Weignerová, L.; Fliedrová, B.; Kuzma, M.; Křen, V. *Beilstein J. Org. Chem.* **2012,** *8,* 428–432. doi:10.3762/bjoc.8.48
6. Braitsch, M.; Kähli, H.; Kontaxis, G.; Fischer, M.; Kawada, T.; Konrat, R.; Schmid, W. *Beilstein J. Org. Chem.* **2012,** *8,* 448–455. doi:10.3762/bjoc.8.51
7. Nokami, T.; Shibuya, A.; Saigusa, Y.; Manabe, S.; Ito, Y.; Yoshida, J.-i. *Beilstein J. Org. Chem.* **2012,** *8,* 456–460. doi:10.3762/bjoc.8.52
8. Bini, D.; Cardona, F.; Forcella, M.; Parmeggiani, C.; Parenti, P.; Nicotra, F.; Cipolla, L. *Beilstein J. Org. Chem.* **2012,** *8,* 514–521. doi:10.3762/bjoc.8.58
9. Dey, S.; Jayaraman, N. *Beilstein J. Org. Chem.* **2012,** *8,* 522–527. doi:10.3762/bjoc.8.59
10. Fiege, K.; Lünsdorf, H.; Atarijabarzadeh, S.; Mischnick, P. *Beilstein J. Org. Chem.* **2012,** *8,* 551–566. doi:10.3762/bjoc.8.63
11. Premathilake, H. D.; Demchenko, A. V. *Beilstein J. Org. Chem.* **2012,** *8,* 597–605. doi:10.3762/bjoc.8.66
12. Nishida, Y.; Shingu, Y.; Mengfei, Y.; Fukuda, K.; Dohi, H.; Matsuda, S.; Matsuda, K. *Beilstein J. Org. Chem.* **2012,** *8,* 629–639. doi:10.3762/bjoc.8.70
13. Jasiński, M.; Lentz, D.; Reissig, H.-U. *Beilstein J. Org. Chem.* **2012,** *8,* 662–674. doi:10.3762/bjoc.8.74
14. Koester, D. C.; Werz, D. B. *Beilstein J. Org. Chem.* **2012,** *8,* 675–682. doi:10.3762/bjoc.8.75
15. Stanetty, C.; Wolkerstorfer, A.; Amer, H.; Hofinger, A.; Jordis, U.; Claßen-Houben, D.; Kosma, P. *Beilstein J. Org. Chem.* **2012,** *8,* 705–711. doi:10.3762/bjoc.8.79
16. Kupper, C. E.; Rosencrantz, R. R.; Henßen, B.; Pelantová, H.; Thönes, S.; Drozdová, A.; Křen, V.; Elling, L. *Beilstein J. Org. Chem.* **2012,** *8,* 712–725. doi:10.3762/bjoc.8.80
17. van der Kaaden, M.; Breukink, E.; Pieters, R. J. *Beilstein J. Org. Chem.* **2012,** *8,* 732–737. doi:10.3762/bjoc.8.82
18. Weissenborn, M. J.; Wehner, J. W.; Gray, C. J.; Šardzik, R.; Eyers, C. E.; Lindhorst, T. K.; Flitsch, S. L. *Beilstein J. Org. Chem.* **2012,** *8,* 753–762. doi:10.3762/bjoc.8.86
19. Khatuntseva, E. A.; Men'shov, V. M.; Shashkov, A. S.; Tsvetkov, Y. E.; Stepanenko, R. N.; Vlasenko, R. Y.; Shults, E. E.; Tolstikov, G. A.; Tolstikova, T. G.; Baev, D. S.; Kaledin, V. A.; Popova, N. A.; Nikolin, V. P.; Laktionov, P. P.; Cherepanova, A. V.; Kulakovskaya, E. V.; Nifantiev, N. E. *Beilstein J. Org. Chem.* **2012,** *8,* 763–775. doi:10.3762/bjoc.8.87
20. Marano, G.; Gronewold, C.; Frank, M.; Merling, A.; Kliem, C.; Sauer, S.; Wiessler, M.; Frei, E.; Schwartz-Albiez, R. *Beilstein J. Org. Chem.* **2012,** *8,* 787–803. doi:10.3762/bjoc.8.89
21. Westerlind, U. *Beilstein J. Org. Chem.* **2012,** *8,* 804–818. doi:10.3762/bjoc.8.90
22. Beckmann, H. S. G.; Möller, H. M.; Wittmann, V. *Beilstein J. Org. Chem.* **2012,** *8,* 819–826. doi:10.3762/bjoc.8.91
23. Lütteke, T. *Beilstein J. Org. Chem.* **2012,** *8,* 915–929. doi:10.3762/bjoc.8.104
24. Marradi, M.; Cicchi, S.; Sansone, F.; Casnati, A.; Goti, A. *Beilstein J. Org. Chem.* **2012,** *8,* 951–957. doi:10.3762/bjoc.8.107
25. Ziegler, T.; Heber, U. *Beilstein J. Org. Chem.* **2012,** *8,* 1059–1070. doi:10.3762/bjoc.8.118
26. Moore, C. J.; Auzanneau, F.-I. *Beilstein J. Org. Chem.* **2012,** *8,* 1134–1143. doi:10.3762/bjoc.8.126
27. Zou, L.; Zheng, R. B.; Lowary, T. L. *Beilstein J. Org. Chem.* **2012,** *8,* 1219–1226. doi:10.3762/bjoc.8.136
28. Esposito, D.; Hurevich, M.; Castagner, B.; Wang, C.-C.; Seeberger, P. H. *Beilstein J. Org. Chem.* **2012,** *8,* 1601–1609. doi:10.3762/bjoc.8.183
29. Gallas, K.; Pototschnig, G.; Adanitsch, F.; Stütz, A. E.; Wrodnigg, T. M. *Beilstein J. Org. Chem.* **2012,** *8,* 1619–1629. doi:10.3762/bjoc.8.185
30. Wierzejska, J.; Motogoe, S.-i.; Makino, Y.; Sengoku, T.; Takahashi, M.; Yoda, H. *Beilstein J. Org. Chem.* **2012,** *8,* 1831–1838. doi:10.3762/bjoc.8.210

31. Yin, J.; Eller, S.; Collot, M.; Seeberger, P. H. *Beilstein J. Org. Chem.* **2012,** *8,* 2067–2071. doi:10.3762/bjoc.8.232
32. Wehner, J. W.; Lindhorst, T. K. *Beilstein J. Org. Chem.* **2012,** *8,* 2149–2155. doi:10.3762/bjoc.8.242
33. Fürniss, D.; Mack, T.; Hahn, F.; Vollrath, S. B. L.; Koroniak, K.; Schepers, U.; Bräse, S. *Beilstein J. Org. Chem.* **2013,** *9,* 56–63. doi:10.3762/bjoc.9.7
34. Collot, M.; Eller, S.; Weishaupt, M.; Seeberger, P. H. *Beilstein J. Org. Chem.* **2013,** *9,* 97–105. doi:10.3762/bjoc.9.13
35. Leonori, D.; Seeberger, P. H. *Beilstein J. Org. Chem.* **2013,** *9,* 332–341. doi:10.3762/bjoc.9.38
36. Bernardi, A.; Jiménez-Barbero, J.; Casnati, A.; De Castro, C.; Darbre, T.; Fieschi, F.; Finne, J.; Funken, H.; Jaeger, K.-E.; Lahmann, M.; Lindhorst, T. K.; Marradi, M.; Messner, P.; Molinaro, A.; Murphy, P.; Nativi, C.; Oscarson, S.; Penadés, S.; Peri, F.; Pieters, R. J.; Renaudet, O.; Reymond, J.-L.; Richichi, B.; Rojo, J.; Sansone, F.; Schäffer, C.; Turnbull, W. B.; Velasco-Torrijos, T.; Vidal, S.; Vincent, S.; Wennekes, T.; Zuilhof, H.; Imberty, A. *Chem. Soc. Rev.* **2013,** *42,* 4709–4727. doi:10.1039/C2CS35408J
37. http://www.cost.eu/domains_actions/cmst/Actions/CM1102.

License and Terms

Beilstein Journal of Organic Chemistry

Synthesis of a sucrose dimer with enone tether; a study on its functionalization

Zbigniew Pakulski, Norbert Gajda, Magdalena Jawiczuk, Jadwiga Frelek, Piotr Cmoch and Sławomir Jarosz*

Full Research Paper

Open Access

Address:
Institute of Organic Chemistry, Polish Academy of Sciences, ul. Kasprzaka 44/52, 01-224 Warsaw, Poland

Email:
Sławomir Jarosz* - slawomir.jarosz@icho.edu.pl

* Corresponding author

Keywords:
CD-spectroscopy; Cotton effect; multivalent glycosystems; osmylation; stereoselective synthesis; sucrose

Beilstein J. Org. Chem. **2014,** *10,* 1246–1254.
doi:10.3762/bjoc.10.124

Received: 05 March 2014
Accepted: 30 April 2014
Published: 28 May 2014

This article is part of the Thematic Series "Multivalent glycosystems for nanoscience".

Guest Editor: A. Casnati

Abstract

The reaction of appropriately functionalized sucrose phosphonate with sucrose aldehyde afforded a dimer composed of two sucrose units connected via their C6-positions ('the glucose ends'). The carbonyl group in this product (enone) was stereoselectively reduced with zinc borohydride and the double bond (after protection of the allylic alcohol formed after reduction) was oxidized with osmium tetroxide to a diol. Absolute configurations of the allylic alcohol as well as the diol were determined by circular dichroism (CD) spectroscopy using the in situ dimolybdenum methodology.

Introduction

Molecular recognition is one of the most important phenomena in stereoselective processes. Chiral crown ethers (or analogs) are particularly useful in enantioselective reactions [1,2] as well as differentiation of chiral guests [3,4]. From all of the chiral platforms designed for such receptors, sugars are the most promising due to their availability and biocompatibility. Up to date only monosaccharides have found a wide application in the synthesis of crown ether analogs [5,6]. The disaccharide scaffold is much less pronounced [7].

During the past decade we have become engaged in the preparation of the analogs of crown and aza-crown ethers with sucrose scaffold. It is based on a selective protection of 1',2,3,3',4,4'-hexa-*O*-benzylsucrose (**1**) either at the glucose (C-6) [8] or fructose (C-6') [9] end and further transformations to a variety of macrocycles (**2**–**4**; Figure 1). Such receptors exhibit interesting complexing properties towards chiral ammonium salts including amino acids [10-14]. More complex sucrose macrocycles, such as **5**, are available, although in rather low yield [15].

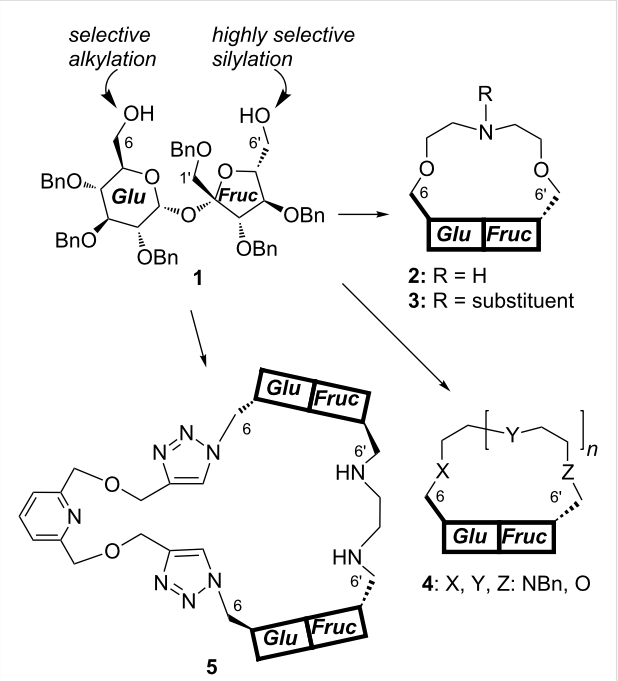

Figure 1: Examples of sucrose-based macrocycles.

In this paper we present an approach to other derivatives containing two sucrose units. This type of dimers may be eventually used for the construction of macrocycles by (simple) connecting their C-6' (fructose) ends.

Results and Discussion

Coupling of two sugar units can be performed by a number of methods. The best one in our hands was the Wittig-type methodology shown in Figure 2. The properly activated sugar is converted into phosphorane or phosphonate which – upon reaction with an aldehyde derived from another monosaccharide – provides higher carbon sugar (HCS) enone [16-18].

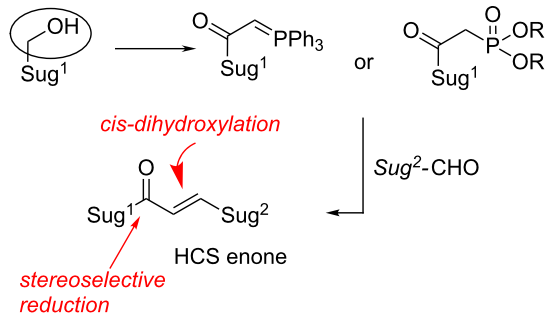

Figure 2: Synthesis of higher sugar precursors by a Wittig-type methodology.

Application of this methodology to selectively protected 2,3,3',4,4'-penta-*O*-benzylsucrose allowed us to elongate the parent disaccharide at either terminal position (1',6', and 6') by relatively small (C2 or C7) unit and prepare so-called higher sucroses in good yields [19,20]. A similar approach is used now for a more convenient hexa-*O*-benzyl derivative which is easily silylated at the 'fructose end' providing alcohol **6** [8]. This alcohol was converted into aldehyde **7** [21] (route a in Scheme 1) and separately into phosphonate **9** (route b). Reaction of both synthons under the mild PTC conditions [22-24] afforded the respective enone **10** in good yield (Scheme 1).

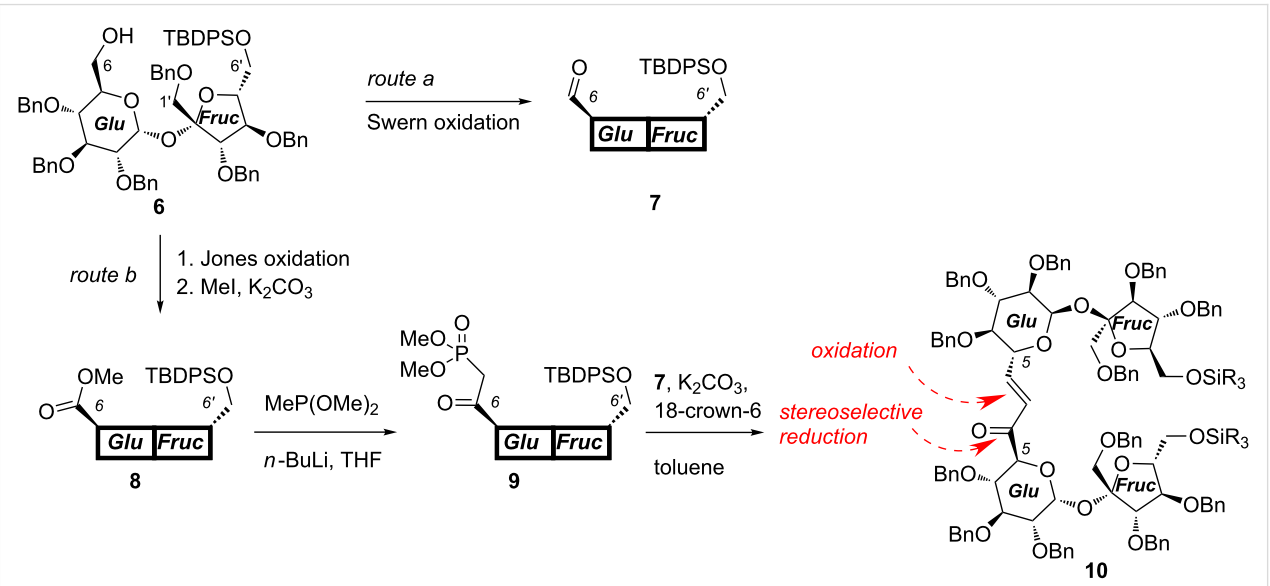

Scheme 1: Synthesis of higher sugar enone **10**.

Functionalization of the three-carbon atom unit connecting the C5-positions of both sucrose units required reduction of the carbonyl group of the enone system and oxidation of the double bond.

We have already reported that reduction of higher carbon sugar enones of the D series with zinc borohydride is highly selective and provides the corresponding allylic alcohols with the *R* configuration at the newly created stereogenic center, as the only products. This can be rationalized assuming the cyclic model of such reduction [25] shown in Scheme 2. We expected, therefore, also very high selectivity in the reduction of **10**.

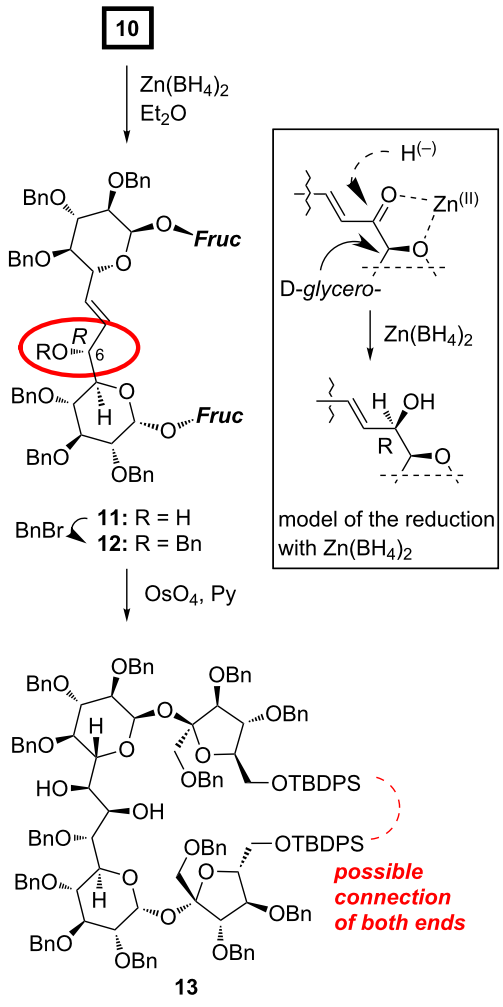

Scheme 2: Synthesis of the diol **13** containing two sucrose units.

Indeed, treatment of enone **10** with $Zn(BH_4)_2$ under the standard conditions afforded allylic alcohol **11** as single stereoisomer in 65% yield. Based on our model, the *R*-configuration might be safely assigned to the new stereogenic center. This assignment was further verified independently by circular dichroism spectroscopy (CD) using the in situ dimolybdenum methodology (see next chapter).

Next steps of the synthesis consisted of the protection of the C6–OH as benzyl ether (to **12**) and osmylation of the double bond. The *cis*-dihydroxylation provided, as single stereoisomer, a diol to which structure **13** could be assigned on the basis of the Kishi rule [26] (Scheme 2). It postulates that the attack of OsO_4 occurs from the side opposite to hydroxy (alkoxy) substituent(s) flanking the double bond. Since in **12**, both alkoxy units act in the same direction, very high diastereoselectivity is not surprising. The assignment of the configuration of this diol was further confirmed also by the CD methodology; this is discussed in the next chapter.

Determination of the absolute configuration of **11** and **13**

It is widely acceptable that the circular dichroism (CD) spectroscopy utilizing the in situ dimolybdenum methodology offers the hard proof of the absolute configuration of the *vic*-diols [27-29]. In this methodology, dimolybdenum tetraacetate acts as auxiliary chromophore allowing the application of electronic circular dichroism (ECD) to (otherwise in ECD non-observable) *vic*-diols. $Mo_2(OAc)_4$ when mixed with a chiral diol ligand forms complexes active in ECD in which a transfer of ligand chirality to the in situ-formed complex occurs in solution. Thus, stereochemistry of *vic*-diols can be easily assigned based on the helicity rule developed for this class of compounds. This rule correlates the positive/negative signs of Cotton effects (CE) occurring in the 300–400 nm spectral range in the ECD spectra with the positive/negative sign of the O–C–C–O torsion angle of the diol unit of resultant complexes with the Mo_2-core. The basic assumption leading to the assignment of the absolute configuration (AC) based only on the ECD spectra with the Mo_2-core preferring the gauche conformation of the diol units with both O–C–C–C fragments in an antiperiplanar arrangement (Figure 3). This arrangement is favored, for steric reasons, i.e., to avoid any interaction with the carboxylate ligands remaining in the stock complex. As a result of the structure–ECD spectra relationship, it is possible to assign the AC of the diol moiety unambiguously on the basis of the ECD spectra alone.

In the past few years, this simple but, above all, efficient and effective method is becoming more and more recognized as evidenced by the steadily increasing number of reports in the literature about its successful application in the determination of the AC of 1,2-diols [30-32].

Therefore, in assignment of the AC of compounds under the present study (**13**, **14** and **16**), we decided just to take advantage of the in situ methodology.

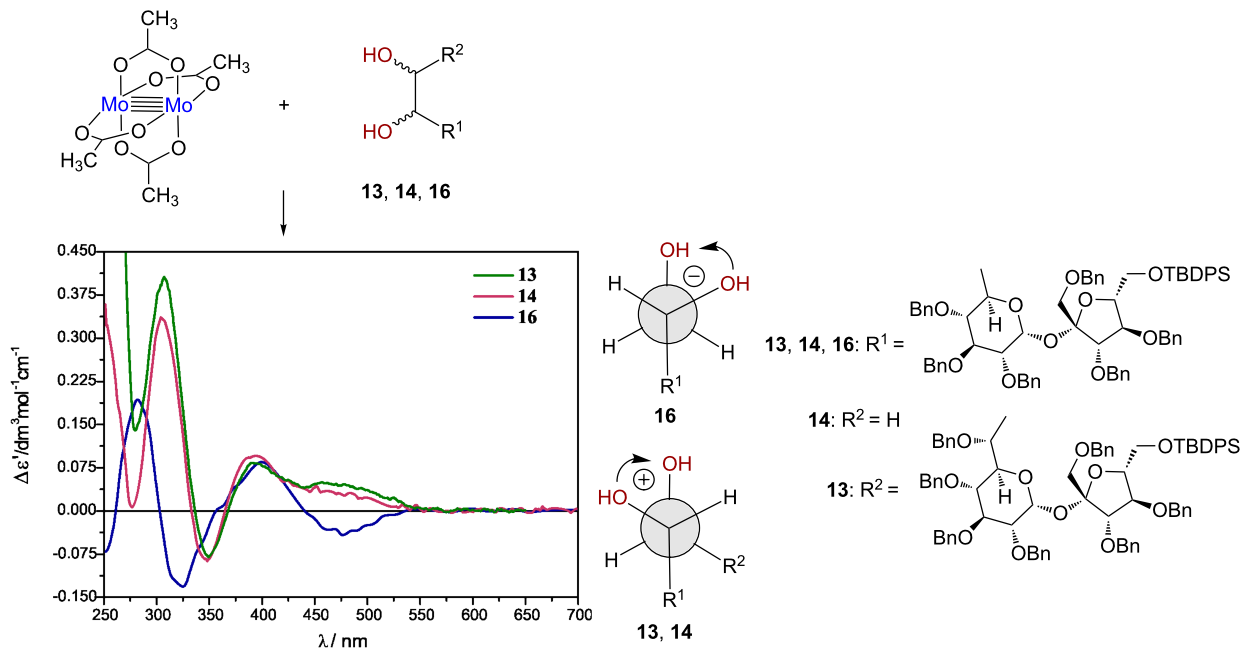

Figure 3: CD spectra of in situ formed chiral complexes of **13** (green line), **14** (purple line) and **16** (blue line) with dimolybdenum tetraacetate recorded in DMSO; right: preferred gauche conformation of the diols **13**, **14** and **16** in the complex with Mo_2-core.

This method was used to prove indirectly the 6*R* configuration at the newly created stereogenic center in allylic alcohol **11**. The double bond in **11** was cleaved with ozone and the resulting ozonide was reduced with $NaBH_4$; this sequence afforded sucrose *vic*-diol **14** and (as a byproduct) sucrose alcohol **6** (Scheme 3).

The positive sign of the Cotton effect at around 307.0 nm recorded for the complex of the diol **14** with $Mo_2(OAc)_4$ unambiguously pointed at the 6*R* configuration (Figure 3). However, to exclude any errors we have also prepared **14** and epimeric alcohol **16**; its synthesis is shown in Scheme 3.

First, aldehyde **7** was converted into olefin **15** by treatment with the simplest Wittig reagent: $Ph_3P{=}CH_2$. Subsequent osmylation of the double bond in **15** provided two stereoisomeric diols in a 1:1 ratio; the first one was identical in all respects with the diol obtained from degradation of **11**.

The resultant ECD spectra of the Mo_2-core with compounds **13** and **16** are shown in Figure 3. Based on the positive CE's at 308.5 nm for **13** and negative at 310 nm for **16**, respectively, the positive (negative) sign of the O–C–C–O torsion angle has been attributed to these diols. In the next step, based on the preferred *gauche* conformation of the diol unit with both O–C–C–C fragments in an antiperiplanar arrangement as shown in Figure 3, we were able to assign unambiguously the (7*R*,8*R*) AC to diol **13** and (6*S*) to **16**.

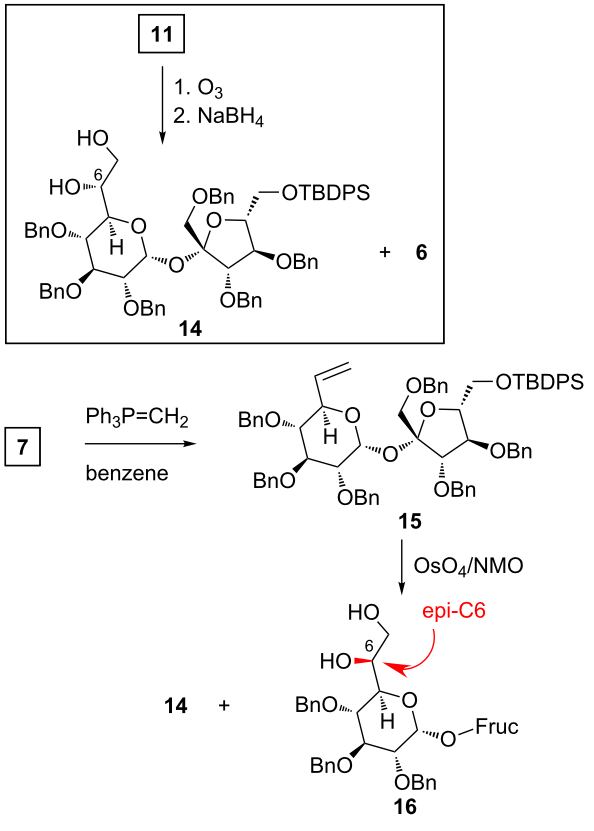

Scheme 3: Synthesis of model sucrose diols.

Conclusion

Coupling of two properly activated sucrose sub-units afforded the dimer in which both glucose-rings were connected via an enone linker. The dimer was then converted into a (partially protected) triol via a stereoselective reduction of the carbonyl group and highly selective *cis*-dihydroxylation of the double bond. The configuration at each new stereogenic center was determined by CD spectroscopy using the so-called dimolybdenum methodology which allows for fast, easy, and effective assignment of the absolute configuration of *vic*-diols. We have confirmed the usefulness of this simple methodology which can be applied even in cases when other spectroscopic methods fail.

It is worthy to point out that this methodology, which is used in the synthesis of more simple derivatives such as higher carbon sugars, was also applicable for the preparation of the sucrose dimer.

Experimental

General methods

All reported NMR spectra were recorded with a Varian-Vnmrs-600 MHz spectrometer (at 600 and 150 MHz for ^{1}H and ^{13}C NMR spectra, respectively) for solutions in $CDCl_3$ at room temperature. Chemical shifts (δ, ppm) were determined relative to TMS as the internal standard. Most of the resonances were assigned by COSY (^{1}H–^{1}H) and gradient selected HSQC and HMBC correlations. Mass spectra were recorded with an ESI/MS Mariner (PerSeptive Biosystem) mass spectrometer. Elemental analyses were obtained using a Perkin-Elmer 2400 CHN analyzer. Optical rotations were measured with a Jasco P-2000 digital polarimeter for solutions in $CHCl_3$ (c = 0.3) at room temperature. Flash and column chromatographic separations were performed on silica gel (Merck, 230–400 mesh). Progress of the reactions was monitored by thin-layer chromatography (TLC) performed on aluminum plates covered with silica gel (60 F254, Merck).

The ECD spectra were acquired at room temperature in DMSO (for UV-spectroscopy, Fluka) on a Jasco J-715 spectropolarimeter and were collected at 0.5 nm/step with an integration time of 0.25 s over the range 235–800 nm with 200 nm/min scan speed, 5 scans. For the ECD standard measurements the chiral diols (~3.6 mg, ca. 0.003 M) was mixed with stock complex $[Mo_2(O_2CCH_3)_4]$ (Mo1) (~0.9 mg, ca. 0.002 M) and dissolved in DMSO (1 mL) so that the molar ratio of the stock complex to ligand was about 1:1.5 in general. Quantitative values could not be obtained with the in situ dimolybdenum method since the concentration of the chiral complex formed in solution and its actual structure were unknown. So the ECD data are given as the Δε' values, which are calculated in the usual manner by means of the equation $\Delta\varepsilon' = \Delta A/c \times d$, A being the absorption, c the molar concentration of the chiral ligand, assuming 100% complexation, and d the path length of the cell.

The numbering of the atoms in sucrose dimers is as followed. The bottom part (green) is marked A and the top marked as B. The original numbering of the sucrose skeleton in both parts is retained (i.e., the glucose part is numbered C1–C6 and fructose C1'–C6').

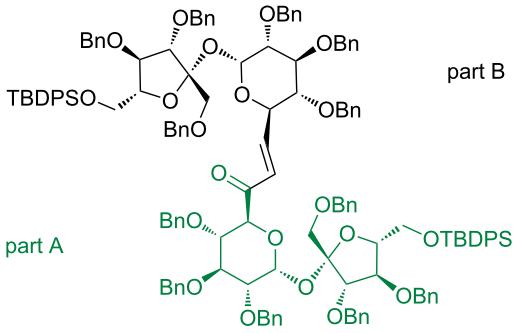

10

Synthesis of phosphonate 9. To a cooled −78 °C solution of dimethyl methylphosphonate (110 μL, 1.0 mmol) in THF (7 mL) a 2.5 M solution of butyllithium in hexane (0.4 mL, 1.0 mmol) was added and the mixture was stirred for 15 min. Then, a solution of **8** (325 mg, 0.28 mmol) in THF (5 mL) was slowly added and the mixture was stirred for additional 30 min. Reaction was quenched by addition of a saturated solution of NaCl (5 drops). The mixture was concentrated, and the residue was purified by column chromatography (hexane–ethyl acetate, 10:1 → 1:1) to afford title compound **9** (227 mg, 65%) as a foam. $[\alpha]_D^{20}$ 16.2.; ^{1}H NMR δ 7.64–7.61 (m, 4H, Ar), 7.35–7.18 (m, 36H, aryl-H), 6.08 (d, 1H, $J_{1,2}$ = 3.6 Hz, H-1), 4.86–4.38 (m, 12H, PhCH_2), 4.54 (d, 1H, $J_{5,4}$ = 9.9 Hz, H-5), 4.48 (d, 1H, $J_{3,4}$ = 7.5 Hz, H-3'), 4.45 (dd, 1H, $J_{4,3}$ = 7.5, $J_{4,5}$ = 15.0 Hz, H-4'), 4.03 (dd, 1H, $J_{6,5}$ = 3.8, $J_{6,6'}$ 11.5 Hz, H-6'), 3.94 (m, 2H, H-3, H-5'), 3.85 (dd, 1H, $J_{6,5}$ = 4.1 Hz, $J_{6,6'}$ = 11.5 Hz, H-6'), 3.71 (dd, 1H, $J_{4,3}$ = 9.1 Hz, $J_{4,5}$ = 9.9 Hz, H-4), 3.67 (d, 1H, J_{gem} = 10.8 Hz, H-1'), 3.62 (d, 3H, $J_{H,P}$ = 11.1 Hz, OCH_3), 3.61 (d, 3H, $J_{H,P}$ = 11.2 Hz, OCH_3), 3.56 (d, 1H, J_{gem} = 10.8 Hz, H-1'), 3.43 (dd, 1H, $J_{2,1}$ = 3.6, $J_{2,3}$ = 9.7 Hz, H-2), 3.26 (dd, 1H, $J_{7,7'}$ = 15.7 Hz, $J_{H,P}$ = 20.3 Hz, H-7), 2.97 (dd, 1H, $J_{7,7'}$ = 15.7 Hz, $J_{H,P}$ = 20.8 Hz, H-7), 1.06 (s, 9H, *t*-Bu); ^{13}C NMR δ 198.5 (d, J 7.4 Hz, C=O), 138.7, 138.5, 138.2, 138.1, 137.8, 137.7, 135.6, 135.4, 133.1, 132.7, 129.8, 129.8, 128.6–127.5 (Ar), 104.5 (C-2'), 89.2 (C-1), 83.3 (C-3'), 81.5 (C-3), 80.8 (C-4'), 80.5 (C-5'), 79.5 (C-2), 77.9 (C-4), 75.7 (PhCH_2), 74.9 (d, J 5.0 Hz, C-5), 74.8 (PhCH_2), 73.5 (PhCH_2), 73.4 (PhCH_2), 72.9 (PhCH_2), 72.0 (PhCH_2), 72.0 (C-1'), 63.5

(C-6'), 52.8 (d, J = 6.3 Hz, OCH_3), 52.6 (d, J = 6.4 Hz, OCH_3), 37.9 (d, J = 136.9 Hz, C-7), 26.9 (*t*-Bu-CH_3), 19.2 (*t*-Bu-C); ^{31}P NMR ($CDCl_3$) δ 23.5; anal. calcd for $C_{73}H_{81}O_{14}PSi$ (1241.51): C, 70.62; H, 6.58; found: C, 70.44; H, 6.79.

Synthesis of ketone 10. To a solution of aldehyde **7** (200 mg, 0.18 mmol), phosphonate **9** (220 mg, 0.18 mmol), and 18-crown-6 (70 mg) in toluene (25 mL) potassium carbonate (300 mg) was added and the suspension was stirred at rt for 4 days. The solvents were evaporated and the residue was purified by column chromatography (hexane–ethyl acetate, 40:1 → 5:1) to afford title compound **10** as a foam (287 mg; 73%). $[\alpha]_D^{20}$ 41.8; ^{1}H NMR δ 7.62–7.61 (m, 8H, Ar), 7.28–7.06 (m, 73H, Ar, =C*H*-CO), 6.75 (dd, 1H, J = 1.8 Hz, 15.7 Hz, =C*H*), 5.90 (d, 1H, J = 3.5 Hz, H-1A), 5.82 (d, 1H, J = 3.5 Hz, H-1B), 4.74–4.26 (m, 24H, 12 × PhCH_2), 4.67 (d, 1H, J = 10.2 Hz, H-5A), 4.58 (d, 1H, J = 12.3 Hz, H-5B), 4.37–4.26 (m, 4H, furanose), 4.00–3.80 (m, 8H, H-3A, H-3B, 4 × H-6', 2 × furanose), 3.77 (d, 1H, J = 11.0 Hz, H-1'B), 3.68 (d, 1H, J = 10.9 Hz, H-1'A), 3.50 (dd, 1H, J = 9.1 Hz, 10.0 Hz, H-4A), 3.46 (d, 1H, J = 10.9 Hz, H-1'A), 3.42–3.38 (m, 2H, H-1'B, H-2A), 3.25 (dd, 1H, J = 3.5 Hz, 9.6 Hz, H-2A), 2.97 (dd, 1H, J = 9.1 Hz, 9.9 Hz, H-4B), 1.03 (s, 9H, *t*-Bu), 1.02 (s, 9H, *t*-Bu); ^{13}C NMR δ 195.2 (C=O), 144.7 (=*C*H-CO), 138.9, 138.8, 138.4, 138.3, 138.2, 138.1, 138.1, 138.0, 137.9, 137.9, 137.8, 137.7, 135.6, 135.6, 135.5, 133.4, 133.3, 133.2, 133.1, 129.7, 129.7, 129.7, 129.6, 128.4–127.4 (Ar), 124.8 (=*C*H) 105.1 (C-2'A), 104.8 (C-2'B), 90.3 (C-1A), 90.2 (C-1B), 84.4, 83.9, 83.3, 83.2, 81.8 (C-4B), 81.7, 81.7, 81.5 (C-3A), 81.4 (C-3B), 79.8 (C-2A, C-2B), 79.6 (C-4A), 75.7 (Ph*C*H_2), 75.4 (Ph*C*H_2), 74.9 (C-5A, Ph*C*H_2), 74.4 (Ph*C*H_2), 73.5 (Ph*C*H_2), 73.4 (Ph*C*H_2), 73.1 (Ph*C*H_2), 73.0 (Ph*C*H_2), 72.6 (Ph*C*H_2), 72.4 (Ph*C*H_2), 72.1 (Ph*C*H_2),71.8 (Ph*C*H_2), 70.6 (C-1'), 70.4 (C-1'), 69.8 (C-5B), 65.3 (C-6'), 65.0 (C-6'), 27.0 (*t*-Bu), 27.0 (*t*-Bu), 19.3 (CH_3), 19.3 (CH_3); anal. calcd for $C_{141}H_{148}O_{21}Si_2$ (2234.91): C, 75.78; H, 6.68; found: C, 75.59; H, 6.80.

Stereoselective reduction of ketone 10. To an ice-cooled solution of ketone **10** (270 mg, 0.12 mmol) in Et_2O (15 mL), an etheral solution of zinc borohydride (0.6 mmol) was added and the mixture was stirred at 0 °C for 1 h. Water (10 drops) was added to decompose excess of hydride, the solvents were evaporated, and the residue was purified by column chromatography (hexane–ethyl acetate, 10:1 → 5:1) to afford title compound **11** (176 mg, 65%) as a foam. $[\alpha]_D^{20}$ 40.4; ^{1}H NMR δ 7.63–7.61 (m, 8H, Ar), 7.30–7.05 (m, 72H, Ar), 5.97 (dd, 1H, J = 7.9 Hz, 15.6 Hz, =C*H*-CHOH), 5.83 (d, 2H, J = 3.6 Hz, H-1A, H-1B), 5.76 (dd, 1H, J = 5.5 Hz, 15.6 Hz, =C*H*), 4.80–4.73 (m, 5H, PhCH_2), 4.63–4.41 (m, 17H, PhCH_2, H-3', H-5B), 4.39–4.34 (m, 6H, PhCH_2, H-3', H-3', H-4', H-6A), 4.32–4.28 (m, 1H, H-4'), 4.25 (dd, 1H, J = 2.2 Hz, 10.3 Hz, H-5A), 4.13 (d, 1H, J = 10.9 Hz, PhCH_2), 4.06–4.04 (m, 1H, H-5'), 3.99–3.95 (m, 2H, 2 × H-6'), 3.92–3.89 (m, 2H, H-5', H-6'), 3.86–3.79 (m, 3H, H-3A, H-1', H-3B), 3.65 (d, 1H, J = 11.0 Hz, H-1'), 3.52 (d, 1H, J = 11.0 Hz, H-1'), 3.49 (d, 1H, H-1'), 3.35 (dd, 1H, J = 3.5 Hz, 9.6 Hz, H-2B), 3.27–3.24 (m, 1H, H-4A), 3.21–3.16 (m, 2H, H-2A, H-4B), 1.03 (s, 9H, *t*-Bu), 1.02 (s, 9H, *t*-Bu); ^{13}C NMR δ 139.0, 138.9, 138.6, 138.6, 138.5, 138.4, 138.3, 138.1, 138.0, 137.9, 137.8, 137.7, 135.7, 135.6, 135.5, 135.5, 133.5, 133.3, 133.3, 132.8, 131.3 (=*C*H), 130.4 (=*C*H-CHOH), 129.8, 129.7, 129.7, 129.6, 128.5–127.3 (Ar), 105.0 (C-2'), 104.5 (C-2'), 90.2 (C-1B), 89.0 (C-1A), 84.5 (C-3'), 83.6 (C-4'), 83.1 (C-4'), 82.3 (C-3A), 82.2 (C-4B), 81.8 (C-5'), 81.6 (C-3'), 81.5 (C-3B), 81.0 (C-5'), 80.4 (C-2A), 80.0 (C-2B), 78.4 (C-4A), 75.5 (Ph*C*H_2), 75.4 (Ph*C*H_2), 74.6 (Ph*C*H_2), 74.4 (Ph*C*H_2), 73.6 (Ph*C*H_2), 73.4 (Ph*C*H_2), 73.4 (C-5A), 73.1 (Ph*C*H_2), 73.0 (Ph*C*H_2), 72.7 (Ph*C*H_2), 72.6 (Ph*C*H_2), 71.8 (Ph*C*H_2), 71.7 (Ph*C*H_2), 71.5 (C-6A), 71.4 (C-1'), 70.5 (C-1'), 70.0 (C-5B), 65.8 (C-6'), 63.7 (C-6'), 27.0 (*t*-Bu), 27.0 (*t*-Bu), 19.3 (CH_3), 19.3 (CH_3); anal. calcd for $C_{141}H_{150}O_{21}Si_2$ (2236.92): C, 75.71; H, 6.76; found: C, 75.51; H, 6.63.

Benzylation of 11. To a solution of alcohol **11** (82 mg, 0.037 mmol) in DMF (1 mL), sodium hydride (60% suspension in mineral oil, 7 mg) was added and the mixture was stirred for 30 min at rt. Benzyl bromide (11 µL, 0.092 mmol) was added, and stirring was continued overnight. Excess of sodium hydride was decomposed with methanol (0.5 mL). The product was isolated by column chromatography (hexane–ethyl acetate, 10:1 → 5:1) to afford **12** (34 mg, 40%) as a foam. $[\alpha]_D^{20}$ 21.8 (*c* 0.9, CH_2Cl_2); ^{1}H NMR δ 7.67–7.63 (m, 8H, Ar), 7.28–7.00 (m, 77H, Ar), 5.93–5.89 (m, 2H, H-1B, =C*H*-CHOH), 5.63–5.59 (m, 2H, H-1A, =C*H*), 4.79–4.50 (m, 13H, H-5B, PhCH_2), 4.47–4.16 (m, 18H, H-5A, PhCH_2), 4.10–3.75 (m, 12H, H-6A, 4 × H-6', H-3B, 2 × H-1', H-3A, 2 × furanose, PhC*H*), 3.56–3.52 (m, 2H, 2 × H-1'), 3.41 (dd, 1H, J = 3.6, 9.7 Hz, H-2B), 3.19–3.14 (m, 2H, H-4A, H-4B), 2.92 (dd, 1H, J = 3.5, 9.6 Hz, H-2A), 1.03 (s, 9H, *t*-Bu), 1.03 (s, 9H, *t*-Bu); ^{13}C NMR δ: 139.0, 138.8, 138.7, 138.6, 138.5, 138.4, 138.3, 138.3, 138.3, 138.3, 138.2, 138.0, 137.8, 135.6, 135.5, 135.5, 135.5, 134.4 (=*C*H), 133.7, 133.6, 133.4, 133.2, 129.7, 129.6, 129.6, 129.6, 128.3–127.0 (Ar), 104.4 (C-2'), 104.4 (C-2'), 90.1 (C-1A), 89.9 (C-1B), 84.5, 84.1, 83.2, 82.2, 82.0 (C-3A), 82.0 (C-4B), 81.6 (C-3B, C-6A), 80.4 (C-2A), 79.9 (C-2B), 78.6, 78.2 (C-4A), 75.6 (Ph*C*H_2), 75.2 (Ph*C*H_2), 74.6 (Ph*C*H_2), 74.2 (Ph*C*H_2), 73.6 (Ph*C*H_2), 73.2 (Ph*C*H_2), 73.1 (Ph*C*H_2), 73.0 (Ph*C*H_2), 72.7 (Ph*C*H_2), 72.6 (C-5A), 72.5 (Ph*C*H_2), 71.9 (Ph*C*H_2), 71.8 (Ph*C*H_2), 71.0 (C-1'), 70.3, 70.2 (C-1'), 69.9, 66.7 (C-6'), 65.6 (C-6'), 27.0 (*t*-Bu), 26.9 (*t*-Bu), 19.3 (CH_3), 19.3 (CH_3); anal. calcd for $C_{148}H_{156}O_{21}Si_2$ (2327.05): C, 76.39; H, 6.76; found: C, 76.44; H, 6.73.

Dihydroxylation of the double bond of 12. Olefin **12** (60 mg, 0.026 mmol) and OsO_4 (30 mg, 0.120 mmol) were dissolved in pyridine (4 mL), and stirred for 48 h. The solvent was evaporated, the residue was dissolved in ethyl acetate (10 mL), to which sat. aq $Na_2S_2O_3$ (1 mL) was added, and the suspension was stirred for 2 days. The organic layer was separated, solvents were evaporated to dryness and the residue was purified by column chromatography (hexane–ethyl acetate, 5:1) to afford **13** (44 mg, 73%) as colorless glass. $[\alpha]_D^{20}$ 22.8; ^{1}H NMR δ 7.64–7.59 (m, 8H, Ar), 7.27–6.98 (m, 77H, Ar), 5.83 (bs, 1H, H-1A), 5.80 (d, 1H, $J_{1,2}$ = 3.5 Hz, H-1B), 4.82–4.69 (m, 5H, PhCH_2), 4.65–4.49 (m, 11H, PhCH_2, sugar-H), 4.45–4.34 (m, 10H, PhCH_2, 2 × sugar-H), 4.29–4.23 (m, 7H, PhCH_2, 5 × sugar-H), 4.08–4.05 (m, 2H, PhCH_2, sugar-H), 4.01–3.95 (m, 6H, 3 × H-6', 3 × sugar-H), 3.89–3.78 (m, 4H, H-1', H-3A, H-3B, H-6'), 3.67 (d, 1H, J = 11.1 Hz, H-1'), 3.58–3.55 (m, 2H, H-1', H-1'), 3.37 (dd, 1H, J = 3.6 Hz, 9.6 Hz, H-2B), 3.36–3.32 (m, 2H, H-2A, sugar-H), 1.02 (s, 9H, *t*-Bu), 1.01 (s, 9H, *t*-Bu); ^{13}C NMR δ 139.1, 139.0, 138.9, 138.8, 138.6, 138.3, 138.2, 138.2, 138.0, 137.9, 137.7, 137.6, 135.6, 135.6, 135.5, 135.5, 133.6, 133.4, 133.3, 132.9, 129.7, 129.7, 129.6, 129.5, 128.4-127.1 (Ar), 105.1 (C-2'), 104.7 (C-2'), 90.7 (C-1B), 89.4 (C-1A), 84.4, 83.5, 82.5 (C-3B), 82.0, 81.9, 81.6 (C-3A), 81.2, 80.4 (C-2B), 79.7 (C-2A), 79.3, 78.6, 75.5 (PhCH_2), 75.3 (PhCH_2), 74.6 (PhCH_2), 74.3, 74.3 (PhCH_2), 73.5 (PhCH_2), 73.2 (PhCH_2), 73.1 (PhCH_2), 73.1 (PhCH_2), 72.7 (PhCH_2), 72.5 (PhCH_2), 71.9 (PhCH_2), 71.8 (PhCH_2), 70.9 (C-1'), 70.7, 70.1 (C-1'), 69.7, 68.2, 66.4 (C-6'), 64.2 (C-6'), 27.0 (*t*-Bu), 19.3 (CH_3), 19.2 (CH_3); MS (ESI): 2383.08 $[M + Na]^+$; anal. calcd for $C_{148}H_{158}O_{23}Si_2$ (2361.06): C, 75.29; H, 6.75; found: C, 75.29; H, 6.79.

Synthesis of olefin 15. To a suspension of methyltriphenylphosphonium bromide (895 mg, 2.50 mmol) in benzene (20 mL) a 2.5 M solution of BuLi in hexane (0.95 mL, 2.30 mmol) was added and the mixture was stirred at rt for 90 min. A solution of aldehyde **7** (298 mg, 0.27 mmol) in benzene (5 mL) was added, the mixture was stirred for another 45 min, quenched with water (100 µL), concentrated, and the residue was purified by column chromatography (hexane–ethyl acetate, 15:1 → 10:1) to afford **15** (172 mg, 58%) as a foam. $[\alpha]_D^{20}$ 24.0; ^{1}H NMR δ 7.67–7.64 (m, 4H, Ar), 7.35–7.18 (m, 36H, Ar), 5.77–5.72 (m, 2H, H-1,6), 5.12–5.09 (m, 1H, H-7), 5.02–5.00 (m, 1H, H-7), 4.82–4.50 (m, 11H, PhCH_2), 4.45–4.43 (m, 3H, H-3',5,PhC*H*), 4.30 (t, 1H, $J_{4,3}$ = $J_{4,5}$ = 7.4 Hz, H-4'), 4.05–4.02 (m, 1H, H-5'), 3.94 (dd, 1H, $J_{6,5}$ = 4.8 Hz, $J_{6,6'}$ = 11.1 Hz, H-6'), 3.90–3.87 (m, 2H, H-3,6'), 3.69 (d, 1H, J_{gem} = 11.0 Hz, H-1'), 3.50 (d, 1H, J_{gem} = 11.0 Hz, H-1'), 3.44 (dd, 1H, $J_{2,1}$ = 3.7 Hz, $J_{2,3}$ = 9.7 Hz, H-2), 3.16 (dd, 1H, $J_{4,3}$ = 9.4 Hz, $J_{4,5}$ = 9.5 Hz, H-4), 1.06 (s, 9H, *t*-Bu); ^{13}C NMR δ 138.9, 138.6, 138.4, 138.3, 138.0, 135.7, 135.6, 135.6, 133.5, 133.3, 129.6, 129.6, 128.3–127.5 (Ar), 117.0 (C-7), 104.3 (C-2'), 89.2 (C-1), 83.8 (C-3'), 82.5 (C-4), 82.3 (C-4'), 81.6 (C-3), 81.2 (C-5'), 80.0 (C-2), 75.6 (PhCH_2), 74.8 (PhCH_2), 73.4 (PhCH_2), 72.9 (PhCH_2), 72.6 (PhCH_2), 72.3 (PhCH_2), 71.4 (C-1',5), 64.9 (C-6'), 26.9 (*t*-Bu-CH_3), 19.3 (*t*-Bu-*C*); anal. calcd for $C_{71}H_{76}O_{10}Si$ (1117.47): C, 76.31; H, 6.86; found: C, 76.42; H, 6.99.

Ozonolytic cleavage of the double bond in sucrose dimer 11. Determination of the configuration at the carbinol center. Ozone was passed through a cooled solution of **11** (51 mg, 0.023 mmol) in CH_2Cl_2 (10 mL) until the blue color persisted (10 min). Dimethyl disulfide (210 µL) was added, the mixture was stirred for 10 min, concentrated, and the residue was dissolved in methanol (10 mL). Sodium borohydride (40 mg) was added, the mixture was stirred for 1 h, concentrated, and the crude product was purified by column chromatography (hexane–ethyl acetate, 7:3) to afford sucrose **6** (16 mg, 63%) and diol **14** (18 mg, 69%), both as foam.

Synthesis of diols 14 and 16. To a solution of **15** (145 mg, 0.13 mmol) in THF (10 mL), *tert*-butyl alcohol (500 µL), water (50 µL), NMO (80 mg, 0.68 mmol), and OsO_4 (8 wt % in *t*-BuOH, 150 µL, 0.035 mmol) were added, and the mixture was stirred at rt for 18 h. Saturated aq $Na_2S_2O_3$ (0.2 mL) was added, the mixture was stirred for 1 h at rt, concentrated, and the products were isolated by column chromatography (hexane–ethyl acetate, 5:1 → 3:1) to afford of **14** (60 mg; 40%) and **16** (58 mg 39%), both as foam.

Data for **14**: $[\alpha]_D^{20}$ 32.6; ^{1}H NMR δ 7.64–7.62 (m, 4H, aryl-H), 7.36–7.14 (m, 36H, Ar), 6.04 (d, 1H, $J_{1,2}$ = 3.8 Hz, H-1), 4.95–4.39 (m, 10H, PhCH_2), 4.47–4.45 (m, 4H, H-3',4',PhCH_2), 4.14 (dd, 1H, $J_{5,4}$ = 10.2, $J_{5,6}$ = 4.1 Hz, H-5), 4.03 (dd, 1H, $J_{6,5}$ = 3.4, $J_{6,6'}$ = 11.6 Hz, H-6'), 3.93–3.89 (m, 2H, H-3,5'), 3.84–3.79 (m, 2H, H-6,6'), 3.65–3.62 (m, 2H, H-1',7), 3.55 (d, 1H, J_{gem} = 10.8 Hz, H-1'), 3.49–3.43 (m, 3H, H-2,4,7), 1.07 (s, 9H, *t*-Bu); ^{13}C NMR δ 138.6, 138.2, 138.0, 137.9, 137.8, 137.3, 135.7, 135.4, 133.0, 132.6, 129.8, 129.7, 128.7–127.6 (Ar), 104.3 (C-2'), 88.2 (C-1), 82.9 (C-3'), 82.0 (C-3), 80.3 (C-5'), 80.1 (C-2,4'), 79.0 (C-4), 75.5 (PhCH_2), 74.7 (PhCH_2),73.4 (PhCH_2), 73.1 (PhCH_2), 72.8 (PhCH_2), 72.3 (C-1'), 72.2 (C-6), 71.9 (PhCH_2), 71.3 (C-5), 63.0 (C-6'), 62.9 (C-7), 26.9 (*t*-Bu-CH_3), 19.2 (*t*-Bu-*C*); anal. calcd for $C_{71}H_{78}O_{12}Si$ (1151.49): C, 74.06; H, 6.83; found: C, 74.00; H, 6.79.

Data for **16**: $[\alpha]_D^{20}$ 21.6; ^{1}H NMR δ 7.64–7.62 (m, 4H, Ar), 7.37–7.16 (m, 36H, aryl-H), 6.04 (d, 1H, $J_{1,2}$ = 3.6 Hz, H-1), 4.93–4.40 (m, 12H, PhCH_2), 4.40 (d, 1H, J = 6.5 Hz, H-3'), 4.32 (t, 1H, $J_{4,3}$ = $J_{4,5}$ = 6.7 Hz, H-4'), 4.03–3.99 (m, 2H, H-5,6'), 3.95 (t, 1H, $J_{3,2}$ = $J_{3,4}$ = 9.4 Hz, H-3), 3.92–3.91 (m,

1H, H-5'), 3.81 (dd, 1H, $J_{6,5}$ = 4.0 Hz, $J_{6,6'}$ = 11.4 Hz, H-6'), 3.74–3.72 (m, 1H, H-6), 3.70–3.66 (m, 2H, H-1',4), 3.55 (d, 1H, J_{gem} = 10.9 Hz, H-1'), 3.48–3.42 (m, 3H, H-2,7,7), 1.07 (s, 9H, *t*-Bu); ^{13}C NMR δ 138.8, 138.5, 138.3, 137.9, 137.7, 137.5, 135.7, 135.5, 132.9, 132.7, 129.8, 129.8, 128.4–127.5 (Ar), 104.8 (C-2'), 89.3 (C-1), 83.2 (C-3'), 81.4 (C-3), 81.1 (C-4'), 80.8 (C-5'), 79.9 (C-2), 77.3 (C-4), 75.5 (Ph*C*H$_2$), 75.1 (Ph*C*H$_2$), 73.5 (Ph*C*H$_2$), 73.2 (Ph*C*H$_2$), 72.5 (Ph*C*H$_2$), 72.0 (Ph*C*H$_2$), 71.9 (C-5), 71.6 (C-1'), 68.9 (C-6), 64.5 (C-7), 63.1 (C-6'), 26.9 (*t*-Bu-*C*H$_3$), 19.2 (*t*-Bu-*C*); anal. calcd for $C_{71}H_{78}O_{12}Si$ (1151.49): C, 74.06; H, 6.83; found: C, 73.94; H, 6.66.

Both compounds were further characterized as diacetates: **14-Ac** and **16-Ac**.

Data for **14-Ac**: $[\alpha]_D^{20}$ 33.3; ^{1}H NMR δ 7.66–7.64 (m, 4H, Ar), 7.34–7.21 (m, 36H, aryl-H), 5.82 (d, 1H, $J_{1,2}$ = 3.6 Hz, H-1), 5.48 (m, 1H, H-6), 4.93–4.55 (m, 10H, PhC*H*$_2$), 4.46–4.42 (m, 3H, H-3', PhC*H*$_2$), 4.15 (dd, 1H, $J_{5,4}$ = 10.3 Hz, $J_{5,6}$ = 1.4 Hz, H-5), 4.03–3.96 (m, 3H, H-5', H-6', H-7), 3.91 (dd, 1H, $J_{6,5}$ = 4.7, $J_{6,6'}$ = 10.9 Hz, H-6'), 3.88 (t, 1H, $J_{3,2}$ = $J_{3,4}$ = 9.2 Hz, H-3), 3.67 (d, 1H, $J_{1,1}$ = 11.0 Hz, H-1'), 3.51 (d, 1H, $J_{1,1}$ = 11.0 Hz, H-1'), 3.49 (dd, 1H, $J_{4,3}$ = 9.2 Hz, $J_{4,5}$ = 10.3 Hz, H-4), 3.39 (dd, 1H, $J_{2,1}$ = 3.6 Hz, $J_{2,3}$ = 9.7 Hz, H-2), 1.96 (s, 3H, CH$_3$), 1.84 (s, 3H, CH$_3$), 1.05 (s, 9H, *t*-Bu); ^{13}C NMR δ 170.5 (C=O), 169.8 (C=O), 138.6, 138.4, 138.2, 138.1, 138.0, 137.9, 135.7, 135.5, 133.3, 133.0, 129.7, 129.6, 128.3-127.5 (Ar), 104.2 (C-2'), 89.0 (C-1), 83.7 (C-3'), 82.0 (C-3), 81.9 (C-4'), 81.0 (C-5'), 79.8 (C-2), 77.6 (C-4), 75.6 (Ph*C*H$_2$), 74.6 (Ph*C*H$_2$), 73.3 (Ph*C*H$_2$), 73.1 (Ph*C*H$_2$), 72.8 (Ph*C*H$_2$), 72.1 (Ph*C*H$_2$), 71.4 (C-1'), 71.1 (C-6), 70.9 (C-5), 64.6 (C-6'), 63.2 (C-7), 26.9, 20.9, 20.8, 19.2; anal. calcd for $C_{75}H_{82}O_{14}Si$ × ½H_2O (1253.57): C, 72.38; H, 6.72; found: C, 72.51; H, 6.36. HRMS (ESI) calc. for $C_{75}H_{86}NO_{14}Si$ [M + NH_4]$^+$: 1252.5818; found: 1252.5825.

Data for **16-Ac**: $[\alpha]_D^{20}$ 13.1; ^{1}H NMR ($CDCl_3$) δ 7.65–7.63 (m, 4H, Ar), 7.34–7.20 (m, 36H, Ar), 6.09 (d, 1H, $J_{1,2}$ = 3.5 Hz, H-1), 5.48 (ddd, 1H, *J* = 1.5 Hz, 2.9 Hz, 9.2 Hz, H-6), 4.88–4.42 (m, 12H, PhC*H*$_2$), 4.42–4.38 (m, 2H, H-3', H-4'), 4.28 (dd, 1H, $J_{7,6}$ = 9.1 Hz, $J_{7,7}$ = 12.0 Hz, H-7), 4.11 (dd, 1H, $J_{5,4}$ = 10.1 Hz, $J_{5,6}$ = 1.3 Hz, H-5), 4.06 (dd, 1H, $J_{7,6}$ = 3.1 Hz, $J_{7,7}$ = 12.0 Hz, H-7), 4.02 (dd, 1H, $J_{6,5}$ = 4.2 Hz, $J_{6,6'}$ = 11.4 Hz, H-6'), 3.97–3.93 (m, 2H, H-3, H-5'), 3.85 (dd, 1H, $J_{6,5}$ = 4.1 Hz, $J_{6,6'}$ = 11.4 Hz, H-6'), 3.74 (d, 1H, $J_{1,1}$ = 10.8 Hz, H-1'), 3.53 (d, 1H, $J_{1,1}$ = 10.8 Hz, H-1'), 3.48 (dd, 1H, $J_{2,1}$ = 3.5 Hz, $J_{2,3}$ = 9.7 Hz, H-2), 3.33 (dd, 1H, $J_{4,3}$ = 8.9 Hz, $J_{4,5}$ = 10.1 Hz, H-4), 2.08 (s, 3H, CH$_3$), 1.95 (s, 3H, CH$_3$), 1.06 (s, 9H, *t*-Bu); ^{13}C NMR ($CDCl_3$) δ 170.3 (C=O), 170.2 (C=O), 138.5, 138.3, 138.3, 138.2, 137.8, 137.7, 135.6, 135.5, 133.2, 132.7, 129.7, 129.6, 128.5–127.5 (Ar), 104.6 (C-2'), 89.1 (C-1), 83.7 (C-3'), 81.6 (C-3), 81.3 (C-4'), 80.8 (C-5'), 79.8 (C-2), 76.9 (C-4), 75.6 (Ph*C*H$_2$), 75.0 (Ph*C*H$_2$), 73.5 (Ph*C*H$_2$), 73.3 (Ph*C*H$_2$), 72.8 (Ph*C*H$_2$), 71.8 (Ph*C*H$_2$), 71.4 (C-1'), 70.2 (C-5), 69.0 (C-6), 64.8 (C-7), 63.7 (C-6'), 26.9, 21.0, 20.8, 19.2; anal. calcd for $C_{75}H_{82}O_{14}Si$ × ½H_2O (1253.57): C, 72.38; H, 6.72; found: C, 72.34; H, 6.29. HRMS (ESI) calc. for $C_{75}H_{86}NO_{14}Si$ [M + NH_4]$^+$: 1252.5818; found: 1252.5819.

Supporting Information

Supporting Information File 1

The ^{1}H and ^{13}C NMR spectra of all new compounds (**9**–**16Ac**).
[http://www.beilstein-journals.org/bjoc/content/supplementary/1860-5397-10-124-S1.pdf]

Acknowledgements

The support from Grant: POIG.01.01.02-14-102/09 (part-financed by the European Union within the European Regional Development Fund) and N N204 187439 (from the Ministry of Science and Higher Education) is acknowledged.

References

1. Ooi, T.; Maruoka, K. *Angew. Chem., Int. Ed.* **2007,** *46,* 4222–4266. doi:10.1002/anie.200601737
2. Rapi, Z.; Démuth, B.; Keglevich, G.; Grün, A.; Drahos, L.; Sóti, P. L.; Bakó, P. *Tetrahedron: Asymmetry* **2014,** *25,* 141–147. doi:10.1016/j.tetasy.2013.12.007
3. Zhang, X. X.; Bradshaw, J. S.; Izatt, R. M. *Chem. Rev.* **1997,** *97,* 3313–3362. doi:10.1021/cr960144p
4. Cheng, C.; Cai, Z.; Peng, X.-S.; Wong, H. N. C. *J. Org. Chem.* **2013,** *78,* 8562–8573. doi:10.1021/jo401240k
5. Jarosz, S.; Listkowski, A. *Curr. Org. Chem.* **2006,** *10,* 643–662. doi:10.2174/138527206776359702
6. Bako, P.; Keglevich, G.; Rapi, Z.; Toke, L. *Curr. Org. Chem.* **2012,** *16,* 297–304. doi:10.2174/138527212799499877
7. Jarosz, S.; Potopnyk, M. A.; Kowalski, M. Sucrose as chiral platform in the synthesis of macrocyclic receptors. In *Carbohydrate Chemistry-Chemical and Biological Approaches;* Rauter, A. P.; Lindhorst, T.; Queneau, Y., Eds.; RSC Publishing, 2014; Vol. 40, pp 236–256. doi:10.1039/9781849739986-00236
See for a recent review.
8. Jarosz, S.; Listkowski, A. *Can. J. Chem.* **2006,** *84,* 492–496. doi:10.1139/v06-035
9. Jarosz, S.; Listkowski, A.; Lewandowski, B. *Phosphorus, Sulfur Silicon Relat. Elem.* **2009,** *184,* 1285–1295. doi:10.1080/10426500902856370
10. Queneau, Y.; Jarosz, S.; Lewandowski, B.; Fitremann, J. *Adv. Carbohydr. Chem. Biochem.* **2007,** *61,* 217–292. doi:10.1016/S0065-2318(07)61005-1
11. Jarosz, S.; Lewandowski, B. *Carbohydr. Res.* **2008,** *343,* 965–969. doi:10.1016/j.carres.2008.01.016

12. Potopnyk, M. A.; Lewandowski, B.; Jarosz, S. *Tetrahedron: Asymmetry* **2012,** *23,* 1474–1479. doi:10.1016/j.tetasy.2012.10.003
13. Lewandowski, B.; Jarosz, S. *Chem. Commun.* **2008,** 6399–6401. doi:10.1039/b816476b
14. Potopnyk, M. A.; Jarosz, S. *Eur. J. Org. Chem.* **2013,** 5117–5126. doi:10.1002/ejoc.201300427
15. Lewandowski, B.; Jarosz, S. *Org. Lett.* **2010,** *12,* 2532–2535. doi:10.1021/ol100749m
16. Jarosz, S. *J. Carbohydr. Chem.* **2001,** *20,* 93–107. doi:10.1081/CAR-100103951
17. Jarosz, S.; Mach, M. *J. Chem. Soc., Perkin Trans. 1* **1998,** 3943–3948. doi:10.1039/a807190j
18. Jarosz, S. *Curr. Org. Chem.* **2008,** *12,* 985–994. doi:10.2174/138527208785161187
19. Jarosz, S.; Mach, M.; Frelek, J. *J. Carbohydr. Chem.* **2000,** *19,* 693–715. doi:10.1080/07328300008544111
20. Mach, M.; Jarosz, S. *J. Carbohydr. Chem.* **2001,** *20,* 411–424. doi:10.1081/CAR-100105713
21. Synthesis of this aldehyde was already reported by us as intermediate in the preparation of the uronate **8** (see ref. [8]).
22. Makosza, M.; Fedorynski, M. *Adv. Catal.* **1987,** *35,* 375–422. doi:10.1016/S0360-0564(08)60097-8
23. Makosza, M. *Pure Appl. Chem.* **2000,** *72,* 1399–1403. doi:10.1351/pac200072071399
24. Makosza, M.; Fedoryński, M. *Catal. Rev.: Sci. Eng.* **2003,** *45,* 321–367. doi:10.1081/CR-120025537
25. Jarosz, S. *Carbohydr. Res.* **1988,** *183,* 201–207. doi:10.1016/0008-6215(88)84074-6
26. Cha, J. K.; Christ, W. J.; Kishi, Y. *Tetrahedron* **1984,** *40,* 2247–2255. doi:10.1016/0040-4020(84)80008-3
27. Frelek, J.; Pakulski, Z.; Zamojski, A. *Tetrahedron: Asymmetry* **1996,** *7,* 1363–1372. doi:10.1016/0957-4166(96)00153-X
28. Frelek, J.; Ikekawa, N.; Takatsuto, S.; Snatzke, G. *Chirality* **1997,** *9,* 578–582. doi:10.1002/(SICI)1520-636X(1997)9:5/6<578::AID-CHIR27>3.0.CO;2-K
29. Frelek, J.; Klimek, A.; Ruśkowska, P. *Curr. Org. Chem.* **2003,** *7,* 1081–1104. doi:10.2174/1385272033486576
30. Jawiczuk, M.; Górecki, M.; Suszczyńska, A.; Karchier, M.; Jaźwiński, J.; Frelek, J. *Inorg. Chem.* **2013,** *52,* 8250–8263. doi:10.1021/ic401170m
31. Biela, A.; Oulaïdi, F.; Gallienne, E.; Górecki, M.; Frelek, J.; Martin, O. R. *Tetrahedron* **2013,** *69,* 3348–3354. doi:10.1016/j.tet.2012.12.082
32. Schönemann, W.; Gallienne, E.; Ikeda-Obatake, K.; Asano, N.; Nakagawa, S.; Kato, A.; Adachi, I.; Górecki, M.; Frelek, J.; Martin, O. R. *ChemMedChem* **2013,** *8,* 1805–1817. doi:10.1002/cmdc.201300327

License and Terms

Beilstein Journal of Organic Chemistry

Human dendritic cell activation induced by a permannosylated dendron containing an antigenic GM_3-lactone mimetic

Renato Ribeiro-Viana[‡1], Elena Bonechi[‡2], Javier Rojo[1], Clara Ballerini[2], Giuseppina Comito[3], Barbara Richichi[*4] and Cristina Nativi[4]

Full Research Paper

Open Access

Address:
[1]Glycosystems Laboratory, Instituto de Investigaciones Químicas (IIQ), CSIC – Universidad de Sevilla, Américo Vespucio 49, 41092 Sevilla, Spain, [2]Department of NEUROFARBA, University of Florence, Viale Pieraccini 6, 50134 Firenze, Italy, [3]Department of Biochemical Science, University of Florence, Viale Morgagni 50, 50134 Florence, Italy and [4]Department of Chemistry, University of Florence, Via della Lastruccia 13, 50019 Sesto Fiorentino (FI), Italy

Email:
Barbara Richichi[*] - barbara.richichi@unifi.it

* Corresponding author ‡ Equal contributors

Keywords:
cancer immunotherapy; DC-SIGN; DC targeting; glycodendron; GM_3-lactone mimetic; multivalent glycosystems; multivalent interactions

Beilstein J. Org. Chem. **2014,** *10,* 1317–1324.
doi:10.3762/bjoc.10.133

Received: 19 February 2014
Accepted: 30 April 2014
Published: 10 June 2014

This article is part of the Thematic Series "Multivalent glycosystems for nanoscience".

Guest Editor: V. Křen

Abstract

Vaccination strategies based on dendritic cells (DCs) armed with specific tumor antigens have been widely exploited due the properties of these immune cells in coordinating an innate and adaptive response. Here, we describe the convergent synthesis of the bifunctional multivalent glycodendron **5**, which contains nine residues of mannose for DC targeting and one residue of an immunogenic mimetic of a carbohydrate melanoma associated antigen. The immunological assays demonstrated that the glycodendron **5** is able to induce human immature DC activation in terms of a phenotype expression of co-stimulatory molecules expression and MHCII. Furthermore, DCs activated by the glycodendron **5** stimulate T lymphocytes to proliferate in a mixed lymphocytes reaction (MLR).

Introduction

Cancer immunotherapy [1] attempts to induce a long-lasting antitumor immunity and boost the immune response overcoming the tumor induced immunosuppression. The immune system, apart from very few exceptions, fails to taking an adequate course of action against tumors. Tumor cells are indeed poor antigen-presenting cells (APCs). Additionally, in

neoplastic diseases the so-called "escape mechanisms" [2-4] enable tumor cells to elude tumor-bearing immunosurveillance of the host. A better understanding of the interactions between cancer and immune cells may lead to more efficient immunotherapy strategies [5,6].

In this context, the discovery of human cancer-specific antigens [7,8] has represented a challenge for the design of tailored cancer vaccines and it has allowed the development of antigen-specific immunotherapy strategies. This approach offers the advantage that the immune response induced by such antigens should presumably be limited to tumor cells bearing antigenic epitopes. To induce a persistent and efficient tumor immune response and generate a pool of tumor antigen specific activated immune cells, a complex cross-talk between the innate and the adaptive immune system is a prerequisite. In this context, during the last two decades, dendritic cells (DCs) have clearly been identified as essential candidates to generate therapeutic immunity against tumors [9-12].

DCs are the principal antigen-presenting cells (APCs) in the immune system where they play a central role because they are able to control self-tolerance as well as induce an effective immune response [13,14]. They provide an essential link between innate and adaptive immune responses [13]. They survey the environment and, based on the typical non-clonal recognition receptors of the innate immune system, they take up the non-self agents and transmit the resulting information to both B and T cells of the adaptive immune system. DCs contribute to the peripheral tolerance and this might be determined by their functional status. Therefore, DC activation is crucial to their function. During activation, DCs up-regulate MHCII molecules and co-stimulatory factors, both of which are mandatory to achieve a complete immunostimulatory function. Since the discovery of their key role in immunogenicity in 1973 by R. Steinman [15], DCs have been identified as "nature's adjuvants". Today, they are considered natural targets for antigen delivery and therapeutic vaccination against cancer [9,10].

Several approaches have been investigated to pulse DCs with target antigens with the aim to induce robust and long-lasting CD4+ and CD8+ T cell responses against tumors [9,10]. In general, the first step of DC vaccination strategies is to arm DCs with tumor-specific antigens. This issue has successfully been achieved by either culturing ex vivo DCs [16,17] from bone marrow precursors or more recently by targeting in vivo DC receptors with specific mAbs conjugated to tumor antigens [18,19]. In both cases, the development of a powerful DCs-based vaccination protocol requires a careful evaluation of the exact conditions necessary for their optimal maturation into potent immunostimulatory APCs. In particular, a strict control must be exercised over the form of the antigen loaded onto DCs, the antigen quantity, the persistence, the timing and the pathways essential for enhancing DC maturation and for licensing the antigen-loaded DCs in the T cell zone of lymph nodes [10].

Concerning the DCs maturation step, triggering C-type lectin receptors (CLRs) is crucial to enhance the antitumor immunity [10,20]. In particular, dendritic cell-specific ICAM-3 grabbing non-integrin (DC-SIGN), which belongs to the class of CLRs, is expressed mainly on the surface of immature DCs and plays a crucial role in the uptake of specific pathogens. DC-SIGN is able to bind in a Ca^{2+}-dependent manner mannose and fucose residues on highly glycosylated proteins expressed on pathogens by means of its carbohydrate recognition domain (CRD) [21]. CLRs are antigen-uptake receptors. Moreover, the signaling pathways downstream induced by these receptors play a pivotal role in tailoring the immune response to break tumor-induced immunosuppression [22]. Therefore, a combination of DC-SIGN ligands and specific tumor-associated antigens could successfully target DCs and trigger an efficient antitumor response.

Melanoma has long been considered a promising target for immunotherapeutic approaches and has been a major focus of clinical development efforts in the realm of immunotherapy [23-25]. GM_3-ganglioside **1** (Figure 1), the major glycosphingolipid in normal melanocytes, is overexpressed in melanoma cells with metastatic potential [26,27]. It has been considered a carbohydrate melanoma-associated antigen and widely investigated as a key component of a potential vaccine against melanoma disease [28].

The GM_3 metabolite, named GM_3-lactone **2** (Figure 1) has also been found in melanoma cells as a minor component [29,30]. Although more immunogenic than GM_3-ganglioside **1**, GM_3-lactone **2** failed as an immunostimulant because under physiological conditions the available amount of lactone is below the recognition threshold and therefore scarcely effective as an immunostimulant.

Several years ago [31], we reported on the conformational analysis and the synthesis of thioether **3** (Figure 1), a hydrolytically stable mimetic of the GM_3-lactone **2**. Structurally simpler than the native antigen, the mimetic **3** presents the folded shape characteristics of the GM_3-lactone and in addition it is stable under physiological conditions [31]. We conjugated the mimetic **3** to the immunogenic protein KLH and demonstrated that the corresponding KLH-glycoconjugated **4** (Figure 1) was able to elicit in vivo antimelanoma antibodies [32].

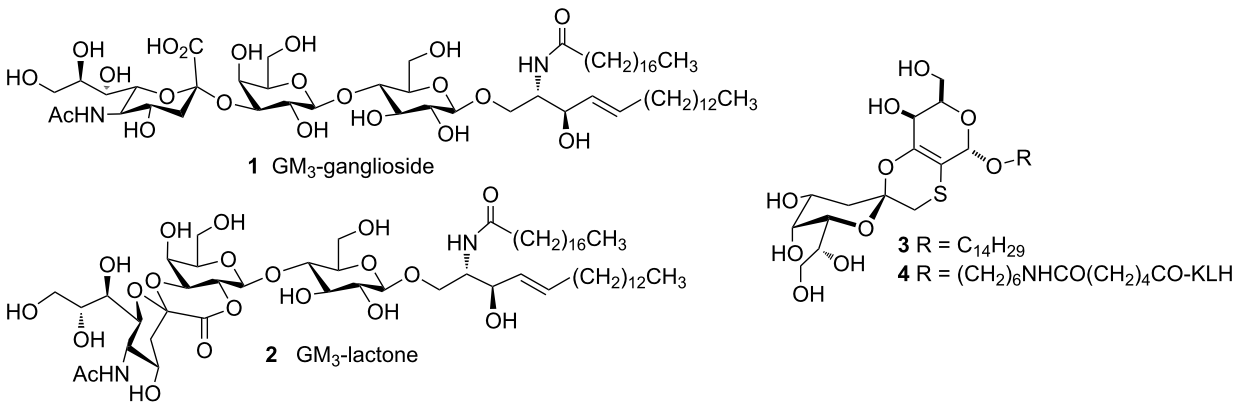

Figure 1: Structure of GM_3-ganglioside **1**, GM_3-lactone **2**, GM_3-lactone mimetic **3**, and GM_3-lactone mimetic conjugated to KLH protein (**4**).

More recently [33], we established that the multivalent presentation of this synthetic mimetic positively interferes with human melanoma cell (A375) adhesion, migration and resistance to apoptosis, showing a clear amplification of the biological properties of the monovalent synthetic antigen as an immunomodulator as well as an anti-adhesive agent in melanoma progression.

Taking into account all these data and relying on recent results on the use of mannose-based glycodendrons as vectors for antigen delivery to DCs [34], we report here on the convergent synthesis of the bifunctional multivalent glycodendron **5** (Scheme 1) and on human DC activation and related mixed-lymphocyte reaction (MLR) induced by the antigenic glycodendron **5**.

Results and Discussion

Glycodendron **5** (Scheme 1) is a bifunctional compound containing nine residues of mannose for DC targeting and one residue of the mimetic **3** as a carbohydrate melanoma-associated antigen. We have previously demonstrated that a glycodendron bearing nine copies of the monosaccharide mannose can be taken up by DCs in a receptor-dependent manner by means of the lectin DC-SIGN [34]. This dendron has the adequate size and valency to efficiently interact with this receptor. Dendron **7** (Scheme 1), presenting an azido group at the focal position, was synthesized as previously described [35]. This functionalization permits, in a further step, the conjugation of any molecule conveniently functionalized with an alkyne group by a Cu(I) azide–alkyne cycloaddition (CuAAC) reaction. Then, the mimetic **6** with a butyne group at the anomeric position, which is required for the conjugation to the glycodendron **7** (Scheme 1), was also prepared as already reported [33]. The synthesis of the tricyclic spiro unit of **6** was efficiently performed relying on a totally diastereoselective inverse electron-demand [4 + 2] hetero-Diels–Alder reaction , as described in [31].

The synthesis of compound **5** is depicted in Scheme 1. The mimetic **6** was deprotected with sodium carbonate at room temperature. Without further purification the resulting syrup was conjugated with the glycodendron **7** by a CuAAC reaction with $CuSO_4$ as a copper source, sodium ascorbate to reduce Cu(II) to Cu(I) in situ, and tris[(1-benzyl-1*H*-1,2,3-triazol-4-yl)methyl]amine (TBTA) to stabilize Cu(I). The solution was treated with a resin (Quadrasil MP) to remove any trace of copper that could cause interferences in the biological assays. After purification by size exclusion chromatography by using a LH-20 column, the bifunctional glycodendron **5** was obtained in 86% yield and characterized by NMR and MS (electrospray).

We tested in vitro human myeloid DCs (see methods) for an activation with LPS (positive control, 1 μg/mL), the bifunctional multivalent glycodendron **5** and **7** (negative control). Two doses (10 μg and 50 μg) of each compound were used. Our data showed that **5**, but not **7**, induces DC activation in terms of phenotype expression of MHC class II molecules, CD80 and CD86 co-stimulatory molecules and CD83 activation marker, as observed with positive control (Figure 2, upper panels, one experiment representative of three independent ones). To test the functional activity of the differently treated DCs, we performed on the same cells mixed lymphocytes reactions (MLR) (see Experimental) and checked the proliferative T lymphocyte response after allo-stimulation. As depicted in Figure 2, DCs treated with LPS or glycodendron **5** fully stimulate T lymphocytes, whereas **7** does not stimulate T lymphocytes (Figure 2, lower panel, one experiment representative of three independent experiments).

In the development of immunotherapy as an emerging strategy to treat tumours, DCs are an object of great interest because they can be used as APCs to stimulate the immune system against a specific tumor antigen. For this purpose, DCs can be

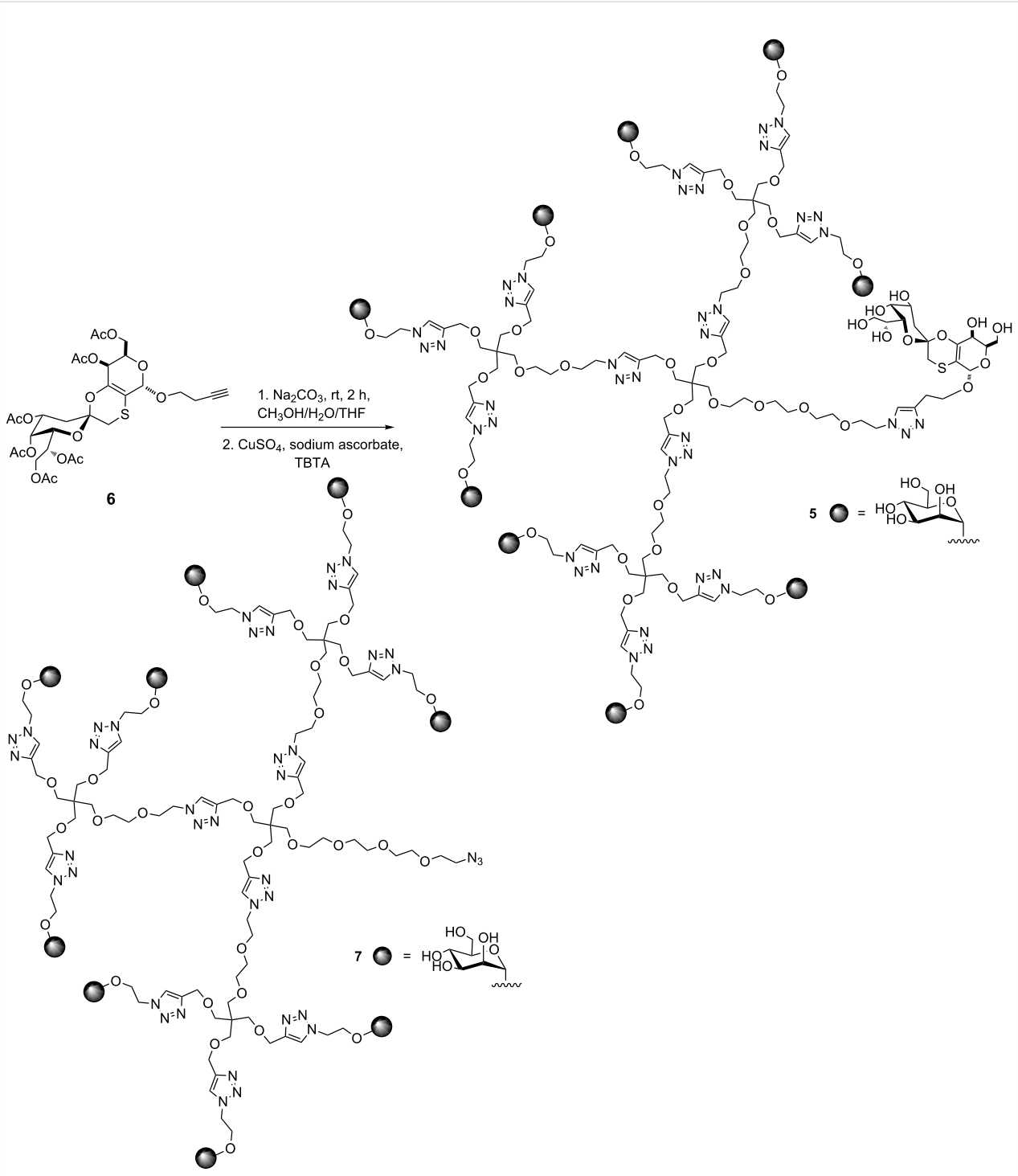

Scheme 1: Synthesis of the bifunctional multivalent glycodendron **5**.

pulsed ex vivo with the corresponding tumor antigen. However, this strategy is complicated and expensive, requiring the isolation of patients' DCs, the pulsing of DCs with the antigen, and their reinsertion. Another approach envisages the targeting of DCs in vivo by using a selective vector combined with a cargo tumor antigen. This second strategy requires a system which should be able to selectively target DCs in vivo. In this work, we have shown how to combine in a single entity a mannosylated dendron able to selectively interact with DCs through DC-SIGN armed with a synthetic antigen. This ditopic glyco-

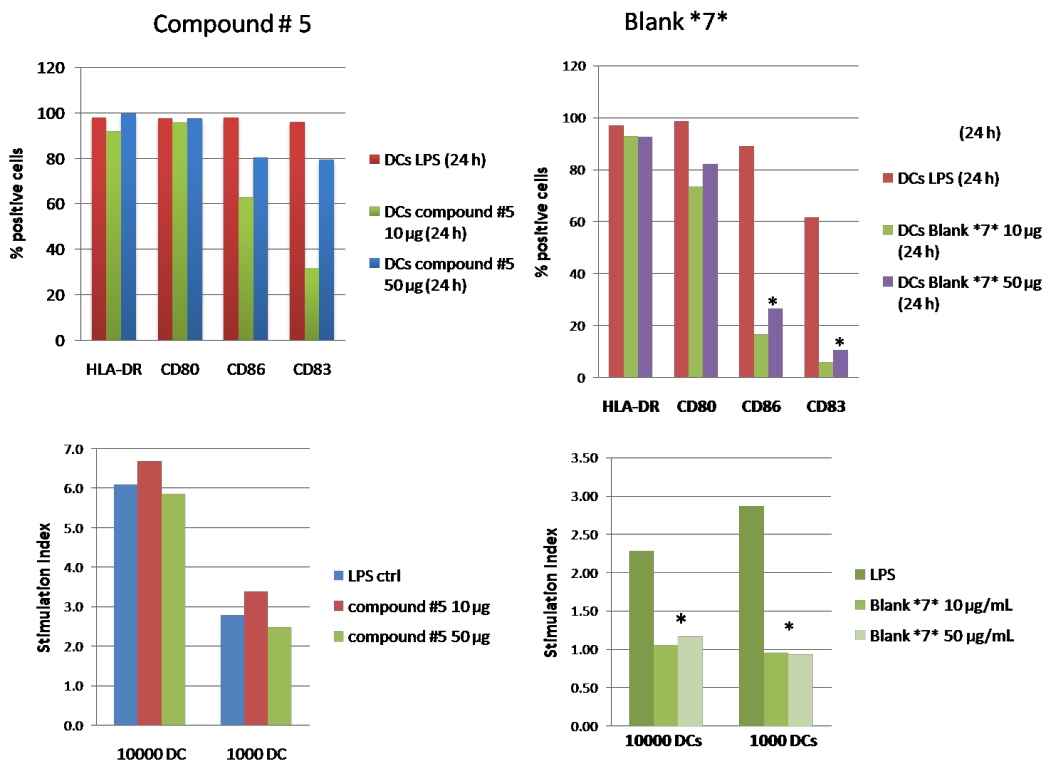

Figure 2: Upper panels: percentage of expression of dendritic cell markers (HLA-DR ECD, CD80 FITC, CD86 PE and CD83 PC5). Cell phenotypes, expressed as the percentage of positive cells for CD80, CD86 and HLA-DR, did not change when activation took place in the presence of compound **5** (left) at 10 or 50 µg/mL compared to LPS. CD83, an activation marker, was fully expressed at the higher dose of treatment. Compound **7** did not activate DCs when compared to LPS (right), differences between CD83 and CD86 expression are statistically significant at the two doses tested (*$p < 0.05$). One experiment is representative of three independent ones. Lower panels: mixed lymphocytes reaction (MLR). Compound **5** (left) at the dose of 10 or 50 µg/mL did not affect T lymphocyte proliferative response. As expected from the phenotype, scaffold (right) treated DCs at the dose of 10 or 50 µg/mL, significantly reduces the proliferative response (*$p < 0.05$). One experiment is representative of three independent ones. The analysis was performed by an unpaired t-test indicating that the mean is statistically significant at $p < 0.05$.

dendron **5** demonstrated to be correctly designed to activate dendritic cells and stimulate T cells. Biological data clearly showed that the multivalent glycodendron **5** activates human immature DCs, induces the expression of all co-stimulatory molecules and MHCII, whereas the negative control **7** does not. Indeed, DCs need both MHC II and co-stimulation properly expressed on their surface to correctly integrate signals and activate T lymphocytes. If DCs do not sufficiently express one or more activation factors, their function may be impaired [36]. From a functional point of view, DCs activated by **5** stimulate T lymphocytes so that they proliferate in a classical MLR assay as LPS-activated cells (golden standard). When we tested the scaffold molecule alone (blank **7** in Figure 2) the phenotypic expression of DCs of co-stimulatory molecules and their T cell allo-stimulation ability was significantly impaired. Based on the data gathered in the experiments outlined here we conclude that the maturation/stimulation of DCs is specifically linked to the presence of the mimetic antigen residue and not determined by the scaffold alone.

Conclusion

Here, we reported on the convergent synthesis of the ditopic multivalent glycodendron **5**, which contains an immunogenic mimetic of a carbohydrate melanoma associated antigen. We demonstrated that the immunogenic carbohydrate-based mimetic is able to induce human DCs activation if properly presented to DCs. Moreover, we showed that this activation is mediated by a permannosylated dendron interacting with the surface receptor DC-SIGN. These promising and preliminary biological results pave the way to the design of glycodendritic structures bearing antigen cargos as a selective vector to target APCs for stimulating immune responses. Further experiments must be performed to verify that the DCs activated by the multivalent ditopic glycodendron **5** are able to induce a strong pro-inflammatory response in vivo, thereby breaking the tolerance toward self antigens as melanoma and bypassing the tolerogenic environment normally established by the tumor activity. We envisage that this kind of compounds based on multivalent ditopic glycodendrons might be used to address the preparation

of a synthetic vaccine against melanoma. In addition, this strategy might be applied to other diseases in immunotherapy.

Experimental

Reagents were purchased from Sigma–Aldrich and Fluka and were used without purification. Synthetic compounds were purified by Sephadex (LH20). Thin-layer chromatography (TLC) was carried out with pre-coated Merck F_{254} silica gel plates. Reaction completion was observed by TLC with phosphomolibdic acid, 10% sulfuric acid in methanol or anisaldehyde as development reagents. ^{1}H NMR and ^{13}C NMR spectra were recorded on a Bruker Avance DRX 500 MHz spectrometer. Chemical shifts (δ) for ^{1}H NMR and ^{13}C NMR spectra are expressed in ppm relative to the residual solvent signal according to the indirect referencing method of the manufacturer. Signals are abbreviated as s, singlet; bs, broad singlet; d, doublet; t, triplet; q, quartet; m, multiplet. Mass spectra were obtained with a Bruker ion-trap Esquire 6000 apparatus (ESI).

Synthesis

The preparation of compounds **6** [33] and **7** [35] was realized as previously described.

Synthesis of Glycodendron **5**

To a solution of mimetic **6** (0.006 g, 0.009 mmol) in a mixture of methanol/THF/water (1:1:1, 1.2 mL), sodium carbonate (46 mg, 0.40 mmol) was added. The solution was stirred at room temperature for 2 h. After that, resin IRA-120 H^+ was added to reach pH 5. The reaction mixture was filtrated, and the solvent evaporated. The resulting syrup, glycodendron **7** (30 mg, 0.008 mmol), $CuSO_4{\cdot}5H_2O$ (0.4 mg, 0.001 mmol), TBTA (2.5 mg, 0.004 mmol) and sodium ascorbate (1 mg, 0.004 mmol) were dissolved in 0.8 mL of THF/H_2O 1:1. After 2.5 h, a small amount of metal scavenger resin (Quadrasil MP) was added, and after further 5 minutes under stirring at room temperature the mixture was filtered on a cotton pad and the solution was purified by size exclusion chromatography (LH-20, MeOH 100%), furnishing 28.4 mg (86% yield, calculated over two steps) of the glycondendron **5** as a white foam. $[\alpha]^{25}_D$ +23.9 (*c* 1, H_2O/MeOH 1:1)

^{1}H NMR (500 MHz, D_2O) δ 8.01 (s, 9H, $H_{triazol}$), 7.96 (s, 3H, $H_{triazol}$), 7.89 (s. 1H, $H_{triazol}$), 5.09 (s, 1H, H-1_{gal}), 4.85 (s, 9H, H-1_{mann}), 4.65–4.55 (m, 18H, $O_{mann}CH_2C\underline{H}_2N$), 4.56–4.45 (m, 32H, $OC\underline{H}_2C_{triazol}$, $O_{linker}CH_2CH_2N$, $OCH_2C_{triazol}$), 4.25–4.21 (m, 1H, H-$3_{sial.ac}$), 4.08–4.04 (m, 9H, $O_{mann}CH_2CH_2N$), 3.91–3.86 (m, 15H, $O_{mann}CH_2CH_2N$, $O_{linker}CH_2CH_2N$), 3.85–3.83 (m, 9H, H-2_{mann}), 3.75–3.43 (m, 79H, H-6_{mann}, H-3_{mann}, H-5_{mann}, $O_{pentaerythritol}CH_2CH_2$, $O_{pentaerythritol}CH_2CH_2$, $OC\underline{H}_{2linker}$, CH_2O_{1gal}, H-4_{gal}, H-5_{gal}, H-6_{gal}, H-$4_{sial.ac}$, H-$5_{sial.ac}$, H-$6_{sial.ac}$, H-$7_{sial.ac}$), 3.39–3.33 (m, 24H, $CH_{2pentaerythritol}$), 3.30–3.27 (m, 8H, $CH_{2pentaerythritol}$), 3.09–3.04 (m, 9H, H-4_{mann}), 2.99–2.95 (m, 4H, SCH_2, $C_{triazol}CH_2CH_2O$), 2.04–1.97 (m, 1H, H-$2_{sial\ ac}$), 1.91–1.84 (m, 1H, H-$2_{sial\ ac}$); ^{13}C NMR (125 MHz, D_2O) δ 144.3 ($C_{triazol}$), 142.4 (O-*C*=C-S), 125.3 ($C_{triazol}$), 105.3 (O-C=*C*-S), 99.6 (C-1_{mann}), 95.8 (C-1_{gal}), 92.7 (C-$1_{sial.ac.}$), 72.8 (C-4_{mann}), 70.4 (C-3_{mann}), 69.91 (C-2_{mann}), 69.7 ($CH_{2pentaerythritol}O_{linker}$), 68.9 ($CH_2O$), 68.8 ($CH_2O$), 68.7 ($CH_2O$), 68.7 ($CH_2O$), 68.4 ($CH_{2pentaerythritol}$), 66.4 (C-$5_{mann}$), 65.8 (CHO), 65.5 ($O_{mann}CH_2CH_2N$, OCH_2CH_2N), 63.6 ($OCH_2C_{triazol}$), 60.7 (C-6_{mann}), 50.0 ($O_{mann}CH_2CH_2N$, OCH_2CH_2N, OCH_2CH_2N), 44.8 ($C_{pentaerythritol}$), 35.4 (C-$2_{sial.ac.}$), 32.9 (SCH_2), 35.3 ($C_{triazol}CH_2CH_2$); ESIMS (*m*/*z*): calcd for $C_{166}H_{269}N_{39}O_{86}S$, 4217; found, 2142.1 $[M + 2Cl)^{2-}$, 1440.4 $[M + 3Cl]^{3-}$.

Dendritic cell activation assay

Cells

DCs were generated from human monocytes of healthy donors as previously described [37]. Briefly, anti-CD14+ monocytes were positively sorted by magnetic microbeads (Miltenyi Biotec). Monocytes (at the density of 1×10^6 cells/mL) were cultured for 6 days in medium (complete RPMI, 10% FCS) supplemented with GM-CSF (1000 U/mL, Labogen) and IL-4 (1000 U/mL, Labogen), At day 7, DCs were activated by 24 hours of incubation with LPS (1 μg/mL, Sigma–Aldrich), compound **5** and scaffold **7** (two doses, 50 and 10 μg/mL).

DC phenotype

The DC phenotype was analyzed by flow cytometry with a 4 color EpicsXL cytometer (Beckman–Coulter), equipped with Expo 32 software. Cell surface markers were labelled with monoclonal antibodies (Immunotech) directed against the following antigens (the tags are given in parentheses): CD80 (FITC), CD86 (PE), HLA-DR (ECD), CD83 (PC5). Cell vitality was tested with propidium iodide (PI, molecular probes). The cells were labelled in PBS with 1% FCS for 15 min at room temperature (rt), washed twice and immediately analyzed. For each test at least 10000 events were acquired.

Mixed lymphocyte reaction (MLR)

CD4+ T cells were negatively selected from peripheral blood mononuclear cells (PBMCs) by using the T cell isolation kit II from Miltenyi Biotec. Mixed lymphocyte reaction (MLR) was performed in 96-well U bottom plates (Nunc). 1×10^5 CD4+ T cells were incubated for 5 days in RPMI with 10% FCS together with 1×10^4 to 1×10^3 allogeneic DCs. Experiments were conducted in quadruplicate. At day 5, the proliferative response was measured by the [3H]-thymidine ([3H]-Thy, 1 μCi/mL, Amersham) incorporation test. [3H]-Thy was added for the last 8 h of incubation. Plates were then harvested (TomtecMacIII) on glass fiber filters (Perkin Elmer), and [3H]-

Thy uptake was measured by liquid scintillation in a Microbeta 1450 Trimux counter (Wallac). The proliferative response is reported as a stimulation index (SI, mean cpm response/mean cpm background).

Statistics

Data were expressed as mean + SD values. Statistical analysis was performed by using Student's t-test where appropriate.

Acknowledgements

We acknowledge a Marie Curie contract to RRV. JR is grateful to MINECO (grant CTQ2011-23410) and EU ITN CARMUSYS (grant 213592) for funding. BR and CN thank AIRC 2012 and Ente Cassa di Risparmio di Firenze. We also acknowledge the European FEDER funds and COST CM1102.

References

1. Mellman, I.; Coukos, G.; Dranoff, G. *Nature* **2011,** *480,* 480–489. doi:10.1038/nature10673
2. Rabinovich, G. A.; Gabrilovich, D.; Sotomayor, E. M. *Annu. Rev. Immunol.* **2007,** *25,* 267–296. doi:10.1146/annurev.immunol.25.022106.141609
3. Igney, F. H.; Krammer, P. *J. Leukocyte Biol.* **2002,** *71,* 907–920.
4. Poggi, A.; Zocchi, M. R. *Arch. Immunol. Ther. Exp.* **2006,** *54,* 323–333. doi:10.1007/s00005-006-0038-7
5. Croci, D. O.; Fluck, M. F. Z.; Rico, M. J.; Matar, P.; Rabinovich, G. A.; Scharovsky, O. G. *Cancer Immunol. Immunother.* **2007,** *56,* 1687–1700. doi:10.1007/s00262-007-0343-y
6. Kim, R.; Emi, M.; Tanabe, K. *Immunology* **2007,** *121,* 1–14. doi:10.1111/j.1365-2567.2007.02587.x
7. Heimburg-Molinaro, J.; Lum, M.; Vijay, G.; Jain, M.; Almogren, A.; Rittenhouse-Olson, K. *Vaccine* **2011,** *29,* 8802–8826. doi:10.1016/j.vaccine.2011.09.009
8. Buonaguro, L.; Petrizzo, A.; Tornesello, M. L.; Buonaguro, F. M. *Clin. Vaccine Immunol.* **2011,** *18,* 23–34. doi:10.1128/CVI.00286-10
9. Palucka, K.; Banchereau, J. *Nat. Rev. Cancer* **2012,** *12,* 265–277. doi:10.1038/nrc3258
10. Gilboa, E. *J. Clin. Invest.* **2007,** *117,* 1195–1203. doi:10.1172/JCI31205
11. Fong, L.; Engleman, E. G. *Annu. Rev. Immunol.* **2000,** *18,* 245–273. doi:10.1146/annurev.immunol.18.1.245
12. Figdor, C. G.; de Vries, I. J. M.; Lesterhuis, W. J.; Melief, C. J. M. *Nat. Med.* **2004,** *10,* 475–480. doi:10.1038/nm1039
13. Banchereau, J.; Steinman, R. M. *Nature* **1998,** *392,* 245–252. doi:10.1038/32588
14. Steinman, R. M.; Banchereau, J. *Nature* **2007,** *449,* 419–426. doi:10.1038/nature06175
15. Steinman, R. M.; Cohn, Z. A. *J. Exp. Med.* **1973,** *137,* 1142–1162. doi:10.1084/jem.137.5.1142
16. Higano, C. S.; Schellhammer, P. F.; Small, E. J.; Burch, P. A.; Nemunaitis, J.; Yuh, L.; Provost, N.; Frohlich, M. W. *Cancer* **2009,** *115,* 3670–3679. doi:10.1002/cncr.24429
17. Kantoff, P. W.; Higano, C. S.; Shore, N. D.; Berger, E. R.; Small, E. J.; Penson, D. F.; Redfern, C. H.; Ferrari, A. C.; Dreicer, R.; Sims, R. B.; Xu, Y.; Frohlich, M. W.; Schellhammer, P. F. *N. Engl. J. Med.* **2010,** *363,* 411–422. doi:10.1056/NEJMoa1001294
18. Shortman, K.; Lahoud, M. H.; Caminschi, I. *Exp. Mol. Med.* **2009,** *41,* 61–66. doi:10.3858/emm.2009.41.2.008
19. Dudziak, D.; Kamphorst, A. O.; Heidkamp, G. F.; Buchholz, V. R.; Trumpfheller, C.; Yamazaki, S.; Cheong, C.; Liu, K.; Lee, H.-W.; Park, C. G.; Steinman, R. M.; Nussenzweig, M. C. *Science* **2007,** *315,* 107–111. doi:10.1126/science.1136080
20. van Vliet, S. J.; García-Vallejo, J. J.; van Kooyk, Y. *Immunol. Cell Biol.* **2008,** *86,* 580–587. doi:10.1038/icb.2008.55
21. Figdor, C. G.; van Kooyk, Y.; Adema, G. J. *Nat. Rev. Immunol.* **2002,** *2,* 77–84. doi:10.1038/nri723
22. Geijtenbeek, T. B. H.; Gringhuis, S. I. *Nat. Rev. Immunol.* **2009,** *9,* 465–479. doi:10.1038/nri2569
23. Mansh, M. *Yale J. Biol. Med.* **2011,** *84,* 381–389.
24. Salcedo, M.; Bercovici, N.; Taylor, R.; Vereecken, P.; Massicard, S.; Duriau, D.; Vernel-Pauillac, F.; Boyer, A.; Baron-Bodo, V.; Mallard, E.; Bartholeyns, J.; Goxe, B.; Latour, N.; Leroy, S.; Prigent, D.; Martiat, P.; Sales, F.; Laporte, M.; Bruyns, C.; Romet-Lemonne, J.-L.; Abastado, J.-P.; Lehmann, F.; Velu, T. *Cancer Immunol. Immunother.* **2006,** *55,* 819–829. doi:10.1007/s00262-005-0078-6
25. Mackensen, A.; Herbst, B.; Chen, J.-L.; Köhler, G.; Noppen, C.; Herr, W.; Spagnoli, G. C.; Cerundolo, V.; Lindemann, A. *Int. J. Cancer* **2000,** *86,* 385–392. doi:10.1002/(SICI)1097-0215(20000501)86:3<385::AID-IJC13>3.0.CO;2-T
26. Harada, Y.; Sakatsume, M.; Nores, G. A.; Hakomori, S.-i.; Taniguchi, M. *Jpn. J. Cancer Res.* **1989,** *80,* 988–992. doi:10.1111/j.1349-7006.1989.tb01638.x
27. Tardif, M.; Coulombe, J.; Soulieres, D.; Rousseau, A. P.; Pelletier, G. *Int. J. Cancer* **1996,** *68,* 97–101. doi:10.1002/(SICI)1097-0215(19960927)68:1<97::AID-IJC17>3.0.CO;2-3
28. Mazorra, Z.; Mesa, C.; Fernández, A.; Fernández, L. E. *Cancer Immunol. Immunother.* **2008,** *57,* 1771–1780. doi:10.1007/s00262-008-0503-8
29. Nores, G. A.; Dohi, T.; Taniguchi, M.; Hakomori, S. I. *J. Immunol.* **1987,** *139,* 3171–3176.
30. Harada, Y.; Sakatsume, M.; Taniguchi, M. *Jpn. J. Cancer Res.* **1990,** *81,* 383–387. doi:10.1111/j.1349-7006.1990.tb02579.x
31. Toma, L.; Di Cola, E.; Ienco, A.; Legnani, L.; Lunghi, C.; Moneti, G.; Richichi, B.; Ristori, S.; Dell'Atti, D.; Nativi, C. *ChemBioChem* **2007,** *8,* 1646–1649. doi:10.1002/cbic.200700208
32. Arcangeli, A.; Toma, L.; Contiero, L.; Crociani, C.; Legnani, L.; Lunghi, C.; Nesti, E.; Moneti, G.; Richichi, B.; Nativi, C. *Bioconjugate Chem.* **2010,** *21,* 1432–1438. doi:10.1021/bc900557v
33. Richichi, B.; Comito, G.; Cerofolini, L.; Gabrielli, G.; Marra, A.; Moni, L.; Pace, A.; Pasquato, L.; Chiarugi, P.; Dondoni, A.; Toma, L.; Nativi, C. *Bioorg. Med. Chem.* **2013,** *21,* 2756–2763. doi:10.1016/j.bmc.2013.03.021
34. Ribeiro-Viana, R.; Garcia-Vallejo, J. J.; Collado, D.; Pérez-Inestrosa, E.; Bloem, K.; van Kooyk, Y.; Rojo, J. *Biomacromolecules* **2012,** *13,* 3209–3219. doi:10.1021/bm300998c
35. Ribeiro-Viana, R.; Sánchez-Navarro, M.; Luczkowiak, J.; Koeppe, J. R.; Delgado, R.; Rojo, J.; Davis, B. G. *Nat. Commun.* **2012,** *3,* No. 1303. doi:10.1038/ncomms2302
36. Schmidt, S. V.; Nino-Castro, A. C.; Schultze, J. L. *Front. Immunol.* **2012,** *3,* No. 274. doi:10.3389/fimmu.2012.00274
37. Aldinucci, A.; Rizzetto, L.; Pieri, L.; Nosi, D.; Romagnoli, P.; Biagioli, T.; Mazzanti, B.; Saccardi, R.; Beltrame, L.; Massacesi, L.; Cavalieri, D.; Ballerini, C. *J. Immunol.* **2010,** *185,* 5102–5110. doi:10.4049/jimmunol.1001332

Beilstein Journal of Organic Chemistry

Design and synthesis of multivalent neoglycoconjugates by click conjugations

Feiqing Ding, Li Ji, Ronny William, Hua Chai and Xue-Wei Liu*

Full Research Paper

Open Access

Address:
Division of Chemistry and Biological Chemistry, School of Physical and Mathematical Sciences, Nanyang Technological University, 21 Nanyang Link, Singapore 637371

Email:
Xue-Wei Liu* - xuewei@ntu.edu.sg

* Corresponding author

Keywords:
click conjugations; copper-catalyzed; microwave irradiation; multivalent glycosystems; neoglycoconjugates; one-pot

Beilstein J. Org. Chem. **2014,** *10,* 1325–1332.
doi:10.3762/bjoc.10.134

Received: 24 February 2014
Accepted: 21 May 2014
Published: 10 June 2014

This article is part of the Thematic Series "Multivalent glycosystems for nanoscience".

Guest Editor: B. Turnbull

Abstract

A highly stereoselective $BF_3{\cdot}OEt_2$-promoted tandem hydroamination/glycosylation on glycal scaffolds has been developed to form propargyl 3-tosylamino-2,3-dideoxysugars in a one-pot manner. Subsequent construction of multivalent 3-tosylamino-2,3-dideoxy-neoglycoconjugates with potential biochemical applications was presented herein involving click conjugations as the key reaction step. The copper-catalyzed regioselective click reaction was tremendously accelerated with assistance of microwave irradiation.

Introduction

Oligosaccharides and glycopeptides are the key constituents of the cellular membrane and extracellular matrix, and play a pivotal role in various key cellular events such as cell–cell recognition, host–pathogen or host–symbiont interactions, molecular recognition of antibodies and metastasis [1-5]. The construction of a 1,4-disubstituted-1,2,3-triazole unit via a copper(I)-catalyzed modern version of the Huisgen-type azide–alkyne cycloaddition [6-10] has been considered to be a powerful ligation method for glycoconjugation [11-16]. In addition to the simplicity of this reaction and the ease of purification, 1,4-disubstituted-1,2,3-triazoles, the regiospecific product of this reaction, exhibit similarities to the ubiquitous amide moiety found in nature. However, unlike amides, the triazole moiety proved to be robust and resistant to chemical and enzymatic cleavage [17-20]. Moreover, the inertness of both azide and alkyne groups towards a majority of functional groups connected to the core of a variety of biomolecules also renders the click reaction particularly suitable for covalently linking bioactive molecular entities [21,22]. For example, the click strategy is especially versatile for the effective construction of complex glycosylated structures such as clusters, dendrimers, polymers, peptides and macrocycles. In all the cases the triazole ring plays a crucial role in combining divergent units together to establish a complex molecular architecture [23-31].

The α-GalNAc-linked glycopeptides, α-*N*-glycosidically linked to the polypeptide chain through the amido nitrogen of an asparagine residue at the *N*-terminal [32], were found to be the most important semi-synthetic glycoconjugates, usually modified from their naturally occurring parent precursors [33-39]. Over the years, many structural analogues of this class of antibiotics have been synthesized. In addition, triazoles are considered as peptidic linkage surrogates. Surprisingly, despite the enormous research interests associated with their synthesis, only a few examples of oligosaccharides and glycopeptides mimics have so far been prepared by a click chemistry strategy [40-48]. Most recently, we developed a strategy for the synthesis of 3-amino-2,3-dideoxysugars using a regio- and stereoselective tandem hydroamination/glycosylation of the glycal shown in Figure 1 [49-53]. Extending the synthetic utility of this protocol, herein, we wish to report the synthetic modification of α-GalNAc-linked glycopeptides to 3-tosylamino-2,3-dideoxyneoglycoconjugates via click conjugations (Figure 2).

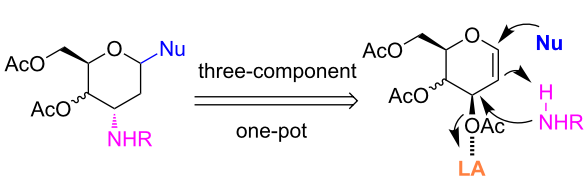

Figure 1: Our reported strategy for quick access to 3-amino-2,3-dideoxysugars via regio- and stereoselective tandem hydroamination/glycosylation of glycals.

Given the success in using "click chemistry" in the glycosylation reactions, we aspired to apply the highly efficient triazole formation employing an azide **3** and a suitable alkyne appended to the 3-amino-2,3-dideoxysugars moiety **2** (Figure 3). In continuation of our previous work, herein we report a direct and reliable synthetic approach to multivalent 3-tosylamino-2,3-dideoxyneoglyco conjugates **4** with potential biochemical applications involving click conjugations as the key reaction step (Figure 3).

Results and Discussion

Primarily, we successfully synthesized propargyl 3-*p*-toluenesulfonamido-4,6-di-*O*-acetyl-2,3-dideoxy-α-D-allohexopyranoside (**2a**) in gram scale via $BF_3{\cdot}OEt_2$-promoted one-pot three-component α-selective tandem hydroamination/glycosylation reaction (Scheme 1). In fact, when 3,4,6-tri-*O*-acetyl-D-glucal (**1a**), propargyl alcohol and *p*-toluenesulfonamide were

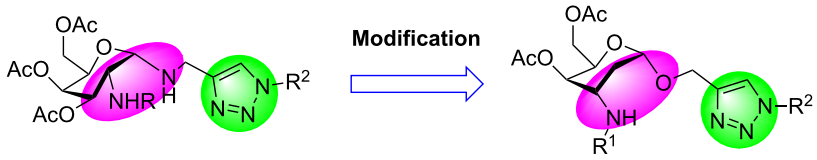

Figure 2: Synthetic modification of α-GalNAc linked glycopeptides to 3-tosylamino-2,3-dideoxyneoglycoconjugates via click conjugation.

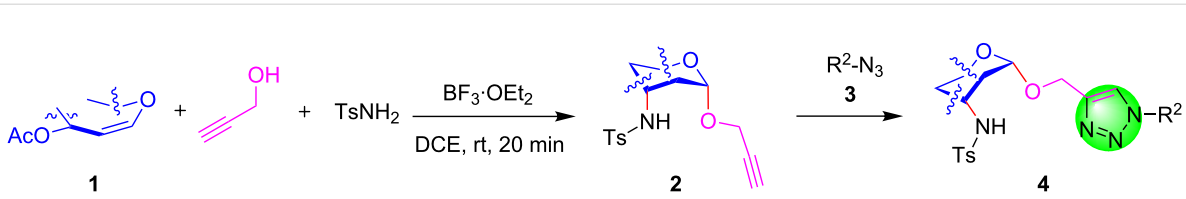

Figure 3: Our proposal for access to 3-tosylamino-2,3-dideoxyneoglycoconjugates via tandem hydroamination/glycosylation of glycals followed by click conjugations.

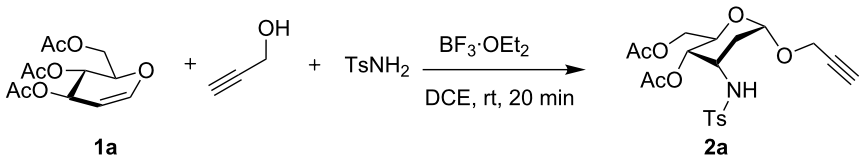

Scheme 1: Synthesis of propargyl 3-tosylamino-2,3-dideoxy-α-D-allohexopyranoside (**2a**).

subjected to a one-pot reaction in the presence of 2.2 equiv of $BF_3{\cdot}OEt_2$ in DCE at room temperature for 20 min, the desired aminoglycoside **2a** was obtained in good yield with exclusive α-stereoselectivity [50]. Later, a systematic screening was executed using 3-tosylamino-2,3-dideoxysugar **2a** and benzyl azide (**3a**) as our model system under varied conditions of catalysts, additives, solvents and reaction temperatures (Table 1). The initial evaluation involved no catalyst and additives at 100 °C and DMF, MeCN/H_2O 3:1 or MeOH as the solvent system, which resulted in unsuccessful reactions (Table 1, entries 1–3). However, a trace amount of the desired product was detected in the presence of 10 mol % of copper(I) iodide (Table 1, entry 4). The combination of $CuSO_4{\cdot}5H_2O$ (10 mol %) and sodium ascorbate (10 mol %) was found to be a suitable catalyst leading regiospecifically to the 1,4-disubstituted-1,2,3-triazole **4a** with moderate yield of 46% in *t*-BuOH/H_2O 1:1 after 20 hours at 70 °C (Table 1, entry 5). The yield was further improved to 97% by employing DMF as solvent in a shorter period of 12 hours (Table 1, entry 6). Encouraged by these results, we attempted to improve the assemblies and to shorten the reaction times further; reactions were subjected to microwave irradiation, which is best known to accelerate transition metal-catalyzed homogeneous reactions [54]. Microwave-assisted organic reactions are rapidly becoming recognized as a valuable tool for facilitating a wide variety of organic transformations [55,56]. Finally, we found that the rate of conversion accelerated dramatically when microwave irradiation was used under 70 °C. To our delight under microwave conditions and in DMF with addition of 1 mol % of $CuSO_4{\cdot}5H_2O$ and 10 mol % of sodium ascorbate, a quantative yield of desired 3-tosylamino-2,3-dideoxyneoglycoconjugate **4a** was obtained in 15 min (Table 1, entry 7).

Next, the required α-propargyl 3-tosylamino-2,3-dideoxyglycosides **2** were synthesized by $BF_3{\cdot}OEt_2$-promoted one-pot three-component tandem hydroamination/glycosylation reaction on a glycal scaffold including tri-*O*-acetyl-D-glucal (**1a**), tri-*O*-acetyl-D-allal (**1b**), tri-*O*-acetyl-D-galactal (**1c**), di-*O*-acetyl-D-rhamnal (**1d**), hexa-*O*-acetyl-D-maltal (**1e**). Accordingly, a series of α-propargyl 3-tosylamino-2,3-dideoxyglycosides **2a**–**2d** were obtained exclusively with α-stereoselectivity in good yields (Table 2, entries 1–5).

With pure α-propargyl 3-tosylamino-2,3-dideoxyglycosides and the optimized conditions in hand, we focused on performing a Huisgen cycloaddition reaction. The scope and generality of this method to prepare 3-tosylamino-2,3-dideoxyneoglycoconjugates **4** with the assistance of copper sulfate and sodium ascorbate was examined extensively. A range of α-alkyne-3-tosylamino-2,3-dideoxysugars and azides with various substituent groups (R^2) were screened and the summarized results are shown in Table 3. Overall, the yields obtained were from good to excellent while preserving the anomeric selectivity and regioselectivity. In general, the analogous reaction of a set of azides with different substituent groups (**3a**–**3e**) with α-propargyl 3-tosylamino-2,3-dideoxy glycosides **2** afforded the corresponding 3-tosylamino-2,3-dideoxyneoglycoconjugates (**4a**–**4h)** in good to excellent yields with exclusive anomeric selectivity (Table 3, entries 1–8). This encouraging result prompted us to apply these conditions to alkyne **2a** and a series of azido-linked monosaccharides **3f**, **3g** and **3h** as well as the propargyl disaccharide **2d** with α-GlaNAc azido **3g** which were also obtained in good yields and selectivities (Table 3, entries 9–13). Subsequently, to shorten the reaction times, we subjected all the click conjugations to microwave irradiation. All the reac-

Table 1: Optimization for synthesis of 3-tosylamino-2,3-dideoxyneoglycoconjugate **4a**.

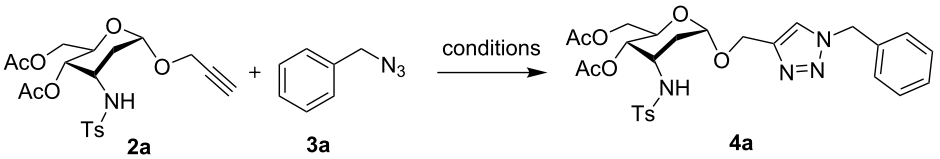

2a **3a** **4a**

Entry	Catalyst (mol %)	Solvent	Temperature (°C)	Time (h)	Yield (mol %)[a]
1	none	DMF	100	20	NR[b]
2	none	MeCN/H_2O	100	20	NR[b]
3	none	MeOH	100	20	NR[b]
4	CuI (10)	THF	60	12	trace
5	$CuSO_4{\cdot}5H_2O$ (1)	*t*-BuOH/H_2O	70	20	46
6	$CuSO_4{\cdot}5H_2O$ (1)	DMF	70	12	97
7	$CuSO_4{\cdot}5H_2O$ (1)	DMF	70[c]	0.25	98

[a]Isolated yield after purification. [b]NR = no reaction. [c]Assisted by microwave irradiation, 200 W.

Table 2: One-pot synthesis of α-propargyl 3-tosylamino-2,3-dideoxyglycosides **2**.

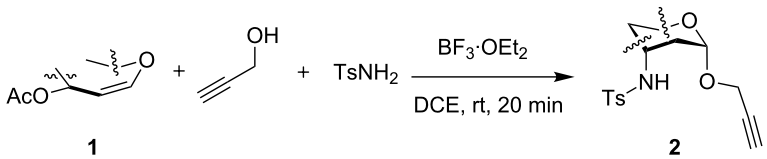

1 **2**

Entry	1	2	Yield (%)[a]
1	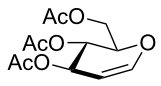 **1a**	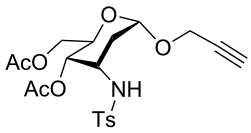 **2a**	86
2	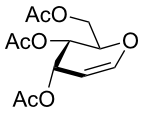 **1b**	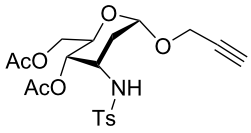 **2a**	84
3	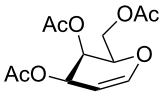 **1c**	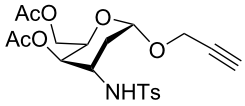 **2b**	81
4	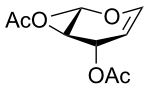 **1d**	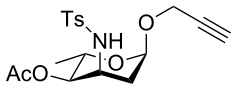 **2c**	74
5	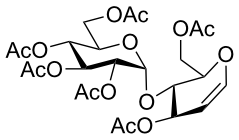 **1e**	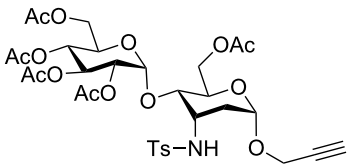 **2d**	67

[a]Isolated yields after purification.

tions were completed in considerably shorter reaction times of less than 30 min for the Huisgen cycloaddition of alkenes and azides catalyzed by copper sulfate and sodium ascorbate, affording the corresponding products in good to excellent yields in each case (Table 3, method B). This result showed that the synthesis of 3-tosylamino-2,3-dideoxyneoglycoconjugates via copper-catalyzed Huisgen cycloaddition is highly efficient under microwave irradiation.

In carbohydrate recognition events, higher multivalent interactions are absolutely essential as the monovalent affinities of carbohydrate monosaccharides are comparatively low and weak. To enhance this multivalent effect, thereby increasing the binding efficiencies of carbohydrates with the coupling counterparts, there has been a constant development of new glycoconjugates such as glycodendrimers [57]. Hence, as continuation of previous encouraging results, we have further designed the use of noncarbohydrate diazide **5a** in the cycloaddition reaction with the α-propargyl 3-tosylamino-2,3-dideoxyalloside **2a** and α-propargyl 3-tosylamino-2,3,6-trideoxy-α-L-ribohexopyranoside **2c** (Scheme 2) to obtain divalent 3-tosylamino-2,3-dideoxyneoglycoconjugates **6a** and **6b** in 83% and 61% yield respectively. The synthesis of trivalent 3-tosylamino-2,3-dideoxyneoglycoconjugates **6c** was also feasible by using triazide **5b** in 66% yield (Scheme 3). Interestingly, for all the reactions under microwave irradiation, reaction times were reduced to 15 minutes. As such, this novel synthetic protocol provides a straightforward access to a wide range of 3-tosyl-

Table 3: Scope for synthesis of 3-tosylamino-2,3-dideoxyneoglycoconjugates.

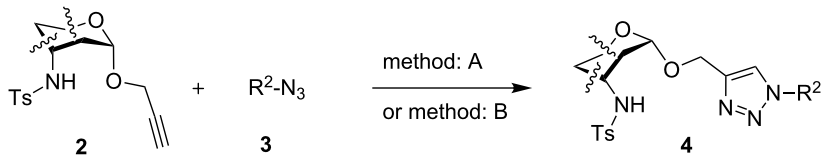

2 **3** **4**

Entry	**2**	**3**	**4**	Yield (%)[a]	
				A[b]	B[c]
1	**2a**	**3a**	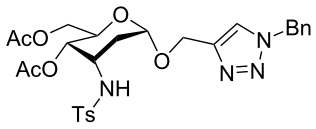 **4a**	97	98
2	**2b**	**3a**	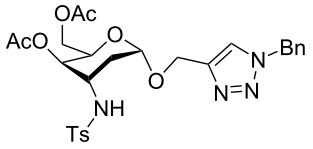 **4b**	89	93
3	**2c**	**3a**	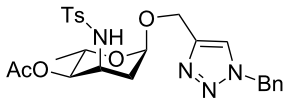 **4c**	74	81
4	**2d**	**3a**	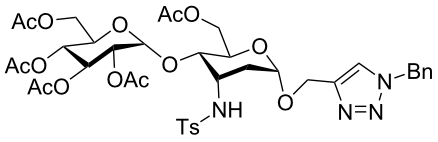 **4d**	71	78
5	**2a**	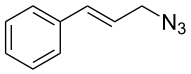 **3b**	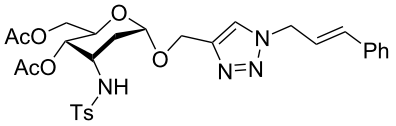 **4e**	82	85
6	**2a**	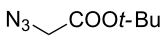 **3c**	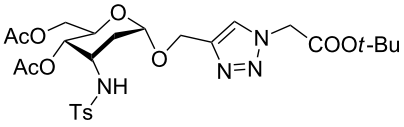 **4f**	91	92
7	**2a**	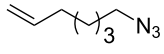 **3d**	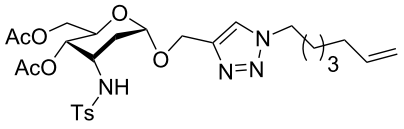 **4g**	86	89
8	**2a**	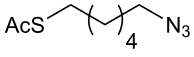 **3e**	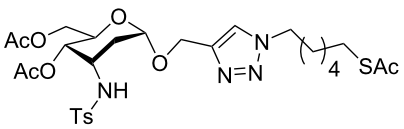 **4h**	87	92

Table 3: Scope for synthesis of 3-tosylamino-2,3-dideoxyneoglycoconjugates. (continued)

9	**2a**	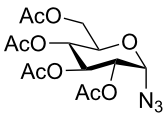 **3f**	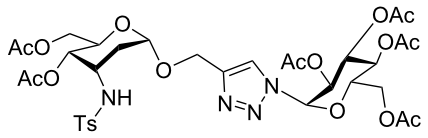 **4i**	76	80
10	**2a**	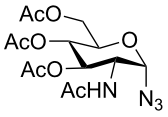 **3g**	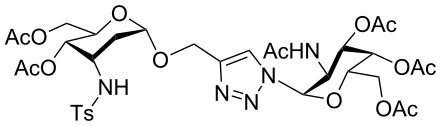 **4j**	93	95
11	**2d**	**3g**	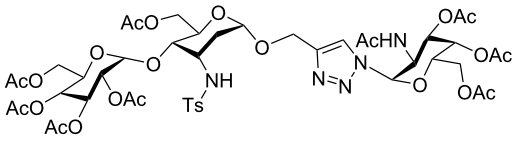 **4k**	80	82
12	**2a**	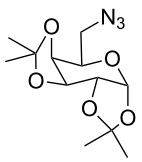 **3h**	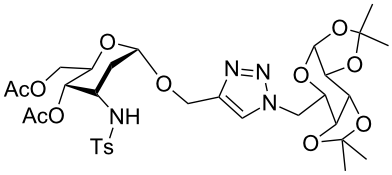 **4l**	72	78

[a]Isolated yields after purification. [b]70 °C under conventional heating, 12 hours. [c]70 °C under microwave irradiation, 200 W, 15 minutes.

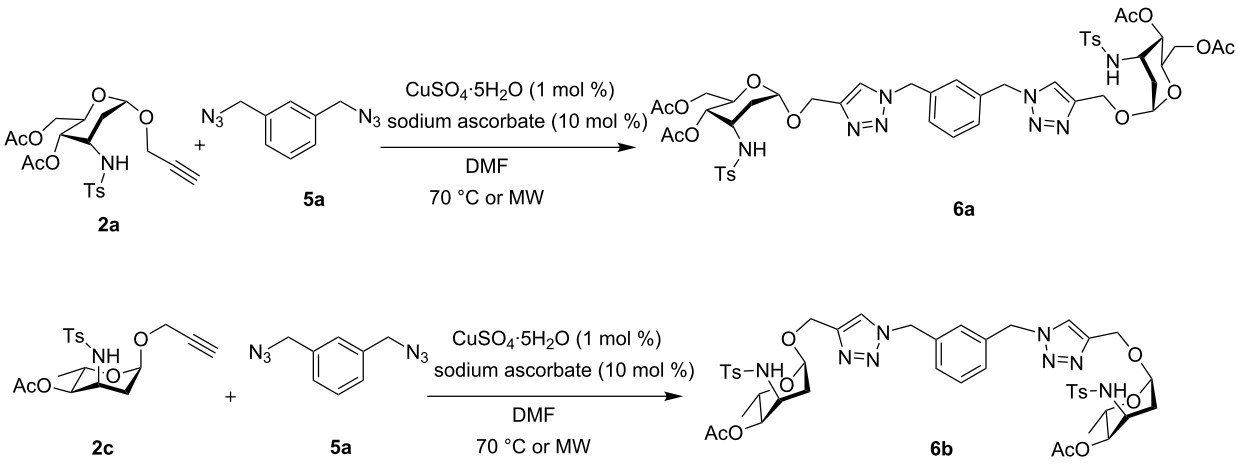

Scheme 2: Synthesis of divalent 3-tosylamino-2,3-dideoxyneoglycoconjugates **6a** and **6b**.

amino-2,3-dideoxyneoglycoconjugate derivatives which may find numerous biochemical applications [40-48].

Conclusion

In conclusion, it has been established that the construction of well-defined multivalent, anomerically pure 3-amino-2,3-dideoxyneoglycoconjugate architectures was successfully achieved by using cycloaddition reactions of alkynes and azides. It is expected that this strategy will find extensive applications in glycoscience, because triazole-linked glycoconjugates can exhibit very interesting biological properties, offering a convenient access toward oligosaccharides, glycopeptide

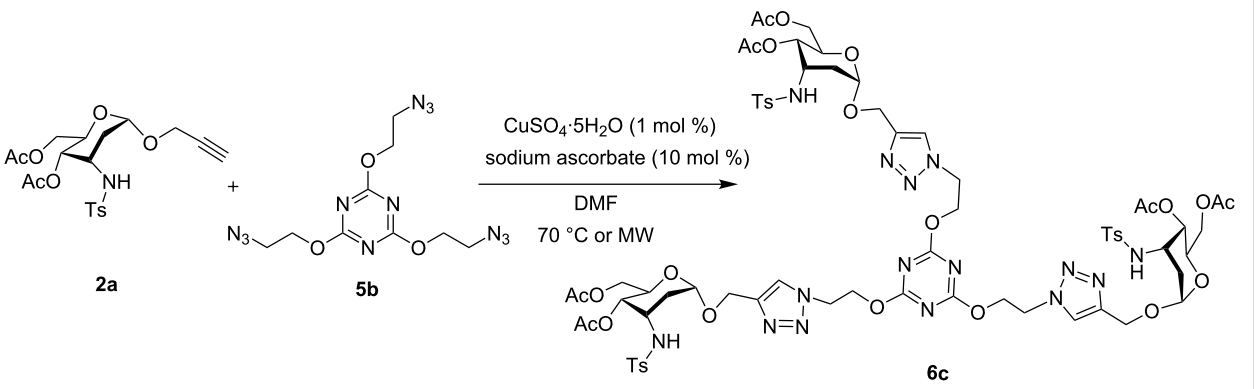

Scheme 3: Synthesis of trivalent 3-tosylamino-2,3-dideoxyneoglycoconjugate **6c**.

mimics, or multivalent carbohydrate systems [40-48]. Their further application in molcecular biosystems is currently underway and the results will be reported in due course.

Supporting Information

Supporting Information File 1

Experimental, analytical data and ^{1}H NMR and ^{13}C NMR spectra for all new compounds.
[http://www.beilstein-journals.org/bjoc/content/supplementary/1860-5397-10-134-S1.pdf]

Acknowledgements

We gratefully acknowledge Nanyang Technological University (RG50/08) and the Ministry of Education, Singapore (MOE 2009-T2-1-030) for the financial support of this research.

References

1. Driguez, H.; Thiem, J. *Glycoscience;* Springer: Berlin, 1999; Vol. 1–2.
2. Ernst, B.; Hart, G.; Sinaý, P. *Carbohydrates in Chemistry and Biology;* Wiley, 2000; Vol. 1–4. doi:10.1002/9783527618255
3. Wang, P. G.; Bertozzi, C. R. *Glycochemistry: Principles, Synthesis, and Applications;* Marcel Dekker: New York, NY, 2001.
4. Kiessling, L. L.; Gestwicki, J. E.; Strong, L. E. *Angew. Chem., Int. Ed.* **2006,** *45,* 2348. doi:10.1002/anie.200502794
5. Gruner, S. A. W.; Locardi, E.; Lohof, E.; Kessler, H. *Chem. Rev.* **2002,** *102,* 491. doi:10.1021/cr0004409
6. Huisgen, R. *1,3*-Dipolar cycloaddition – Introduction, survey, mechanism. In *1,3-Dipolar Cycloaddition Chemistry;* Padwa, A., Ed.; Wiley, 1984; Vol. 1, pp 1–176.
7. Meldal, M.; Tornøe, C. W. *Chem. Rev.* **2008,** *108,* 2952. doi:10.1021/cr0783479
8. Rostovtsev, V.; Green, L. G.; Fokin, V. V.; Sharpless, K. B. *Angew. Chem., Int. Ed.* **2002,** *41,* 2596. doi:10.1002/1521-3773(20020715)41:14<2596::AID-ANIE2596>3.0.CO;2-4
9. Kolb, H. C.; Finn, M. G.; Sharpless, K. B. *Angew. Chem., Int. Ed.* **2001,** *40,* 2004. doi:10.1002/1521-3773(20010601)40:11<2004::AID-ANIE2004>3.0.CO;2-5
10. Tornøe, C. W.; Christensen, C.; Meldal, M. *J. Org. Chem.* **2002,** *67,* 3057. doi:10.1021/jo011148j
11. Davis, B. G. *J. Chem. Soc., Perkin Trans. 1* **1999,** 3215. doi:10.1039/A809773I
12. Turnbull, W. B.; Stoodart, J. F. *Rev. Mol. Biotechnol.* **2002,** *90,* 231. doi:10.1016/S1389-0352(01)00062-9
13. Roy, R.; Baek, M.-G. *Rev. Mol. Biotechnol.* **2002,** *90,* 291. doi:10.1016/S1389-0352(01)00065-4
14. Bezouška, K. *Rev. Mol. Biotechnol.* **2002,** *90,* 269. doi:10.1016/S1389-0352(01)00064-2
15. Dedola, S.; Nepogodiev, S. A.; Field, R. A. *Org. Biomol. Chem.* **2007,** *5,* 1006. doi:10.1039/b618048p
16. Dondoni, A. *Chem.–Asian J.* **2007,** *2,* 700. doi:10.1002/asia.200700015
17. Patani, G. A.; LaVoie, E. J. *Chem. Rev.* **1996,** *96,* 3147. doi:10.1021/cr950066q
18. Tron, G. C.; Pirali, T.; Billington, R. A.; Canonico, P. L.; Sorba, G.; Genazzani, A. A. *Med. Res. Rev.* **2008,** *28,* 278. doi:10.1002/med.20107
19. Wilkinson, B. L.; Bornaghi, L. F.; Poulsen, S.-A.; Houston, T. A. *Tetrahedron* **2006,** *62,* 8115. doi:10.1016/j.tet.2006.06.001
20. Jung, K.-H.; Schmidt, R. R. Glycosyltransferase Inhibitors. In *Carbohydrate-Based Drug Discovery;* Wong, C.-H., Ed.; Wiley-VCH Verlag GmbH & Co KGaA: Weinheim, 2003; pp 609 ff.
21. Kiick, K. L.; Saxon, E.; Tirrell, D. A.; Bertozzi, C. R. *Proc. Natl. Acad. Sci. U. S. A.* **2002,** *99,* 19. doi:10.1073/pnas.012583299
22. Jewett, J. C.; Bertozzi, C. R. *Chem. Soc. Rev.* **2010,** *39,* 1272. doi:10.1039/b901970g
23. Kolb, H. C.; Sharpless, K. B. *Drug Discovery Today* **2003,** *8,* 1128. doi:10.1016/S1359-6446(03)02933-7
24. Whiting, M.; Muldoon, J.; Lin, Y.-C.; Silverman, S. M.; Lindstrom, W.; Olson, A. J.; Kolb, H. C.; Finn, M. G.; Sharpless, K. B.; Elder, J. H.; Fokin, V. V. *Angew. Chem., Int. Ed.* **2006,** *45,* 1435. doi:10.1002/anie.200502161
25. Oh, K.; Guan, Z. *Chem. Commun.* **2006,** 3069. doi:10.1039/b606185k
26. Bock, V. D.; Speijer, D.; Hiemstra, H.; van Maarseveen, J. H. *Org. Biomol. Chem.* **2007,** *5,* 971. doi:10.1039/b616751a

27. Angell, Y. L.; Burgess, K. *Chem. Soc. Rev.* **2007,** *36,* 1674. doi:10.1039/b701444a
28. Nagarajan, S.; Das, T. M. *Carbohydr. Res.* **2009,** *344,* 1028. doi:10.1016/j.carres.2009.03.009
29. Nagarajan, S.; Arjun, P.; Raaman, N.; Das, T. M. *Carbohydr. Res.* **2010,** *345,* 1988. doi:10.1016/j.carres.2010.07.016
30. Prasad, V.; Kale, R. R.; Kumar, V.; Tiwari, V. K. *Curr. Org. Synth.* **2010,** *7,* 506. doi:10.2174/157017910792246063
31. Pandey, V. P.; Bisht, S. S.; Mishra, M.; Kumar, A.; Siddiqi, M. I.; Verma, A.; Mittal, M.; Sane, S. A.; Gupta, S.; Tripathi, R. P. *Eur. J. Med. Chem.* **2010,** *45,* 2381. doi:10.1016/j.ejmech.2010.02.018
32. Shibata, S.; Takeda, T.; Natori, Y. *J. Biol. Chem.* **1988,** *263,* 12483.
33. Pajk, S.; Garvas, M.; Štrancar, J.; Pečar, S. *Org. Biomol. Chem.* **2011,** *9,* 4150. doi:10.1039/c0ob01173h
34. Kumar, G. D. K.; Baskaran, S. *J. Org. Chem.* **2005,** *70,* 4520. doi:10.1021/jo0502697
35. Yan, R.-B.; Yang, F.; Wu, Y.; Zhang, L.-H.; Ye, X.-S. *Tetrahedron Lett.* **2005,** *46,* 8993. doi:10.1016/j.tetlet.2005.10.103
36. Alix, A.; Chassaing, S.; Pale, P.; Sommer, J. *Tetrahedron* **2008,** *64,* 8922. doi:10.1016/j.tet.2008.06.086
37. Wilkinson, B. L.; Stone, R. S.; Capicciotti, C. J.; Thaysen-Andersen, M.; Matthews, J. M.; Packer, N. H.; Ben, R. N.; Payne, R. J. *Angew. Chem., Int. Ed.* **2012,** *51,* 3606. doi:10.1002/anie.201108682
38. Liu, S.; Wang, W.; von Moos, E.; Jackman, J.; Mealing, G.; Monette, R.; Ben, R. N. *Biomacromolecules* **2007,** *8,* 1456. doi:10.1021/bm061044o
39. Bouvet, V. R.; Ben, R. N. In *Antifreeze Glycoprotein Analogues: Synthesis. In Vitro Testing and Applications;* Roy, R., Ed.; American Chemical Society, Oxford University Press: Washington, D.C., 2004; p 151.
40. Santoyo-González, F.; Hernández-Mateo, F. *Top. Heterocycl. Chem.* **2007,** *7,* 133. doi:10.1007/7081_2007_050
41. Chen, Q.; Yang, F.; Du, Y. *Carbohydr. Res.* **2005,** *340,* 2476. doi:10.1016/j.carres.2005.08.013
42. Gouin, S. G.; Bultel, L.; Falentin, C.; Kovensky, J. *Eur. J. Org. Chem.* **2007,** 1160. doi:10.1002/ejoc.200600814
43. Hotha, S.; Kashyap, S. *J. Org. Chem.* **2006,** *71,* 364. doi:10.1021/jo051731q
44. Ortega-Muñoz, M.; Lopez-Jaramillo, J.; Hernandez-Mateo, F.; Santoyo-Gonzalez, F. *Adv. Synth. Catal.* **2006,** *348,* 2410. doi:10.1002/adsc.200600254
45. Touaibia, M.; Wellens, A.; Shiao, T. C.; Wang, Q.; Sirois, S.; Bouckaert, J.; Roy, R. *ChemMedChem* **2007,** *2,* 1190. doi:10.1002/cmdc.200700063
46. Guo, Z.; Lei, A.; Zhang, Y.; Xu, Q.; Xue, X.; Zhang, F.; Liang, X. *Chem. Commun.* **2007,** 2491. doi:10.1039/b701831b
47. Nepogodiev, S. A.; Dedola, S.; Marmuse, L.; de Oliveira, M. T.; Field, R. A. *Carbohydr. Res.* **2007,** *342,* 529. doi:10.1016/j.carres.2006.09.026
48. Pietrzik, N.; Schips, C.; Ziegler, T. *Synthesis* **2008,** 519. doi:10.1055/s-2008-1032150
49. Ding, F.; William, R.; Wang, F.; Ma, J.; Ji, L.; Liu, X.-W. *Org. Lett.* **2011,** *13,* 652. doi:10.1021/ol102891t
50. Ding, F. Q.; William, R.; Wang, S.; Gorityala, B. K.; Liu, X.-W. *Org. Biomol. Chem.* **2011,** *9,* 3929. doi:10.1039/c1ob05068k
51. Ding, F.; William, R.; Cai, S.; Ma, J.; Liu, X.-W. *J. Org. Chem.* **2012,** *77,* 5245. doi:10.1021/jo300791v
52. Ding, F.; William, R.; Liu, X.-W. *J. Org. Chem.* **2013,** *78,* 1293. doi:10.1021/jo302619b
53. Ding, F.; Cai, S.; William, R.; Liu, X.-W. *RSC Adv.* **2013,** *3,* 13594. doi:10.1039/C3RA40595H
54. Pérez-Balderas, F.; Ortega-Muñoz, M.; Morales-Sanfrutos, J.; Hernández-Mateo, F.; Calvo-Flores, F. G.; Calvo-Asin, J. A.; Isac-García, J.; Santoyo-González, F. *Org. Lett.* **2003,** *5,* 1951. doi:10.1021/ol034534r
55. Lidström, P.; Tierney, J.; Wathey, B.; Westman, J. *Tetrahedron* **2001,** *57,* 9225. doi:10.1016/S0040-4020(01)00906-1
56. Kappe, C. O.; Pieber, B.; Dallinger, D. *Angew. Chem., Int. Ed.* **2013,** *52,* 1088. doi:10.1002/anie.201204103
57. Chabre, Y. M.; Roy, R. *Curr. Top. Med. Chem.* **2008,** *8,* 1237. doi:10.2174/156802608785848987

License and Terms

Beilstein Journal of Organic Chemistry

Glycosystems in nanotechnology: Gold glyconanoparticles as carrier for anti-HIV prodrugs

Fabrizio Chiodo[*1,§], Marco Marradi[1,2], Javier Calvo[3], Eloisa Yuste[4,5] and Soledad Penadés[*1,2]

Full Research Paper

Open Access

Address:
[1]Laboratory of GlycoNanotechnology, Biofunctional Nanomaterials Unit, CIC biomaGUNE, Paseo Miramón 182, 20009, San Sebastián, Spain, [2]Networking Research Center on Bioengineering, Biomaterials and Nanomedicine (CIBER-BBN), Paseo Miramón 182, 20009, San Sebastián, Spain, [3]Technological Platform of Mass Spectrometry, CIC biomaGUNE, Paseo Miramón 182, 20009, San Sebastián, Spain, [4]AIDS Research Unit, Institut d'Investigacions Biomediques August Pi i Sunyer, Barcelona, Spain and [5]HIVACAT, Barcelona, Spain

Email:
Fabrizio Chiodo[*] - chiodo.fabrizio@gmail.com; Soledad Penadés[*] - spenades@cicbiomagune.es

* Corresponding author
§ Present address: Department of Parasitology, Leiden University Medical Center, 2333 ZA, Leiden, Netherlands

Keywords:
drug-delivery system; gold glyconanoparticles; HAART; HIV; multivalent glycosystems; reverse transcriptase inhibitors

Beilstein J. Org. Chem. **2014,** *10,* 1339–1346.
doi:10.3762/bjoc.10.136

Received: 13 March 2014
Accepted: 22 May 2014
Published: 12 June 2014

This article is part of the Thematic Series "Multivalent glycosystems for nanoscience".

Guest Editor: A. Casnati

Abstract

The therapeutic approach for the treatment of HIV infection is based on the highly active antiretroviral therapy (HAART), a cocktail of antiretroviral drugs. Notwithstanding HAART has shown different drawbacks like toxic side effects and the emergence of viral multidrug resistance. Nanotechnology offers new tools to improve HIV drug treatment and prevention. In this scenario, gold nanoparticles are an interesting chemical tool to design and prepare smart and efficient drug-delivery systems. Here we describe the preparation and antiviral activity of carbohydrate-coated gold nanoparticles loaded with anti-HIV prodrug candidates. The nucleoside reverse transcriptase inhibitors abacavir and lamivudine have been converted to the corresponding thiol-ending ester derivatives and then conjugated to ~3 nm glucose-coated gold nanoparticles by means of "thiol-for-thiol" ligand place exchange reactions. The drugs-containing glyconanoparticles were characterized and the pH-mediated release of the drug from the nanoparticle has been determined. The antiviral activity was tested by evaluating the replication of NL4-3 HIV in TZM-bl infected cells. The proof-of-principle presented in this work aims to introduce gold glyconanoparticles as a new multifunctional drug-delivery system in the therapy against HIV.

Introduction

Acquired immune deficiency syndrome (AIDS), caused by human immunodeficiency virus type-1 (HIV-1) [1] continues to be a major leading pandemic disease worldwide with approximately 34 million people living with HIV [2]. Due to its incredible genetic variance and the specificity for CD4+ T cells, this virus is responsible for 800.000 deaths per year. In addition to sexual preventions, the strategies used to inhibit viral replication in human CD4+ T cells consist in the highly active antiretroviral therapy (HAART) [3] and the design of a vaccine that should protect people among all the different HIV strains [4,5]. Although great results have been obtained by the use of the HAART regimes since 1996, there are still several problems to solve, such as toxic side-effects of the HAART drugs and the emergence of multidrug resistance. Nowadays the safest prevention against sexual infection relies on physical barriers, but recently a new type of protection based on microbicides has started to be developed. Microbicides are a new class of chemical–physical barrier in clinical development that can be directly applied to the vagina or rectum before sexual intercourses in order to prevent the transmission of HIV [6]. Recently, a conventional anti-HIV drug used for HAART was explored as potential microbicide. A gel formulation containing 1% of the reverse transcriptase inhibitor tenofovir has shown good results in the prevention of HIV infections of women in South Africa [7].

One of the greatest challenges of antiretroviral and microbicide therapy is to develop drug-delivery systems (DDSs) with high efficacy and therapeutic selectivity [8] to overcome the drawbacks of HAART. Nanotechnology allows the construction of novel systems that could bring changes in this scenario. Over the last years, different nano-constructions have been designed as prophylactic agents against HIV. Some of these nanomaterials like polymeric nanoparticles, lipid nanoparticles and nanofibers have shown the ability to improve solubility, stability and permeability of anti-HIV drugs [9,10], but also to reduce the viral load by the activation of latently infected CD4+ T-cells [11].

Gold nanoparticles have been explored in biomedicine as multivalent and multifunctional scaffolds [12,13]. Thanks to their relative inertness and low toxicity gold nanoparticles have been widely explored to conjugate biomolecules on their surface, because the chemistry of their surface is easy to control [12]. The application of gold nanoparticles as a DDS is an expanding field due to the inert properties of the gold core, their controlled fabrication, and multifunctionality [14]. This last property allows the design of particles simultaneously containing multiple chemotherapeutics and targeting moieties. Few studies have described the application of gold nanoparticles for HIV treatment. In 2008 gold nanoparticles were used as carrier for an anti-HIV drug [15]. An inactive derivative of the inhibitor TAK-779 (the active part of the drug was modified to link it to the gold surface) was multimerized on gold nanoparticles that showed surprisingly anti-HIV activity, probably due to the high-local concentration of the drug derivative on the gold surface. Other inorganic nanomaterials have also been explored as carriers for therapeutic drugs against HIV. For example, silver nanoparticles coated with poly(vinyl)pyrrolidone were found to be effective against different HIV-strains [16]. Aptamer-conjugated gold nanoparticles were also exploited as effective inhibitors of viral enzymes [17].

We have previously described the usefulness of carbohydrate-coated gold nanoparticles (GNPs) as a carrier for different structures related to HIV envelope [18]. GNPs coated with oligomannosides of the gp120 (*manno*-GNPs) were able to inhibit the DC-SIGN-mediated HIV-1 *trans*-infection of human T-cells [19] and gold glyconanoparticles coated with sulfated ligands showed to interfere with the adhesion/fusion of HIV during its entry [20]. Our methodology for preparing GNPs allows the construction of particles simultaneously containing carbohydrates, peptides and targeting molecules in a controled way [21]. The use of biocompatible gold glyconanoparticles as scaffolds for the antiviral drugs could bring some important benefits such as the improvement of the solubility in water and biological media of the drugs and the improvement of cellular uptake due to the presence of carbohydrates on the GNPs. In addition a local increase of the drug concentration on the gold surface could also improve their antiviral activity. We reasoned that the presence of multiple antiretroviral molecules on carbohydrate-coated gold nanoparticles could lead to a drug-delivery system and/or microbicides able to inhibit viral replication or to prevent sexual infection. We have previously demonstrated that glucose-coated gold nanoparticles are water-soluble and non-cytotoxic to different cell lines at the tested concentrations [22]. Glucose-coated nanomaterials have been proposed as good intracellular delivery tool and the internalization and uptake of glucose-coated nanoparticles have been described on different cell lines [23-26]. In addition glucose-coated gold nanoparticles did not elicit any immune response in animal models [27,28]. We thus decided to use them as a scaffold to insert antiretroviral drugs to construct new multivalent anti-HIV systems.

Here we describe the preparation of anti-HIV prodrug candidates and their assembly on ~3 nm glucose-coated gold nanoparticles as a potential drug-delivery system. As antiviral drugs, the nucleoside analog reverse transcriptase inhibitors

(NRTIs) abacavir (ABC) and lamivudine (3TC) were selected. NRTIs are drugs that compete in the cytoplasm as triphosphates with endogenous nucleoside substrates acting as chain terminators in the DNA polymerisation reaction catalyzed by HIV-1 RT [3]. Both drugs were transformed in ester derivatives to prepare the GNPs. The pH-mediated release of the drugs from the GNPs surface was evaluated and cellular experiments demonstrated that abacavir and lamivudine ester derivatives tailored onto the gold gluconanoparticles have an antiviral activity similar to the free drugs.

Results and Discussion

Preparation of anti-HIV prodrug-GNPs

As a proof-of-principle for a further exploration of gold glyconanoparticles as drug-delivery system, we prepared glucose-coated gold nanoparticles and functionalized them with in clinical use antiviral drugs abacavir (ABC) and lamivudine (3TC). The drugs were functionalized at the primary hydroxy groups with 11-mercaptoundecanoic acid to obtain the prodrug candidate with an easy hydrolysable ester group that allows the release of the drug from the GNPs by enzymatic or pH mediated hydrolysis. 11-Mercaptoundecanoic acid was chosen as bifunctional aliphatic linker between the drugs and the gold nanoparticles. Aliphatic ester prodrugs of the anti-HIV drug zidovudine have previously shown to promote intestinal lymph transport (a major reservoir for HIV) [29] and some alkyl and alkyloxyalkyl esters of nucleotides or acyclic nucleoside phosphonates have been explored in clinical studies [30]. In order to obtain the ester derivatives, 11-(acetylthio)undecanoic acid, obtained from 11-bromoundecanoic acid and potassium thioacetate [31], was reacted with ABC and 3TC in DMF in the presence of 1-ethyl-3-(3-dimethylaminopropyl)carbodiimide (EDC) and 4-dimethylaminopyridine (DMAP) to obtain the ester derivative in ~75% yield. After purification, the protecting group of the thiol was removed with hydrazine acetate to give the corresponding ester prodrug candidates with a free thiol-ending group fundamental for their gold chemo-adsorption (Figure 1 and Supporting Information File 1).

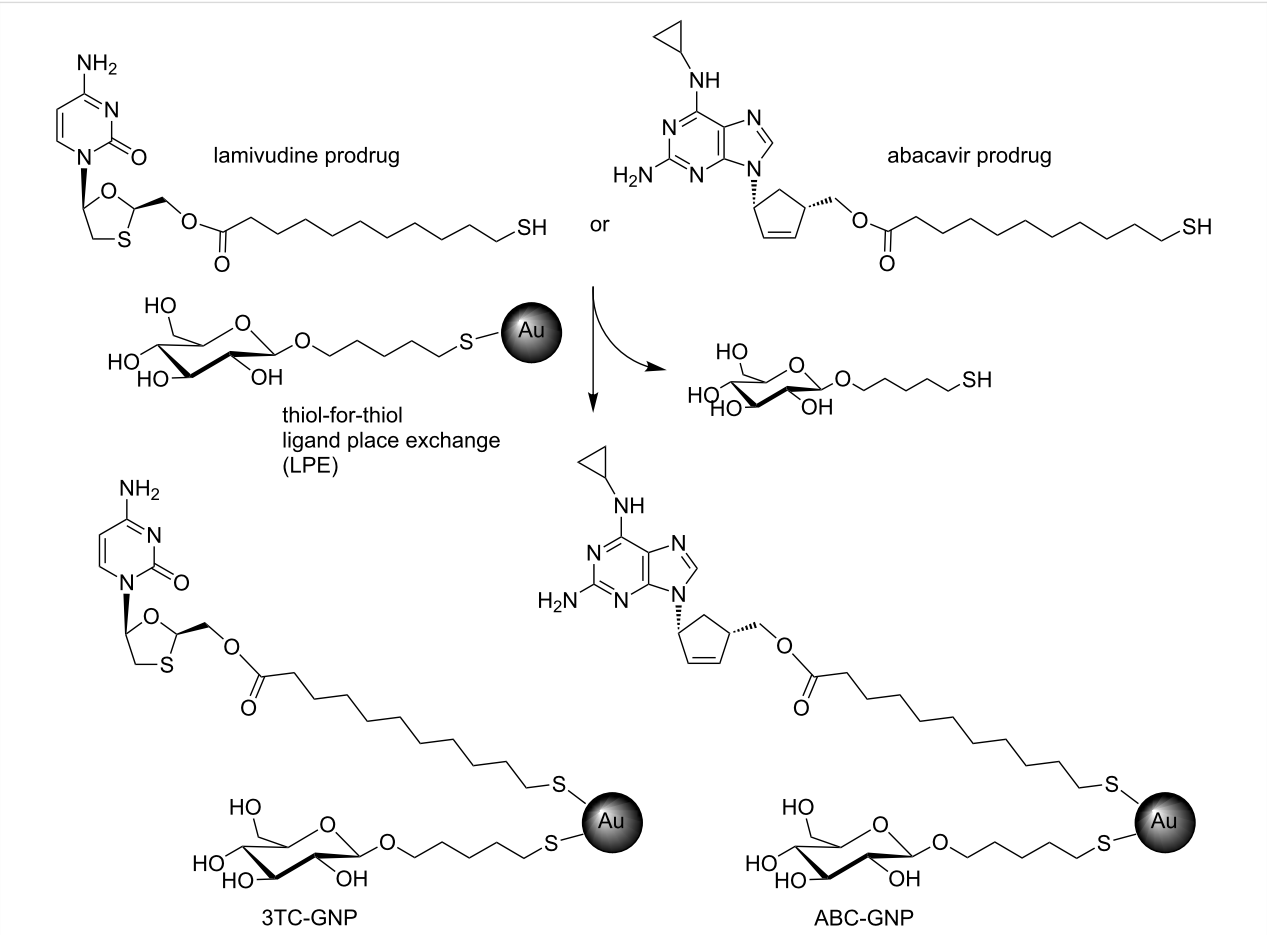

Figure 1: The prepared lamivudine (3TC) and abacavir (ABC) potential prodrugs and the corresponding 3TC- and ABC-GNPs prepared by ligand place exchange (LPE) reactions. Glucose-GNPs were incubated for 22 h with 0.1 equiv of ABC or 3TC thiol-ending drug derivatives. The reaction conditions allowed the "thiol-for-thiol" ligand exchange on the gold surface by replacing some glucose ligands on the glucose-GNPs with the prodrug candidates.

Abacavir (ABC) and lamivudine (3TC) were functionalized at the primary hydroxy groups through an ester bond that will be cleaved by cellular esterase activity or acid conditions in the cellular medium (or vaginal acidic pH). The primary hydroxy group of these NRTIs is fundamental for their antiviral activity: its intracellular enzymatic phosphorylation will form triphosphate derivatives that are the real chain terminators of HIV reverse transcriptase [3].

Due to the presence of an ester group in the prepared drug derivatives, $NaBH_4$ could not be used as reducing agent for the in situ preparation of these gold nanoparticles [32,33]. The ABC- and 3TC-GNPs were then prepared by the so-called "thiol-for-thiol" ligand place exchange (LPE) reaction [34]. The LPE reaction methodology allows the insertion of thiol ending ligands (the thiol-ending prodrug candidates) on pre-formed GNPs (GNPs fully covered by a glucose conjugate [35]) by a "thiol-for-thiol" exchange on the gold surface (Figure 1) following a reported methodology [24]. Preformed glucose-GNPs were incubated with 0.1 equivalents of ABC or 3TC conjugate with respect to the glucose conjugates on the GNP. This amount allowed the insertion of ~10% of the thiol-ending drugs. After precipitation and washings with EtOH, the GNPs were dissolved in a 90:10 mixture of water/DMSO to ensure a better GNPs water-dispersion that was also used for the cellular experiments. The GNPs dimension was evaluated by electron microscopy (Supporting Information File 1) showing an average gold diameter of ~3 nm. The GNPs contain around 10% of ABC or 3TC were analysed by HPLC and mass spectrometry (see next paragraph). The ester derivatives were not detected in the EtOH washings after the GNPs precipitation (by MALDI–MS and ^{1}H NMR) indicating that practically all the drug conjugates were linked on the gold surface.

Drug quantification and release of the drug from GNPs

We studied the stability of the GNPs containing ABC or 3TC (around 10%) in 1 N HCl at different times by liquid chromatography–mass spectrometry (LC–MS, Figure 2). A solution of drugs-GNPs (2 mg/mL) in water was treated with 1 N HCl and 1:1000 dilution aliquots (10 μL) of the GNP solutions were injected into the chromatograph. The free drugs were quantified by mass spectrometry with an internal standard (for detailed ion chromatograms and mass spectra see Supporting Information File 1). In the absence of HCl, the GNPs did not release the drugs showing no peaks in the LC–MS spectra. The pH-mediated delivery of the drugs from the GNPs was followed for 2–3 days until a plateau in the kinetic curve of the drug release was reached (Figure 2). Calibration curves of the free drugs were performed in triplicate by LC–MS (Supporting Information File 1). The release of the drug from a 2 μg/mL GNP dilution after 150–170 h was estimated to be around 150–200 nM from the LC–MS quantification. These experiments were performed in triplicate and repeated with two different GNP batches showing similar results. The pH-mediated release confirmed the estimation of ~10% of the drug on the gold surface and from these results the estimated amount of drug per 1 mg of GNPs was calculated to be ~0.1 μmol (the detailed calculation is given in Supporting Information File 1).

Cellular experiments with lamivudine (3TC) and abacavir (ABC)-GNPs

TZM-bl cells (derived HeLa-cell immortalized cell line that expresses high levels of CD4 and co-receptors CXCR4 and CCR5) were incubated for 30 min with different amounts of drug-GNPs (expressed as drug concentration, from 0.1 to 10 μM), followed by the addition of NL4-3 HIV virus encoding

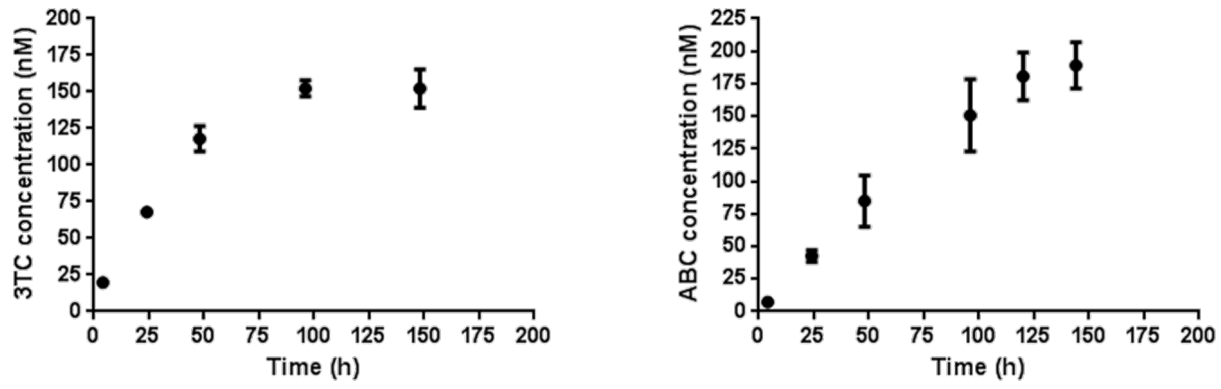

Figure 2: Time course release of free 3TC and ABC from the corresponding GNPs in 1 N HCl, detected by HPLC–MS measurements. Left: Release of 3TC from 2 μg/mL 3TC-GNPs for ~150 h. Right: release of ABC from 2 μg/mL ABC–GNPs for 170 h until a stable drug concentration in the release medium is reached. Both experiments were performed in triplicate.

for luciferase used as reporter gene. The free drugs and prodrug candidates were also tested in the same experiment. The viral replication was followed by the luciferase activity setting 100% of viral replication (luciferase activity) for untreated TZM-bl cells. Figure 3 shows the decrease of viral replication (correlated with the percentage of luciferase activity) of the abacavir and lamivudine-GNPs. Free abacavir and the corresponding ABC-GNPs showed similar IC_{50} values of 5 μM and 8 μM, respectively (Figure 3 left and Table 1). Surprisingly, the abacavir derivative seems to induce viral replication. With the presented data we are not able to explain this result, but it may be due to the amphiphilic properties of the drug derivative. Notwithstanding, the inactive abacavir-derivative showed antiviral activity when coupled on GNPs; a similar effect was previously observed for an inactive derivative of TAK-779 [15]. Free lamivudine and the corresponding GNPs showed IC_{50} values of 0.35 μM and 1 μM, respectively (Figure 3 right and Table 1), while the lamivudine derivative showed an IC_{50} value of 0.2 μM. The antiviral activity of the free drugs and the drugs-GNPs were in the same order of magnitude, while the control glucose-GNPs were not able to exhibit any antiviral activity at the tested concentrations (data not shown). In spite of the fact that no improvement of viral replication inhibition was obtained with respect to the free drug (probably due to the low loading of the drugs on the GNPs) these data indicate that the antiviral activity after conjugation is maintained and that gold glyconanoparticles can be considered as a promising drug delivery system.

After 30 min of pre-incubation with TZM-bl cells, the drug-loaded glyconanoparticles showed an NRTi activity as the free drugs at similar concentration. This activity suggests that the drug is delivered from the GNPs into the TZM-bl cells and has been triphosphorylated to active metabolites that can compete with the natural substrate of RT avoiding the RNA retrotranscription, e.g., the viral replication. Abacavir and lamivudine (being NRTi) inhibit the HIV reverse transcriptase enzyme competitively and act as a chain terminator in DNA synthesis. The lack of a 3'-OH group in the nucleoside analogue (NRTi) inhibits the formation of the 5' to 3' phosphodiester linkage (essential for the elongation of the DNA chain) terminating the growth of viral DNA [3].

Table 1: Antiviral activity of tested molecules calculated as IC_{50} from the cellular experiments.

Molecule tested	IC_{50}
abacavir	5 μM
abacavir derivative	–[a]
abacavir-GNP	8 μM
lamivudine	0.35 μM
lamivudine derivative	0.2 μM
lamivudine-GNP	1 μM

[a]The abacavir derivative showed the ability to induce viral replication.

Conclusion

The preparation and characterization of ~3 nm glucose-coated gold nanoparticles loaded with anti-HIV abacavir and lamivudine ester prodrug candidates is described. The effects of multimerization of the HIV drug derivatives on biocompatible and water-dispersible glyconanomaterials have been tested. The

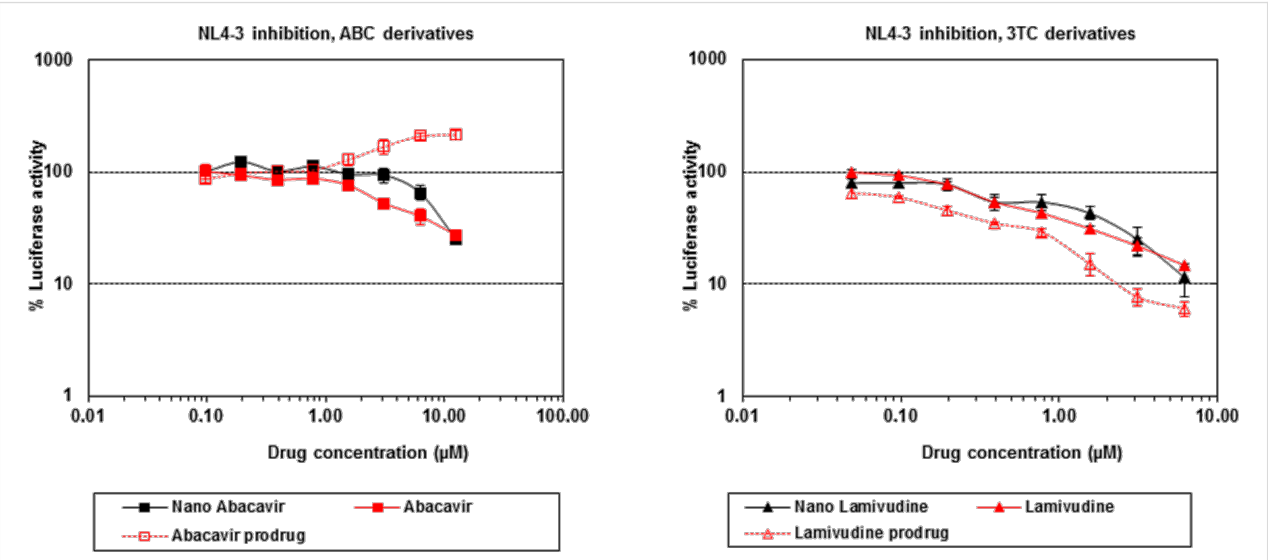

Figure 3: Cellular experiments: The two graphs show the percentage of luciferase activity decrease in the presence of increasing amounts of GNPs. ABC-GNPs (left) show an antiviral activity with an IC_{50} of 8 μM. 3TC–GNPs (right) show an antiviral activity with an IC_{50} of 1 μM.

drugs were released from the glyconanoparticles in acidic conditions and were able to inhibit viral replication in cellular assays with IC_{50} values (in terms of drug concentration) similar to the free drugs (less than 10 μM). These data support the strategy of developing a drug delivery system based on the coupling of ester derivatives onto gold glyconanoparticles and open the way to re-design more complex GNPs with improved activity carrying different antiviral inhibitors at the same time. In addition, other types of molecules able to block different steps of the viral replication can be introduced on the GNPs surface as previously shown with the microbicide candidates sulfate and *manno*-GNPs [19,20]. The combination of the gold glyconanoparticle properties with the advantage of multiple presentations of drugs, opens-up the possibility for generating multivalent nano delivery systems against HIV, combining on the same nanoparticle scaffold different antiviral inhibitors. Further experiments need to be performed to investigate the molecular mechanisms of the described antiviral activity. A cellular tracking of the GNPs could give a molecular explanation of their behavior in the intracellular milieu. The described proof-of-principle aims to a further exploration of gold glyconanoparticles as a new multifunctional tool in the world of drug-delivery system against HIV.

Experimental

General methods: All chemicals were purchased as reagent grade from Sigma-Aldrich, except chloroauric acid (Strem Chemicals), and were used without further purification. NMR analyses were performed with a Bruker DRX 500 MHz spectrometer with a broad band inverse (BBI) probe at 25 °C. Chemical shifts (δ) are given in ppm relative to the residual signal of the solvent used. Coupling constants (*J*) are reported in Hz. Splitting patterns are described by using the following abbreviations: br, broad; s, singlet; d, doublet; t, triplet; q, quartet; m, multiplet. For transmission electron microscopy (TEM) examinations, a single drop (10 μL) of an aqueous solution (ca. 0.1 mg/mL in milli-Q water) of drugs-GNPs was placed onto an ultrathin carbon film (<3 nm thickness) supported by a lacey carbon film on a 400 mesh copper grid (Ted Pella). The solution on the grid was left to dry in air for 14 hours at room temperature. TEM analysis was carried out in a JEOL JEM-2100F-UHR, operated at 200 kV. UV–vis spectra were carried out with a Beckman Coulter DU 800 spectrometer. The mass spectrometry detection was carried out in positive ion mode with electrospray ionization. The capillary and the cove voltages were set to 100 and 30 V, respectively. The desolvation gas was set to 600 L/h at 120 °C. The cone gas was set to 50 L/h and the ion source temperature at 120 °C. The instrument was operated in W mode with a resolution higher than 10.000. Data were obtained in centroid mode from *m*/*z* 50 to 1000 using a acquisition rate of 1 s/scan. The extracted-ion chromatograms for each compound were obtained with a mass tolerance window of ±0.1 Da (*m*/*z* 230.06 for 3TC, *m*/*z* 287.16 for ABC, 244.09 for cytidine, *m*/*z* 205.1 for tryptophan). An Acquity UPLC coupled to LCT Premier XE mass spectrometer (Waters, Mildford, MA) was employed for the drug quantification. The chromatographic separations were performed on a 100 × 2.1 mm Acquity BEH 1.7 μm C18 column (Waters, Mildford, MA). The gradient elution buffers were A (water and 0.1% formic acid) and B (methanol). The column temperature was set to 35 °C and eluted with a linear gradient consisted of 95% A over 0.5 min, 95–5% over 0.5–7 min, 5% over 7–8 min, returned to 95% for 0.5 min and kept for a further 1.5 min before next injection. Total run was 10 min, volume injection 5 μL and the flow rate 300 μL/mL.

Synthesis and characterization of thiol-ending prodrugs and GNPs: The preparation and characterization of the abacavir and lamivudine prodrug candidates and the corresponding GNPs is described in the Supporting Information File 1.

LC–MS analysis: GNPs and calibration curve samples were spiked with 10 μL of the appropriate internal standard solution before the LC–MS analysis (tryptophan and cytidine at 1 μM were used for quantification of 3TC and ABC, respectively). Calibration curves were designed over the range of 1–200 nM in triplicate. All the standard solutions were above the lower limit of quantification and within a linear range of quantification ($R^2 > 0.998$). Peak ratios of the drug and the internal standard were calculated and the calibration curves adjusted by fitting these ratios to the concentrations by a linear regression method.

Cellular viral inhibition assay: The ability of lamivudine and abacavir-GNPs to block HIV-1 infection was tested using a luciferase reporter cell line (TZM-bl) as described in [36]. TZM-bl is a Hela cell line that stably expresses CD4, CCR5 and CXCR4 (viral receptor and co-receptors). These cells also contain separate integrated copies of the luciferase and β-galactosidase genes under the control of the HIV-1 promoter [37-40]. Drugs, ester derivatives and GNPs were incubated with HIV-1 virus (NL4-3 strain) in triplicate for 30 min at 37 °C. The virus–drug mixture was added (1:1 by volume) to 10,000 TZM-bl cells per well. The plate was then placed into a humidified chamber within a CO_2 incubator at 37 °C. The luciferase activity was measured from cell lysates when the levels were sufficiently over the background to give reliable measurements (at least 10 fold) using Luciferase Assay System (Promega) and following the manufacturer's recommendations. A virus equivalent to 4 ng of p24 capsid protein (quantified by an antigen-capture assay; Innogenetics, Belgium) of the NL4-3 strain of HIV-1 was chosen as the lowest level of viral input sufficient to

give a clear luciferase signal within the linear range at day 3 post-infection. Infectivity was measured in triplicate and reported as the percentage of luciferase activity compared to the luciferase activity corresponding to the wells with virus and no drug. The concentration of drug required to inhibit 50% of the viral infectivity (IC_{50}) was determined.

Supporting Information

Supporting Information File 1

Synthesis and characterization of thiol-ending prodrugs and GNPs; HPLC–MS chromatograms, mass spectra and drugs calibration curves; calculation of drug-loading on GNPs.
[http://www.beilstein-journals.org/bjoc/content/supplementary/1860-5397-10-136-S1.pdf]

Acknowledgements

We thank Dr. Miguel Ángel von Wichmann from Hospital Donostia (San Sebastián) for his suggestions and scientific support. Financial support from the EU (grant CHAARM), the MINECO (grant No. CTQ2011-27268) and the Department of Industry of the Basque Country (Grant No. ETORTEK2011) is acknowledged. F.C. was supported by the Spanish Ministry of Science and Innovation, MICINN (Grant No. CTQ2008-04638). M.M. and S.P. acknowledge EU COST Action CM1102.

References

1. Gallo, R. C.; Montagnier, L. *N. Engl. J. Med.* **2003,** *349,* 2283–2285. doi:10.1056/NEJMp038194
2. Data and statistics from WHO webpage. http://www.who.int/hiv/data/en/ (accessed Jan 1, 2014).
3. De Clercq, E. *Curr. Opin. Pharmacol.* **2010,** *10,* 507–515. doi:10.1016/j.coph.2010.04.011
4. Munier, C. M. L.; Andersen, C. R.; Kelleher, A. D. *Drugs* **2011,** *71,* 387–414. http://link.springer.com/article/10.2165/11585400-000000000-00000/fulltext.html
5. Walker, B. D.; Burton, D. R. *Science* **2008,** *320,* 760–764. doi:10.1126/science.1152622
6. Balzarini, J.; Van Damme, L. *Lancet* **2007,** *369,* 787–797. doi:10.1016/S0140-6736(07)60202-5
7. Abdool Karim, Q.; Abdool Karim, S. S.; Frohlich, J. A.; Grobler, A. C.; Baxter, C.; Mansoor, L. E.; Kharsany, A. B. M.; Sibeko, S.; Mlisana, K. P.; Omar, Z.; Gengiah, T. N.; Maarschalk, S.; Arulappan, N.; Mlotshwa, M.; Morris, L.; Taylor, D. *Science* **2010,** *329,* 1168–1174. doi:10.1126/science.1193748
8. Allen, T. M.; Cullis, P. R. *Science* **2004,** *303,* 1818–1822. doi:10.1126/science.1095833
9. Pelgrift, R. Y.; Friedman, A. J. *Adv. Drug Delivery Rev.* **2013,** *65,* 1803–1815. doi:10.1016/j.addr.2013.07.011
10. Date, A. A.; Destache, C. J. *Biomaterials* **2013,** *34,* 6202–6228. doi:10.1016/j.biomaterials.2013.05.012
11. Lisziewicz, J.; Tőke, E. R. *Nanomed. Nanotechnol. Biol. Med.* **2013,** *9,* 28–38. doi:10.1016/j.nano.2012.05.012
12. Boisselier, E.; Astruc, D. *Chem. Soc. Rev.* **2009,** *38,* 1759–1782. doi:10.1039/b806051g
13. Dykman, L.; Khlebtsov, N. *Chem. Soc. Rev.* **2012,** *41,* 2256–2282. doi:10.1039/c1cs15166e
14. Duncan, B.; Kim, C.; Rotello, V. M. *J. Controlled Release* **2010,** *148,* 122–127. doi:10.1016/j.jconrel.2010.06.004
15. Bowman, M.-C.; Ballard, T. E.; Ackerson, C. J.; Feldheim, D. L.; Margolis, D. M.; Melander, C. *J. Am. Chem. Soc.* **2008,** *130,* 6896–6897. doi:10.1021/ja710321g
16. Elechiguerra, J. L.; Burt, J. L.; Morones, J. R.; Camacho-Bragado, A.; Gao, X.; Lara, H. H.; Yacaman, M. J. *J. NanoBiotechnology* **2005,** *3,* No. 6. doi:10.1186/1477-3155-3-6
17. Shiang, Y.-C.; Ou, C.-M.; Chen, S.-J.; Ou, T.-Y.; Lin, H.-J.; Huang, C.-C.; Chang, H.-T. *Nanoscale* **2013,** *5,* 2756–2764. doi:10.1039/c3nr33403a
18. Di Gianvincenzo, P.; Chiodo, F.; Marradi, M.; Penadés, S. *Methods Enzymol.* **2012,** *509,* 21–40. doi:10.1016/B978-0-12-391858-1.00002-2
19. Martínez-Ávila, O.; Bedoya, L. M.; Marradi, M.; Clavel, C.; Alcamí, J.; Penadés, S. *ChemBioChem* **2009,** *10,* 1806–1809. doi:10.1002/cbic.200900294
20. Di Gianvincenzo, P.; Marradi, M.; Martínez-Ávila, O.; Bedoya, L. M.; Alcamí, J.; Penadés, S. *Bioorg. Med. Chem. Lett.* **2010,** *20,* 2718–2721. doi:10.1016/j.bmcl.2010.03.079
21. Marradi, M.; Chiodo, F.; García, I.; Penadés, S. *Chem. Soc. Rev.* **2013,** *42,* 4728–4745. doi:10.1039/c2cs35420a
22. Arnáiz, B.; Martínez-Ávila, O.; Falcon-Perez, J. M.; Penadés, S. *Bioconjugate Chem.* **2012,** *23,* 814–825. doi:10.1021/bc200663r
23. de la Fuente, J. M.; Alcántara, D.; Penadés, S. *IEEE Trans. Nanobiosci.* **2007,** *6,* 275–281. doi:10.1109/TNB.2007.908981
24. Irure, A.; Marradi, M.; Arnáiz, B.; Genicio, N.; Padro, D.; Penadés, S. *Biomater. Sci.* **2013,** *1,* 658–668. doi:10.1039/c3bm60032g
25. Murray, R. A.; Qiu, Y.; Chiodo, F.; Marradi, M.; Penadés, S.; Moya, S. E. *Small* **2014**. doi:10.1002/smll.201303604
26. Moros, M.; Hernáez, B.; Garet, E.; Dias, J. T.; Sáez, B.; Grazú, V.; González-Fernández, A.; Alonso, C.; de la Fuente, J. M. *ACS Nano* **2012,** *6,* 1565–1577. doi:10.1021/nn204543c
27. Safari, D.; Marradi, M.; Chiodo, F.; Dekker, H. A. T.; Shan, Y.; Adamo, R.; Oscarson, S.; Rijkers, G. T.; Lahmann, M.; Kamerling, J. P.; Penadés, S.; Snippe, H. *Nanomedicine* **2012,** *7,* 651–662. doi:10.2217/nnm.11.151
28. Chiodo, F.; Marradi, M.; Tefsen, B.; Snippe, H.; van Die, I.; Penadés, S. *PLoS One* **2013,** *8,* e73027. doi:10.1371/journal.pone.0073027
29. Bibby, D. C.; Charman, W. N.; Charman, S. A.; Iskander, M. N.; Porter, C. J. H. *Int. J. Pharm.* **1996,** *144,* 61–70. doi:10.1016/S0378-5173(96)04720-5
30. Tichý, T.; Andrei, G.; Dračínský, M.; Holý, A.; Balzarini, J.; Snoeck, R.; Krečmerová, M. *Bioorg. Med. Chem.* **2011,** *19,* 3527–3539. doi:10.1016/j.bmc.2011.04.016
31. Tahir, M. N.; Théato, P.; Müller, W. E. G.; Schröder, H. C.; Janshoff, A.; Zhang, J.; Huth, J.; Tremel, W. *Chem. Commun.* **2004,** 2848–2849. doi:10.1039/b410283e
32. Barrientos, A. G.; de la Fuente, J. M.; Rojas, T. C.; Fernández, A.; Penadés, S. *Chem.–Eur. J.* **2003,** *9,* 1909–1921. doi:10.1002/chem.200204544

33. Marradi, M.; Martín-Lomas, M.; Penadés, S. *Adv. Carbohydr. Chem. Biochem.* **2010,** *64,* 211–290. doi:10.1016/S0065-2318(10)64005-X
34. Hostetler, M. J.; Templeton, A. C.; Murray, R. W. *Langmuir* **1999,** *15,* 3782–3789. doi:10.1021/la981598f
35. Martínez-Ávila, O.; Hijazi, K.; Marradi, M.; Clavel, C.; Campion, C.; Kelly, C.; Penadés, S. *Chem.–Eur. J.* **2009,** *15,* 9874–9888. doi:10.1002/chem.200900923
36. Marradi, M.; Di Gianvincenzo, P.; Enríquez-Navas, P. M.; Martínez-Ávila, O. M.; Chiodo, F.; Yuste, E.; Angulo, J.; Penadés, S. *J. Mol. Biol.* **2011,** *410,* 798–810. doi:10.1016/j.jmb.2011.03.042
37. Takeuchi, Y.; McClure, M. O.; Pizzato, M. *J. Virol.* **2008,** *82,* 12585–12588. doi:10.1128/JVI.01726-08
38. Wei, X.; Decker, J. M.; Liu, H.; Zhang, Z.; Arani, R. B.; Kilby, J. M.; Saag, M. S.; Wu, X.; Shaw, G. M.; Kappes, J. C. *Antimicrob. Agents Chemother.* **2002,** *46,* 1896–1905. doi:10.1128/AAC.46.6.1896-1905.2002
39. Derdeyn, C. A.; Decker, J. M.; Sfakianos, J. N.; Wu, X.; O'Brien, W. A.; Ratner, L.; Kappes, J. C.; Shaw, G. M.; Hunter, E. *J. Virol.* **2000,** *74,* 8358–8367. doi:10.1128/JVI.74.18.8358-8367.2000
40. Platt, E. J.; Wehrly, K.; Kuhmann, S. E.; Chesebro, B.; Kabat, D. *J. Virol.* **1998,** *72,* 2855–2864. http://jvi.asm.org/content/72/4/2855.full

License and Terms

Beilstein Journal of Organic Chemistry

Molecular recognition of surface-immobilized carbohydrates by a synthetic lectin

Melanie Rauschenberg, Eva-Corrina Fritz, Christian Schulz, Tobias Kaufmann and Bart Jan Ravoo*

Full Research Paper

Open Access

Address:
Organic Chemistry Institute, Westfälische Wilhelms-Universität Münster, Corrensstrasse 40, 48149 Münster, Germany

Email:
Bart Jan Ravoo* - b.j.ravoo@uni-muenster.de

* Corresponding author

Keywords:
carbohydrates; lectins; molecular recognition; microarrays; multivalent glycosystems; peptides

Beilstein J. Org. Chem. **2014,** *10,* 1354–1364.
doi:10.3762/bjoc.10.138

Received: 19 February 2014
Accepted: 22 May 2014
Published: 16 June 2014

This article is part of the Thematic Series "Multivalent glycosystems for nanoscience".

Guest Editor: J.-L. Reymond

Abstract

The molecular recognition of carbohydrates and proteins mediates a wide range of physiological processes and the development of synthetic carbohydrate receptors ("synthetic lectins") constitutes a key advance in biomedical technology. In this article we report a synthetic lectin that selectively binds to carbohydrates immobilized in a molecular monolayer. Inspired by our previous work, we prepared a fluorescently labeled synthetic lectin consisting of a cyclic dimer of the tripeptide Cys-His-Cys, which forms spontaneously by air oxidation of the monomer. Amine-tethered derivatives of *N*-acetylneuraminic acid (NANA), β-D-galactose, β-D-glucose and α-D-mannose were microcontact printed on epoxide-terminated self-assembled monolayers. Successive prints resulted in simple microarrays of two carbohydrates. The selectivity of the synthetic lectin was investigated by incubation on the immobilized carbohydrates. Selective binding of the synthetic lectin to immobilized NANA and β-D-galactose was observed by fluorescence microscopy. The selectivity and affinity of the synthetic lectin was screened in competition experiments. In addition, the carbohydrate binding of the synthetic lectin was compared with the carbohydrate binding of the lectins concanavalin A and peanut agglutinin. It was found that the printed carbohydrates retain their characteristic selectivity towards the synthetic and natural lectins and that the recognition of synthetic and natural lectins is strictly orthogonal.

Introduction

In comparison to proteins and nucleic acids, carbohydrates have traditionally received less attention in the scientific community. However, it is increasingly apparent that carbohydrates and glycoconjugates are involved in a multitude of physiological and pathological processes and offer an enormous potential to encrypt biological information [1-4]. In contrast to the linear nucleic acids and proteins, carbohydrates usually form branched oligomers or polymers which are joined together by a variety of

linkages. The vast amount of resulting carbohydrate oligomers and polymers offers a virtually unlimited number of encodings. In nature, carbohydrates are often linked to lipids, peptides or proteins. These conjugates are found inside cells, on cell membranes as well as in extracellular fluids and matrices. Surprisingly, the general understanding of the function of carbohydrates in cell biology is still lagging far behind our knowledge of proteins and nucleic acids. This backlog is mainly due to the complexity of biological carbohydrates. Additionally, established analytical and synthetic methods in protein and nucleic acid research such as automated sequencing, automated synthesis and high-throughput microarray screening are lacking in glycobiology [5]. However, during the last decade, these methods have also been adapted to carbohydrates [6-8].

Carbohydrate microarrays on chips proved to be a particularly useful tool in glycomics [9-11] since their description in 2002 by several groups [12-17]. Microarrays normally consist of carbohydrates immobilized in an ordered and well defined format on a flat surface. The arrays can be considered as minimal models of cell surfaces that are compatible with high-throughput analysis techniques and can be used to study carbohydrate–protein/antibody interactions, to detect enzymes cleaving glycosidic bonds, to study cell–cell adhesions mediated by carbohydrates as well as to screen for selective inhibitors of carbohydrate–protein interactions [18]. The immobilization of carbohydrates can be divided into noncovalent and covalent attachment routes. While carbohydrates simply adhere to the surface when using the noncovalent strategy, the covalent attachment leads to the fabrication of highly stable arrays because a chemical bond is formed between the substrate and the carbohydrates. Fabrication of carbohydrate microarrays can be achieved either by microspotting of carbohydrates on activated surfaces or by using printing techniques on activated substrates. The first approach can be realized by robotic printers [19,20] generating high density chips with a large number of different spots. Read out is performed with an array scanner using fluorescence microscopy or surface plasmon resonance.

In recent years, microcontact printing (μCP) [21-24] has gained importance as a replication method for biological microarrays such as protein [25,26] and DNA microarrays [27-30]. Our group has shown that also simple carbohydrate microarrays can be conveniently prepared by μCP if reactive glycosides are printed on a suitable target self-assembled monolayer (SAM) [31,32]. Amongst others, we reported carbohydrate microarrays fabricated by cycloaddition of alkynes on azide-terminated SAMs [33], by Diels–Alder reaction of cyclopentadienes and furans on maleimide-terminated SAMs [34], by thiol–ene click reaction of functionalized thiols on alkene-terminated SAMs [35] as well as by strain promoted cycloadditions on azide- and nitriloxide-terminated SAMs [36] using μCP. Homogenous spots, high-edge resolution, good reproducibility and short reaction times can be easily achieved by using μCP. These advantages render this method a versatile tool for the fabrication of simple carbohydrate microarrays.

"Synthetic lectins" as artificial carbohydrate receptors would be highly valuable as drugs in various therapies and as recognition units in diagnostics and sensing. However, the development of synthetic lectins poses a phenomenal challenge for supramolecular chemistry [37] because a carbohydrate receptor in order to be useful must not only compete with the strong hydration of carbohydrates in water but also discriminate closely related isomers. It is obvious that the de-novo design of a "synthetic lectin" is very difficult. The most remarkable synthetic lectins to date have been prepared by Davis and co-workers, who recently synthesized a cage-like receptor that binds glucose in water with excellent selectivity versus other simple carbohydrates (for example, ~50:1 versus galactose) which also has sufficient affinity for glucose sensing at the concentrations found in blood [38]. On the other hand, we have described a dynamic combinatorial approach to the identification of biomimetic carbohydrate receptors [39]. To this end, we explored a dynamic combinatorial library of cyclic peptides to select receptors that are assembled from tripeptides under thermodynamic equilibrium. Amongst others, we identified a synthetic lectin (HisHis) that binds *N*-acetylneuraminic acid (NANA) [18]. HisHis is a cyclic hexapeptide which is easily obtained from the air oxidation of the tripeptide Cys-His-Cys (see Figure 1). It should be noted that in this case HisHis is obtained as a mixture of two isomers, in which the tripeptides are either oriented in parallel or antiparallel direction. The parallel isomer is shown in Figure 1. We have recently synthesized and isolated the parallel and antiparallel isomers of HisHis and found that both isomers can bind NANA in a cooperative 1:2 complex (1 molecule of HisHis and 2 molecules of NANA) [40]. The binding constants are $K_1 = 143\ M^{-1}$ and $K_2 = 5.08 \times 10^3\ M^{-1}$ for the parallel isomer and $K_1 = 94\ M^{-1}$ and $K_2 = 990\ M^{-1}$ for the antiparallel isomer at neutral pH in water [40]. We also found that the parallel isomer of HisHis (but not the antiparallel isomer) binds β-D-galactose in a 1:1 complex with $K = 7.96 \times 10^3\ M^{-1}$ [40]. NMR spectroscopy and DFT calculations indicate that the interaction of the peptide with the carbohydrates is based primarily on hydrogen bonding [40]. It should be emphasized that NANA is a particularly interesting carbohydrate since it belongs to the class of sialic acids which are often the terminal carbohydrates in glycoproteins and glycolipids on the cell surface. Sialic acids are involved in the communication of cells with their environment [41] and selective detection, binding and blocking of sialic acids on the cell surface is of significant biomedical interest.

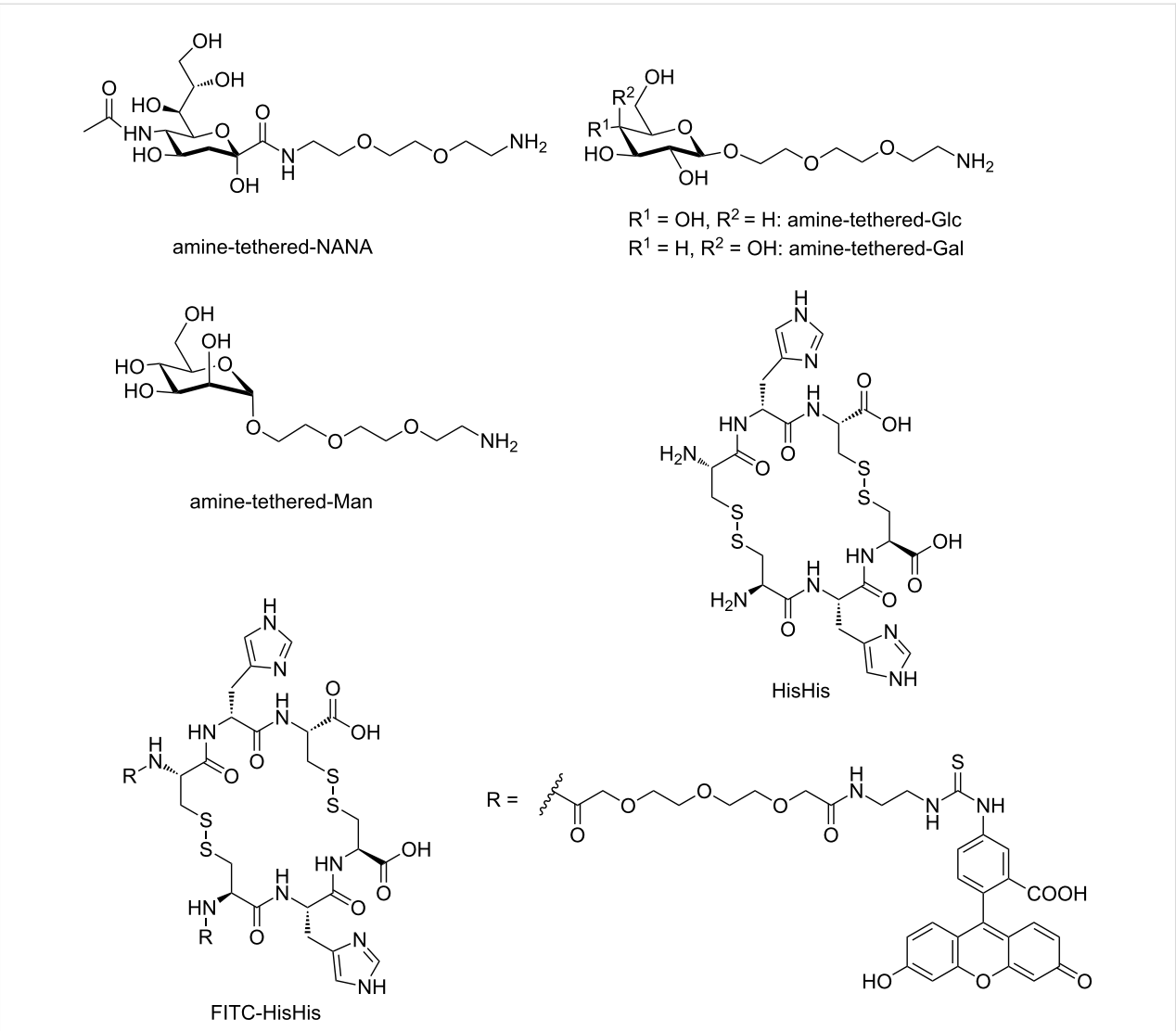

Figure 1: Molecular structures of carbohydrates (NANA, Glc, Gal, Man) immobilized on epoxide SAMs, NANA-binding synthetic lectin (HisHis), and the FITC-labeled synthetic lectin (FITC HisHis). For simplicity, only the parallel isomer of HisHis is shown.

It is the aim of this report to investigate whether the synthetic lectin HisHis is able to selectively bind to NANA immobilized on a substrate which serves as a model for a cell surface. To this end, we prepared a set of simple carbohydrate microarrays as well as fluorescein-isothiocyanate labeled HisHis (FITC-HisHis) and studied the selectivity and affinity of HisHis towards immobilized NANA in comparison with the glycosides of glucose (Glc), galactose (Gal) and mannose (Man) (Figure 1). In this study, we exploit the epoxide ring opening reaction of amine-tethered carbohydrates on epoxide-terminated SAMs [42] to print carbohydrate microarrays on silicon and glass substrates. Epoxide-terminated SAMs are particularly versatile for the fabrication of biological arrays [43,44] and we have recently demonstrated that epoxide-terminated substrates are easily modified using μCP [45]. The incubation of the synthetic lectin FITC-HisHis as well as two natural lectins on the immobilized carbohydrates provides insight into the affinity and selectivity of lectin–carbohydrate interaction.

Results and Discussion

The synthetic lectin HisHis was prepared by air oxidation of the tripeptide Cys-Hys-Cys (synthesized by solid phase peptide synthesis) as described previously [39]. Fluorescein-labeled FITC-HisHis was obtained by labeling of Cys-His-Cys with fluorescein isothiocyanate, which was achieved by using an Fmoc-protected oligo(ethylene glycol) spacer synthesized in four steps from commercially available ethylenediamine (see Supporting Information File 1). The introduction of this water soluble spacer should ensure the unhindered formation of the cyclic synthetic lectin FITC-HisHis from the FITC-labeled Cys-

His-Cys by air oxidation. The spectroscopic and analytical data obtained for FITC-HisHis are fully consistent with the molecular structure (see Supporting Information File 1). Successful incorporation of the fluorophore was also evident in the UV–vis spectrum of the precursor FITC-labeled Cys-His-Cys (see Figure S1 in the Supporting Information File 1). We note that if prepared directly by air oxidation from Cys-His-Cys, HisHis as well as FITC-HisHis consist of a mixture of two isomers, in which the two tripeptides are arranged in parallel or antiparallel direction, respectively. We have recently synthesized and isolated the parallel and antiparallel HisHis isomers and found that both isomers can bind NANA in a 1:2 complex with slightly stronger binding by the parallel HisHis compared to the antiparallel HisHis [40]. Isothermal titration calorimetry (ITC) confirmed that the interaction of FITC-HisHis (mixture of isomers) and NANA is characterized by the same stoichiometry (1:2) and nearly the same binding constants (K_1 = 163 M^{-1} and $K_2 = 5.36 \times 10^3$ M^{-1}) were obtained. ITC data are provided in Supporting Information File 1. These findings indicate that the introduction of the FITC label does not affect the formation of the synthetic lectin HisHis and its interaction with NANA. Since the mixture of isomers is much more easily synthesized than the individual isomers and since both isomers are potent binders of NANA, all experiments described in this report where performed with the mixture of parallel and antiparallel isomers of FITC-HisHis.

In order to study the affinity of the synthetic lectin HisHis on the surface, four carbohydrates (NANA, Glc, Gal, Man, see Figure 1) were selected for the fabrication of carbohydrate arrays. To provide carbohydrate inks suitable for microcontact printing (μCP), NANA was conjugated via its C1 carboxylic acid moiety, whereas the other carbohydrates were conjugates as β-glycosides (Glc, Gal) and α-glycosides (Man), respectively. In order to flexibly attach the carbohydrates on the substrate and to ensure unhindered carbohydrate–lectin interactions, oligo(ethylene glycol) spacers were introduced. Oligo(ethylene glycol) chains are flexible, water-soluble and do not interact with lectins [46]. A nucleophilic primary amine function was introduced on the terminus of the spacer in order to ensure reaction with the epoxide-functionalized substrate upon μCP. The NANA ink was prepared by solution phase peptide coupling using the DIPCDI/Oxyma pure® coupling protocol. The glucose (Glc), galactose (Gal) and mannose (Man) inks were synthesized as described in Supporting Information File 1.

The effective immobilization of the amine-terminated carbohydrate inks requires a surface functionalized with epoxides. Epoxides are stable under ambient conditions yet highly reactive towards amines at elevated temperatures and epoxide SAMs on silicon oxide surfaces can be obtained in only one step from an epoxy-terminated trimethoxysilane. The most common approaches to fabricate epoxide SAMs is by dip-coating or vapor condensation. However, this leads to the formation of thick films of aggregated molecular layers with undefined surface morphology [47-50]. Therefore, the epoxide SAMs were prepared by the method of Julthongpiput et al. because well-defined monolayers of epoxides on glass and silicon substrates can be obtained by using (3-glycidoxypropyl)trimethoxysilane in toluene [42]. The successful surface modification was verified by contact angle and XPS measurements (see Supporting Information File 1) which are in accordance with literature data [42].

The μCP protocol to fabricate carbohydrate microarrays was optimized to provide a highly effective combination of stamp, ink and substrate. In view of the fact that the epoxide ring opening reaction with amines is much faster at elevated temperatures, the surface of oxidized, patterned PDMS stamps was coated with 2-[methoxy(polyethyleneoxy)propyl]trimethylsilane (PEG silane) [51]. The PEG coated stamps provided optimal wetting of the stamp by the carbohydrate ink solution, while preventing contamination of the substrate by PDMS residues. Moreover, it was observed that oxidized stamps without such a PEG coating adhered irreversibly to the epoxide substrates, possible due to reaction of the epoxide substrate with the oxidized PDMS surface. In the optimized μCP protocol, the PEG coated stamps were wetted with a 20 mM ethanolic solution of carbohydrate inks (NANA, Glc, Gal or Man) and triethylamine, and dried after 1 min incubation time. After placing the stamps on the epoxide-terminated SAMs on cleaned and activated glass or silicon substrates, the substrate and stamp were placed in an oven at 60 °C for 4 h. Finally, the stamp was removed from the substrate at room temperature. In order to prepare microarrays with two carbohydrates, the printing step was repeated with a second carbohydrate ink on a flat stamp to functionalize the remaining epoxide surface (Figure 2). After printing, the surfaces were rinsed extensively to remove any residual physisorbed material.

Immobilization of carbohydrates on the epoxide-terminated SAMs was investigated by several methods. Printing of a polar carbohydrate on the epoxide surface should lead to increased hydrophilicity exclusively in the printed areas which can be detected by water condensation experiments. Figure 3 shows optical microscopy pictures of epoxide SAMs onto which NANA ink or Gal ink were printed with a structured stamp (10 μm dots spaced by a 5 μm gap). It is obvious that the water condensed on the surface is found exclusively in the areas where the hydrophilic NANA or Gal were printed. Furthermore, quantification of the surface hydrophilicity was performed by water contact angle measurements. To this end, a flat PDMS

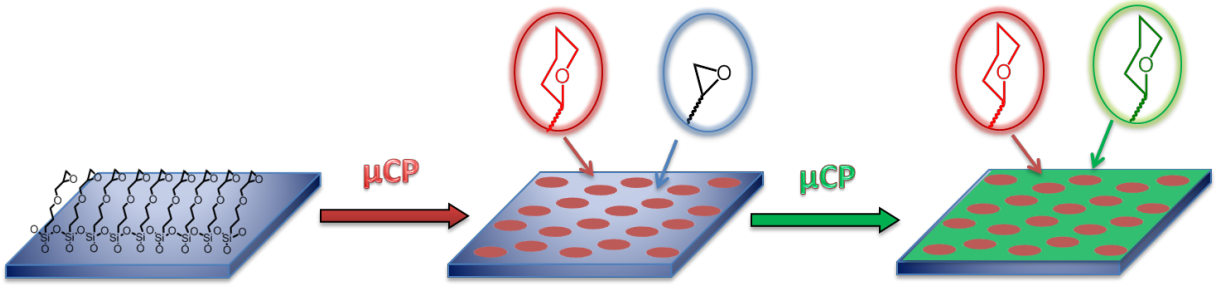

Figure 2: Schematic representation of the preparation of a simple carbohydrate microarray by μCP of amine-functionalized carbohydrate inks on epoxide-terminated SAM ("microcontact chemistry"). The first carbohydrate (red) is printed with a patterned PDMS stamp, the second carbohydrate (green) is printed in the interspaces with a flat PDMS stamp.

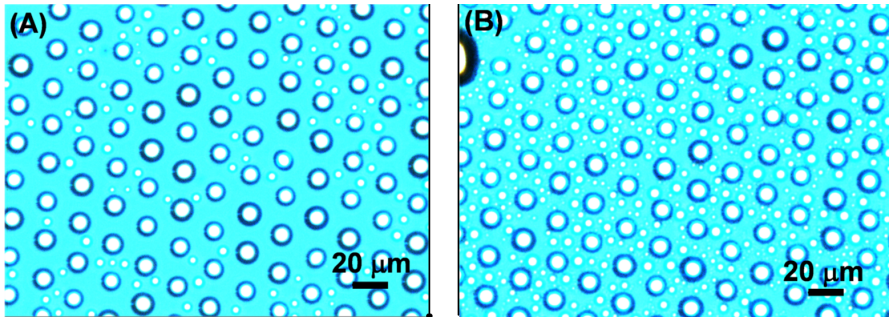

Figure 3: Optical microscopy images of water droplets selectively condensed in the areas where (A) the NANA ink and (B) the Gal ink were patterned by μCP on an epoxide-terminated SAM.

stamp was used to obtain a homogenous carbohydrate surface after μCP for 4 h at 60 °C. After printing, the contact angles decreased from 61°/33° (advancing/receding) for the epoxide-terminated SAMs to ~30°/~12° for the carbohydrate-functionalized SAMs (with minor differences for the different carbohydrate inks). Data for all contact angle measurements can be found in Table S1 in Supporting Information File 1.

Further information on the printing process was obtained from X-ray photoelectron spectroscopy (XPS) of Si-wafers functionalized with an epoxide-terminated SAM and printed with NANA ink using a PEG coated flat stamp (see Figure S3 and Figure S4 in Supporting Information File 1). While nearly no N(1s) signal was detected in the epoxide-terminated SAM, a clear N(1s) signal can be observed when the NANA ink is printed. The C(1s) peak shows a splitting into the C–C (285 eV), C–O (287 eV), C=C, C=O and residual epoxide C–O signals (289 eV) as expected for the NANA-terminated SAM [52].

In addition, atomic force microscopy (AFM) of patterned epoxide SAMs was performed to verify the success of the printing process. The AFM height profiles of a pattern of NANA ink printed with a patterned stamp (10 μm stripes that are spaced by a 5 μm gap) as well as a cross printed pattern obtained by a successive print at 90° angle with two identically patterned stamps (5 μm stripes that are spaced by a 10 μm gap) using the Glc ink and the Gal ink are shown in Figure 4. A clear pattern in accordance with the shape and dimensions of the used stamps can be seen. If printing of the carbohydrate ink results in a very dense layer of carbohydrates aligned mostly perpendicular to the surface, the height difference of printed and nonprinted areas should be around 1 nm. The observed height differences are significantly less which indicates that the carbohydrates are tilted relative to the surface normal and that the printed layers exhibit a lower than maximal surface coverage. This is most likely due to a combination of factors, i.e., quality of the base epoxide SAM, reaction time with the amine inks, and steric bulk of the carbohydrates compared to the triethylene glycol linker. We note that these observations are consistent with our earlier reports on the immobilization of glycosides on SAMs by μCP [33-36].

Having established that one or more carbohydrate inks can be patterned on epoxide-terminated SAMs by μCP, we turned our attention to the investigation of the interaction of synthetic and natural lectins with the immobilized carbohydrates. To this end, bifunctional surfaces were fabricated by μCP of a the first ink in

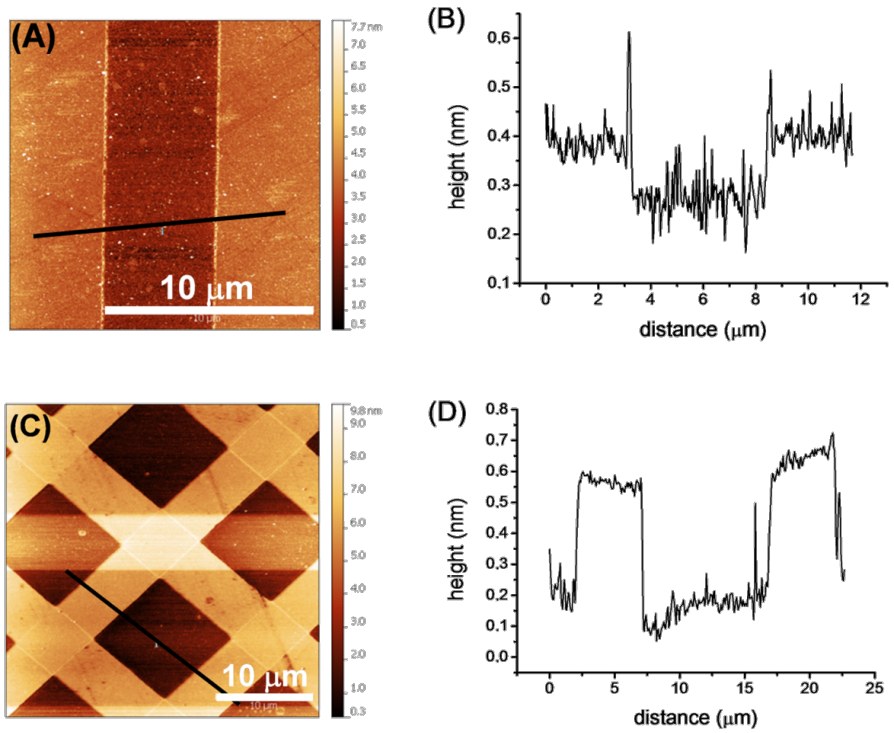

Figure 4: (A) AFM height image (zoom) of NANA ink in 10 µm stripes on an epoxide-terminated SAM; (B) Height profile of the black line shown in (A); (C) AFM height image of Glc ink and Gal ink cross printed in 5 µm stripes on an epoxide-terminated SAM; (D) Height profile of the black line shown in (C).

a dot pattern (10 µm dots spaced by a 5 µm gap) and filling up the interspaces with the second ink by using µCP with a flat stamp. In a first set of experiments, NANA ink was printed in a dot pattern and the remaining area was functionalized by printing Man ink with a flat stamp. In a reverse experiment, Man ink was printed in dots and the remaining area was functionalized with NANA ink. After incubation of these carbohydrate arrays with the synthetic lectin FITC-HisHis, fluorescence was observed exclusively in the areas where the NANA ink had been printed. No significant fluorescence was observed in the area where the Man ink had been printed (Figure 5). This observation confirms – for the first time – that the synthetic lectin HisHis binds selectively to NANA, and not to Man, also when the carbohydrate is immobilized on a surface. We note that no fluorescence was detected when the inks were printed onto bare glass slides (instead of epoxide-functionalized glass slides) or when printing was performed without inking the PEG coated PDMS stamp. In a second set of experiments, NANA ink was printed in dots and the remaining area was functionalized with Glc ink, and vice versa. Again it was observed that HisHis binds exclusively to NANA, and not to Glc (see Figure 8A). In a third set of experiments, Gal ink was printed in dots and the remaining area was functionalized with Man ink, and vice versa. As expected, it was observed that FITC-HisHis binds to Gal, and not to Man (Figure 5). In our preceding work, we had observed that the parallel isomer of HisHis binds to β-galactosides [40].

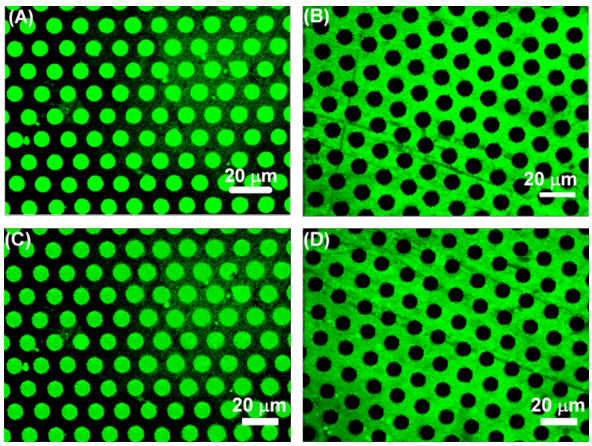

Figure 5: Fluorescence images of bifunctional carbohydrate microarrays incubated with FITC-HisHis. (A) NANA (dots 10 × 5 µm) and Man (background); (B) Man (dots 10 × 5 µm) and NANA (background); (C) Gal (dots 10 × 5 µm) and Man (background); (D) Man (dots 10 × 5 µm) and Gal (background).

In order to confirm the interaction between HisHis and NANA with surface plasmon resonance (SPR) spectroscopy a commercially available polycarboxylate hydrogel sensor surface was

employed, which is known to be particularly advantageous for low molecular weight compounds due to the signal amplification caused by multiple binding events in the hydrogel on the sensor. The functionalization of the polycarboxylate hydrogel with amine terminated NANA was performed by *N*-hydroxysuccinimide (NHS) activation and subsequent peptide coupling. Indeed, using the hydrogel sensor a small but significant SPR signal increase was observed upon the addition of HisHis (see Figure S5 in Supporting Information File 1). The initial rate and extent of surface binding correlated with the concentration of HisHis (0.5–2.0 mM) applied to the sensor. However, it was not possible to obtain sufficiently reproducible data to perform a quantitative analysis of the peptide–carbohydrate interaction. The poor quality of the SPR signal is certainly due to the low molecular weight of HisHis which limits any further SPR investigations.

Additionally, bifunctionalized carbohydrate surfaces were incubated simultaneously with FITC-HisHis, TRITC-ConA, and FITC-PNA to elucidate whether selective binding of the synthetic lectin to glycosides is also observed in the presence of natural lectins. In Figure 6, the overlays of fluorescence images are shown. In each experiment, FITC-HisHis is detected exclusively on the NANA and the Gal areas, whereas TRITC-ConA binds to Man and FITC-PNA binds to Gal only. These observations demonstrate that selective recognition between HisHis and NANA or Gal is not in any way disturbed by the presence of a second lectin and that the synthetic lectin HisHis and the natural lectins ConA and PNA operate orthogonally.

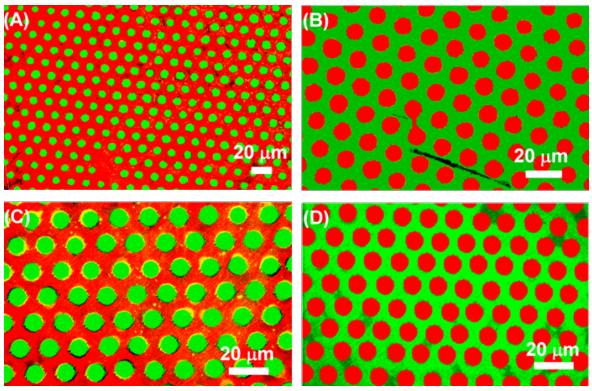

Figure 6: Overlay of fluorescence images of bifunctional carbohydrate microarrays; (A) NANA (dots 10 × 5 µm) and Man (background) incubated with FITC-HisHis and TRITC-ConA; (B) Man (dots 10 × 5 µm) and NANA (background) incubated with FITC-HisHis and TRITC-ConA; (C) Gal (dots 10 × 5 µm) and Man (background) incubated with FITC-HisHis and TRITC-ConA; (D) Man (dots 10 × 5 µm) and Gal (background) incubated with FITC-PNA and TRITC-ConA.

Additionally, the selectivity of the FITC-HisHis was tested with a set of competition experiments on a microarray of NANA dots with Man background (Figure 7). If the recognition process between FITC-HisHis and NANA or Gal is selective, incubation with a large excess of the two carbohydrates should lead to release of the surface-bound synthetic lectin from a microarray displaying NANA or Gal. In this case, the detected fluorescence pattern should vanish after washing the microarrays with concentrated solutions of NANA and Gal. As is shown in Figure 7B,C, FITC-HisHis is indeed displaced from the microarray when a solution of 250 mM NANA or a solution of 500 mM methyl β-D-galactoside solution is used to rinse the microarray. The original fluorescence pattern can be restored by incubation with FITC-HisHis (Figure 7D) and this process is reversible over several cycles. Upon simultaneous incubation of the microarray with NANA or methyl β-D-galactoside and FITC-HisHis, no fluorescent pattern was detected (Figure 7E,F). This indicates that the synthetic lectin HisHis is saturated by the excess of carbohydrate which is present in solution and can therefore no longer bind to the carbohydrates on the microarray. Conversely, it would be expected that carbohydrates which do not show any interaction with HisHis should not lead to a decrease in the fluorescence of FITC-HisHis on the microarray and this is indeed observed for methyl α-D-mannoside, methyl β-D-glucoside, methyl β-D-fucoside, trehalose, sucrose as well as *N*-acetylglucosamine (see Figure 7G–L). These experiments demonstrate two important points: firstly, they attest the selectivity as well as the affinity of HisHis for immobilized NANA and Gal, and secondly, these results show that even a very simple microarray provides a versatile screening tool.

Finally, in addition to the mono- and disaccharides described above, the selectivity of the synthetic lectin HisHis was tested by using two heparins. These polymers display a particularly high carbohydrate epitope density. While one polymer (wild type, WT, 6.61 µg μL^{-1}) has a negatively charged sulfonate group at the terminus, the second one (KO, 6.12 µg μL^{-1}) does not possess this group and is therefore charge neutral. After 5 h incubation of a microarray of NANA (10 µm dots spaced by a 5 µm gap) and Glc (background) with three different dilutions of WT and KO, the fluorescence images were recorded (Figure 8). No significant effect is observed when the polysaccharides are diluted by a factor of 1000 or a factor of 100, but a 10 times dilution of KO and WT (0.661 µg μL^{-1} and 0.612 µg μL^{-1}) leads to a strong decrease of the FITC-HisHis fluorescence on the microarray (Figure 8C,F). No loss in fluorescence was detected when the wafer was incubated for 5 h with the same amount of Milli-Q water. These data demonstrate that heparin-type polysaccharides can compete with the interaction of the synthetic lectin HisHis and the carbohydrate NANA. The concentration dependence of displacement assay indicates the high affinity of HisHis for NANA in the

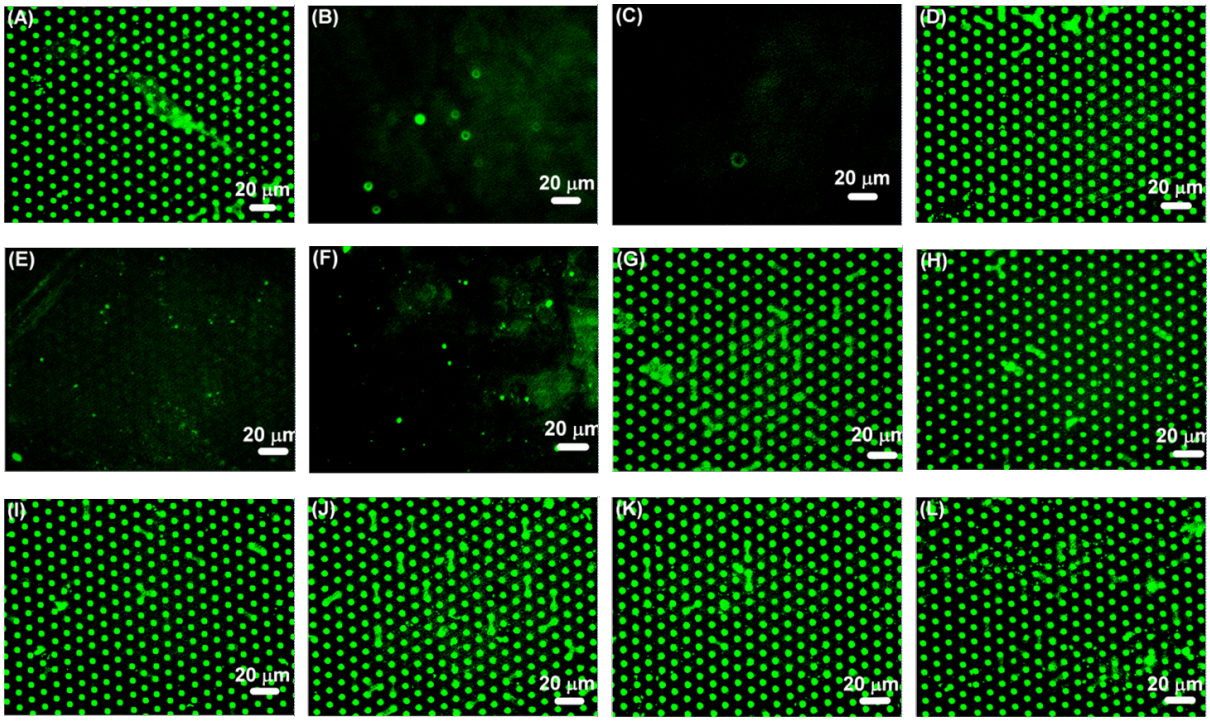

Figure 7: Fluorescence images of a microarray consisting of NANA (dots 5 × 3 μm) and Man (background). (A) Incubation with FITC-HisHis; (B) washing of (A) with 250 mM NANA; (C) washing of (A) with 500 mM methyl β-D-galactoside; (D) incubation of (B) with FITC-HisHis; (E) simultaneous incubation with FITC-HisHis and NANA; (F) simultaneous incubation with FITC-HisHis and methyl β-D-galactoside; (G) washing of (A) with 500 mM methyl α-D-mannoside; (H) washing of (A) with 500 mM methyl β-D-glucoside; (I) washing of (A) with 500 mM methyl β-D-fucoside; (J) washing of (A) with 500 mM trehalose; (K) washing of (A) with 500 mM sucrose; (L) washing of (A) with 500 mM *N*-acetylglucosamine.

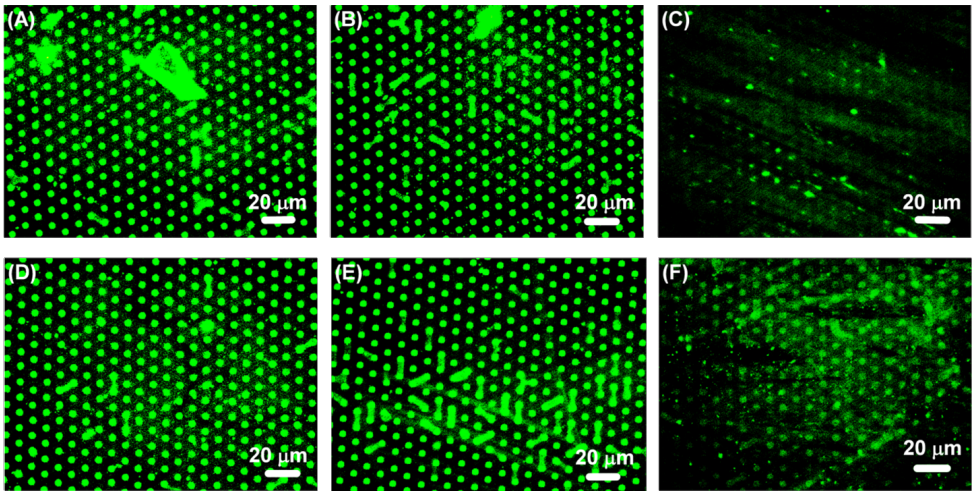

Figure 8: Fluorescence images of a microarray of NANA (dots 5 × 3 μm) and Glc (background), first incubated with FITC-HisHis and subsequently incubated for 5 h with (A) a 1000-fold dilution of KO (0.00612 μg μL^{-1}); (B) a 100-fold dilution of KO (0.0612 μg μL^{-1}); (C) a 10-fold dilution of KO (0.612 μg μL^{-1}); (D) a 1000-fold dilution of WT (0.00661 μg μL^{-1}); (E) a 100-fold dilution of WT (0.0661 μg μL^{-1}); (F) a 10-fold dilution of WT (0.661 μg μL^{-1}).

microarray. Thus, the results obtained from the microarray support our earlier finding that the interaction of HisHis and NANA is 1:2 [39], so that HisHis is likely to bind divalently to the microarray surface.

Conclusion

In summary, we have investigated the molecular recognition of surface immobilized carbohydrates by a synthetic lectin. To this end, amine-tethered carbohydrates were printed on epoxide

SAMs by μCP. Using tailor-made PDMS stamps and an optimized printing protocol, simple carbohydrate microarrays could readily be obtained by μCP. Consistent with measurements in solution, the microarrays showed high selectivity of the synthetic lectin HisHis for NANA and Gal versus Glc and Man. Both the selectivity and the high affinity of the synthetic lectin could be demonstrated in competition experiments with monosaccharides, disaccharides and heparin-type polysaccharides. The results obtained here demonstrate – for the first time – the high selectivity and affinity of a synthetic lectin for two different carbohydrates immobilized in a simple microarray. We contend that this is a significant development in the search for synthetic lectins that operate under physiological conditions.

Experimental

General: Chemicals were purchased from Sigma Aldrich, Acros Organics, Iris Biotech and ABCR and used without further purification. Silicon wafers (B-doped, 100-orientation, resistivity 20–30 Ω) were kindly donated by Siltronic AG. The heparins KO and WT were kindly donated by Prof. Dr. Rupert Hallmann (Westfälische Wilhelms-Universität Münster). Milli-Q water was prepared from distilled water using a PureLab UHQ deionization system (Elga). Tetramethylrhodamine isothiocyanate-labeled concanavalin A (TRITC-ConA) was purchased from Sigma Aldrich. Fluorescein isothiocyanate-labeled peanut agglutinin (FITC-PNA) was obtained from Vector Laboratories. Detailed information concerning the synthesis and analysis of carbohydrates and peptides is provided in Supporting Information File 1.

SAM preparation: Epoxide-terminated SAMs were prepared as reported in literature [42]. Glass slides as well as Si-wafers were cut into small pieces of around 1.6 × 2.6 cm^2, cleaned with detergent and dried. After sonification in pentane, acetone and Milli-Q water, the slides were put into a freshly prepared piranha solution (H_2O_2/H_2SO_4 = 1:3) for 30 min. The wafers were then thoroughly washed with water, dried and immersed in a 0.3 vol % solution of (3-glycidoxypropyl)trimethoxysilane in toluene for 24 h. Excess silane was removed by sonification in abs. ethanol for 20 min. After washing the slides with abs. ethanol, and drying, they were kept at least 24 h under ambient conditions before printing.

Stamp preparation: Poly(dimethylsiloxane) (PDMS) stamps were prepared by mixing PDMS with a curing agent (Sylgard 184, Dow Corning) in a 10:1 ratio and pouring the viscous mixture on a patterned silicon master. After removing the air in vacuum, the PDMS was cured at 80 °C overnight and peeled off after cooling. The patterned areas were cut out with a knife and oxidized in a UV-ozonizer (PSD-UV, Novascan Technologies Inc.) for 55 min after which they were stored under water. Coating of the stamps with 2-[methoxy(poly(ethyleneoxy))propyl]trimethylsilane was done by incubating the oxidized and dried stamps in a 1 vol % solution of the silane in abs. ethanol for 2 h, after which they were washed with abs. ethanol and dried [51]. Flat PDMS stamps were fabricated as described above by using a flat silicon wafer as master.

Microcontact printing: The surface of the freshly oxidized or coated PDMS stamp was covered with 2 to 3 drops of ethanolic solutions of the ink (20 mM) and triethylamine (20 mM) and incubated for 1 min. After blow-drying, they were placed on the according SAM. Printing was performed by placing the substrates together with the stamp in an oven which was tempered to 60 °C for 4 h. After removing the stamp from the substrate, with dichloromethane (DCM), abs. ethanol and Milli-Q water and dried. Subsequent printing steps were carried out as described above. After the last print, the substrates were sonicated in DCM, abs. ethanol and Milli-Q water, and dried.

Lectin carbohydrate interactions: As described in [34], in order to reduce non-specific protein adsorption, the arrays were incubated with a 3% bovine serum albumin (BSA) solution in PBS buffer (pH 7.5, 0.1% Tween 20) for 30 min and washed two times with PBS buffer prior to lectin screening. The surfaces of the carbohydrate arrays were covered by a solution of 1 mM FITC HisHis and 1 μg of labeled lectin (TRITC ConA or FITC PNA) in 100 μL of HEPES buffer (20 mM HEPES, pH 7.5, 0.15 M NaCl, 1.0 mM $CaCl_2$). In the case of ConA, $MnCl_2$ was added to a concentration of 1 mM. After 90 min, the arrays were washed with the same buffer, rinsed with Milli-Q water, dried, and analyzed.

Selectivity studies: The carbohydrate chips were incubated with a 1 mM solution of FITC HisHis for 1 min, washed with phosphate buffer (100 mM, pH 7.4) to remove unbound receptor, dried and analyzed. Afterwards, the wafer was washed three times with 500 μL mono- or disaccharide solution, dried and analyzed again. 100 μL of the heparin polymer (KO and WT) solutions were put on glass slides which were afterwards covered with a beaker. After 5 h at room temperature, the glass slides were washed with Milli-Q water, dried and analyzed.

Contact angle measurements: Water contact angles were measured using the sessile drop method on a DSA 100 goniometer (Krüss GmbH Wissenschaftliche Laborgeräte, Hamburg/Germany). The advancing and receding contact angles were measured on glass and silicon substrates, and at least three measurements were performed for every sample.

Determination of the angles was done using the software Drop Shape Analysis.

X-ray photoelectron spectroscopy (XPS): X-ray photoelectron spectra were recorded on a Kratos Axis Ultra system (Kratos Analytical, Manchester/UK). Monochromatized Al Ka radiation (1486.6 eV) as the excitation source and a pass energy of 20 meV for narrow scans were used. The obtained spectra were analyzed using the Casa XPS (version 2.3.15, Casa software Ltd, Teignmouth/UK) software and were referenced to the C(1s)-peak of the saturated hydrocarbons by setting it to 285 eV. All measurements were carried out on silicon substrates.

Atomic force microscopy (AFM): AFM images were measured with a Nano Wizzard 3 system (JPK Instruments AG, Berlin/Germany) in combination with processing software Gwyddion (http://www.gwyddion.net, version 2.25). All measurements were carried out on silicon substrates.

Fluorescence microscopy: Fluorescence microscopy images were made by using an Olympus inverted research microscope CKX41 (Olympus, Shinjuku, Tokyo/Japan) equipped with a mercury burner U-RFL-T as light source and a DX 20 L-FW camera (Kappa opto-electronics GmbH, Gleichen/Germany) for image acquisition. The camera was controlled by the program Kappa CameraControl (version 2.7.5.7032). All experiments were carried out on glass substrates.

Supporting Information

Supporting Information File 1

Experimental procedures, characterization data and additional spectra.
[http://www.beilstein-journals.org/bjoc/content/supplementary/1860-5397-10-138-S1.pdf]

Acknowledgements

Silicon wafers were kindly donated by Siltronic AG (Burghausen, Germany) and the heparin polymers WT and KO were kindly donated by Prof. Dr. Rupert Hallmann (Westfälische Wilhelms-Universität Münster). The Deutsche Forschungsgemeinschaft is acknowledged for financial support (SFB 858). This work was supported by COST CM1005 “Supramolecular Chemistry in Water”.

References

1. Varki, A. *Glycobiology* **1993,** *3,* 97. doi:10.1093/glycob/3.2.97
2. Laine, R. A. *Glycobiology* **1994,** *4,* 759. doi:10.1093/glycob/4.6.759
3. Houseman, B. T.; Mrksich, M. *Top. Curr. Chem.* **2002,** *218,* 1. doi:10.1007/3-540-45010-6_1
4. Lindhorst, T. K. *Essentials of Carbohydrate Chemistry and Biochemistry;* Wiley-VCH: Weinheim, 2007.
5. Seeberger, P. H.; Werz, D. W. *Nature* **2007,** *446,* 1046. doi:10.1038/nature05819
6. Venkataraman, G.; Shiver, Z.; Raman, R.; Sasisekharan, R. *Science* **1999,** *286,* 537. doi:10.1126/science.286.5439.537
7. Seeberger, P. H. *Chem. Soc. Rev.* **2008,** *37,* 19. doi:10.1039/b511197h
8. Park, S.; Lee, M.-R.; Shin, I. *Chem. Commun.* **2008,** 4389. doi:10.1039/b806699j
9. Bidlingmaier, S.; Snyder, M. *Chem. Biol.* **2002,** *9,* 400. doi:10.1016/S1074-5521(02)00133-3
10. Love, K. R.; Seeberger, P. H. *Angew. Chem., Int. Ed.* **2002,** *41,* 3583. doi:10.1002/1521-3773(20021004)41:19<3583::AID-ANIE3583>3.0.CO;2-P
11. Kiessling, L. L.; Cairo, C. W. *Nat. Biotechnol.* **2002,** *20,* 234. doi:10.1038/nbt0302-234
12. Houseman, B. T.; Mrksich, M. *Chem. Biol.* **2002,** *9,* 443. doi:10.1016/S1074-5521(02)00124-2
13. Park, S.; Shin, I. *Angew. Chem., Int. Ed.* **2002,** *41,* 3180. doi:10.1002/1521-3773(20020902)41:17<3180::AID-ANIE3180>3.0.CO;2-S
14. Wang, D.; Liu, S.; Trummer, B. J.; Deng, C.; Wang, A. *Nat. Biotechnol.* **2002,** *20,* 275. doi:10.1038/nbt0302-275
15. Fukui, S.; Feizi, T.; Galustian, C.; Lawson, A. M.; Chai, W. *Nat. Biotechnol.* **2002,** *20,* 1011. doi:10.1038/nbt735
16. Willats, W. G. T.; Rasmussen, S. E.; Kristensen, T.; Mikkelsen, J. D.; Knox, J. P. *Proteomics* **2002,** *2,* 1666. doi:10.1002/1615-9861(200212)2:12<1666::AID-PROT1666>3.0.CO;2-E
17. Houseman, B. T.; Gawalt, E. S.; Mrksich, M. *Langmuir* **2003,** *19,* 1522. doi:10.1021/la0262304
18. Shin, I.; Park, S.; Lee, M. *Chem.–Eur. J.* **2005,** *11,* 2894. doi:10.1002/chem.200401030
19. Heise, C.; Bier, F. F. *Top. Curr. Chem.* **2005,** *261,* 1. doi:10.1007/128_007
20. Pirrung, M. C. *Angew. Chem., Int. Ed.* **2002,** *41,* 1276. doi:10.1002/1521-3773(20020415)41:8<1276::AID-ANIE1276>3.0.CO;2-2
21. Kumar, A.; Whitesides, G. M. *Appl. Phys. Lett.* **1993,** *63,* 2002. doi:10.1063/1.110628
22. Ruiz, S. A.; Chen, C. S. *Soft Matter* **2007,** *3,* 168. doi:10.1039/b613349e
23. Perl, A.; Reinhoudt, D. N.; Huskens, J. *Adv. Mater.* **2009,** *21,* 2257. doi:10.1002/adma.200801864
24. Kaufmann, T.; Ravoo, B. J. *Polym. Chem.* **2010,** *1,* 371. doi:10.1039/b9py00281b
25. Bernard, A.; Delamarche, E.; Schmid, H.; Michel, B.; Bosshard, R. H.; Biebuyck, H. *Langmuir* **1998,** *14,* 2225. doi:10.1021/la980037l
26. Ludden, M. J. W.; Mulder, A.; Schulze, K.; Subramaniam, V.; Tampé, R.; Huskens, J. *Chem.–Eur. J.* **2008,** *14,* 2044. doi:10.1002/chem.200701478
27. Lange, S. A.; Benes, V.; Kern, D. P.; Höber, J. K. H.; Bernard, A. *Anal. Chem.* **2004,** *76,* 1641. doi:10.1021/ac035127w
28. Thibault, C.; Le Berre, V.; Casimirius, S.; Trévisol, E.; François, J.; Vieu, C. *J. Nanobiotechnol.* **2005,** *3,* No. 7. doi:10.1186/1477-3155-3-7

29. Rozkiewicz, D. I.; Gierlich, J.; Burley, G. A.; Gutsmiedl, K.; Carell, T.; Ravoo, B. J.; Reinhoudt, D. N. *ChemBioChem* **2007,** *8,* 1997. doi:10.1002/cbic.200700402
30. Rozkiewicz, D. I.; Brugman, W.; Kerkhoven, R. M.; Ravoo, B. J.; Reinhoudt, D. N. *J. Am. Chem. Soc.* **2007,** *129,* 11593. doi:10.1021/ja073574d
31. Ravoo, B. J. *J. Mater. Chem.* **2009,** *19,* 8902. doi:10.1039/b908564e
32. Wendeln, C.; Ravoo, B. J. *Langmuir* **2012,** *28,* 5527. doi:10.1021/la204721x
33. Michel, O.; Ravoo, B. J. *Langmuir* **2008,** *24,* 12116. doi:10.1021/la802304w
34. Wendeln, C.; Heile, A.; Arlinghaus, H. F.; Ravoo, B. J. *Langmuir* **2010,** *26,* 4933. doi:10.1021/la903569v
35. Wendeln, C.; Rinnen, S.; Schulz, C.; Arlinghaus, H. F.; Ravoo, B. J. *Langmuir* **2010,** *26,* 15966. doi:10.1021/la102966j
36. Wendeln, C.; Singh, I.; Rinnen, S.; Schulz, C.; Arlinghaus, H. F.; Burley, G. A.; Ravoo, B. J. *Chem. Sci.* **2012,** *3,* 2479. doi:10.1039/c2sc20555f
37. Davis, A. P.; Wareham, R. S. *Angew. Chem., Int. Ed.* **1999,** *38,* 2978. doi:10.1002/(SICI)1521-3773(19991018)38:20<2978::AID-ANIE2978>3.0.CO;2-P
38. Ke, C.; Destecroix, H.; Crump, M. P.; Davis, A. P. *Nat. Chem.* **2012,** *4,* 718. doi:10.1038/nchem.1409
39. Rauschenberg, M.; Bomke, S.; Karst, U.; Ravoo, B. J. *Angew. Chem., Int. Ed.* **2010,** *49,* 7340. doi:10.1002/anie.201002847
40. Rauschenberg, M.; Bandaru, S.; Waller, M. P.; Ravoo, B. J. *Chem.–Eur. J.* **2014,** *20,* 2770. doi:10.1002/chem.201303777
41. Schauer, R.; Kelm, S.; Reuter, G.; Roggentin, P.; Shaw, L. In *Biology of the Sialic Acids;* Rosenberg, A., Ed.; Plenum Press: New York, 1995; pp 7–67. doi:10.1007/978-1-4757-9504-2_2
42. Tsukruk, V. V.; Luzinov, I.; Julthongpiput, D. *Langmuir* **1999,** *15,* 3029. doi:10.1021/la981632q
43. Angenendt, P.; Glökler, J.; Murphy, D.; Lehrach, H.; Cahill, D. J. *Anal. Biochem.* **2002,** *309,* 253. doi:10.1016/S0003-2697(02)00257-9
44. Preininger, C.; Sauer, U. *Sens. Actuators, B* **2003,** *90,* 98. doi:10.1016/S0925-4005(03)00049-2
45. Kaufmann, T.; Gokmen, M. T.; Rinnen, S.; Arlinghaus, H. F.; Du Prez, F. E.; Ravoo, B. J. *J. Mater. Chem.* **2012,** *22,* 6190. doi:10.1039/c2jm16807c
46. Prime, K. L.; Whitesides, G. M. *J. Am. Chem. Soc.* **1993,** *115,* 10714. doi:10.1021/ja00076a032
47. Elender, G.; Kühner, M.; Sackmann, E. *Biosens. Bioelectron.* **1996,** *11,* 565. doi:10.1016/0956-5663(96)83292-1
48. Salmon, L.; Thominette, F.; Pays, M. F.; Verdu, J. *Compos. Sci. Technol.* **1997,** *57,* 1119. doi:10.1016/S0266-3538(97)00038-9
49. Petrunin, M. A.; Nazarov, A. P. *Mater. Res. Soc. Symp. Proc.* **1994,** *351,* 305. doi:10.1557/PROC-351-305
50. Lee, J.-H.; Shim, H.-W.; Choi, H.-S.; Son, Y.-A.; Lee, C.-S. *J. Phys. Chem. Solids* **2008,** *69,* 1581. doi:10.1016/j.jpcs.2007.10.124
51. Delamarche, E.; Donzel, C.; Kamounah, F. S.; Wolf, H.; Geissler, M.; Stutz, R.; Schmidt-Winkel, P.; Michel, B.; Mathieu, H. J.; Schaumburg, K. *Langmuir* **2003,** *19,* 8749. doi:10.1021/la034370n
52. Dhayal, M.; Ratner, D. M. *Langmuir* **2009,** *25,* 2181. doi:10.1021/la8031122

License and Terms

Beilstein Journal of Organic Chemistry

Biantennary oligoglycines and glyco-oligoglycines self-associating in aqueous medium

Svetlana V. Tsygankova[1], Alexander A. Chinarev[1], Alexander B. Tuzikov[1], Nikolai Severin[2], Alexey A. Kalachev[3], Juergen P. Rabe[2], Alexandra S. Gambaryan[4] and Nicolai V. Bovin[*1]

Full Research Paper

Open Access

Address:
[1]Shemyakin-Ovchinnikov Institute of Bioorganic Chemistry, ul. Miklukho-Maklaya 16/10 Moscow V-437, 117997, Russia, [2]Department of Physics, Humboldt University Berlin, Newtonstr. 15, D-12489, Berlin, Germany, [3]Plasmachem GmbH, Rudower Chaussee 29, D-12489 Berlin, Germany and [4]M. P. Chumakov Institute of Poliomyelitis and Viral Encephalitides, 142782 Moscow Region, Russia

Email:
Nicolai V. Bovin[*] - bovin@carb.ibch.ru

* Corresponding author

Keywords:
glycopeptides; influenza virus; multivalent glycosystems; oligoglycine; polyglycine II; self-assembling; tectomers

Beilstein J. Org. Chem. **2014,** *10,* 1372–1382.
doi:10.3762/bjoc.10.140

Received: 28 February 2014
Accepted: 09 May 2014
Published: 17 June 2014

This article is part of the Thematic Series "Multivalent glycosystems for nanoscience". A part of this work was presented at 17th European Carbohydrate Symposium “EuroCarb17” [1].

Guest Editor: B. Turnbull

Abstract

Oligoglycines designed in a star-like fashion, so-called tri- and tetraantennary molecules, were found to form highly ordered supramers in aqueous medium. The formation of these supramers occurred either spontaneously or due to the assistance of a mica surface. The driving force of the supramer formation is hydrogen bonding, the polypeptide chain conformation is related to the folding of helical polyglycine II (PG II). Tri- and tetraantennary molecules are capable of association if the antenna length reach 7 glycine (Gly) residues. Properties of similar biantennary molecules have not been investigated yet, and we compared their self-aggregating potency with similar tri- and tetraantennary analogs. Here, we synthesized oligoglycines of the general formula R-Gly_n-X-Gly_n-R (X = -HN-$(CH_2)_m$-NH-, m = 2, 4, 10; n = 1–7) without pendant ligands (R = H) and with two pendant sialo-ligands (R = sialic acid or sialooligosaccharide). Biantennary oligoglycines formed PG II aggregates, their properties, however, differ from those of the corresponding tri- and tetraantennary oligoglycines. In particular, the tendency to aggregate starts from Gly_4 motifs instead of Gly_7. The antiviral activity of end-glycosylated peptides was studied, and all capable of assembling glycopeptides demonstrated an antiviral potency which was up to 50 times higher than the activity of peptide-free glycans.

Introduction

Recently, we have synthesized and described tetraantennary [2] and triantennary [3] oligoglycines capable of spontaneous or surface-promoted formation of flat layers in aqueous medium. These layers are one or two molecules thick. The stability was attributed to the formation of a network of hydrogen bonds. This class of supramers has been called tectomers. Tectomers in

a layer are packed by polyglycine II type (PG II) [4,5]. Their helical polypeptide chain fundamentally differs from the canonical α-helix. The association of symmetrical tetra- and triantennary (star-like) oligoglycines spontaneously proceeds only when the number of glycine (Gly) residues in a chain (*n*) is equal or greater to seven. Oligoglycines with an antennae size less than seven do either not associate at all or require extremely favorable conditions, in particular surface promotion. Yet, the properties of similar biantennary molecules were not investigated. Here, we synthesized biantennary oligoglycines and studied them in order to determine the necessary and sufficient conditions for self-association. More specifically, we investigated the combination of structure elements, such as the *n* value, the type of terminal substituents, and the type of structural motifs (core), where the antennae are connected to each other. The knowledge of the rules found for the unsubstituted assembly of oligoglycines may be suitable for us for the design of corresponding sialo derivartives, which are candidate therapeutics for the blocking of the influenza virus [6].

Results and Discussion

Synthesis of biantennary oligoglycines and their glyco derivatives

The synthesized biantennary oligoglycines and their glyco derivatives are presented in Figure 1. Analogously to tri- and tetraantennary molecules, oligoglycine antennas are connected according to the 'head-to-head' principle, i.e., by their C-termini, so that the two amino groups are terminal. The

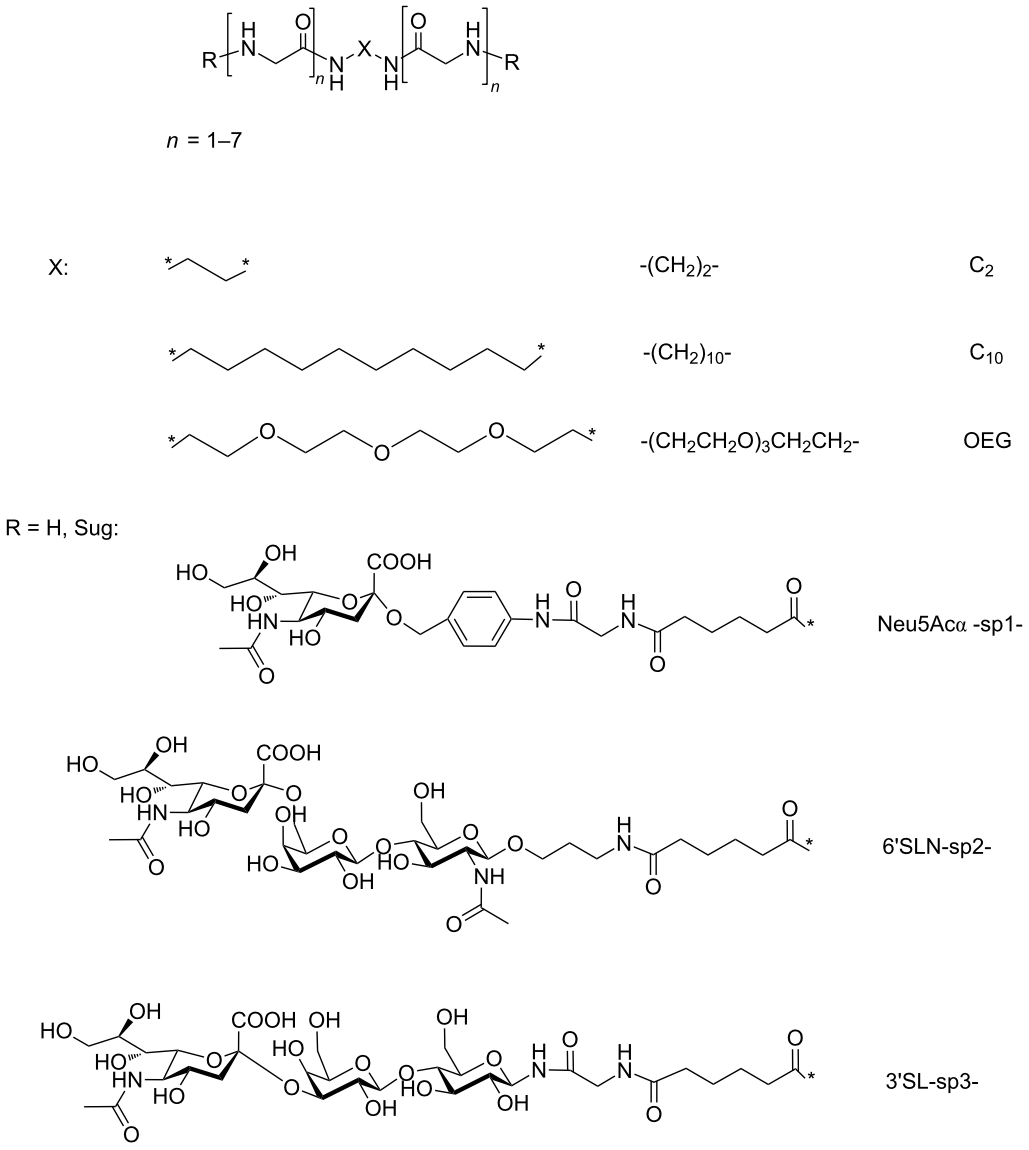

Figure 1: The structure of biantennary oligoglycines and their glyco derivatives (sp = spacer group).

obtained compounds differ threefold. Firstly, they differ by core X nature: hydrophilic oligoethylene glycol (OEG), hydrophobic flexible decamethylene (C_{10}), or short ethylene (C_2). Secondly, the length of oligoglycine antennas, i.e., the number of glycine residues in a chain (n = 1–7) is different. Thirdly, the substances differ by the presence or absence of carbohydrate fragment (Sug), containing α-*N*-acetylneuraminic moiety (Neu5Acα).

Diamines NH_2–X–NH_2 were the starting substances for the synthesis, oligoethylene glycol diamine was obtained from ditosylate as described in [7,8]. The synthesis of biantennary oligoglycines was carried out by means of the activated esters method (Scheme 1) [9]. The glycine chains were elongated stepwise by their N-terminus by using *N*-oxysuccinimidyl esters (BocGlyONSu or $BocGly_2ONSu$, Boc = *tert*-butyloxycarbonyl). Boc-peptides were isolated from the reaction mixture by the removal of the solvent and the re-crystallization of the reaction product from aqueous methanol (yields 75–95%). In the case of poorly soluble products the impurities and starting materials were washed off with methanol (yields 60–90%). In the case of an oil-like substance (X = OEG, n = 2) chromatography on silica gel was performed. The quantitative removal of Boc groups was achieved by the treatment of the obtained peptides with trifluoroacetic acid. Salt forms (trifluoroacetates or hydrochlorides) of diamino derivatives were obtained by sedimentation from an aqueous solution by methanol (yield ≥95%). At later stages of elongation the salts were converted to the respective free bases by treatment with a slight excess of triethylamine. The preparation of oligoglycines with a chain length exceeding five glycine residues for the derivatives with core C_{10} and six residues for core C_2 failed due to their low solubility and, consequently, the impossibility of separating them from the intermediates of the synthesis.

Sialo conjugates of biantennary oligoglycines were obtained from the corresponding diamines and derivatives of α-*N*-acetylneuraminic acid (Sug-ONp), where the carboxyl group of the spacer was activated with 4-nitrophenol (Np) (Scheme 1). The synthesis of these compounds was described in [10,11]. Owing to the poor solubility of the diamine form of oligoglycines with cores C_2 and C_{10} in DMSO, the reaction was carried out in a saturated aqueous solution of lithium bromide, which prevented the formation of hydrogen bonds and thus increased the solubility of oligoglycines. Glycopeptides were isolated from the reaction mixture by gel-permeation chromatography (yields 70–75%). The peptide modification by the amino group with mono- or oligosaccharides dramatically increased their solubility in water. This may support their antiviral action (see below), because glycopeptides act topically, in the respiratory tract, and are administered as a spray.

We then investigated the ability of synthesized biantennary oligoglycines to assemble in aqueous media as well as the antiviral activity of glycoderivatives.

Study of biantennary oligoglycines association in solution by dynamic light scattering

The size of the particles formed by the biantennary oligoglycines in solution was measured with the dynamic light scattering method (DLS). We found that the ability of association depends on the number of the glycine units in the antennae, the nature of the core, the pH, and the peptide concentration.

It is known that the charge of terminal amino groups of the protonated form of oligoglycines hinders association. To overcome this obstacle an equimolar quantity of $NaHCO_3$ or Na_2CO_3 was added to aqueous solutions of oligoglycine salts. In the absence of the base, pH values of oligoglycine salt solutions varied from 3.5 to 4.5 (hereinafter denoted as pH < 5). In the case of the addition of one base equivalent per one amino group the solution becomes neutral (pH 6.5), in the case of two Na_2CO_3 equivalents the pH value is more than 8.5 (basic solution, denoted as pH > 8.5).

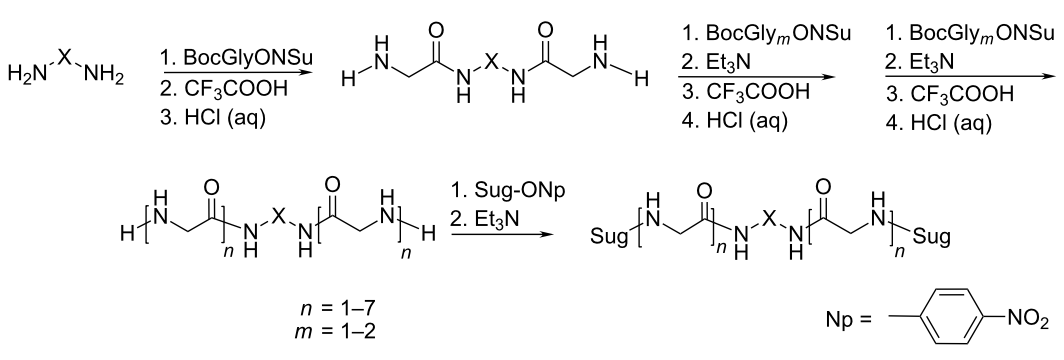

Scheme 1: Synthesis of biantennary oligoglycines and their glycoderivatives.

At $n < 4$ peptides with an oligoethylene glycol core and the cores C_2 and C_{10} did not form associates in aqueous medium in all the studied ranges of pH and concentration (0.1–1.0 mg/mL).

Biantennary oligoglycines, cores C_2 and C_{10}, $n \geq 4$, are capable of forming associates (700–900 nm) in acidic solutions in the studied concentration range, except for H-$Gly_4NH(CH_2)_{10}NHGly_4$-H·2HCl, which associates in concentrations ≥0.5 mg/mL.

Molecules with the core C_2 (n = 4–6) and C_{10} (n = 5) associate so rapidly in neutral and basic media that a precipitate is formed (data for peptide with n = 5 are given in Figure 2a). Only the peptide H-$Gly_4NH(CH_2)_{10}NHGly_4$-H in concentration ≤0.1 mg/mL is capable of forming associates (800–1200 nm) stable in aqueous media (Figure 2a,b).

Study of biantennary peptides association using scanning force microscopy

Scanning force microscopy (SFM) elucidates information not only about the association process both in solution and on a surface, but also about fine details of the formed architectures. Of particular interest are cases characterized by the active participation of the surface in accelerating the self-assembly. To discriminate the processes taking place on the surface from similar processes in liquid volume, measurements were carried out immediately after the deprotonation of oligoglycine salts at incubation times insufficient for a spontaneous association in solution (found out as ≤1 min). The solution was placed on a freshly cleaved surface of mica or graphite, exposed for fixed time intervals (denoted as t_{exp}), followed by the removal of the liquid phase from the surface and the scanning of the sample in tapping mode in air. The contact mode of scanning was used for experiments in a liquid cell. Experiments in a liquid cell allowed us to study the kinetics of the process without a possible distortion of the nanostructures resulting from the drying of the sample.

The Raman spectra (Figure 3) of biantennary oligoglycines capable of association as well as the spectra of tri- and tetraantennary peptides described earlier display bands at 884, 1261, 1382, 1424 and 1654 cm^{-1}, which are characteristic and specific for crystalline PG II. Based on the presence of these bands we conclude that the structure organization of associates formed in solution corresponds to PG II. The sensitivity of routine Raman scattering method is insufficient for the work with oligoglycine monolayers, so indirect methods were used in order to attribute formed material to a PG II structure. More specifically, geometrical parameters of the layers were determined by using SFM and compared with: 1) those for tectomers (attributed to PG II, see above) formed in solution and 2) calculated values for different, not only PG II, models. As shown below for particular examples, in most cases spontaneous and surface-mediated assembly led to associates of PG II structure, i.e., tectomers.

The formation of the PG II structure for oligoglycines with a short rigid spacer C_2 is only possible if the molecule is extended, i.e., antennas are pointing in opposite directions (conformation "1 + 1", Figure 4a). The presence of a flexible core (C_{10}, OEG) allows the molecule to adopt the conformation "2 + 0", which is characterized by unidirectional oligoglycine antennas. The hydrophobic side of the tectomer should initiate the formation of the second layer with the opposite orientation

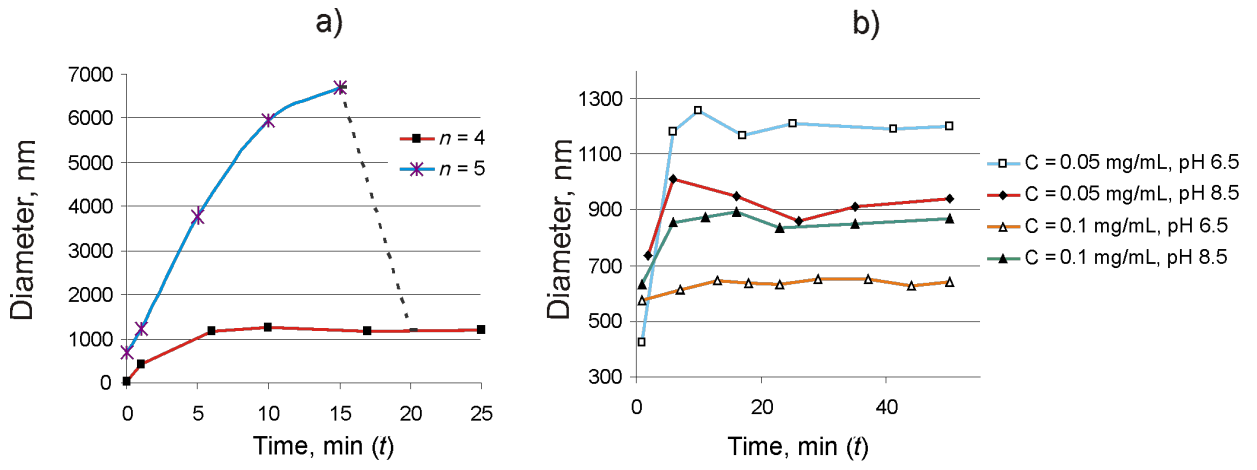

Figure 2: Dynamics of associate formation by biantennary oligoglycines H-Gly_n-$NH(CH_2)_{10}NH$-Gly_n-H. a) n = 4–5, in aqueous solution at pH 6.5 and a concentration of 0.1 mg/mL at t = 0 and pH < 5 before the addition of base and at t > 0 and pH 6.5 after the addition of base. The region of sedimentation is marked with a dotted line. b) n = 4, in aqueous solution at pH 6.5 and 8.5.

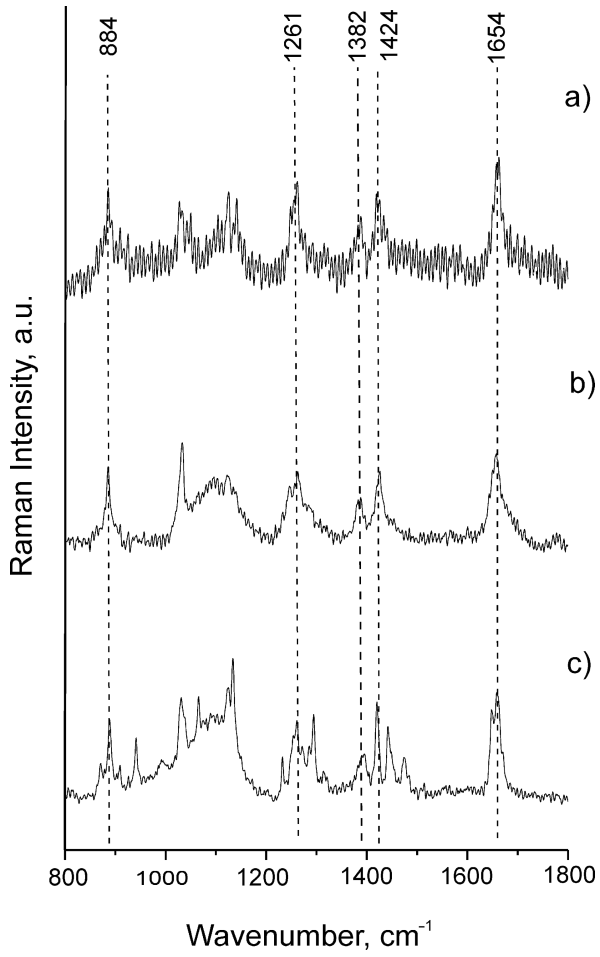

Figure 3: Raman spectra of a) [H-Gly$_7$-NHCH$_2$]$_4$C; b) H-Gly$_4$-NH(CH$_2$)$_2$NH-Gly$_4$-H; c) H-Gly$_4$-NH(CH$_2$)$_{10}$NH-Gly$_4$-H. The spectra contain characteristic bands at 884, 1261, 1382, 1424 and 1654 cm^{-1}, corresponding to the structure PG II [12]. Spectra were recorded for the samples in solid phase.

of the monomer in aqueous solutions (Figure 4b) in order to minimize the thermodynamically unfavorable contact with water.

It was demonstrated for biantennary oligoglycines that a concentration of 0.1 mg/mL is optimal for the study of the dynamics of tectomer growth on a mica surface. At higher concentrations the growth both in solution and on the surface proceeded so rapidly that the dynamics study was considered impossible. No tectomer structure was observed under acidic conditions (pH < 5), whereas under neutral and basic conditions the reaction proceeded similarly in terms of both the velocity and the morphology of formed tectomers. The oligoethylene glycol derivatives H-Gly$_n$-NH(CH$_2$CH$_2$O)$_3$CH$_2$CH$_2$NH-Gly$_n$-H (n = 2–7), non-associating in aqueous solutions as well as oligoglycines with cores C$_2$ and C$_{10}$ (n < 4) did not form associates on a mica surface under all studied ranges of pH (from 4.5 to 8.5).

According to dynamic light scattering data (see above) only peptide H-Gly$_4$NH(CH$_2$)$_{10}$NHGly$_4$-H was capable of forming tectomers in neutral and basic solutions which were unchanged in an aqueous phase for a long time. Figure 5 demonstrates the dynamics of layer growth on mica with the characteristic formation of islet structures (t_{exp} = 0.5 min, Figure 5a), growing laterally (t_{exp} = 1 min, Figure 5b), and covering the whole surface with an even layer (t_{exp} = 2 min, Figure 5c). Presumably, longer times (t_{exp} > 2 min) are characterized by the appearance of multilayer tectomers resulting from the sorption of associates formed in solution. The multilayer tectomers can be readily removed by washing with buffer solution (pH 6.5 or 9.0). The morphology of the first layer remains unchanged and the available defects ('holes') are preserved. The layer height is 3.7–4.0 nm, which may correspond to both mono- and bilayer (conformations "1 + 1" and "2 + 0", respectively, see Figure 4).

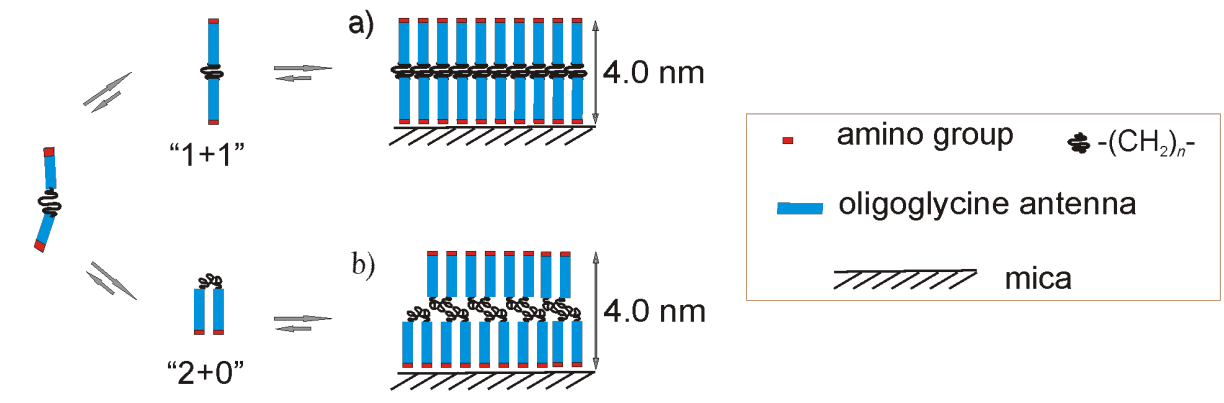

Figure 4: Model of the formation of tectomer layers by biantennary oligoglycines on a mica surface. The heights are given for H-Gly$_4$NH(CH$_2$)$_{10}$NHGly$_4$-H.

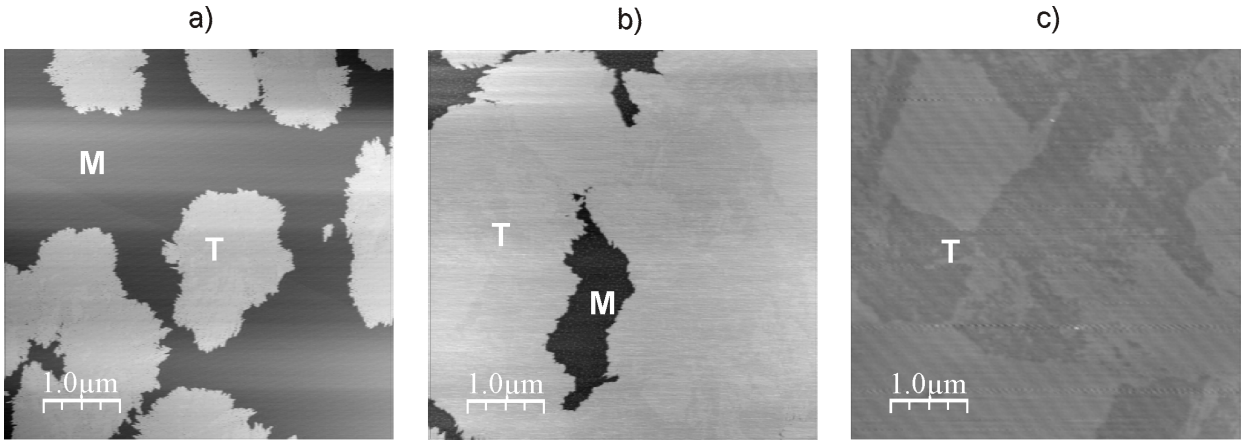

Figure 5: Growth of the tectomer formed by the peptide H-Gly$_4$-NH(CH$_2$)$_{10}$-NHGly$_4$-H (concentration 0.1 mg/mL) on a mica surface at pH 6.5, with tapping mode, SFM on air, and a t_{exp} of a) 0.5 min, b) 1 min, c) 2 min. Here, the shown field is completely covered with tectomer layer; its roughness found to be ± 0.1 nm. T indicates the tectomer layer, M the uncovered mica regions.

The dynamics of H-Gly$_4$NH(CH$_2$)$_{10}$NHGly$_4$-H association was studied in more detail in a liquid cell (Figure 6). After 3 min the surface was virtually completely covered with a uniform defect-free layer. It should be noted that the stepwise surface profile (typical for bilayer structures) was not observed in a liquid cell. The layer morphology was identical to the one observed in experiments in air (Figure 5).

Dynamic light scattering data give evidence that in neutral aqueous solutions the association of compounds H-Gly$_5$-NH-X-NH-Gly$_5$-H (cores C_2 and C_{10}) leads to the formation of large aggregates. By means of SFM it was demonstrated that the peptide with core C_2 formed islet-like tectomers on mica surface (t_{exp} = 10 min) with a height of 3.3 nm and planar dimensions of 500–700 nm (Figure 7a). The compound with core C_{10} associated more rapidly (Figure 7b), though the surface was not completely covered (t_{exp} = 10 min). This is in contrast to the structure analog with four glycines in the antenna, where a time period of only two minutes was sufficient for complete covering. The measured heights fit the model "1 + 1".

The obtained data give evidence that mica promotes the formation of tectomers from biantennary oligoglycines in neutral and basic solutions. Layer growth proceeds due to the surface co-participation. In the case of the molecule H-Gly$_4$-NH(CH$_2$)$_{10}$NH-Gly$_4$-H growth continues until the surface is completely covered, whereas in the bulk of the liquid phase

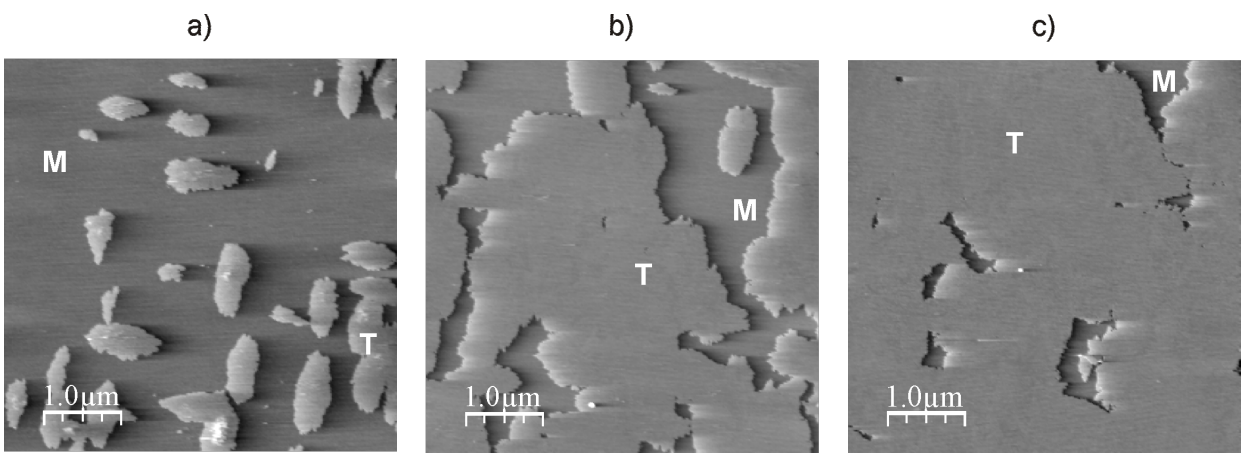

Figure 6: Growth of the tectomer formed by peptide H-Gly$_4$-NH(CH$_2$)$_{10}$NH-Gly$_4$-H (concentration 0.1 mg/mL) on a mica surface in a liquid cell at pH 6.5. Phase SFM images were taken with a) t_{exp} = 1 min, b) t_{exp} = 2 min and c) t_{exp} = 3 min where t_{exp} is the time after the experiment was started. T indicates the tectomer layer, M the uncovered mica regions.

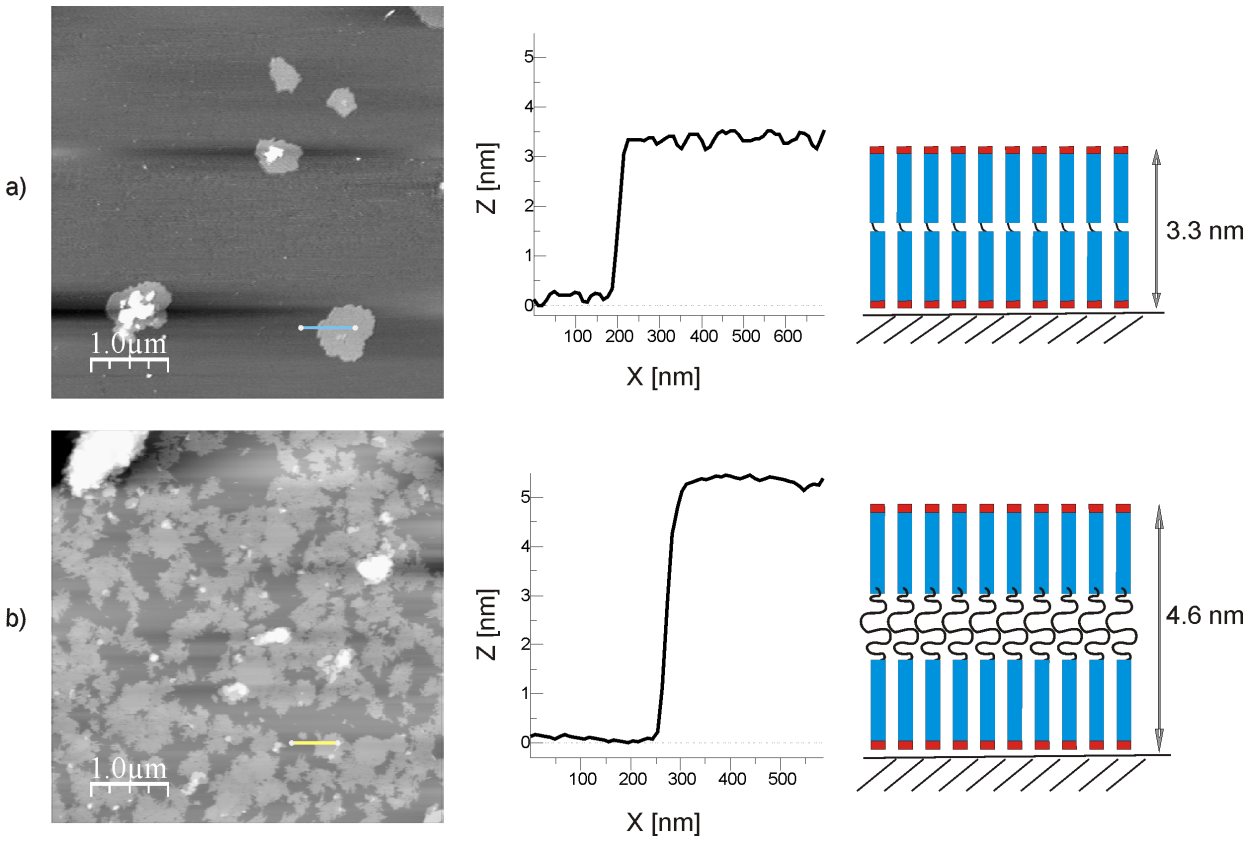

Figure 7: SFM images of associates formed by peptides a) H-Gly_5-$NH(CH_2)_2NH$-Gly_5-H and b) H-Gly_5-$NH(CH_2)_{10}NH$-Gly_5-H (concentration 0.1 mg/mL) on a mica surface at pH 6.5 with t_{exp} = 10 min SFM tapping mode in air, and an incubation time in solution of 1 min. Surface profiles, schematic layer models, and their calculated heights are given on the right.

dimensions remain unchanged over time according to dynamic light scattering data.

There are no direct data pointing at the particular conformation ("1 + 1" or "2 + 0") the peptide monomer has in the layer (Figure 4). The height value does not allow for the unambiguous assignment of one of the proposed models. Nevertheless, all intrinsic data supports the model "1 + 1": 1) the steps typical for a bilayer profile are not present in the SFM images, 2) intense washing does not lead to the formation of half-height structures, 3) the lack of any association on a graphite surface where the formation of "2 + 0" is expected to be preferable (see below).

Mica promotes the assembling of amino-terminated chains due to the negative charge of the surface. In contrast, graphite did not participate in the association of biantennary oligoglycines, we observed only irregular associates formed in solution. This experimental result is unexpected, because the formation of a monolayer with the monomer conformation "2 + 0" is favorable according to molecular dynamics simulations [13].

Minimal size of Gly_n fragment providing association

In the case of biantennary molecules association formally starts from the value n = 4, but, in fact, this value is supposedly equal to 8 because biantennary peptides form a polyglycine structure in the extended conformation "1 + 1". It is noteworthy that related polymers, nylons with the formula -$NH(CH_2)_xCO$- are known to form a PG II structure [14], i.e., additional methylene groups (-$(CH_2)_x$- instead of -CH_2-) have no significant influence on its ability to form PG II. The association of tri- and tetraantennary peptides leads to structures with the monomer conformations "2 + 2" and "3 + 0", respectively. The association starts from n = 7. Presumably, the first and closest to forking Gly residue takes a distorted conformation and does not take part in the formation of hydrogen bonds with neighboring residues. In the case of tetraantennary oligoglycines the plane of one pair of antennas is rotated by 90° [8] with respect to another pair, so that the glycines cannot form a continuous chain. On the other hand, in the biantennary analog the chain Gly_4-X-Gly_4 has the ability to form a PG II structure despite the core fragment -$(CH_2)_n$-.

The nature of the core fragment X in H-Gly$_n$-X-Gly$_n$-H

Biantennary molecules with core C_{10} form tectomers on a mica surface more readily than the molecules with core C_2 and an equal number of glycines. The more flexible core C_{10} should lead to a entropy driven destabilization. The opposite effect observed in reality is most probably caused by van der Waals interactions of hydrophobic fragments C_{10} closely situated in the PG II structure. The oligoethylene glycol core abolishes the formation of a PG II structure, presumably due to competitive hydrogen bonding with spatially close oligoglycine fragments.

Spontaneous and surface-promoted association

The formation of tectomers on mica proceeds considerably more rapidly than association in solution (the formation of associates in solutions just starts when assembling on the surface is already finished), i.e., the mica surface obviously plays an active role in the process. Tectomer growth starts from the formation of islet structures that increase in lateral direction and cover the whole surface in an even layer. This growth is limited only by the dimensions of the support itself. It should be noted that graphite, in contrast to mica, does not promote association.

Effect of pH value

Depending on the pH value, the free terminal group of the oligoglycine chain can be heavily charged, weakly charged, or neutral. In acidic solutions antennas are repulsed due to the positive charge, which hinders tectomer assembly or even abolishes it. The pH value effects not only the ability to assemble but also the morphology of forming supramers. Thus, in neutral solutions biantennary oligoglycines form multilayer tectomers. The process is unstoppable at the stage of the monolayer formation. At the same time, monolayer tectomers are exclusively formed in basic solutions.

Concentration range

Most parts of the experiments were carried out in the concentration range of 0.1–1.0 mg/mL. A concentration of 0.1 mg/mL was used for the adequate comparison of association of all investigated peptides. The association in the liquid phase proceeds slower at low concentrations leading to an increased size of the formed supramers.

In summary, based on our investigations related to unglycosylated molecules we can conclude that the association of biantennary oligoglycines is affected by several factors. 1) Mica but not graphite promotes the formation of tectomers. 2) The spatial organization of oligoglycine molecules in supramers corresponds to PG II conformation. 3) Not less than four glycine residues in each of two antennas are required for the assembling of monomer layers into surface tectomer layers or into long-living associates in solution. 4) Oligoethylene glycol core 'inhibits' the association both in the liquid phase and on a mica surface.

Antiviral activity of glycoderivatives

The idea of antiadhesion influenza virus therapy is based on the inhibition or the blocking of the binding of the influenza virus with target cells [15]. Monovalent oligosaccharides are incapable of an efficient competition for analogous glycans on the cell surface due to the low binding constant with viral hemagglutinin. An attractive way of increasing the affinity of a blocker (inhibitor) is the design of multivalent receptor analogs such as the oligoglycine-based tectomers described above. A first success for an application in this regard was achieved by inhibiting the influenza virus by sialo derivatives of the associating tetraantennary peptides, which demonstrated an antiviral activity three orders of magnitude higher than the activity of non-associating analogs [2]. Similar triantennary molecules with sialo-glycan located in the molecule "head", however, appear to display a low activity [16]. Thus, it was interesting to study the antiviral activity of sialo derivatives of biantennary oligoglycines in relation to their propensity to associate in aqueous solutions.

The fact that a sialylated biantennary peptide is capable of association in an aqueous solution similarly to glycan-free peptides is confirmed by DLC data. The average size of the sialoglycopeptide aggregates in aqueous solution was about 1 μm (data not shown).

The antiviral activity of biantennary glycopeptides was studied by means of a fetuin binding inhibition test (FBI-test) [17] (the glycoprotein fetuin contains several sialylated carbohydrate chains). In this test, the glycopeptides inhibited the binding of a fetuin peroxidase conjugate to a virus immobilized on a plastic (related to the corresponding monomer). Results are given in Table 1. The activity of associating sialooligoglycines with core C_2 was only 3–6 times higher than the activities of their non-associated counterparts (n = 2–4) and the monomeric reference sialoside, Neu5AcαBn. The compound with core C_{10} and n = 4 demonstrated the highest activity from the studied biantennary glycopeptides, which was 50 times higher than the activity of the monomer. The activity of bivalent derivatives with core OEG and n = 2–5 did not exceed that of monovalent sialoside. However, the activity increased dramatically when n = 6 (up to 50 times), although it was still orders of magnitude smaller compared to the high activity of polymeric inhibitors [18]. As sialooligoglycines of the OEG series did not associate in aqueous solution, we suppose that the reason for the increased activity is related to a critical distance, which facilitates the real-

Table 1: Relative activity of biantennary glycopeptides in the influenza virus receptor binding inhibition assay [17].

Compound[a]	Core, X (*n*, number of glycine residues in antenna)	Virus	Relative activity
Neu5AcαOBn			1(150)[b]
Neu5Acα-sp1-Gly$_n$-X-Gly$_n$-sp1-Neu5Acα	C_2 (2–4)	(A/H3N2/29/90)	1
	C_2 (5)		3
	C_2 (6)		6
Neu5Acα-sp1-Gly$_n$-X-Gly$_n$-sp1-Neu5Acα	C_{10} (1–3)		1
	C_{10} (4)		50
	C_{10} (5)		25
6'SLN			1(150)[b]
6'SLN-sp2-Gly$_n$-X-Gly$_n$-sp2-6'SLN	OEG (2, 4)	(A/H1N1/NIB23)	1
	OEG (5)		1
	OEG (6)		40
3'SL			1(150)[b]
3'SL-sp3-Gly$_n$-X-Gly$_n$-sp3-3'SL	OEG (2, 4)	(A/H5N2)	1
	OEG (5)		1
	OEG (6)		50

[a]Abbreviations: sp1 = -$OCH_2(p\text{-}C_6H_4)NHCOCH_2NH\text{-}CO(CH_2)_4CO$; Bn – benzyl; sp2 = -$O(CH_2)_3NHCO(CH_2)_4CO$; 6'SLN = Neu5Acα2-6Galβ1-4GlcNAcβ; sp3 = -$NHCOCH_2NHCO(CH_2)_4CO$; 3'SL = Neu5Acα2-3Galβ1-4Glcβ. [b]Values of IC_{50}, μM, for monomeric Neu5AcαOBn, 6'SLN and 3'SL are given in parentheses.

ization of a divalent interaction of this bivalent molecule with a viral hemagglutinin. Indeed, a simple calculation demonstrates that this distance in a maximally extended molecule with $n = 6$ is about 100 Å. This distance value corresponds to the distance between the carbohydrate binding sites in one molecule of a hemagglutinin homotrimer and slightly exceeds the distance between a couple of hemagglutinin trimmers, which are closely situated on the virion surface.

Experimental

Reagents and solvents were bought from Merck and Sigma–Aldrich. Activated esters BocGlyONSu and BocGly$_2$ONSu were prepared as described earlier [9] from glycine or glycylglycine (Acros). Ethylenediamine and 1,10-diaminodecane were supplied from Sigma-Aldrich, and diamine $NH_2(CH_2CH_2O)_3CH_2CH_2NH_2$ (**1**) was synthesized from ditosylate $TosO(CH_2CH_2O)_3CH_2CH_2OTos$ (Sigma–Aldrich) according to the described methods [7,8].

Silica gel (Kieselgel 60, Merck, Germany) was used for low-pressure column chromatography. Sephadex LH-20 (Pharmacia Biotech, Austria) was employed for gel chromatography. Thin-layer chromatography (TLC) was performed on foil plates covered with silica gel (Kieselgel 60, Merck, Germany).

^{1}H NMR spectra were recorded on a Bruker spectrometer (600, 700, 800 MHz) at 303 K. Chemical shifts (δ) for characteristic signals in ^{1}H NMR spectra are given in ppm and spin–spin coupling constants (*J*) in Hz. The scale of the chemical shifts was calibrated against the signals of residual protons of solvents ($CDCl_3$: δ 7.26 ppm; DMSO-d_6: δ 2.50 ppm; D_2O: δ 4.75 ppm). Mass-spectra were recorded on the time-of-flight spectrometer Vision-2000 (Thermo Bioanalysis, UK) with MALDI with 2,6-dihydroxybenzoic acid as reference. Raman spectra were recorded on a spectrometer Ramanor HG-2S (Jobin Yvon) with the monochromator Anaspec 300S and argon (λ = 514.5 nm, Spectra Physics, model 164-03).

Synthesis of biantennary oligoglycines

Protocol 1: Elongation of the oligoglycine chain (Boc-Gly$_n$NH-X-NHGly$_n$-Boc; n = 1–7, X = C_2, C_{10} and OEG). Et_3N (8 mmol) followed by BocGlyONSu or BocGly$_2$ONSu (3 mmol) were added to a solution of diamine (1 mmol) in dimethyl sulfoxide (DMSO; 5 mL). The reaction mixture was stirred until the disappearance of the starting diamine (1–24 h, TLC control) and the solvent was removed under vacuum. The dry residue was suspended in methanol, filtered, dissolved in water, sedimentated with methanol, and dried in vacuo.

Protocol 2: Preparation of oligoglycines (HCl·Gly$_n$NH-X-NHGly$_n$·HCl; n = 1–7, X = C_2, C_{10} and OEG). The Boc-derivative (0.5 mmol) was dissolved in trifluoroacetic acid (5 mL), the reaction mixture was kept for 2 h at room temperature, co-evaporated with toluene (2 × 10 mL) and 1 M HCl aqueous solution

(1–2 mL), and finally with a mixture iPrOH/methanol 1:1 (2 × 10 mL). The obtained product was sedimentated from the aqueous solution by the addition of methanol and dried in vacuo.

Synthesis of associating glycopeptides

Protocol 3: Neu5Acα-sp1-ONp, 3'SL-sp3-ONp or 6'SLN-sp2-ONp (4 μmol) were added to a solution of diamine (1 μmol) in DMSO or saturated aqueous solution of LiBr (200 μL). NEt_3 (4 μmol) was added until a pH of 8 was reached, and the mixture was stirred for 24 h at room temperature. Exclusion chromatography on Sephadex LH-20 (eluent: 0.1 M solution of NH_3 in the mixture acetonitrile/water, 1:1). Fractions containing pure product were combined and evaporated. Dry residue was dissolved in water and freeze-dryed.

Dynamic light scattering experiments

The light scattering of aqueous solutions of biantennary oligoglycines was studied with an analyzer of submicron particle size "Malvern HPPS" (UK). After the preparation of aqueous (Milli-Q) solutions of oigoglycine salts in a concentration of 0.01–0.1 mg/mL, the instrument reading was recorded (t = 0, pH < 5). Then, 1–2 equiv of base (0.1 M aqueous solution of $NaHCO_3$ or Na_2CO_3) per amino group was added to the solution of the analyzed oligoglycine salt (t > 0, pH 6–8), and instrument readings were recorded in fixed periods of time. In the case of the formation of large associates (intense opalescence, sedimentation), whose dimensions exceeded the working limit of the instrument, the experiment was stopped.

For experiments with biantennary sialooligoglycines their aqueous (Milli-Q) solutions with a concentration of 0.1 mg/mL were used.

Scanning force microscopy (SFM)

The samples were imaged with a Nanoscope IIIa instrument (Digital Instruments, USA). Commercial silicon nitride cantilevers with force constants of 0.06, 0.12, and 0.32 Nm^{-1} were used for the measurements in contact mode in liquid cell. Cantilevers with a resonance frequency of about 300 kHz and a force constant of 42 Nm^{-1} were used for the SFM tapping mode in air. Software WSxM (Nanotec Electronica, Spain) was employed for the image treatment. Pure water (Fluka) was used for the preparation of solutions.

Scanning in air. 1–2 equiv of 0.1 M of aqueous solution of $NaHCO_3$ or Na_2CO_3 per amino group (pH ~ 6–8) was added for the deprotonation to a freshly prepared solution of oligoglycine salt (0.1–1.0 mg/mL; pH < 5), and incubated for a specified time period in the range of 0 to 90 min. Then the solution was applied on the freshly cleaved mica or graphite, and kept for a specified period of time within the range of 0 to 10 min. Liquid was removed from the surface by spin coating or in nitrogen flow. Structures formed on the surface were visualized in tapping mode SFM.

Scanning in liquid cell. A plate of freshly cleaved mica (1 × 1 cm^2) was placed in a liquid cell. The cell was filled with water (25 μL) and the instrument was set up. Then, water was changed with a freshly prepared solution of deprotonated peptide (see scanning in air above) and the surface was scanned in contact mode SFM in fixed time periods.

The influenza virus receptor-binding inhibition assay was carried out as described in [17].

Supporting Information

Supporting Information File 1

Descriptions of the synthesis of individual compounds.
[http://www.beilstein-journals.org/bjoc/content/supplementary/1860-5397-10-140-S1.pdf]

Acknowledgments

This study was partly supported by the Russian Academy of Sciences Presidium Program Molecular and Cell Biology. The authors would like to thank Dr. Ekaterina A. Obraztsova for the Raman analysis and Dr. Galina V. Pazynina for valuable discussions about the experimental design and the results.

References

1. Tsygankova, S. V.; Chinarev, A. A.; Tuzikov, A. B.; Gambaryan, A. S.; Bovin, N. V. "Self-assembling glycopeptides" presented at the 17th European Carbohydrate Symposium "EuroCarb17", Tel Aviv, Israel, July 7–11, 2013, P-55.
2. Tuzikov, A. B.; Chinarev, A. A.; Gambaryan, A. S.; Oleinikov, V. A.; Klinov, D. V.; Matsko, N. B.; Kadykov, V. A.; Ermishov, M. A.; Demin, I. V.; Demin, V. V.; Rye, P. D.; Bovin, N. V. *ChemBioChem* **2003,** *4,* 147–154. doi:10.1002/cbic.200390025
3. Bovin, N. V.; Tuzikov, A. B.; Chinarev, A. A. *Nanotechnologies in Russia* **2008,** *3,* 291–302. doi:10.1134/S1995078008050042
4. Bamford, C. H.; Brown, L.; Cant, E. M.; Elliott, A.; Hanby, W. E.; Malcolm, B. R. *Nature* **1955,** *176,* 396–397. doi:10.1038/176396a0
5. Crick, F. H. C.; Rich, A. *Nature* **1955,** *176,* 780–781. doi:10.1038/176780a0
6. Bovin, N. V.; Tuzikov, A. B.; Chinarev, A. A.; Gambaryan, A. S. *Glycoconjugate J.* **2004,** *21,* 471–478. doi:10.1007/s10719-004-5537-3
7. Katritzky, A. R.; Singh, S. K.; Meher, N. K.; Doskocz, J.; Suzuki, K.; Jiang, R.; Sommen, G. L.; Ciaramitaro, D. A.; Steel, P. J. *ARKIVOC* **2006,** *(v),* 43–62. doi:10.3998/ark.5550190.0007.505

8. Katritzky, A. R.; Meher, N. K.; Hanci, S.; Gyanda, R.; Tala, S. R.; Mathai, S.; Duran, R. S.; Bernard, S.; Sabri, F.; Singh, S. K.; Doskocz, J.; Ciaramitaro, D. A. *J. Polym. Sci., Part A: Polym. Chem.* **2008,** *46,* 238–256. doi:10.1002/pola.22376
9. Gershkovich, A. A.; Kibirev, V. C. *Chemical synthesis of peptides;* Naukova Dumka: Kiev, Ukraine, 1992.
10. Chinarev, A. A.; Tuzikov, A. B.; Gambaryan, A. S.; Matrosovich, M. N.; Imberty, A.; Bovin, N. V. In *Sialobiology and Other Novel Forms of Glycosylation;* Ynoue, Y.; Lee, Y. C.; Troy, F. A., II., Eds.; Gakushin Publishing Co.: Osaka, 1999; pp 135–143.
11. Bovin, N. V.; Chinarev, A. A.; Tuzikov, A. B. Multiligand constructs. WO Patent WO/2010/043230, Oct 13, 2008.
12. Krimm, S.; Bandekar, J. In *Advanced Protein Chemistry;* Anfinsen, C. B.; Edsall, J. T.; Richards, F. M., Eds.; Academic Press: New York; Vol. 38, pp 181–364.
13. Gus'kova, O. A.; Khalatur, P. G.; Khokhlov, A. R.; Chinarev, A. A.; Tsygankova, S. V.; Bovin, N. V. *Russ. J. Bioorg. Chem.* **2010,** *36,* 574–580. doi:10.1134/S1068162010050043
14. Bella, J.; Puiggali, J.; Subirana, J. A. *Polymer* **1994,** *35,* 1291–1297. doi:10.1016/0032-3861(94)90026-4
15. Mammen, M.; Choi, S.-K.; Whitesides, G. M. *Angew. Chem., Int. Ed.* **1998,** *37,* 2754–2794. doi:10.1002/(SICI)1521-3773(19981102)37:20<2754::AID-ANIE2754>3.0.CO;2-3
16. Chugunov, P. A.; Chinarev, A. A.; Tuzikov, A. B.; Formanovsky, A. A.; Prokhorov, V. V.; Gambaryan, A. S.; Bovin, N. V. *Mendeleev Commun.* **2009,** *19,* 62–63. doi:10.1016/j.mencom.2009.03.002
17. Gambaryan, A. S.; Matrosovich, M. N. *J. Virol. Methods* **1992,** *39,* 111–123. doi:10.1016/0166-0934(92)90130-6
18. Gambaryan, A. S.; Tuzikov, A. B.; Piskarev, V. E.; Yamnikova, S. S.; Lvov, D. K.; Robertson, J. S.; Bovin, N. V.; Matrosovich, M. N. *Virology* **1997,** *232,* 345–350. doi:10.1006/viro.1997.8572

License and Terms

Beilstein Journal of Organic Chemistry

Synthesis of the first examples of iminosugar clusters based on cyclopeptoid cores

Mathieu L. Lepage[1], Alessandra Meli[2], Anne Bodlenner[1], Céline Tarnus[3], Francesco De Riccardis[2], Irene Izzo[*2] and Philippe Compain[*1,4]

Letter

Open Access

Address:
[1]Laboratoire de Synthèse Organique et Molécules Bioactives (SYBIO), Université de Strasbourg/CNRS (UMR 7509), Ecole Européenne de Chimie, Polymères et Matériaux, 25 rue Becquerel, 67087 Strasbourg, France, [2]Department of Chemistry and Biology, University of Salerno, Via Giovanni Paolo II, 132, I-84084 Fisciano Salerno, Italy, [3]Université de Haute Alsace, Laboratoire de Chimie Organique et Bioorganique, EA4466, ENSCMu, 3, rue Alfred Werner, 68093 Mulhouse Cedex, France and [4]Institut Universitaire de France, 103 Bd Saint-Michel, 75005 Paris, France

Email:
Irene Izzo[*] - iizzo@unisa.it; Philippe Compain[*] - philippe.compain@unistra.fr

* Corresponding author

Keywords:
cyclopeptoids; glycosidases; iminosugars; inhibitors; multivalency; mutivalent glycosystems

Beilstein J. Org. Chem. **2014,** *10,* 1406–1412.
doi:10.3762/bjoc.10.144

Received: 24 February 2014
Accepted: 20 May 2014
Published: 23 June 2014

This article is part of the Thematic Series "Multivalent glycosystems for nanoscience".

Guest Editor: B. Turnbull

Abstract

Cyclic *N*-propargyl α-peptoids of various sizes were prepared by way of macrocyclizations of linear *N*-substituted oligoglycines. These compounds were used as molecular platforms to synthesize a series of iminosugar clusters with different valency and alkyl spacer lengths by means of Cu(I)-catalysed azide–alkyne cycloadditions. Evaluation of these compounds as α-mannosidase inhibitors led to significant multivalent effects and further demonstrated the decisive influence of scaffold rigidity on binding affinity enhancements.

Introduction

Within a few years, the field of multivalent glycosidase inhibitors has witnessed tremendous advancement. Since the report in 2009 of the first quantifiable multivalent effect in glycosidase inhibition [1,2], the pace of progress has been breath-taking with the discovery of iminosugar clusters showing outstanding affinity enhancements of up to four orders of magnitude over the parent monovalent analogues [3-7]. The best results were obtained with multivalent systems based on C_{60} [3], β-cyclodextrin [4,5] and porphyrin [7] cores, and with nanoparticles prepared by self-assembly of iminosugar-based glycopolypetides [6]. So far, the largest multivalent effect (up to 610-fold relative inhibition potency increase on a valency-

corrected basis) has been achieved on jack bean α-mannosidase with β-cyclodextrin-based analogues displaying 14 copies of 1-deoxynojirimycin (DNJ) [4]. Applications of the inhibitory multivalent effect to glycosidases of therapeutic interest were promptly performed and promising results were obtained in the field of Gaucher disease, the most common lysosomal storage disorder [8,9]. In 2013, the first description of a multivalent effect for correcting protein folding defects in cells was reported with trivalent DNJ clusters [10]. These compounds were found to overcome the processing defect of the mutant CFTR protein involved in cystic fibrosis, and to be up to 2 orders of magnitude more efficient as CFTR correctors than the clinical candidate miglustat (*N*-Bu-DNJ, **1**, Figure 1).

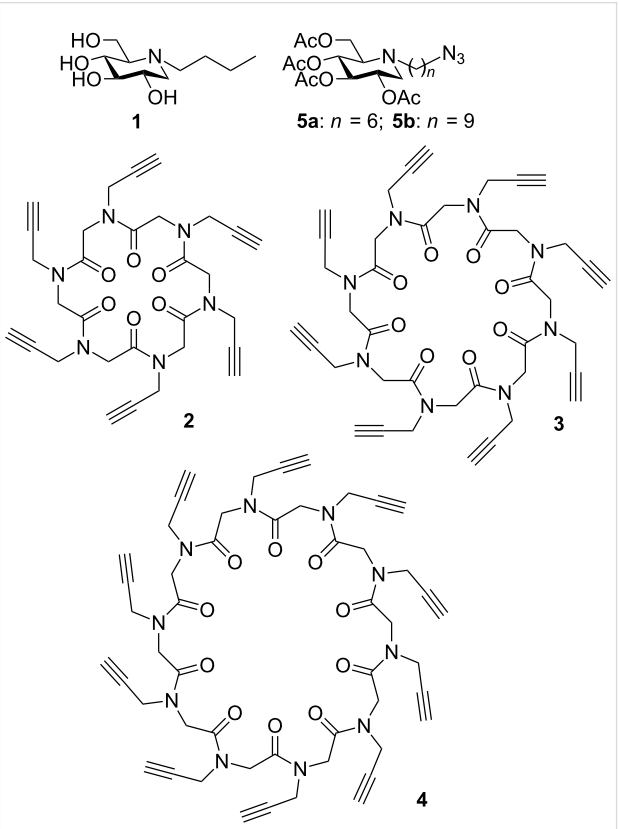

Figure 1: *N*-Bu-DNJ (**1**), azide-armed DNJ derivatives **5** and cyclopeptoid scaffolds **2**–**4**.

The mechanisms underlying the inhibitory multivalent effect were studied with different methods such as isothermal titration calorimetry, competitive lectin-enzyme assays, X-ray crystallography or atomic force spectroscopy [7,11-13]. At this stage of research, one of the main challenges in the field is to design optimal systems that not only display large multivalent effects but also possess the desired properties for particular applications. In this context, the choice of the scaffold is crucial as it defines the valency, the size and the shape of the multivalent architectures. Due to their broad chemical diversity, rapid and convenient synthetic access, improved proteolytic stability and cell permeability over peptides, *N*-substituted glycine oligomers, called peptoids [14-17], appear as promising scaffolds for the synthesis of glycoconjugates of biological interest [14-18]. Combination of these advantages has led to many examples of biologically active peptoids [19-21]. So far, some syntheses of *N*-, *O*-, *C*- and *S*-linked glycopeptoids have been reported [22-31] and few of them are related to cyclopeptoids [32,33]. One of the most intriguing features of peptoids is their capacity to generate cyclic structures, which can expand the utility of this platform to multivalent chemical achitectures [34]. Conformation, size, charge and branching of these cyclic scaffolds influence the pharmacological profile of the products [35-39]. Moreover, macrocyclization enforces the rigidity of the more flexible linear peptoid skeleton and generally produces enhancement in biological activities [21,37]. In this context cyclopeptoids **2**–**4** appear as ideal building blocks because of their simplicity of synthesis and easy functionalization by click reaction (Figure 1). In the present paper, we report the synthesis of the first examples of cyclopeptoid-based iminosugar clusters. The influence of valency, size, linker and scaffold structure on jack bean α-mannosidase inhibition was evaluated with a series of 6- to 10-valent DNJ derivatives with two different alkyl spacer lengths (C_6 or C_9).

Results and Discussion

Our synthetic strategy was based on a convergent approach involving the attachment of azide-armed iminosugars **5** onto polyalkyne "clickable" scaffolds **2**–**4** by Cu(I)-catalyzed azide–alkyne cycloaddition (CuAAC) reactions [40,41] (Figure 1). *N*-alkyl derivatives of DNJ were logically chosen as the peripheral ligands because of the therapeutic relevance of these compounds [42]. In addition, most of the glycosidase inhibitor clusters published in the literature are based on these binding motifs [1-7,11,43] providing thus the opportunity to assess the relevance of cyclopeptoid cores by comparison with the other platforms already described.

Scaffold synthesis

The linear precursors of cyclic scaffolds (**2**–**4,** Figure 1) were prepared using the sub-monomer approach developed by Zuckerman et al. [44] through a two-step sequence, repeated iteratively, to obtain the desired oligomers (Scheme 1). Each monomer is constructed on the 2-chlorotrityl resin from *C*- to *N*-terminus using *N*,*N'*-diisopropylcarbodiimide (DIC)-mediated acylation with bromoacetic acid, followed by amination with the propargyl amine. After the completion of synthesis, the oligomers were cleaved from the resin using a 4:1 solution of CH_2Cl_2/hexafluoroisopropanol (HFIP). Macrocyclizations of the linear *N*-substituted oligoglycines **6**–**8** proceeded smoothly

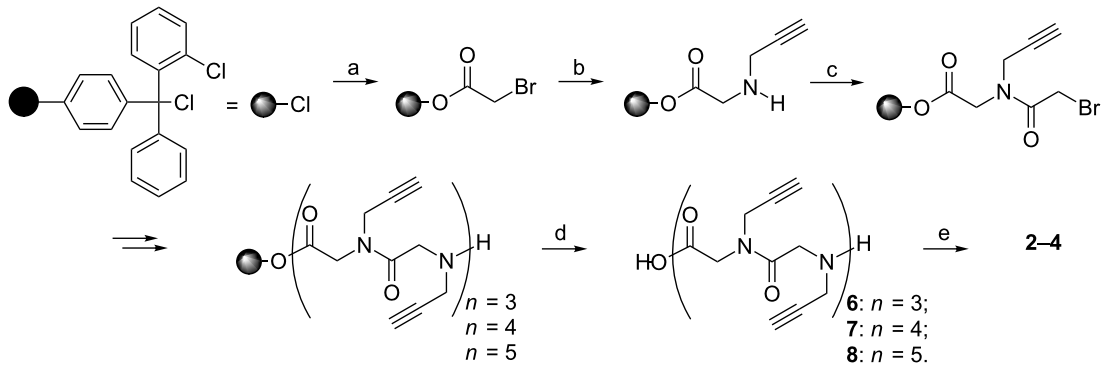

Scheme 1: Sub-monomer approach for the synthesis of cyclopeptoids **2**–**4**: DIPEA = *N*,*N*-diisopropylethylamine; DIC = *N*,*N*′-diisopropylcarbodiimide; HATU *O*-(7-azabenzotriazole-1-yl)-*N*,*N*,*N*′,*N*′-tetramethyluronium hexafluorophosphate. (a) bromoacetic acid, DIPEA, CH_2Cl_2; (b) propargylamine (10 equiv), DMF; (c) bromoacetic acid, DIC, DMF; (d) CH_2Cl_2/HFIP (4:1); (e) HATU, DIPEA, DMF.

giving, under high dilution conditions (3.0×10^{-3} M) and in the presence of the efficient coupling agent HATU, the desired cyclic peptoids **2**–**4** (Scheme 1). After purification, compounds **2**–**4** were recovered in 31%, 32% and 12% overall yield respectively.

DNJ cluster synthesis

The last stages of the DNJ cluster synthesis were based on a robust two-step process, recently developed in our group for the preparation of iminosugar click clusters [4,5,9-11]. The first step of the process involved the attachment of peracetylated azido iminosugars **5** [4] onto polyalkyne scaffolds **2**–**4** by microwave-assisted CuAAC reaction (Scheme 2).

The multiconjugation reaction proceeded smoothly to afford the six desired DNJ clusters **9** in 69–95% yields. With the exception of octavalent iminosugars **9c** (*n* = 6) and **9d** (*n* = 9), these compounds showed complex ^{1}H NMR spectra at room temperature as exemplified by compound **9a** (Figure 2i). This phenomenon, already observed for *N*-substituted cyclic α-peptoid derivatives [35-39], indicated the presence of more than one conformer in slow exchange on the NMR time scale. It is well known that the conformational heterogeneity is due to tertiary amide bonds, which can isomerize more readily than secondary amides, and to the absence of amide protons, which stabilize secondary structure by backbone hydrogen bonding [15,16]. As we have previousy demonstrated, this heterogeneity can be reduced by metal chelation [35,38]. Addition of an excess of sodium picrate to **9a** indeed dramatically simplified the ^{1}H NMR spectrum by inducing the formation of a sodium complex with a 6-fold symmetry (Figure 2ii).

Subsequent *O*-deacetylation of compounds **9** using anion exchange Amberlite IRA-400 (OH^-) resin provided the final deprotected iminosugar clusters **10** in high yields without affecting the potentially labile amide bond.

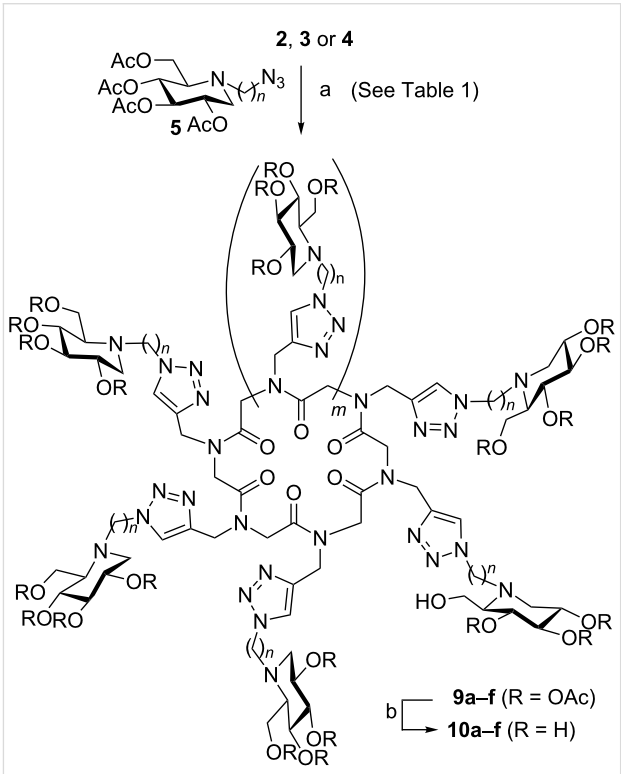

Scheme 2: Synthesis of DNJ clusters **10**: (a) $CuSO_4 \cdot 5H_2O$ cat., sodium ascorbate, DMF/H_2O (5:1), MW, 80 °C; (b) Amberlite IRA 400 (OH^-), MeOH/H_2O (1:1), 40 °C. Overall yields from compounds **2**, **3** or **4**: **10a** (*n* = 6, *m* = 1) 95%; **10b** (*n* = 9, *m* = 1) 83%; **10c** (*n* = 6, *m* = 3) 69%; **10d** (*n* = 9, *m* = 3) 80%; **10e** (*n* = 6, *m* = 5) 70%; **10f** (*n* = 9, *m* = 5) 80%.

As indicated in the introduction, the best multivalent effects in glycosidase inhibition observed so far were obtained with jack

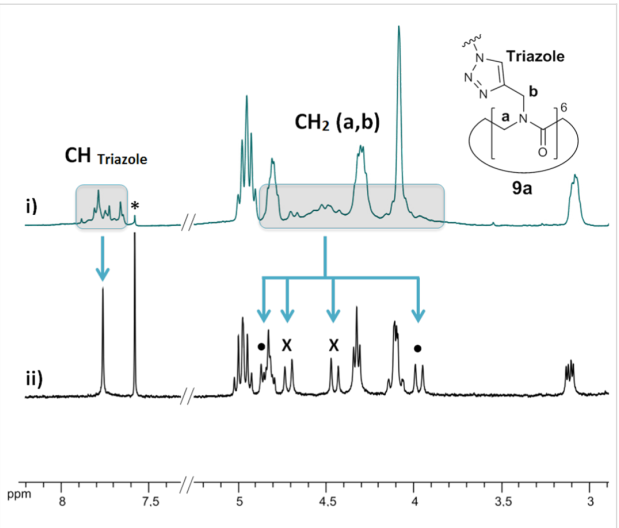

Figure 2: i) Partial ^{1}H NMR spectrum (400 MHz, $CD_3CN/CDCl_3$ 9:1) of compound **9a**; ii) Partial ^{1}H NMR spectrum (400 MHz, $CD_3CN/CDCl_3$ 9:1) of compound **9a** with sodium picrate (11 equiv). * Residual solvent peak for $CDCl_3$. • and X are assigned to protons a or b.

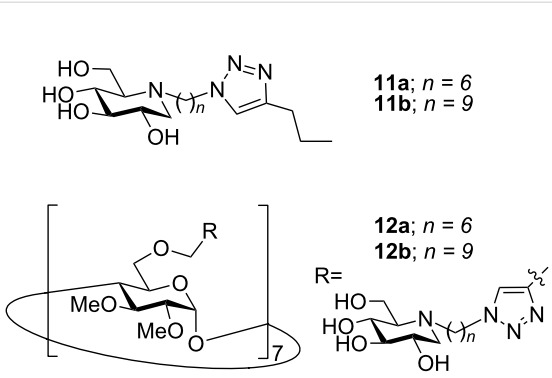

Figure 3: Monovalent models **11** and 7-valent DNJ derivatives **12**.

bean α-mannosidase [1-7,11,12]. Accordingly, in order to complete these compelling investigations, evaluation of the inhibition potency of multivalent iminosugars **10** was performed on this peculiar enzyme (Table 1). Related monovalent controls **11** [3,4] as well as 7-valent β-cyclodextrin-based DNJ clusters **12** [4] have been included for comparative purposes (Figure 3). Our results clearly point out that all cyclopeptoid-based clusters **10** display a significant multivalent effect ($rp/n > 1$), with 6-valent iminosugar **10a** as a single exception.

Increasing the valency (from 6 to 10) or the linker length (from C_6 to C_9) resulted in increased inhibition potencies when compared to the corresponding monovalent models **11**, the best result being obtained with 10-valent DNJ cluster **10f** with a C_9 linker ($rp/n \sim 4$). However, the binding enhancements were found to be 2- to 31-fold lower than the ones observed with the related 7-valent DNJ clusters **12** with identical alkyl spacer length but a different core (β-cyclodextrin). These results may indicate that the ligand spatial presentation in cyclopeptoid-based iminosugars **10** is not optimal to achieve a substantial multivalent effect. It has been shown recently that the use of rigid scaffolds such as porphyrin or C_{60} could lead to large multivalent effects (up to 200-fold on a valency-corrected basis) [3,7]. The modest inhibition enhancements observed with DNJ-cyclopeptoid conjugates **10** could thus be due to the high flexibility of their amide backbone [14-17].

Conclusion

In conclusion, we have reported the efficient synthesis of the first examples of cyclopeptoid-based iminosugar clusters and

Table 1: Relative inhibition potency of cyclopeptoid-based clusters **10** and inhibitory activity (K_i, μM) against jack bean α-mannosidase.

Compound	Valency	Linker length	K_i (μM)	rp[a]	rp/n[b]
11a	1	C_6	322 [3,4]	–	–
10a	6	C_6	65 ± 24	4.9	0.8
10c	8	C_6	21 ± 2	15	1.9
10e	10	C_6	15 ± 10[c]	21	2.1
12a	7	C_6	7.7 [4]	42	6.0
11b	1	C_9	188 [3,4]	–	–
10b	6	C_9	11 ± 1	17	2.8
10d	8	C_9	8 ± 3	23	2.9
10f	10	C_9	5 ± 1	38	3.8
12b	7	C_9	0.36 [4]	522	75

[a]Relative inhibition potency = K_i (monovalent reference)/K_i (glycocluster). [b]rp/n = Relative inhibition potency/number of iminosugar units. [c]Single determination of K_i without duplicate.

their evaluation as α-mannosidase inhibitors. Modest but significant inhibitory multivalent effects were observed for most of the compounds evaluated. This study further highlights the decisive impact of the scaffold rigidity on binding affinity enhancements. In connection with our recent work in the field of rare genetic diseases [8-10], further evaluation of neoglycopeptoids in cell systems are currently underway in our laboratory. The intrinsic advantages of cylopeptoid scaffolds including improved cell permeability and proteolytic stability are indeed expected to be most beneficial for this exploratory work.

Experimental

General information

NMR spectra were recorded on Bruker 300, 400 and 500 MHz spectrometers with solvent peaks as reference. Carbon multiplicities were assigned by distortionless enhancement by polarization transfer (DEPT) experiments. The ^{1}H signals were assigned by 2D experiments (COSY). ESI–HRMS mass spectra were carried out on a Bruker MicroTOF spectrometer. Purifications were performed with silica gel 60 (230–400 mesh, 0.040–0.063 mm).

General procedure for the synthesis of cyclopeptoid-based iminosugar click clusters **9a–f**

To a solution of the cyclopeptoid **2, 3** or **4** (typically 5 to 15 mg) and ligand **5a** or **5b** (1.1 equiv/alkyne moiety) in DMF (typically 0.5 to 1 mL) in a microwave vial was added a bright yellow suspension of $CuSO_4{\cdot}5H_2O$ (10 mol %/alkyne moiety) and sodium ascorbate (20 mol %/alkyne moiety) in water (typically 0.1 to 0.2 mL). The mixture was stirred and heated under microwave irradiation for 3 h at 80 °C. The mixture was concentrated, diluted in a 9:1:1 (v/v/v) mixture of MeCN/water/30 wt %-NH_4OH and filtrated with the same eluent (25 mL) on a small pad of SiO_2 (typically 1 cm thick), whose top surface became blue after copper complexation with NH_3. The filtrate was concentrated and then filtrated on another pad of SiO_2 (typically 1 cm wide and 2 cm thick), eluting it with AcOEt/PE 4:6 (25 mL) to recover clean unclicked ligand **5a** or **5b**, and then with MeCN/water 8:2 (25 mL) to afford iminosugar click clusters **9a–f** as pale brown translucent wax after concentration.

General procedure for the synthesis of deprotected cyclopeptoid-based iminosugar click clusters **10a–f**

To a solution of acetate-protected iminosugar click clusters **9a–f** in a 1:1 mixture of water/MeOH (typically 600 µL/µmol) was added Amberlite IRA400 (OH^-) (5.5*n* g/mmol of substrate; *n* = number of acetate groups). The suspension was softly stirred overnight at 40 °C. Then the mixture was filtrated and the filtrate was concentrated to afford deprotected iminosugar click clusters **10a–f** in quantitative yields.

Compound **9a**

$[\alpha]_D^{18}$ +6.2 (*c* 1, $CHCl_3$); ^{1}H NMR ($CD_3CN/CDCl_3$ 9:1 + 11 equiv sodium picrate, 400 MHz) δ 7.76 (s, 6H, H-1'), 4.97 (m, *J* = 10.3 Hz, 12H, H-3, H-4), 4.85 (d, *J* = 16.3 Hz, 6H, H-3' or H-5'), 4.83 (td, *J* = 9.8, 5.3 Hz, 6H, H-2), 4.71 (d, *J* = 16.3 Hz, 6H; H-3' or H-5'), 4.45 (d, *J* = 16.3 Hz, 6H, H-3' or H-5'), 4.32 (t, *J* = 7.0 Hz, 12H, H-12), 4.10 (dd, *J* = 19.4, 13.0 Hz, 12H, H-6), 3.97 (d, *J* = 16.3 Hz, 6H, H-3' or H-5'), 3.11 (dd, *J* = 11.1, 5.3 Hz, 6H, H-1a), 2.70 (m, 6H, H-7a), 2.68 (d, *J* = 8.8 Hz, 6H, H-5), 2.51 (m, 6H, H-7b), 2.35 (dd, *J* = 12.7, 11.1 Hz, 6H, H-1b), 1.95 (s, 72H, AcO), 1.85 (m, 12H, H-11), 1.40 (m, 12H, H-8), 1.28 (m, 24H, H-9, H-10) ppm; ^{13}C NMR ($CD_3CN/CDCl_3$ 9:1, 100 MHz) δ 171.4, 170.94, 170.88, 170.6, 170.6–168.9, 144.4–142.8, 124.7–123.8, 75.3, 70.5, 70.2, 62.1, 60.5, 53.4, 52.3, 50.8, 50.3–48.5, 44.9–42.6, 30.9, 27.3, 27.0, 25.2, 21.1 ppm; HRMS–ESI (*m*/*z*): $[M + 2H]^{2+}$ calcd for $C_{150}H_{224}N_{30}O_{54}$ 1654.7847; found: 1654.7827.

Compound **10a**

$[\alpha]_D^{20}$ −28.0 (*c* 0.1, H_2O/DMSO 1:1 + 0.1% TFA); ^{1}H NMR (D_2O + 0.1% TFA, 500 MHz) δ 8.21–7.60 (m, 6H, H-1'), 5.20–3.72 (br m, 12H, H-3' and H-5'), 4.35 (s, 12H, H-12), 3.85 (s, 12H, H-6), 3.59 (s, 6H, H-2), 3.43 (s, 6H, H-4), 3.31 (s, 6H, H-3), 3.16 (s, 6H, H-1a), 2.91 (s, 6H, H-7a), 2.78 (s, 6H, H-7b), 2.56 (s, 12H, H-1b and H-5), 1.84 (s, 12H, H-11), 1.51 (s, 12H, H-8), 1.25 (s, 24H, H-9 and H-10) ppm; ^{13}C NMR (D_2O + 0.1% TFA, 125 MHz) δ 173.4–169.3, 145.6–142.8, 127.4–124.6, 78.9, 70.4, 69.3, 66.8, 57.5, 55.9, 53.9, 51.9, 51.5–49.3, 46.3–43.3, 30.9, 27.3, 26.8, 24.0 ppm; HRMS–ESI (*m*/*z*): $[M + 2H]^{2+}$ calcd for $C_{102}H_{174}N_{30}O_{30}$ 1150.6579; found: 1150.6626.

Supporting Information

Supporting Information File 1

Mannosidase inhibition assay procedures, synthesis and NMR spectra of all new compounds.
[http://www.beilstein-journals.org/bjoc/content/supplementary/1860-5397-10-144-S1.pdf]

Acknowledgements

This work was supported by the Institut Universitaire de France (IUF), the CNRS (UMR 7509), the University of Strasbourg, the Agence Nationale de la Recherche (ANR, grant number 11-BS07-003-02), and a doctoral fellowship from the French Department of Research to Mathieu L. Lepage. We also thank Michel Schmitt and Lionel Allouche for NMR measurements and Hélène Nierengarten for MS measurements. We thank the University of Salerno (FARB) and the Italian MIUR (PRIN 20109Z2XRJ_006) for financial support. We thank Dr. Patrizia

Iannece for ESI–MS and Miss. Dagmara Lubowiecka for experimental work (University of Salerno).

References

1. Diot, J.; Garcia-Moreno, M. I.; Gouin, S. G.; Ortiz Mellet, C.; Haupt, K.; Kovensky, J. *Org. Biomol. Chem.* **2009,** *7,* 357–363. doi:10.1039/b815408b
2. Compain, P.; Bodlenner, A. *ChemBioChem* **2014,** in press. doi:10.1002/cbic.201402026
   See for a review on the multivalent effect in glycosidase inhibition.
3. Compain, P.; Decroocq, C.; Iehl, J.; Holler, M.; Hazelard, D.; Mena Barragán, T.; Ortiz Mellet, C.; Nierengarten, J.-F. *Angew. Chem., Int. Ed.* **2010,** *49,* 5753–5756. doi:10.1002/anie.201002802
4. Decroocq, C.; Rodríguez-Lucena, D.; Russo, V.; Mena Barragán, T.; Ortiz Mellet, C.; Compain, P. *Chem.–Eur. J.* **2011,** *17,* 13825–13831. doi:10.1002/chem.201102266
5. Joosten, A.; Schneider, J. P.; Lepage, M. L.; Tarnus, C.; Bodlenner, A.; Compain, P. *Eur. J. Org. Chem.* **2014,** 1866–1872. doi:10.1002/ejoc.201301583
6. Bonduelle, C.; Huang, J.; Mena-Barragán, T.; Ortiz Mellet, C.; Decroocq, C.; Etamé, E.; Heise, A.; Compain, P.; Lecommandoux, S. *Chem. Commun.* **2014,** *50,* 3350–3352. doi:10.1039/c3cc48190e
7. Brissonet, Y.; Ortiz Mellet, C.; Morandat, S.; Garcia-Moreno, M. I.; Deniaud, D.; Matthews, S. E.; Vidal, S.; Sestak, S.; El Kirat, K.; Gouin, S. G. *J. Am. Chem. Soc.* **2013,** *135,* 18427–18435. doi:10.1021/ja406931w
8. Decroocq, C.; Rodríguez-Lucena, D.; Ikeda, K.; Asano, N.; Compain, P. *ChemBioChem* **2012,** *13,* 661–664. doi:10.1002/cbic.201200005
9. Joosten, A.; Decroocq, C.; de Sousa, J.; Schneider, J.; Etamé, E.; Bodlenner, A.; Butters, T. D.; Compain, P. *ChemBioChem* **2014,** *15,* 309–319. doi:10.1002/cbic.201300442
10. Compain, P.; Decroocq, C.; Joosten, A.; de Sousa, J.; Rodríguez-Lucena, D.; Butters, T. D.; Bertrand, J.; Clément, R.; Boinot, C.; Becq, F.; Norez, C. *ChemBioChem* **2013,** *14,* 2050–2058. doi:10.1002/cbic.201300312
11. Decroocq, C.; Joosten, A.; Sergent, R.; Mena Barragán, T.; Ortiz Mellet, C.; Compain, P. *ChemBioChem* **2013,** *14,* 2038–2049. doi:10.1002/cbic.201300283
12. Rísquez-Cuadro, R.; García Fernández, J. M.; Nierengarten, J.-F.; Ortiz Mellet, C. *Chem.–Eur. J.* **2013,** *19,* 16791–16803. doi:10.1002/chem.201303158
13. Moreno-Clavijo, E.; Carmona, A. T.; Moreno-Vargas, A. J.; Molina, L.; Wright, D. W.; Davies, G. J.; Robina, I. *Eur. J. Org. Chem.* **2013,** 7328–7336. doi:10.1002/ejoc.201300878
14. Nielsen, P. E., Ed. *Pseudo-Peptides in Drug Discovery;* Wiley-VCH: Weinheim, 2004.
15. Fowler, S. A.; Blackwell, H. E. *Org. Biomol. Chem.* **2009,** *7,* 1508–1524. doi:10.1039/B817980H
16. Culf, A. S.; Ouellette, R. J. *Molecules* **2010,** *15,* 5282–5335. doi:10.3390/molecules15085282
17. Seo, J.; Lee, B.-C.; Zuckermann, R. N. *Compr. Biomater.* **2011,** *2,* 53–76. doi:10.1016/B978-0-08-055294-1.00256-7
18. Marcaurelle, L. A.; Bertozzi, C. R. *Chem.–Eur. J.* **1999,** *5,* 1384–1390. doi:10.1002/(SICI)1521-3765(19990503)5:5<1384::AID-CHEM1384>3.0.CO;2-X
19. Yoo, B.; Kirshenbaum, K. *Curr. Opin. Chem. Biol.* **2008,** *12,* 714–721. doi:10.1016/j.cbpa.2008.08.015
20. Zuckermann, R. N.; Kodadek, T. *Curr. Opin. Mol. Ther.* **2009,** *11,* 299–307.
21. Huang, M. L.; Shin, S. B. Y.; Benson, M. A.; Torres, V. J.; Kirshenbaum, K. *ChemMedChem* **2012,** *7,* 114–122. doi:10.1002/cmdc.201100358
22. Saha, U. K.; Roy, R. *Tetrahedron Lett.* **1995,** *36,* 3635–3638. doi:10.1016/0040-4039(95)00620-R
23. Yuasa, H.; Kamata, Y.; Kurono, S.; Hashimoto, H. *Bioorg. Med. Chem. Lett.* **1998,** *8,* 2139–2144. doi:10.1016/S0960-894X(98)00364-3
24. Dechantsreiter, M. A.; Burkhart, F.; Kessler, H. *Tetrahedron Lett.* **1998,** *39,* 253–254. doi:10.1016/S0040-4039(97)10566-4
25. Burger, K.; Böttcher, C.; Radics, G.; Hennig, L. *Tetrahedron Lett.* **2001,** *42,* 3061–3063. doi:10.1016/S0040-4039(01)00351-3
26. Norgren, A. S.; Budke, C.; Majer, Z.; Heggemann, C.; Koop, T.; Sewald, N. *Synthesis* **2009,** *3,* 488–494. doi:10.1055/s-0028-1083302
27. Ahn, M.; Murugan, R. N.; Nan, Y. H.; Cheong, C.; Sohn, H.; Kim, E.-H.; Hwang, E.; Ryu, E. K.; Kang, S. W.; Shin, S. Y.; Bang, J. K. *Bioorg. Med. Chem. Lett.* **2011,** *21,* 6148–6153. doi:10.1016/j.bmcl.2011.08.012
28. Khan, S. N.; Kim, A.; Grubbs, R. H.; Kwon, Y.-U. *Org. Lett.* **2012,** *14,* 2952–2955. doi:10.1021/ol300808c
29. Ham, H. O.; Park, S. H.; Kurutz, J. W.; Szleifer, I. G.; Messersmith, P. B. *J. Am. Chem. Soc.* **2013,** *135,* 13015–13022. doi:10.1021/ja404681x
30. Singhamahapatra, A.; Sahoo, L.; Loganathan, D. *J. Org. Chem.* **2013,** *78,* 10329–10336. doi:10.1021/jo401720s
31. Fürniss, D.; Mack, T.; Hahn, F.; Vollrath, S. B. L.; Koroniak, K.; Schepers, S.; Bräse, S. *Beilstein J. Org. Chem.* **2013,** *9,* 56–63. doi:10.3762/bjoc.9.7
32. Comegna, D.; De Riccardis, F. *Org. Lett.* **2009,** *11,* 3898–3901. doi:10.1021/ol901524k
33. Cecioni, S.; Faure, S.; Darbost, U.; Bonnamour, I.; Parrot-Lopez, H.; Roy, O.; Taillefumier, C.; Wimmerova, M.; Praly, J.-P.; Imberty, A.; Vidal, S. *Chem.–Eur. J.* **2011,** *17,* 2146–2159. doi:10.1002/chem.201002635
34. Levine, P. M.; Carberry, T. P.; Holub, J. M.; Kirshenbaum, K. *Med. Chem. Commun.* **2013,** *4,* 493–509. doi:10.1039/c2md20338c
35. Maulucci, N.; Izzo, I.; Bifulco, G.; Aliberti, A.; De Cola, C.; Comegna, D.; Gaeta, C.; Napolitano, A.; Pizza, C.; Tedesco, C.; Flot, D.; De Riccardis, F. *Chem. Commun.* **2008,** 3927–3929. doi:10.1039/b806508j
36. De Cola, C.; Licen, S.; Comegna, D.; Cafaro, E.; Bifulco, G.; Izzo, I.; Tecilla, P.; De Riccardis, F. *Org. Biomol. Chem.* **2009,** *7,* 2851–2854. doi:10.1039/b905665c
37. Comegna, D.; Benincasa, M.; Gennaro, R.; Izzo, I.; De Riccardis, F. *Bioorg. Med. Chem.* **2010,** *18,* 2010–2018. doi:10.1016/j.bmc.2010.01.026
38. Izzo, I.; Ianniello, G.; De Cola, C.; Nardone, B.; Erra, L.; Vaughan, G.; Tedesco, C.; De Riccardis, F. *Org. Lett.* **2013,** *15,* 598–601. doi:10.1021/ol3034143
39. Della Sala, G.; Nardone, B.; De Riccardis, F.; Izzo, I. *Org. Biomol. Chem.* **2013,** *11,* 726–731. doi:10.1039/c2ob26764k
40. Kolb, H. C.; Finn, M. G.; Sharpless, K. B. *Angew. Chem., Int. Ed.* **2001,** *40,* 2004–2021. doi:10.1002/1521-3773(20010601)40:11<2004::AID-ANIE2004>3.0.CO;2-5
    Angew. Chem. **2001,** *113,* 2056–2075. doi:10.1002/1521-3757(20010601)113:11<2056::AID-ANGE2056>3.0.CO;2-W

41. Tornøe, C. W.; Christensen, C.; Meldal, M. *J. Org. Chem.* **2002,** *67,* 3057–3064. doi:10.1021/jo011148j
42. Compain, P.; Martin, O. R., Eds. *Iminosugars: from Synthesis to Therapeutic Applications;* Wiley & Sons: Chichester, 2007. doi:10.1002/9780470517437
43. Cardona, F.; Isoldi, G.; Sansone, F.; Casnati, A.; Goti, A. *J. Org. Chem.* **2012,** *77,* 6980–6988. doi:10.1021/jo301155p
See for a recent example of multivalent pyrrolidinols based oncalix[4]arene scaffolds.
44. Zuckermann, R. N.; Kerr, J. M.; Kent, S. B. H.; Moos, W. H. *J. Am. Chem. Soc.* **1992,** *114,* 10646–10647. doi:10.1021/ja00052a076

License and Terms

Beilstein Journal of Organic Chemistry

Carbohydrate PEGylation, an approach to improve pharmacological potency

M. Eugenia Giorgi, Rosalía Agusti and Rosa M. de Lederkremer*

Review

Open Access

Address:
CIHIDECAR-CONICET, Departamento de Química Orgánica, Facultad de Ciencias Exactas y Naturales, Universidad de Buenos Aires, Pabellón II, Ciudad Universitaria, 1428 Buenos Aires, Argentina

Email:
Rosa M. de Lederkremer* - lederk@qo.fcen.uba.ar

* Corresponding author

Keywords:
bioavailability; carbohydrates; conjugates; glycoPEGylation; multivalent glycosystems; multivalent PEGylation

Beilstein J. Org. Chem. **2014,** *10,* 1433–1444.
doi:10.3762/bjoc.10.147

Received: 25 February 2014
Accepted: 26 May 2014
Published: 25 June 2014

This article is part of the Thematic Series "Multivalent glycosystems for nanoscience".

Guest Editor: A. Casnati

Abstract

Conjugation with polyethylene glycol (PEG), known as PEGylation, has been widely used to improve the bioavailability of proteins and low molecular weight drugs. The covalent conjugation of PEG to the carbohydrate moiety of a protein has been mainly used to enhance the pharmacokinetic properties of the attached protein while yielding a more defined product. Thus, glycoPEGylation was successfully applied to the introduction of a PEGylated sialic acid to a preexisting or enzymatically linked glycan in a protein. Carbohydrates are now recognized as playing an important role in host–pathogen interactions in protozoal, bacterial and viral infections and are consequently candidates for chemotherapy. The short in vivo half-life of low molecular weight glycans hampered their use but methods for the covalent attachment of PEG have been less exploited. In this review, information on the preparation and application of PEG-carbohydrates, in particular multiarm PEGylation, is presented.

Introduction

In recent years, the modification of biotherapeutics by covalent conjugation with polyethyleneglycol (PEG) known as PEGylation has emerged as an effective strategy to improve the therapeutic potential of drugs through less frequent dosing [1-3]. PEG is a biologically inert, non-immnunogenic linear polyether diol that confers proteins greater solubility in aqueous and organic media. It is being used in pharmaceutical areas not only to enhance water solubility and reduce immunogenicity but also to increase in vivo circulation half-life by preventing enzymatic degradation and renal clearance [4]. Numerous examples of bioconjugation with PEG have been reported including, among others, proteins located in adenovirus coat for vaccine development [5], antibodies or antibody fragments to prolong their circulating half-lives in vivo [6] and selective alkylation and acylation of amino groups in a somatostatin analog using two different PEG reagents [7]. Also, PEGylation of low molecular weight drugs in order to increase solubility [8], prolong the in vivo action [9] or for targeting drug delivery [10] has been

described. The potent anti-inflammatory drug dexamethasone was coupled to a multifunctional PEG, prepared by a click reaction, for treatment of rheumatoid arthritis [11]. A heterobifunctional PEG has been conjugated with both paclitaxel, a potent anticancer drug, and alendronate, a bone-targeting biphosphonate, in order to obtain strong bone tropism and fast drug release [12]. An enzymatic method using a microbial transglutaminase was described for PEGylation of human growth hormone [13].

Glycans have been recognized as immunodominant epitopes in antigenic glycoconjugates [14]. Carbohydrates participate in molecular recognition events such as host–pathogen interactions, responsible for mammal infections, and are candidates for chemotherapy [15]. Moreover, synthesis of multivalent carbohydrate ligands provide higher affinity for receptors as described for Shiga-like toxins [16] and other systems [17].

Several excellent reviews have been published on PEGylation of proteins, including PEG-drugs in the market [2,18-21]. However, PEGylation of carbohydrate molecules has been less exploited and studies have been focused on polysaccharides or on carbohydrates linked to proteins. A review dedicated to PEGylated chitosan derivatives has been published [22].

In the present review we present different approaches used for modification of glycans by covalent conjugation with PEG reagents, in particular with multiarm PEGs, with the aim to increase the loading of the active sugar. Multivalent glycomolecules have proven to mediate or inhibit a variety of biological or pathological processes [17,23].

Review

Polyethylene glycol (PEG) derivatives

Polyethyleneglycol is an amphiphilic polymer consisting of repeating units of ethylene oxide which may be assembled in linear or branched structures to give a range of PEGs with different shapes and molecular weights (Figure 1). PEG must be activated for further conjugation by substitution of terminal OH by a functional group that could react with an appropriate site in the molecule to be conjugated, maintaining its biological activity. Examples of activated PEGs are shown in Figure 2. Multiarm PEGs have the advantage of presenting several sites for conjugation and, in the higher MW conjugates, the arms are far away enough from each other to allow independent interaction with the target site.

GlycoPEGylation of proteins

PEGylation of proteins is usually performed on the ε-amine group of lysine or on the unprotected α-amino of the *N*-terminal

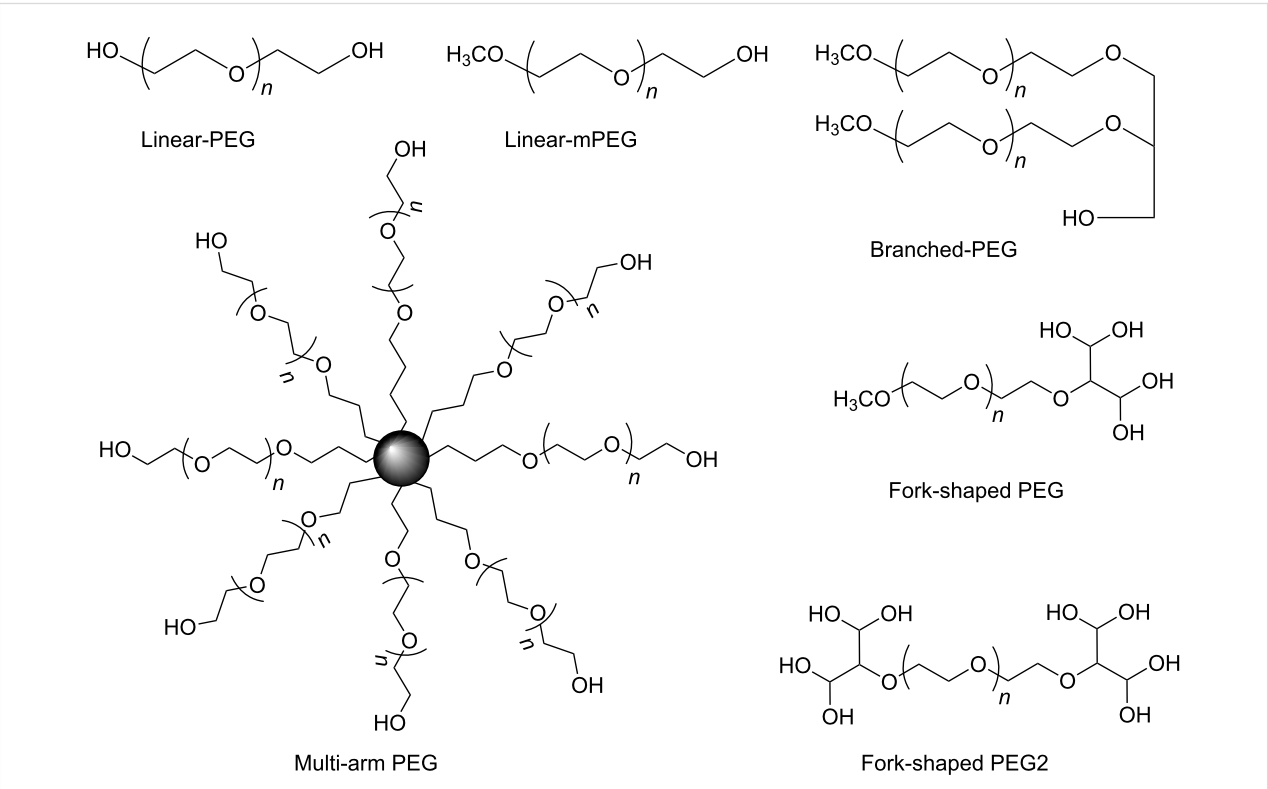

Figure 1: Types of PEG utilized for derivatization of drugs and peptides.

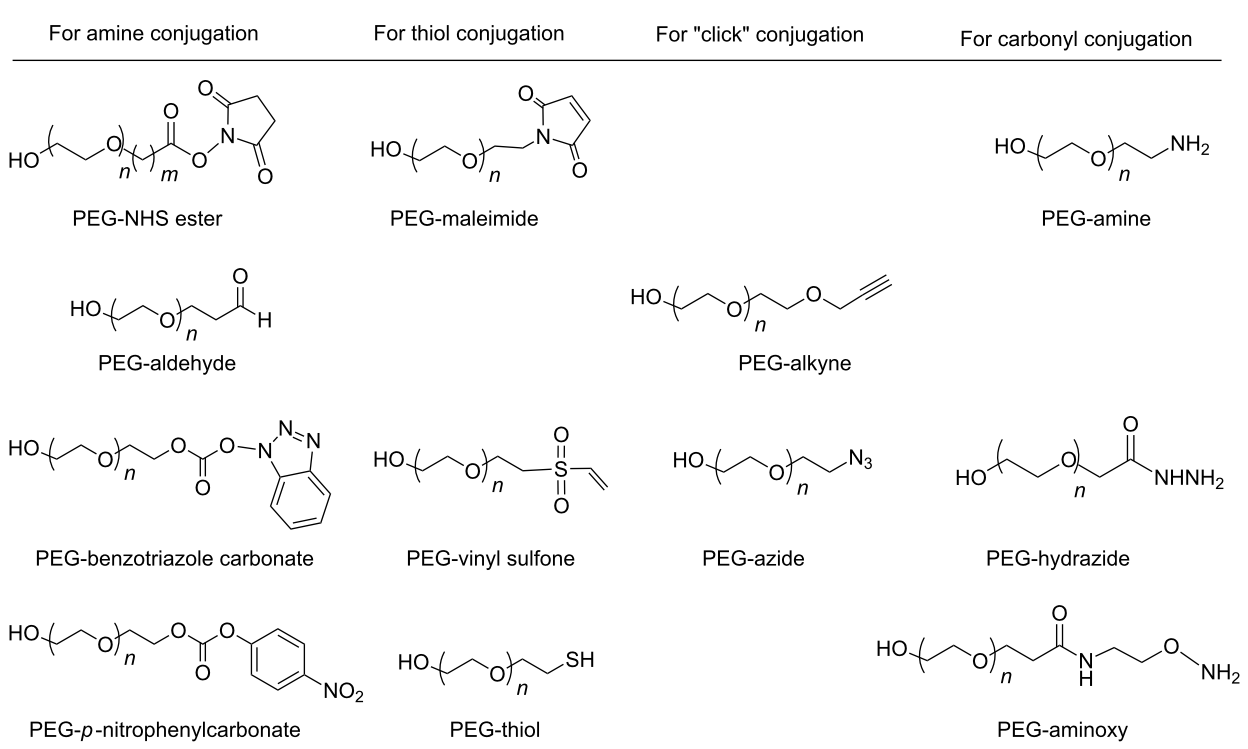

Figure 2: Activated PEG derivatives for conjugation.

amino acid using *N*-hydroxysuccinimidyl (NHS) activated PEGs or aldehyde PEGs. This conjugation leads to heterogeneous products, depending on the number of lysine residues in the molecule. Random PEGylation may have undesired steric effects, shielding active sites in the protein or disrupting its tertiary structure [24].

PEGylation may be also directed to the side-chain amide nitrogen of Asn. In order to improve the pharmacokinetic properties of a protein, *N*-PEGylation may be used additively to *N*-glycosylation since both modifications stabilize the protein by different mechanisms [25]. Also, glutamine residues on intact or chimeric proteins can be combined with alkylamino-PEG derivatives by the use of a transglutaminase [26].

Several methods have been developed for site-directed PEGylation. One of the most popular involves the reaction of the thiol group in one or two cysteine residues with appropriate PEG derivatives. The cysteine could be originally present in the protein or introduced by mutagenesis [27,28]. The C-terminus of the human growth hormone was PEGylated using a two-step strategy in which a linker was first incorporated by a carboxypeptidase-catalyzed transpeptidation and then used for the ligation of the PEG moiety [29]. A more specific and irreversible attachment of a single PEG molecule has been achieved by the use of a [3 + 2] cycloaddition reaction of an alkyne-bearing PEG reagent and an azide-functionalized tyrosine residue genetically incorporated on human superoxide dismutase-1 [30].

GlycoPEGylation, targeting carbohydrate sites, was conceived to produce a more homogeneous product with lower steric effects [31]. The strategy is based on the finding that certain PEGylated nucleotide-sugars are effectively transferred to a glycan acceptor by the corresponding glycosyltransferase.

A modified sialic acid PEGylated at the 5'-amino position in the CMP nucleotide (CMP-SA-5-NHCOCH$_2$NHPEG) can be transferred to a glycan acceptor in a glycoprotein by a sialyltransferase [32,33]. A chemoenzymatic method for its preparation is shown in Scheme 1. It is based on the coupling of Fmoc-glycylmannosamine with pyruvate catalized by SA-aldolase to afford the *N*-protected sialic acid. After reaction with CTP catalyzed by CMP-sialic acid synthetase, the nucleotide is deprotected and the free amine is utilized as a locus to PEG attachment.

The introduction of the PEGylated sialic acid into the glycoprotein takes place in two steps. First, an *O*-glycan is introduced enzymatically and second, PEGylated sialic acid is transferred to the glycan by a sialyltransferase. The serine or threonine residues in the *O*-glycosylation sites serve as acceptors for GalNAc using a convenient GalNAc transferase. This unit can

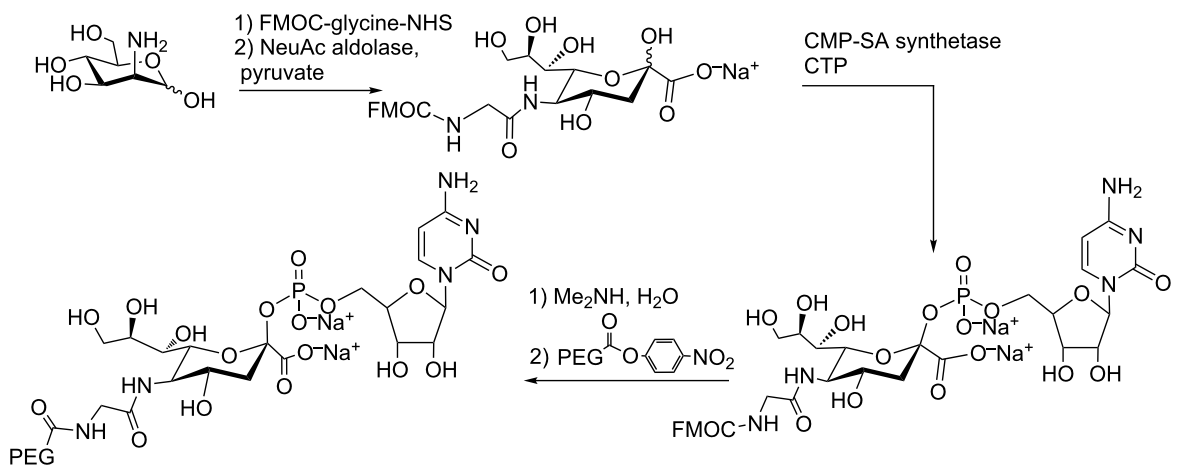

Scheme 1: Chemoenzymatic method for the preparation of PEG-CMP-SA, adapted from [32,33].

be galactosylated by a galactosyltransferase and both, the monosaccharide and the disaccharide, may be acceptors for PEG-sialic acid (Scheme 2). This technique was applied to polypeptides used clinically and has the advantage that it is easier to produce a recombinant protein using *E. coli* than to obtain the glycosylated forms in eukaryotic cells [31].

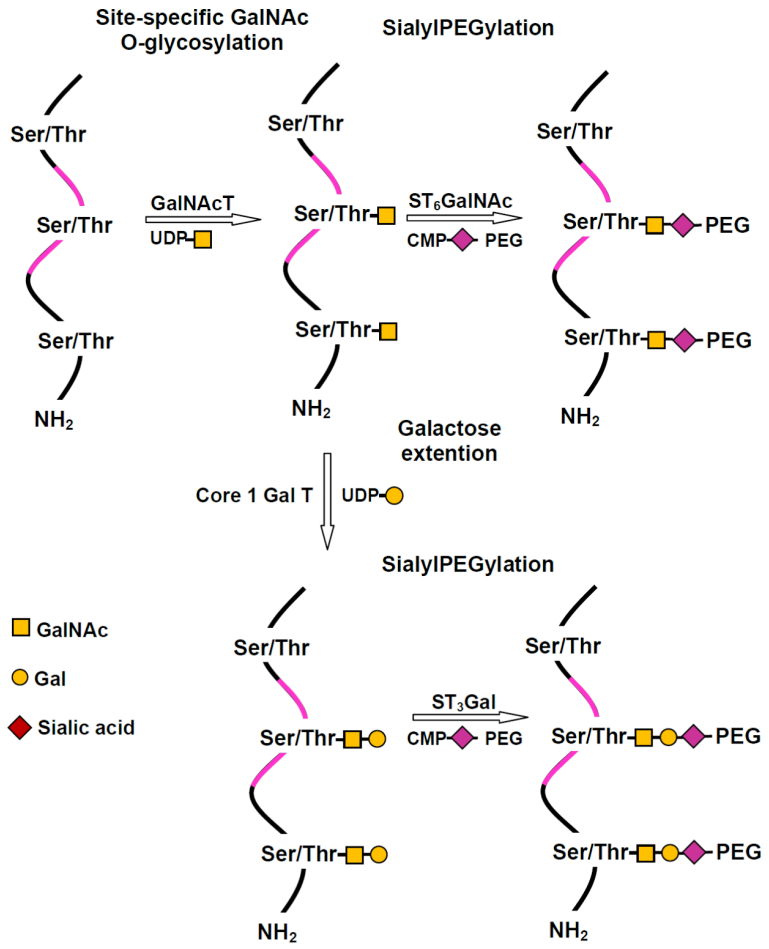

Scheme 2: GlycoPEGylation by sequential in vitro, enzyme mediated, *O*-glycosylation followed by transfer of PEGylated sialic acid, adapted from [31].

Chemical glycation of a protein and PEGylation after periodate oxidation

A small glycan may be also introduced by chemical ligation to an inaccessible aminoacid in a natural protein, like Cys^{34} in human serum albumin. The glycan may be oxidized by periodate to afford aldehyde groups for selective multiple coupling with a PEG hydrazide (PEG-Hz), as shown in Scheme 3 [34]. Analysis of the PEGylated species showed more than 90% conversion, whereas less than 30% of the protein was PEGylated by direct conjugation of the albumin with commercial PEG-maleimide. The PEG-Hz may undergo pH controlled hydrolysis which also depends on the number of units in the linked sugar. Therefore release of the active protein may be controlled by the structure of the sugar linker.

PEGylation of native glycosylated proteins

PEGylation of native glycoproteins may be performed by enzymatic or chemical modification of the glycan.

a) Enzymatic modification of the glycan

Enzymatic PEGylation of a glycoprotein can be performed in three steps. First, the sialic acid is removed from the native protein with a sialidase and subsequently Sia-PEG is transfered to the uncovered terminal Gal units of the linked glycan taking

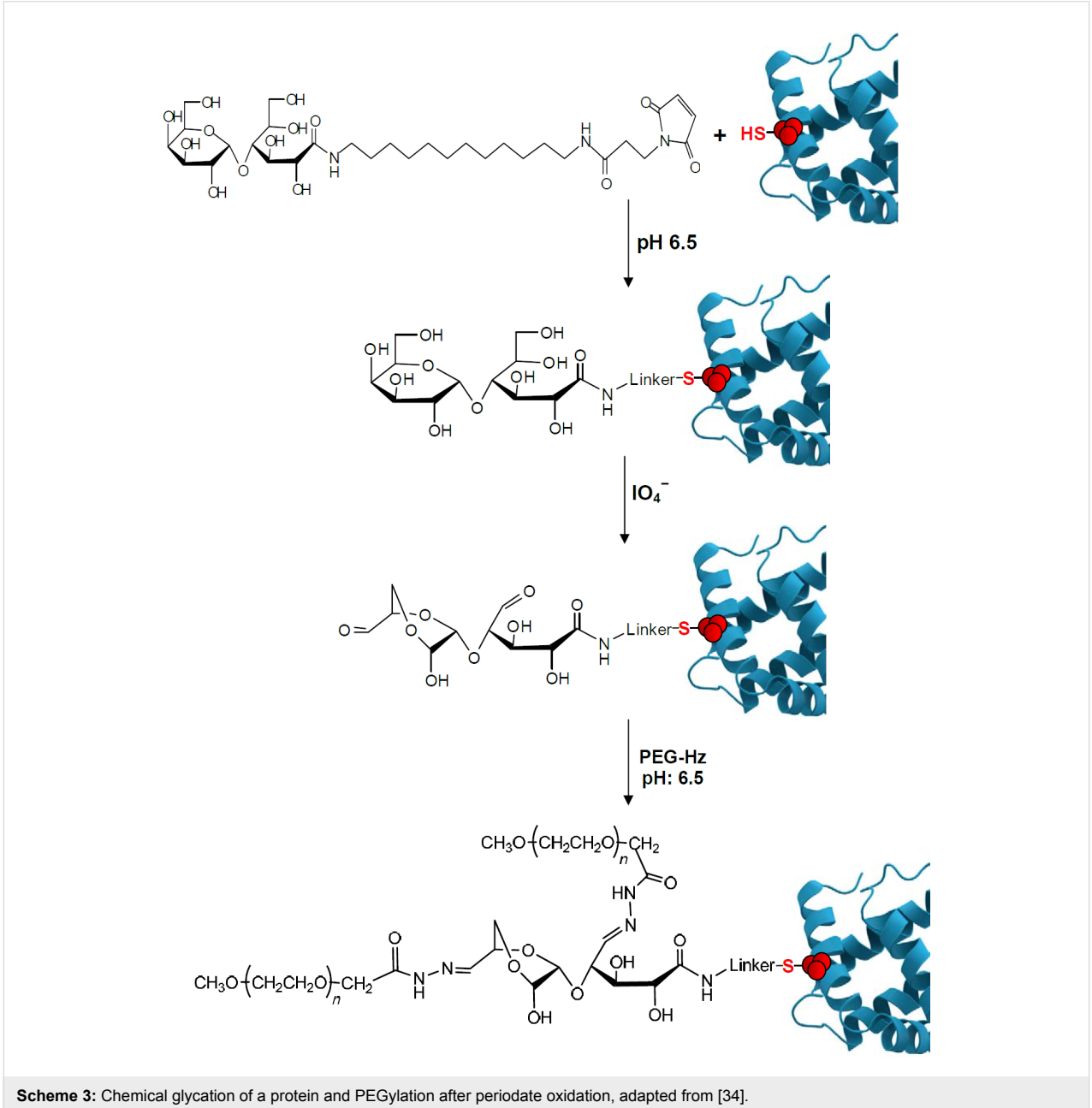

Scheme 3: Chemical glycation of a protein and PEGylation after periodate oxidation, adapted from [34].

advantage of the substrate promiscuity of the sialyltransferase ST3GalIII [35,36]. The reaction is kinetically controlled and the number of PEGs added depends on the reaction time. Finally, the unreacted galactose residues should be blocked with sialic acid to avoid hepatic clearance by the asialoglycoprotein receptor. More recently, the same group modified genetically the coagulation factor VIII used to treat Hemophilia A, in order to obtain a unique *O*-linked glycan for selective modification with PEGylated sialic acid [37].

Alternatively, a terminal galactose may be oxidized at C-6 with galactose oxidase to create the reactive site in the glycan that could react with an activated PEG (Scheme 4A). As galactose is usually substituted with sialic acid, the latter procedure was applied before or after sialidase treatment [38].

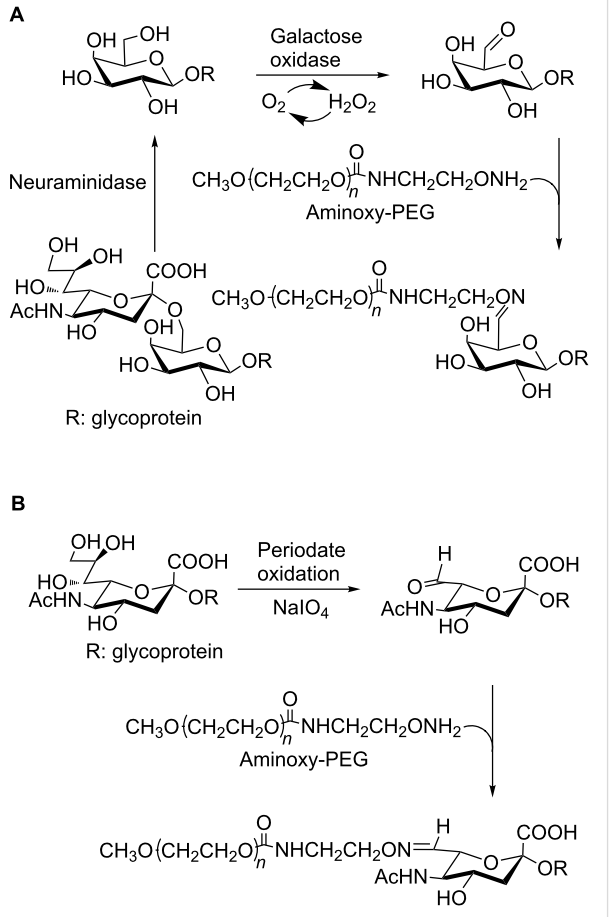

Scheme 4: PEGylation of native glycosylated proteins after modification of the glycan. (A) Enzymatic modification of the glycan; (B) Chemical modification of the glycan, adapted from [38].

b) PEGylation after chemical modification of the sugar chain of a glycoprotein

In this approach, a reactive group is created in the sugar of an *O*- or *N*-linked glycan by a chemical modification. The terminal residue of the *N*-linked carbohydrate in ricin A-chain has been PEGylated by mild oxidation with periodate followed by reaction with hydrazide-derivatized PEG [39]. The carbohydrate-specifically modified ricin showed better pharmacokinetic properties than the peptide amino-PEGylated or the unmodified ricin. The same technique was applied to glucose oxidase (GOx), a glycosylated dimeric protein. In this case the hydrazone was further stabilized by reduction with cyanoborohydride to afford a bioconjugate with retention of its activity as a biosensor of glucose [40]. A similar strategy was applied to the recombinant human thyroid-stimulating hormone (rhTSH, Thyrogen). Terminal sialic acids were oxidized with sodium periodate to generate aldehydes, which reacted with aminoxi-PEGs (Scheme 4B). The use of this PEGylating agent, instead of hydrazide-PEGs, generated a more stable oxime linkage with the carbohydrate aldehydes. Similar to the other gonadotropins, TSH is a glycosylated protein, and the role of the *N*-linked oligosaccharides is well established. The effect of PEG size and mono- vs multi-PEGylation was compared both in vitro and in vivo. The best performing of the products, a 40-kDa mono-PEGylated sialic acid-mediated conjugate, exhibited a 5-fold lower affinity which was however compensated by a 23-fold increase of circulation half-life [38].

PEGylation of low-molecular weight carbohydrates: Enzymatic esterification of two hydroxy methylene groups present in pentofuranose derivatives with a PEG dimethyl ester yielded sugar-PEG copolymers used for drug encapsulation. The carbohydrate monomer was obtained by a multistep synthesis starting from the easily available diacetone glucose (Scheme 5) [41].

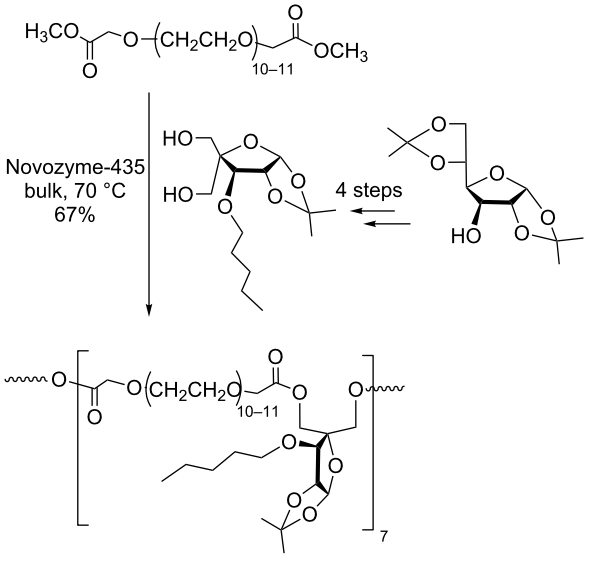

Scheme 5: PEGylation of a pentofuranose derivative, adapted from [41].

Galactose has been PEGylated and introduced in the surface of polystyrene nanoparticles in order to increase the interaction with galactose receptors. *p*-Aminophenyl β-D-galactopyranoside was coupled with a bifunctional PEG activated on one end with NHS for the combination with the aniline and a FMOC-protected amino group on the other end. After deprotection, the amine reacted with the carboxylic groups on the surface of the nanoparticles (Scheme 6) [42]. A similar approach was developed recently using poly(amidoamine) dendrimers for selective delivery of chemotherapeutic agents into hepatic cancer cells [43].

Mannose was also PEGylated in order to target drugs specifically to mannose receptors present in liver endothelial cells. Mannosyl PEGylated polyethylenimine (PEI) conjugates were synthesized either by direct coupling the mannose and the PEG chain to the PEI backbone (Figure 3A) or by attaching the mannose to PEI via a PEG chain spacer (Figure 3B). This system was used to deliver small interfering RNA (siRNA) into a murine macrophage cell line [44].

Mannose residues as their 2-aminoethyl glycosides were attached by reductive amination to the surface of copolymer

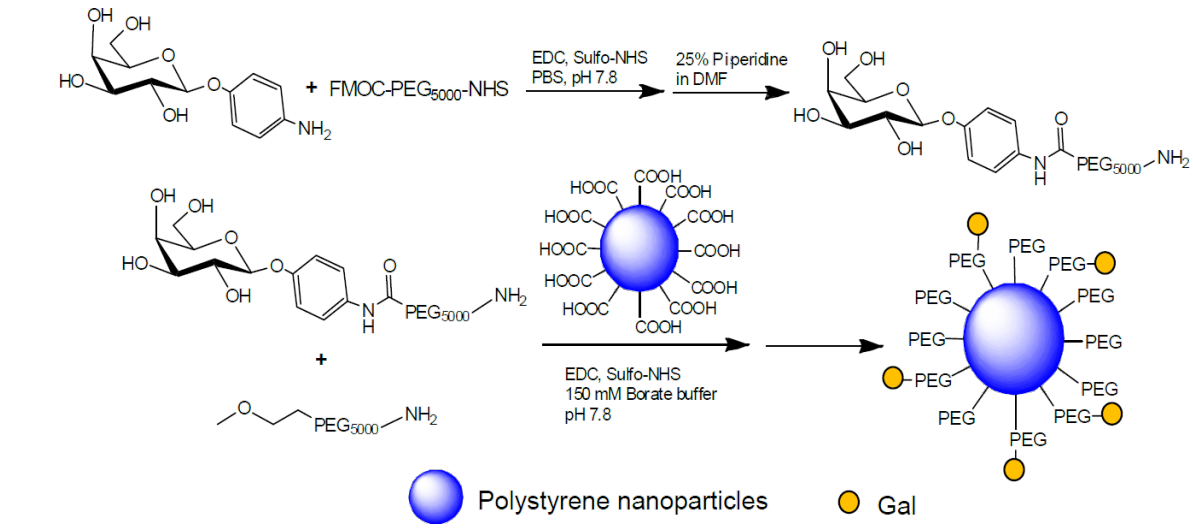

Scheme 6: Galactosyl PEGylation of polystyrene nanoparticles, adapted from [42].

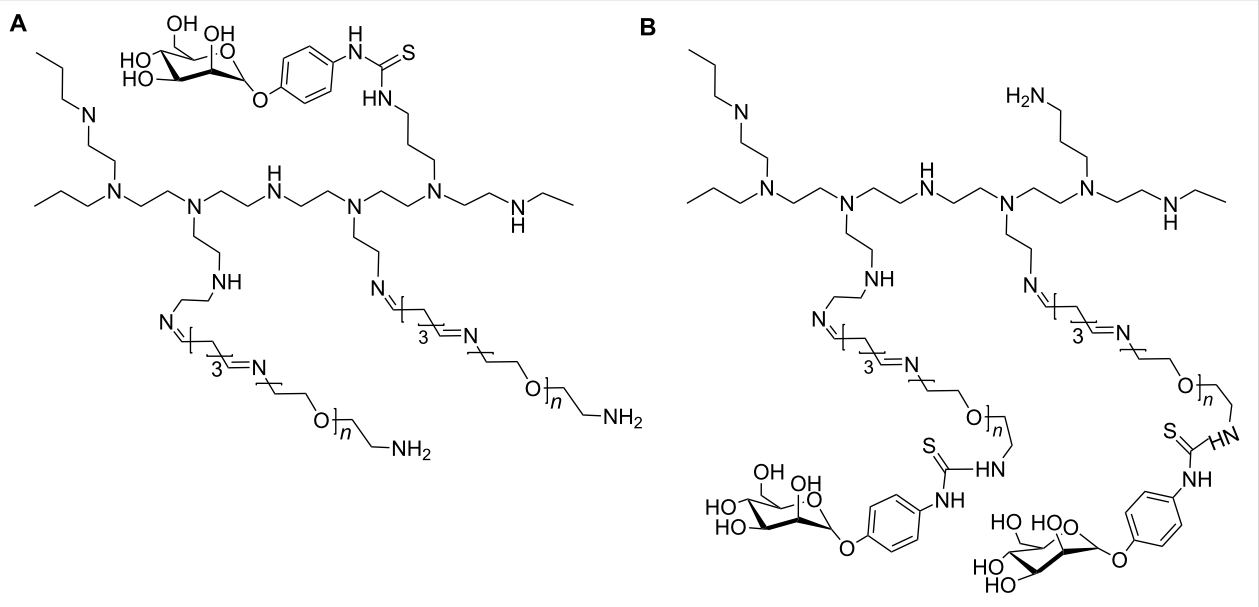

Figure 3: Mannosyl PEGylated polyethylenimine for delivery systems. (A) Mannose and PEG are independently linked to the PEI backbone; (B) Mannose is attached to PEI via a PEG chain, adapted from [44].

micelles of PEG with poly-ε-caprolactone for targeting dendritic cells and macrophages (Figure 4) [45]

Both mannose and galactose were attached to PEGylated nanoparticles by click-chemistry between their propargyl glycosides and a gold nanoparticles derivatized with an azide-functionalized PEG [46]. Also, several unprotected carbohydrate units of mannose, fucose or lactose, have been incorporated into the surface of PEGylated dendritic polymers by means of click chemistry. The larger dendrimer generations have demonstrated an increased capacity to aggregate lectins [47].

Analogs of lactose have been reported as inhibitors of the enzyme trans-sialidase (TcTS) [48], a virulence factor of *Trypanosoma cruzi* [49-51]. It was shown that lactitol prevented apoptosis caused by TcTS although it is rapidly eliminated from the circulatory system [52]. With the aim to improve bioavailability, PEGylation of lactose analogs was performed using two approaches, both depending on the formation of an amide bond. In one case the amino group was provided by the sugar and the carboxylic acid by a NHS-activated PEG and in the other approach an amino-functionalized PEG reacted with lactobionolactone (Scheme 7) [53].

Using linear PEGs of MW 5000 Da, no enhancement in the permanence in blood was observed. However, improved biovailability with retention of inhibition of TcTS was achieved by PEGylation with multiarm PEGs of MW 40000 (Scheme 8) [54]. In these complex conjugates, the degree of substitution is determined by ^{1}H NMR spectroscopy. The identification of signals that disappear or are shifted when conjugation takes place, together with the appearance of new signals due to the sugar in well-separated regions of the spectrum are used to confirm the extent of derivatization of the multiarm PEGs.

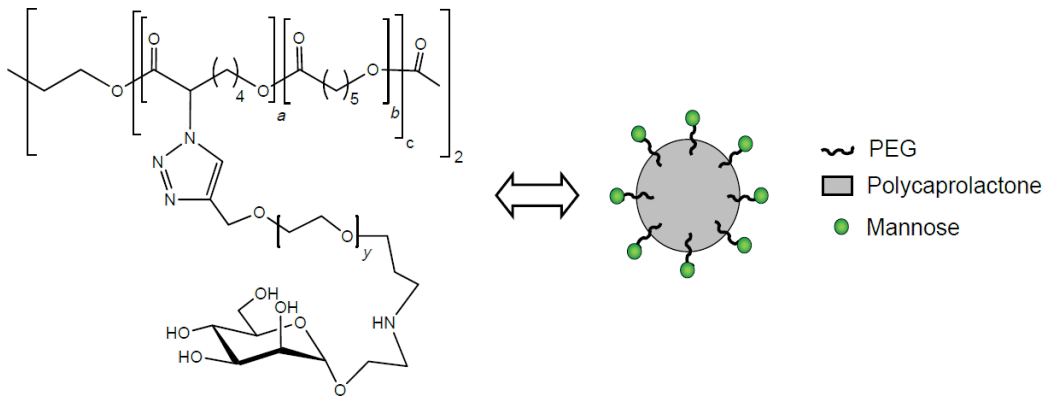

Figure 4: PEGylated mannose derivatives, adapted from [45].

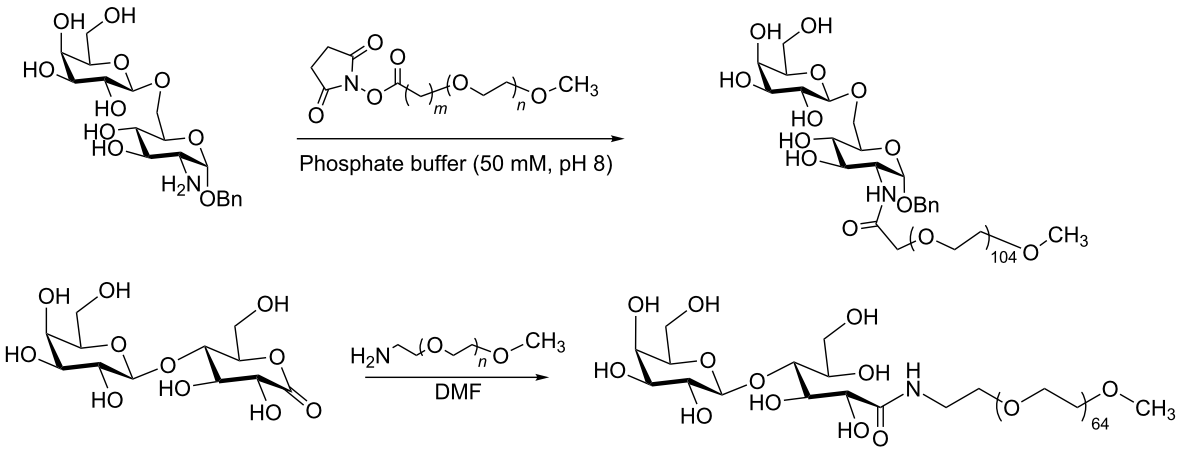

Scheme 7: PEGylation of lactose analogs [53].

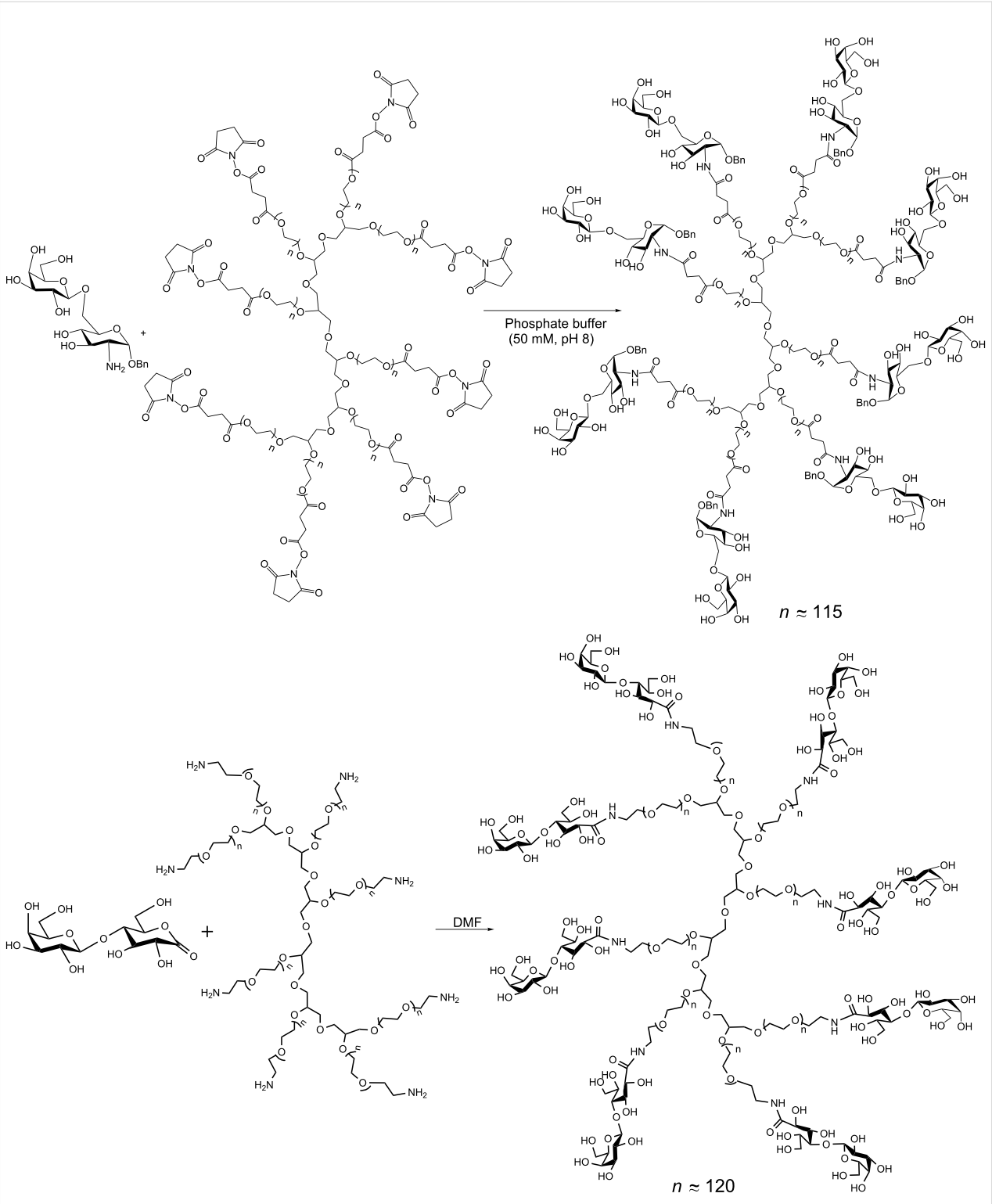

Scheme 8: Conjugation of lactose analogs with dendritic PEGs [54].

PEGylation of polysaccharides: PEGylation of chitosan and chitosan derivatives for pharmaceutical applications was described [22]. Chitosan is the polysaccharide obtained from the abundant chitin by alkali or enzymatic degradation. It consists of a backbone of β-(1→4)-linked D-glucosamine units with a variable degree of *N*-acetylation. The protonated amino

groups of chitosan favor interaction with negatively charged cellular surfaces. The amino groups of chitosan may be derivatized with PEG chains, thus modifying the physicochemical properties. Chitosan was first modified in the amino group of the glucosamine units with a PEG-aldehyde to yield an imine (Schiff base), which was subsequently reduced to PEG-g-chitosan with sodium cyanoborohydride [55], allowing retention of net charge. PEGylation can also be accomplished by condensation of the free amino groups with activated PEGs, such as PEG-NHS or PEG-*p*-nitrophenyl carbonate, converting the protonable amines into neutral amide or carbamate linkers.

Even though PEGylation of chitosan via the amino group is the most commonly used method a number of examples of polysaccharide derivatisation on the hydroxy groups have been reported. Chitosan-*O*-poly(ethylene glycol) graft copolymers were synthesized from *N*-phthaloylchitosan by etherification with poly(ethylene glycol) monomethyl ether (mPEG) iodide obtaining different degrees of *O*-substitution [56]. Several strategies were designed to obtain regioselective PEGylation at C-6 of the glucosamine unit [57]. Other methods of PEGylation included, among others, free radical polymerization of C-6 of the glucosamine residues with poly(ethylenglycol) acrylate [58]; free-radical polymerization of C-1 of glucosamine with mPEG [59] and 1,3-dipolar cycloaddition between the azide of an *N*-azidated chitosan and mPEG derivatives containing a triazolyl moiety [60].

Chitosan, partially substituted with lactobionic acid, bearing a galactose, provides a ligand for the asialoglycoprotein receptor of liver cells. Lactobionic acid formed an amide bond with the glucosamine residue, and the non-substituded amino groups of the galactosylated chitosan (GC) were further coupled with activated hydrophilic PEG to enhance its stability (Figure 5) [61].

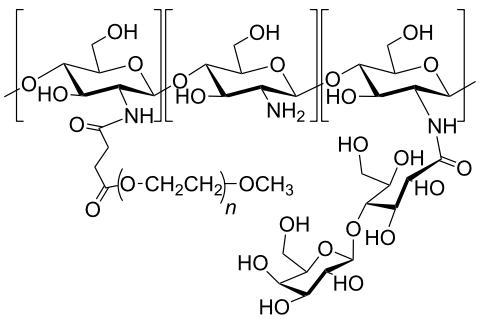

Figure 5: PEGylated chitosan derivative, adapted from [61].

Bifunctional PEGs were used to introduce a bioactive molecule, for instance biotine, coumarin, cholesterol or mannose into the distal end of a PEG-chitosan complex (Figure 6) [62].

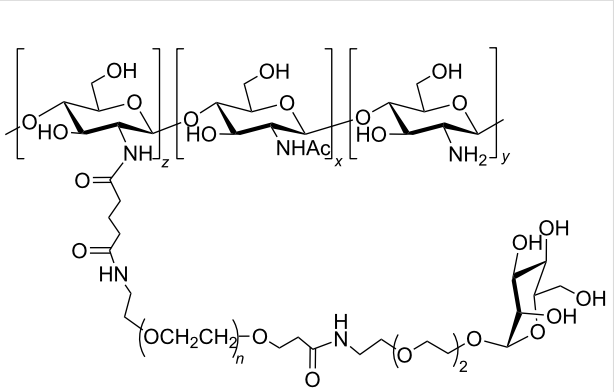

Figure 6: Chitosan/PEG functionalized with a mannose at the distal end, adapted from [62].

Fructans have been PEGylated by reaction of hydroxy-activated polysaccharides with amino-terminated methoxy PEGs. The reaction was applied to inulin [63] and to a polysaccharide from Radix Ophiopogonis [64] for improving their pharmacokinetic properties. A similar activation of the sugar has been previously applied to a dextran for further PEGylation. Hydrogels with supramolecular structures have been obtained by inclusion complexation of the PEG grafted dextrans with α-cyclodextrins. The unique thermoreversible sol-transition properties of the gels were considered interesting for drug delivery applications [65].

Conclusion

The advantage of PEGylation of glycan structures attached to proteins is the possibility to restrict the reaction to the glycosylated site affording a product with the benefits that PEGylation can impart without the loss of activity due to random multistep PEGylation of proteins. The examples presented in this review on the PEGylation of carbohydrates show improvement of some properties such as bioavailability of drugs, in particular enzyme inhibitors, or creation of polymers with encapsulating properties for drugs. Apparently, the benefits of PEGylation were yet not extended to carbohydrate based drugs in the market. In particular, multiarm PEGylation with more available sites for glycan linking can be exploited for improvement of interaction of carbohydrates with cell receptors. We hope that this review on sugar PEGylation will provoke further studies on the subject.

Acknowledgements

This work was supported by grants from Agencia Nacional de Promoción Científica y Tecnológica (ANPCyT), National Research Council (CONICET) and Universidad de Buenos Aires. R. M. de Lederkremer and R. Agustí are research members of CONICET.

References

1. Fishburn, C. S. *J. Pharm. Sci.* **2008,** *97,* 4167–4183. doi:10.1002/jps.21278
2. Veronese, F. M.; Pasut, G. *Drug Discovery Today* **2008,** *5,* e57–e64. doi:10.1016/j.ddtec.2009.02.002
3. Jevševar, S.; Kunstelj, M.; Porekar, V. G. *Biotechnol. J.* **2010,** *5,* 113–128. doi:10.1002/biot.200900218
4. Greenwald, R. B. *J. Controlled Release* **2001,** *74,* 159–171. doi:10.1016/S0168-3659(01)00331-5
5. Wonganan, P.; Croyle, M. A. *Viruses* **2010,** *2,* 468–502. doi:10.3390/v2020468
6. Chapman, A. P. *Adv. Drug Delivery Rev.* **2002,** *54,* 531–545. doi:10.1016/S0169-409X(02)00026-1
7. Morpurgo, M.; Monfardini, C.; Hofland, L. J.; Sergi, M.; Orsolini, P.; Dumont, J. M.; Veronese, F. M. *Bioconjugate Chem.* **2002,** *13,* 1238–1243. doi:10.1021/bc0100511
8. Greenwald, R. B.; Pendri, A.; Conover, C. D.; Lee, C.; Choe, Y. H.; Gilbert, C.; Martinez, A.; Xia, J.; Wu, D.; Hsue, M. *Bioorg. Med. Chem.* **1998,** *6,* 551–562. doi:10.1016/S0968-0896(98)00005-4
9. Marcus, Y.; Sasson, K.; Fridkin, M.; Shechter, Y. *J. Med. Chem.* **2008,** *51,* 4300–4305. doi:10.1021/jm8002558
10. Dixit, V.; Van den Bossche, J.; Sherman, D.; Thompson, D. H.; Andres, R. P. *Bioconjugate Chem.* **2006,** *17,* 603–609. doi:10.1021/bc050335b
11. Liu, X.-M.; Quan, L.-d.; Tian, J.; Laquer, F. C.; Coborowski, P.; Wang, D. *Biomacromolecules* **2010,** *11,* 2621–2628. doi:10.1021/bm100578c
12. Clementi, C.; Miller, K.; Mero, A.; Satchi-Fainaro, R.; Pasut, G. *Mol. Pharmaceutics* **2011,** *8,* 1063–1072. doi:10.1021/mp2001445
13. Mero, A.; Schiavon, M.; Veronese, F. M.; Pasut, G. *J. Controlled Release* **2011,** *154,* 27–34. doi:10.1016/j.jconrel.2011.04.024
14. Song, X.; Heimburg-Molinaro, J.; Cummings, R. D.; Smith, D. F. *Curr. Opin. Chem. Biol.* **2014,** *18,* 70–77. doi:10.1016/j.cbpa.2014.01.001
15. Kawasaki, N.; Itoh, S.; Hashii, N.; Takakura, D.; Qin, Y.; Huang, X.; Yamaguchi, T. *Biol. Pharm. Bull.* **2009,** *32,* 796–800. doi:10.1248/bpb.32.796
16. Kitov, P. I.; Sadowska, J. M.; Mulvey, G.; Armstrong, G. D.; Ling, H.; Pannu, N. S.; Read, R. J.; Bundle, D. R. *Nature* **2000,** *403,* 669–672. doi:10.1038/35001095
17. Bernardi, A.; Jiménez-Barbero, J.; Casnati, A.; De Castro, C.; Darbre, T.; Fieschi, F.; Finne, J.; Funken, H.; Jaeger, K.; Lahmann, M.; Lindhorst, T. K.; Marradi, M.; Messner, P.; Molinaro, A.; Murphy, P. V.; Nativi, C.; Oscarson, S.; Penadés, S.; Peri, F.; Pieters, R. J.; Renaudet, O.; Reymond, J.; Richichi, B.; Rojo, J.; Sansone, F.; Schaffer, C.; Turnbull, W. B.; Velasco-Torrijos, T.; Vidal, S.; Vincent, S.; Wennekes, T.; Zuilhof, H.; Imberty, A. *Chem. Soc. Rev.* **2013,** *42,* 4709–4727. doi:10.1039/c2cs35408j
18. Pasut, G.; Veronese, F. M. *J. Controlled Release* **2012,** *161,* 461–472. doi:10.1016/j.jconrel.2011.10.037
19. Joralemon, M. J.; McRae, S.; Emrick, T. *Chem. Commun.* **2010,** *46,* 1377–1393. doi:10.1039/b920570p
20. Banerjee, S. S.; Aher, N.; Patil, R.; Khandare, J. J. *Drug Delivery* **2012,** *2012,* No. 103973. doi:10.1155/2012/103973
21. Li, W.; Zhan, P.; De Clercq, E.; Lou, H.; Liu, X. *Prog. Polym. Sci.* **2013,** *38,* 421–444. doi:10.1016/j.progpolymsci.2012.07.006
22. Casettari, L.; Vllasaliu, D.; Castagnino, E.; Stolnik, S.; Howdle, S.; Illum, L. *Prog. Polym. Sci.* **2012,** *37,* 659–685. doi:10.1016/j.progpolymsci.2011.10.001
23. Chabre, Y. M.; Roy, R. Design and Creativity in Synthesis of multivalent neoglycoconjugates. In *Adv. Carbohydr. Chem. Biochem.;* Horton, D., Ed.; Academic Press Elsevier: Amsterdam, The Netherlands, 2010; Vol. 63, pp 165–393.
24. Veronese, F. M.; Caliceti, P.; Schiavon, O.; Sartore, L. Preparation and Properties of Monomethoxypoly(Ethylene Glycol)-Modified Enzymes for Therapeutic Applications. In *Poly(Ethylene Glycol) Chemistry: Biotechnical and Biomedical Applications;* Milton Harris, J., Ed.; Topics in Applied Chemistry; Plenum Press: New York, NY, USA, 1992; pp 127–137. doi:10.1007/978-1-4899-0703-5_9
25. Price, J. L.; Powers, E. T.; Kelly, J. W. *ACS Chem. Biol.* **2011,** *6,* 1188–1192. doi:10.1021/cb200277u
26. Sato, H. *Adv. Drug Delivery Rev.* **2002,** *54,* 487–504. doi:10.1016/S0169-409X(02)00024-8
27. Tsutsumi, Y.; Onda, M.; Nagata, S.; Lee, B.; Kreitman, R. J.; Pastan, I. *Proc. Natl. Acad. Sci. U. S. A.* **2000,** *97,* 8548–8553. doi:10.1073/pnas.140210597
28. Kuan, C.; Wang, Q.; Pastan, I. *J. Biol. Chem.* **1994,** *269,* 7610–7616.
29. Peschke, B.; Zundel, M.; Bak, S.; Clausen, T. R.; Blume, N.; Pedersen, A.; Zaragoza, F.; Madsen, K. *Bioorg. Med. Chem.* **2007,** *15,* 4382–4395. doi:10.1016/j.bmc.2007.04.037
30. Deiters, A.; Cropp, A. T.; Summerer, D.; Mukherji, M.; Schultz, P. G. *Bioorg. Med. Chem. Lett.* **2004,** *14,* 5743–5745. doi:10.1016/j.bmcl.2004.09.059
31. DeFrees, S.; Wang, Z.; Xing, R.; Scott, A. E.; Wang, J.; Zopf, D.; Gouty, D. L.; Sjoberg, E. R.; Panneerselvam, K.; Brinkman-Van der Linden, E. C. M.; Bayer, R. J.; Tarp, M. A.; Clausen, H. *Glycobiology* **2006,** *16,* 833–843. doi:10.1093/glycob/cwl004
32. DeFrees, S.; Zopf, D.; Bayer, R. J.; Bowe, C.; Hakes, D.; Chen, X. GlycoPEGylation methods and protein/peptides produced by the methods. U.S. Patent 2004/0132640 A1, July 8, 2004.
33. DeFrees, S.; Felo, M. Nucleotide sugar purification using membranes. U.S. Patent WO2007056191 A2, May 18, 2007.
34. Salmaso, S.; Semenzato, A.; Bersani, S.; Mastrotto, F.; Scomparin, A.; Caliceti, P. *Eur. Polym. J.* **2008,** *44,* 1378–1389. doi:10.1016/j.eurpolymj.2008.02.021
35. Østergaad, H.; Bjelke, J. R.; Hansen, L.; Petersen, L. C.; Pedersen, A. A.; Elm, T.; Møller, F.; Hermit, M. B.; Holm, P. K.; Krogh, T. N.; Petersen, J. M.; Ezban, M.; Sørensen, B. B.; Andersen, M. D.; Agersø, H.; Ahamdian, H.; Balling, K. W.; Christiansen, M. L. S.; Knobe, K.; Nichols, T. C.; Bjørn, S. E.; Tranholm, M. *Blood* **2011,** *118,* 2333–2341. doi:10.1182/blood-2011-02-336172
36. Stennicke, H. R.; Østergaad, H.; Bayer, R. J.; Kalo, M. S.; Kinealy, K.; Holm, P. K.; Sørensen, B. B.; Zopf, D.; Bjørn, S. E. *Thromb. Haemostasis* **2008,** *100,* 920–928. doi:10.1160/TH08-04-0268
37. Stennicke, H. R.; Kjalke, M.; Karpf, D. M.; Balling, K. W.; Johasen, P. B.; Elm, T.; Øvlisen, K.; Möller, F.; Holmberg, H. L.; Gudme, C. N.; Persson, E.; Hilden, I.; Pelzer, H.; Rahbek-Nielsen, H.; Jespersgaard, C.; Bogsnes, A.; Pedersen, A. A.; Kristensen, A. K.; Peschke, B.; Kappers, W.; Rode, K.; Thim, L.; Tranholm, M.; Ezban, M.; Olsen, E. H. N.; Bjørn, S. E. *Blood* **2013,** *121,* 2108–2116. doi:10.1182/blood-2012-01-407494
38. Park, A.; Honey, D. M.; Hou, L.; Bird, J. J.; Zarazinski, C.; Searles, M.; Braithwaite, C.; Kingsbury, J. S.; Kyazike, J.; Culm-Merdek, K.; Greene, B.; Stefano, J. E.; Qiu, H.; McPherson, J. M.; Pan, C. Q. *Endocrinology* **2013,** *154,* 1373–1383. doi:10.1210/en.2012-2010

39. Youn, Y. S.; Na, D. H.; Yoo, S. D.; Song, S.-C.; Lee, K. C. *Int. J. Biochem. Cell Biol.* **2005,** *37,* 1525–1533. doi:10.1016/j.biocel.2005.01.014
40. Ritter, D. W.; Roberts, J. R.; McShane, M. J. *Enzyme Microb. Technol.* **2013,** *52,* 279–285. doi:10.1016/j.enzmictec.2013.01.004
41. Bhatia, S.; Mohr, A.; Mathur, D.; Parmar, V. S.; Haag, R.; Prasad, A. K. *Biomacromolecules* **2011,** *12,* 3487–3498. doi:10.1021/bm200647a
42. Popielarski, S. R.; Pun, S. H.; Davis, M. E. *Bioconjugate Chem.* **2005,** *16,* 1063–1070. doi:10.1021/bc050113d
43. Medina, S. H.; Tiruchinapally, G.; Chevliakov, M. V.; Yuksel Durmaz, Y.; Stender, R. N.; Ensminger, W. D.; Shewach, D. S.; ElSayed, M. E. H. *Adv. Healthcare Mater.* **2013,** *2,* 1337–1350. doi:10.1002/adhm.201200406
44. Kim, N.; Jiang, D.; Jacobi, A. M.; Lennox, K. A.; Rose, S. D.; Behlke, M. A.; Salem, A. K. *Int. J. Pharm.* **2012,** *427,* 123–133. doi:10.1016/j.ijpharm.2011.08.014
45. Freichels, H.; Alaimo, D.; Auzély-Velty, R.; Jérôme, C. *Bioconjugate Chem.* **2012,** *23,* 1740–1752. doi:10.1021/bc200650n
46. Richards, S.; Fullam, E.; Besra, G. S.; Gibson, M. I. *J. Mater. Chem. B* **2014,** *2,* 1490–1498. doi:10.1039/c3tb21821j
47. Fernandez-Megia, E.; Correa, J.; Riguera, R. *Biomacromolecules* **2006,** *7,* 3104–3111. doi:10.1021/bm060580d
48. Agusti, R.; Paris, G.; Ratier, L.; Frasch, A. C. C.; de Lederkermer, R. M. *Glycobiology* **2004,** *14,* 659–670. doi:10.1093/glycob/cwh079
49. Frasch, A. C. C. *Parasitol. Today* **2000,** *16,* 282–286. doi:10.1016/S0169-4758(00)01698-7
50. Tomlinson, S.; Pontes de Carvalho, L. C.; Vandekerckhove, F.; Nussenzweig, V. *J. Immunol.* **1994,** *153,* 3141–3147.
51. Pereira-Chioccola, V. L.; Acosta-Serrano, A.; Correira de Almeida, I.; Ferguson, M. A.; Souto-Padron, T.; Rodrigues, M. M.; Travassos, L. R.; Schenkman, S. *J. Cell Sci.* **2000,** *113,* 1299–1307.
52. Mucci, J.; Risso, M. G.; Leguizamón, M. S.; Frasch, A. C. C.; Campetella, O. *Cell. Microbiol.* **2006,** *8,* 1086–1095. doi:10.1111/j.1462-5822.2006.00689.x
53. Giorgi, M. E.; Ratier, L.; Agusti, R.; Frasch, A. C.; de Lederkremer, R. M. *Glycoconjugate J.* **2010,** *27,* 549–559. doi:10.1007/s10719-010-9300-7
54. Giorgi, M. E.; Ratier, L.; Agusti, R.; Frasch, A. C.; de Lederkremer, R. M. *Glycobiology* **2012,** *22,* 1363–1373. doi:10.1093/glycob/cws091
55. Harris, J. M.; Struck, E. C.; Case, M. G.; Paley, S.; van Alstine, J. M.; Brooks, D. E. *J. Polym. Sci., Polym. Chem. Ed.* **1984,** *22,* 341–352. doi:10.1002/pol.1984.170220207
56. Gorochovceva, N.; Makuška, R. *Eur. Polym. J.* **2004,** *40,* 685–691. doi:10.1016/j.eurpolymj.2003.12.005
57. Makuška, R.; Gorochovceva, N. *Carbohydr. Polym.* **2006,** *64,* 319–327. doi:10.1016/j.carbpol.2005.12.006
58. Shantha, K. L.; Harding, D. R. K. *Carbohydr. Polym.* **2002,** *48,* 247–253. doi:10.1016/S0144-8617(01)00244-2
59. Kong, X.; Li, X.; Wang, X.; Liu, T.; Gu, Y.; Guo, G.; Luo, F.; Zhao, X.; Wei, Y.; Qian, Z. *Carbohydr. Polym.* **2010,** *79,* 170–175. doi:10.1016/j.carbpol.2009.07.037
60. Kulbokaite, R.; Ciuta, G.; Netopilik, M.; Makuska, R. *React. Funct. Polym.* **2009,** *69,* 771–778. doi:10.1016/j.reactfunctpolym.2009.06.010
61. Park, I. K.; Kim, T. H.; Park, Y. H.; Shin, B. A.; Choi, E. S.; Chowdhury, E. H.; Akaike, T.; Cho, C. S. *J. Controlled Release* **2001,** *76,* 349–362. doi:10.1016/S0168-3659(01)00448-5
62. Fernandez-Megia, E.; Novoa-Carballal, R.; Quiñoá, E.; Riguera, R. *Biomacromolecules* **2007,** *8,* 833–842. doi:10.1021/bm060889x
63. Sun, G.; Lin, X.; Wang, Z.; Feng, Y.; Xu, D.; Shen, L. J. *J. Biomater. Sci., Polym. Ed.* **2011,** *22,* 429–441. doi:10.1163/092050610X487729
64. Lin, X.; Wang, S.; Jiang, Y.; Wang, Z.-j.; Sun, G.-l.; Xu, D.-s.; Feng, Y.; Shen, L. *Eur. J. Pharm. Biopharm.* **2010,** *76,* 230–237. doi:10.1016/j.ejpb.2010.07.003
65. Huh, K. M.; Ooya, T.; Lee, W. K.; Sasaki, S.; Kwon, I. C.; Jeong, S. Y.; Yui, N. *Macromolecules* **2001,** *34,* 8657–8662. doi:10.1021/ma0106649

License and Terms

Beilstein Journal of Organic Chemistry

Multichromophoric sugar for fluorescence photoswitching

Stéphane Maisonneuve[1], Rémi Métivier[*1], Pei Yu[2], Keitaro Nakatani[1] and Juan Xie[*1]

Full Research Paper

Open Access

Address:
[1]PPSM, ENS Cachan, CNRS, UMR8531, 61 avenue du Président Wilson, 94235 Cachan cedex, France and [2]LCI, ICMMO, CNRS, Université Paris-Sud, 15 rue Georges Clémenceau, 91405 Orsay Cedex, France

Email:
Rémi Métivier[*] - metivier@ppsm.ens-cachan.fr; Juan Xie[*] - joanne.xie@ens-cachan.fr

* Corresponding author

Keywords:
click chemistry; energy transfer; fluorophore; monosaccharide; photochromism

Beilstein J. Org. Chem. **2014,** *10,* 1471–1481.
doi:10.3762/bjoc.10.151

Received: 07 March 2014
Accepted: 28 May 2014
Published: 30 June 2014

This article is part of the Thematic Series "Multivalent glycosystems for nanoscience".

Guest Editor: J.-L. Reymond

Abstract

A multichromophoric glucopyranoside **2** bearing three dicyanomethylenepyran (DCM) fluorophores and one diarylethene (DAE) photochrome has been prepared by Cu(I)-catalyzed alkyne–azide cycloaddition reaction. The fluorescence of **2** was switched off upon UV irradiation, in proportion with the open to closed form (OF to CF) conversion extent of the DAE moiety. A nearly 100% Förster-type resonance energy transfer (FRET) from all three DCM moieties to a single DAE (in its CF) moiety was achieved. Upon visible irradiation, the initial fluorescence intensity was recovered. The observed photoswiching is reversible, with excellent photo resistance.

Introduction

The development of functional nanomaterials is nowadays a very attractive field of fundamental and applied research. The chemical functions at the molecular level yield properties, which are translated in terms of specific electronic or optical functions to the materials and device level. One of the challenges is to synthesize organic nano-architectures with a high degree of structural order and well-defined properties yielding high-performance functions, for both economic and environmental saving reasons. Saccharides are polyfunctional molecules with well-defined stereogenic centres in one molecular unit, and constitute "platforms" on which multiple functional moieties can be attached. Among many applications, the use of photochemical devices based on sugar derivatives is particularly appealing for the development of supramolecular systems for optical data storage media. Photochromic molecules are particularly efficient photo-driven switches, as they can commute upon light excitation between two distinct molecular species (states A and B, Figure 1) with the possibility to cycle up to one million "round trips", showing different physical and chemical properties, the most noticeable one being the absorp-

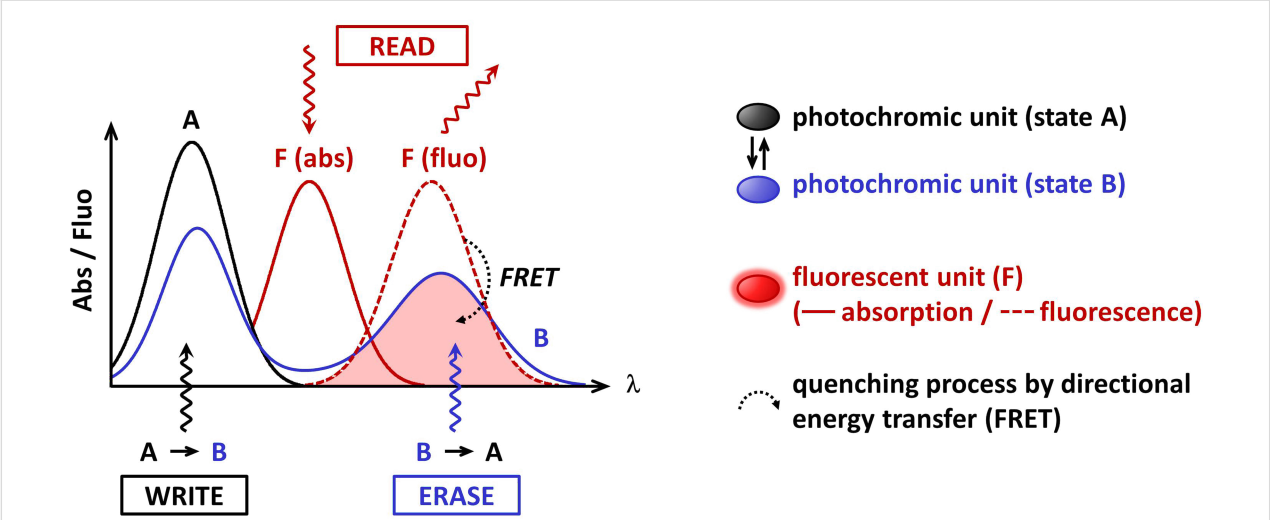

Figure 1: Requirements on absorption and emission spectral features of the photochromic and fluorescent units of the platform to induce efficient fluorescence photoswitching by energy transfer process (FRET).

tion change [1]. Indeed, they usually shuttle between a colorless and a colored form. Combining them with fluorescent compounds provides an added value to their photophysical function. Actually, fluorescence allows the possibility to reach high sensitivity and very low detection levels, down to the single molecule limit, whereas absorption spectroscopy requires a high number of active molecules [2]. If structural and spectral features of the fluorophore and the photochromic compound fit well together, the fluorescence can be switched ON and OFF: quenching of the fluorescence through a Förster-type resonance energy transfer (FRET) process from the former to the latter would occur, when the photochromic moiety is in the colored form (state B, Figure 1). At the opposite, in the colorless form (state A), the absence of FRET would keep the fluorescence alive, showing that the combination of these two functional molecules leads to a photon-driven fluorescence switch.

Previously, we have synthesized a fluorescent-photochromic dyad (**1**, Figure 2) combining a DCM fluorophore (4-dicyanomethylene-2-*tert*-butyl-6-(*p*-dialkylaminostyryl)-4*H*-

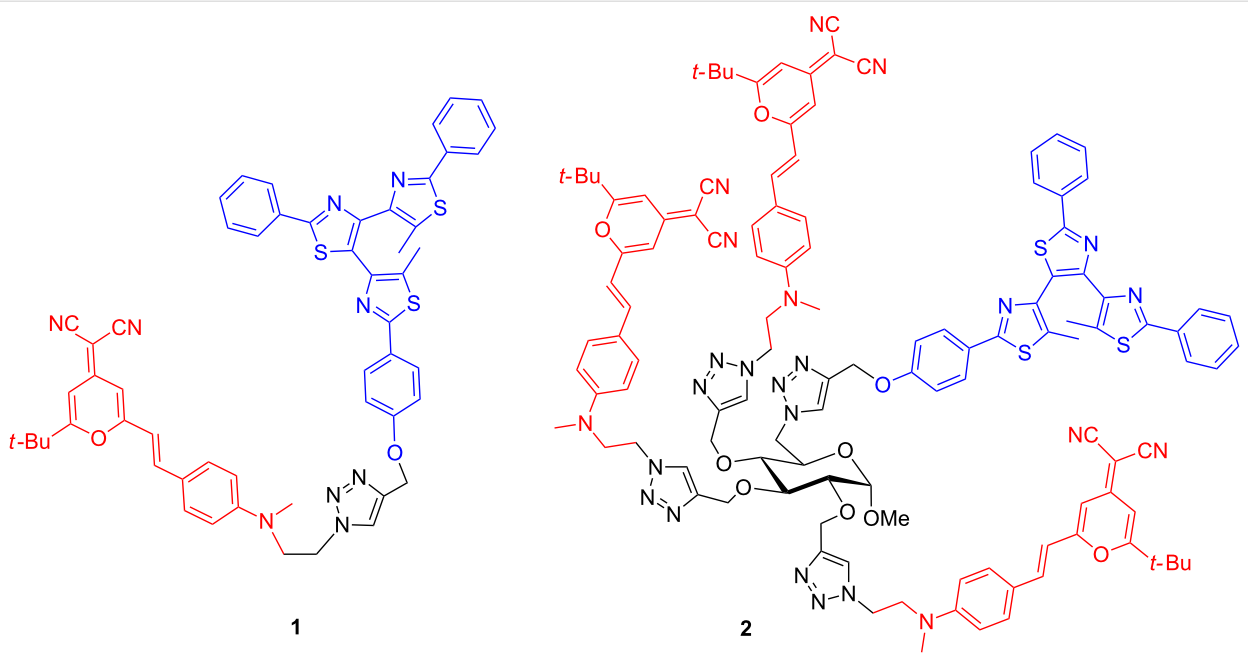

Figure 2: Bifunctional fluorescent-photochromic molecules **1** and **2**.

pyran) [3] with a photochromic diarylethene (DAE) which showed a photoreversible two-way FRET controlled by the state of the photochromic moiety, and 49% quenching of the fluorescence upon UV irradiation [4]. Bifunctional molecules built on two distinct (photochrome and fluorophore) moieties have also been reported by other groups [5-9]. The fluorophore vs photochrome ratio in reported bifunctional systems is 1:1 [4-7] or 2:1 [8,9]. Other strategies to assemble interacting fluorophores and photochromes (supramolecular systems, nanoparticles, polymer materials) are also reported [10-13]. FRET operates at distances of a few nanometers around the photochromic moiety (in its state B, Figure 1), which is related to the Förster radius. It means that in a suitably designed molecular system, one single photochromic unit can quench several fluorophores present within this distance. In a situation where one photochromic unit is surrounded by several fluorophores, we can take advantage of this phenomenon both to increase the brightness of the fluorescent molecular system and to turn "ON" and "OFF" several fluorophores with one given photochromic molecule. This is valuable in terms of photon (thus energy) saving, since "switching a few photochromes leads to quenching many fluorophores". In this perspective, we decided to design a multichromophoric glycopyranoside bearing three DCM fluorophores and one photochromic bis(dithiazole)ethane [14-16] (compound **2**, Figure 2) so as to take advantage of this sugar-based "platform" to get a specific molecular architecture and to study the energy transfer and photo-switching efficiency. To the best of our knowledge, readily available monosaccharides have been rarely used to develop multichromophoric supramolecular systems. Only one artificial light-harvesting antenna system grafted on the α-D-glucopyranoside has been reported [17].

Results and Discussion

Synthesis of multichromophoric sugars

Synthesis of organic nano-architectures with a high degree of structural order and defined properties is challenging because sophisticated multistep experimental procedures are often implicated. Recently, the Cu(I)-catalyzed alkyne–azide cycloaddition reaction (CuAAC, an excellent example of click chemistry) has been demonstrated as a robust and highly efficient ligation tool to conjugate various azido- and alkyne-functionalized moieties [18-20]. Monosaccharides can be readily functionalized with several propargyl groups to synthesize, using click chemistry, multivalent neoglycoconjugates for recognition studies with carbohydrate-binding proteins (lectins) [21-24] or to develop light-harvesting antenna systems [17]. In order to introduce three DCM fluorophores and one photochromic species into the glycopyranoside scaffold, methyl 6-*O*-trityl-α-D-glucopyranoside **3** was chosen as starting material (Scheme 1). *O*-Propargylation followed by microwave-assisted CuAAC with azido-functionalized DCM fluorophore **5** [25] in the presence of copper sulfate and sodium ascorbate led to the fluorescent glucoside **6**. The trityl group was then removed by a catalytic amount of acetyl chloride in a mixture of MeOH and CH_2Cl_2. Subsequent activation as mesylated followed by "microwave-assisted" nucleophilic substitution with sodium azide afforded the corresponding 6-azido sugar **8** which was treated with alkyne-functionalized photochromic diarylethene **9** [26] to furnish the target compound **2** in 68% yield. The structure of this compound has been confirmed by NMR and HRMS spectra.

Photophysical studies

The fluorescent glucoside derivative **6**, bearing three DCM fluorophores, is used as a model fluorescent compound. Its absorption spectrum in acetonitrile, plotted in Figure 3a, shows a main large band peaking at 455 nm. It exhibits a wide fluorescence spectrum between 550 nm and 700 nm, with a maximum located at 610 nm (Figure 3b), associated with a fluorescence quantum yield $\Phi_F = 0.12$. These spectroscopic characteristics are rather comparable to the absorption and fluorescence features of the fluorophore **5** [4]. The photophysical properties of the photochromic model compound **9** have been described in a previous report [4]. Briefly, the diarylethene **9** is originally in its colorless open form (**9**-OF), with an absorption spectrum in acetonitrile located in the UV range ($\lambda_{max} = 317$ nm, Figure 3c, full black line). In this state, **9**-OF is moderately fluorescent in the blue region ($\lambda_{max} = 440$ nm, $\Phi_F = 0.016$, Figure 3d). Under irradiation at 335 nm, **9**-OF undergoes a cyclisation photoreaction yielding the molecule in its colored and non-fluorescent closed form (**9**-CF), as revealed by the appearance of a large absorption band peaking in the 500–700 nm range (Figure 3c, full blue line). The photostationary state (PSS) reached under 335 nm illumination is composed of 91% of **9**-CF and 9% of **9**-OF (Figure 3c, dashed line). The target compound **2** can be considered as the assembly of the fluorescent model derivative **6** and the photochromic model compound **9**. Indeed, before any UV irradiation, the absorption spectrum of **2** in its open form (**2**-OF) represents the overlay of the absorption feature of **6** and **9**-OF: as displayed in Figure 3e (full line), the absorption band at 455 nm matches to the three fluorophores, whereas the absorption bands at 286 nm and 325 nm correspond mostly to the photochromic diarylethene moiety. The fluorescence spectrum of **2**-OF shows a very weak blue emission band between 400 nm and 500 nm from the diarylethene unit, and a rather strong red emission band peaking at 610 nm from the three DCM dyes (Figure 3f). This dual emission will be discussed further, by a careful analysis of excitation spectra (vide infra). Figure 4a and b show that upon increasing irradiation times at 335 nm, an absorption band at 600 nm emerges, corresponding to the photochromic moiety in its thermally stable closed form, and the fluorescence emission is concomitantly quenched by

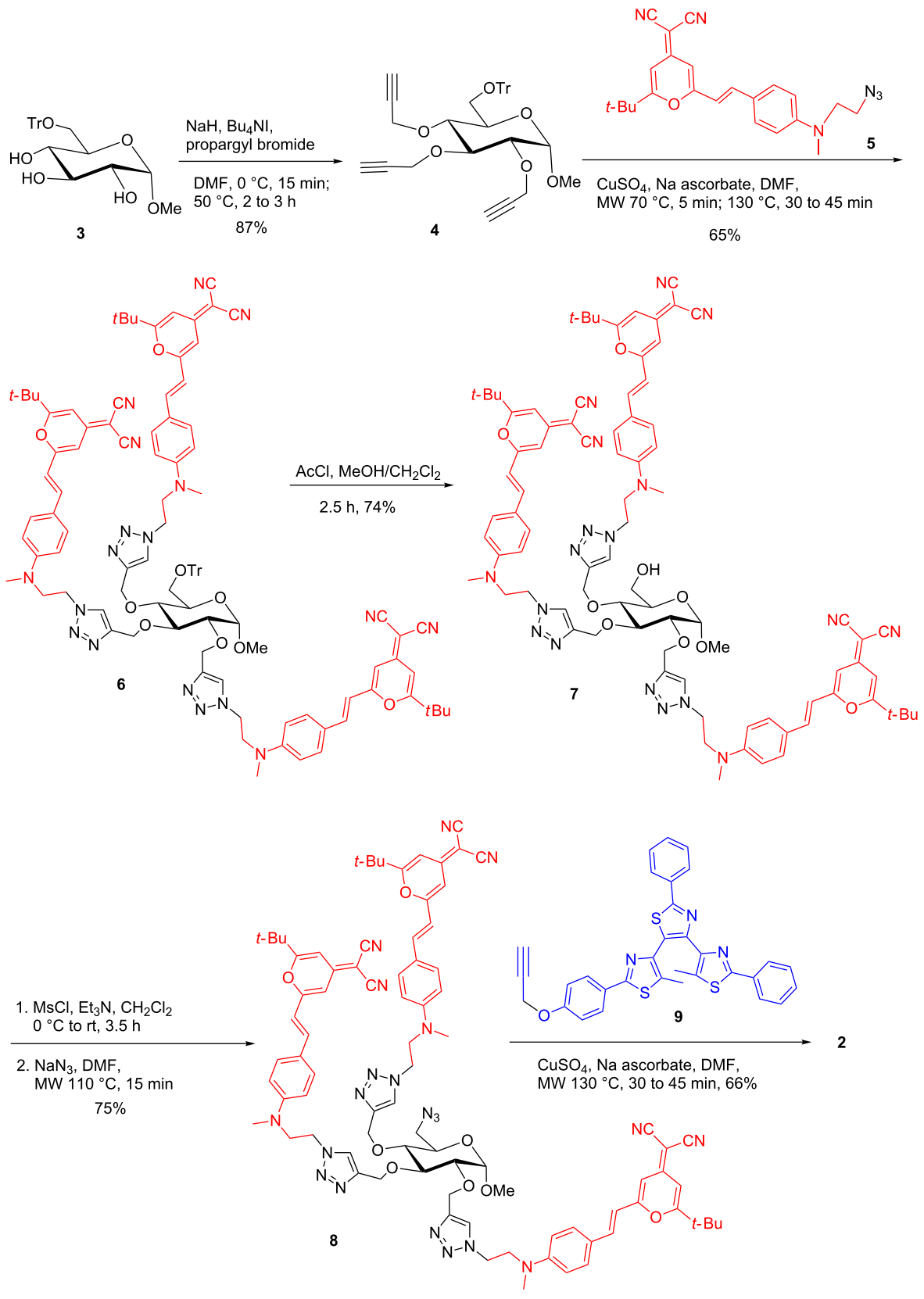

Scheme 1: Synthesis of multichromophoric glucopyranoside **2**.

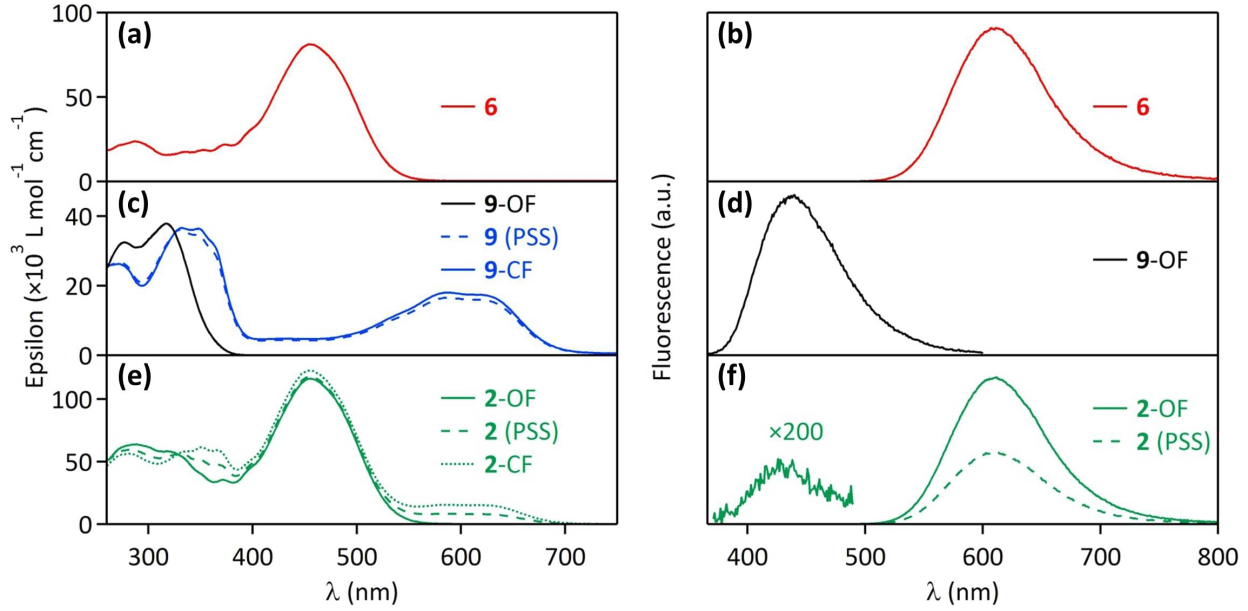

Figure 3: Absorption and fluorescence spectra of compounds **6**, **9**, and **2** in CH_3CN: (a) absorption spectrum of **6**; (b) emission spectrum of **6** (λ_{exc} = 450 nm); (c) absorption spectra of **9**-OF, **9** at the photostationary state (PSS) under 335 nm illumination, isolated **9**-CF; (d) emission spectrum of **9**-OF (λ_{exc} = 325 nm); (e) absorption spectra of **2**-OF, **2** at the photostationary state (PSS) under 335 nm illumination (no noticeable change has been observed over 5 days, indicating the thermal stability of **2**), **2**-CF (obtained by extrapolation of the ^{1}H NMR vs UV–visible absorption experiment, see text for details); (f) emission spectra of **2**-OF and **2** at the photostationary state (PSS) under 335 nm illumination (λ_{exc} = 325 nm).

51%. As displayed in Figure 3, the emission band of the fluorophores in the 550–700 nm range overlaps well the absorption band of the photochromic derivative in its closed form, in the same spectral region. Therefore, the fluorescence quenching observed for the compound **2** under UV irradiation can be easily interpreted as the consequence of a FRET process from the DCM fluorophores (donors) to the diarylethene derivative in its colored closed form (acceptor), which plays the role of the quencher. The multichromophoric system **2** is completely reversible: under irradiation at 575 nm, the cycloreversion reaction **2**-CF → **2**-OF occurs, the absorption band centered at 610 nm drops back to zero and the fluorescence of the sample is fully recovered (Figure 4c and d). As shown in Figure 4e and f, several UV–visible irradiation cycles were applied to the system without any degradation of its photophysical properties, revealing its excellent fatigue resistance.

^{1}H NMR spectra were recorded under increasing irradiation times at 335 nm in order to follow the photoisomerisation of compound **2** (Figure 5), and corresponding UV–visible absorption spectra were measured, in order to correlate the absorption changes with the OF → CF conversion yield. Under 335 nm illumination, new signals appear near 5.2 ppm (for OCH_2 group) and 6.5 to 8.0 ppm which are induced by the photocyclisation of the photochromic moiety from the open to the closed form. Due to higher concentration of NMR sample, the maximum conversion reached was about 39%. Such combined ^{1}H NMR vs UV–visible absorption data allowed us to extrapolate the absorption spectrum of the dyad molecule in its pure closed form **2**-CF, as plotted in Figure 3e (dotted line). It appears that the PSS obtained for the compound **2** with a light-irradiation at 335 nm corresponds to a mixture of 53% of **2**-CF and 47% of **2**-OF. Such a conversion yield has to be compared to the fluorescence quenching of **2** observed after irradiation at 335 nm (51% fluorescence quenching, vide supra). Therefore, the incomplete fluorescence quenching is due to a limited photochromic conversion yield under UV light. Furthermore, since the photochromic conversion yield (53%) corresponds almost to the fluorescence quenching (51%), the FRET process appears to be extremely efficient: under irradiation at 335 nm, half of the multichromophoric system is still in its initial open form **2**-OF, associated with a strong fluorescence emission, and another half are promoted in their closed form **2**-CF, whose fluorescence is almost totally quenched by FRET.

This phenomenon is well-supported by time-resolved fluorescence measurements. Fluorescence decay curves of **6**, **2**-OF, and **2** after irradiation at 335 nm were recorded in acetonitrile by the time-correlated single photon counting method (TCSPC) at λ_{exc} = 475 nm, and analyzed by a sum of three exponential components (Table 1). The model fluorescent glucoside derivative **6** shows a main time-constant at τ_1 = 1.00 ns, a second

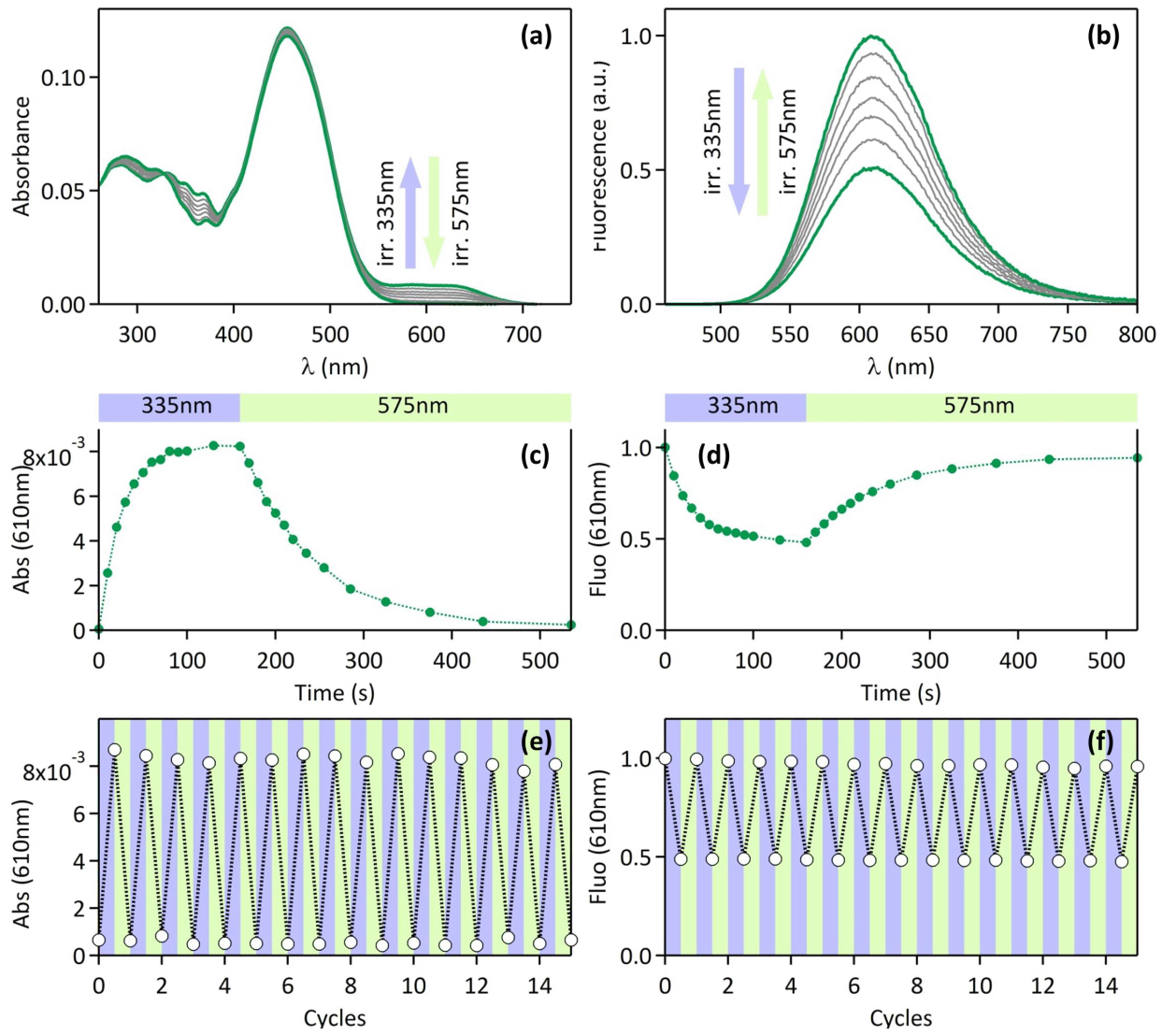

Figure 4: Absorption and fluorescence changes of compound **2** (1.0 μM in CH_3CN) upon UV–visible irradiation: (a) absorption and (b) emission spectra (λ_{exc} = 450 nm) under increasing irradiation times at 335 nm; (c) time-evolution profile of absorption and (d) emission upon irradiation at 335 nm and 575 nm; (e) fatigue resistance followed by the absorption band at 610 nm and (f) the emission band at 610 nm under alternate 355 nm/575 nm irradiation cycles. Irradiation conditions at 335 nm: (a–d) 2.7 mW cm^{-2} and (e,f) 40 s at 7.2 mW cm^{-2}. Irradiation conditions at 575 nm: (a–d) 3.1 mW cm^{-2} and (e,f) 120 s at 9.5 mW cm^{-2}.

component at τ_2 = 0.35 ns, and a minor time-constant at τ_3 = 0.04 ns. The latter one has been neglected in the following discussion, since it is very close to the time-resolution of our instrument, and associated with a very low fraction of intensity (0.02). The two other time-constants are attributed to the *E*-isomer (τ_1) and the *Z*-isomer (τ_2) of the fluorophores, which is consistent with our previous studies [4]. The fluorescence decays of **2**-OF and **2** after irradiation at 335 nm are plotted in Figure 6a, and the result of a global three-exponential fitting procedure is displayed on Table 1. The three time-constants obtained by this method are in the same range as the ones determined for **6**: τ_1 = 1.26 ns, τ_2 = 0.47 ns, τ_3 = 0.05 ns, associated with the fraction of the intensities comparable to **6**. In a similar manner, the two significant contributions correspond to the *E* and *Z*-isomers of the fluorophores, respectively. Interestingly, the fluorescence decay curves of **2** before and after UV irradiation are overlapping, and the results of the fitting are identical in both cases, despite the fact that the fluorescence intensity is decreased by a factor of two (51% fluorescence quenching, vide supra). Such an observation is compatible with a static FRET quenching process. Indeed, when the PSS is reached under 335 nm irradiation, the population of **2**-OF molecules represents 47% of the whole system, behaves as the initial non-irradiated molecules and contributes to the fluorescence decay,

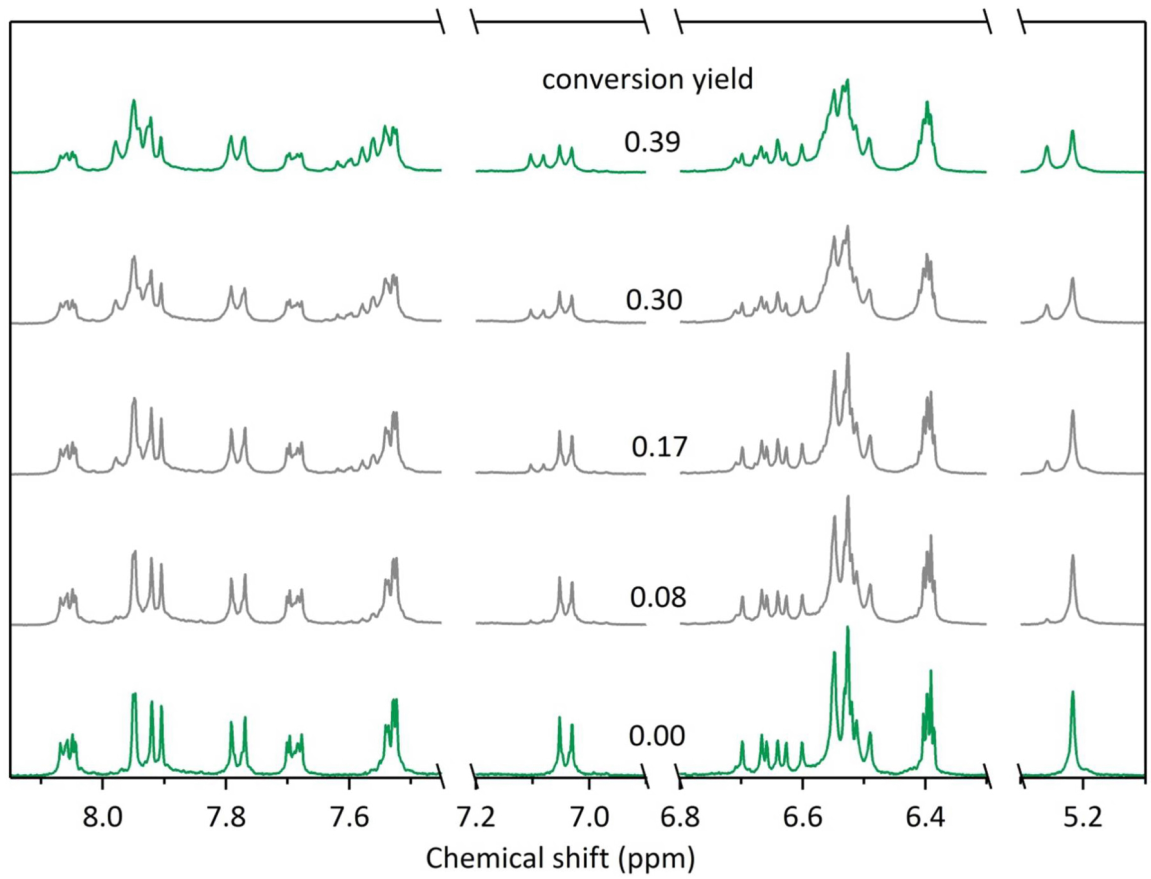

Figure 5: Partial ^{1}H NMR spectra of compound **2** (11 µM in CD_3CN/DMSO-d_6 4:1) before and after increasing irradiation times at 335 nm (from bottom to top). The conversion yield at each irradiation time is deduced from the integration of signals around 5.2–5.3 and 7.0–7.1 ppm.

Table 1: Fluorescence decay parameters of compounds **6** and **2** in CH_3CN.

	τ_1/ns (a_1, f_1[a])	τ_2/ns (a_2, f_2[a])	τ_3/ns (a_3, f_3[a])	χ^2_R
6	1.00 (0.43, 0.79)	0.35 (0.29, 0.19)	0.04 (0.28, 0.02)	1.08
2-OF[b]	1.26 (0.40, 0.75)	0.47 (0.33, 0.23)	0.05 (0.27, 0.02)	1.16
2 (PSS under irradiation at 335 nm)[b]	1.26 (0.35, 0.74)	0.47 (0.30, 0.23)	0.05 (0.35, 0.03)	1.12

[a]The fraction of intensities f_i is defined as follows: $f_i = a_i\tau_i/\Sigma a_j\tau_j$. [b]Results obtained by means of a global fitting procedure.

whereas the population of **2**-CF molecules (53% of the system) is fully quenched through a very efficient FRET process, its contribution to the emission signal is negligible, and its decay-time is obviously below the time-resolution of our instrument. As a conclusion, the FRET process from the fluorophores to the closed form of the photochromic diarylethene is close to 100% in the molecule **2**.

Fluorescence excitation spectra provide another evidence of FRET intramolecular phenomenon within the compound **2**. Indeed, the excitation spectrum of the model fluorescent glucoside **6**, displayed in Figure 6b (red curve), resembles to the shape of its absorption spectrum, with a large band centered at 455 nm. However, the excitation spectrum of the molecule **2**-OF recorded at λ_{em} = 620 nm (corresponding to the fluorophore emission) shows an additional contribution in the 250–350 nm range, which corresponds to the open form of the photochromic moiety, revealing a FRET process from the open form of the diarylethene unit (donor) to the DCM fluorophores (acceptors). This energy transfer pathway is actually allowed by the favorable spectral overlap in the 400–500 nm range between the blue emission of the photochromic moiety in its open form (see Figure 3d) and the absorption of the fluorophores (see Figure 3a). As evidenced previously on **1** [4], this "reverse"

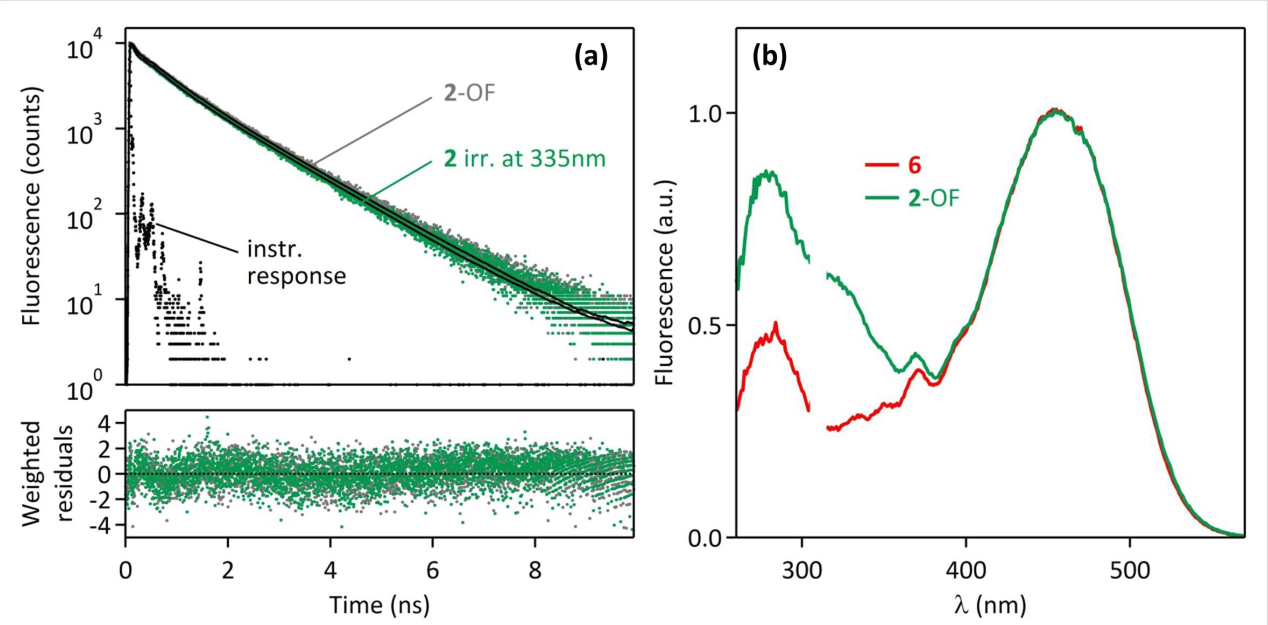

Figure 6: (a) Fluorescence decays (λ_{exc} = 475 nm, λ_{em} = 610 nm) of compound **2**-OF, and **2** after irradiation at 335 nm in CH_3CN (7 mW cm^{-2}). (b) Normalized excitation spectra (λ_{em} = 620 nm) of **6** (red line) and **2**-OF (green line) in CH_3CN.

FRET explains why the emission of the photochromic moiety is almost absent in the fluorescence spectrum of the dyad **2**-OF (Figure 3f).

Finally, the limited conversion yield of the molecule **2** under irradiation in the UV (53%), compared to the model photochromic compound **9** (conversion yield = 91%) can be explained by this efficient double FRET effect: (i) the energy transfer from the open form of the photochromic unit to the fluorophores tends to deactivate the photochromic activity of **2**-OF, and (ii) the energy transfer from the fluorophores to the closed form of the photochromic unit contributes to favor the CF → OF cycloreversion reaction. Consequently, the PSS of **2** when irradiated at 335 nm is much lower than the photochromic moiety **9** alone, because of the highly efficient FRET processes.

Conclusion

Through click chemistry, we have successfully introduced three DCM fluorophores and a DAE photochrome on the methyl α-D-glucopyranoside in good yield. The multichromophoric compound **2** can be reversibly switched upon UV and visible irradiation, and showed an excellent fatigue resistance. Under UV irradiation at 335 nm, the fluorescence was decreased by 51%. This value corresponds to the photochromic conversion yield at this photostationary state, with 53% of the DAE molecules promoted to their closed form. We therefore demonstrated that, at the molecular level, one single DAE moiety in the closed form induces the full fluorescence quenching of all three DCM moieties, by a FRET yield close to unity. This study is supported by time-resolved fluorescence experiments. This result represents a step forward, compared to our previous report on the 1/1 system **1**. The increase of the OF to CF conversion extent of the photochromic unit is among our future perspectives, since this could lead to a better ON vs OFF fluorescence contrast. By a careful molecular engineering, combining photophysical analysis and synthetic work, we are endeavoring to tune optimally the fluorophore/photochrome ratio. Glycosides, and more generally sugar molecules, may further provide appropriate "platforms".

Experimental

General details

Commercially available solvents and reagents were used without further purification. Compounds **3** [27], **5** [25] and **9** [26] were prepared according to the literature. Melting points were measured on a Kofler bench. Optical rotations were measured using a JASCO P-2000 polarimeter. Column chromatography was performed on Carlo Erba Silica Gel 60A (40–63 µm). Analytical thin-layer chromatography was performed on E. Merck aluminum percolated plates of Silica Gel 60F-254 with detection by UV. ^1H and ^{13}C NMR spectra were recorded on a Jeol ECS-400 spectrometer. HRMS–ESI spectra were recorded on a Bruker microTOF-Q II spectrometer or Bruker maXis using standard conditions.

Absorption spectra were recorded on a Cary-5000 spectrophotometer from Agilent Technologies. Corrected emission spectra

were performed on a Fluorolog FL3-221 spectrofluorometer from Horiba Jobin-Yvon. The fluorescence quantum yields were determined by using quinine sulfate dihydrate in sulfuric acid (0.5 N) as a standard at λ_{exc} = 325 nm (Φ_F = 0.546) and coumarin 540A in ethanol as a standard at λ_{exc} = 450 nm (Φ_F = 0.544). Photochromic reactions were induced in situ by a continuous irradiation Hg–Xe lamp (Hamamatsu, LC6 Lightningcure, 200 W) equipped with narrow band interference filters of appropriate wavelengths (Semrock FF01-335/7-25 for λ_{irr} = 335 nm; FF01-575/25-25 for λ_{irr} = 575 nm). The irradiation power was measured using a photodiode from Ophir (PD300-UV). The photoconversion was followed by a combination of ^{1}H NMR and UV–visible absorption spectra, realized by successive irradiation at 335 nm for a total time of 20 min. Fluorescence intensity decays were obtained by the time-correlated single-photon counting (TCSPC) method with femtosecond laser excitation using a set-up composed of a Ti:Sa laser (Tsunami, Spectra-Physics) pumped by a doubled Nd:YAG cw-laser (Millennia, Spectra-Physics), pumped itself by two laser diode arrays. Light pulses at 950 nm were selected by optoacoustic crystals at a repetition rate of 4 MHz, and then doubled at 475 nm by non-linear crystals. Fluorescence photons were detected through a band-pass filter 370–500 nm (a monochromator set at 620 nm, respectively) by means of a Hamamatsu MCP R3809U photomultiplier, connected to a constant-fraction discriminator. The time-to-amplitude converter was purchased from Tennelec. In the present investigation, the channel width was set to 3.1 ps. The instrumental response function was recorded before each decay measurement with a fwhm (full width at half-maximum) of ~25 ps. The fluorescence data were analyzed using the Globals software package developed at the Laboratory for Fluorescence Dynamics at the University of Illinois at Urbana-Champaign, which includes reconvolution analysis and non-linear least-squares minimization method. The shortest fluorescence decay time accessible by our instrumental set-up and our data analysis method was estimated to be around 10 ps (time-resolution).

Methyl 2,3,4-tri-*O*-propargyl-6-*O*-trityl-α-D-glucopyranoside (**4**)

To a stirred solution of methyl 6-*O*-trityl-α-D-glucopyranoside (**3**, 3.08 g, 7.05 mmol) in distilled DMF (60 mL) under argon in an ice bath, were added Bu_4NI (3.07 g, 8.32 mmol) and propargyl bromide (80% solution in toluene, 2.3 mL, 20.65 mmol). The NaH (60% in mineral oil, 1.02 g, 25.5 mmol) was then added slowly by portions. After 15 min, the mixture was heated at 50 °C over 2 to 3 h (brown to black color). After evaporation under vacuum, the residue was partitioned in a mixture of EtOAc/H_2O (200:200 mL) and the aqueous layer was extracted with EtOAc (2 × 100 mL). The organic layers were combined, washed with brine, dried over $MgSO_4$ and evaporated under vacuum to give the crude product which was purified by column chromatogrphy using a mixture of petroleum ether (PE):EtOAc (95:5, 9:1, 8:2) to give 87% of the desired compound (3.36 g, 6.10 mmol) as white solid, mp 96–97 °C; R_f = 0.64 (PE/EtOAc = 4:1); $[\alpha]_D$ +51 (*c* 0.5, $CHCl_3$); ^{1}H NMR (400 MHz, $CDCl_3$) δ 2.23 (t, *J* = 2.3 Hz, 1H, CH≡), 2.45 (t, *J* = 2.3 Hz, 1H, CH≡), 2.50 (t, *J* = 2.3 Hz, 1H, CH≡), 3.12 (dd, *J* = 5.0, 10.1 Hz, 1H, H-6), 3.46 (s, 3H, OMe), 3.45–3.49 (m, 1H, H-6'), 3.53 (t, *J* = 9.2 Hz, 1H, H-4), 3.68 (dd, *J* = 3.7, 9.6 Hz, 1H, H-2), 3.69–3.72 (m, 1H, H-5), 3.78 (t, *J* = 9.2 Hz, 1H, H-3), 4.08 (dd, *J* = 2.8, 15.1 Hz, 1H, OCH), 4.25 (dd, *J* = 2.8, 15.1 Hz, 1H, OCH), 4.40–4.45 (m, 4H, 2×OCH_2), 4.97 (d, *J* = 3.7 Hz, 1H, H-1), 7.21–7.32 (m, 9H, H_{Ar}), 7.47–7.49 (m, 6H, H_{Ar}) ppm; ^{13}C NMR (100 MHz, $CDCl_3$) δ 55.05 (OMe), 58.83, 59.94, 60.59 (OCH_2), 62.83 (C-6), 69.80 (C-5), 74.31, 75.06 (C_q), 77.36 (C-4), 79.46 (C-2), 79.87, 79.99, 80.19 (CH≡), 81.75 (C-3), 86.49 (C_q), 97.79 (C-1), 127.11, 127.95, 128.86 (CH_{Ar}), 144.11 (C_q) ppm; HRMS–ESI (*m*/*z*): $[M + Na]^+$ calcd for 573.2253; found: 573.2244.

DCM-functionalized methyl 6-*O*-trityl-α-D-glucopyranoside **6**

To a solution of **4** (1.01 g, 1.83 mmol) in distilled DMF (15 mL), were added the azido-DCM **5** (2.23 g, 5.57 mmol), $CuSO_4$ (110.9 mg, 0.44 mmol) and Na ascorbate (188 mg, 0.95 mmol). The reaction mixture was stirred at 70 °C during 5 min then at 130 °C during 30 to 45 min under microwave irradiation (700 rpm, monitoring by TLC), and poured into distilled water after cooling to room temperature. The precipitate was then filtred through a cellulose acetate filter (porosity 2 μm) under vacuum and washed with water, then purified by column chromatography using pure EtOAc, then EtOAc/acetone (gradient 9:1, 8:2, 5:5) then EtOAc/EtOH (7:3) to give 65% of the desired compound (2.09 g, 1.19 mol) as a red solid; mp 164–166 °C; R_f = 0.29 (EtOAc/acetone = 9:1); $[\alpha]_D$ +12 (*c* 0.5, $CHCl_3$); ^{1}H NMR (400 MHz, acetone-d_6) δ 1.38 (s, 27H, $H_{t\text{-}Bu}$), 2.84 (s, 3H, NMe), 2.85 (s, 3H, NMe), 2.85 (s, 3H, NMe), 3.10 (dd, *J* = 4.6, 10.1 Hz, 1H, H-6), 3.39–3.40 (m, 1H, H-6'), 3.41 (s, 3H, OMe), 3.50 (t, *J* = 9.5 Hz, 1H, OCH), 3.55 (dd, *J* = 3.7, 9.6 Hz, H-2), 3.62–3.70 (m, 2H, 2×OCH), 3.82–3.99 (m, 6H, 3×NCH_2), 4.34 (d, *J* = 11.4 Hz, 1H, NCH), 4.58–4.86 (m, 11H, NCH, 2×NCH_2, 3×OCH_2), 4.98 (d, *J* = 3.7 Hz, 1H, H-1), 6.45–6.46 (m, 3H, 3×CH=), 6.56–6.73 (m, 9H, 9×CH=), 6.81 (d, *J* = 16.0 Hz, 1H, CH=), 6.86 (d, *J* = 16.0 Hz, 1H, CH=), 6.87 (d, *J* = 16.0 Hz, 1H, CH=), 7.21–7.33 (m, 10H, 10×CH=), 7.39 (s, 1H, $H_{Triazole}$), 7.41–7.53 (m, 14H, 14×CH=), 8.15 (s, 1H, $H_{Triazole}$), 8.17 (s, 1H, $H_{Triazole}$) ppm; ^{13}C NMR (100 MHz, acetone-d_6) δ 28.14 ($Me_{t\text{-}Bu}$), 37.26 (C_q), 38.63, 38.78 (NMe), 47.99, 48.12, 48.18, 52.89 (NCH_2), 55.14 (OMe), 57.61 (C_q), 63.50 (C-6), 64.41, 66.39, 66.98 (OCH_2), 69.68 (C_q), 70.96 (C-5), 78.46, 80.40,

81.91 (C-2,3,4), 87.03 (C_q), 98.37 (C-1), 102.62, 106.02, 106.07, 112.67, 112.75, 114.21, 114.33 (CH=), 116.13, 116.18, 123.98, 124.07 (C_q), 124.81, 125.29, 125.45 ($CH_{Triazole}$), 127.86, 128.66, 129.56, 130.79, 130.84, 139.11, 139.22 (CH=), 145.00, 145.56, 145.91, 146.14, 151.13, 151.18, 157.49, 157.49, 161.50, 161.55, 173.02 (C_q) ppm; HRMS–ESI (*m*/*z*): $[M + H]^+$ calcd for 1751.8463; found: 1751.8397.

DCM-functionalized methyl α-D-glucopyranoside **7**

To a stirred solution of compound **6** (940 mg, 0.54 mmol) in a mixture of CH_2Cl_2/MeOH (10/10 mL) cooled in an ice bath, was added acetyl chloride (115 µL, 1.61 mmol). After 2.5 h, the reaction was quenched by addition of a saturated $NaHCO_3$ solution (5 mL). The mixture was extracted with CH_2Cl_2. The organic layers were combined, washed with brine, dried over $MgSO_4$ and evaporated under vacuum. The product was purified by column chromatography using pure EtOAc followed by a mixture of EtOAc/acetone (gradient 9:1, 8:2, 7:3, 6:4) to give 74% of the desired compound (600 mg, 0.40 mmol) as a red solid; mp 156–158 °C; R_f = 0.22 (EtOAc/acetone = 4:1); $[\alpha]_D$ +25 (*c* 0.5, $CHCl_3$); ^{1}H NMR (400 MHz, $CDCl_3$) δ 1.37 (s, 27H, $H_{t\text{-}Bu}$), 2.89 (s, 3H, NMe), 2.91 (s, 3H, NMe), 2.92 (s, 3H, NMe), 3.37 (s, 3H, OMe), 3.47 (dd, *J* = 3.2, 9.6 Hz, 1H, H-2), 3.52–3.54 (m, 2H, H-3,4), 3.73 (s, 2H, H-6,6'), 3.80–3.83 (m, 1H, H-5), 3.92–3.94 (m, 6H, 3×NCH_2), 4.58–4.60 (m, 6H, 3×NCH_2), 4.74–4.97 (m, 7H, H-1, 3×OCH_2), 6.45–6.65 (m, 16H, 16×CH=), 7.25–7.42 (m, 8H, 8×CH=), 7.63 (s, 1H, $H_{Triazole}$), 7.87 (s, 1H, $H_{Triazole}$), 8.00 (s, 1H, $H_{Triazole}$) ppm; ^{13}C NMR (100 MHz, $CDCl_3$) δ 28.18 ($Me_{t\text{-}Bu}$), 36.70 (C_q), 38.59, 38.66, 38.74 (NMe), 47.49, 47.57, 52.53 (NCH_2), 55.22 (OMe), 57.89, 57.94 (C_q), 61.18 (C-6), 64.13, 65.75, 66.27 (OCH_2), 69.60 (C_q), 70.71, 77.36 (C-3,4), 79.39 (C-2), 81.42 (C-5), 97.51 (C-1), 102.43, 105.81, 111.98, 112.03, 113.81 (CH=), 115.70, 115.81, 115.86, 123.30, 123.35, 123.41 (C_q), 123.86, 124.43, 124.74 ($CH_{Triazole}$), 129.91, 137.95, 138.02 (CH=), 144.90, 145.32, 145.42, 149.84, 149.92, 149.98, 156.83, 160.01, 160.01, 160.05, 172.04 (C_q) ppm. HRMS–ESI (*m*/*z*): $[M + H]^+$ calcd for 1509.7367; found: 1509.7332; $[M + 2H]^{2+}$ calcd for 755.3720; found: 755.3715.

DCM-functionalized methyl 6-azido-6-deoxy-α-D-glucopyranoside **8**

To a stirred solution of compound **7** (414 mg, 0.27 mmol) in CH_2Cl_2 (2 mL) were added Et_3N (125 µL, 0.90 mmol) and MsCl (52 µL, 0.67 mmol). After stirring 3.5 h, the mixture was treated with 10 mL of water and the aqueous layer was extracted with CH_2Cl_2 (3 × 20 mL). The organic layers were combined, washed with brine, dried over $MgSO_4$ and evaporated under vacuum to a crude mesylate which was used without purification for the next step. To a solution of crude mesylate in DMF (3 mL) was added sodium azide (29.9 mg, 0.46 mmol) and the mixture was stirred at 110 °C during 15 min under microwave irradiation (700 rpm, monitoring by TLC). After cooling to room temperature, the reaction mixture was poured into 20 to 25 mL of distilled water. The precipitate was then filtred through cellulose acetate filter (porosity 2 µm) under vacuum and washed with water. The product was purified by column chromatography using EtOAc/acetone (gradient 1:0 to 9:1) to give 75% of the desired compound (328 mg, 0.21 mmol) as a red solid; mp 156–158 °C; R_f = 0.49 (EtOAc/acetone = 4:1); $[\alpha]_D$ +9 (*c* 0.5, $CHCl_3$); ^{1}H NMR (400 MHz, $CDCl_3$) δ 1.37 (s, 27H, $H_{t\text{-}Bu}$), 2.91 (s, 3H, NMe), 2.92 (s, 3H, NMe), 2.92 (s, 3H, NMe), 3.31–3.51 (m, 3H, H-4,6,6'), 3.39 (s, 3H, OMe), 3.49 (dd, *J* = 3.7, 9.6 Hz, 1H, H-2), 3.64–3.69 (m, 1H, H-5), 3.79 (t, *J* = 9.6 Hz, 1H, H-3), 3.90–3.97 (m, 6H, 3×NCH_2), 4.57–4.64 (m, 6H, 3×NCH_2), 4.65–4.97 (m, 7H, 3×OCH_2, H-1), 6.46–6.66 (m, 16H, 16×CH=), 7.26–7.42 (m, 8H, 8×CH=), 7.69 (s, 1H, $H_{Triazole}$), 7.89 (s, 1H, $H_{Triazole}$), 8.00 (s, 1H, $H_{Triazole}$) ppm; ^{13}C NMR (100 MHz, $CDCl_3$) δ 28.16 ($Me_{t\text{-}Bu}$), 36.68 (C_q), 38.54, 38.65, 38.71 (NMe), 47.51 (NCH_2), 51.22 (C-6), 52.52 (NCH_2), 55.39 (OMe), 57.84, 57.91, 57.91 (C_q), 64.26, 65.87, 66.28 (OCH_2), 69.57 (C_q), 69.83 (C-5), 77.37 (C_q), 78.00 (C-4), 79.29 (C-2), 81.08 (C-3), 97.43 (C-1), 102.41, 105.80, 111.95, 112.01, 113.73, 113.78 (CH=), 115.70, 115.83, 123.31, 123.37 (C_q), 124.13, 124.43, 124.77 ($CH_{Triazole}$), 129.89 (C_q), 137.89, 137.93, 138.02 (CH=), 144.81, 144.86, 145.27, 149.86, 149.96, 149.96, 156.80, 159.97, 160.03, 172.02 (C_q) ppm; HRMS–ESI (*m*/*z*): $[M + H]^+$ calcd for 1534.7432; found: 1534.7381; $[M + 2H]^{2+}$ calcd for 767.8753; found: 767.8746.

DCM and DAE-functionalized methyl α-D-glucopyranoside **2**

To a solution of compound **8** (51.1 mg, 0.033 mmol) in DMF (2 mL) were added the photochromic compound **9** (62.0 mg, 0.111 mmol), $CuSO_4$ (2.5 mg, 0.010 mmol) and Na ascorbate (6.8 mg, 0.034 mmol). The reaction mixture was stirred at 70 °C during 5 min then at 130 °C during 30 to 45 min under microwave irradiation (700 rpm, monitoring by TLC), and poured into distilled water after cooling to room temperature. The precipitate was then filtred through a cellulose acetate filter (porosity 2 µm) under vacuum and washed with water, then purified by column chromatogrphy using EtOAc:ethanol (9:1) to give 66% of the desired compound (45.8 mg, 0.022 mmol) as a red solid; mp 181–183 °C; R_f = 0.53 (EtOAc/acetone = 4:1); $[\alpha]_D$ +45 (*c* 0.5, $CHCl_3$); ^{1}H NMR (400 MHz, $CDCl_3$) δ 1.36 (s, 27H, $H_{t\text{-}Bu}$), 2.09 (s, 3H, Me), 2.54 (s, 3H, Me), 2.88 (s, 3H, NMe), 2.90 (s, 3H, NMe), 2.92 (s, 3H, NMe), 2.97 (t, *J* = 9.6 Hz, 1H, H-4), 3.21 (s, 3H, OMe), 3.35 (dd, *J* = 3.2, 9.6 Hz, 1H, H-2), 3.79–3.93 (m, 8H, H-3,5, 3×NCH_2), 4.45–4.81 (m, 13H, H-1,6,6', 3×NCH_2, 2×OCH_2), 4.93 (d,

J = 11.4 Hz, 1H, OCH), 4.97 (d, J = 11.5 Hz, 1H, OCH), 5.26 (s, 2H, OCH_2), 6.45–6.64 (m, 15H, 15×CH=), 7.02 (d, J = 8.7 Hz, 2H, 2×CH=), 7.26–7.49 (m, 15H, 15×CH=), 7.77–7.79 (m, 4H, 4×CH=), 7.88 (d, 2H, J = 8.7 Hz, 2×CH=), 7.97 (s, 1H, $H_{Triazole}$), 8.03–8.09 (m, 3H, 3×CH=) ppm; ^{13}C NMR (100 MHz, $CDCl_3$) δ 12.46, 12.94 (Me), 28.25 ($Me_{t\text{-}Bu}$), 36.77 (C_q), 38.79, 38.88 (NMe), 47.56, 47.68 (NCH_2), 50.54 (C-6), 52.56, 52.62, 52.72 (NCH_2), 55.56 (OMe), 58.20, 58.28 (C_q), 62.07, 64.23, 65.96, 66.27 (OCH_2), 68.89 (CH), 69.65 (C_q), 77.36, 79.31, 81.05 (OCH), 97.56 (C-1), 102.54, 112.21, 113.95, 114.05, 114.09, 115.29 (CH=), 115.71, 115.87, 123.51, 123.55, 123.60, 123.66 (C_q), 124.57, 124.68, 124.94, 126.41, 126.72, 128.20, 128.89, 129.08, 129.95, 130.40 (CH=), 133.59, 133.68 (C_q), 137.89, 137.95, 138.02 (CH=), 143.90, 144.78, 144.99, 145.06, 149.85, 156.89, 160.02, 163.93, 164.13, 167.30, 172.08 (C_q) ppm; HRMS–ESI (m/z): $[M + 2H]^{2+}$ calcd for 1048.4254; found: 1048.4247; $[M + 3H]^{3+}$ calcd for 699.2860; found: 699.2845.

References

1. Irie, M., Ed. Photochromism: Memories and Switches. *Chem. Rev.* **2000,** *100,* 1683–1890. doi:10.1021/cr980068l
2. Fukaminato, T. *J. Photochem. Photobiol., C* **2011,** *12,* 177–208. doi:10.1016/j.jphotochemrev.2011.08.006
3. Guo, Z.; Zhu, W.; Tian, H. *Chem. Commun.* **2012,** *48,* 6073–6084. doi:10.1039/c2cc31581e
4. Ouhenia-Ouadahi, K.; Métivier, R.; Maisonneuve, S.; Jacquart, A.; Xie, J.; Léaustic, A.; Yu, P.; Nakatani, K. *Photochem. Photobiol. Sci.* **2012,** *11,* 1705–1714. doi:10.1039/c2pp25129a
5. Bossi, M.; Belov, V.; Polyakova, S.; Hell, S. W. *Angew. Chem., Int. Ed.* **2006,** *45,* 7462–7465. doi:10.1002/anie.200602591
6. Berberich, M.; Krause, A.-M.; Orlandi, M.; Scandola, F.; Würthner, F. *Angew. Chem., Int. Ed.* **2008,** *47,* 6616–6619. doi:10.1002/anie.200802007
7. Irie, M.; Fukaminato, T.; Sasaki, T.; Tamai, N.; Kawai, T. *Nature* **2002,** *420,* 759–760. doi:10.1038/420759a
8. Jiang, G.; Wang, S.; Yan, W.; Jiang, L.; Song, Y.; Tian, H.; Zhu, D. *Chem. Mater.* **2006,** *18,* 235–237. doi:10.1021/cm052251i
9. Golovkova, T. A.; Kozlov, D. V.; Neckers, D. C. *J. Org. Chem.* **2005,** *70,* 5545–5549. doi:10.1021/jo050540k
10. Wu, S.; Luo, Y.; Zeng, F.; Chen, J.; Chen, Y.; Tong, Z. *Angew. Chem., Int. Ed.* **2007,** *46,* 7015–7018. doi:10.1002/anie.200701396
11. Del Guerzo, A.; Olive, A. G. L.; Reichwagen, J.; Hopf, H.; Desvergne, J.-P. *J. Am. Chem. Soc.* **2005,** *127,* 17984–17985. doi:10.1021/ja0566228
12. Fölling, J.; Polyakova, S.; Belov, V.; van Blaaderen, A.; Bossi, M. L.; Hell, S. W. *Small* **2008,** *4,* 134–142. doi:10.1002/smll.200700440
13. Métivier, R.; Badré, S.; Méallet-Renault, R.; Yu, P.; Pansu, R. B.; Nakatani, K. *J. Phys. Chem. C* **2009,** *113,* 11916–11926. doi:10.1021/jp902344x
14. Wu, Y.; Xie, Y.; Zhang, Q.; Tian, H.; Zhu, W.; Li, A. D. Q. *Angew. Chem., Int. Ed.* **2014,** *53,* 2090–2094. doi:10.1002/anie.201309915
15. Nakashima, T.; Kajiki, Y.; Fukumoto, S.; Taguchi, M.; Nagao, S.; Hirota, S.; Kawai, T. *J. Am. Chem. Soc.* **2012,** *134,* 19877–19883. doi:10.1021/ja309275q
16. Snegir, S. V.; Marchenko, A. A.; Yu, P.; Maurel, F.; Kapitanchuk, O. L.; Mazerat, S.; Lepeltier, M.; Léaustic, A.; Lacaze, E. *J. Phys. Chem. Lett.* **2011,** *2,* 2433–2436. doi:10.1021/jz200875c
17. Bonaccorsi, P.; Aversa, M. C.; Barattucci, A.; Papalia, T.; Puntoriero, F.; Campagna, S. *Chem. Commun.* **2012,** *48,* 10550–10552. doi:10.1039/c2cc35555h
18. Kolb, H. C.; Finn, M. G.; Sharpless, K. B. *Angew. Chem., Int. Ed.* **2001,** *40,* 2004–2021. doi:10.1002/1521-3773(20010601)40:11<2004::AID-ANIE2004>3.0.CO;2-5
19. Tornøe, C. W.; Christensen, C.; Meldal, M. *J. Org. Chem.* **2002,** *67,* 3057–3064. doi:10.1021/jo011148j
20. Wu, P.; Feldman, A. K.; Nugent, A. K.; Hawker, C. J.; Scheel, A.; Voit, B.; Pyun, J.; Fréchet, J. M. J.; Sharpless, K. B.; Fokin, V. V. *Angew. Chem., Int. Ed.* **2004,** *43,* 3928–3932. doi:10.1002/anie.200454078
21. Wu, P.; Chen, X.; Hu, N.; Tam, U. C.; Blixt, O.; Zettl, A.; Bertozzi, C. R. *Angew. Chem., Int. Ed.* **2008,** *47,* 5022–5025. doi:10.1002/anie.200705363
22. Gao, Y.; Eguchi, A.; Kakehi, K.; Lee, Y. C. *Bioorg. Med. Chem.* **2005,** *13,* 6151–6157. doi:10.1016/j.bmc.2005.06.036
23. Perez-Balderas, F.; Morales-Sanfrutos, J.; Hernandez-Mateo, F.; Isac-García, J.; Santoyo-Gonzalez, F. *Eur. J. Org. Chem.* **2009,** 2441–2453. doi:10.1002/ejoc.200801170
24. Ortega-Muñoz, M.; Perez-Balderas, F.; Morales-Sanfrutos, J.; Hernandez-Mateo, F.; Isac-García, J.; Santoyo-Gonzalez, F. *Eur. J. Org. Chem.* **2009,** 2454–2473. doi:10.1002/ejoc.200801169
25. Yu, Y.; Bogliotti, N.; Maisonneuve, S.; Tang, J.; Xie, J. *Tetrahedron Lett.* **2013,** *54,* 1877–1883. doi:10.1016/j.tetlet.2013.01.119
26. Ouhenia-Ouadahi, K.; Yasukuni, R.; Yu, P.; Laurent, G.; Pavageau, C.; Grand, J.; Guérin, J.; Léaustic, A.; Félidj, N.; Aubard, J.; Nakatani, K.; Métivier, R. *Chem. Commun.* **2014,** *50,* 7299–7302. doi:10.1039/c4cc02179g
27. Collins, D. J.; Hibberd, A. I.; Skelton, B. W.; White, A. H. *Aust. J. Chem.* **1998,** *51,* 681–694. doi:10.1071/C97156

License and Terms

Beilstein Journal of Organic Chemistry

Postsynthetic functionalization of glycodendrons at the focal point

Thisbe K. Lindhorst* and Katharina Elsner

Full Research Paper

Open Access

Address:
Otto Diels Institute of Organic Chemistry, Christiana Albertina University of Kiel, Otto-Hahn-Platz 3–4, D-24098 Kiel

Email:
Thisbe K. Lindhorst* - tklind@oc.uni-kiel.de

* Corresponding author

Keywords:
amphiphilic glycomimetics; cross metathesis; glycodendrons; multivalent glycoconjugates; multivalent glycosystems

Beilstein J. Org. Chem. **2014,** *10,* 1482–1487.
doi:10.3762/bjoc.10.152

Received: 12 March 2014
Accepted: 10 June 2014
Published: 01 July 2014

This article is part of the Thematic Series "Multivalent glycosystems for nanoscience".

Guest Editor: B. Turnbull

Abstract

Glycodendrons are multivalent glycoconjugates bearing an orthogonal functional group at the focal point of the molecule. This allows for their postsynthetic elaboration to achieve amphiphilic glycolipid mimetics, for example, which eventually can be applied in biology, biophysics, or material science. Here, postsynthetic modification of di- and tetravalent polyether glycodendrons has been explored using etherification, thiol-ene reaction and in particular olefin cross metathesis.

Introduction

In addition to nucleic acids and proteins, molecular life is based on a third important class of compounds, the carbohydrates. Carbohydrates are involved in numerous biological recognition processes, where they are often displayed in the form of multivalent conjugates such as on the surface of cells [1]. To investigate multivalency in carbohydrate recognition, multivalent glycomimetics, for example the glycodendrimers, have become valuable tools during the last two decades [2]. Typical glycodendrimers consist of (hyper)branched dendritic core molecules which are decorated with specific sugars in their periphery [3-5]. In addition to dendrimers, also so-called dendrons have been frequently applied for the synthesis of multivalent glycoconjugates [6]. Dendrons resemble a branched fragment of a whole dendrimer with an orthogonal functional group (FG) at the focal point of the molecular fragment (Figure 1a). This molecular architecture comprises the possibility to anchor a multivalent glycoconjugate to a scaffold or surface, respectively, after suitable postsynthetic modification at the focal point of the molecule. Moreover, such an approach opens the door to a number of intriguing applications of multivalent glycoconjugates such as incorporation into a supramolecular assembly, for example films, liposomes, or membranes.

Focal functionalization of dendrons can be performed prior to modification of the multivalent dendron periphery, or as postsynthetic modification. However, postsynthetic functionaliza-

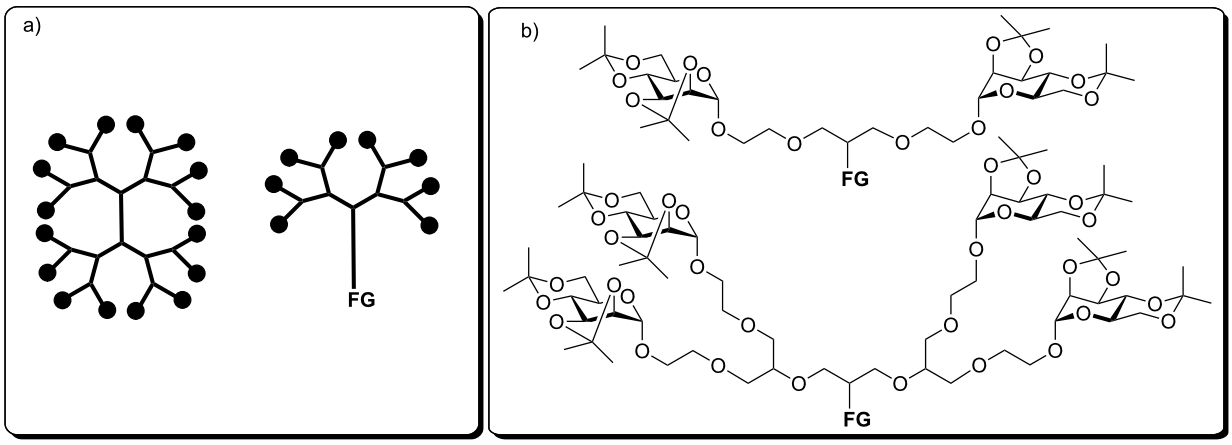

Figure 1: a) Dendrons (right) are branched fragments of dendrimers (left), featuring a functional group (FG) at their focal point which can be orthogonal to all other functionalities of the molecule; b) di- and tetravalent polyether glycodendrons equipped with protected α-D-mannosyl residues were employed to test postsynthetic modification at the focal point; FG: double bond, OH.

tion of the focal point of a rather bulky molecule is not necessarily facile owing to steric hindrance, and therefore has been employed to a lesser extent until to date. Consequently, we have commenced a study on postsynthetic modification of di- and tetravalent polyether glycodendrons, functionalized with a focal double bond or hydroxy group, respectively (Figure 1b).

Results and Discussion

The principal synthesis of the employed polyether glycodendrons has been published earlier by us [7,8]. It is based on Williamson etherification of methallyldichloride (MDC, **1**, 3-chloro-2-chloromethyl-1-propene) [9] using the isopropylidene-protected hydroxyethyl mannoside **2** to furnish the divalent glycodendron **3** (Scheme 1). Then, ozonolysis yields the

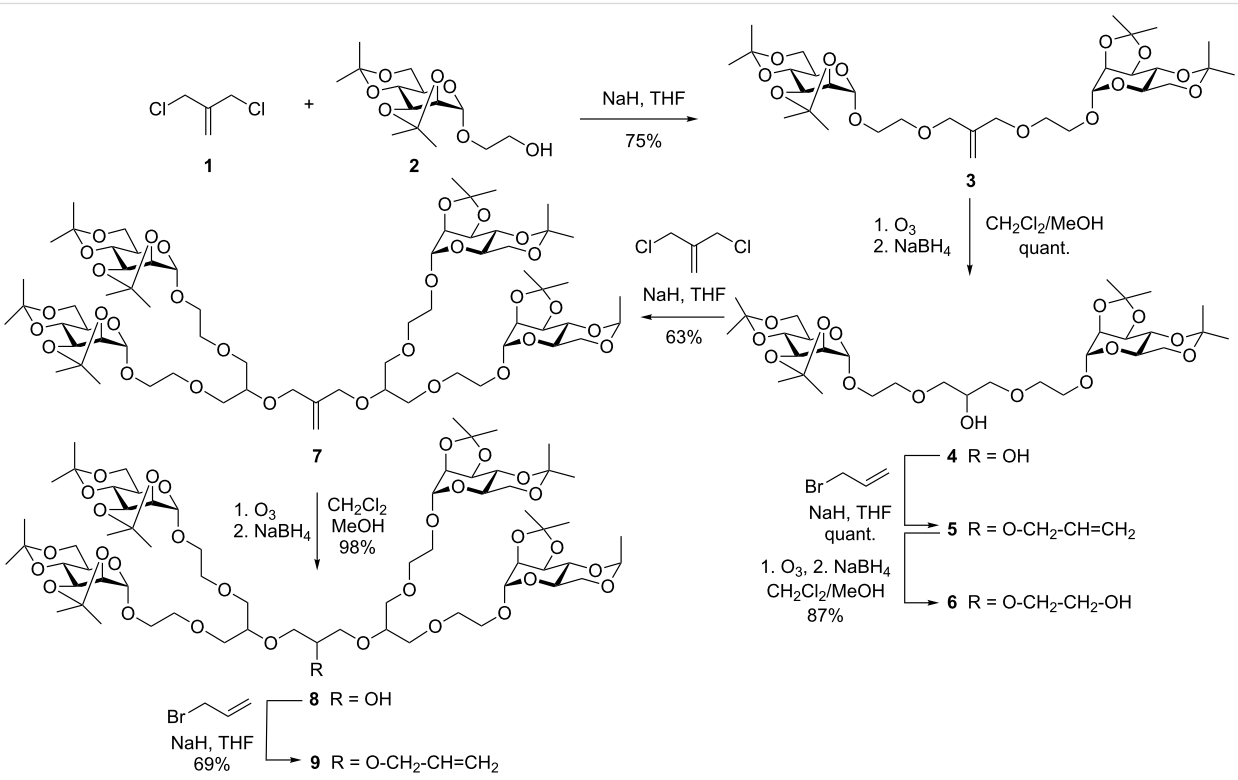

Scheme 1: Synthesis of the starting material for postsynthetic focal point functionalization; published yields [7] were partly improved. Glycodendron **9** was obtained for the first time (cf. Experimental part).

alcohol **4** in a quantitative reaction, which can be further modified at the focal hydroxy group, leading to **5** after allylation and to the primary alcohol **6** in the following ozonolysis step. However, the alcohol **4** can also be employed in another etherification reaction with MDC to deliver glycodendron **7** of the next dendron generation. This in turn, can be further elaborated to give the alcohol **8** and the formerly unknown glycodendron alkene **9**.

Initially, postsynthetic focal point modification of glycodendrons was attempted by direct etherification employing long chain alkyl bromides. Williamson etherification of **4** using tetradecanyl bromide led to **10** in only 33% yield, and the same reaction starting with the primary alcohol **6** led to **11** in a somewhat better yield of 44% (Scheme 2). When the tetravalent glycodendron **3** was employed in the same experiment, yields remained below 10%. The focal point apparently is disadvantaged in this reaction. Under those reaction conditions that resulted in at least some yield, degradation of the starting material concomitantly occurred. Also other standard reactions of organic chemistry did not proceed as expected in case of the glycodendrons **3**–**9**. However, the so-called "thiol-ene" reaction [10] gave reliable results with both bivalent and tetravalent glycodendrons. The radical addition of mercaptododecane to either **3** or **7**, employing AIBN as radical starter, led to the amphiphilic thioethers **12** and **13**, respectively, in fair yields. Deprotection conditions employing TFA in water left the thioethers intact. These results were encouraging for further postsynthetic modification of glycodendrons.

In a second part of our study we have investigated olefin cross metathesis [11] of polyether di- and tetravalent glycodendrons **5** and **9** with terminal alkenes of different chain length (Scheme 3). Indeed, reaction of **5** and 1-decene using Grubbs' catalyst (5%) led to the alkene **14** in 81% and the analogous reaction with 1-pentadecene and 10% Grubbs' catalyst furnished **15** in 64% yield. Interestingly, in both cases, the *trans*-configured alkenes were the only cross-coupling products obtained. This might be due to the specific structure of the used substrates, as sterically hindered olefins are known to enhance *trans*-selectivity in metathesis [12]. The same reactions were successful with the tetravalent glycodendron **9** yielding the

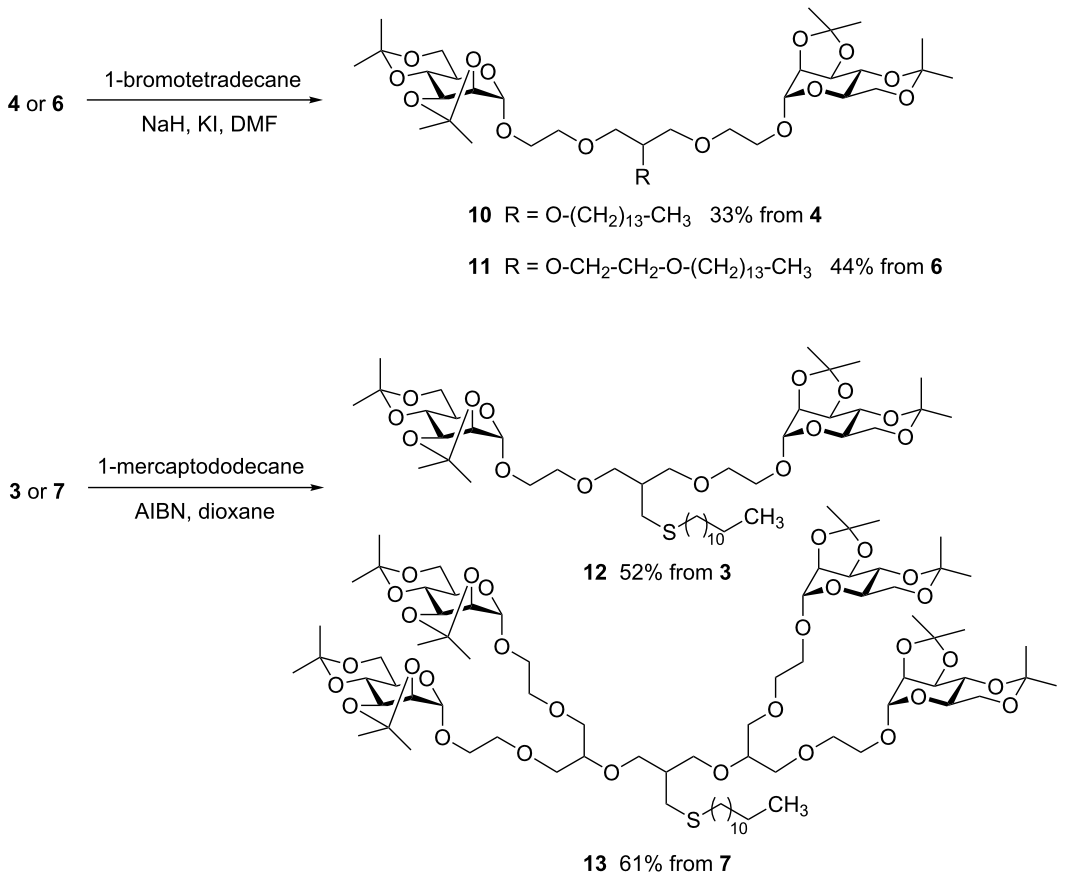

Scheme 2: Initial syntheses of amphiphilic glycodendrons.

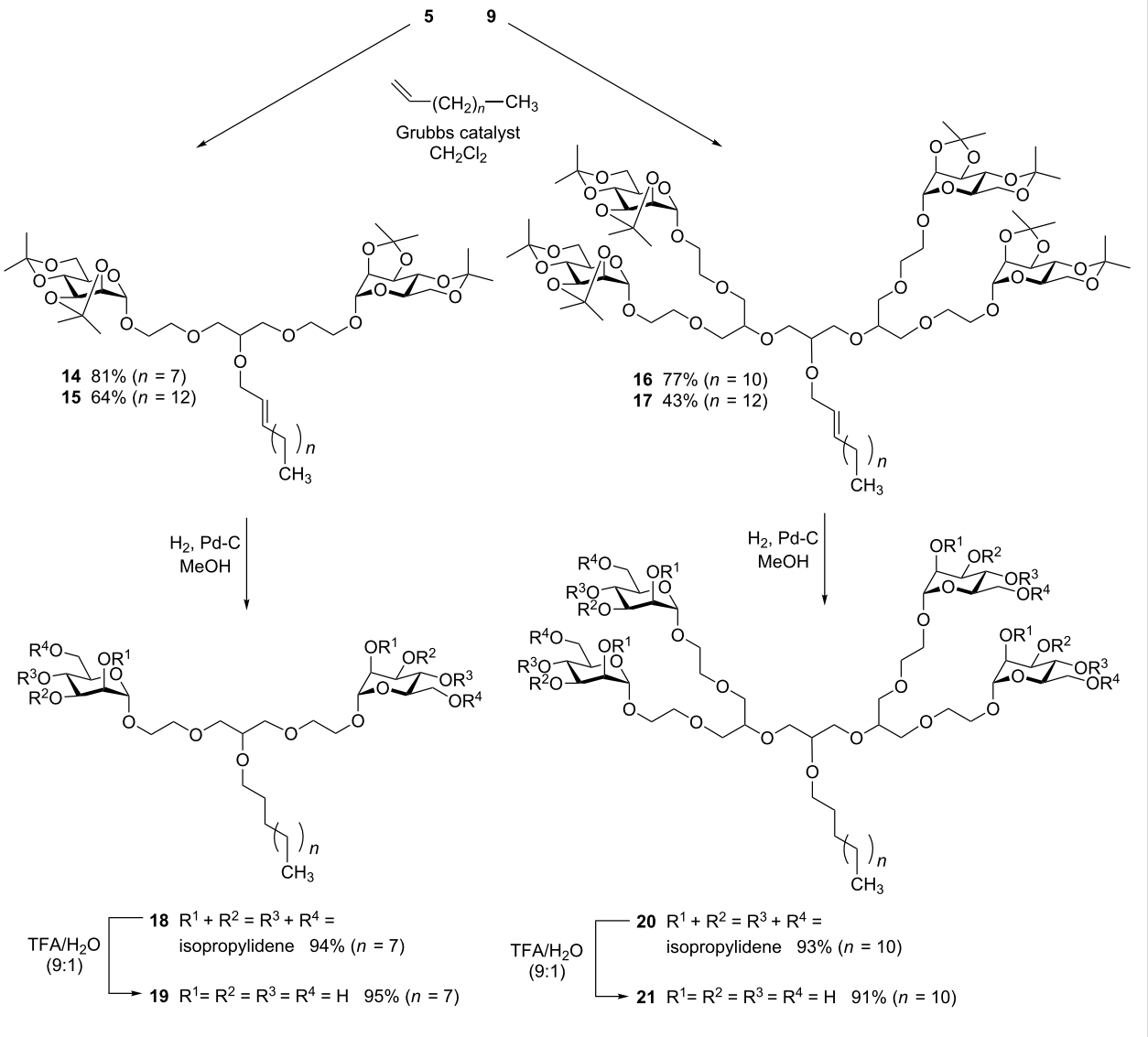

Scheme 3: Postsynthetic focal modification of glycodendrons (I) using using olefin cross metathesis.

cross coupling products **16** and **17** in 77% and 43% respective yields. Again, only the *trans*-metathesis products were obtained. The cross-coupled alkenes **14** and **16** were carried on in catalytic hydrogenation reactions for reduction of the double bond, followed by deprotection of the sugar isopropylidene protecting groups. This supplied the di- and tetravalent amphiphilic glycodendrons **19** and **21**, which can eventually be explored in glycoarray fabrication [13] or in another supramolecular context such as in glycomicelles [14].

To also achieve the synthesis of branched glycolipid mimetics which are suitable for incorporation into lipid bilayers, the di- and tetravalent glycodendrons **6** and **9** were then cross-coupled with the mono-allylated glycerol triether **22** (Scheme 4). The alkene **22** can be derived from commercially available glycerol-monoallyl ether according to the literature [15]. Metathesis with the divalent glycodendron **6** led to the desired product **23** as *cis*/*trans* mixture in 38% yield, while the glycerol ether dimer was obtained as the main product (not shown). The analogous result was obtained with the tetravalent glycodendron **9** leading to the hetero-cross coupling product **24** as the minor and the homo-cross coupling product as the dominating product. Nevertheless, metathesis allows to achieve these quite complex branched glycolipid mimetics, **23** and **24**, on a multi-100 mg scale. The following hydrogenation of the double bond was carried out in order to resolve the diastereomeric *cis/trans* mixtures leading to the saturated products **25** and **26** in high yields. Then deprotection of the sugar isopropylidene protecting groups furnished the

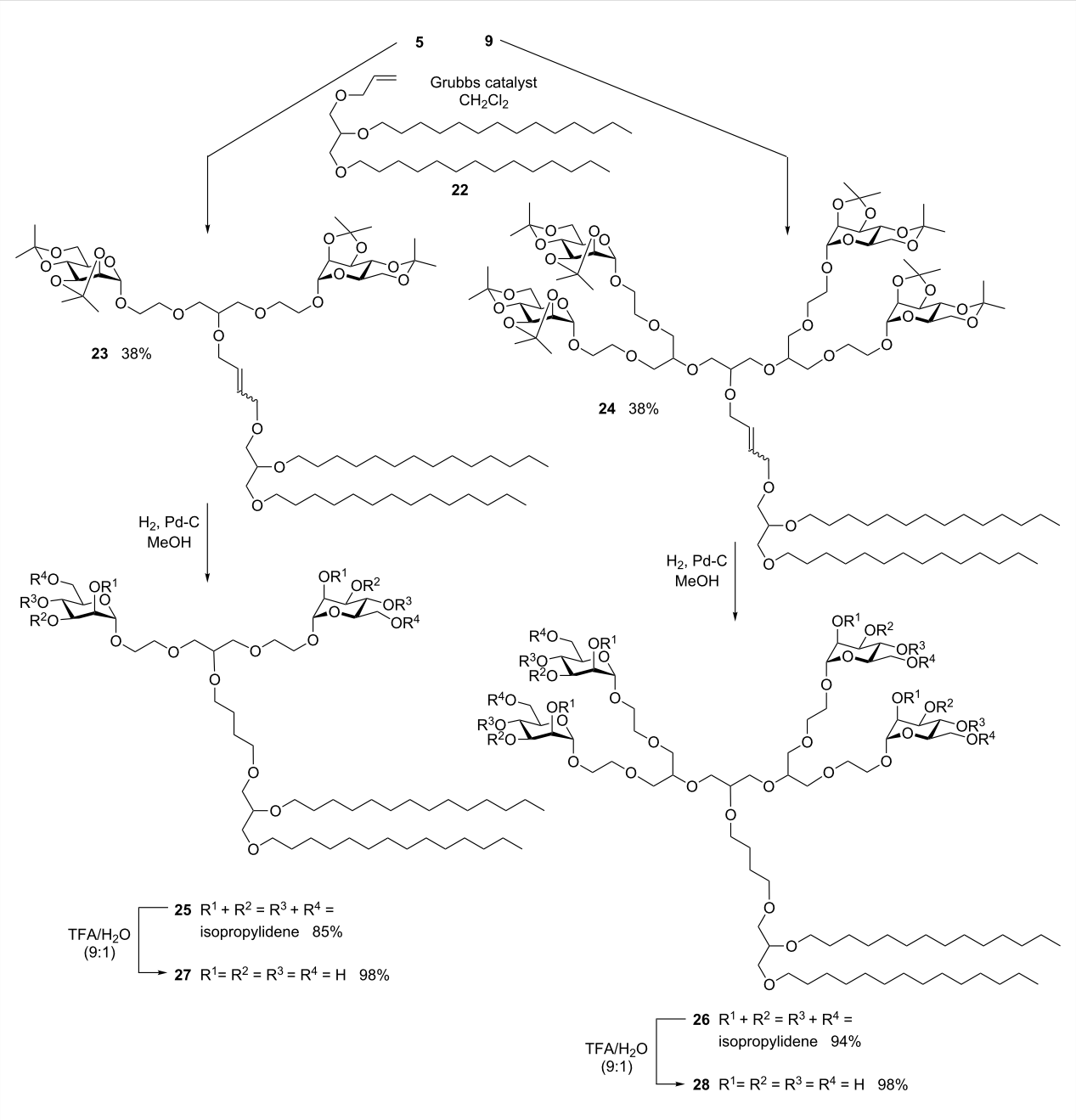

Scheme 4: Postsynthetic focal modification of glycodendrons (II) using olefin cross metathesis.

di- and tetravalent amphiphilic glycodendrons **27** and **28**. Purification of the unprotected products was facilitated by gel permeation chromatography (GPC).

Conclusion

In conclusion, it was shown that readily available polyether glycodendrons can be refined employing suitable postsynthetic modification of the focal point. We have illustrated, that alkylation, thiol-ene reaction and in particular olefin cross metathesis leads to di- and tetravalent glycolipid mimetics that are amenable to a variety of applications, employing Langmuir films [16], self-assembled monolayers (SAMs) [17-19] or lipid bilayers [20], for example. We will eventually optimize some of the described reactions where necessary and validate the described procedures for modification of more complex glycodendrons, including the use of alternative protecting groups. Certainly, thiol-ene and metathesis reaction should be particularly useful also for oligosaccharide glycodendrons, which might be even more sensitive than the herein used molecules.

Supporting Information

Supporting Information File 1

Detailed experimental procedures and full NMR interpretation of all synthesised compounds.
[http://www.beilstein-journals.org/bjoc/content/supplementary/1860-5397-10-152-S1.pdf]

Acknowledgements

Support by the Fonds of the Chemical Industry (FCI) is gratefully acknowledged.

References

1. Kiessling, L. L.; Gestwicki, J. E.; Strong, L. E. *Angew. Chem.* **2006,** *118,* 2408–2429. doi:10.1002/ange.200502794
Angew. Chem., Int. Ed. **2006,** *45,* 2348–2368. doi:10.1002/anie.200502794
2. Bernardi, A.; Jiménez-Barbero, J.; Casnati, A.; De Castro, C.; Darbre, T.; Fieschi, F.; Finne, J.; Funken, H.; Jaeger, K.-E.; Lahmann, M.; Lindhorst, T. K.; Marradi, M.; Messner, P.; Molinaro, A.; Murphy, P. V.; Nativi, C.; Oscarson, S.; Penadés, S.; Peri, F.; Pieters, R. J.; Renaudet, O.; Reymond, J.-L.; Richichi, B.; Rojo, J.; Sansone, F.; Schäffer, C.; Turnbull, W. B.; Velasco-Torrijos, T.; Vidal, S.; Vincent, S.; Wennekes, T.; Zuilhof, H.; Imberty, A. *Chem. Soc. Rev.* **2013,** *42,* 4709–4727. doi:10.1039/c2cs35408j
3. Röckendorf, N.; Lindhorst, T. K. *Top. Curr. Chem.* **2001,** *217,* 201–238. doi:10.1007/3-540-45003-3_6
4. Lindhorst, T. K. *Top. Curr. Chem.* **2002,** *218,* 201–235. doi:10.1007/3-540-45010-6_7
5. Chabre, Y. M.; Roy, R. *Chem. Soc. Rev.* **2013,** *42,* 4657–4708. doi:10.1039/c3cs35483k
6. Ribeiro-Viana, R.; Sánchez-Navarro, M.; Luczkowiak, J.; Koeppe, J. R.; Delgado, R.; Rojo, J.; Davis, B. G. *Nat. Commun.* **2012,** *3,* No. 1303. doi:10.1038/ncomms2302
7. Boysen, M. M. K.; Elsner, K.; Sperling, O.; Lindhorst, T. K. *Eur. J. Org. Chem.* **2003,** 4376–4386. doi:10.1002/ejoc.200300413
8. Elsner, K.; Boysen, M. M. K.; Lindhorst, T. K. *Carbohydr. Res.* **2007,** *342,* 1715–1725. doi:10.1016/j.carres.2007.05.005
9. Grasyon, S. M.; Fréchet, J. M. J. *J. Am. Chem. Soc.* **2000,** *122,* 10335–10344. doi:10.1021/ja001903v
10. Dondoni, A.; Marra, A. *Chem. Soc. Rev.* **2012,** *41,* 573–586. doi:10.1039/c1cs15157f
11. Grubbs, R. H.; Chang, S. *Tetrahedron* **1998,** *54,* 4413–4450. doi:10.1016/S0040-4020(97)10427-6
12. Crowe, W. E.; Goldberg, D. R.; Zhang, Z. J. *Tetrahedron Lett.* **1996,** *37,* 2117–2120. doi:10.1016/0040-4039(96)00230-4
13. Grabosch, C.; Kolbe, K.; Lindhorst, T. K. *ChemBioChem* **2012,** *13,* 1874–1879. doi:10.1002/cbic.201200365
14. Schwekendiek, K.; Kobarg, H.; Daumlechner, L.; Sönnichsen, F. D.; Lindhorst, T. K. *Chem. Commun.* **2011,** *47,* 9399–9401. doi:10.1039/c1cc13246f
15. Cassel, S.; Debaig, C.; Benvegnu, T.; Chaimbault, P.; Lafosse, M.; Plusquellec, D.; Rollin, P. *Eur. J. Org. Chem.* **2001,** 875–896. doi:10.1002/1099-0690(200103)2001:5<875::AID-EJOC875>3.0.CO;2-R
16. Guo, C. X.; Boullanger, P.; Jiang, L.; Liu, T. *Colloids Surf., A* **2007,** *293,* 152–156. doi:10.1016/j.colsurfa.2006.07.019
17. Love, J. C.; Estroff, L. A.; Kriebel, J. K.; Nuzzo, R. G.; Whitesides, G. M. *Chem. Rev.* **2005,** *105,* 1103–1170. doi:10.1021/cr0300789
18. Ban, L.; Pettit, N.; Li, L.; Stuparu, A. D.; Cai, L.; Chen, W.; Guan, W.; Wang, P. G.; Mrksich, M. *Nat. Chem. Biol.* **2012,** *8,* 769–773. doi:10.1038/nchembio.1022
19. Grabosch, C.; Kind, M.; Gies, Y.; Schweighöfer, F.; Terfort, A.; Lindhorst, T. K. *Org. Biomol. Chem.* **2013,** *11,* 4006–4015. doi:10.1039/c3ob40386f
20. Jayaramam, N.; Maiti, K.; Naresh, K. *Chem. Soc. Rev.* **2013,** *42,* 4640–4656. doi:10.1039/c3cs00001j

License and Terms

Beilstein Journal of Organic Chemistry

Efficient routes toward the synthesis of the D-*rhamno*-trisaccharide related to the A-band polysaccharide of *Pseudomonas aeruginosa*

Aritra Chaudhury, Sajal K. Maity and Rina Ghosh*

Full Research Paper

Open Access

Address:
Department of Chemistry, Jadavpur University, Kolkata 700 032, India

Email:
Rina Ghosh* - ghoshrina@yahoo.com

* Corresponding author

Keywords:
A-band polysaccharide; D-*rhamno*-trisaccharide; deoxygenation on thioglycoside; multivalent glycosystems; one-pot sequential glycosylation; *Pseudomonas aeruginosa*

Beilstein J. Org. Chem. **2014,** *10,* 1488–1494.
doi:10.3762/bjoc.10.153

Received: 27 February 2014
Accepted: 11 June 2014
Published: 01 July 2014

This article is part of the Thematic Series "Multivalent glycosystems for nanoscience".

Guest Editor: B. Turnbull

Abstract

The present work describes efficient avenues for the synthesis of the trisaccharide repeating unit [α-D-Rha*p*-(1→3)-α-D-Rha*p*-(1→3)-α-D-Rha*p*] associated with the A-band polysaccharide of *Pseudomonas aeruginosa.* One of the key steps involved 6-*O*-deoxygenation of either partially or fully acylated 4,6-*O*-benzylidene-1-thiomannopyranoside by radical-mediated redox rearrangement in high yields and regioselectivity. The D-*rhamno*-thioglycosides so obtained allowed efficient access to the trisaccharide target via stepwise glycosylation as well as a one-pot glycosylation protocol. In a different approach, a 4,6-*O*-benzylidene D-*manno*-trisaccharide derivative was synthesized, which upon global 6-*O*-deoxygenation followed by deprotection generated the target D-*rhamno*-trisaccharide. The application of the reported regioselective radical-mediated deoxygenation on 4,6-*O*-benzylidene D-*manno* thioglycoside (hitherto unexplored) has potential for ramification in the field of synthesis of oligosaccharides based on 6-deoxy hexoses.

Introduction

With the firm establishment of the critical roles played by oligosaccharides in diverse biological processes [1-4], the field of oligosaccharide synthesis has seen a rapid development over the last two decades [5-7]. The D-rhamnoside motif is of particular interest with its presence established in the LPS/EPS systems of various bacterial strains which are pathogenic towards both plants and animals. These species include the *Burkholderia cepacia* complex [8], *P. aeruginosa* [9], *Helicobacter pylori* [10], *Citrobacter freundii* [11], *Campylobacter fetus* [12], *Stenotrophonas maltophilia* [13], *Xanthomonas campestri* [14] and *Brucella sp.* [15].

P. aeruginosa has long been established as an opportunistic pathogen which infects humans having compromised immunity

with fatal consequences in a majority of cases. Its high persistence against a wide variety of antibiotics is also well documented. It has also been observed how the colonized form of this species in cystic fibrosis lungs, through non-expression of *O*-antigens, offer high persistence often rendering *O*-antigen-based vaccines ineffective. But the conservation of the A-band polysaccharide even in the colonized form makes this repeating unit a viable candidate for A-band polysaccharide-based vaccines which can avoid the vulnerability applicable to their *O*-antigen-based counterparts [16]. Hence, the A-band polysaccharide [16] of *P. aeruginosa* which has been characterized previously as a repeating combination of [→2)-α-D-Rha*p*-(1→3)-α-D-Rha*p*-(1→3)-α-D-Rha*p*] (Figure 1) provides for a synthetic target whose efficient synthesis is worth pursuing. It is to be noted that synthesis of a tetrasaccharide, α-D-Rha*p*-(1→2)-α-D-Rha*p*-(1→3)-α-D-Rha*p*-(1→3)-α-D-Rha*p* [17] and a trisaccharide, α-D-Rha*p*-(1→3)-α-D-Rha*p*-(1→2)-α-D-Rha*p* [18] related to the A-band polysaccharide of *P. aeruginosa* were made with a view to develop glycoconjugate vaccines, but none have ultimately materialized into valid vaccine candidates.

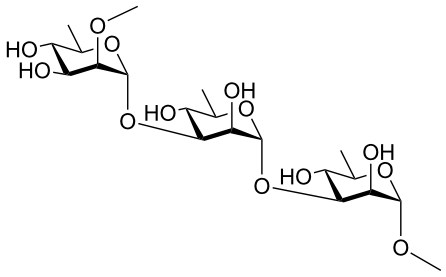

Figure 1: Repeating unit of the A-band polysaccharide of *P. aeruginosa*.

Thus, we targeted the trisaccharide [α-D-Rha*p*-(1→3)-α-D-Rha*p*-(1→3)-α-D-Rha*p*] as our synthetic goal toward construction of a probable vaccine candidate against *P. aeruginosa.*

The synthesis of the D-rhamnose-based oligosaccharide from the D-mannose motif has received substantial attention over the last decade. The problem of β-D-rhamnoside synthesis has been greatly addressed by Crich et al. [19-23]. But, Crich's global deoxygenating strategy, despite its ultimate efficiency, still requires synthetic modification on the conventional 4,6-*O*-benzylidene framework involving reagents which are rather expensive. Moreover, additional steps are required for the preparation of these adequately derivatized mannose-based systems from which the D-rhamnose motif may be accessed. Other reports on the D-rhamnose-based synthesis have also surfaced in recent times [24,25]. Apart from this, the synthesis of monomeric D-rhamnose has been highly streamlined by Roy et al. in 2007 [26], and further improvement on this method was reported by Kiefel et al. in 2011 [27]. However, the deoxygenation protocol involving halogenation under Mitsunobu conditions was found to be inefficient when applied to thioglycosides directly. Moreover, the use of stoichiometric amounts of the toxic tin hydride for radical-based reductive dehalogenation as required by the above method appeared undesirable especially in the preparative stages where reactions have to be set up on a large scale. On the other hand, Kiefel's method requires four steps for the conversion of D-mannose to D-rhamnose on which further manipulations are required to reach the adequately designed derivatives. This makes the starting material preparations rather long drawn.

Keeping these limitations in mind we selected the protocol devised by Pedersen et al. [28] and subsequently studied by Dang et al. [29-32] which seemed to address all the inadequacies described above. However, the compatibility of the method with thioglycosides had to be verified. Upon application, and much to our delight, it was found that thioglycosides responded equally well compared to their *O*-glycosidic counterparts. It may be mentioned here that the response of thioglycosides towards this method was not reported in the original observation [28]. To the best of our knowledge, this method has not yet been applied directly on thioglycosides. So, having established an easy means to access D-*rhamno*-thioglycosides from their D-*manno*-counterparts, we set about devising efficient routes to reach the target trisaccharide. The following section bears elaboration of our efforts.

Results and Discussion

Deoxygenation at the C-6 position of D-mannose derivatives bearing conventional or Crich's modified 4,6-*O*-benzylidene protection [19-23] has been the principal philosophy behind the synthesis of the D-rhamnose [19-23,30,33-39] motif. This is a natural choice not only because it allows simultaneous selective blockage of the O-4 and O-6 positions but also sets up the model on which various deoxygenation protocols may be tried. The linkage pattern and stereochemistry at the glycosidic positions on the target dictate the presence of acyl protection on the O-2 position as shown in Scheme 1.

We began our synthesis targeting two pivotal intermediates **1a** and **1b** which were obtained using previously reported methods [40,41] and then proceeding forward to the monomeric building blocks required according to the retrosynthetic analysis (Figure 2).

The procedures used and the results obtained to reach the intermediate targets have been summarized in Scheme 1. Accordingly, compounds **2** and **3b** [42] were obtained uneventfully

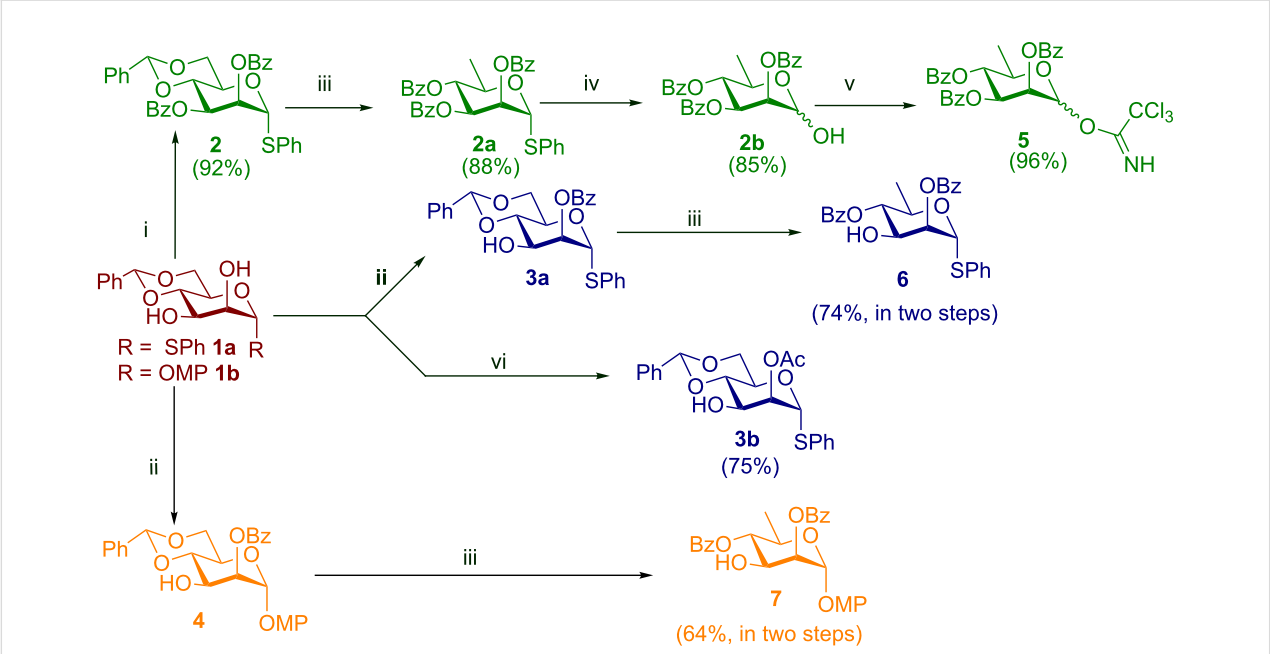

Scheme 1: Preparation of the monomeric building blocks; reagents and conditions: i) Pyr., BzCl, 0 °C–rt; ii) $PhC(OMe)_3$, CSA, MeCN, 0 °C–rt, 80% AcOH (aq), 25 °C; iii) DTBP, TIPST, octane, reflux; iv) TCCA, acetone–H_2O, rt; v) CCl_3CN, DBU, DCM; vi) $MeC(OEt)_3$, CSA, MeCN, 0 °C–rt, 80% AcOH (aq), 25 °C.

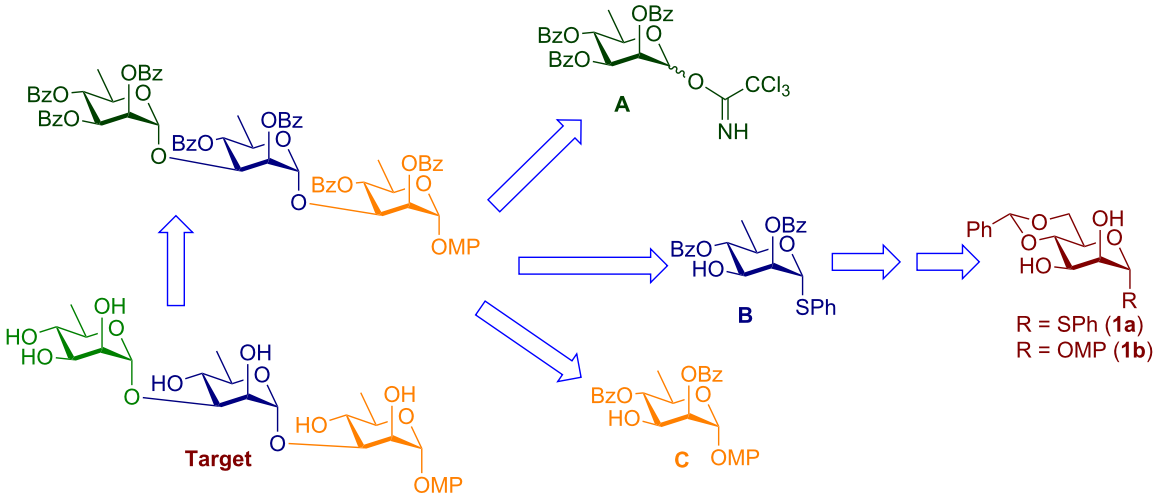

Figure 2: Retrosynthetic analysis.

from **1a** in 92% and 75%, respectively (Scheme 1). All attempts to place an acetyl protection at the O-2 position of **1b** with high yield failed. The poor yield was presumed to be due to the migration of the 2-*O*-acetyl group to the O-3 position leading to a mixture which was hard to separate. Hence we switched to *O*-benzoyl protection which was found to be less susceptible to migration [25]. The 2-*O*-benzoylated compound **4** was prepared by conversion of **1b** into its corresponding methyl 2,3-orthobenzoate derivative followed by the selective cleavage of the same with 80% aq AcOH. Compound **3a** which is the phenyl thioglycoside analogue of **4** was also accessed similarly. Both the compounds were next converted to their rhamnoside counterparts **6** and **7** [44], respectively by treatment with di-*tert*-butyl peroxide (DTBP) and triisopropylsilanethiol (TIPST) under reflux in octane over 2–3 h [30] in overall 74% and 64% yields, respectively, over two steps. It is worth noting here that during column chromatographic purification after AcOH-mediated cleavage of the orthobenzoate derivative some losses were incurred due to

the migration of the 2-*O*-benzoyl group to the O-3 position. However the susceptibility of the benzoyl group to migration was much lower than that of its acetate analogue.

The same problem persisted even in the rhamnosides **6** and **7**. Hence, to minimize the loss during purification, the chromatographic purification was reserved until the end of the deoxygenation step. Thus, the intermediate compounds **3a** and **4** were used without purification by column chromatography. Compound **2** was deoxygenated to its rhamnosyl counterpart **2a** in a high yield (88%). Next, the thioglycoside was hydrolyzed to the hemiacetal **2b** with trichloroisocyanuric acid (TCCA) in acetone–H_2O [43] in 85% yield and was further converted almost quantitatively to the corresponding trichloroacetimidate **5** [44]. Having arrived at the monomeric building blocks **5**, **6**, and **7** we carried forward to the rhamnose-based disaccharide **8** which being a thioglycoside would subsequently serve as the glycosyl donor in the next step. Accordingly, **5** and **6** were coupled almost quantitatively to give **8**. The disaccharide so obtained was then coupled with **7** to give the protected trisaccharide **9** in 90% yield using a *N*-iodosuccinimide-trimethylsilyl trifluoromethanesulfonate (NIS-TMSOTf) combination as the activating reagent. The target trisaccharide was then obtained via deprotection under the Zémplen conditions to give **10** quantitatively, as is summarized in Scheme 2.

However, in the interest of time and economy of resources consumed, a one-pot synthesis is always desirable. Accordingly, further optimization of the glycosylation protocol was achieved by carrying out the whole glycosylation process in one-pot leading to the target trisaccharide **9** in 79% yield (Scheme 3). In this case the disaccharide synthesis was set up as described previously, and then the second acceptor **7** was introduced into the reaction mixture at −50 °C after which NIS and TMSOTf were added successively at the same temperature. The temperature was then raised upto −10 °C, and the reaction mixture was stirred for another 1 h at that temperature to give the target trisaccharide as summarized in Scheme 3.

At this point, our search for overall synthetic efficiency was greatly augmented by a change of approach. Since, multiple deoxygenations had been observed by Dang et al. [30] on trehalose derivatives previously, we figured that we could access the rhamnose-based trisaccharide directly from a suitably derivatized *manno*-trisaccharide bearing the three 4,6-*O*-benzylidene protecting groups by a single global deoxygenation step. Accordingly, we coupled the monomeric units **2**, **3b** [45] and **4** to reach the mannose-based trisaccharide **12** (Scheme 4). The deoxygenation protocol, being incompatible with the *O*-benzyl protecting group, required an acyl protection profile on O-2 and O-3 positions. Such an arrangement was also in agreement with the stereochemical requirements at the anomeric positions of our target trisaccharide.

Since compounds **2** and **3b** bear structural similarity with each other it was expected that they would have similar reactivity towards glycosylative activation. Hence, a preactivation-based glycosylation protocol was devised for the first step leading to

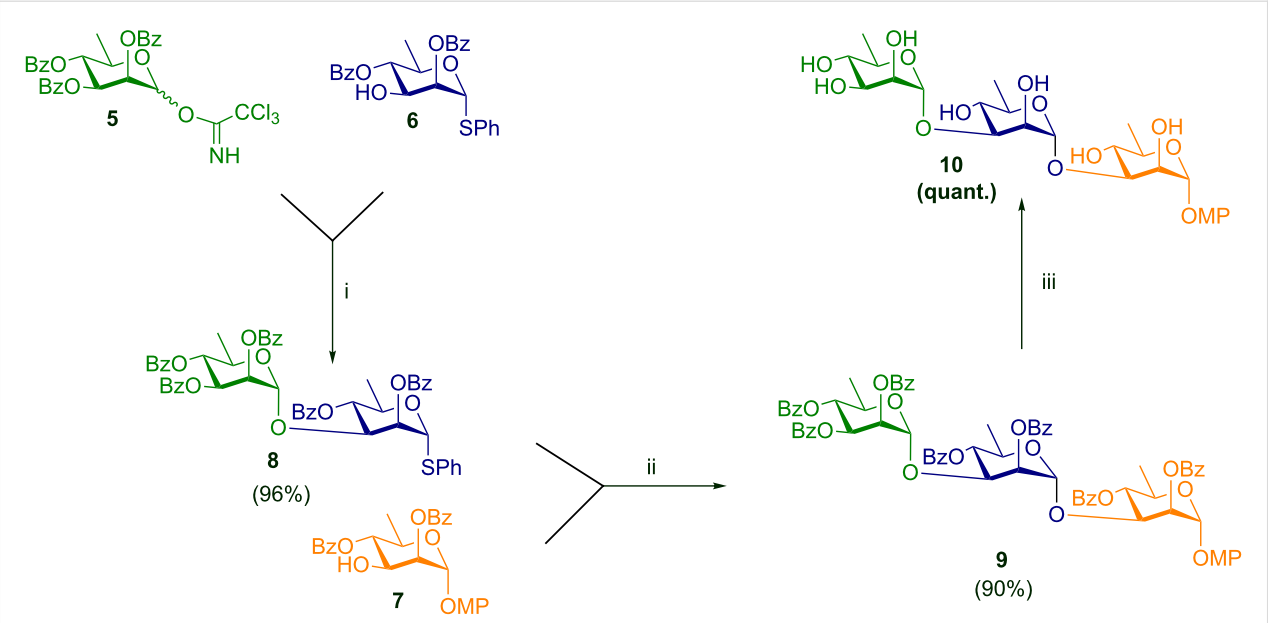

Scheme 2: Sequential stepwise synthesis of the trisaccharide; reagents and conditions: i) TMSOTf, DCM, molecular sieves 4 Å, N_2, −50 °C; ii) NIS, TMSOTf, DCM, molecular sieves 4 Å, N_2, −10 °C; iii) NaOMe, MeOH, rt, 12 h.

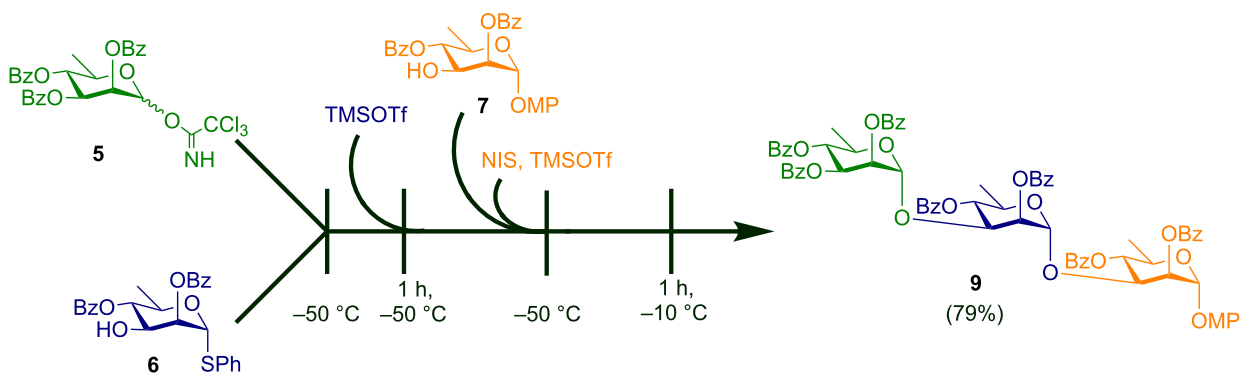

Scheme 3: Synthesis of the trisaccharide by sequential one-pot glycosylation reactions; reagents and conditions: i) (a) TMSOTf, DCM, molecular sieves 4 Å, N_2, −50 °C; (b) NIS, TMSOTf, −50 °C, DCM, molecular sieves 4 Å, N_2, −10 °C.

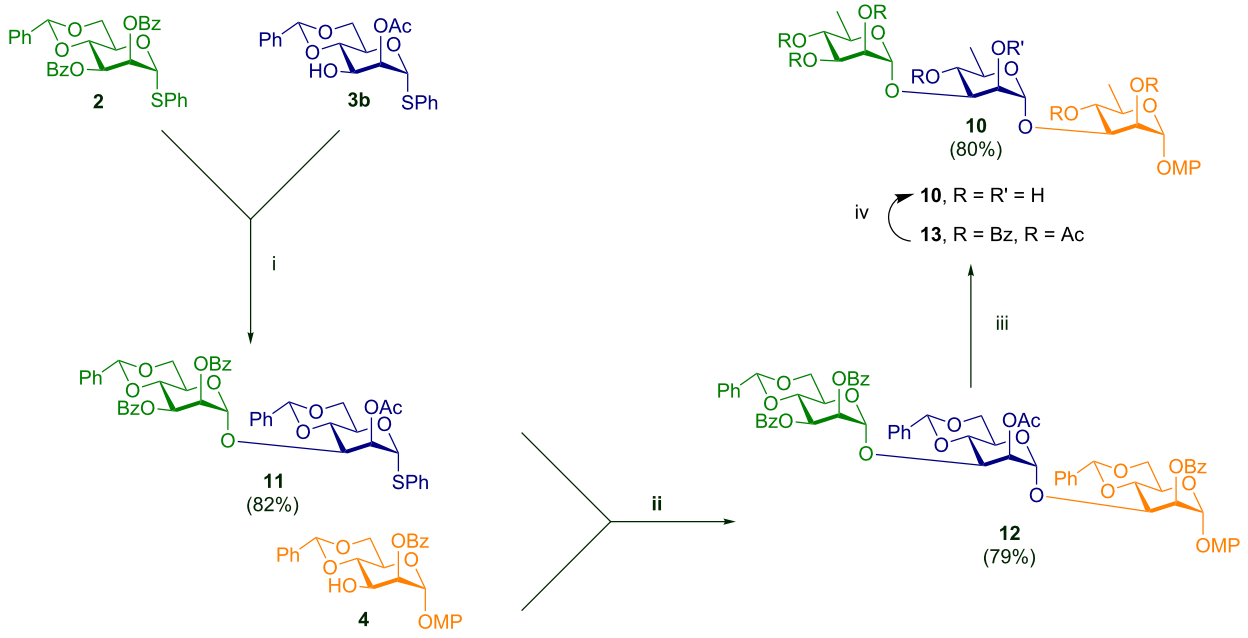

Scheme 4: Synthesis of the target trisaccharide via global deoxygenation strategy; reagents and conditions: i) BSP, Tf_2O, –60 °C, DCM, molecular sieves 4 Å, N_2, –78 °C; ii) NIS, TMSOTf, DCM, molecular sieves 4 Å, N_2, −10 °C; iii) DTBP, TIPST, octane, reflux, 3 h; iv) NaOMe, MeOH, rt, 12 h.

the disaccharide **11** using 1-benzenesulfinyl piperidine–triflic anhydride (BSP–Tf_2O) [46]. The subsequent step was carried out using NIS–TMSOTf to give the mannose-based trisaccharide **12**. This trisaccharide was next deoxygenated globally to give the rhamnose-based trisaccharide **13** with high yield (80%). This was then deprotected under the Zémplen conditions to yield **10** quantitatively as is summarized in Scheme 4.

^{1}H NMR in MeOH-d_4 of the target trisaccharide **10** showed the anomeric protons of the consecutive rhamnose residues from the non-reducing end appearing at δ 5.09, 5.06 and 5.30 ppm, respectively. ^{13}C NMR in the same solvent revealed that the chemical shifts of the anomeric carbons of the two consecutive rhamnose units from the non-reducing end coincided at δ 102.3 ppm (as also evidenced from HSQC data) with the corresponding $^1J_{C1\text{-}H1}$ of 170.4 Hz and that of the anomeric carbon of the reducing end monomer unit appeared at 98.9 ppm with the corresponding $^1J_{C1\text{-}H1}$ of 170.2 Hz. The value at δ 102.3 ppm can be corroborated with the reported [16] C_1-chemical shifts at δ 103.19 and 103.43 with $^1J_{C1\text{-}H1}$ of 173 Hz, exhibited in D_2O corresponding to the two [→3)-α-D-Rha*p*-(1→] units in the A-band polysaccharide of *P. aeruginosa*. The small difference in the chemical shifts and the corresponding $^1J_{C1\text{-}H1}$ values may be attributed to the difference in the solvents (MeOH-d_4 and D_2O), chosen in these two cases for recording NMR. Comparing and considering the NMR data in these two cases

we surmised that all the three anomeric carbons are α-configured [47].

Conclusion

In short, we have described three different efficient routes to access the A-band trisaccharide associated with *P. aeruginosa*. The radical-based 6-deoxygenation protocol on 4,6-*O*-benzylidene (hitherto unexplored on thioglycosides) was utilized to arrive at the D-*rhamno*-thioglycoside derivatives from their D-*manno*-counterparts. This, along with a similar global 6-deoxygenation strategy on D-*manno*-trisaccharide derivative (bearing 4,6-*O*-benzylidene protection on each mannose unit) offer great potential in future oligosaccharide syntheses based on 6-deoxy hexoses.

Supporting Information

Supporting Information File 1

Experimental details for the preparation of compounds **2a**, **2b**, **3a**, **4**, **6**–**13** and the corresponding characterization data.
[http://www.beilstein-journals.org/bjoc/content/supplementary/1860-5397-10-153-S1.pdf]

Supporting Information File 2

^{1}H and ^{13}C NMR of compounds **2a**, **4**, **6**, **8**–**13** and 2D NMR (COSY, HSQC and HMBC) of compound **10**.
[http://www.beilstein-journals.org/bjoc/content/supplementary/1860-5397-10-153-S2.pdf]

Acknowledgements

The authors are grateful to CSIR, New Delhi, India for providing a fellowship (SRF) to AC and funding of project (No. 2382/01/10/2010 EMR II) to RG. Financial assistance from DST-SERB, India to RG and supports from CAS-UGC, India and FIST-DST, India to the Department of Chemistry, Jadavpur University, Kolkata are also acknowledged.

References

1. Varki, A. *Glycobiology* **1993,** *3,* 97–130. doi:10.1093/glycob/3.2.97
2. Varki, A.; Cummings, D. C.; Esko, J. D.; Freeze, H. H.; Stanley, P.; Bertozzi, C. R.; Hart, G. W.; Etzler, M. E. *Essentials of Glycobiology;* Cold Spring Harbor Press: New York, 2009.
3. Seeberger, P. H.; Werz, D. B. *Nature* **2007,** *446,* 1046–1051. doi:10.1038/nature05819
4. Fuster, M. M.; Esko, J. D. *Nat. Rev. Cancer* **2005,** *5,* 526–542. doi:10.1038/nrc1649
5. Zhu, X.; Schmidt, R. R. *Angew. Chem., Int. Ed.* **2009,** *48,* 1900–1934. doi:10.1002/anie.200802036
6. Nicolaou, K. C.; Mitchell, H. J. *Angew. Chem., Int. Ed.* **2001,** *40,* 1576–1624. doi:10.1002/1521-3773(20010504)40:9<1576::AID-ANIE15760>3.0.CO;2-G
7. Hsu, C.-H.; Hung, S.-C.; Wu, C.-Y.; Wong, C.-H. *Angew. Chem., Int. Ed.* **2011,** *50,* 11872–11923. doi:10.1002/anie.201100125
8. Herasimenka, Y.; Cescutti, P.; Impallomeni, G.; Campana, S.; Taccetti, G.; Ravenni, N.; Zanetti, F.; Rizzo, R. *J. Cystic Fibrosis* **2007,** *6,* 145–152. doi:10.1016/j.jcf.2006.06.004
9. Yokota, S.-i.; Kaya, S.; Sawada, S.; Kawamura, T.; Araki, Y.; Ito, E. *Eur. J. Biochem.* **1987,** *167,* 203–209. doi:10.1111/j.1432-1033.1987.tb13324.x
10. Kocharova, N. A.; Knirel, Y. A.; Widmalm, G.; Jansson, P. E.; Moran, A. P. *Biochemistry* **2000,** *39,* 4755–4760. doi:10.1021/bi992635k
11. Kocharova, N. A.; Borisova, S. A.; Zatonsky, G. V.; Shashkov, A. S.; Knirel, Y. A.; Kholodkova, E. V.; Staniskavsky, E. S. *Carbohydr. Res.* **1998,** *306,* 331–333. doi:10.1016/S0008-6215(97)10049-0
12. Senchenkova, S. N.; Shashkov, A. S.; Knirel, Y. A.; Mcgovern, J. J.; Moran, A. P. *Eur. J. Biochem.* **1996,** *239,* 434–438. doi:10.1111/j.1432-1033.1996.0434u.x
13. Winn, A. M.; Wilkinson, S. G. *Carbohydr. Res.* **1996,** *294,* 109–115. doi:10.1016/S0008-6215(96)90623-0
14. Molinaro, A.; Silipo, A.; Lanzetta, R.; Newman, M.-A.; Dow, M. J.; Parrilli, M. *Carbohydr. Res.* **2003,** *338,* 277–281. doi:10.1016/S0008-6215(02)00433-0
15. Kihlberg, J.; Bundle, D. R. *Carbohydr. Res.* **1992,** *216,* 67–78. doi:10.1016/0008-6215(92)84151-H
16. Arsenault, T. L.; Hughes, D. W.; MacLean, D. B.; Szarek, W. A.; Kropinski, A. M. B.; Lam, J. S. *Can. J. Chem.* **1991,** *69,* 1273–1280. doi:10.1139/v91-190
17. Tsvetkov, Y. E.; Backinowsky, L. V.; Kochetkov, N. K. *Carbohydr. Res.* **1989,** *193,* 75–90. doi:10.1016/0008-6215(89)85108-0
18. Zou, W.; Sen, A. K.; Szarek, W. A.; MacLean, D. B. *Can. J. Chem.* **1993,** *71,* 2194–2200. doi:10.1139/v93-275
19. Picard, S.; Crich, D. *Chimia* **2011,** *65,* 59–64. doi:10.2533/chimia.2011.59
20. Crich, D.; Bowers, A. A. *Org. Lett.* **2006,** *8,* 4327–4330. doi:10.1021/ol061706m
21. Crich, D.; Bowers, A. A. *J. Org. Chem.* **2006,** *71,* 3452–3463. doi:10.1021/jo0526688
22. Crich, D.; Yao, Q. *J. Am. Chem. Soc.* **2004,** *126,* 8232–8236. doi:10.1021/ja048070j
23. Crich, D.; Li, L. *J. Org. Chem.* **2009,** *74,* 773–781. doi:10.1021/jo8022439
24. Bedini, E.; Carabellese, A.; Barone, G.; Parrilli, M. *J. Org. Chem.* **2005,** *70,* 8064–8070. doi:10.1021/jo051153d
25. Bedini, E.; Carabellese, A.; Corsaro, M. M.; De Castro, C.; Parrilli, M. *Carbohydr. Res.* **2004,** *339,* 1907–1915. doi:10.1016/j.carres.2004.06.010
26. Fauré, R.; Shiao, T. C.; Damerval, S.; Roy, R. *Tetrahedron Lett.* **2007,** *48,* 2385–2388. doi:10.1016/j.tetlet.2007.01.122
27. Zunk, M.; Kiefel, M. J. *Tetrahedron Lett.* **2011,** *52,* 1296–1299. doi:10.1016/j.tetlet.2011.01.064
28. Jeppesen, L. M.; Lundt, I.; Pedersen, C. *Acta Chem. Scand.* **1973,** *27,* 3579–3585. doi:10.3891/acta.chem.scand.27-3579
29. Roberts, B. P.; Smits, T. M. *Tetrahedron Lett.* **2001,** *42,* 3663–3666. doi:10.1016/S0040-4039(01)00540-8
30. Dang, H.-S.; Roberts, B. P.; Sekhon, J.; Smits, T. M. *Org. Biomol. Chem.* **2003,** *1,* 1330–1341. doi:10.1039/b212303g
31. Fielding, A. J.; Franchi, P.; Roberts, B. P.; Smits, T. M. *J. Chem. Soc., Perkin Trans. 2* **2002,** 155–163. doi:10.1039/B106140M

32. Cai, Y.; Dang, H.-S.; Roberts, B. P. *J. Chem. Soc., Perkin Trans. 1* **2002,** 2449–2458. doi:10.1039/b208200b
33. Hanessian, S.; Plessas, N. R. *J. Org. Chem.* **1969,** *34,* 1035–1044. doi:10.1021/jo01256a059
34. Hanessian, S.; Plessas, N. R. *J. Org. Chem.* **1969,** *34,* 1045–1053. doi:10.1021/jo01256a060
35. Hanessian, S.; Plessas, N. R. *J. Org. Chem.* **1969,** *34,* 1053–1058. doi:10.1021/jo01256a061
36. Chana, J. S.; Collins, P. M.; Farnia, F.; Peacock, D. J. *J. Chem. Soc., Chem. Commun.* **1988,** 94–96. doi:10.1039/c39880000094
37. Binkley, R. W.; Goewey, G. S.; Johnston, J. C. *J. Org. Chem.* **1984,** *49,* 992–996. doi:10.1021/jo00180a008
38. Hanessian, S. *Org. Synth.* **1987,** *65,* 243–250.
39. Hullar, T. L.; Siskin, S. B. *J. Org. Chem.* **1970,** *35,* 225–228. doi:10.1021/jo00826a046
40. Niu, Y.; Wang, N.; Cao, X.; Ye, X.-S. *Synlett* **2007,** 2116–2120. doi:10.1055/s-2007-984903
41. Shivatare, S. S.; Chang, S.-H.; Tsai, T.-I.; Ren, C.-T.; Chuang, H.-Y.; Hsu, L.; Lin, C.-W.; Li, S.-T.; Wu, C.-Y.; Wong, C.-H. *J. Am. Chem. Soc.* **2013,** *135,* 15382–15391. doi:10.1021/ja409097c
42. Franzyk, H.; Meldal, M.; Paulsen, H.; Bock, K. *J. Chem. Soc., Perkin Trans. 1* **1995,** 2883–2898. doi:10.1039/p19950002883
43. Basu, N.; Maity, S. K.; Chaudhury, A.; Ghosh, R. *Carbohydr. Res.* **2013,** *369,* 10–13. doi:10.1016/j.carres.2013.01.001
44. Fauré, R.; Shiao, T. C.; Lagnoux, D.; Giguère, D.; Roy, R. *Org. Biomol. Chem.* **2007,** *5,* 2704–2708. doi:10.1039/b708365c
45. Chevalier, R.; Esnault, J.; Vandewalle, P.; Sendid, B.; Colombel, J.-F.; Poulain, D.; Mallet, J.-M. *Tetrahedron* **2005,** *61,* 7669–7677. doi:10.1016/j.tet.2005.05.098
46. Crich, D.; Smith, M. *J. Am. Chem. Soc.* **2001,** *123,* 9015–9020. doi:10.1021/ja0111481
47. Kasai, R.; Okihara, M.; Asakawa, J.; Mizutani, K.; Tanaka, O. *Tetrahedron* **1979,** *35,* 1427–1432. doi:10.1016/0040-4020(79)85038-3

License and Terms

Beilstein Journal of Organic Chemistry

Bis(β-lactosyl)-[60]fullerene as novel class of glycolipids useful for the detection and the decontamination of biological toxins of the *Ricinus communis* family

Hirofumi Dohi*[1], Takeru Kanazawa[1], Akihiro Saito[2], Keita Sato[3], Hirotaka Uzawa[4], Yasuo Seto[3] and Yoshihiro Nishida*[1]

Full Research Paper

Open Access

Address:
[1]Department of Nanobiology, Graduate School of Advanced Integration Science, Chiba University, 1-33 Yayoi-cho, Inage-ku, Chiba 263−8522, Japan, [2]Department of Materials and Life Science, Shizuoka Institute of Science and Technology, 2200-2 Toyosawa, Fukuroi, Shizuoka 437-8555, Japan, [3]National Research Institute of Police Science, 6-3-1 Kashiwanoha, Kashiwa, Chiba 277-0882, Japan and [4]Nanosystem Research Institute, National Institute of Advanced Industrial Science and Technology (AIST), 1-1-1 Higashi, Tsukuba, 305-8565, Japan

Email:
Hirofumi Dohi* - hdohi@faculty.chiba-u.jp; Yoshihiro Nishida* - YNishida@faculty.chiba-u.jp

* Corresponding author

Keywords:
fullerene; multivalent glycosystems; oligosaccharides; proteotoxins; ricin

Beilstein J. Org. Chem. **2014,** *10,* 1504–1512.
doi:10.3762/bjoc.10.155

Received: 28 February 2014
Accepted: 22 May 2014
Published: 03 July 2014

This article is part of the Thematic Series "Multivalent glycosystems for nanoscience".

Guest Editor: J.-L. Reymond

Abstract

Glycosyl-[60]fullerenes were first used as decontaminants against ricin, a lactose recognition proteotoxin in the *Ricinus communis* family. A fullerene glycoconjugate carrying two lactose units was synthesized by a [3 + 2] cycloaddition reaction between C_{60} and the azide group in 6-azidohexyl β-lactoside per-*O*-acetate. A colloidal aqueous solution with brown color was prepared from deprotected bis(lactosyl)-C_{60} and was found stable for more than 6 months keeping its red color. Upon mixing with an aqueous solution of *Ricinus communis* agglutinin (RCA_{120}), the colloidal solution soon caused precipitations, while becoming colorless and transparent. In contrast, a solution of concanavalin A (Con A) caused no apparent change, indicating that the precipitation was caused specifically by carbohydrate–protein interactions. This notable phenomenon was quantified by means of sodium dodecyl sulfate polyacrylamide gel electrophoresis (SDS-PAGE), and the results were discussed in terms of detection and decontamination of the deadly biological toxin in the *Ricinus communis* family.

Introduction

Carbohydrate-binding proteins (lectins) and proteotoxins, e.g., verotoxins [1,2] and cholera toxins [3], can cause serious damages to human cells. The carbohydrate binding proteins are able to interact with cell-surface glycoconjugates such as glycoproteins and glycolipids to aggregate the cells. Proteotoxins penetrate into the target cells after binding with glycoconjugates and disturb vital cell functions. Ricin, a proteotoxin isolated from the castor bean of the *Ricinus communis* family, is one of the strongest biological toxins and is registered as a scheduled compound in the Chemical Weapon Convention [4]. Ricin consists of a subunit A with ribonuclease activity and a subunit B possessing carbohydrate-binding domains specific to β-lactosyl linkage [5,6]. In the past years, the development of proteotoxin infection inhibitors based on carbohydrate molecules has attracted great interest [7,8]. In particular, multivalent biomaterials carrying more than two carbohydrate ligands have been designed [9-15] and proven to enhance protein–carbohydrate interactions by means of glycocluster effects [16-18].

More recently, our research group has reported on attempts of applying these glycomaterials for both the detection and the decontamination of biological toxins in an assumed polluted scene [19-21]. In the present study, we attempted to apply our *N*-glycosyl-[60]fullerenes [22-25], which were designed as a novel class of glycolipids with notable biological and physical properties. For example, bis(α-D-mannopyranosyl)-[60]fullerene is capable of forming a liposome-like supramolecule in aqueous media and exhibits a strong binding activity to an α-mannose-binding lectin (concanavalin A, Con A) as the result not only of carbohydrate cluster effects but also of a unique spatial arrangement of the bis(mannosyl) linkage on the [60]fullerene surface [25]. In this paper, we describe our first synthesis of bis(β-lactosyl)-[60]fullerene and its potential as a tool for detecting and decontaminating the deadly biological toxin, ricin.

Results and Discussion

In our preceding studies [24,25], we have shown that bis(α-mannosyl)-[60]fullerene can be obtained by a coupling reaction between 1-azidoalkyl per-*O*-acetyl-glycoside and C_{60} together with [5,6]- and [6,6]-junction isomers of mono(α-mannosyl)-[60]fullerene. The bis(glycosyl)adduct is more polar than the two monoadducts and can be easily separated by silica gel column chromatography. Taking these preceding results into account, we prepared the bis(β-lactosyl)-[60]fullerene (bis-Lac-C_{60}, Figure 1) in the present study.

Synthesis of bis(per-*O*-acetyl-β-lactosyl)-[60]fullerene **4**

The bis(lactosyl)-fullerene has been prepared from lactosyl trichloroacetimidate **1** [26] following a pathway as shown in Scheme 1 [25]. The coupling reaction between **1** and 6-chloro-1-hexanol was conducted in the presence of trimethylsilyl trifluoromethanesulfonate (TMSOTf) to yield β-lactoside **2**. The nucleophilic substitution of the terminal chloride group in **2** with sodium azide afforded glycosyl azide **3**. The thermal cycloaddition of the azide group to C_{60} was conducted by boiling in chlorobenzene to obtain a mixture of the three main products, which were identified as a mixture of [5,6]- and [6,6]-fused isomers of monoadducts and the targeted bisadduct **4** in TLC analysis. **4** was purified with chromatography on silica gel and identified with NMR and MS spectroscopy as the desired bis(per-*O*-acetyl-β-lactosyl)-[60]fullerene (Experimental and Supporting Information Information file 1).

Preparation of colloidal suspension of bis(β-lactosyl)-[60]fullerene (bis-Lac-C_{60})

All acetyl groups in **4** were removed with sodium methoxide in a mixture of dichloromethane and methanol. During this process, the reaction mixture deposited aggregates of bis-Lac-C_{60}, which were collected by filtration and washed thoroughly

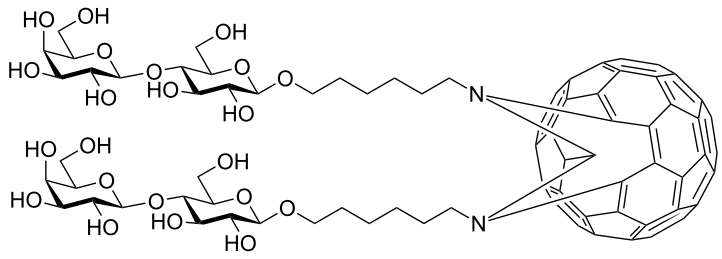

Figure 1: Structure of bis(β-lactosyl)-[60]fullerene (bis-Lac-C_{60}).

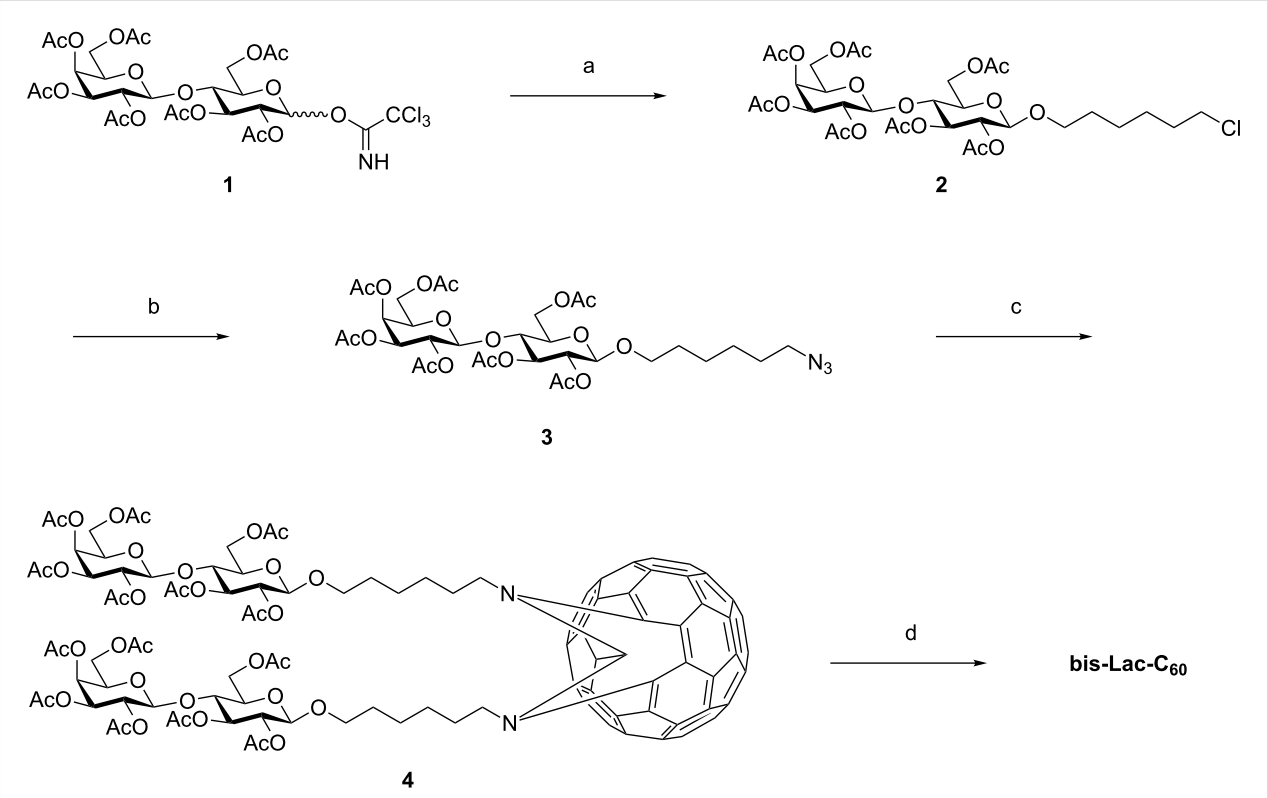

Scheme 1: Synthesis of bis-Lac-C_{60}. Reagents and conditions: (a) 6-chloro-1-hexanol, TMSOTf, CH_2Cl_2, −40 °C, 1 h, 48%; (b) NaN_3, DMF, 60 °C, 16 h, 93%; (c) C_{60}, chlorobenzene, reflux, 7 h, 14%; (d) NaOMe, CH_2Cl_2, MeOH, 5 h.

with methanol. The aggregates were diluted with dimethyl sulfoxide (DMSO) and dialyzed against distilled water for 2 days to give a colloidal suspension of bis-Lac-C_{60} with a deep brown color. The derived suspension was stable for at least 6 months when stored at 4 °C in the dark. Dynamic light scattering (DLS) analysis indicated that the colloidal suspension might involve spherical particles with two different sizes, smaller particles with a diameter range of 30–50 nm (av 39.6 ± 6.7 nm) and larger particles with a diameter range of 150–170 nm (av 162 ± 29 nm). We observed analogous results for colloidal suspensions of mono- and bis(α-D-mannopyranosyl)-[60]fullerenes in both AFM (atomic force microscopy) and DLS analyses. Probably, the smaller particles are bilayer vesicles that are stable in DMSO and pyridine while they can be destructed in parts by treatment with surfactants such as Triton-X [25]. These nano-sized constructs tend to attract each other to form the larger particles, and this tendency seems to be pronounced in polar aqueous solvents.

Precipitation assay for the colloidal suspension of bis-Lac-C_{60} with proteins of the *Ricinus communis* family

With the colloidal suspension of bis-Lac-C_{60} in hand, precipitation tests were conducted with *Ricinus communis* agglutinin (RCA_{120}) [27], ricin and concanavalin A (Con A) [28]. RCA_{120} is a ricin-like lectin and able to bind β-galactose residues. Con A is an α-mannose-specific lectin. When RCA_{120} (10 μL, 20 μg mL^{-1}) was added to this suspension (0.1 mL, 300 μM), the suspension soon gave rise to dark brown precipitate (Figure 2a). The precipitate was collected by centrifugation, washed thoroughly with water, and then applied to SDS-PAGE. A clear band was observed at the region matching with RCA_{120}, supporting that this lectin was directly associated with the sedimentation. Also upon the addition of ricin, a similar phenomenon could be observed, even though the precipitation took a prolonged time (ca. 15 min) in comparison with the case of RCA_{120} (ca. 2 min). Apparently, the proteotoxin possesses a lower ability to crosslink the [60]fullerene vesicles into larger sediments, though the reason is unknown. In contrast, no precipitation could be found in the negative control, which were composed of the same PBS buffer solution albeit free from these proteins. In addition, Con A in the same PBS buffer solution could not induce any sedimentation (Figure 2b and Figure 2c). These observations allowed us to expect that the sedimentary phenomenon might arise from species-specific interactions of the *Ricinus communis* proteins with the lactose cluster arrayed on the surface of the [60]fullerene vesicles. In nature, there are a lot of β-lactose-binding proteins. Not only to

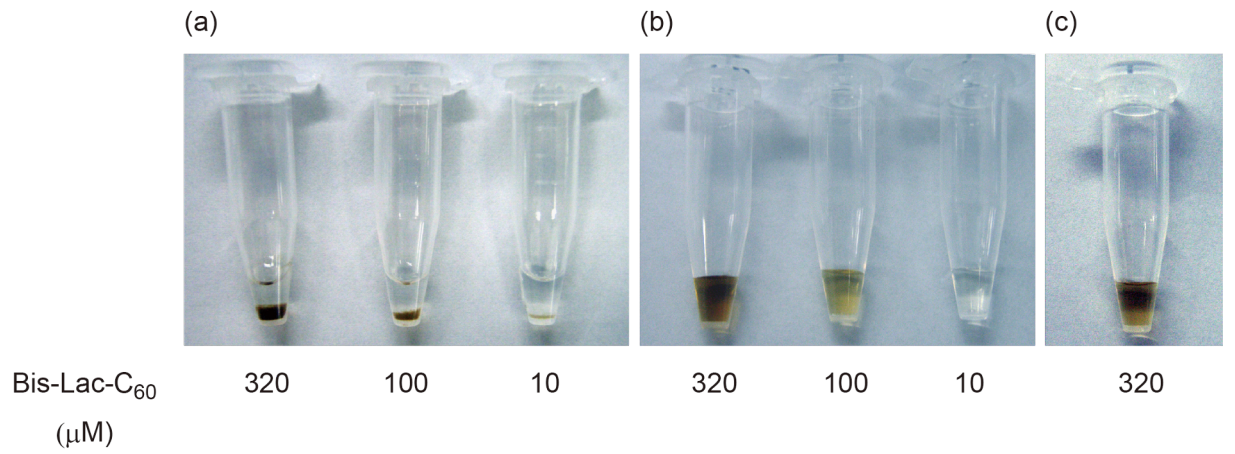

Figure 2: Precipitation assay of bis-Lac-C_{60} colloidal solution. The tubes were allowed to stand for 10 min after the addition of proteins or buffer. (a) 10 μL of 20 μg mL^{-1} RCA_{120} solution; (b) 10 μL of 10 μg mL^{-1} Con A solution; (c) 10 μL of 100 mM PBS buffer.

the *Ricinus communis* proteins but also to many other β-lactose or β-D-galactose-binding proteins, the β-lactose cluster arrayed on the surface of the [60]fullerene vesicles may become an ideal ligand. In this context, the sedimentary reaction is not specific to the proteins from the *Ricinus communis* family. Probably, in an assumed polluted scene, the colloidal suspension of the bis(β-lactosyl)-[60]fullerene will be useful to check the presence of ricin-like proteins.

Quantitative analysis of ricin protein in the bis-Lac-C_{60} colloidal suspension by means of SDS-PAGE

The above results have suggested that the *Ricinus communis* toxins and probably also other lactose-binding proteins can crosslink the vesicles of bis-Lac-C_{60} and then deposit aggregates at the bottom. If this holds true, the vesicles of bis-Lac-C_{60} can serve as decontaminants to remove ricin and related proteins from dangerous areas contaminated with biological toxins. In this section, we report on the examination of the behavior of ricin protein in the bis-Lac-C_{60} suspension by estimating its distribution (%) in both the supernatant and the aggregate after the sedimentation. The test samples were prepared in a manner as summarized in Figure 3. A ricin solution was added to the suspension of bis-Lac-C_{60} at different concentrations in the range of 1–100 μM. The mixtures were allowed to stand for 10 min and then centrifuged at 10 000*g* for 10 min. The amount of ricin remaining in the aqueous phase was quantified from the intensity of the protein band in SDS-PAGE. The amounts were calibrated with standard samples with known concentrations.

Though Bradford and Lowry methods might be useful for this kind of protein assays, the strong UV–vis absorbance of the C_{60} chromophore interfered with these established methodologies.

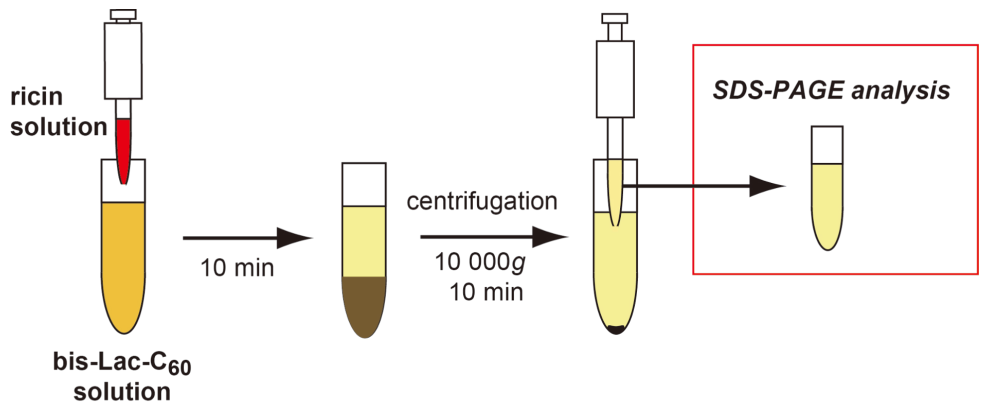

Figure 3: Schematic image for the quantitative analysis of ricin protein in the colloidal suspension of bis-Lac-C_{60}.

Therefore, we undertook an alternative way by means of the SDS-PAGE.

The results summarized in Table 1 show that the ricin protein was partitioned into two phases, i.e., solid phase (precipitates) and liquid phase (supernatants), after the sedimentation. Its distribution (%) in the solid phase increased with the concentration of bis-Lac-C_{60}. At 100 μM, most of the protein (94%) was deposited at the bottom as aggregates (run 4 in Table 1). These results support our previous suggestion that the sedimentary reaction in the colloidal suspension is based on toxin–lactose interactions and thus is useful for a simple detection of the biological toxin.

Table 1: Distribution (%) of ricin protein (0.1 mg mL^{-1}) after sedimentation in the colloidal suspension of bis-Lac-C_{60} at different concentrations.

run	bis-Lac-C_{60} (μM)	distribution of ricin (%)	
		precipitate	supernatant
1	1	26	74
2	10	31	69
3	50	74	26
4	100	94	6

Glyco-nanotechnology for locking the deadly toxin at the bottom

In an assumed situation of bioterrorism, the total time required for the identification and the decontamination is one of the key factors for minimizing possible damages from contaminated biological toxins. Obviously, a simple and highly effective method is required for this purpose. We have recognized in the above study that the colloidal suspension of bis-Lac-C_{60} can deposit ricin in more than 90% efficiency in a structural form of "protein–lactose aggregates." This means that the bis(β-lactosyl)-[60]fullerene can provide us with a promising tool to tackle the deadly toxin. At the end of this study, we attempted to establish our protocol for the rapid detection and the efficient decontamination of ricin and ricin-like proteins. The overall protocol examined here is schemed in Figure 4. Though this is similar to that already shown in Figure 3, the total manipulation time was shortened to 20 min and the decontamination efficiency was improved by a brine-induced salting-out effect.

First, an aqueous ricin solution was added to the colloidal suspension of bis-Lac-C_{60}. For the first 2 minutes, the suspension gave no apparent sediment. Upon addition of brine, the mixture soon generated precipitates. After standing for another 3 minutes, the mixture was centrifuged and analyzed with SDS-PAGE in the same manner as described previously (see also Experimental). By changing concentrations of both brine and bis-Lac-C_{60} solutions, we optimized the conditions for locking this toxin at the bottom effectively.

The results are summarized in Table 2. At a constant bis-Lac-C_{60} concentration (183 μM or 363 μM), the decontamination efficiency (%) increased with the concentration of brine. The efficiency reached 99% at 500 mM brine concentration and 363 μM bis-Lac-C_{60} (run 6 in Table 2). Consequently, the modified procedure enabled us to decontaminate ricin with >99% efficiency within 20 min.

Table 2: Efficiency (%) in the decontamination of ricin.

run	bis-Lac-C_{60} (μM)	brine (mM)	efficiency[a] (%)
1	183	100	89.1
2	183	200	97.9
3	183	500	98.4
4	363	100	89.3
5	363	200	97.8
6	363	500	99.3

[a]The efficiency (%) was determined from the distribution (%) of ricin partitioned in the aqueous phase after sedimentation and centrifugation.

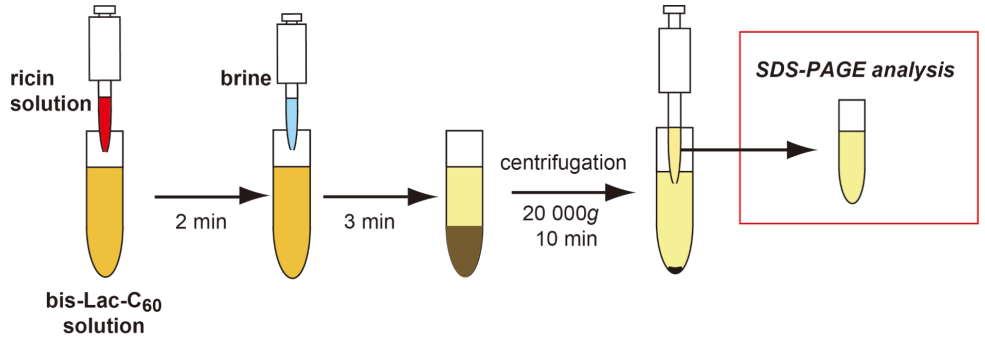

Figure 4: A modified procedure for the rapid detection and the efficient decontamination of ricin and ricin-like proteins.

Conclusion

A bis(β-lactosyl)-[60]fullerene was synthesized and evaluated as a novel class of glycolipid in the form of a red-colored colloidal suspension in aqueous medium. Its potency was obvious in the precipitation assay by using *Ricinus communis* proteins, which soon precipitated at the bottom while the red-colored suspension changed to colorless transparent solution. The observed phenomenon, which is based on multivalent protein–lactose interactions, prompted us to apply this glycolipid as a tool for the rapid detection and the decontamination of ricin and other biological toxins. By using an SDS-PAGE analysis, we successfully quantified distributions (%) of ricin in the aqueous and the solid phase. With this analytical tool in hands, we have also optimized the reaction conditions and proposed two protocols. The first protocol facilitates the detection, the second protocol allows for both the detection and the decontamination. The latter enabled us to deposit the toxin at the bottom of polluted solutions with efficiency greater than 99%. Obviously, the lactosyl-[60]fullerene provides us with a simple and powerful tool for tackling such dangerous toxins that aggregate our cells and/or penetrate into cells by a common way of protein–carbohydrate interactions.

Experimental

Safety consideration: Ricin is a highly toxic protein and was used with permission from the Minister of Economy, Trade and Industry of Japan. It should be handled using protective clothing in a fume hood, and should be decontaminated with an autoclave apparatus after examination.

General: All reactions were conducted under a dry argon atmosphere. All chemicals involved in the bis(lactosyl)-fullerene synthesis were purchased from Wako Pure Chemical Industries Co., Ltd., Tokyo Chemical Industry Co., Ltd. (Japan) and Sigma-Aldrich Co. (USA) and used without further purification. All reactions were monitored by thin-layer chromatography (TLC) on an aluminum sheet silica gel (60 F_{254} Merck, Sigma-Aldrich) by using UV-light detection and ethanolic phosphomolybdic acid or a *p*-anisaldehyde solution and heat as developing reagents. Flash column chromatography was performed on a silica gel (Merck 60 Å, particle size: 0.040–0.063 mm) by using toluene/ethyl acetate, hexane/ethyl acetate, cyclohexane/ethyl acetate, and chloroform/methanol mixtures as eluents. ^{1}H NMR (500 MHz), ^{13}C NMR (125 MHz), and 2D NMR spectra were recorded with a JNM-LA-500s or JNM-ECA-500 spectrometer (JEOL, Japan). Unless otherwise stated, NMR spectra were recorded at 22 °C in $CDCl_3$ with tetramethylsilane (TMS) as an internal standard and a digital resolution of 0.30 Hz. The following abbreviations correspond to spin multiplicities: s = singlet, d = doublet, t = triplet, m = multiplet, br = broad, and bs = broad singlet. FABMS spectra were recorded on a JEOL JMS-AX-500 spectrometer. HRMS–ESI spectra were recorded with a Thermo Scientific Exactive mass spectrometer. FTIR spectra were recorded on a JASCO FTIR-230 spectrometer (Japan) as KBr films. Ricin (2.5 mg mL^{-1}) was obtained from Honen Corporation (now J-Oil Mills, Inc., Tokyo, Japan) in a 10 mmol L^{-1} potassium phosphate buffer (pH 7.2) containing 0.8% (w/v) sodium chloride and 0.02% (w/v) potassium chloride.

6-Chlorohexyl 2,3,6,2',3',4',6'-hepta-*O*-acetyl-β-lactoside (2): A suspension of glycosyl imidate **1** (4.65 g, 5.96 mmol), 6-chloro-1-hexanol (2.37 mL, 17.9 mmol), and molecular sieves 4 Å (3.00 g) in dichloromethane (30 mL) was stirred for 1 h. After cooling to −40 °C, TMSOTf (53.8 μL, 0.298 mmol) was added to the suspension and the mixture was stirred for another 1 h. After quenching with triethylamine, the reaction mixture was diluted with chloroform and filtered through a Celite pad. The filtrate was washed with brine, the organic layer was dried over $MgSO_4$, filtered, and concentrated in vacuo. The residue was chromatographed on silica gel by using cyclohexane/ethyl acetate 3:2 to give glycoside **2** as a white solid (2.16 g, 48%): $[\alpha]_D$ −11.4 (*c* 1.0, $CHCl_3$); ^{1}H NMR (500 MHz, $CDCl_3$) δ 5.35 (dd, $J_{3',4'}$ = 3.4 Hz, $J_{4',5'}$ = 0.9 Hz, 1H, H-4'), 5.19 (t, $J_{2,3} = J_{3,4}$ = 9.2 Hz, 1H, H-3), 5.11 (dd, $J_{1',2'}$ = 7.9 Hz, $J_{2',3'}$ = 10.7 Hz, 1H, H-2'), 4.97 (dd, $J_{2',3'}$ = 10.4 Hz, $J_{3',4'}$ = 3.4 Hz, 1H, H-3'), 4.88 (dd, $J_{1,2}$ = 7.9 Hz, $J_{2,3}$ = 9.5 Hz, 1H, H-2), 4.49 (d, $J_{1',2'}$ = 7.9 Hz, 1H, H-1'), 4.49 (m, 1H, H-6a), 4.45 (d, $J_{1,2}$ = 7.9 Hz, 1H, H-1), 4.15–4.06 (m, 3H, H-6b, H-6'a and H-6'b), 3.89–3.82 (m, 2H, H-5' and –CH_2–), 3.79 (t, $J_{3,4} = J_{4,5}$ = 9.7 Hz, 1H, H-4), 3.60 (dq, $J_{4,5}$ = 9.8 Hz, $J_{5,6}$ = 2.1 and 4.9 Hz, 1H, H-5), 3.53 (t, *J* = 6.7 Hz, 2H, –CH_2–Cl), 3.49–3.44 (dt, *J* = 6.4 and 9.5 Hz, 1H, –OCH_2–), 2.15, 2.12, 2.06, 2.04, and 1.97 (s×5, 15H, –OCOCH_3), 2.05 (s, 6H, –OCOCH_3), 1.79–1.73 (m, 2H, –CH_2–), 1.61–1.54 (m, 2H, –CH_2–), 1.46–1.41 (m, 2H, –CH_2–), 1.37–1.32 (m, 2H, –CH_2–); ^{13}C NMR (125 MHz, $CDCl_3$) δ 170.35, 170.31, 170.12, 170.04, 169.77, 169.56, 169.06, 101.05, 100.55, 76.29, 72.81, 72.58, 71.70, 70.97, 70.66, 69.85, 69.10, 66.59, 62.00, 60.77, 44.90, 32.44, 29.20, 26.46, 25.08, 20.82, 20.77, 20.66, 20.58, 20.46; HRMS–FAB (*m*/*z*): $[M + K - H]^+$ calcd for $C_{32}H_{47}O_{18}Cl$, 793.2088; found, 793.2040.

6-Azidohexyl 2,3,6,2',3',4',6'-hepta-*O*-acetyl-β-lactoside (3): A suspension of compound **2** (2.16 g, 2.86 mmol) and sodium azide (372 mg, 5.72 mmol) in *N*,*N*-dimethylformamide (10 mL) was stirred at 60 °C for 16 h. The reaction mixture was diluted with ethyl acetate and the organic layer was washed with brine twice, dried over $MgSO_4$, filtered, and concentrated in vacuo. The residue was chromatographed on silica gel by using toluene/ethyl acetate 1:1 to give azide **3** as a white solid (2.02 g, 93%). $[\alpha]_D$ −11.1 (*c* 1.13, $CHCl_3$); ^{1}H NMR (500 MHz, $CDCl_3$)

δ 5.31 (dd, $J_{3',4'}$ = 3.4 Hz, $J_{4',5'}$ = 0.9 Hz, 1H, H-4'), 5.16 (t, $J_{2,3} = J_{3,4}$ = 9.5 Hz, 1H, H-3), 5.08 (dd, $J_{1',2'}$ = 8.0 Hz, $J_{2',3'}$ = 10.6 Hz, 1H, H-2'), 4.92 (dd, $J_{2',3'}$ = 10.3 Hz, $J_{3',4'}$ = 3.4 Hz, 1H, H-3'), 4.85 (dd, $J_{1,2}$ = 7.7 Hz, $J_{2,3}$ = 9.5 Hz, 1H, H-2), 4.46 (d, $J_{1',2'}$ = 8.0 Hz, 1H, H-1'), 4.46 (m, 1H, H-6a), 4.42 (d, $J_{1,2}$ = 7.7 Hz, 1H, H-1), 4.12–4.03 (m, 3H, H-6b, H-6'a and H-6'b), 3.86–3.78 (m, 2H, H-5' and –CH_2–), 3.76 (t, $J_{3,4} = J_{4,5}$ = 9.5 Hz, 1H, H-4), 3.56 (dq, $J_{4,5}$ = 9.7 Hz, $J_{5,6}$ = 2.0 and 5.2 Hz, 1H, H-5), 3.53 (dt, J = 6.6 and 9.5 Hz, 2H, –CH_2–N_3), 3.23 (t, J = 6.9 Hz, 1H, –OCH_2–), 2.12, 2.03, 2.00, 1.93, and 2.09 (s×5, 15H, –OCOCH_3), 2.01 (s, 6H, –OCOCH_3), 1.55 (m, 4H, –CH_2–), 1.33 (m, 4H, –CH_2–); ^{13}C NMR (125 MHz, $CDCl_3$) δ 170.41, 170.21, 170.13, 169.86, 169.64, 169.14, 101.14, 100.64, 76.39, 72.88, 72.66, 71.78, 71.05, 70.73, 69.95, 69.17, 66.67, 62.09, 60.87, 51.39, 29.30, 28.83, 26.44, 25.47, 20.95, 20.89, 20.77, 20.71, 20.58; HRMS–ESI (*m*/*z*): $[M + Na]^+$ calcd for $C_{32}H_{47}N_3O_{18}$, 784.2752; found, 764.2747.

***per-O*-Acetyl bis-Lac-C_{60} 4:** A suspension of compound **3** (588 mg, 0.772 mmol) and C_{60} (278 mg, 0.386 mmol) in chlorobenzene (117 mL) was stirred until complete dissolution of C_{60}. The mixture was freeze-deaerated and heated under reflux for 7 h. After cooling to ambient temperature, the mixture was concentrated in vacuo. The residue was purified by silica gel column chromatography by using a toluene:ethyl acetate gradient (1:0→3:1→2:1→1:1) to afford bisadduct **4** as a black solid (243 mg, 14%) and compound **3** (179 mg, 30%): ^{1}H NMR (500 MHz, $CDCl_3$) δ 5.35 (d, J = 3.1 Hz, 1H, H-4'), 5.21 (t, $J_{2,3} = J_{3,4}$ = 9.3 Hz, 1H, H-3), 5.11 (dd, $J_{1',2'}$ = 7.9 Hz, $J_{2',3'}$ = 10.4 Hz, 1H, H-2'), 4.96 (dd, $J_{2',3'}$ = 10.4 Hz, $J_{3',4'}$ = 3.4 Hz, 1H, H-3'), 4.90 (dd, $J_{1,2}$ = 8.3 Hz, $J_{2,3}$ = 9.5 Hz, 1H, H-2), 4.50–4.48 (m, 3H, H-1, H-6, and H-1'), 4.16–4.00 (m, 4H, H-6, H-6'×2, and –CH_2–), 3.91–3.77 (m, 3H, H-4, H-5', and –CH_2–), 3.63–3.58 (m, 1H, H-5), 3.55–3.46 (m, 1H), 2.15, 2.13, 2.06, 2.05, and 1.97 (s×5, 21H, –OCOCH_3), 1.49 (b, 1H, –CH_2–), 0.87 (b, 1H, –CH_2–); ^{13}C NMR (125 MHz, $CDCl_3$) δ 170.32, 170.31, 170.11, 170.03, 169.77, 169.55, 169.05, 147.59, 146.81, 145.10, 144.97, 144.86, 144.60, 144.54, 144.17, 144.11, 144.09, 143.94, 143.72, 143.53, 143.33, 142.66, 142.00, 141.55, 141.23, 139.54, 139.32, 138.95, 138.79, 137.11, 135.18, 134.56, 132.86, 130.48, 129.01, 128.19, 125.27, 101.07, 100.62, 77.22, 76.31, 72.84, 72.62, 71.73, 70.97, 70.64, 70.02, 69.69, 69.10, 66.57, 62.01, 60.75, 51.60, 29.47, 29.41, 29.38, 27.09, 25.82, 20.92, 20.84, 20.78, 20.64, 20.51; HRMS–ESI (*m*/*z*): $[M + Na]^+$ calcd for $C_{124}H_{94}N_2O_{36}$, 2209.5484; found, 2209.5467.

Bis−Lac C_{60}: Sodium methoxide (5 mg, 93 μmol) was added to a solution of **7** (7 mg, 3 μmol) in dichloromethane (2 mL) and methanol (0.5 mL), and the mixture was stirred. The reaction was monitored by TLC and FTIR visualization of the decrease of the peak originating from the carboxyl group. After 5 h of stirring, a black precipitate was collected by filtration and washed with methanol to give bis-Lac-C_{60} as a black solid.

Preparation of the colloidal suspension of bis-Lac-C_{60}: Bis-Lac-C_{60} (7 mg, 3 μmol) was dissolved in dimethyl sulfoxide (2 mL), and the solution was poured into a dialysis tube (Cellulose Dialyzer Tubing VT351, molecular weight cut-off: 3500, Nacalai Tesque, Inc., Japan) suffused with distilled water (20 mL). After 2 days of dialysis, the solution was subjected to ultrafiltration at 3,000*g* for 15 min by using an Amicon Ultra-15 device (molecular weight cut: off 5000, Millipore, Co., USA). The concentrate was transferred into a measuring flask, and the total volume was adjusted with distilled water to give a bis-Lac-C_{60} dispersion colloidal suspension at the desired concentration.

Precipitation assay for the colloidal suspension of bis-Lac-C_{60} with proteins of the *Ricinus communis* family: A solution of RCA_{120} in water (10 μL, 20 μg mL^{-1}), Con A in water (10 μL, 10 μg mL^{-1}), or PBS buffer (10 μL, 100 mM) was separately added to the 320 μM colloidal suspension of bis-Lac-C_{60} (100 μL) in Eppendorf tubes. The mixtures were vigorously shaken by means of a vortex mixer and allowed to stand for 5 min before careful physical examination.

SDS-PAGE analysis of the precipitate generated by the addition of RCA_{120} solution to the colloidal suspension of bis-Lac-C_{60}: An RCA_{120} solution (60 μL, 1 mg mL^{-1}) in water was added to a bis-Lac-C_{60} colloidal suspension in water (300 μM, 940 μL), and the mixture was vigorously shaken by using a vortex mixer and allowed to stand for 10 min. The mixture was centrifuged at 10,000*g* for 20 min, and the supernatant was removed. Water (1 mL) was added to the residual black pellet, which was vigorously dispersed. The black suspension (10 μL) was mixed with a buffer containing SDS (10 μL), and the mixture was heated to 90 °C for 10 min. An RCA_{120} solution (1 mg mL^{-1}) was also denatured by the same procedure. Each solution (10 μL) was applied to the polyacrylamide gel (14%) and electrophoresed for 1 h. The gel was dyed with Coomassie Brilliant Blue (CBB).

Quantitative analysis of ricin in the colloidal suspension of bis-Lac-C_{60}: A ricin solution (1.67 mg mL^{-1}, 60 μL) was added to each bis-Lac-C_{60} colloidal suspension (940 μL), and the mixture was shaken vigorously and allowed to stand for 10 min. After centrifugation of the mixture at 10,000*g* for 10 min, the supernatant (100 μL) was collected and concentrated with a centrifugal vacuum concentrator. Ricin solutions (100 μL) at concentrations of 50, 25, 10, 5, 1, and 0.5 μg mL^{-1} were also prepared to construct the calibration curve and concentrated with a centrifugal vacuum concentrator. All concentrated residues were denatured with SDS (20 μL) at

90 °C for 10 min, and each solution (10 μL) was applied to the polyacrylamide gel (14%). The gel was dyed with Flamingo solution, and band intensities were estimated by using a laser excitation imaging kit. The residual ricin concentration in the bis-Lac-C_{60} colloidal suspension was determined by means of the calibration curve, which shows the ricin intensities at each concentration.

Estimation of decontamination efficiency by using a salting-out agent: A ricin solution (2.5 mg mL^{-1}, 60 μL) was added to each bis-Lac-C_{60} solution (940 μL), and the mixture was shaken and allowed to stand for 2 min. Brine (100 μL) was added to the mixture, shaken vigorously, and allowed to stand for 3 min. After centrifugation of the mixture at 20,000*g* for 10 min, the supernatant (100 μL) was collected and concentrated with a centrifugal vacuum concentrator. Ricin solutions (1 mL) at concentrations of 50, 25, 10, 5, 1, and 0.5 μg mL^{-1} were prepared and separately mixed with brine (100 μL) as control solutions. These solutions (100 μL) were collected and concentrated with a centrifugal vacuum concentrator, respectively. Subsequent procedures to determine the concentration of ricin were carried out according to the protocol mentioned in the previous section. The decontamination efficiency against ricin (%) was calculated by the formula [ricin concentration of centrifuged supernatant (μM)/concentration of initial ricin solution (μM)] × 100 (%).

Supporting Information

Supporting Information File 1

Copies of ^{1}H and ^{13}C NMR spectra for compounds **2**, **3** and **4**.
[http://www.beilstein-journals.org/bjoc/content/supplementary/1860-5397-10-155-S1.pdf]

Acknowledgements

This research was supported by the Program Special Coordination Funds for Promoting Science and Technology from the Ministry of Education, Culture, Sports, Science and Technology (MEXT) of Japan. We thank Ms. S. Kado (Center for Analytical Instrumentation, Chiba University) for her technical support regarding the MS spectra.

References

1. Lingwood, C. A.; Law, H.; Richardson, S.; Petric, M.; Brunton, J. L.; Degrandis, S.; Karmali, M. *J. Biol. Chem.* **1987,** *262,* 8834–8839.
2. Cohen, A.; Hannigan, G. E.; Williams, B. R. G.; Lingwood, C. A. *J. Biol. Chem.* **1987,** *262,* 17088–17091.
3. Merritt, E. A.; Sarfaty, S.; Van Den Akker, F.; L'Hoir, C.; Martial, J. A.; Hol, W. G. J. *Protein Sci.* **1994,** *3,* 166–175. doi:10.1002/pro.5560030202
4. Chemical weapon convention. Organization for the prohibition of chemical weapons. http://www.opcw.org.
5. Montfort, W.; Villafranca, J. E.; Monzingo, A. F.; Ernst, S. R.; Katzin, B.; Rutenber, E.; Xuong, N. H.; Hamlin, R.; Robertus, J. D. *J. Biol. Chem.* **1987,** *262,* 5398–5403.
6. Endo, Y.; Mitsui, K.; Motizuki, M.; Tsurugi, K. *J. Biol. Chem.* **1987,** *262,* 5908–5912.
7. Fan, E.; Merritt, E. A.; Verlinde, C. L. M. J.; Hol, W. G. J. *Curr. Opin. Struct. Biol.* **2000,** *10,* 680–686. doi:10.1016/S0959-440X(00)00152-4
8. Miller, D. J.; Ravikumar, K.; Shen, H.; Suh, J.-K.; Kerwin, S. M.; Robertus, J. D. *J. Med. Chem.* **2002,** *45,* 90–98. doi:10.1021/jm010186s
9. Dohi, H.; Nishida, Y.; Mizuno, M.; Shinkai, M.; Kobayashi, T.; Takeda, T.; Uzawa, H.; Kobayashi, K. *Bioorg. Med. Chem.* **1999,** *7,* 2053–2062. doi:10.1016/S0968-0896(99)00129-7
10. Dohi, H.; Nishida, Y.; Takeda, T.; Kobayashi, K. *Carbohydr. Res.* **2002,** *337,* 983–989. doi:10.1016/S0008-6215(02)00093-9
11. Mammen, M.; Choi, S.-K.; Whitesides, G. M. *Angew. Chem., Int. Ed.* **1998,** *37,* 2754–2794. doi:10.1002/(SICI)1521-3773(19981102)37:20<2754::AID-ANIE2754>3.0.CO;2-3
12. Bernardi, A.; Jiménez-Barbero, J.; Casnati, A.; De Castro, C.; Darbre, T.; Fieschi, F.; Finne, J.; Funken, H.; Jaeger, K.-E.; Lahmann, M.; Lindhorst, T. K.; Marradi, M.; Messner, P.; Molinaro, A.; Murphy, P. V.; Nativi, C.; Oscarson, S.; Penadés, S.; Peri, F.; Pieters, R. J.; Renaudet, O.; Reymond, J.-L.; Richichi, B.; Rojo, J.; Sansone, F.; Schäffer, C.; Turnbull, W. B.; Velasco-Torrijos, T.; Vidal, S.; Vincent, S.; Wennekes, T.; Zuilhof, H.; Imberty, A. *Chem. Soc. Rev.* **2013,** *42,* 4709–4727. doi:10.1039/c2cs35408j
13. Branson, T. R.; Turnbull, W. B. *Chem. Soc. Rev.* **2013,** *42,* 4613–4622. doi:10.1039/c2cs35430f
14. Richards, S.-J.; Jones, M. W.; Hunaban, M.; Haddleton, D. M.; Gibson, M. I. *Angew. Chem., Int. Ed.* **2012,** *51,* 7812–7816. doi:10.1002/anie.201202945
15. Marradi, M.; Chiodo, F.; García, I.; Penadés, S. *Chem. Soc. Rev.* **2013,** *42,* 4728–4745. doi:10.1039/c2cs35420a
16. Lee, Y. C.; Lee, R. T. *Acc. Chem. Res.* **1995,** *28,* 321–327. doi:10.1021/ar00056a001
17. Lee, R. T.; Lee, Y. C. *Glycoconjugate J.* **2000,** *17,* 543–551. doi:10.1023/A:1011070425430
18. Lee, R. T.; Lee, Y. C. Enhanced Biochemical Affinities of Multivalent Neoglycoconjugates. In *Neoglycoconjugates: Preparation and Applications;* Lee, Y. C.; Lee, R. T., Eds.; Academic Press: San Diego, 1994; pp 23–50. doi:10.1016/B978-0-12-440585-1.50005-X
19. Seto, Y. *J. Health Sci.* **2011,** *57,* 311–333. doi:10.1248/jhs.57.311
20. Nagatsuka, T.; Uzawa, H.; Ohsawa, I.; Seto, Y.; Nishida, Y. *ACS Appl. Mater. Interfaces* **2010,** *2,* 1081–1085. doi:10.1021/am900846r
21. Nagatsuka, T.; Uzawa, H.; Sato, K.; Ohsawa, I.; Seto, Y.; Nishida, Y. *ACS Appl. Mater. Interfaces* **2012,** *4,* 832–837. doi:10.1021/am201493q
22. Yashiro, A.; Nishida, Y.; Ohno, M.; Eguchi, S.; Kobayashi, K. *Tetrahedron Lett.* **1998,** *39,* 9031–9034. doi:10.1016/S0040-4039(98)02047-4
23. Kato, H.; Yashiro, A.; Mizuno, A.; Nishida, Y.; Kobayashi, K.; Shinohara, H. *Bioorg. Med. Chem. Lett.* **2001,** *11,* 2935–2939. doi:10.1016/S0960-894X(01)00583-2

24. Nishida, Y.; Mizuno, A.; Kato, H.; Yashiro, A.; Ohtake, T.; Kobayashi, K. *Chem. Biodiversity* **2004,** *1,* 1452–1464. doi:10.1002/cbdv.200490106
25. Kato, H.; Kaneta, N.; Nii, S.; Kobayashi, K.; Fukui, N.; Shinohara, H.; Nishida, Y. *Chem. Biodiversity* **2005,** *2,* 1232–1241. doi:10.1002/cbdv.200590093
26. González Núñez, F.; Campos Valdes, M. T.; Aruca, E.; Schmidt, R. R.; Verez Bencomo, V. *J. Carbohydr. Chem.* **2003,** *22,* 395–406. doi:10.1081/CAR-120025326
27. Schofield, C. L.; Mukhopadhyay, B.; Hardy, S. M.; McDonnell, M. B.; Field, R. A.; Russell, D. A. *Analyst* **2008,** *133,* 626–634. doi:10.1039/b715250g
28. Hardman, K. D.; Ainsworth, C. F. *Biochemistry* **1972,** *11,* 4910–4919. doi:10.1021/bi00776a006

License and Terms

Beilstein Journal of Organic Chemistry

Why a diaminopyrrolic tripodal receptor binds mannosides in acetonitrile but not in water?

Diogo Vila-Viçosa[1], Oscar Francesconi[2] and Miguel Machuqueiro[*1]

Full Research Paper

Open Access

Address:
[1]Centro de Química e Bioquímica, Departamento de Química e Bioquímica, Faculdade de Ciências, Universidade de Lisboa, 1749-016 Lisboa, Portugal, Phone: +351-21-7500112. Fax: +351-21-7500088 and [2]Dipartimento di Chimica, Università di Firenze, Polo Scientifico e Tecnológico, 50019 Sesto Fiorentino, Firenze, Italy

Email:
Miguel Machuqueiro[*] - machuque@fc.ul.pt

* Corresponding author

Keywords:
conformational analysis; constant-pH MD; mannose; multivalent glycosystems; pH; synthetic receptor

Beilstein J. Org. Chem. **2014,** *10,* 1513–1523.
doi:10.3762/bjoc.10.156

Received: 26 February 2014
Accepted: 28 May 2014
Published: 03 July 2014

This article is part of the Thematic Series "Multivalent glycosystems for nanoscience".

Guest Editor: A. Casnati

Abstract

Intermolecular interactions involving carbohydrates and their natural receptors play important roles in several biological processes. The development of synthetic receptors is very useful to study these recognition processes. Recently, it was synthetized a diaminopyrrolic tripodal receptor that is selective for mannosides, which are obtained from mannose, a sugar with significant relevance in living systems. However, this receptor is significantly more active in acetonitrile than in water. In this work, we performed several molecular dynamics and constant-pH molecular dynamics simulations in acetonitrile and water to evaluate the conformational space of the receptor and to understand the molecular detail of the receptor–mannoside interaction. The protonation states sampled by the receptor show that the positive charges are always as distant as possible in order to avoid large intramolecular repulsions. Moreover, the conformational space of the receptor is very similar in water above pH 4.0 and in acetonitrile. From the simulations with the mannoside, we observe that the interactions are more specific in acetonitrile (mainly hydrogen bonds) than in water (mainly hydrophobic). Our results suggest that the readiness of the receptor to bind mannoside is not significantly affected in water (above pH 4.0). Probably, the hydrogen bond network that is formed in acetonitrile (which is weaker in water) is the main reason for the higher activity in this solvent. This work also presents a new implementation of the stochastic titration constant-pH molecular dynamics method to a synthetic receptor of sugars and attests its ability to describe the protonation/conformation coupling in these molecules.

Introduction

The recognition of specific carbohydrates is an important step in several biological processes [1]. To better understand these recognition processes, several synthetic receptors have been developed over the years [1-6]. Most of these were developed for glucose since it is one of the most common sugars in living systems [7] and the preferred monosaccharide for energy

storage [8]. However, mannose is essential for various biological functions, such as molecular recognition, being one of the most abundant sugars in glycoconjugates [9,10].

In 2011, Roelens' group [11-13] synthetized and tested a chiral diaminopyrrolic tripodal receptor that showed high binding affinities to mannosides (Figure 1). This particular receptor is significantly more active in acetonitrile (ACN) than in water [14]. In fact, this receptor family [11-13] could only be tested in water at slightly acidic conditions, due to solubility reasons, and proved to be very inefficient [14]. Unraveling the molecular details of these host–guest interactions is crucial to understand their different performances when changing the solvent and to identify the molecular determinants behind the reported high affinities.

Simulation methods, namely the so-called constant-pH molecular dynamics (CpHMD) methods, have been used to understand the molecular detail of several phenomena in the last years [15-24]. Since MD simulations deal with pH in a limited way, simply by setting a fixed protonation state in the beginning of the simulation, the use of one of these methods is mandatory. The stochastic titration constant-pH MD method [15,21] takes advantage from the complementarity between molecular mechanics/molecular dynamics (MM/MD) simulations, that correctly samples the conformational space of a system according to a classic potential energy function, and Poisson–Boltzmann/Monte Carlo methods, that can efficiently treat multiple protonation equilibria on rigid structures [25,26]. This way, it is possible to deal with pH as an external parameter that is fixed in our simulations since the protonation state of the titrable groups is allowed to periodically change during the simulation capturing the coupling between protonation and conformation. This method was already successfully applied to peptides and proteins in recent years [15,21,27-36].

The interaction of sugar molecules with receptors has been studied and shown that the recognition process involves many hydrogen bonds between the two molecules [1,37]. Aqvist et al, using MM/MD simulations, showed that the major contribution to the binding energy between both glucose and galactose to a proteic receptor, came from hydrogen bonds [38]. Moreover, Lerbret et al, suggested that hydrogen bonds are strongly related with the influence of sugar molecules in lysozyme structure [39,40].

In this work, we performed an exhaustive conformational study of a chiral diaminopyrrolic tripodal receptor (Figure 1) in both water and acetonitrile. We used MM/MD simulations in the organic solvent and constant-pH MD to simulate the receptor in water at several pH values. Moreover, the interaction between the receptor and octyl α-D-mannoside (the receptor binds strongly both α and β anomers [12]) was also studied in these two solvents. These two approaches intend to address two working hypothesis: the receptor is active in acetonitrile but not in water due to the different conformational behavior in the two environments or due to specific interactions that are (un)favored when changing the solvent. This work also extends, for the first time, the use of the stochastic titration constant-pH MD method to artificial molecules, in particular to diaminopyrrolic receptors.

Results and Discussion

Titration curve of the receptor

The titration curve of the receptor was obtained by averaging the occupancy of all titrable amine groups at each pH value

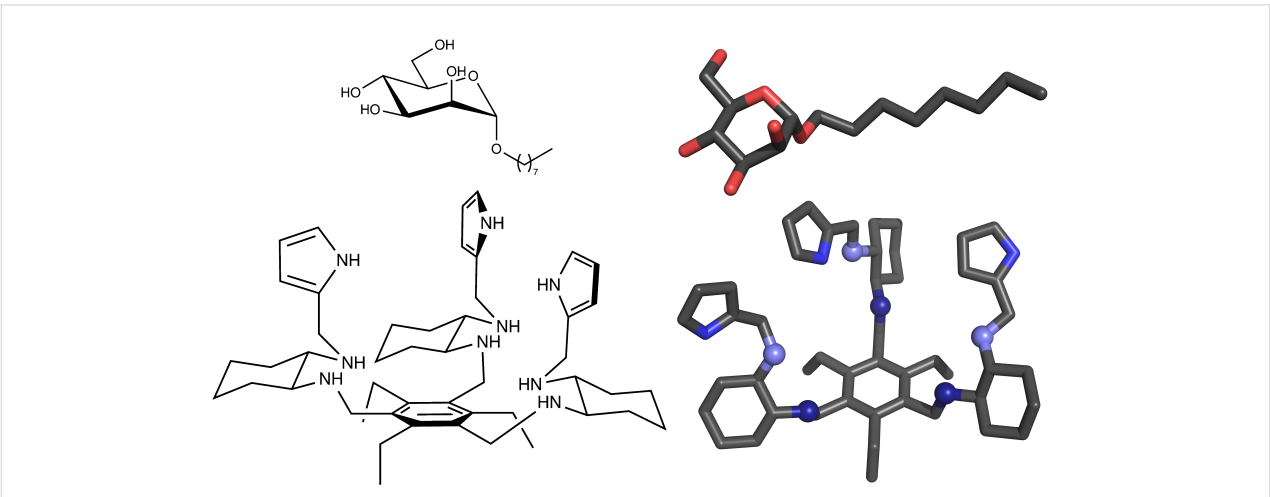

Figure 1: Octyl α-D-mannoside (mannoside) and diaminopyrrolic tripodal receptor molecules. 2D and 3D representations are shown. In 3D, all hydrogen atoms were omitted for clarity, and titrable amino groups are shown in spheres with first generation in dark blue and second in light blue.

over 270 ns (last 90 ns of each replicate). The total titration curve (Figure 2a) shows a clear plateau between pH 4.0 and 7.0, approximately. In these range, the total protonation is ~3 meaning that half of the titrable groups are protonated and the total charge of the receptor is 3. At an extremely high (low) pH value the molecule is completely deprotonated (protonated) which means that the protonation range is completely sampled. From the total titration curve, we can also conclude that our receptor is only close to neutrality at pH 10.0. From the individual titration curves of the first and second generation residues (Figure 1), we can determine which of these groups are being protonated at each pH value (Figure 2b). We observe that, in the plateau between pH 4.0 and 7.0, the second generation has an average protonation of 75% and the first, 25%. The higher charge in the second generation amine groups is expected since these groups are more exposed to the solvent, interacting less with each other, which means that they are easier to ionize. In the case of the first generation amino groups, they are much closer to each other, with limited conformational freedom, resulting in much lower pK_a values.

The small number of titrable sites in the receptor allows us to analyze in detail the population of each possible microstate. In particular, from the populations of all simulated pH values, it is possible to draw a diagram to represent which states are more populated at each number of titrable protons present in the molecule (Figure 3). For example, when the molecule has one proton, it can be in one amino group of the first generation or in the second generation. However, if the molecule has two protons, they can be both in the first generation, both in the second generation, in different generations but in the same arm, or in different arms of the molecule (by arms we consider the diaminopyrrolic groups attached to the center phenyl group). From Figure 3, we observe that, in general, the position of protons (positive charges) is such that repulsion is minimized. For example, with two protons, the preferred state is the one with two second generation amino groups protonated which allows the two charges to be more distant to each other. Interestingly, there are many states that are almost not populated. In particular, with five protons, the state with three protons in the first generation is almost not populated since this state implies the presence of three positive charges in a very small space. With one proton, the preferred state is the one with the proton in the second generation which is more exposed to the solvent. However, since the global charge of the receptor is only one in this state, both microstates are significantly populated. With two and four protons, the observations are similar since in both cases the microstates with the second generation amino groups protonated are preferred and the ones with protons in different arms are also significantly populated. In these states, there are two microstates that are almost not populated due to the high

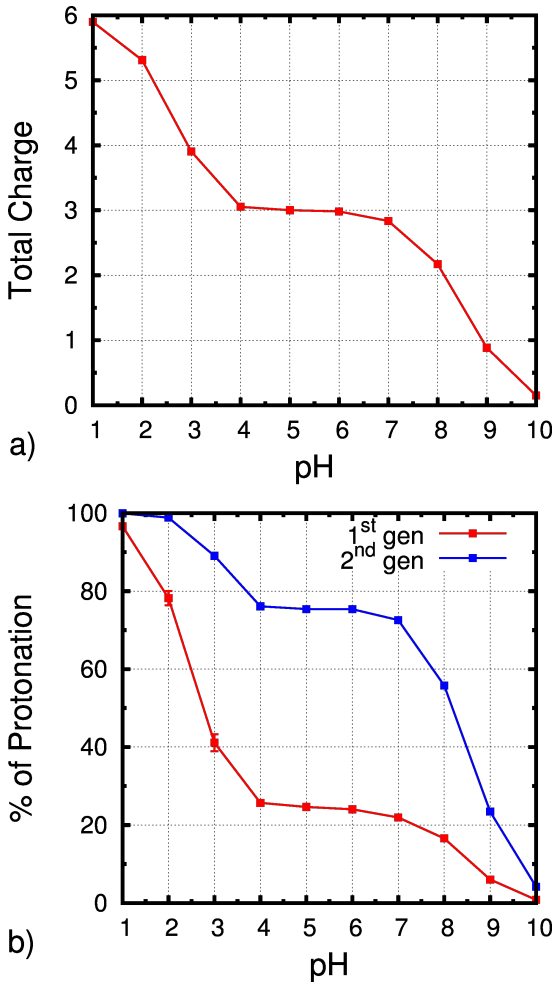

Figure 2: Full titration curve of the receptor (a) and the correspondent percentage of protonation in each generation (b).

repulsion when protonating two groups in the same arm or in the first generation. Finally, with three protons, only three (out of six) microstates are significantly populated and these are the ones that allow for smaller repulsion, as observed in the previous cases. This analysis was also performed for each pH value (see Supporting Information File 1) and the observations are completely analogous to the described above. As expected, geometrically constrained titrable sites show strong interactions due to electrostatic repulsion which results in shifted pK_a values and in some forbidden (not sampled) protonation states. These results illustrate the usefulness of the constant-pH MD methodologies and expose the strong limitations of classic MM/MD simulations to deal with such systems.

Conformational analysis of the receptor

As expected, both in ACN and in water at all simulated pH values, the receptor shows a large conformational variability. The radius of gyration (R_g) indicates how "open" is the struc-

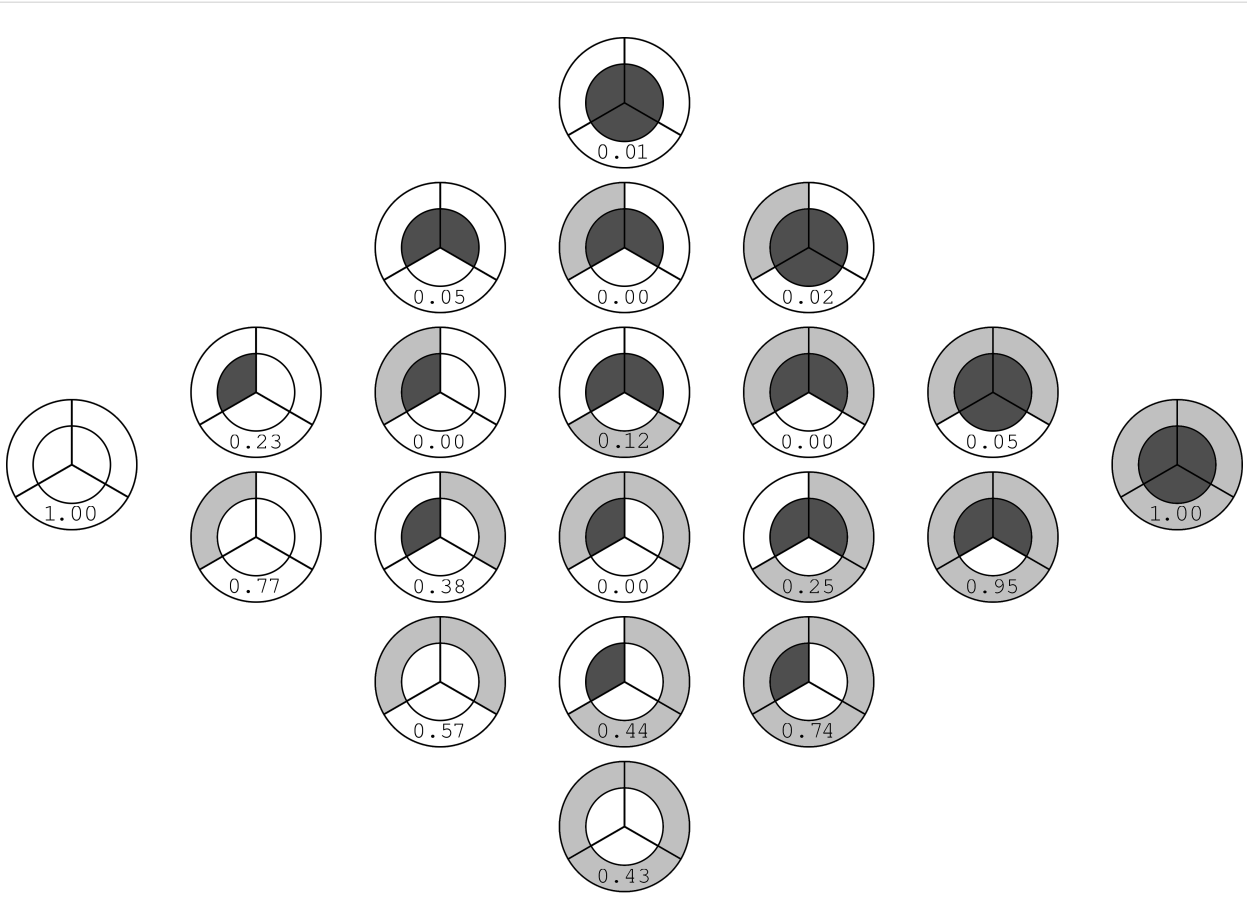

Figure 3: Diagram representing the population of all microstates at each number of titrable protons (*n*) present in the molecule.

ture: a large R_g indicates that the receptor is in an extended conformation. Our results show that the receptor samples a large interval of R_g (Figure 4 and Supporting Information File 1). In fact, in most simulations, the molecule can sample "closed" conformations with R_g around 0.50 nm or more "open" with R_g larger than 0.65 nm. However, at lower pH values, in particular at pH 1.0, the distribution of R_g is much narrower and deviated to larger R_g values. As mentioned above, at pH 1.0, the residues are almost completely charged and this generates significant repulsion between the arms which increases the R_g. At pH 10.0, the receptor is able to sample a very low R_g region (a shoulder in the histogram) that is almost inaccessible in the ACN simulations. These closed and packed conformations are favored when the receptor is neutral and is potentiated by its hydrophobicity, which does not happen in the organic solvent. Interestingly, above pH 4.0, the distribution of R_g is very similar in all simulations and comparable with the simulations in ACN. This observation suggest that the conformational space, in terms of R_g, is similar in water (above pH 4.0) and in ACN. In other words, the receptor is able to accommodate up to 3 protons without any

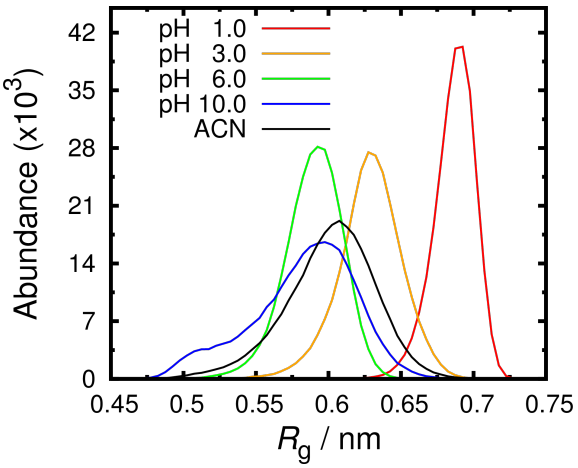

Figure 4: Radius of gyration (R_g) histograms for the receptor in water at pH 1.0, 3.0, 6.0, 10.0 and in ACN. The R_g curves at the pH values not shown are well behaved and respect the observed trend.

major influence in the preferred positions of its arms. This suggests that the reason hindering the receptor to bind sugars in water should not be its conformational readiness to establish specific intermolecular interactions.

To further characterize the conformational behavior of the receptor in water and ACN, we combined two broadly used properties, namely R_g and RMSD, to obtain 2D-energy landscapes for each pH value and ACN (Figure 5 and Supporting Information File 1). In agreement with the R_g data, at low pH values, all sampled structures have both high R_g and RMSD. This means that, in more open conformations, the structure is also very different to the reference. Hence, in all these landscapes, we observe a correlation between RMSD and R_g properties. As the pH increases, more closed and lower RMSD structures are sampled. This is also in agreement with the R_g data which shows that the conformational space of the receptor at high pH values is similar to the one in ACN.

Both R_g and energy landscapes data identify the position of the arms as a good descriptor of the receptor conformational space. Hence, we represented the positions of pyrrolic nitrogen atoms relative to the phenyl ring in 900 conformations (Figure 6 and Supporting Information File 1). This result illustrates that, at low pH values, the arms are very distant to each other since they are positively charged and, as pH increases, more closed structures are sampled. Moreover, as observed before, the sampled positions at high pH values are very similar to the ones in ACN.

The described conformational analyses of the receptor suggest that the behavior in water, at low protonation, is similar to the

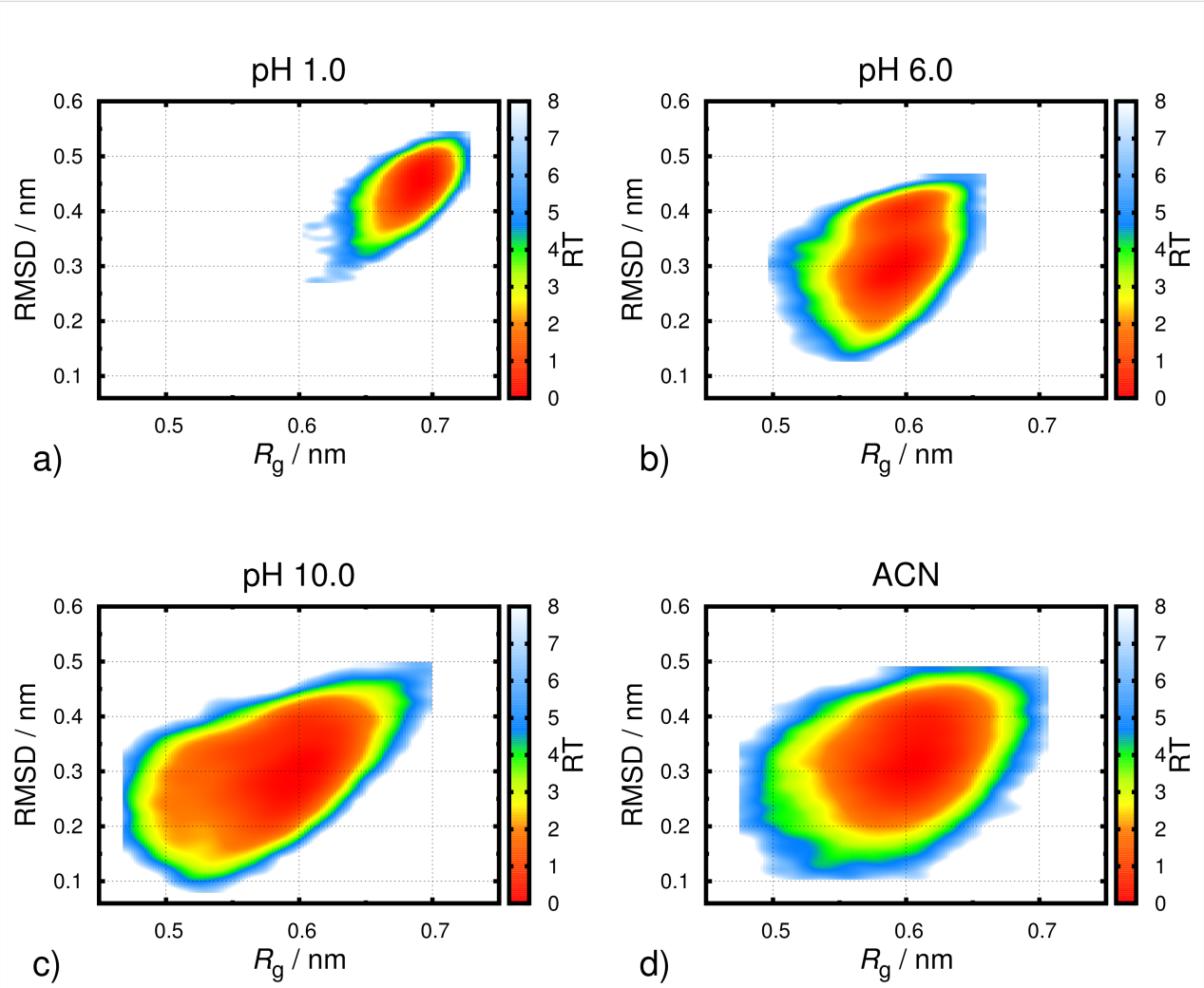

Figure 5: Free energy profiles for the receptor at pH 1.0 (a), 6.0 (b), 10.0 (c) and ACN (d) using RMSD and R_g as structural coordinates. The RMSD was calculated using the NMR derived structure as reference.

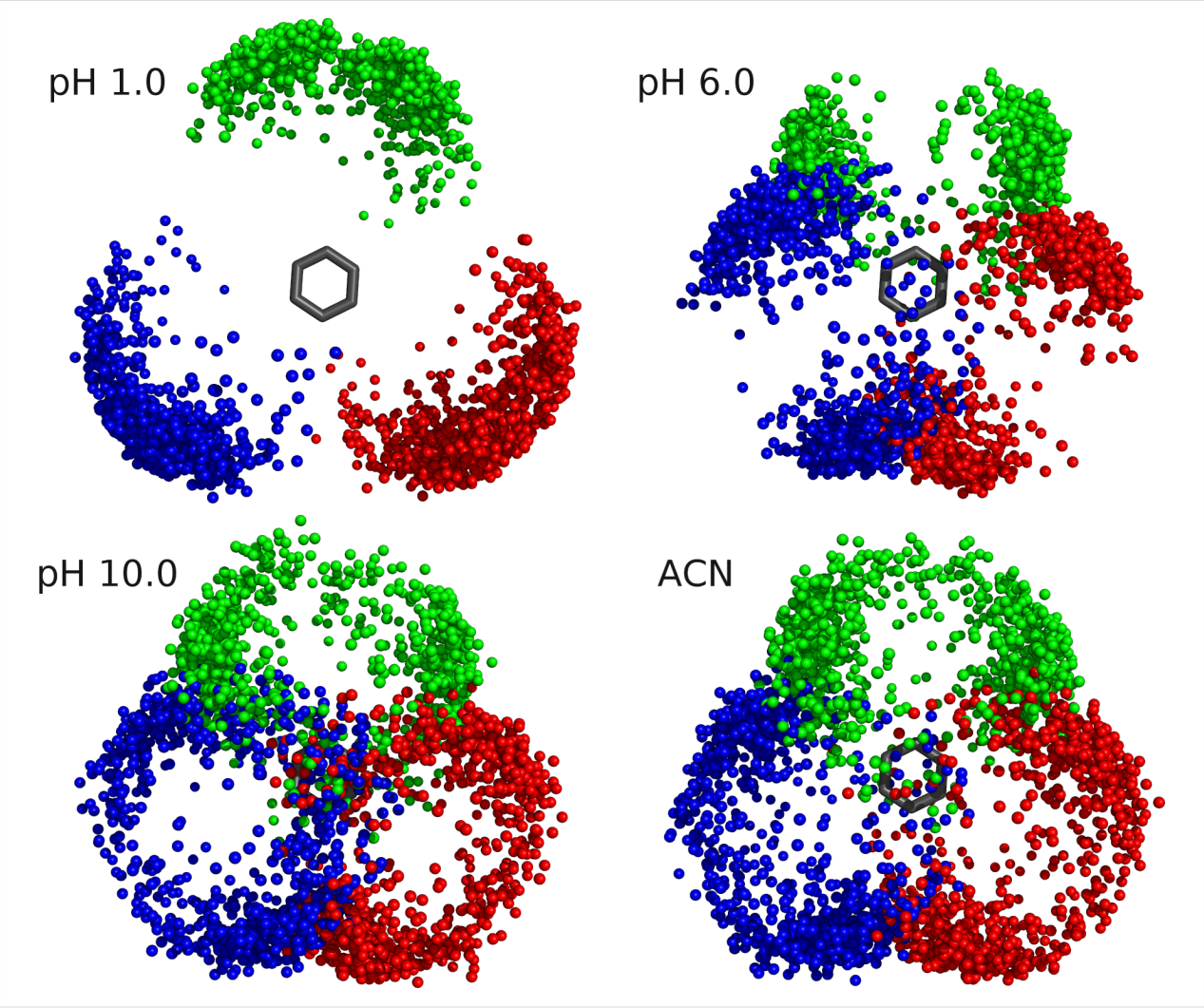

Figure 6: Schematic representation of the receptor arms positions. Pyrrolic nitrogen atoms positions relative to the phenyl ring in 900 conformations at pH 1.0, 6.0, 10.0 and in ACN.

observed in ACN. This suggests that, from a conformational point of view, the receptor would be able to bind the mannoside, both in water and ACN. However, as mentioned above, it was observed that this interaction is favorable in ACN but not in water. This may be explained by the different interactions that occur in water and ACN.

Receptor/mannoside interactions

To understand the molecular detail of the interaction between receptor and mannoside, several MM/MD simulations in water and ACN were performed without restraints (data not shown). In these simulations the residence time of the mannoside was very short (in the sub ns timescale). In addition, the binding event was never observed in our unrestrained simulations. Since entropy plays a crucial role in binding events they can be too slow and inaccessible in our computational timescale. Hence, to gain better insights into the molecular detail of the interaction between sugar and receptor, we performed the receptor + mannoside simulations (see Experimental section) with a position restraint between the phenyl group of the receptor and the sugar ring in the mannoside. This way, we were able to sample the interactions between the ligand and the receptor more efficiently and draw conclusions regarding the specificity of this event. In these simulations, we tested four protonation states (see Experimental section) from which W^{q3a} and W^{q3b} refer to the slightly acidic conditions analogous to experiments [14].

The histogram of the number of hydrogen bonds in ACN and water (Figure 7) suggests that in ACN the interaction is stronger. The number of conformations with more than 1 hydrogen bond is higher in ACN. Since donors and acceptors for hydrogen bonds in the mannoside are all in the head group, this result suggests that the interaction with the receptor is more specific in ACN. In water, with increased ionization, the

receptor samples more open conformations favoring interactions involving only one arm (1–2 hydrogen bonds) and preventing structures with more hydrogen bonds.

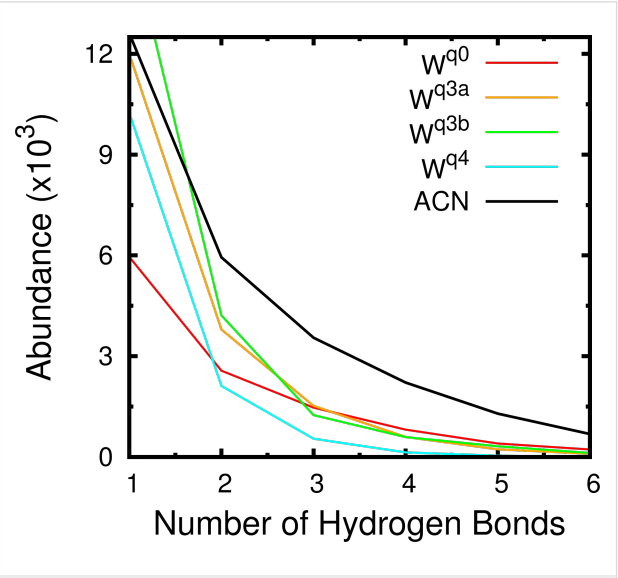

Figure 7: Histogram of the hydrogen bonds between receptor and mannoside in ACN and water (at different protonation states).

We also calculated the histogram of the distance between the center of mass of the last 4 atoms of the carbon chain of the mannoside and the 6 atoms of the phenyl ring (Figure 8). These histograms show a clear preference for lower distances in water for the fully deprotonated state (W^{q0}). In W^{q0}, the interaction

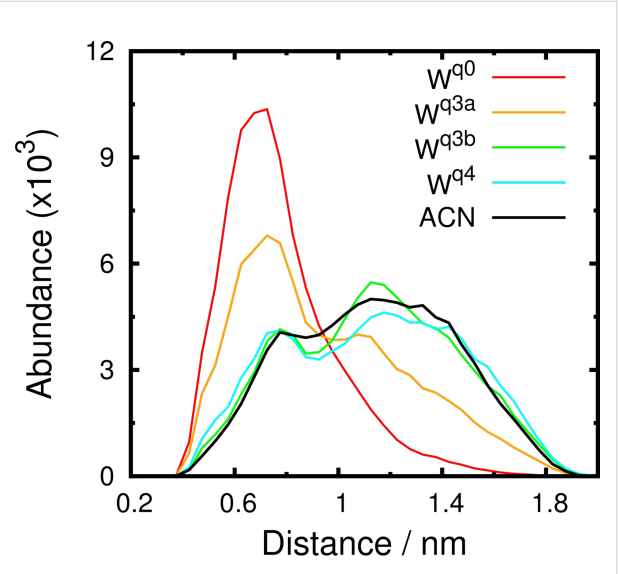

Figure 8: Distance histograms between the center of mass of the last 4 atoms of the carbon chain of the mannoside and the 6 atoms of the phenyl ring in the receptor. Calculations were done in ACN and water (at different protonation states).

between the carbon chain and the phenyl ring is stronger and stabilized by more close conformations. The protonation of the 1st generation amino groups (W^{q3b} and W^{q4}) induces a higher solvent exposure which destabilizes the mentioned hydrophobic interaction. As a result, these systems behave like ACN where there is no significant interaction. These observations are illustrated with two typical conformations in W^{q0} and ACN (Figure 9). In ACN, a strong interaction between the sugar ring and the arms of the receptor is observed and, in water, the carbon chain lays close to the ring stabilized by the hydrophobic effect.

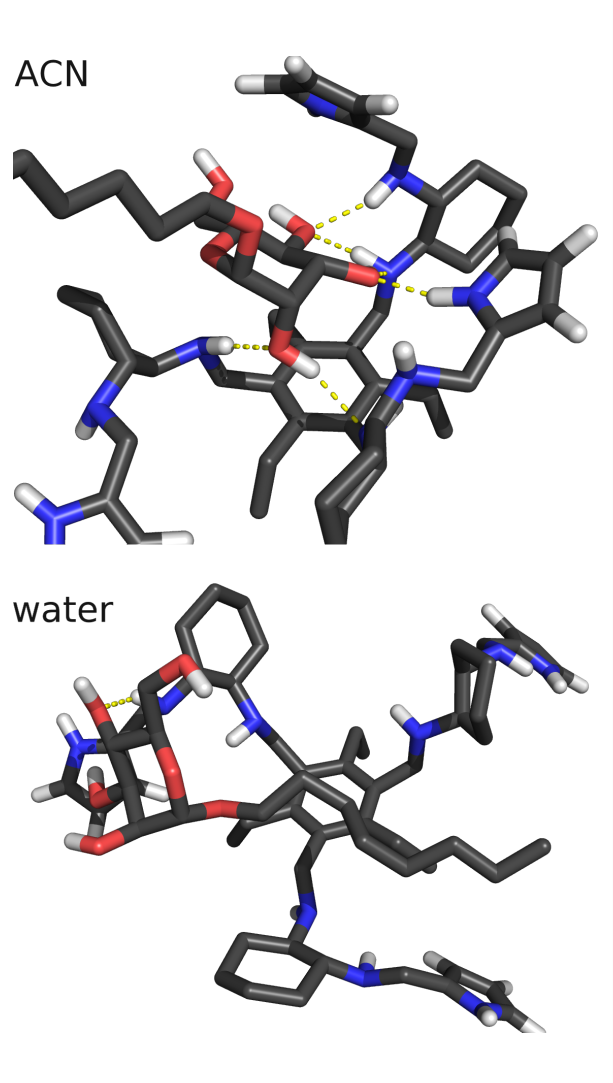

Figure 9: Typical conformations in water and ACN. The selected conformations have 6 hydrogen bonds in ACN and 1 in water.

Altogether, these results show that, in ACN, hydrogen bonds are stronger and, probably, the main responsible for the intermolecular interaction. In water, hydrophobic effects may play an important role, rendering the interactions between the carbon

chain and the phenyl group a structural determinant when all 1st generation amino groups are neutral.

Conclusion

In this work, we performed a full pH titration of the diaminopyrrolic tripodal receptor and a detailed analysis of the conformational dependence of this molecule with pH. We also studied the interaction between the receptor and the mannoside. Our results show that there is no significant difference in the conformational space of the receptor in ACN and in water (at pH > 4.0). Interestingly, in the presence of the mannoside, the number of hydrogen bonds between the two molecules is significantly larger in ACN than in water. This is probably the reason that the receptor is able to be selective towards mannoside in the organic solvent. There are several works, both theoretical [38-40] and experimental [1-6,37,41,42], showing that the interaction between sugars and their receptors is mainly driven by hydrogen bonds. In fact, there are several experimental structures of mannosides similar to the one used in this work in the protein data bank that also show a significant hydrogen bond network stabilizing the interaction between the sugar molecule and the protein (PDB IDs: 4avi [41], 1tr7 [42], 1uwf [42]). These observations indicate that the cause hindering the receptor to be active in water lies in the incapacity to form sufficient hydrogen bonds with the mannoside. Probably, the high propensity to form hydrogen bonds with water and the high flexibility of the arms of the receptor, are the main reasons that explain its low binding affinity in aqueous solvent.

This work also presents a new application of the stochastic titration constant-pH molecular dynamics method to a synthetic receptor for sugars. This method was able to describe the protonation/conformation coupling by correctly sample the occupation of titrable residues at the desired pH value.

Experimental

Simulations setup

As indicated in the introduction, two sets of simulations were performed (Table 1): A set of constant-pH MD simulations at 10 pH values (3 replicates of 100 ns each) and a set of MM/MD simulations in both water (at different protonation states) and acetonitrile (10 replicates of 100 ns each). The choice of protonation states was based on the pH-dependent proton distribution in the receptor from the constant-pH MD simulations. The fully deprotonated state (W^{q0}) is typical of a high pH value (~10), the two states with 3 protons (W^{q3a} and W^{q3b}) are typical of intermediate pH values (~4–7), and the 4 protons state (W^{q4}) is representative of pH 3.0. This pH assignment to the protonation states was done according to the population analysis obtained in the constant-pH MD simulations (see Supporting Information File 1).

Constant-pH MD settings

All constant-pH MD simulations were performed using the stochastic titration constant-pH MD method implemented for the GROMACS package, developed by Baptista et al. [15,21]. These simulations ran following a stop-and-go procedure that alters between a protonation state calculation where the new states are obtained from a Monte Carlo run using Poisson–Boltzmann derived energy terms and two MM/MD runs (one with the solute frozen to allow it to adapt to the new protonation states – 0.2 ps and another of the unconstrained system – 2.0 ps). All six amino groups were titrated at all simulated pH values.

Table 1: Summary of the simulations used in this work. All replicates were run for 100 ns.

Solute	Simulation method	Solvent	Protonation state	pH	Replicates
receptor	Constant-pH MD	Water (1268 molecules)	NA	1, 2, 3, 4, 5, 6, 7, 8, 9 and 10	3 per pH
receptor + mannoside	MD	ACN (535 molecules)	Fully deprotonated	NA	3
		Water (1926 molecules)	Fully deprotonated (W^{q0})		10
			3 protons in 2nd generation (W^{q3a})		
			2 protons in 2nd generation and 1 in 1st (W^{q3b})		
			3 protons in 2nd generation and 1 in 1st (W^{q4})		
		ACN (612 molecules)	Fully deprotonated		

MM/MD settings (MM/MD simulations and MM/MD part of constant-pH MD simulations)

The MM/MD simulations were performed using GROMACS 4.0.7 [43,44] and adapted parameters from the GROMOS $56A_{CARBO}$ [45,46] force field. In all the constant protonation simulations, the neutral secondary amino groups were built in the R configuration. In the constant-pH MD simulations, the chirality of the amino groups is not important due to the continuous exchange of protons. A time step of 2 fs was used in the leap-frog algorithm. A rhombic dodecahedral simulation box with periodic boundary conditions was used. The non-bonded interactions were treated using a twin-range cutoff of 0.8/1.4 nm and the neighbor lists were updated every 5 steps (10 fs). Electrostatic long range interactions were treated with a generalized reaction field [47] with an ionic strength of 0.1 M and a relative dielectric constant of 54 for systems with water [48] and 35.84 for systems solvated with acetonitrile [49]. The v-rescale temperature coupling was used (298.0 K) with a coupling constant of 0.1 with solvent and solute separately coupled to the bath. The Berendsen coupling bath [50] was used to treat pressure (1 bar) with coupling constant 0.5. Isothermal compressibility of 4.50×10^{-5} bar^{-1} for water and 8.17×10^{-5} bar^{-1} for acetonitrile [51,52] were used. All bonds were constrained using the P-LINCS algorithm [53].

The energy minimization steps were performed using a combination of both steepest descent and limited-memory Broyden–Fletcher–Goldfarb–Shanno methods. The initiation was performed in 3 steps of 100 ps, 200 ps, and 200 ps with different restraints.

In the receptor + mannoside simulations, a distance restraint of 100 kJ mol^{-1} nm^{-2} was used between all pairs of atoms in the two rings (6 in substituted phenyl group in the receptor and 6 in the sugar ring of the mannoside). Hence, a penalty was added when the distance between any pair of atoms in the two rings exceeded 1.0 nm. The used function for this energy penalty is quadratic between 1.0 and 1.2 nm and linear above 1.2 nm. This restraint creates a sphere around the receptor that maintains the two molecules close to each other. It is important to mention that within this sphere, no unphysical restrain forces are applied to the interacting molecules.

PB/MC settings

The PB/MC calculations were done as previously described [26]. The MEAD 2.2.9 [25] software package was used for PB calculations performed with the atomic charges and radii taken from the MM/MD force field. The model compound pK_a value used (10.64 for all equivalent amino groups) is the pK_a of the dimethylamine [54]. It was used a dielectric constant of 2 for the solute and 80 for the solvent. Grid spacing of 0.1 nm, in the coarser calculation, and 0.025 nm, in the focusing procedure, were used in the finite difference method [55]. The molecular surface was determined using a rolling probe of 0.14 nm and the Stern layer was 0.2 nm. The temperature used was 298 K and the ionic strength was 0.1 M.

The MC calculations were performed using the PETIT (version 1.5) [56] software with 10^5 steps for each calculation. Each step consisted of a cycle of random choices of protonation state (including tautomeric forms) for all individual sites and for pairs of sites with a coupling above 2.0 pK_a units [56,57], followed by the acceptance/rejection step according to Metropolis criterion [58]. The last protonation state is then used for the MM/MD part.

Analyses

The last 90 ns of each simulation were used for analyses. Several tools from the GROMACS software package [43,44] were used and others were developed in-house. The RMSD calculations followed a previously published procedure [59] that takes into account the symmetry of the receptor. The PyMOL 0.99RC6 software (http://www.pymol.org) was used to obtain rendered conformational images.

Energy landscapes were obtained from different 2D spaces by computing kernel estimates of the data probability densities [60] on grids of 2 pm^2 bins, using a Gaussian kernel. The probability density surface was then converted to an energy surface according to:

$$E(\vec{x}) = -RT \ln \frac{P(\vec{x})}{P_{max}}$$

where $\vec{x}$ is a coordinate in a 2D space and P_{max} is the maximum of the probability density function, $P(\vec{x})$.

The calculations of correlation-corrected errors for averages were computed using standard methods based on the auto-correlation function of the property measured to determine the number of independent blocks in the simulations [61].

Supporting Information

Supporting Information File 1

Diagrams with the population of each microstate, histograms of R_g, free energy profiles and schematic representation of the position of the arms at all pH values.
[http://www.beilstein-journals.org/bjoc/content/supplementary/1860-5397-10-156-S1.pdf]

Acknowledgments

The authors thank Cristina Nativi and Stefano Roelens for the NMR derived structure and useful discussions. We also thank António M. Baptista for several fruitful discussions and Rafael Nunes for the careful reading of the manuscript. Finally, we thank Sara R. R. Campos and Luís C. S. Filipe for several tools used to obtain the energy landscapes. We acknowledge financial support from Fundação para a Ciência e Tecnologia, through project PEst-OE/QUI/UI0612/2013 and grant SFRH/BD/81017/2011, and COST program through action CMST/COST-Action/CM1102.

References

1. Davis, A. P.; Wareham, R. S. *Angew. Chem., Int. Ed.* **1999,** *38,* 2978. doi:10.1002/(SICI)1521-3773(19991018)38:20<2978::AID-ANIE2978>3.0.CO;2-P
2. Davis, A. P. *Org. Biomol. Chem.* **2009,** *7,* 3629. doi:10.1039/b909856a
3. Jin, S.; Cheng, Y.; Reid, S.; Li, M.; Wang, B. *Med. Res. Rev.* **2010,** *30,* 171. doi:10.1002/med.20155
4. Mazik, M. *Chem. Soc. Rev.* **2009,** *38,* 935. doi:10.1039/b710910p
5. Nakagawa, Y.; Ito, Y. *Trends Glycosci. Glycotechnol.* **2012,** *24,* 1. doi:10.4052/tigg.24.1
6. Walker, D. B.; Joshi, G.; Davis, A. P. *Cell. Mol. Life Sci.* **2009,** *66,* 3177. doi:10.1007/s00018-009-0081-8
7. Collins, P. M.; Ferrier, R. J. *Monosaccharides: their chemistry and their roles in natural products;* Wiley & Sons: Chichester, New York, 1995.
8. Lehninger, A. L.; Nelson, D. L.; Cox, M. M. *Lehninger principles of biochemistry,* 4th ed.; W. H. Freeman: New York, 2005.
9. Dwek, R. A. *Chem. Rev.* **1996,** *96,* 683. doi:10.1021/cr940283b
10. Varki, A. *Glycobiology* **1993,** *3,* 97. doi:10.1093/glycob/3.2.97
11. Ardá, A.; Cañada, F. J.; Nativi, C.; Francesconi, O.; Gabrielli, G.; Ienco, A.; Jiménez-Barbero, J.; Roelens, S. *Chem.–Eur. J.* **2011,** *17,* 4821. doi:10.1002/chem.201002872
12. Nativi, C.; Cacciarini, M.; Francesconi, O.; Moneti, G.; Roelens, S. *Org. Lett.* **2007,** *9,* 4685. doi:10.1021/ol701959r
13. Nativi, C.; Francesconi, O.; Gabrielli, G.; Vacca, A.; Roelens, S. *Chem.–Eur. J.* **2011,** *17,* 4814. doi:10.1002/chem.201002871
14. Nativi, C.; Francesconi, O.; Roelens, S. Personal communication regarding the inability of the receptor to bind the mannoside in water.
15. Baptista, A. M.; Teixeira, V. H.; Soares, C. M. *J. Chem. Phys.* **2002,** *117,* 4184. doi:10.1063/1.1497164
16. Börjesson, U.; Hünenberger, P. H. *J. Chem. Phys.* **2001,** *114,* 9706. doi:10.1063/1.1370959
17. Bürgi, R.; Kollman, P. A.; van Gunsteren, W. F. *Proteins: Struct., Funct., Bioinf.* **2002,** *47,* 469. doi:10.1002/prot.10046
18. Dlugosz, M.; Antosiewicz, J. M. *Chem. Phys.* **2004,** *302,* 161. doi:10.1016/j.chemphys.2004.03.031
19. Dlugosz, M.; Antosiewicz, J. M.; Robertson, A. D. *Phys. Rev. E* **2004,** *69,* 021915. doi:10.1103/PhysRevE.69.021915
20. Lee, M. S.; Salsbury, F. R., Jr.; Brooks, C. L., III. *Proteins: Struct., Funct., Bioinf.* **2004,** *56,* 738. doi:10.1002/prot.20128
21. Machuqueiro, M.; Baptista, A. M. *J. Phys. Chem. B* **2006,** *110,* 2927. doi:10.1021/jp056456q
22. Mongan, J.; Case, D. A.; McCammon, J. A. *J. Comput. Chem.* **2004,** *25,* 2038. doi:10.1002/jcc.20139
23. Stern, H. A. *J. Chem. Phys.* **2007,** *126,* 164112. doi:10.1063/1.2731781
24. Vorobjev, Y. N. *J. Comput. Chem.* **2012,** *33,* 832. doi:10.1002/jcc.22909
25. Bashford, D.; Gerwert, K. *J. Mol. Biol.* **1992,** *224,* 473. doi:10.1016/0022-2836(92)91009-E
26. Teixeira, V. H.; Cunha, C. A.; Machuqueiro, M.; Oliveira, A. S. F.; Victor, B. L.; Soares, C. M.; Baptista, A. M. *J. Phys. Chem. B* **2005,** *109,* 14691. doi:10.1021/jp052259f
27. Campos, S. R. R.; Baptista, A. M. *J. Phys. Chem. B* **2009,** *113,* 15989. doi:10.1021/jp902991u
28. Campos, S. R. R.; Machuqueiro, M.; Baptista, A. M. *J. Phys. Chem. B* **2010,** *114,* 12692. doi:10.1021/jp104753t
29. Carvalheda, C. A.; Campos, S. R. R.; Machuqueiro, M.; Baptista, A. M. *J. Chem. Inf. Model.* **2013,** *53,* 2979. doi:10.1021/ci400479c
30. Henriques, J.; Costa, P. J.; Calhorda, M. J.; Machuqueiro, M. *J. Phys. Chem. B* **2013,** *117,* 70. doi:10.1021/jp3082134
31. Machuqueiro, M.; Baptista, A. M. *Biophys. J.* **2007,** *92,* 1836. doi:10.1529/biophysj.106.092445
32. Machuqueiro, M.; Baptista, A. M. *Proteins: Struct., Funct., Bioinf.* **2008,** *72,* 289. doi:10.1002/prot.21923
33. Machuqueiro, M.; Baptista, A. M. *J. Am. Chem. Soc.* **2009,** *131,* 12586. doi:10.1021/ja808463e
34. Machuqueiro, M.; Baptista, A. M. *Proteins: Struct., Funct., Bioinf.* **2011,** *79,* 3437. doi:10.1002/prot.23115
35. Vila-Viçosa, D.; Campos, S. R. R.; Baptista, A. M.; Machuqueiro, M. *J. Phys. Chem. B* **2012,** *116,* 8812. doi:10.1021/jp3034837
36. Vila-Viçosa, D.; Teixeira, V. H.; Santos, H. A. F.; Machuqueiro, M. *J. Phys. Chem. B* **2013,** *117,* 7507. doi:10.1021/jp401066v
37. Nakagawa, Y.; Doi, T.; Masuda, Y.; Takegoshi, K.; Igarashi, Y.; Ito, Y. *J. Am. Chem. Soc.* **2011,** *133,* 17485. doi:10.1021/ja207816h
38. Aqvist, J.; Mowbray, S. L. *J. Biol. Chem.* **1995,** *270,* 9978.
39. Lerbret, A.; Affouard, F.; Hédoux, A.; Krenzlin, S.; Siepmann, J.; Bellissent-Funel, M.-C.; Descamps, M. *J. Phys. Chem. B* **2012,** *116,* 11103. doi:10.1021/jp3058096
40. Lerbret, A.; Bordat, P.; Affouard, F.; Hédoux, A.; Guinet, Y.; Descamps, M. *J. Phys. Chem. B* **2007,** *111,* 9410. doi:10.1021/jp071946z
41. Wellens, A.; Lahmann, M.; Touaibia, M.; Vaucher, J.; Oscarson, S.; Roy, R.; Remaut, H.; Bouckaert, J. *Biochemistry* **2012,** *51,* 4790. doi:10.1021/bi300251r
42. Bouckaert, J.; Berglund, J.; Schembri, M.; De Genst, E.; Cools, L.; Wuhrer, M.; Hung, C.-S.; Pinkner, J.; Slättegård, R.; Zavialov, A.; Choudhury, D.; Langermann, S.; Hultgren, S. J.; Wyns, L.; Klemm, P.; Oscarson, S.; Knight, S. D.; De Greve, H. *Mol. Microbiol.* **2005,** *55,* 441. doi:10.1111/j.1365-2958.2004.04415.x
43. Berendsen, H. J. C.; van der Spoel, D.; van Drunen, R. *Comput. Phys. Commun.* **1995,** *91,* 43. doi:10.1016/0010-4655(95)00042-E
44. Hess, B.; Kutzner, C.; van der Spoel, D.; Lindahl, E. *J. Chem. Theory Comput.* **2008,** *4,* 435. doi:10.1021/ct700301q
45. Hansen, H. S.; Hünenberger, P. H. *J. Comput. Chem.* **2011,** *32,* 998. doi:10.1002/jcc.21675
46. Schmid, N.; Eichenberger, A. P.; Choutko, A.; Riniker, S.; Winger, M.; Mark, A. E.; van Gunsteren, W. F. *Eur. Biophys. J.* **2011,** *40,* 843. doi:10.1007/s00249-011-0700-9
47. Tironi, I. G.; Sperb, R.; Smith, P. E.; van Gunsteren, W. F. *J. Chem. Phys.* **1995,** *102,* 5451. doi:10.1063/1.469273
48. Smith, P. E.; van Gunsteren, W. F. *J. Chem. Phys.* **1994,** *100,* 3169. doi:10.1063/1.466407
49. Barthel, J.; Kleebauer, M.; Buchner, R. *J. Solution Chem.* **1995,** *24,* 1. doi:10.1007/BF00973045

50. Berendsen, H. J. C.; Postma, J. P. M.; van Gunsteren, W. F.; DiNola, A.; Haak, J. R. *J. Chem. Phys.* **1984,** *81,* 3684. doi:10.1063/1.448118
51. Dharmaraju, G.; Narayanaswamy, G.; Raman, G. K. *J. Chem. Eng. Data* **1982,** *27,* 193. doi:10.1021/je00028a028
52. Narayanaswamy, G.; Dharmaraju, G.; Raman, G. K. *J. Chem. Thermodyn.* **1981,** *13,* 327. doi:10.1016/0021-9614(81)90022-7
53. Hess, B. *J. Chem. Theory Comput.* **2008,** *4,* 116. doi:10.1021/ct700200b
54. Hall, H. K., Jr. *J. Am. Chem. Soc.* **1957,** *79,* 5441. doi:10.1021/ja01577a030
55. Gilson, M. K.; Sharp, K. A.; Honig, B. H. *J. Comput. Chem.* **1988,** *9,* 327. doi:10.1002/jcc.540090407
56. Baptista, A. M.; Soares, C. M. *J. Phys. Chem. B* **2001,** *105,* 293. doi:10.1021/jp002763e
57. Baptista, A. M.; Martel, P. J.; Soares, C. M. *Biophys. J.* **1999,** *76,* 2978. doi:10.1016/S0006-3495(99)77452-7
58. Metropolis, N.; Rosenbluth, A. W.; Rosenbluth, M. N.; Teller, A. H.; Teller, E. *J. Chem. Phys.* **1953,** *21,* 1087. doi:10.1063/1.1699114
59. Filipe, L. C. S.; Machuqueiro, M.; Baptista, A. M. *J. Am. Chem. Soc.* **2011,** *133,* 5042. doi:10.1021/ja111001v
60. Silverman, B. W. *Density estimation for statistics and data analysis;* Chapman and Hall: London, New York, 1986.
61. Allen, M. P.; Tildesley, D. J. *Computer simulation of liquids;* Clarendon Press: Oxford, England, 1987.

License and Terms

Beilstein Journal of Organic Chemistry

Synthesis and solvodynamic diameter measurements of closely related mannodendrimers for the study of multivalent carbohydrate–protein interactions

Yoann M. Chabre, Alex Papadopoulos, Alexandre A. Arnold and René Roy*

Full Research Paper

Open Access

Address:
Pharmaqam, Department of Chemistry, Université du Québec à Montréal, P. O. Box 8888, Succ. Centre-ville, Montréal, Québec, Canada H3C 3P8

Email:
René Roy* - roy.rene@uqam.ca

* Corresponding author

Keywords:
carbohydrates; click chemistry; dendrimers; glycodendrimers; lectins; multivalent glycosystems

Beilstein J. Org. Chem. **2014,** *10,* 1524–1535.
doi:10.3762/bjoc.10.157

Received: 04 March 2014
Accepted: 11 June 2014
Published: 04 July 2014

This article is part of the Thematic Series "Multivalent glycosystems for nanoscience".

Guest Editor: B. Turnbull

Abstract

This paper describes the synthesis of three closely related families of mannopyranoside-containing dendrimers for the purpose of studying subtle structural parameters involved in the measurements of multivalent carbohydrate–protein binding interactions. Toward this goal, two trimers **5** and **9**, three 9-mers **12**, **17**, **21**, and one 27-mer **23**, varying by the number of atoms separating the anomeric and the core carbons, were synthesized using azide–alkyne cycloaddition (CuAAc). Compound **23** was prepared by an efficient convergent strategy. The sugar precursors consisted of either a 2-azidoethyl (**3**) or a prop-2-ynyl α-D-mannopyranoside (**7**) derivative. The solvodynamic diameters of 9-mer **12**, **17**, and **21** were determined by pulsed-field-gradient-stimulated echo (PFG-STE) NMR experiments and were found to be 3.0, 2.5, and 3.4 nm, respectively.

Introduction

Multivalent carbohydrate–protein interactions are at the forefront of a wide range of biological events which have triggered a plethora of versatile synthetic methods for the design of potent inhibitors and glycomimetics [1-4]. Among the diverse strategies leading to efficient ligands, glycopolymers [1,5-7], glycodendrimers [7-14], and sugar rods [15,16] have retained most attention. An additional approach that has gained keen interest resides in the modifications of both the aglycon [17-19] and substituent residues [20-22] of the targeted sugar moieties through extensive studies of quantitative structure–activity relationships (QSARs). In most of the studies related to aglycon modifications, it was concluded that aromatic glycosides possessed improved binding properties due to the ubiquitous presence of aromatic amino acids in the cognate binding sites

[23-25]. This is also supported by the recent findings that the sugar backbones themselves also possess a hydrophobic side that orients the sugars in appropriate aromatic amino acid rich pockets [26-28].

Unfortunately, due to the inherent complexity of studying multivalent binding interactions, researchers have used experimental conditions that often biased the intrinsic phenomena under investigations [29]. For instance, when evaluating thermodynamic parameters by isothermal calorimetry (ITC), scientists used either truncated versions of for instance, tetrameric lectins such as ConA, or diluted conditions to avoid precipitation of the complexes [30,31]. Alternatively, the application of surface plasmon resonance (SPR) also creates artificial situations not sufficiently related to the natural cellular events, thus requiring complex mathematical algorithms [32]. Most solid-phase immunoassays (ELLA, ELISA) also fall under the same criticism by providing unusually high (or too close) sugar densities. Also important and in spite of the two decades of glycodendrimer chemistry [7], there is still no general rule to allow predicting which structural parameters would be optimal for the binding interactions.

In order to gain more insight into this direction, we designed herein three families of closely related mannopyranoside clusters (glycodendrimers) aimed at evaluating their relative binding abilities against the hometetrameric leguminous lectin ConA from *Canavalia ensiformis* by inhibition of haemagglutination and by turbidimetry. The latter would allow us to measure relative kinetic factors involved in the cross-linking lattice formation using soluble partners.

Results and Discussion

In order to critically evaluate the subtle structural parameters imparted by glycodendrimers in deciphering their relative thermodynamic and kinetic abilities towards multivalent lectins, we designed three families of closely related mannopyranoside dendrimers. Scheme 1 describes the preparation of trimers **5** and **9** built around benzene-1,3,5-tricarboxamide (BTA or trimesamide core) having respectively nine and ten atoms between the

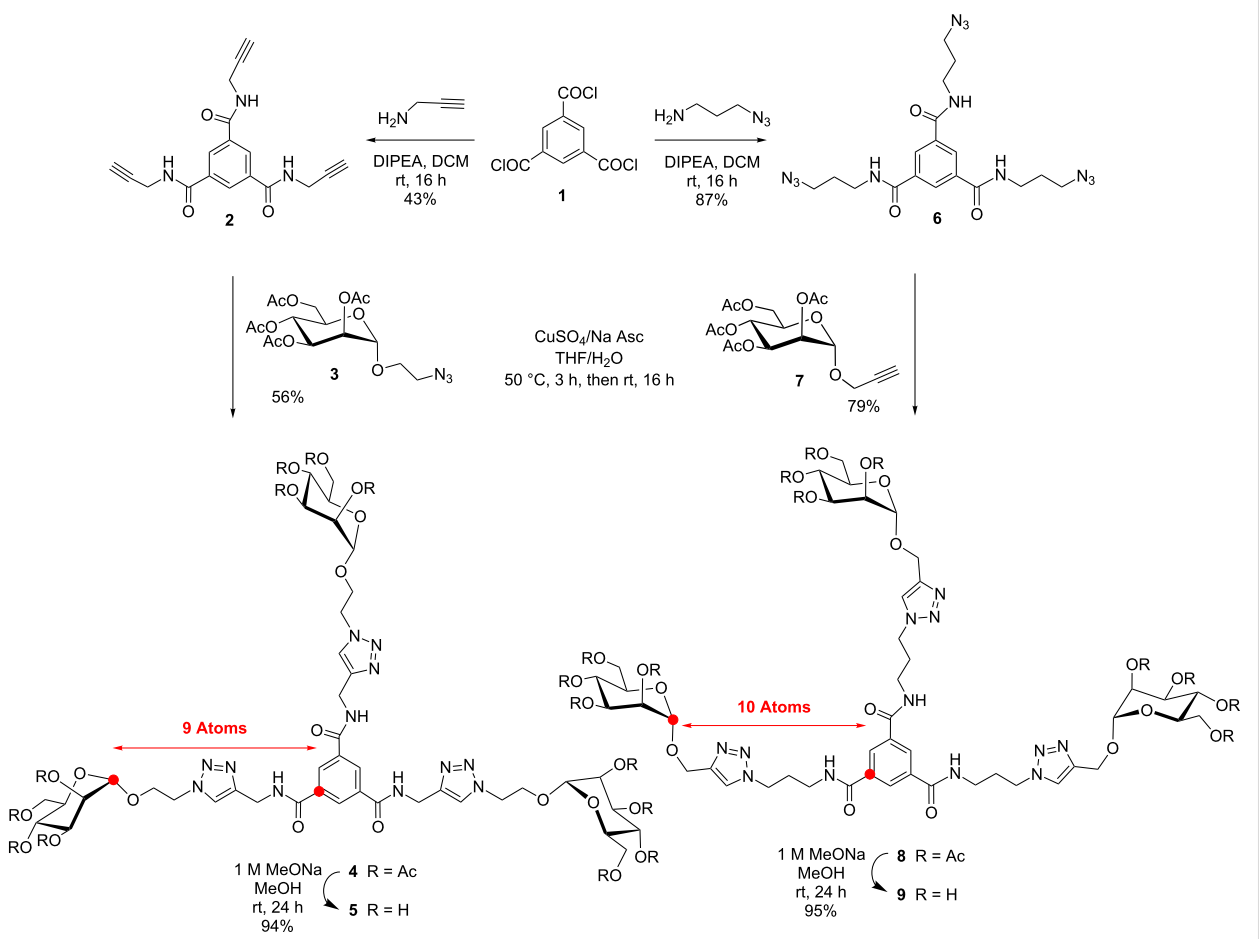

Scheme 1: Synthesis of mannosylated trimers **5** and **9** using trimesic acid core transformed into propargylated (**2**) and azidopropylated (**6**) scaffolds and then coupled by "click chemistry" with either 2-azidoethyl (**3**) or propargyl (**7**) mannopyranosides.

anomeric and the benzene carbon, hence differing by a distance of only ~1.5 Å. Schemes 2–4 illustrate the syntheses of 9-mers **12** and **21** using the same trimesic acid core, together with a phloroglucinol template to initiate the synthesis of homologue **17**, but incorporating 2-amino-2-hydroxymethylpropane-1,3-diol as a branching unit (TRIS) at the G(1) level. Thus, compounds **12**, **17**, and **21** differ by having nine atoms between the anomeric carbon and the focal quaternary carbon of TRIS followed by two, four, and nine atoms to reach the benzene carbon, respectively (~4, 6, and 12 Å). Finally, the synthesis of a 27-mer mannosylated dendrimer **23** is shown in Scheme 5.

The synthesis of **5** was accomplished starting from commercial trimesic acid chloride **1** which was readily transformed into known tripropargyl amide derivative **2** [33] using propargylamine according to Scheme 1. Amide **2** was conjugated to peracetylated 2-azidoethyl α-D-mannopyranoside **3** [34] under classical copper-catalyzed dipolar cycloaddition (CuAAc) to afford **4** in 56% yield. Structure **4** was readily characterized by the absence of acetylenic protons at δ 3.16 ppm, the appearance of identical triazole protons (3H) at δ 7.74 ppm relative to the anomeric signal (3H) at δ 4.81 ppm and corresponding HRMS data. Zemplén deprotection (NaOMe, MeOH) afforded **5** in

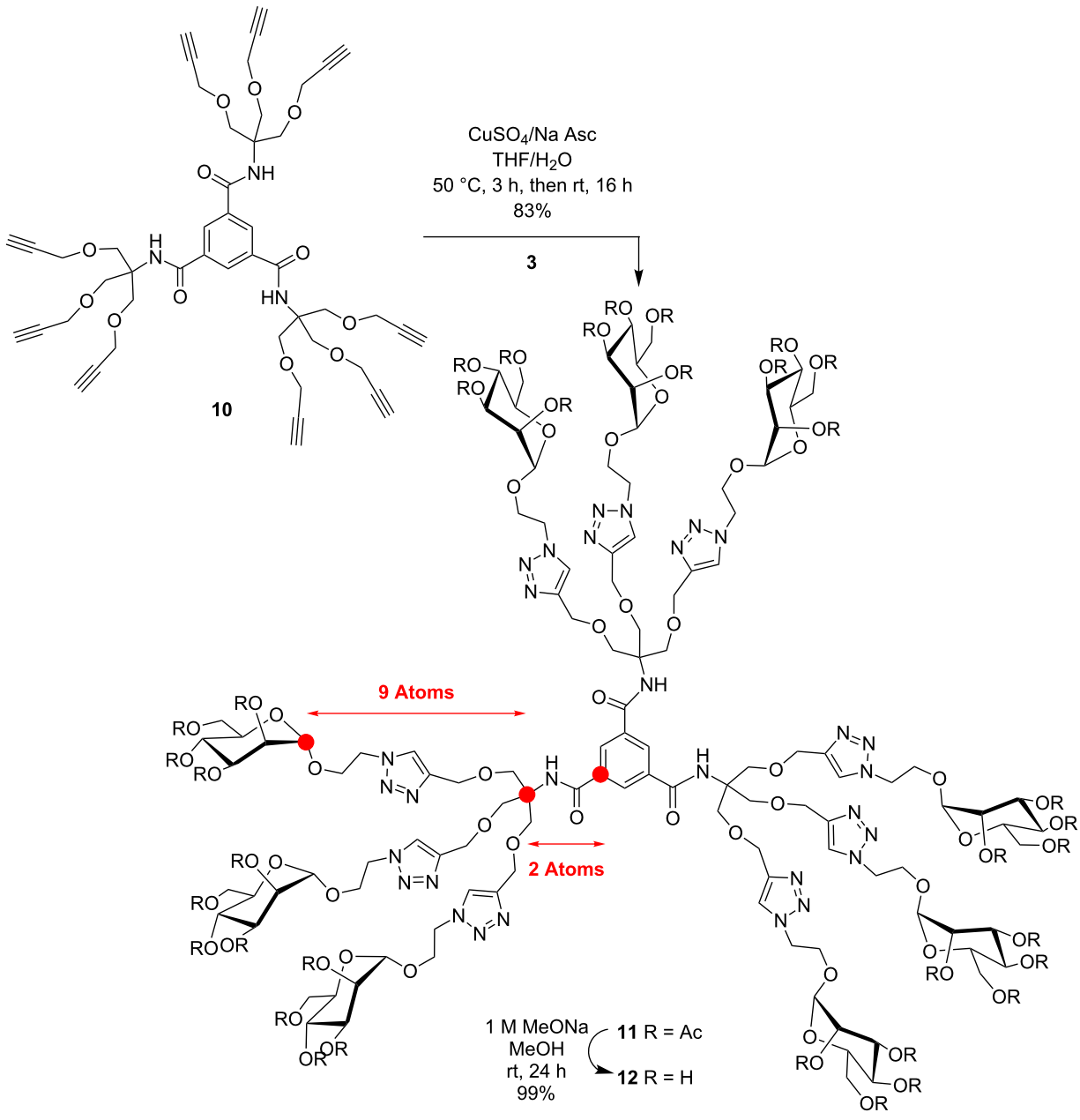

Scheme 2: Divergent CuAAc "click reaction" between propargylated core **10** and azide **3** to afford 9-mer **12**.

94% yield. Synthesis of the related homolog **9**, prepared in 74% overall yield from known **6** [17] by an analogous click chemistry, is also described in Scheme 1. To this end, trichloride **1** was treated as above with 3-azido-1-propanamine to provide **6** in 87% yield. Azide–alkyne cycloaddition of **6** with prop-2-ynyl α-D-mannopyranoside **7** [35] gave **8** (79%) which was de-*O*-acetylated under Zemplén conditions (NaOMe, MeOH, 95%) to give **9**.

The syntheses of 9-mers **12**, **17** and **21** are illustrated in Schemes 2–5 and follow a conceptually identical strategy to the one described above for trimers **5** and **9**. Toward this goal, propargylated 9-mer scaffold **10** [17] was treated under the same CuAAc conditions with azide **3** to provide peracetylated **11** in 83% yield which upon Zemplén de-*O*-acetylation gave **12** in essentially quantitative yield (Scheme 2). Complete spectral characterization (^{1}H, ^{13}C NMR and HRMS) concluded for the

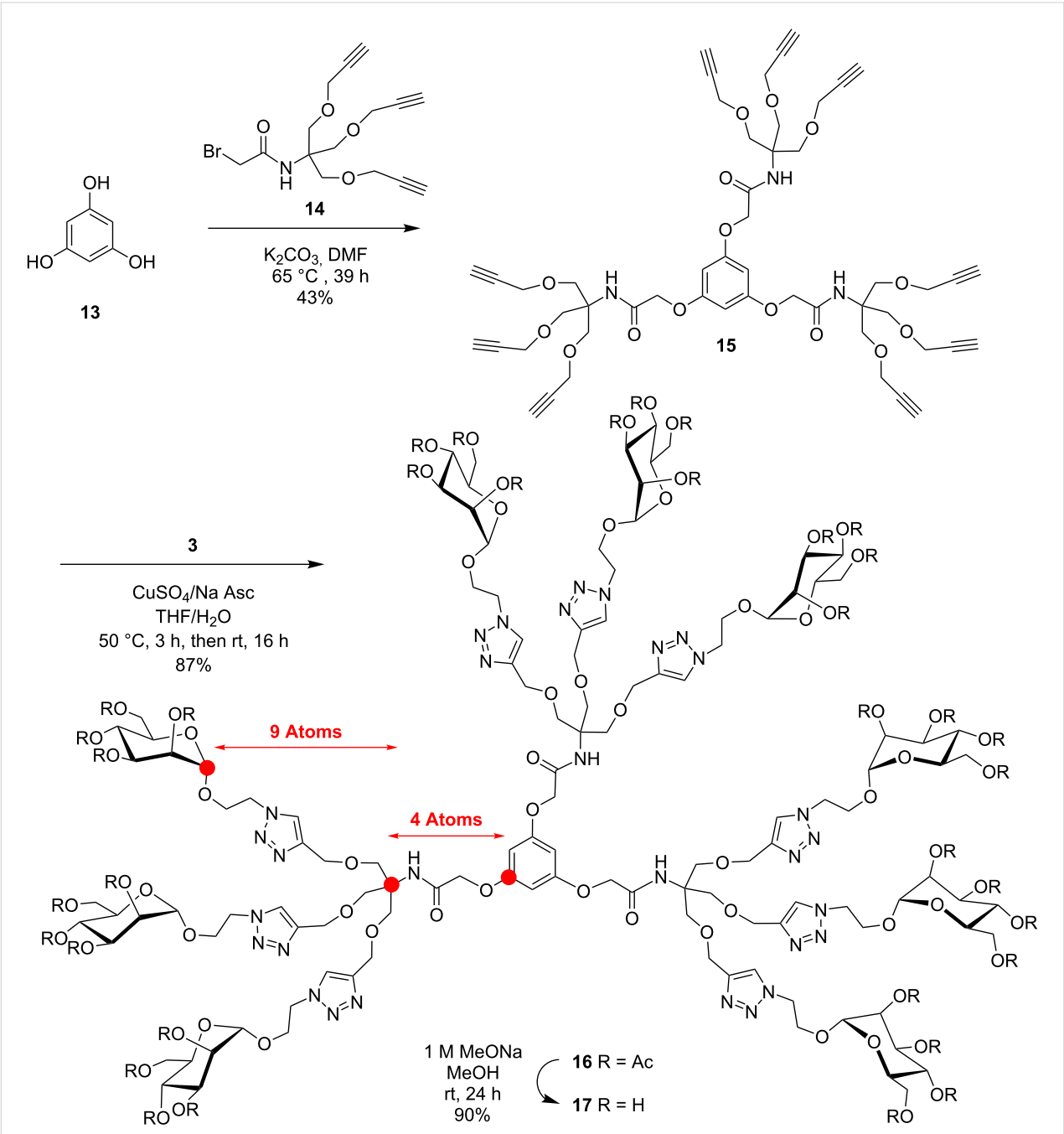

Scheme 3: Divergent CuAAc synthesis of "extended" 9-mer **17** using phloroglucinol (**13**) as core, bromoacylated TRIS as linker and mannopyranosyl-azide **3**.

aforementioned structure having twelve atoms in the linking arm (see Supporting Information File 1).

Analogously, the extended 9-mer glycodendrimer **17**, possessing fourteen atoms between the anomeric carbon and the benzene carbon, was prepared according to Scheme 3. Thus, phloroglucinol (**13**) was carefully *O*-alkylated with the previously synthesized bromoacetylated TRIS derivative **14** [36] using K_2CO_3 in DMF to provide **15** in 43% yield. Again, the structural integrity of **15** was fully assessed by the simplicity of its ^{1}H NMR symmetrical patterns that showed the characteristic singlets for the three amide protons at δ 6.85 ppm, relative to the three benzene protons (δ 6.17 ppm) and the six *O*-acyl protons at δ 4.36 ppm (core) compared with the peripheral acetylenic methylenes (18H), inner methylene of TRIS (18H), and the terminal alkyne protons (9H) at δ 4.16, 3.87, and 2.48 ppm, respectively.

Toward the last and further extended 9-mer **21**, a convergent strategy was rather adopted (Scheme 4). This strategy has the clear advantages of providing an easier purification process from partially substituted end-products together with a better assessment of complete surface group modifications. Hence, known **14** [36] was first cycloadded to mannosylazide **3** under the above CuAAc conditions. The "click reaction" proceeded exceptionally efficiently and provided bromoacylated dendron precursor **18** in 94% yield. Substitution of the bromide by azide also proceeded uneventfully (NaN_3, DMF, rt, 16 h) to afford intermediate glycodendron **19** in 93% yield. Finally, coupling of the propargylated core **2** with azidodendron **19** under the typical CuAAc conditions gave peracetylated intermediate **20** which was readily deprotected to give 9-mer **21** in 84% overall yield. All spectral characteristics concurred to the expected structural integrity of **21** (see Supporting Information File 1).

Finally, a 27-mer mannosylated G(1)-dendrimer **23** was similarly prepared using an accelerated convergent strategy (Scheme 5). This time, the nonapropargylated scaffold **10** was "clicked" under CuAAc with trimeric azidodendron **19** to give **22** in an acceptable yield of 63% after silica gel column chro-

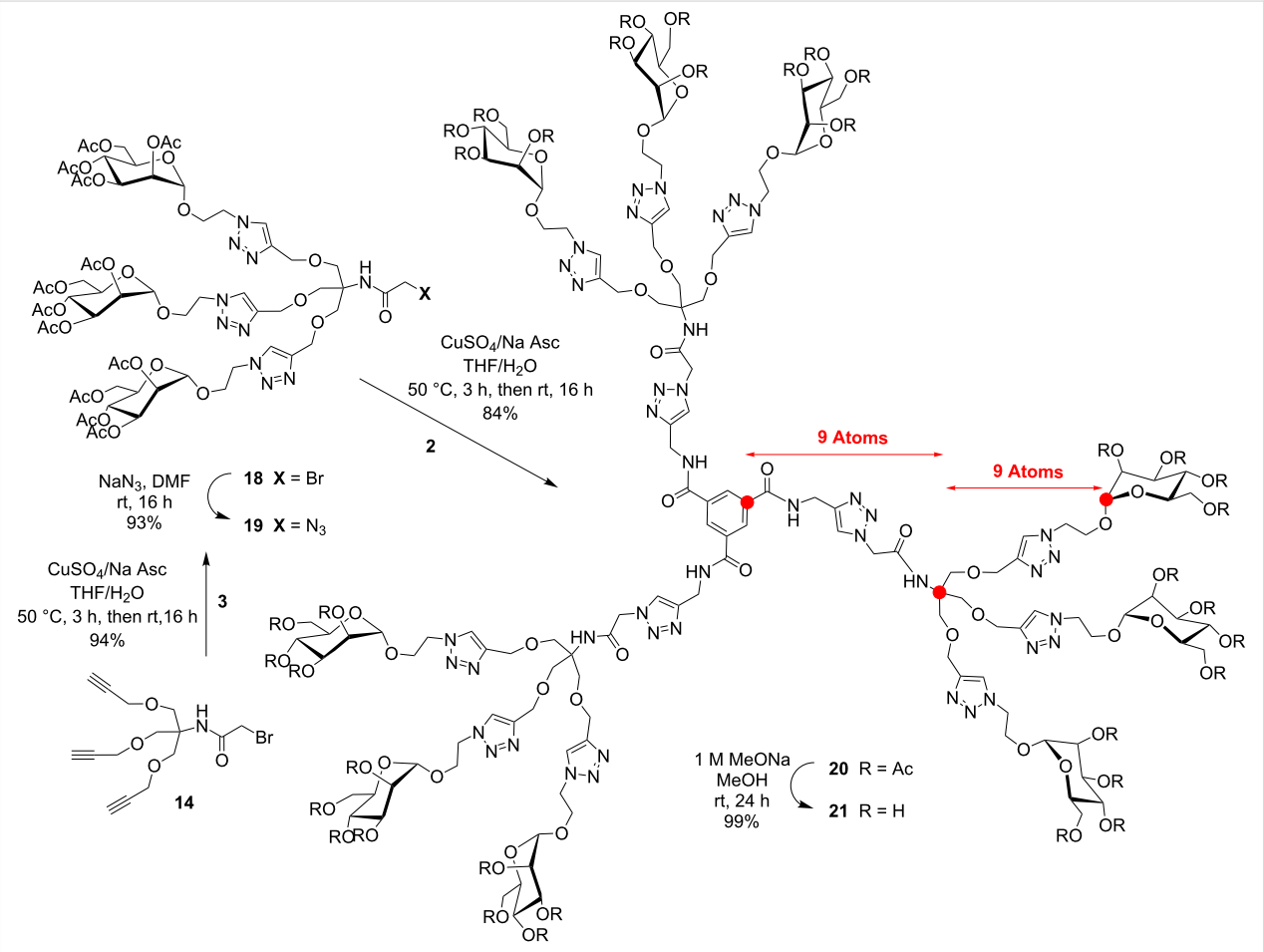

Scheme 4: Convergent synthesis of further "extended" 9-mer **21** using mannosylated bromoacyl dendron **18** transformed into azide **19** followed by CuAAc coupling to tripropargylated core **2**.

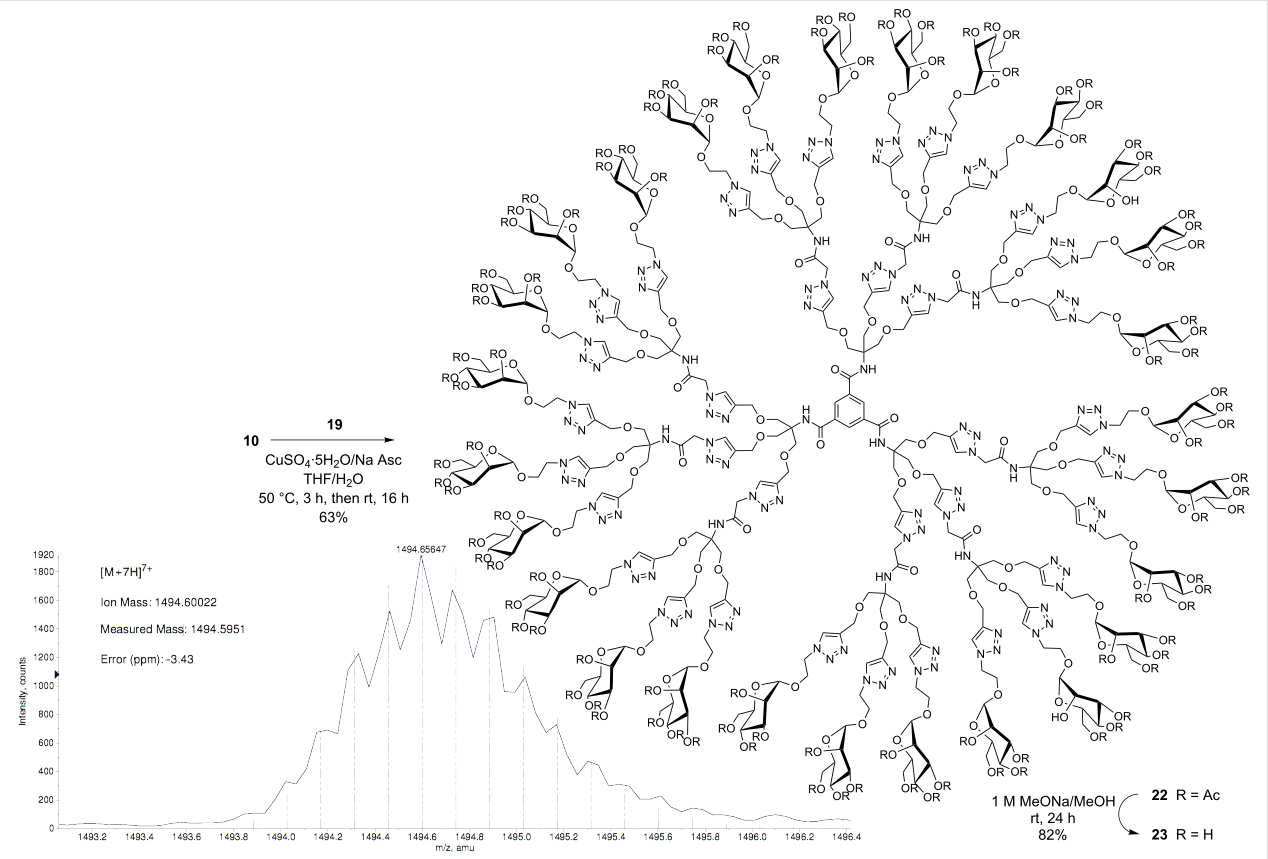

Scheme 5: Convergent assembly of 27-mer **23** using key propargylated scaffold precursors **10** and mannosylated azidodendron **19**. Insert: Zoom section of HRMS ($^+$TOF) spectrum for deprotected G(1)-mannodendrimer **23** illustrating observed and theoretical isotopic distributions for $[M + 7H]^{7+}$ adduct.

matography, corresponding to an excellent 95% yield per individual dendron's incorporation. The complete disappearance of propargylic signals in the ^{1}H NMR spectrum supported complete conversion. Note that working with peracetylated sugar precursors allows less tedious purification practices as opposed to working with unprotected sugars which often necessitate purification by cumbersome dialysis followed by HPLC treatment. Here again, the complete structural integrity of the final product can be readily confirmed from its characteristic spectral identification. Ultimately, dendrimer **23** was deprotected under the usual Zemplén conditions in 82% yield. Once again, all the relative integrations for each proton presented on the surface were in perfect agreement with those of the middle and internal regions. Interestingly, high resolution mass spectrometry ($^+$TOF technique) resulted in the formation of multicharged adducts that matched the expected theoretical patterns, especially the one corresponding to $[M + 7H]^{7+}$, as illustrated in Scheme 5 (insert).

NMR diffusion studies

To accurately estimate the various structural factors involved in the intricate binding interactions between our synthetic multimeric mannosides and ConA, we determined their relative diffusivity measurements by NMR spectroscopy. In fact, diffusion NMR spectroscopy has recently become a method of choice to access information about sizes and shapes of macromolecular species by measuring their diffusion coefficients in a given solvent [17,37]. The size of nonavalent compounds **12**, **17**, and **21**, and more particularly their solvodynamic radii, was thus estimated with the help of pulsed-field-gradient stimulated echo (PFG-STE) NMR experiments using bipolar pulse pairs-longitudinal-eddy-current delay (BPP-LED) in D_2O at 25 °C. Stimulated echoes were used since they avoid signal attenuation due to transverse relaxation while bipolar gradient pulses reduce gradient artefacts [38]. The diffusion rates (D) were calculated from the decay of the signal intensity of the common H-5 proton (δ = 2.98 ppm) located on each epitope with increasing field gradient strength (Figure 1a). In all cases, monoexponential behavior was observed (Figure 1b), which was manifested as a linear decay of the logarithm of the signal intensity as a function of the gradient strength. This behavior is consistent with a spherical and unimolecular character of the glycodendrimers, confirming the absence of aggregation phenomena in aqueous solution under the working concentra-

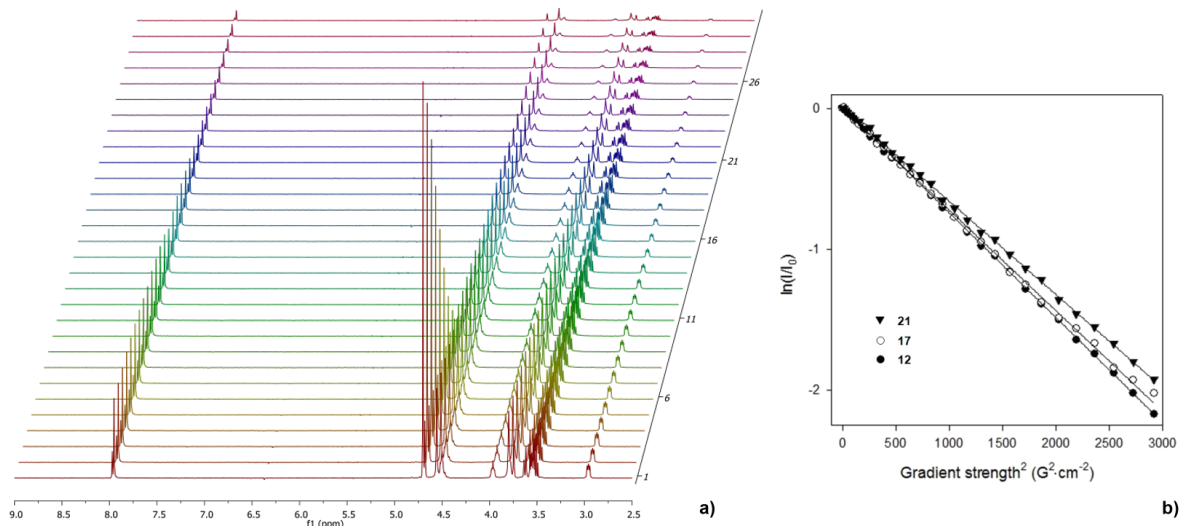

Figure 1: a) Decay of ^{1}H signal for the nonavalent mannosylated compound **12** in D_2O during the PFGSTE experiment. The gradient strength is increased linearly between 1.8 and 54.2 G·cm^{-1}; b) characteristic echo decays of the H-5 resonances (δ = 2.98 ppm) as a function of squared gradient strength located in **12** (full circles) and **21** (full triangles) with δ = 4 ms and Δ = 50 ms (Δ = 40 ms for **17** (circles)). Notably, such linear behavior was also obtained for the decay of the signal intensities of other protons located either in internal regions of the conjugates on aromatic or branching sections, or in the peripheral saccharidic belt (results not shown).

tions. The corresponding solvodynamic diameters ($d_s = 2 \times r_s$) can be calculated using the Stokes–Einstein equation and the viscosity of pure D_2O (Table 1).

As expected, nonavalent conjugates **12**, **17**, and **21** presented solvodynamic diameters in the range of roughly 3 nm when considering the decay of distinctive and common H-5 signals. These values remained consistent with similar congeners described earlier and harboring different epitopes [17]. The variation of the complexity of anchoring functionalities in the middle region with the incorporation of amide functions and triazole groups is responsible for a diameter enhancement for **21** when compared with **12**, as expected. On the other hand, rather counter-intuitive tendencies were observed since the apparently slightly extended structure **17** was measured as the smallest molecule of the family in water. A specific spatial arrangement of the dendrons that emanate from 1,3,5-*O*-alkylations on the aromatic core in **17**, compared to the one generated in BTAs-centered structures **12** and **21**, could explain this observation. Also, these discrepancies might result from the general amphiphilic behavior of this kind of macromolecules [39]. In fact, these glycoclusters shared common structural factors with hydrophilic peripheral moieties and an aromatic central core but the introduction of distinct functionalized linkers may change the overall hydrophobic/hydrophilic balances of the structures. As such, they could engage supplementary intramolecular hydrogen bonding or hydrophobic interactions that could mediate their three-dimensional arrangement in aqueous media. Moreover, it is also reported that the relative spatial distribution of the branches around the C=O-centered BTAs strongly depends on the nature of the substituents [40]. This hypothesis can partly explain the discrepancy observed for the calculated

Table 1: Determination of diffusion data and solvodynamic diameters of nonavalent conjugates **12**, **17**, and **21** by diffusion NMR experiments.

Entry	Compound	D [× 10^{-10} m^2s^{-1}][a,b,c]	Solvodynamic diameter [d_s, nm][d]
1	**12**	1.33	3.0 (2.9)
2	**17**	1.62	2.5 (2.3)
3	**21**	1.17	3.4 (2.9)

[a]See general procedures and Supporting Information File 1 for extraction of the diffusion rate and calibration of the gradient strength. D was determined from the decay of the H-5 resonance (δ = 2.98 ppm). [b]Viscosity of D_2O at 25 °C: $\eta D_2O = 1.097 \times 10^{-3}$ Pa s. [c]The error associated with the measurement was estimated from repeated calculations of the diffusion coefficients to be below 10%. [d]Results in parentheses correspond to the average value calculated from the decays of 4 or 5 different proton signals.

diameter of **21** (Table 1, entry 3). In fact, diffusion data for **21** ranged from 1.61×10^{-10} m^2s^{-1} for central CH_{ar} to 1.17×10^{-10} m^2s^{-1} for H-5, indicating a heterogeneity in diffusivity depending on the proton location within the same molecule. As a consequence, the calculated d_s value based on the utilization of an average value of diffusion data (D) extracted from signal decays of distinct protons located at different levels in the molecule differ from that obtained with the decay of peripheral H-5 signal only. This heterogeneity was less pronounced for **17** and absent for **12** that presented consistent values of D ranging from 1.51 to 1.33×10^{-10} m^2s^{-1} for protons in the core or the periphery. Interestingly, calculation of the extended conformation (MM2, Chem3D) of the linkers in **12**, **17**, and **21** showed lengths of 14.8, 17.1, and 21.8 Å, respectively.

Conclusion

The syntheses of three related families of mannosylated glycoclusters and glycodendrimers were efficiently accomplished around a benzene core and using the CuAAc methods now routinely used in this field [9,41,42]. The targeted compounds were based on trimesic acid scaffold which is known to properly expose the surface sugar groups to tetrameric lectins such as ConA [43] and the LecA lectin from *Pseudomonas aeruginosa* [17]. With these closely related families of mannosylated dendrimers in hand, together with their known relative size in solution, we are now well positioned to evaluate their binding behavior against their cognate proteins and this work will be published in due course [44].

The study of subtle structural variations and the nature of anchoring functions, as observed in diffusivity experiments, could represent a first step towards rational interpretation to explain the differential kinetic behavior within a closely related family of glycoclusters.

Experimental

General remarks

All reactions in organic medium were performed in standard oven-dried glassware under an inert atmosphere of nitrogen using freshly distilled solvents. CH_2Cl_2 was distilled from CaH_2 and DMF from ninhydrin, and kept over molecular sieves. Solvents and reagents were deoxygenated when necessary by purging with nitrogen. Water used for lyophilization of final dendrimers was nanopure grade, purified through Barnstead NANOPure II Filter with Barnstead MegOhm-CM Sybron meter. All reagents were used as supplied without prior purification unless otherwise stated, and obtained from Sigma-Aldrich Chemical Co. Ltd. Reactions were monitored by analytical thin-layer chromatography using silica gel 60 F254 precoated plates (E. Merck) and compounds were visualized by 254 nm light, a mixture of iodine/silica gel and/or mixture of ceric ammonium molybdate solution (100 mL H_2SO_4, 900 mL H_2O, 25 g $(NH_4)_6Mo_7O_{24}H_2O$, 10 g $Ce(SO_4)_2$) and subsequent development by gentle warming with a heat-gun. Purifications were performed by flash column chromatography using silica gel from Silicycle (60 Å, 40–63 μm) with the indicated eluent.

NMR, IR, and MS spectroscopy

^{1}H NMR and ^{13}C NMR spectra were recorded at 300 or 600 MHz and 75 or 150 MHz, respectively, on a Bruker spectrometer (300 MHz) and Varian spectrometer (600 MHz). All NMR spectra were measured at 25 °C in indicated deuterated solvents. Proton and carbon chemical shifts (δ) are reported in ppm and coupling constants (J) are reported in Hertz (Hz). The resonance multiplicity in the ^{1}H NMR spectra are described as "s" (singlet), "d" (doublet), "t" (triplet), and "m" (multiplet) and broad resonances are indicated by "br". Residual protic solvent of $CDCl_3$ (^{1}H, δ 7.27 ppm; ^{13}C, δ 77.0 ppm (central resonance of the triplet)), D_2O (^{1}H, δ 4.79 ppm and 30.89 ppm for CH_3 of acetone for ^{13}C spectra of de-*O*-acetylated compounds), MeOD (^{1}H, δ 3.31 ppm and ^{13}C, δ 49.0 ppm). 2D Homonuclear correlation ^{1}H-^{1}H COSY together with 2D heteronuclear correlation ^{1}H-^{13}C HSQC experiments were used to confirm NMR peak assignments.

Fourier transform infrared (FTIR) spectra were obtained with Thermo-scientific, Nicolet model 6700 equipped with ATR. The absorptions are given in wavenumbers (cm^{-1}). The intensity of the bands is described as s (strong), m (medium) or w (weak). Melting points were measured on a Electrothermal MEL-TEMP apparatus and are uncorrected.

Accurate mass measurements (HRMS) were performed on a LC–MSD–ToF instrument from Agilent Technologies in positive electrospray mode. Low-resolution mass spectra were performed on the same apparatus or on a LCQ Advantage ion trap instrument from Thermo Fisher Scientific in positive electrospray mode (Mass Spectrometry Laboratory (Université de Montréal), or Plateforme analytique pour molécules organiques (Université du Québec à Montréal), Québec, Canada). Either protonated molecular ions $[M + nH]^{n+}$ or adducts $[M + nX]^{n+}$ (X = Na, K, NH_4) were used for empirical formula confirmation.

NMR diffusion measurements were performed at 25 °C on a Varian Inova Unity 600 spectrometer (Varian, Walnut Creek, CA, USA) operating at a frequency of 599.95 MHz for ^{1}H using a 5 mm broadband *z*-gradient temperature-regulated probe. The temperature was calibrated with 1,2-ethanediol according to a standard procedure [38]. The diffusion experiment employed a

bipolar pulse-field gradients stimulated echo sequence as proposed by Wu et al [45]. The gradient pulse duration δ was 4 ms and the diffusion times (Δ) were 40 to 50 ms to ensure that the echo intensities were attenuated by at least 80%. A complete attenuation curve was obtained by measuring 30 gradient strengths, which were linearly incremented between 1.8 and 54.2 Gcm^{-1}. Hard 90° ^1H pulses of 15 μs were used and 36 k data points were recorded with 16 scans acquired for each gradient's strength. A recycle delay of 3.0 s was used. The gradient strength was calibrated by back calculation of the coil constant from diffusion experiments on H_2O traces in D_2O ($D = 1.90 \times 10^{-9}$ m^2 s^{-1}) [46].

Diffusion rates were extracted from the slope of the straight lines obtained by plotting ln(*I*) against the gradient-pulse power squared according to the following equation: $\ln(I) = -D\gamma^2G^2\delta^2(\Delta - \delta/3 - \tau/2) + \ln(I_0)$ where *I* is the relative intensity of a chosen resonance ($I = I_0\exp-[D\gamma^2G^2\delta^2(\Delta - \delta/3 - \tau/2)]$), *G* = gradient strength (*T*/m), γ = proton gyromagnetic ratio, *D* = diffusion rate (m^2 s^{-1}), δ = gradient duration, Δ = diffusion delay, and τ = pulse length for bipolar pulses. All diffusion spectra were processed in Mat NMR [47].

Glycodendrimer synthesis

Procedure A: multiple CuAAc couplings on polypropargylated cores

To a solution of polypropargylated core (1.00 equiv) and complementary azido synthon (1.25 equiv/propargyl) in a THF/H_2O mixture (1:1) were added sodium ascorbate (0.30 equiv/propargyl) and $CuSO_4{\cdot}5H_2O$ (0.30 equiv/propargyl). The reaction mixture was stirred at 50 °C for 3 h then at room temperature for an additional 16 h period. Ethyl acetate (10 mL) was added and the resulting solution was poured in a separatory funnel containing 25 mL of EtOAc and 30 mL of a saturated aqueous solution of NH_4Cl. Organics were washed with (2 × 25 mL) of saturated NH_4Cl_{aq}, water (2 × 20 mL) and brine (1 × 10 mL). The organic phase was then dried over $MgSO_4$ and concentrated under reduced pressure. Column chromatography on silica (DCM/MeOH 100:0 to 90:10) afforded the desired glycocluster.

Procedure B: Zemplén de-*O*-acetylation procedure for insoluble hydroxylated derivatives

The acetylated compound was dissolved in anhydrous MeOH and a solution of sodium methoxide (1 M in MeOH, 5 μL every 20 min until precipitation) was added. An additional 100 μL was then injected and the heterogeneous reaction mixture was stirred at room temperature for 24 h. The solvent was then removed with a Pasteur pipette and a mixture of anhydrous MeOH/DCM (4:1, 5 mL) was added to the residual white foam. A vigorous agitation is maintained for an additional 15 min period. After removal of the solvents with a Pasteur pipette, the residue was dissolved in H_2O (3 mL), and the pH was adjusted to 7 by the addition of ion-exchange resin (Amberlite IR 120 H^+). After filtration, the solvent was removed under vacuum with a rotary evaporator and lyophilized to yield the fully deprotected glycocluster.

Synthesis of peracetylated trivalent derivative 8: To a solution of triazido core **6** (50.0 mg, 109 μmol, 1.00 equiv) and mannoside **7** (158 mg, 409 μmol, 3.75 equiv) in a THF/H_2O mixture (1:1, 6 mL) were added sodium ascorbate (19.4 mg, 98.1 μmol, 0.90 equiv) and $CuSO_4{\cdot}5H_2O$ (24.5 mg, 98.1 μmol, 0.90 equiv). The reaction mixture was stirred at 50 °C for 3 h then at room temperature for an additional 16 h period. Ethyl acetate (10 mL) was added and the resulting solution was poured in a separatory funnel containing 35 mL of EtOAc and 30 mL of a saturated aqueous solution of NH_4Cl. Organics were washed with (2 × 25 mL) of saturated NH_4Cl_{aq}, water (2 × 20 mL) and brine (1 × 10 mL). The organic phase was then dried over $MgSO_4$ and concentrated under reduced pressure. Column chromatography on silica (DCM/MeOH 98:2 to 94:6) afforded the desired compound **8** (138 mg, 86.0 μmol, 79%) as a viscous oil. R_f 0.34 (95:5 DCM/MeOH); ^1H NMR (600 MHz, $CDCl_3$) δ (ppm) 8.27 (s, 3H, CH_{ar}), 7.79 (s, 3H, C$H_{triazole}$), 7.72 (t, *J* = 5.3 Hz, 3H, N*H*), 5.29–5.19 (m, 9H, H_2, H_3, H_4), 4.92 (s_{app}, 3H, H_1), 4.77–4.62 (2 × d, *J* = 12.4 Hz, 6H, OCH_2), 4.54 (t, *J* = 6.4 Hz, 6H, $N_{triazole}CH_2$), 4.28 (dd, *J* = 12.4 Hz, *J* = 5.4 Hz, 3H, H_{6b}), 4.11–4.03 (m, 6H, $H_5 + H_{6a}$), 3.55 (m, 6H, NHCH_2), 2.28 (m, 6H, $CH_2CH_2CH_2$), 2.12, 2.10, 2.02, 1.96 (4s, 36H, COCH_3); $^{13}C\{^1H\}$ NMR (150 MHz, $CDCl_3$) δ (ppm) 170.8, 170.1, 170.0, 169.7 (*C*OCH_3), 166.1 (*C*ONH), 143.5 ($C_{triazole}$), 134.9 (C_{arom}), 128.5 (*C*H$_{arom}$), 123.9 (*C*H$_{triazole}$), 96.7 (C_1), 69.3 (C_2), 69.0 (C_3), 68.7 (C_5), 65.9 (C_6), 62.3 (C_4), 60.7 (O*C*H$_2$), 48.3 (*C*H$_2$N$_{triazole}$), 37.5 (NH*C*H$_2$), 29.9 ($CH_2CH_2CH_2$), 20.9, 20.8, 20.7, 20.7 (CO*C*H$_3$); MS ($^+$TOF-MS, *m*/*z*): $[M + H]^+$ calculated for $C_{69}H_{90}N_{12}O_{33}$, 1615.6; found, 1615.6.

Synthesis of nonapropargylated core 15: To a solution of phloroglucinol (**13**, 10.0 mg, 79.3 μmol, 1.00 equiv) in anhydrous DMF (3 mL) was added under nitrogen anhydrous K_2CO_3 (previously heated at 250 °C under vaccum, 39.5 mg, 285 μmol, 3.60 equiv). After 10 min of vigorous stirring, tripropargylated synthon **14** (93.0 mg, 285 μmol, 3.60 equiv) was added into the solution under inert atmosphere and the reaction mixture was allowed to stir at 65 °C for 39 h. In the end, the dark-brown heterogeneous reaction was poured in 30 mL of EtOAc and organics were washed with a saturated aqueous solution of NH_4Cl (2 × 30 mL) then water (2 × 20 mL) and brine (10 mL). The organic phase was then dried over $MgSO_4$ and concentrated under reduced pressure. Column chro-

matography on silica (EtOAc/hexane 40:60 to 50:50) afforded the desired compound **15** (32.0 mg, 33.8 μmol, 43%) as a colorless oil. R_f 0.27 (1:1 EtOAc/hexane); ^{1}H NMR (300 MHz, $CDCl_3$) δ (ppm) 6.85 (s, 3H, N*H*), 6.17 (s, 3H, CH_{ar}), 4.36 (s, 6H, OCH_2CONH), 4.16 (m, 18H, OCH_2C≡CH), 3.87 (br s, 18H, HNC$_q$CH_2O), 2.48 (m, 9H, OCH$_2$C≡C*H*); ^{13}C{^{1}H} NMR (75 MHz, $CDCl_3$) δ (ppm) 167.3 (*C*ONH), 159.0 (C_{ar}OCH$_2$), 95.8 (*C*H$_{ar}$), 79.4 (OCH$_2$*C*≡CH), 74.9 (OCH$_2$C≡*C*H), 68.3 (HNC$_q$*C*H$_2$O), 67.5 (O*C*H$_2$CONH), 59.2 (C_q), 58.6 (O*C*H$_2$C≡CH); HRMS ($^+$TOF-HRMS, *m*/*z*): [M + H]$^+$ calculated for $C_{51}H_{57}N_3O_{15}$, 952.3862; found, 952.3843 (Δ = −2.10 ppm); [M + Na]$^+$: calculated for 974.3682; found, 974.3662 (Δ = −2.05 ppm).

Synthesis of bromoacylated dendron 18: To a solution of tripropargylated synthon **14** (140.0 mg, 393.0 μmol, 1.00 equiv) and mannoside **3** (616 mg, 1.48 mmol, 3.75 equiv) in a THF/H_2O mixture (1:1, 6 mL) were added sodium ascorbate (70.0 mg, 354 μmol, 0.90 equiv) and $CuSO_4{\cdot}5H_2O$ (88.4 mg, 354 μmol, 0.90 equiv). The reaction mixture was stirred at 50 °C for 3 h then at room temperature for an additional 16 h period. Ethyl acetate (20 mL) was added and the resulting solution was poured in a separatory funnel containing 40 mL of EtOAc and 30 mL of a saturated aqueous solution of NH_4Cl. Organics were washed with 2 × 35 mL of saturated NH_4Cl_{aq}, water (2 × 30 mL) and brine (20 mL). The organic phase was then dried over $MgSO_4$ and concentrated under reduced pressure. Column chromatography on silica (DCM/MeOH 99:1 to 96:4) afforded the desired compound **18** (594 mg, 369.4 μmol, 94%) as a white solid. R_f 0.47 (94:6 DCM/MeOH); mp 68–72 °C (not corrected); ^{1}H NMR (300 MHz, $CDCl_3$) δ (ppm) 7.68 (br s, 3H, C$H_{triazole}$), 6.89 (br s, 1H, N*H*), 5.24–5.18 (m, 9H, H_2, H_3, H_4), 4.80 (d, J = 1.3 Hz, 1H, H_1), 4.61–4.58 (br s, 12H, OCH_2C$_{triazole}$ + N$_{triazole}$CH_2), 4.17–4.00 (m, 11H, OCH_2CH$_2$ + H_{6a} + BrCH_2CONH), 3.94–3.78 (m, 9H, H_{6b} + NHC$_q$CH_2O), 3.60 (m, 3H, H_5), 2.12, 2.08, 2.03, 1.98 (4s, 36H, COCH_3); ^{13}C{^{1}H} NMR (75 MHz, $CDCl_3$) δ (ppm) 170.5, 169.9, 169.9, 169.5, (*C*OCH$_3$), 165.6 (*C*ONH), 145.0 ($C_{triazole}$), 123.7 (*C*H$_{triazole}$), 97.4 (C_1), 69.1 (C_2), 68.9 (C_3), 68.8 (C_5), 68.4 (NHC$_q$*C*H$_2$O), 66.2 (C_6), 65.6 (C_4), 64.6 (O*C*H$_2$C$_{triazole}$), 62.1 (O*C*H$_2$CH$_2$), 60.2 (C_q), 49.6 (*C*H$_2$N$_{triazole}$), 29.7 (*C*H$_2$Br), 20.8, 20.7, 20.6, 20.6 (CO*C*H$_3$); IR (cm^{-1}): 2956, 2937, 2361, 2337, 1751, 1734, 1540, 1370, 1218, 1045, 759; HRMS ($^+$TOF-HRMS, *m*/*z*): [M + 2H]$^{2+}$ calculated for $C_{63}H_{87}BrN_{10}O_{34}$, 804.2358; found, 804.2356 (Δ = −0.18 ppm); [M + H] $^+$ calculated for 1607.4642, found: 1607.4620 (Δ = −1.36 ppm); [M + Na]$^+$ calculated for 1629.4462; found, 1629.4448 (Δ = −0.84 ppm).

Synthesis of azidoacylated dendron 19: To a stirring solution of brominated trivalent dendron **18** (121.0 mg, 75.2 μmol, 1.00 equiv) in dry DMF (1.5 mL) was added under a nitrogen atmosphere sodium azide (7.3 mg, 112 μmol, 1.50 equiv). After stirring overnight at room temperature, the solvent was removed under vaccum. Ethyl acetate (20 mL) was added and the resulting solution was poured in a separatory funnel containing 20 mL of EtOAc and 30 mL of a saturated aqueous solution of NH_4Cl. Organics were washed with 2 × 30 mL of saturated NH_4Cl_{aq}, water (2 × 30 mL) and brine (20 mL). The organic phase was then dried over $MgSO_4$ and concentrated under reduced pressure to furnish the desired compound **19** (110 mg, 69.9 μmol, 93%) as a white solid. R_f 0.47 (94:6 DCM/MeOH); mp 62–65 °C (not corrected); ^{1}H NMR (300 MHz, $CDCl_3$) δ (ppm) 7.68 (br s, 3H, C$H_{triazole}$), 6.69 (br s, 1H, N*H*), 5.27–5.18 (m, 9H, H_2, H_3, H_4), 4.80 (d, J = 1.3 Hz, 1H, H_1), 4.61–4.58 (br s, 12H, OCH_2C$_{triazole}$ + N$_{triazole}$CH_2), 4.23–4.00 (m, 11H, OCH_2CH$_2$ + H_{6a} + N$_3$CH_2CONH), 3.90–3.81 (m, 9H, H_{6b} + NHC$_q$CH_2O), 3.60 (m, 3H, H_5), 2.12, 2.08, 2.03, 1.98 (4s, 36H, COCH_3); ^{13}C{^{1}H} NMR (75 MHz, $CDCl_3$) δ (ppm) 170.4, 169.9, 169.8, 169.5, (*C*OCH$_3$), 166.7 (*C*ONH), 144.9 ($C_{triazole}$), 123.7 (*C*H$_{triazole}$), 97.4 (C_1), 69.0 (C_2), 68.8 (C_3), 68.8 (C_5), 68.4 (NHC$_q$*C*H$_2$O), 66.1 (C_6), 65.6 (C_4), 64.5 (O*C*H$_2$C$_{triazole}$), 62.1 (O*C*H$_2$CH$_2$), 59.9 (C_q), 52.5 (*C*H$_2$N$_3$), 49.5 (*C*H$_2$N$_{triazole}$), 20.7, 20.7, 20.6, 20.6 (CO*C*H$_3$); IR (cm^{-1}): 2934, 2361, 2338, 2107 (N$_3$), 1751, 1734, 1540, 1373, 1218, 1045, 761; HRMS ($^+$TOF-HRMS, *m*/*z*): [M + H]$^+$ calculated for $C_{63}H_{87}N_{13}O_{34}$, 1570.5551; found, 1570.5543 (Δ = −0.51 ppm); [M + Na]$^+$ calculated for 1592.5371; found, 1592.5366 (Δ = −0.31 ppm).

Synthesis of peracetylated 27-mer derivative 22: To a solution of nonapropargylated core **10** (4.6 mg, 5.38 μmol, 1.00 equiv) and trimannosylated dendron **19** (95.0 mg, 60.5 μmol, 11.25 equiv) in a THF/H_2O mixture (1:1, 3 mL) were added sodium ascorbate (2.9 mg, 15 μmol, 2.70 equiv) and $CuSO_4{\cdot}5H_2O$ (3.6 mg, 15 μmol, 0.90 equiv). The reaction mixture was stirred at 50 °C for 3 h then at room temperature for an additional 16 h period. Ethyl acetate (10 mL) was added and the resulting solution was poured in a separatory funnel containing 25 mL of EtOAc and 30 mL of a saturated aqueous solution of NH_4Cl. Organics were washed with 2 × 25 mL of saturated NH_4Cl_{aq}, water (2 × 20 mL) and brine (10 mL). The organic phase was then dried over $MgSO_4$ and concentrated under reduced pressure. Column chromatography on silica (DCM/MeOH 98:2 to 90:10) afforded the desired compound **22** (50.0 mg, 3.33 μmol, 63%) as a yellowish oil. R_f 0.72 (90:10 DCM/MeOH); ^{1}H NMR (600 MHz, $CDCl_3$) δ (ppm) 8.27 (m, 3H, CH_{ar}), 7.79 (s, 9H, C$H_{int\text{-}triazole}$), 7.75 (s, 27H, C$H_{ext\text{-}triazole}$), 7.34–7.31 (m, 12H, N*H*), 5.23–5.18 (m, 81H, H_2, H_3, H_4), 5.05 (br s, 18H, N$_{triazole}$CH_2CONH), 4.81 (s$_{app}$, 27H, H_1), 4.62–4.53 (m, 126H, OCH_2C$_{triazole}$ + N$_{triazole}$CH_2), 4.20–3.64 (m, 207H, OCH_2 + H_6 + NHC$_q$CH_2O + H_5), 2.11, 2.08, 2.01, 1.96 (4s, 324H, COCH_3); ^{13}C{^{1}H} NMR (150 MHz,

$CDCl_3$) δ (ppm) 170.6, 170.5, 170.0, 169.9, 169.9, 169.7, 169.6 ($COCH_3$), 168.4 ($CONH$), 165.4 ($CONH$), 144.9 + 144.8 ($C_{ext\text{-}triazole}$), 144.5 ($C_{int\text{-}triazole}$), 135.6 (C_{arom}), 128.6 (CH_{arom}), 124.9 ($CH_{int\text{-}triazole}$), 124.0 ($CH_{ext\text{-}triazole}$), 97.5 (C_1), 69.1 (C_2), 69.0 (C_3), 68.7 (C_5), 68.4 (NHC_qCH_2O), 66.2 (C_6), 65.6 (C_4), 64.5 ($OCH_2C_{triazole}$), 62.1 (OCH_2), 60.4 (C_q), 52.4 ($Ntria\text{-}_{zole}CH_2CONH$), 49.5 ($CH_2N_{triazole}$), 20.8, 20.8, 20.7, 20.7 ($COCH_3$); MS ($^+$TOF-MS, *m*/*z*): $[M + H]^+$ calculated for $C_{615}H_{834}N_{120}O_{318}$, 14995.8; found, 14995.9.

Synthesis of de-*O*-acetylated 27-mer derivative 23: Acetylated compound **22** (30.0 mg, 2.00 μmol) was dissolved in anhydrous MeOH (3 mL) and a solution of sodium methoxide (1 M in MeOH, 5 μL every 20 min until precipitation) was added. An additional 100 μL was then injected and the heterogeneous reaction mixture was stirred at room temperature for 24 h. The solvent was then removed with a Pasteur pipette and a mixture of anhydrous MeOH/DCM (4:1, 5 mL) was added to the residual white foam. A vigorous agitation is maintained for an additional 15 min period. After removal of the solvent with a Pasteur pipette, the residue was dissolved in 3 mL of H_2O, and the pH was adjusted to 7 with addition of ion-exchange resin (Amberlite IR 120 H^+). After filtration, the solvent was removed under vacuum with a rotary evaporator and lyophilized to yield the fully deprotected 27-mer **23** as a white solid (17.0 mg, 1.63 μmol) in 82% yield. ^{1}H NMR (600 MHz, D_2O) δ (ppm) 8.06 (m, 3H, CH_{ar}), 7.97 (s, 27H, $CH_{ext\text{-}triazole}$), 7.96 (s, 9H, $CH_{int\text{-}triazole}$), 5.14 (br s, 18H, $N_{triazole}CH_2CONH$), 4.75 (s, 27H, H_1), 4.59−4.51 (m, 126H, $OCH_2C_{triazole}$ + $N_{triazole}CH_2$), 4.05–4.03 (m, 27H, $OCHHCH_2N$), 3.83–3.80 (m, 72H, $OCHHCH_2N$ + H_2 + $NHC_qCH_2O_{int}$), 3.71–3.57 (m, 162H, $NHC_qCH_2O_{ext}$ + H_6 + H_4 + H_3), 3.01 (m, 27H, H_5); $^{13}C\{^1H\}$ NMR (150 MHz, D_2O) δ (ppm) 168.8 ($CONH_{int}$), 167.5 ($CONH_{ext}$), 144.7 ($C_{ext\text{-}triazole}$), 144.6 ($C_{int\text{-}triazole}$), 135.7 (C_{arom}), 129.7 (CH_{arom}), 127.0 ($CH_{int\text{-}triazole}$), 126.1 ($CH_{ext\text{-}triazole}$), 100.2 (C_1), 73.5 (C_5), 71.1 (C_3), 70.6 (C_2), 68.2 (NHC_qCH_2O), 68.0 (NHC_qCH_2O), 67.0 ($OCH_2CH_2N_{triazole}$), 66.1 (C_4), 64.2 ($OCH_2C_{triazole}$), 61.3 (C_6), 60.9 (C_q), 52.9 ($N_{triazole}CH_2CONH$), 50.7 ($CH_2N_{triazole}$), 35.7 ($OCHNCH_2C_{triazole}$); HRMS ($^+$TOF-HRMS, *m*/*z*): $[M + 7H]^{7+}$ calculated for $C_{399}H_{204}N_{120}O_{210}$, 1494.6002; found, 1494.5951 (Δ = −3.43 ppm).

Supporting Information

Supporting Information File 1

Experimental procedures, characterization data, NMR, IR and mass spectra and NMR diffusion experiments.
[http://www.beilstein-journals.org/bjoc/content/supplementary/1860-5397-10-157-S1.pdf]

Acknowledgements

This work was supported by a discovery grant from the National Science and Engineering Research Council of Canada (NSERC) and by a Canadian Research Chair in Therapeutic Chemistry. YMC is grateful to the FQRNT (Québec) for a scholarship. We are thankful to Dr. A. Furtos (Université de Montréal) for HRMS determination.

References

1. Roy, R. *Curr. Opin. Struct. Biol.* **1996,** *6,* 692–702. doi:10.1016/S0959-440X(96)80037-6
2. Kiessling, L. L.; Gestwicki, J. E.; Strong, L. E. *Angew. Chem., Int. Ed.* **2006,** *45,* 2348–2368. doi:10.1002/anie.200502794
3. Imberty, A.; Chabre, Y. M.; Roy, R. *Chem.–Eur. J.* **2008,** *14,* 7490–7499. doi:10.1002/chem.200800700
4. Renaudet, O.; Roy, R. *Chem. Soc. Rev.* **2013,** *42,* 4515–4517. doi:10.1039/c3cs90029k
5. Kiessling, L. L.; Grim, J. C. *Chem. Soc. Rev.* **2013,** *42,* 4476–4491. doi:10.1039/c3cs60097a
6. Bovin, N. V.; Gabius, H.-J. *Chem. Soc. Rev.* **1995,** *24,* 413–421. doi:10.1039/cs9952400413
7. Roy, R. *Trends Glycosci. Glycotechnol.* **2003,** *15,* 291–310. doi:10.4052/tigg.15.291
8. Roy, R.; Zanini, D.; Meunier, S. J.; Romanowska, A. *J. Chem. Soc., Chem. Commun.* **1993,** 1869–1872. doi:10.1039/C39930001869
9. Chabre, Y. M.; Roy, R. *Adv. Carbohydr. Chem. Biochem.* **2010,** *63,* 165–393. doi:10.1016/S0065-2318(10)63006-5
10. Chabre, Y. M.; Roy, R. *Curr. Top. Med. Chem.* **2008,** *8,* 1237–1285. doi:10.2174/156802608785848987
11. Lindhorst, T. K. *Top. Curr. Chem.* **2002,** *218,* 201–235. doi:10.1007/3-540-45010-6_7
12. Röckendorf, N.; Lindhorst, T. K. *Top. Curr. Chem.* **2001,** *217,* 201–238. doi:10.1007/3-540-45003-3_6
13. Roy, R. *Polym. News* **1996,** *21,* 226–232.
14. Pieters, R. J. *Org. Biomol. Chem.* **2009,** *7,* 2013–2025. doi:10.1039/b901828j
15. Roy, R.; Das, S. K.; Santoyo-González, F.; Hernández-Mateo, F.; Dam, T. K.; Brewer, C. F. *Chem.–Eur. J.* **2000,** *6,* 1757–1762. doi:10.1002/(SICI)1521-3765(20000515)6:10<1757::AID-CHEM1757>3.0.CO;2-5
16. Roy, R.; Trono, M. C.; Giguère, D. *ACS Symp. Ser.* **2005,** *896,* 137–150. doi:10.1021/bk-2005-0896.ch008
17. Chabre, Y. M.; Giguère, D.; Blanchard, B.; Rodrigue, J.; Rocheleau, S.; Neault, M.; Rauthu, S.; Papadopoulos, A.; Arnold, A. A.; Imberty, A.; Roy, R. *Chem.–Eur. J.* **2011,** *17,* 6545–6562. doi:10.1002/chem.201003402
18. Sirois, S.; Giguère, D.; Roy, R. *Med. Chem.* **2006,** *2,* 481–489. doi:10.2174/157340606778250252
19. Gerland, B.; Goudot, A.; Ligeour, C.; Pourceau, G.; Meyer, A.; Vidal, S.; Gehin, T.; Vidal, O.; Souteyrand, E.; Vasseur, J.-J.; Chevolot, Y.; Morvan, F. *Bioconjugate Chem.* **2014,** *25,* 379–392. doi:10.1021/bc4005365
20. van Hattum, H.; Branderhorst, H. M.; Moret, E. E.; Nilsson, U. J.; Leffler, H.; Pieters, R. J. *J. Med. Chem.* **2013,** *56,* 1350–1354. doi:10.1021/jm301677r
21. Öberg, C. T.; Noresson, A.-L.; Leffler, H.; Nilsson, U. J. *Chem.–Eur. J.* **2011,** *17,* 8139–8144. doi:10.1002/chem.201003247

22. Giguère, D.; André, S.; Bonin, M.-A.; Bellefleur, M.-A.; Provencal, A.; Cloutier, P.; Pucci, B.; Roy, R.; Gabius, H.-J. *Bioorg. Med. Chem.* **2011,** *19,* 3280–3287. doi:10.1016/j.bmc.2011.03.022
23. Sharon, N. *FEBS Lett.* **1987,** *217,* 145–157. doi:10.1016/0014-5793(87)80654-3
24. Arya, P.; Kutterer, K. M. K.; Qin, H.; Roby, J.; Barnes, M. L.; Kim, J. M.; Roy, R. *Bioorg. Med. Chem. Lett.* **1998,** *8,* 1127–1132. doi:10.1016/S0960-894X(98)00182-6
25. Schierholt, A.; Hartmann, M.; Lindhorst, T. K. *Carbohydr. Res.* **2011,** *346,* 1519–1526. doi:10.1016/j.carres.2011.04.023
26. Asensio, J. L.; Ardá, A.; Cañada, F. J.; Jiménez-Barbero, J. *Acc. Chem. Res.* **2013,** *46,* 946–954. doi:10.1021/ar300024d
27. Chen, W.; Enck, S.; Price, J. L.; Powers, D. L.; Powers, E. T.; Wong, C.-H.; Dyson, H. J.; Kelly, J. W. *J. Am. Chem. Soc.* **2013,** *135,* 9877–9884. doi:10.1021/ja4040472
28. Lemieux, R. U. *Acc. Chem. Res.* **1996,** *29,* 373–380. doi:10.1021/ar9600087
29. Reynolds, M.; Pérez, S. *C. R. Chim.* **2011,** *14,* 74–95. doi:10.1016/j.crci.2010.05.020
30. Dam, T. K.; Roy, R.; Das, S. K.; Oscarson, S.; Brewer, C. F. *J. Biol. Chem.* **2000,** *275,* 14223–14230. doi:10.1074/jbc.275.19.14223
31. Dam, T. K.; Roy, R.; Pagé, D.; Brewer, C. F. *Biochemistry* **2002,** *41,* 1351–1358. doi:10.1021/bi015830j
32. Munoz, E. M.; Correa, J.; Fernandez-Megia, E.; Riguera, R. *J. Am. Chem. Soc.* **2009,** *131,* 17765–17767. doi:10.1021/ja9074826
33. Giguère, D.; Patnam, R.; Bellefleur, M.-A.; St-Pierre, C.; Sato, S.; Roy, R. *Chem. Commun.* **2006,** 2379–2381. doi:10.1039/b517529a
34. Hayes, W.; Osborn, H. M. I.; Osborne, S. D.; Rastall, R. A.; Romagnoli, B. *Tetrahedron* **2003,** *59,* 7983–7996. doi:10.1016/j.tet.2003.08.011
35. Touaibia, M.; Wellens, A.; Shiao, T. C.; Wang, Q.; Sirois, S.; Bouckaert, J.; Roy, R. *ChemMedChem* **2007,** *2,* 1190–1201. doi:10.1002/cmdc.200700063
36. Chabre, Y. M.; Contino-Pépin, C.; Placide, V.; Shiao, T. C.; Roy, R. *J. Org. Chem.* **2008,** *73,* 5602–5605. doi:10.1021/jo8008935
37. Cohen, Y.; Avram, L.; Frish, L. *Angew. Chem., Int. Ed.* **2005,** *44,* 520–554. doi:10.1002/anie.200300637
38. Berger, S.; Braun, S. *200 and More NMR Experiments−A Practical Course;* Wiley-VCH: Weinheim, 2004; pp 145–148.
39. Chabre, Y. M.; Roy, R. *Chem. Soc. Rev.* **2013,** *42,* 4657–4708. doi:10.1039/c3cs35483k
40. Cantekin, S.; de Greef, T. F. A.; Palmans, A. R. A. *Chem. Soc. Rev.* **2012,** *41,* 6125–6137. doi:10.1039/c2cs35156k
41. Aragão-Leoneti, V.; Campo, V. L.; Gomes, A. S.; Field, R. A.; Carvalho, I. *Tetrahedron* **2010,** *66,* 9475–9492. doi:10.1016/j.tet.2010.10.001
42. Finn, M. G.; Fokin, V. V., Eds. Click chemistry: function follows form. *Chem. Soc. Rev.* **2010,** *39,* 1221–1408. doi:10.1039/C003740K
43. Corbell, J. B.; Lundquist, J. J.; Toone, E. J. *Tetrahedron: Asymmetry* **2000,** *11,* 95–111. doi:10.1016/S0957-4166(99)00589-3
44. Talga, M. L.; Fan, N.; Fueri, A. L.; Brown, R. K.; Chabre, Y. M.; Bandyopadhyay, P.; Roy, R.; Dam, T. K. *Biochemistry* **2014,** in press. doi:10.1021/6i5001307
45. Wu, D. H.; Chen, A. D.; Johnson, C. S., Jr. *J. Magn. Reson., Ser. A* **1995,** *115,* 260–264. doi:10.1006/jmra.1995.1176
46. Holz, M.; Weingärtner, H. *J. Magn. Reson.* **1991,** *92,* 115–125. doi:10.1016/0022-2364(91)90252-O
47. van Beek, J. D. *J. Magn. Reson.* **2007,** *187,* 19–26. doi:10.1016/j.jmr.2007.03.017

License and Terms

Beilstein Journal of Organic Chemistry

A promising cellulose-based polyzwitterion with pH-sensitive charges

Thomas Elschner and Thomas Heinze*

Full Research Paper

Open Access

Address:
Center of Excellence for Polysaccharide Research, Institute for Organic Chemistry and Macromolecular Chemistry, Friedrich Schiller University of Jena, Humboldtstraße 10, D-07743 Jena, Germany

Email:
Thomas Heinze* - thomas.heinze@uni-jena.de

* Corresponding author

Keywords:
carbonate; cellulose; complexation; multivalent glycosystems; NMR; polyzwitterion

Beilstein J. Org. Chem. **2014,** *10,* 1549–1556.
doi:10.3762/bjoc.10.159

Received: 06 March 2014
Accepted: 12 June 2014
Published: 08 July 2014

This article is part of the Thematic Series "Multivalent glycosystems for nanoscience".

Guest Editor: J.-L. Reymond

Abstract

A novel polyzwitterion possessing weak ionic groups could be efficiently synthesized from cellulose phenyl carbonate. Polyanion, polycation, and polyzwitterion are accessible by orthogonal removal of protecting groups. The molecular structure was proofed by FTIR- and NMR spectroscopy. Characteristic properties of the cellulose derivatives, e.g., acid dissociation constants, isoelectric point and complexation, were investigated by potentiometric titration (pH), nephelometry, rheology and dynamic light-scattering. The formation of pH-responsive interpolyelectrolyte complexes applying polydiallyldimethylammonium chloride was preliminary studied.

Introduction

Ionic polymers are important naturally occurring macromolecules and various synthetic polyelectrolytes play an important role in commercial applications [1]. Naturally occurring biopolymers are for example proteins, nucleotides, and polysaccharides like alginates. Synthetic ionic polymers are widely used in the field of water treatment [2], protein separation, desalination, binding of metal ions, in the oil industry [3] and nanotechnology [4]. In general, these polymers may be divided into water-soluble polyelectrolytes, containing anionic or cationic groups, and polyzwitterions that include both charges. While the addition of low molecular weight electrolyte cause the polyelectrolyte effect, i.e., the shrinking and precipitation of the polyelectrolyte, polyzwitterions show chain expansion and increased solubility (antipolyelectrolyte effect). Moreover, the classification may result from weak and strong ionic groups, and the location of the charges. Polyampholytes possess the charged groups on different monomer units, while polybetaines refer to polymers with opposite charges on one side chain at the same monomer unit [1].

The first statistical, synthetic polyampholytes were obtained in the 1950s by radical polymerization of acrylic- or methacrylic acid and their derivatives [5-7]. 20 years later the first block polyampholytes were synthesized via anionic polymerization of

2-vinylpyridine with trimethylsilyl methacrylate [8,9]. Polybetaines, for example sulfobetaines, could be prepared from the reaction of a tertiary amine (monomer or polymer) and a sultone [10]. Due to their biocompatibility and hemocompatibility polybetaines are attributed to be materials with biomimetic properties [11]. However, polybetaines are mostly not soluble in pure water. Their solubility is often limited to concentrated saline solutions or organic solvents with high hydrogen bond-donating ability (e.g., trifluoroethanol) [12]. Therefore, the processing to yield films or nanoparticles requires ecologically harmful solvents. Thus, a broad variety of synthetic polyampholytes and polybetaines were synthesized, however, they are not soluble in pure water.

The chemical modification of polysaccharides allows the access to novel polyzwitterions where the opposite charges may be located in the same repeating unit, but not in the same side chain. Moreover, regioselective functionalization is possible [13]. In contrast to synthetic polybetaines an increased solubility could be expected for polysaccharide derivatives and, furthermore, biopolymers possess an inherent biocompatibility and biodegradability. While polyzwitterions based on N-functionalized chitosan [14,15] or 6-desoxy-6-aminocelluloses [16] are composed like synthetic polybetaines, a few cellulose-based zwitterions are described where the isoelectric point and the properties in solution could be tuned by varying the substitution pattern [17-20]. However, the polymers contain mostly a permanent cationic- or anionic charge, which may lead to limitations in solubility. Thus, there is an increasing interest in novel biobased, zwitterionic polysaccharide derivatives in research and industry.

In the present work the structure design of novel polyzwitterions based on cellulose carbamate with carboxylic- and primary amino groups is discussed. Starting from cellulose carbonate, the fully protected zwitterion is efficiently synthesized that could be converted into the polyanion, polycation, and polyzwitterion via the orthogonal removal of the protecting groups. The molecular structure of the products is investigated by means of FTIR- and NMR spectroscopy in detail. Moreover, important properties including the acid dissociation constants, the isoelectric point and the aggregation behavior are determined by potentiometric titration (pH), nephelometry, rheology and dynamic light-scattering. Moreover, preliminary studies about stimuli-responsive interpolyelectrolyte complexes are presented.

Results and Discussion

Synthesis

The synthesis of a novel polyzwitterion based on cellulose was performed by activation of the polymer backbone by formation of a carbonate moiety and subsequent introduction of amino- and carboxylic groups using the protected diamine and amino acid. As schematically shown in Figure 1, cellulose phenyl carbonate (**1**, degree of substitution, DS 1.92), obtained by homogeneous conversion of cellulose with phenyl chloroformate in *N*,*N*-dimethylacetamide (DMAc)/LiCl and pyridine [21], was allowed to react with an equimolar mixture of β-alanine ethyl ester (**2**) and *N*-*tert*-butoxycarbonyl-1,2-ethanediamine (**3**). The β-alanine ethyl ester was obtained from the respective commercially available hydrochloride under triethylamine deficiency conditions in order to avoid cross-linking of the polymer chains via carbonate moieties resulting from the strong basicity of the trialkylamine [22]. The aminolysis yields the (3-ethoxy-3-oxopropyl)(*N*-Boc-2-aminoethyl)cellulose carbamate **4** with a $DS_{\beta\text{-alanine ester}}$ of 0.88 and a $DS_{\text{Boc-EDA}}$ of 0.95 that indicates a similar reactivity of the amines applied and the conversion of 95% of the carbonate moieties into the carbamate. Moreover, a random distribution of the substituents within the repeating unit and the polymer backbone can be assumed.

From cellulose carbamate **4**, the polyanion **5**, the polycation **6**, and the polyzwitterion **7a**,**b** may be obtained because of the orthogonal protecting groups. The homogeneous alkaline cleavage of the ethyl ester into (2-carboxyethyl)(*N*-Boc-2-aminoethyl)cellulose carbamate **5** was carried in methanolic/aqueous sodium hydroxide solution to mediate the solubility of educt and product. The acidic cleavage of the Boc group applying gaseous hydrogen chloride leads to the polycation **6**.

Finally, the polyzwitterion (2-carboxyethyl)(2-aminoethyl)-cellulose carbamate **7a** could be obtained by acidic treatment of polyanion **5**. However, the solubility in aprotic organic solvents, like dioxane and CH_2Cl_2, is decreased and the deprotection has to be carried out in trifluoroacetic acid (TFA), followed by a subsequent anion exchange by dialysis of the polymer solution against aqueous sodium chloride and water. **7b** was prepared from the polycation **6** by alkaline treatment, but the acidification of the reaction mixture is required for a convenient isolation of the product **7b**.

Structure characterization

The molecular structure of the products obtained could be revealed by means of FTIR- and NMR spectroscopy. The C=O stretching vibration of the ester- and the carbamate moiety overlap in the IR spectrum to a broad signal at 1716 cm^{-1}. The carboxylate in polyanion **5** can be detected separately from the carbamate linkage (1705 cm^{-1}) at 1581 cm^{-1}. While the C=O peaks in the IR spectrum of the polyzwitterion, arising from the carbamate and the carboxylic group, cannot be resolved, NMR spectroscopy may be applied for detailed structure characteriza-

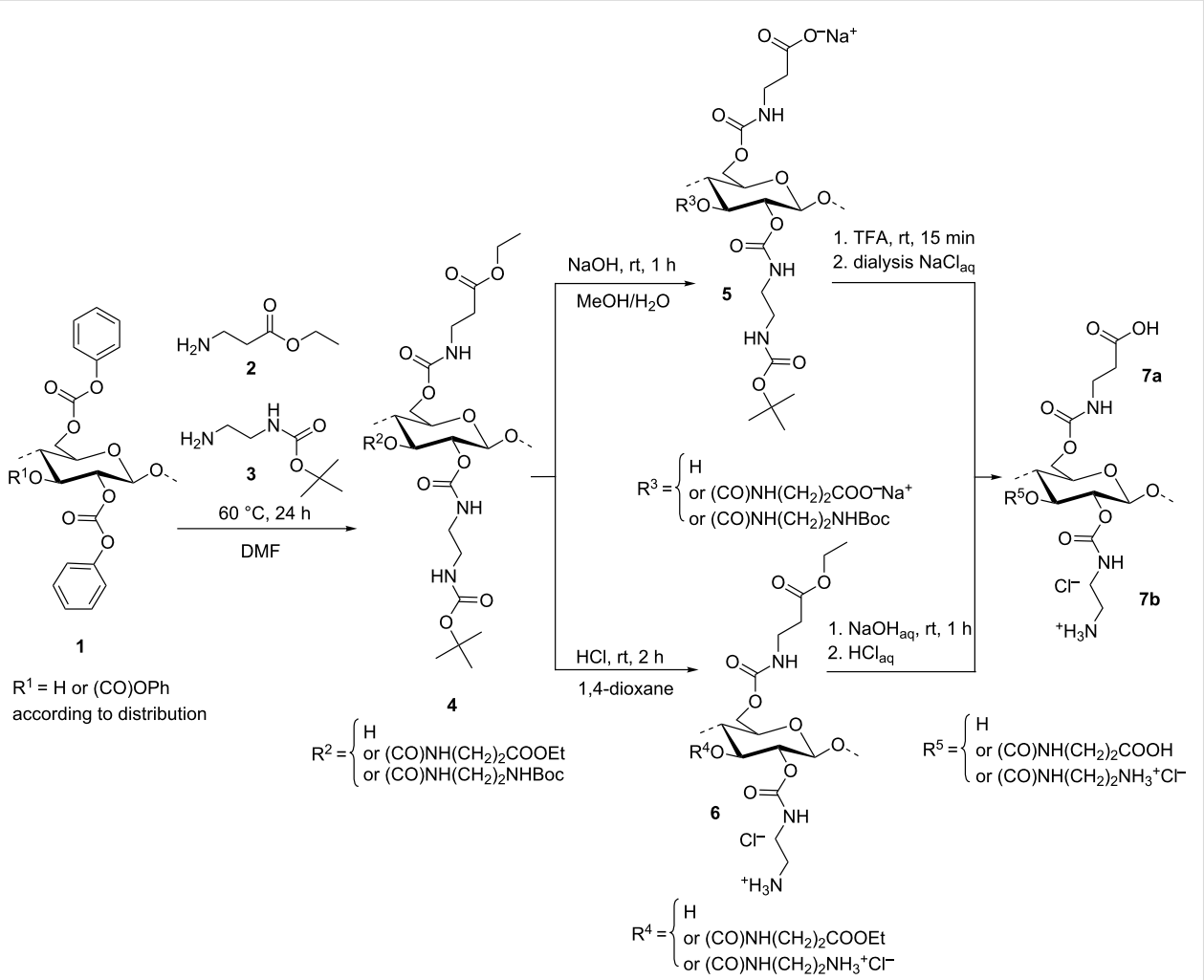

Figure 1: Reaction scheme of the synthesis of anionic, cationic, and ampholytic cellulose carbamates (substituents randomly distributed).

tion. Figure 2 shows the ^{13}C NMR spectra of the (3-ethoxy-3-oxopropyl)(*N*-Boc-2-aminoethyl)- (**4**), the anionic- (**5**), the cationic- (**6**), and the zwitterionic (**7a**) cellulose carbamate. The C=O resonances at 172 and 157 ppm indicate the ester and the carbamate moieties, respectively. Signals arising from the cellulose backbone are visible at 103–101 (C-1), 83–74 (C-2-5) and 63 ppm (C-6). Moreover, the resonances of aliphatic carbon nuclei of the substituents occur at 78.8 (CMe_3), 60.4 (OCH_2), 40.5–34.1 (CH_2), 27.5 ($C(CH_3)_3$), and 13.2 ppm (CH_3). The cleavage of the ethyl ester to the corresponding carboxylate **5** is indicated by a shift of the C=O resonance to lower field. Moreover, the signals belonging to the ethyl group disappear and the peak of the methylene moiety next to the carboxylate is shifted to low field of about 3 ppm. The removal of the Boc group leads to the cation **6** clearly visible by the absence of the resonances at 78 and 28 ppm. After the cleavage of both, the ethyl ester and the Boc moiety, the polyzwitterion **7a** is obtained indicated by the missing resonances. Furthermore, the desired functionalities are still linked to the polymer backbone, proofed by C=O resonances, signals from position 1 to 6 of the repeating unit, and the peaks of four CH_2 groups.

Properties

Acid dissociation constants and isoelectric point

The acid dissociation constants could be determined by potentiometric titration (pH). Moreover, the question arises how the pK_a value is influenced by further substituents. Therefore, the acidity of the ammonium groups of ω-aminoethylcellulose carbamate [23], (3-ethoxy-3-oxopropyl)(2-aminoethyl)cellulose carbamate **6** and the polyzwitterion **7a** were compared. Polycation **6** was titrated forth and back in range from pH 4.3 to 10 (Figure 3). The rising point of inflection, representing the pK_a value of the amino group (9.0), was determined by the first derivative of the curve (dpH/dV) that yields the minimum. To obtain the pK_a value of the amino group in the polyzwitterionic molecule the titration curve of **7a** could be considered. In

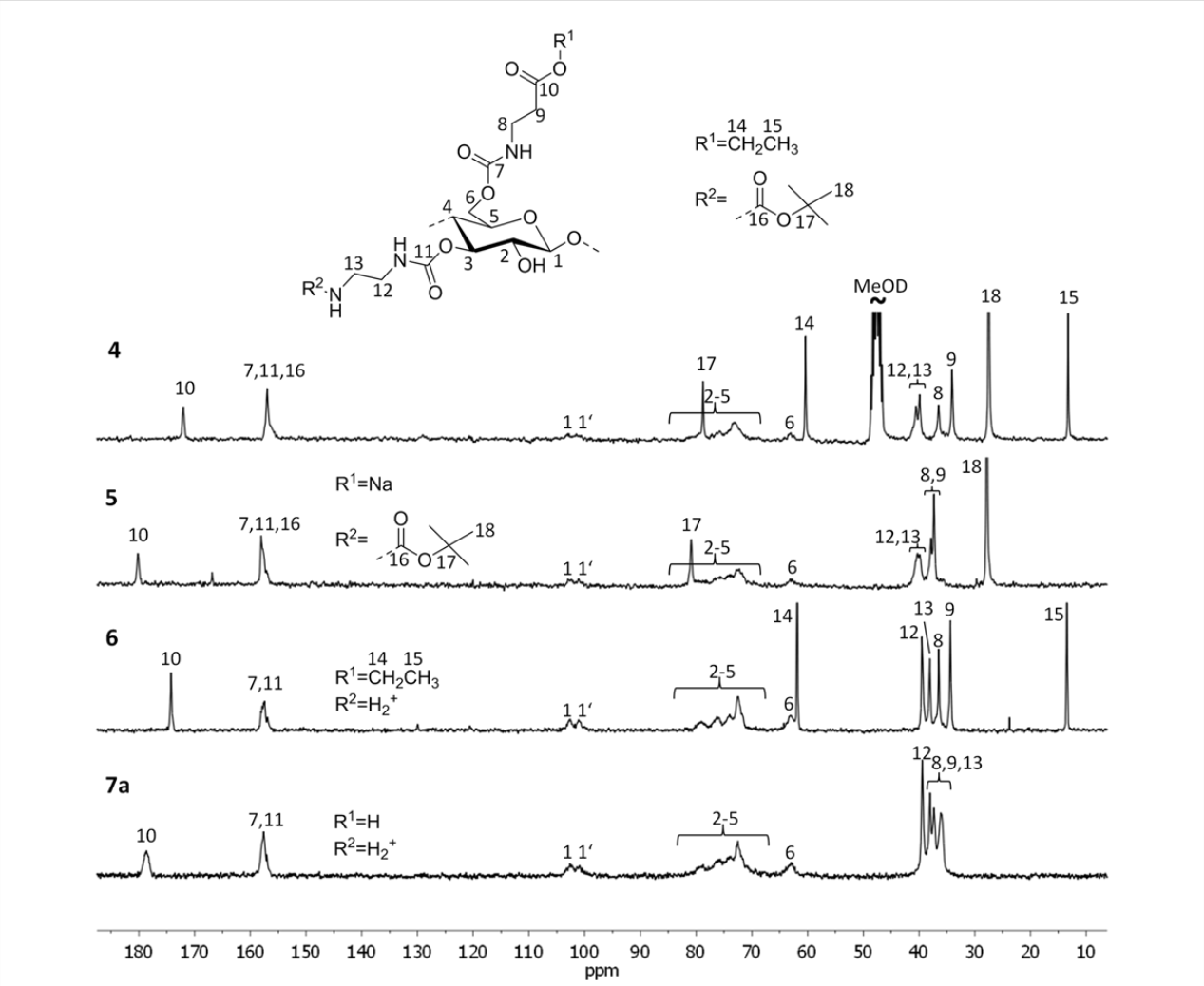

Figure 2: ^{13}C NMR spectra of (3-ethoxy-3-oxopropyl)(*N*-Boc-2-aminoethyl)- (**4**), (2-carboxyethyl)(*N*-Boc-2-aminoethyl)- (**5**), (3-ethoxy-3-oxopropyl)(2-aminoethyl)- (**6**) and (2-carboxyethyl)(2-aminoethyl)cellulose carbamate (**7a**) recorded in MeOD (**4**) or D_2O (**5**–**7a**).

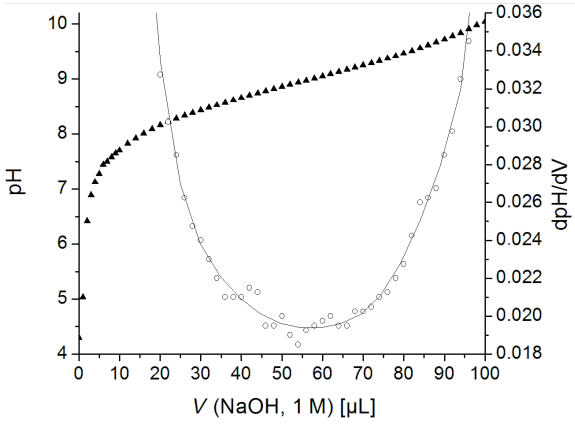

Figure 3: Acid–base titration of (3-ethoxy-3-oxopropyl)(2-aminoethyl)cellulose carbamate (**6**, 0.4%) in 0.2 M aqueous sodium chloride solution: pH (*V* NaOH) ▲ and its first derivative dpH/dV ○.

Figure 4 the minimum of the first derivative at 340 µL indicates a pK_a value of 9.7. Thus, the pK_a increases from 8.6 [23] to 9.0 if the ester moiety is present within the polymer chain and, moreover, the value increases to 9.7 for cellulose carbamate containing carboxylate. The higher affinity of the protons to the polymer chain may be explained by hydrogen bonding to the carboxylic functionalities. The pK_a value of the carboxylic group is 4.0 and could be obtained from the minimum at 230 µL (Figure 4).

To determine the isoelectric point (IP) of the polyzwitterion, the falling point of inflection between the pK_a values has to be considered. In Figure 4 the maximum of dpH/dV at 285 µL indicates an IP of 7.3. Naturally, the summation of the charges of the functional groups has to yield a neutral molecule at the IP and a ratio of carboxylic groups to amino groups of 0.997 was predicted from IP and pK_a values. The consumption of sodium

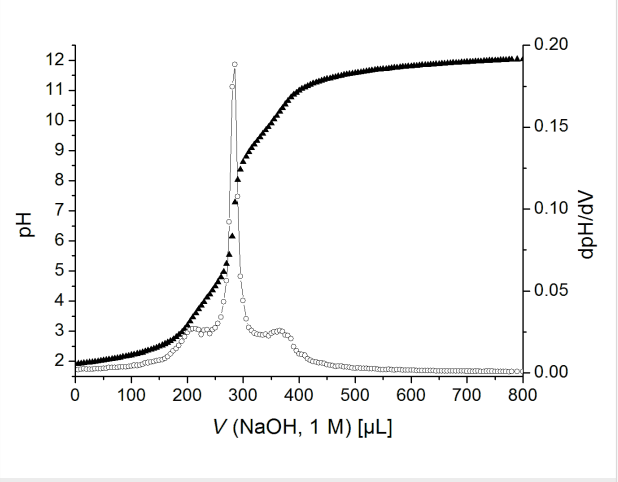

Figure 4: Acid–base titration of (2-carboxyethyl)(2-aminoethyl)cellulose carbamate (**7a**, 0.4%) in 0.2 M aqueous sodium chloride solution: pH (*V* NaOH) ▲ and its first derivative dpH/dV ○.

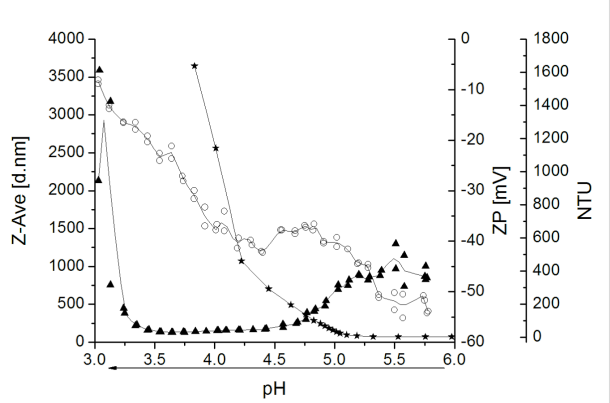

Figure 5: Acid–base titration of (2-carboxyethyl)(*N*-Boc-2-aminoethyl)-cellulose carbamate (**5**, 0.1%) from pH 6 to pH 3 (arrow): turbidity (nephelometric turbidity units, NTU ★), Z-average (d. nm ▲), zeta potential (ZP, mV ○), and interpolation (line) determined by nephelometry and dynamic light scattering (DLS).

hydroxide solution leads to an equal partial $DS_{\beta\text{-alanine}}$ and DS_{EDA} of 0.53. The decrease of the DS values compared to the protected polyzwitterion **4** could be explained by a reduced accessibility of the functional groups in aqueous solution or the cleavage of carbamate moieties from the polymer backbone during acidic and basic treatment. However, the ratio between amino and carboxylic groups is balanced. In addition, the IP was proofed by rheology. The IP is indicated by a minimum of the relative viscosity of a polyzwitterion solution at pH value of 7.7 (Supporting Information File 1).

Precipitation and self-complexation

The pH value influences the solution state of polyanions, polycations, or polyzwitterions. While the polycation **6** is soluble in water at the whole pH range from 3 to 11, aqueous solutions of polyanion **5** show precipitation below pH values of 5 due to the protonation of the carboxylate and the hydrophobic Boc group. Figure 5 reveals an increase of turbidity with decreasing pH value. Moreover, dynamic light scattering (DLS) display details about the aggregates formed. The measurements of dissolved polymer and aggregates with the DLS equipment yield no useful results, but from pH 4.5 to 3.5 nanoparticles with a Z-average diameter of about 200 nm could be detected. During the titration, the zeta potential of the particles increases from −40 to −10 mV according to the protonation of the carboxylate and thus, the compensation of the negative charge of the boundary surface.

Polyzwitterion **7a** shows self-complexation at neutral pH value if no salt is added. Figure 6 illustrates the titration from acidic and alkaline solution and the gap of solubility. In the border from solubility to insolubility at pH value of 5 and 8.5, the turbidity and the Z-average diameter increase significantly. In the pH scale from 4.5 to 6, the zeta potential decreases from +25 to +5 mV due to the deprotonation of the carboxylic moiety. In alkaline solution the zeta potential increases with decreasing pH and the amino groups become protonated. The Z-average diameter seems to decrease with increasing protonation. However, aggregates of widely distributed sizes (high polydispersity) become regular particles due to the electrostatic stabilization indicated by an increase of the absolute value of the zeta potential at pH value of 9. At lower pH values, large aggregates are formed induced by self-complexation.

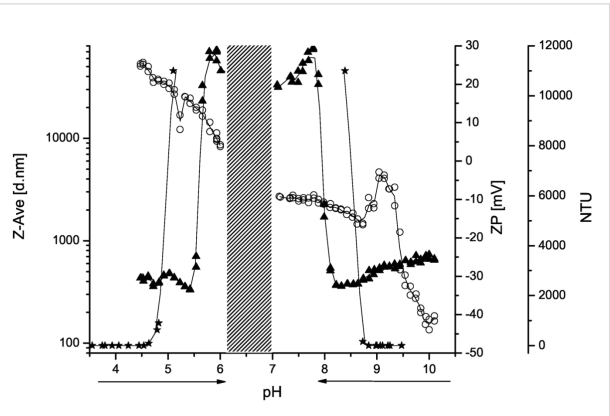

Figure 6: Acid–base titration of (2-carboxyethyl)(2-aminoethyl)cellulose carbamate (**7a**, 0.4% in water) from pH 3.5 to pH 6 and from pH 10 to pH 7 (arrows): turbidity (nephelometric turbidity units, NTU ★), Z-average (d. nm ▲), zeta potential (ZP, mV ○), and interpolation (line) determined by nephelometry and dynamic light scattering (DLS).

Polyelectrolyte complex formation with poly-DADMAC

A permanently charged polycation (polydiallyldimethylammonium chloride, polyDADMAC) was applied to study the forma-

tion of interpolyelectrolyte complexes. In the first experiment a solution of the zwitterionic cellulose derivative **7a** was adjusted to pH 11.5 in order to yield the maximum of negative charges. The addition of polycation causes the formation of particles resulting in an increased turbidity, finally forming macroscopic aggregates (Figure 7). The degree of titration (τ) is defined by the ratio of the amount of polyDADMAC and the amount of carboxylate in the cellulose derivative. Moreover, a solution of **7a** and polyDADMAC (τ = 1) was titrated with aqueous sodium hydroxide solution (Figure 8). In acidic medium, cationic charges are predominant and repulsive interaction of the polymer chains lead to a clear solution. At pH value from 4 to 5 an increase in turbidity indicates the attractive forces between the molecules due to the deprotonation of the carboxylic groups. Thus, the formation of interpolyelectrolyte complexes is switchable in a physiological relevant range of the pH value.

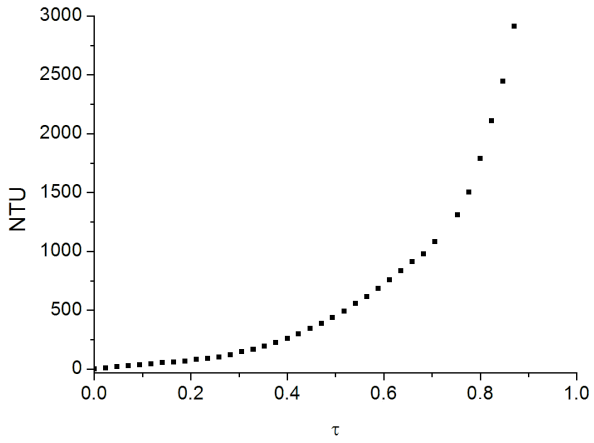

Figure 7: Titration of (2-carboxyethyl)(2-aminoethyl)cellulose carbamate (**7a**, 0.1% in water) at pH 11.5 with polydiallyldimethylammonium chloride (polyDADMAC); turbidity (nephelometric turbidity units, NTU) in dependence on degree of titration (τ).

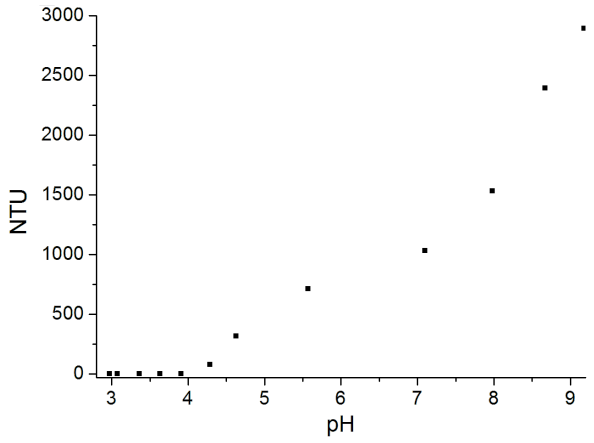

Figure 8: Titration of (2-carboxyethyl)(2-aminoethyl)cellulose carbamate (**7a**, 0.1% in water) and polyDADMAC (equimolar to carboxylic groups) with sodium hydroxide solution; turbidity (nephelometric turbidity units, NTU) in dependence on pH value.

Conclusion

In this work a well soluble cellulose-based polyzwitterion with weak ionic groups could be efficiently synthesized starting from cellulose phenyl carbonate. It became possible to access the polyanion, the polycation, and the polyzwitterion by the orthogonal removal of protecting groups. While IR spectroscopy could not proof the presence of all functional groups, the molecular structure was clearly described by NMR spectroscopy. Potentiometric titration (pH), nephelometry, rheology and dynamic light-scattering revealed physicochemical characteristics of the cellulose derivatives. Acid dissociation constants, isoelectric point and complexation behavior are in good agreement and thus, a well characterized zwitterionic cellulose carbamate with excellent properties was discovered. Preliminary studies show the formation of pH-responsive interpolyelectrolyte complexes applying polydiallyldimethylammonium chloride. The particles are switchable in a physiological relevant range of pH values and are promising nanocarriers in the field of drug delivery that will be a subject of further studies.

Experimental

Materials

Microcrystalline cellulose (Avicel PH-101) with a DP_w of 330 was purchased from Sigma-Aldrich and dried at 60 °C in vaccum. Polydiallyldimethylammonium chloride (Sigma-Aldrich) with a very low molecular weight of M_w < 100000 g/mol was used as received. Other chemicals and solvents were purchased from Sigma-Aldrich, Acros Organics or TCI Europe and were used without further treatment.

Cellulose phenyl carbonate was prepared by esterification of cellulose, dissolved in *N*,*N*-dimethylacetamide (DMAc)/LiCl, applying pyridine and phenyl chloroformate [21]. **1**, DS 1.92 (determined by means of ^{1}H NMR spectroscopy after peracetylation), FTIR (KBr): 1770 cm^{-1} ($\nu_{C=O}$); ^{13}C NMR (63 MHz, DMSO-d_6) δ 153.4, 153.1, 151.5 (C=O), 151.1 (C-Ph), 130.0 (CH-Ph), 126.6 (CH-Ph), 121.5 (CH-Ph), 103.0 (C-1) 99.2 (C-1'), 82-67 (C-2, C-3, C-4, C-5, C-6) ppm.

N-*tert*-Butoxycarbonyl-1,2-ethanediamine (**3**) was obtained according to the procedure described by Krapcho and Kuell [24] and purified by distillation in vaccum (7 mbar, 109 °C). Yield: 67% ^{1}H NMR (250 MHz, $CDCl_3$) δ 5.17 (bs, NH), 3.07 (m, CH_2), 2.71 (m, CH_2), 1.35 (s, CH_3), 1.12 (s, NH_2) ppm; ^{13}C NMR (63 MHz, $CDCl_3$) δ 156.2 (C=O), 79.0 (CMe_3), 43.4 (CH_2), 41.8 (CH_2), 28.3 (CH_3) ppm.

Measurements

NMR spectra were acquired on a Bruker Avance 400 MHz (Bruker Biospin, Rheinstetten, Germany) with 16 scans and 25 mg sample per mL solvent for ^{1}H NMR spectroscopy (room temperature) and up to 200,000 scans for ^{13}C NMR spectroscopy (70 °C) applying up to 100 mg sample per mL solvent. FTIR spectra were recorded on a Nicolet AVATAR 370 DTGS spectrometer (Thermo Scientific, Schwerte, Germany) with the KBr technique. Elemental analyses were performed by a CHNS 932 Analyzer (Leco, Mönchengladbach, Germany). Nephelometric measurements were carried out with a Turbiquant® 3000 IR from Merck (Darmstadt, Germany). The self complexation at different pH values was investigated by potentiometric titration with 0.25 M hydrochloric acid and 0.25 M sodium hydroxide solution using the Zetasizer Nano ZS from Malvern Instruments (Malvern, UK) equipped with a MPT-2 autotitrator. Z-Average diameter and zeta potential were determined by dynamic light scattering (DLS) and obtained by the cumulants method assuming spherical shape. Each measurement was repeated at least two times. Manual potentiometric titrations were performed with a SevenMulti™ pH meter (Mettler Toledo, Gießen, Germany). The viscosity of the polymer solutions was measured with a Haake Mars II cone-plate rheometer (Thermo Scientific, Schwerte, Germany) in controlled rate mode at 20 °C. Shear rates were varied from 0.1 to 1000 s^{-1} in a cycle of increasing and decreasing shear rate over 5 min. The linear range was extrapolated to zero shear viscosity.

Syntheses

Synthesis of (3-ethoxy-3-oxopropyl)(*N*-Boc-2-aminoethyl)cellulose carbamate **4**

In a centrifuge tube β-alanine ethyl ester hydrochloride (11.27 g, 73 mmol) dissolved in 70 mL *N*,*N*-dimethylformamide (DMF) and a solution of triethylamine (5.93 g, 59 mmol) in 20 mL DMF was added. The tube was shaken immediately and allowed to stand for 1 h at room temperature. The precipitate was removed by centrifugation and the clear solution of β-alanine ethyl ester (**2**) was mixed with *N*-*tert*-butoxycarbonyl-1,2-ethanediamine (**3**, 11.73 g, 73 mmol), dissolved in 60 mL DMF.

The solution of the amines **2** and **3** was added rapidly under vigorous stirring to cellulose phenyl carbonate **1** (10 g, DS 1.92, 49 mmol carbonate) dissolved in 150 mL DMF. The reaction mixture was allowed to react for 24 h at 60 °C. After precipitation into 2.5 L of water, the product was isolated by filtration. The product was washed three times with 1 L of water and dried in vacuum at 40 °C. Yield: 90%, $DS_{\beta\text{-alanine ester}}$ 0.88, $DS_{Boc\text{-}EDA}$ 0.95 (determined by elemental analysis from nitrogen content assuming a total DS of 1.83 according to a conversion of carbonate of 95% [21]), FTIR (KBr): 1716 cm^{-1} ($\nu_{C=O}$, carbamate and ester); ^{13}C NMR (100 MHz, MeOD) δ 172.0 (C=O, ester), 157.0 (C=O, carbamate), 103.0 (C-1), 101.4 (C-1'), 83–74 (C-2, C-3, C-4, C-5), 78.8 (CMe_3), 63.0 (C-6), 60.4 (OCH_2), 40.5 (CH_2), 39.9 (CH_2), 36.5 (CH_2), 34.1 (CH_2), 27.5 ($C(CH_3)_3$), 13.2 (CH_3) ppm.

Synthesis of (2-carboxyethyl)(*N*-Boc-2-aminoethyl)cellulose carbamate sodium salt (**5**)

A solution of **4** (1 g) in 15 mL methanol was mixed with 2 g sodium hydroxide dissolved in 5 mL water under nitrogen atmosphere and allowed to react for 1 h at room temperature under stirring. The product was isolated by precipitation into 40 mL 2-propanol and subsequent filtration. The precipitate was washed four times with 2-propanol, pre-dried in vacuum at room temperature, dissolved in 10 mL water, dialyzed against deionized water, and finally lyophilized. Yield: 873 mg (88%), FTIR (KBr): 1705 cm^{-1} ($\nu_{C=O}$, carbamate), 1581 cm^{-1} ($\nu_{C=O}$, carboxylate); ^{13}C NMR (100 MHz, D_2O) δ 180.2 (C=O, carboxylate), 158.0 (C=O, carbamate), 103.0 (C-1), 101.1 (C-1'), 85–66 (C-2, C-3, C-4, C-5), 80.9 (CMe_3), 63.0 (C-6), 40.3 (CH_2), 39.8 (CH_2), 37.9 (CH_2), 37.3 (CH_2), 27.8 ($C(CH_3)_3$) ppm.

Synthesis of (3-ethoxy-3-oxopropyl)(2-aminoethyl)cellulose carbamate hydrochloride **6**

4 (2 g) was dissolved in 60 mL 1,4-dioxane at 60 °C. After cooling to room temperature, a flow of hydrogen chloride was bubbled through the solution for 2 h under stirring. The precipitate was isolated by centrifugation, washed one times with 50 mL dioxane, three times with 50 mL 2-propanol and pre-dried in vacuum at room temperature. The half amount of the product was dissolved in 10 mL water, dialyzed against deionized water and finally lyophilized. Yield: 82%, $DS_{\beta\text{-alanine ester}}$ 0.90, DS_{EDA} 0.80 (determined by elemental analysis from nitrogen- and chlorine content), FTIR (KBr): 1716 cm^{-1} ($\nu_{C=O}$, carbamate and ester); ^{13}C NMR (100 MHz, D_2O) δ 174.2 (C=O, ester), 157.5 (C=O, carbamate), 102.7 (C-1), 101.0 (C-1'), 82–66 (C-2, C-3, C-4, C-5), 63.0 (C-6), 61.8 (OCH_2), 39.5 (CH_2), 38.1 (CH_2), 36.5 (CH_2), 34.4 (CH_2), 13.5 (CH_3) ppm.

Synthesis of (2-carboxyethyl)(2-aminoethyl)cellulose carbamate hydrochloride

7a: **5** (0.5 g) was dissolved in 5 mL TFA under stirring for 15 min. After precipitation into 40 mL cold 2-propanol, the product was immediately isolated by centrifugation, washed four times with 25 mL 2-propanol and pre-dried in vacuum at room temperature. The product dissolved in 5 mL water was dialyzed against saturated sodium chloride solution and deionized water, and finally lyophilized. Yield: 340 mg (82 %), $DS_{\beta\text{-alanine}}$ 0.53, DS_{EDA} 0.53, FTIR (KBr): 1716 cm^{-1} ($\nu_{C=O}$, carbamate and

carboxylic acid); ^{13}C NMR (100 MHz, D_2O) δ 178.7 (C=O, carboxylic acid), 157.6 (C=O, carbamate), 102.6 (C-1), 100.9 (C-1'), 83–67 (C-2, C-3, C-4, C-5), 63.0 (C-6), 39.4 (CH_2), 38.0 (CH_2), 37.3 (CH_2), 36.1 (CH_2) ppm.

7b: 10 mL sodium hydroxide solution (2 g NaOH/10 mL water) was added to the half amount of the product **6** (see procedure above) dissolved in 10 mL water under nitrogen atmosphere. The reaction solution was allowed to react for 1 h at room temperature under stirring. Subsequently, an equimolar amount of hydrochloric acid (50 mmol, 4.2 mL 37%) diluted with 5 mL water was added under cooling with ice and the mixture was precipitated into 200 mL 2-propanol. The product was isolated by centrifugation, washed three times with 50 mL 2-propanol, dried in vacuum at room temperature, dissolved in 10 mL water, dialyzed against deionized water, and finally lyophilized. Yield: 71%

Supporting Information

Supporting Information File 1

Relative viscosity of an aqueous solution of cellulose carbamate **7a** in dependence on pH value.
[http://www.beilstein-journals.org/bjoc/content/supplementary/1860-5397-10-159-S1.pdf]

Acknowledgements

The financial support of the German Science Foundation (DFG, project HE 2054/15-1) is gratefully acknowledged. The authors thank Prof. Dr. Felix H. Schacher and Dr. Holger Wondraczek for the fruitful discussions.

References

1. Lowe, A. B.; McCormick, C. L. *Chem. Rev.* **2002,** *102,* 4177–4190. doi:10.1021/cr020371t
2. Bolto, B.; Gregory, J. *Water Res.* **2007,** *41,* 2301–2324. doi:10.1016/j.watres.2007.03.012
3. Kudaibergenov, S. E.; Ciferri, A. *Macromol. Rapid Commun.* **2007,** *28,* 1969–1986. doi:10.1002/marc.200700197
4. Ballauff, M.; Borisov, O. *Curr. Opin. Colloid Interface Sci.* **2006,** *11,* 316–323. doi:10.1016/j.cocis.2006.12.002
5. Alfrey, T., Jr.; Morawetz, H.; Fitzgerald, E. B.; Fuoss, R. M. *J. Am. Chem. Soc.* **1950,** *72,* 1864. doi:10.1021/ja01160a532
6. Alfrey, T., Jr.; Morawetz, H. *J. Am. Chem. Soc.* **1952,** *74,* 436–438. doi:10.1021/ja01122a046
7. Alfrey, T., Jr.; Fuoss, R. M.; Morawetz, H.; Pinner, H. *J. Am. Chem. Soc.* **1952,** *74,* 438–441. doi:10.1021/ja01122a047
8. Kamachi, M.; Kurihara, M.; Stille, J. K. *Macromolecules* **1972,** *5,* 161–167. doi:10.1021/ma60026a013
9. Kurihara, M.; Kamachi, M.; Stille, J. K. *J. Polym. Sci., Part A: Polym. Chem.* **1973,** *11,* 587–610. doi:10.1002/pol.1973.170110308
10. Roberts, D. W.; Williams, D. L. *Tetrahedron* **1987,** *43,* 1027–1062. doi:10.1016/S0040-4020(01)90041-9
11. Lowe, A. B.; Vamvakaki, M.; Wassall, M. A.; Wong, L.; Billingham, N. C.; Armes, S. P.; Lloyd, A. W. *J. Biomed. Mater. Res.* **2000,** *52,* 88–94. doi:10.1002/1097-4636(200010)52:1<88::AID-JBM11>3.0.CO;2-#
12. Huglin, M. B.; Radwan, M. A. *Polym. Int.* **1991,** *26,* 97–104. doi:10.1002/pi.4990260208
13. Baumann, H.; Liu, C.; Faust, V. *Cellulose* **2003,** *10,* 65–74. doi:10.1023/A:1023084628101
14. Muzzarelli, R. A. A. *Carbohydr. Polym.* **1988,** *8,* 1–21. doi:10.1016/0144-8617(88)90032-X
15. Yin, Q.; Li, Y.; Yin, Q.-J.; Miao, X.; Jiang, B. *J. Appl. Polym. Sci.* **2009,** *113,* 3382–3387. doi:10.1002/app.30010
16. Liu, C.; Baumann, H. *Carbohydr. Res.* **2002,** *337,* 1297–1307. doi:10.1016/S0008-6215(02)00132-5
17. Zheng, G.-Z.; Meshitsuka, G.; Ishizu, A. *J. Polym. Sci., Part B: Polym. Phys.* **1995,** *33,* 867–877. doi:10.1002/polb.1995.090330602
18. Zheng, G.-Z.; Meshitsuka, G.; Ishizu, A. *Polymer* **1996,** *37,* 1629–1634. doi:10.1016/0032-3861(96)83711-6
19. Heinze, T.; Genco, T.; Petzold-Welcke, K.; Wondraczek, H. *Cellulose* **2012,** *19,* 1305–1313. doi:10.1007/s10570-012-9725-1
20. You, J.; Hu, H. Z.; Zhou, J. *Cellulose* **2013,** *20,* 1175–1185. doi:10.1007/s10570-013-9891-9
21. Elschner, T.; Ganske, K.; Heinze, T. *Cellulose* **2013,** *20,* 339–353. doi:10.1007/s10570-012-9819-9
22. Vandoorne, F.; Vercauteren, R.; Permentier, D.; Schacht, E. *Makromol. Chem.* **1985,** *186,* 2455–2460. doi:10.1002/macp.1985.021861205
23. Elschner, T.; Doliška, A.; Bračič, M.; Stana-Kleinschek, K.; Heinze, T. *Carbohydr. Polym.* **2014,** in press. doi:10.1016/j.carbpol.2014.04.101
24. Krapcho, A. P.; Kuell, C. S. *Synth. Commun.* **1990,** *20,* 2559–2564. doi:10.1080/00397919008053205

License and Terms

Beilstein Journal of Organic Chemistry

Orthogonal dual thiol–chloroacetyl and thiol–ene couplings for the sequential one-pot assembly of heteroglycoclusters

Michele Fiore[1], Gour Chand Daskhan[1], Baptiste Thomas[1] and Olivier Renaudet[*1,2]

Full Research Paper

Open Access

Address:
[1]Département de Chimie Moléculaire, UMR-CNRS 5250 & ICMG FR2607, Université Joseph Fourier, PB 53, 38041 Grenoble Cedex 9, France and [2]Institut Universitaire de France, 103 Boulevard Saint-Michel, 75005 Paris, France

Email:
Olivier Renaudet[*] - olivier.renaudet@ujf-grenoble.fr

* Corresponding author

Keywords:
chemoselective ligation; heteroglycocluster; multivalency; multivalent glycosystems; one-pot synthesis

Beilstein J. Org. Chem. **2014,** *10,* 1557–1563.
doi:10.3762/bjoc.10.160

Received: 03 March 2014
Accepted: 10 June 2014
Published: 08 July 2014

This article is part of the Thematic Series "Multivalent glycosystems for nanoscience".

Guest Editor: B. Turnbull

Abstract

We describe the first one-pot orthogonal strategy to prepare well-defined cyclopeptide-based heteroglycoclusters (hGCs) from glycosyl thiols. Both thiol–chloroactetyl coupling (TCC) and thiol–ene coupling (TEC) have been used to decorate cyclopeptides regioselectively with diverse combination of sugars. We demonstrate that the reaction sequence starting with TCC can be performed one-pot whereas the reverse sequence requires a purification step after the TEC reaction. The versatility of this orthogonal strategy has been demonstrated through the synthesis of diverse hGCs displaying alternating binary combinations of α-D-Man or β-D-GlcNAc, thus providing rapid access to attractive heteroglycosylated platforms for diverse biological applications.

Introduction

Multivalent carbohydrate–protein interactions are complex mechanisms that play key roles in biology [1]. To decipher, exploit or inhibit these recognition processes, a large variety of synthetic multivalent glycoconjugates have been developed over the last decade [2-4]. For a long time, these structures have capitalized on the utilization of a core scaffold decorated with identical sugars which are covalently linked through various spacers. While mimicking the multivalent sugar display of biological systems, these structures poorly reflect their inherent heterogenicity which hampers progresses towards the detailed elucidation of carbohydrate–protein interactions and the discovery of more selective ligands. Heteromultivalent ligands, namely heteroglycoclusters (hGCs), represent ideal structures to achieve this purpose [5]. A few recent reports described the construction of various hGCs based on the successive attachment of sugar residues on a core scaffold such as sugar [6,7],

peptide [8-10], dendrimer [11,12], cyclodextrin [13-15] and polymer [16]. The most common synthetic strategy to build such hGCs relies on a fragment-coupling approach using thiol–ene coupling [17], copper(I)-catalyzed alkyne–azide cycloaddition (CuAAC) [18] or S_N2 reaction [19]. In addition, orthogonal chemoselective ligations were proved more attractive strategies to prepare hGCs in high yields, in part because they require less synthetic and purification steps. For example, oxime and CuAAC ligations have been used in our group to prepare tetravalent structures displaying two sugars either in 2:2 or 3:1 relative proportions [20]. In the meanwhile, the group of A. Dondoni has developed a sequential orthogonal TEC in combination with CuAAC for grafting two different sugar motifs on calix[4]arene scaffold [21].

Herein we report a new strategy based on both thiol–chloroactetyl coupling (TCC) and thiol–ene coupling (TEC) to prepare hGCs from glycosyl thiols and cyclopeptide scaffolds displaying chloroacetyl (ClAc) and allyloxycarbonyl (Alloc) groups and vice versa. We demonstrate that cyclopeptides regioselectively decorated with four sugars on one side, and two other sugars on the other side can be obtained either by a stepwise or a one-pot protocol depending on the reaction sequence (Figure 1). It should be mentioned that during the course of this study, the group of R. Roy has demonstrated the orthogonality of these two reactions for the growth of multifuncional dendrimers [22].

Results and Discussion

Owing to their straightforward access, their high nucleophilicity and the stability of thioether conjugates, glycosyl thiols [23,24], α-D-ManSH **1** and β-D-GlcNAcSH **2** have been selected for this study (Scheme 1). Such derivatives have proved to be useful in bioconjugates chemistry [25] and for the preparation of thioether-linked tetravalent glycocyclopeptides which have shown highest inhibition against a model lectin in comparison with analogues bearing oxime and triazole linkage [26]. Glycosyl thiols α-D-ManSH **1** and β-D-GlcNAcSH **2** were prepared from the corresponding bromo peracetyl and chloro peracetyl sugars by treatment with potassium thioacetate followed by de-*O*-acetylation under standard conditions [24].

Cyclopeptide **3** displaying two orthogonal functionalities, i.e., four lysine residues functionalized with Alloc groups [27] pointing on the upper face, and two lysine residues protected with chloroacetyl moiety at the lower face has been prepared. To evaluate the importance of the reaction sequences, we first performed the TEC reaction using α-D-ManSH **1**. This reaction was carried out in a mixture of DMF and H_2O under UV irradiation (λ = 365 nm) in the presence of 2,2-dimethoxy-2-phenylacetophenone (DPAP) as a radical initiator (Scheme 1, route A). In previous studies [26], we observed that the TEC reaction requires the utilization of 3 equivalents of sugar per reaction site to be complete. Disappearance of starting material was indeed observed by reversed-phase HPLC after 45 minutes. The formation of the desired intermediate **4** having two chloroacetyl groups on the other side was confirmed by ESI mass spectrometry (see Supporting Information File 1 and Table 1). As expected, the chloroacetyl groups remained unreactive under these conditions as no partially glycosylated product was observed. Even though the HPLC profile of the crude mixture showed a clean reaction mixture, we were aware that the remaining presence of **1** could lead to the formation of an unwanted mixture of products. However we performed the next TCC reaction without further purification. The reaction occurred with a slight excess of **2** (1.2 equiv per reactive site) in the presence of NaH in dry DMF. Expectedly, this route gave a heterogeneous mixture of inseparable products, thus indicating that removal of the unreacted excess of sugar **1** is mandatory to avoid its addition during the TCC reaction. After purification, compound **4** was obtained in 46% yield and subsequently subjected to the TCC reaction with β-D-GlcNAcSH **2** under conditions described above. Compound **5**, wherein α-D-Man and β-D-GlcNAc occupied at the upper and the lower domains

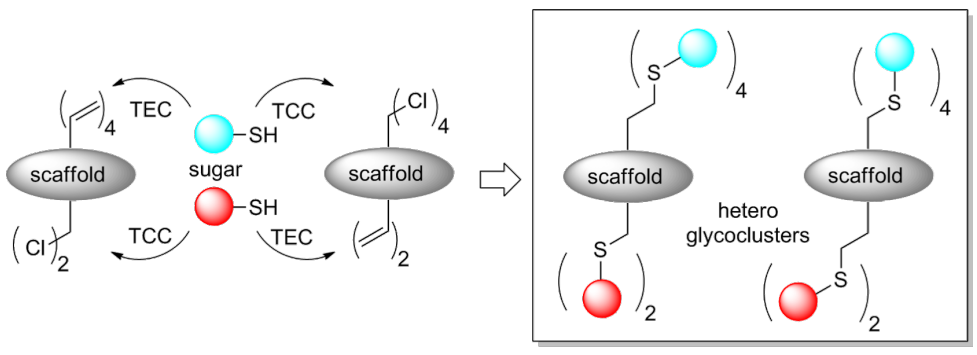

Figure 1: Chemical strategy for the construction of heteroglycoclusters.

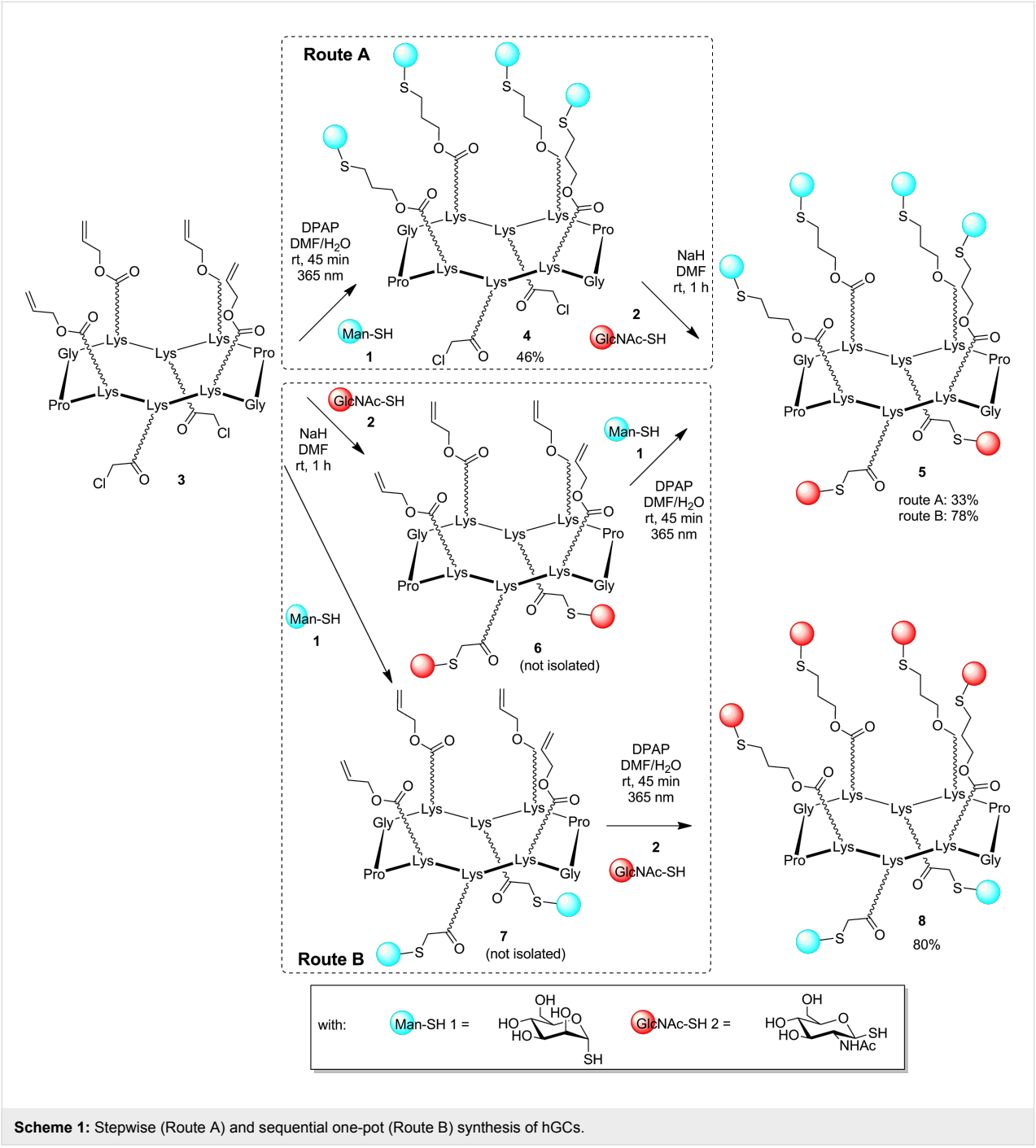

Scheme 1: Stepwise (Route A) and sequential one-pot (Route B) synthesis of hGCs.

of the scaffold, respectively, was obtained after 1 hour as confirmed by HPLC and MS analyses (Table 1).

We decided to investigate whether changing the reaction sequence could allow the one-pot assembly. We thus coupled β-D-GlcNAcSH **2** by TCC as the first step (Scheme 1, route B). Contrary to the previous route, we expected that the presence of unreacted sugar **2** (used in slight excess) might not interfere during the thiol–ene coupling as it should form disulfide adduct spontaneously. Therefore, the crude mixture was neutralized by addition of hydrochloric acid and compound **6** was used without further additional purification. α-D-ManSH **1** was then conjugated by TEC and compound **5** was obtained in 78% after purification. Interestingly no side product corresponding to the addition of **2** on the Alloc group was detected. We concluded that performing reactions in this order (route B) makes the one-pot assembly possible, faster and provides hGCs with higher yields (Table 1).

Table 1: Analytical data of the hGCs.

compound	yield (%)[a]	MS calc[b]	MS found[c]	t_R (min)[d]
4	46 (6.9 mg)	2351.9	2352.0	9.71
5 (route A)	33 (2.6 mg)	2753.1	2753.2	8.24
5 (route B)	78 (13.8 mg)	2753.1	2753.2	8.24
8	80 (10.2 mg)	2835.8	2836.0	8.35
11	77 (13.1 mg)	2666.1	2666.1	8.06
13	54 (14.4 mg)	2747.1	2747.2	8.06

[a]Yields were calculated on isolated compounds after HPLC purification. [b]Calculated mass for $[M + H]^+$. [c]MS analysis was performed by electrospray ionization method in positive mode. [d]RP-HPLC retention time using a linear gradient A–B, 95:5 to 0:100 in 20 min, flow: 1.0 mL/min, λ = 214 nm and 250 nm (column: nucleosil 300-5 C18; solvent A: 0.09% TFA in H_2O, solvent B: 0.09% TFA in 90% acetonitrile).

To verify the efficiency and versatility of this protocol, we decided to perform similar sequence of reactions with cyclopeptide **9** having reactive functionalities in reverse orientation compared to **3**, i.e., four chloroacetyl and two Alloc moieties at the upper and the lower face, respectively (Scheme 2).

α-D-ManSH was used for the TCC reaction and β-D-GlcNAcSH for the subsequent TEC using a similar sequence of reactions described in Scheme 1. The HPLC profile of the crude mixture (Figure 2) showed that the successive TCC and TEC reactions give clean reaction mixtures to provide the hGC **11** with 77% yield.

The same strategy was followed to prepare compound **13** featuring two α-D-Man and four β-D-GlcNAc. No difference of reactivity was observed whatever the scaffold or the glycosyl thiol used. All these products were obtained in good yield after

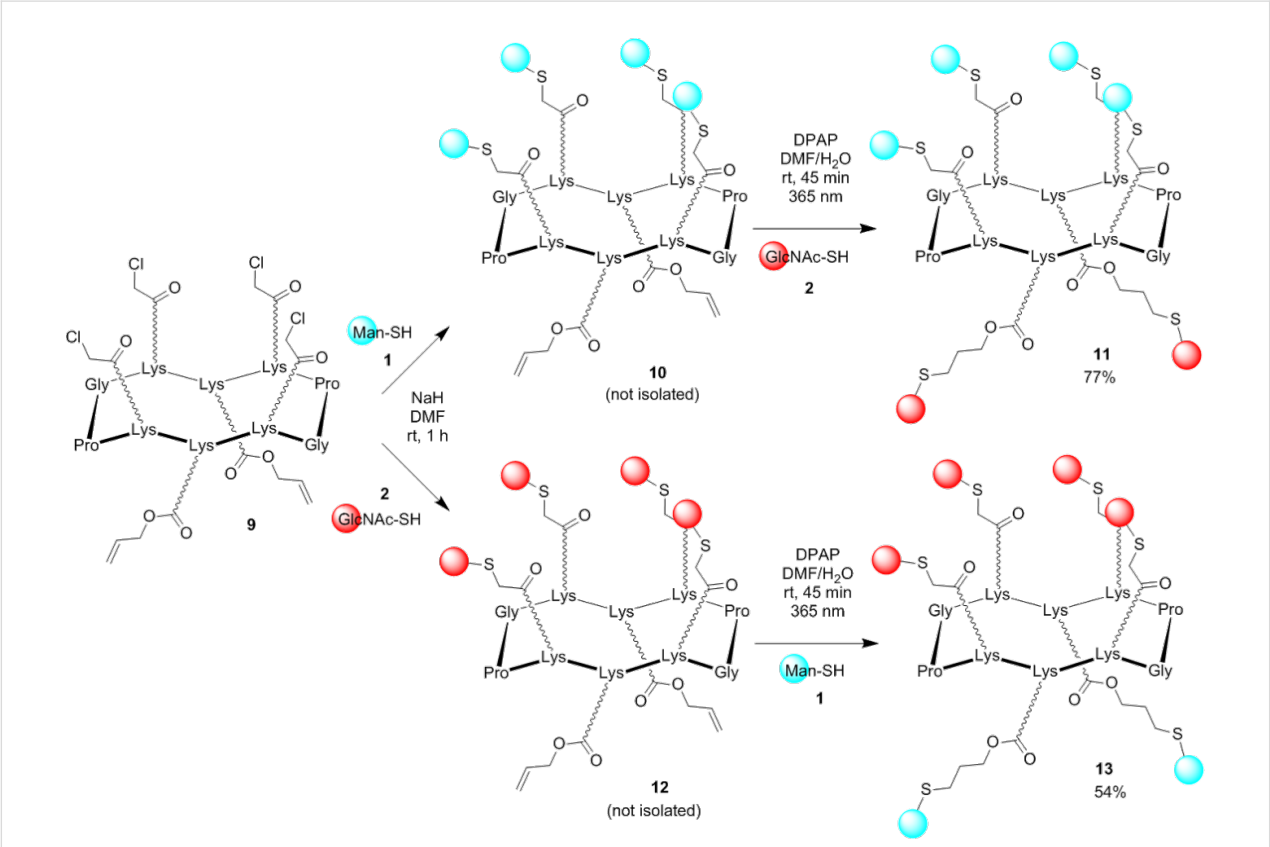

Scheme 2: Synthesis of hGCs **11** and **13**.

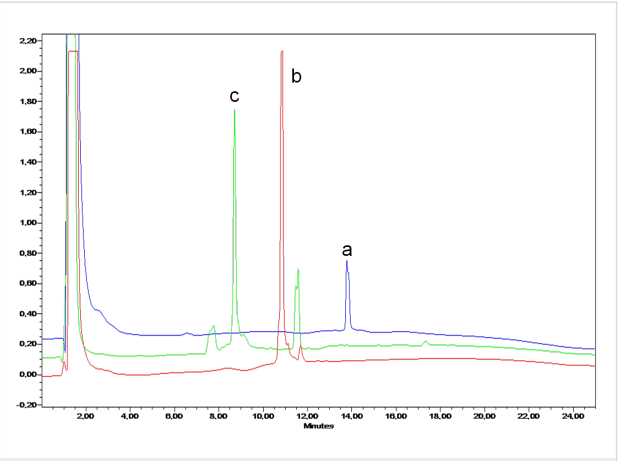

Figure 2: RP-HPLC profile of the one-pot synthesis of hGC **11** (linear A–B gradient: 5 to 100% B in 20 min, λ = 214 nm); (a, blue) cyclodecapeptide precursor **9**; (b, red) crude mixture of intermediate product **10**; (c, green) corresponds to crude mixture after TCC and TEC (**11**).

HPLC purification and gave the expected multicharged ions by electrospray mass spectrometry (Table 1).

Conclusion

In summary, we have developed the first synthesis of hGCs using a one-pot orthogonal chemoselective route by using dual thiol–chloroacetyl and thiol–ene couplings. The effectiveness of this method was demonstrated through the coupling of multiple copies of α-D-ManSH and β-D-GlcNAcSH residues onto both addressable domains of cyclopeptide scaffolds displaying chloroacetyl and allyloxycarbonyl groups. While the first utilization of thiol–ene coupling in a stepwise approach requires an intermediate purification, a sequential one-pot assembly can be performed in good yields by starting with thiol–chloroacetyl coupling. This process is currently used in our laboratory for the construction of mutliantigenic synthetic vaccines against cancers.

Experimental

General details. All chemical reagents were purchased from Aldrich (Saint Quentin Fallavier, France) or Acros (Noisy-Le-Grand, France) and were used without further purification. PyBOP was obtained from Calbiochem-Novabiochem (Merck Biosciences - VWR, Limonest, France). Analytical RP-HPLC was performed on a Waters system equipped with a Waters 600 controller and a Waters 2487 Dual Absorbance Detector. Analysis was carried out at 1.0 mL/min (EC 125/3 nucleosil 300-5 C18) with UV monitoring at 214 nm and 250 nm using a linear A–B gradient (buffer A: 0.09% CF_3CO_2H in water; buffer B: 0.09% CF_3CO_2H in 90% acetonitrile). Preparative separation was carried out at 22 mL/min (VP 250/21 nucleosil 300-7 C18) with UV monitoring at 214 nm and 250 nm using a linear A–B gradient (buffer A: 0.09% CF_3CO_2H in water; buffer B: 0.09% CF_3CO_2H in 90% acetonitrile). Mass spectrometry was performed using electrospray ionization on an Esquire 3000+ Bruker Daltonics in positive mode.

General procedure for solid-phase peptide synthesis. Assembly of all protected peptides was carried out on a synthesizer (Syro II, Biotage) using the Fmoc/*t*-Bu strategy and the Fmoc-Gly-Sasrin^{TM} resin. Coupling reactions were performed using, relative to the resin loading, 3 equiv of Fmoc-protected amino acid activated in situ with 3 equiv of PyBOP and 6 equiv of DIPEA in DMF (10 mL/g resin) for 30 min. Fmoc protecting groups were removed by treatment with a piperidine/DMF solution 1:4 (10 mL/g resin) for 10 min. Synthetic linear peptides were recovered directly upon acid cleavage (1% TFA in CH_2Cl_2). The resins were treated for 3 min repeatedly until the resin beads became dark purple. The combined washings were concentrated under reduced pressure, and white solid peptides were obtained by precipitation from diethyl ether.

General procedure for peptide cyclization. All linear peptides were dissolved in CH_2Cl_2 (0.5 mM) and the pH was adjusted to 8 by addition of DIPEA. PyBOP (1.2 equiv) was added and the solution was stirred at room temperature for 1 h. Evaporation of the solvent and precipitation in diethyl ether afforded the cyclic peptides as white solids.

General procedure for Boc deprotection. All cyclic peptides were dissolved in CH_2Cl_2 and then a solution at 40% of trifluoroacetic acid in CH_2Cl_2 with 2.5% of water as scavenger was added. The reaction was run until disappearance of stating material (1 h). Evaporation of the solvent and precipitation in diethyl ether afforded the cyclic peptides as white solids.

Cyclopeptide 3. To a solution of partial protected cyclopeptide [Lys(Aloc)-Lys-Lys(Aloc)-Pro-Gly-Lys(Aloc)-Lys-Lys(Aloc)-Pro-Gly] (200 mg, 0.142 mmol) in dry DMF (10 mL) was added chloroacetic anhydride (100 mg, 0.304 mmol) and pH adjusted to 8 by adding 100 µL of DIPEA. The brown solution was left stirring for 2 h. The solvent was then evaporated, the brown residue was dissolved in a minimum amount of CH_2Cl_2 and then precipitated in Et_2O. The dark-yellow precipitate was purified by HPLC obtaining **3** (157 mg, 70%) as white foam. Analytical RP-HPLC: t_R = 16.64 min (gradient: 5 to 100% B in 20 min); ESIMS$^+$ (*m*/*z*): $[M + H]^+$ calcd for $C_{70}Cl_2H_{111}N_{16}O_{20}$, 1567.7; found, 1567.7.

Homoglycocluster 4. Route A: Compounds **1** (14 mg, 0.076 mmol) and **3** (10 mg, 0.0064 mmol) were dissolved in dry DMF and DPAP (2.0 mg, 0.008 mmol) was added. The solution was irradiated at 365 nm for 45 min. Compound **4** (6.9 mg, 46%) was obtained as a white foam. Analytical RP-HPLC: t_R =

9.71 min (gradient: 5 to 100% B in 20 min); ESIMS$^+$ (*m*/*z*): [M + H]$^+$calcd for $C_{94}Cl_2H_{158}N_{16}O_{40}S_4$, 2351.9; found, 2352.0.

Heteroglycocluster 5. Route A: Compounds **4** (6.9 mg, 0.029 mmol) and **2** (1.7 mg, 0.0696 mmol) were dissolved in dry DMF (300 µL) and NaH (0.28 mg, 0.0696 mmol) was added. The heterogeneous solution was left stirring 2 h at rt. The crude mixture was then purified at HPLC obtaining **5** (2.6 mg, 33%) as a white foam. Analytical RP-HPLC: t_R = 8.24 min (gradient: 5 to 100% B in 20 min); ESIMS$^+$ (*m*/*z*): [M + H]$^+$ calcd for $C_{110}H_{187}N_{18}O_{60}S_6$, 2753.1; found, 2753.2.

Heteroglycocluster 5. Route B (one-pot assembly). Compounds **2** (3.6 mg, 0.015 mmol) and **3** (10 mg, 0.0064 mmol) were dissolved in dry DMF (300 µL) and NaH (0.5 mg, 0.015 mmol) was added. After stirring 1 h at room temperature, analytical HPLC indicated complete disappearance of **3** and the appearance of a new product corresponding to compound **6**. Analytical HPLC: t_R = 11.34 (gradient: 5 to 100% B in 20 min); ESIMS$^+$ (*m*/*z*): [M + H]$^+$ calcd for $C_{86}H_{139}N_{18}O_{30}S_2$, 1968.0; found, 1969.3. The crude mixture was treated with 1% HCl aqueous solution (150 µL) then compound **1** (14.52 mg, 0.0768 mmol) and DPAP (1.96 mg, 0.0077 mmol) were added. The solution was irradiated at 365 nm for 45 min. Heteroglycocluster **5** was obtained as a white foam after HPLC purification. Yield: 78%; (13.8 mg); analytical HPLC: t_R = 8.24 min (gradient: 5 to 100% B in 20 min); ESIMS$^+$ (*m*/*z*): [M + H]$^+$ calcd for $C_{110}H_{187}N_{18}O_{60}S_6$, 2753.1; found, 2753.2.

Heteroglycocluster 8. Heteroglycocluster **8** wad obtained from **1** (2.4 mg, 0.0122 mmol), **3** (8 mg, 0.0051 mmol) and **2** (14.2 mg, 0.06 mmol) as described for **5**. Yield: 80% (10.2 mg); analytical RP-HPLC: t_R = 8.35 min (gradient: 5 to 100% B in 20 min); ESIMS$^+$ (*m*/*z*): [M + H]$^+$ calcd for $C_{114}H_{193}N_{20}O_{50}S_6$, 2835.8; found, 2836.0.

Cyclopeptide 9. To a solution of the partial protected cyclopeptide [Lys-Lys(Aloc)-Lys-Pro-Gly-Lys-Lys(Aloc)-Lys-Pro-Gly] (871 mg, 0.70 mmol) in dry DMF (40 mL) was added chloroacetic anhydride (601.2 mg, 3.36 mmol) and the pH was adjusted to 8 by adding 250 µL of DIPEA. The brown solution was left stirring for 4 h. Solvent was then evaporated; the brown residue was dissolved in a minimum amount of CH_2Cl_2 and then precipitated in Et_2O. The dark-brown precipitate was purified by HPLC obtaining **9** (459 mg, 42%) as white foam. Analytical RP-HPLC: t_R = 12.67 min (gradient: 5 to 100% B in 20 min); ESIMS$^+$ (*m*/*z*): [M + H]$^+$ calcd for $C_{66}Cl_4H_{105}N_{16}O_{18}$, 1582.7; found, 1582.0.

Heteroglycocluster 11. Heteroglycocluster **11** was obtained from **9** (13 mg, 0.0084 mmol), **1** (8 mg, 0.0402 mmol) and **2** (11.9 mg, 0.0504 mmol) as described for **5**. Yield: 77% (13.1 mg); analytical RP-HPLC: t_R = 8.06 min (gradient: 5 to 100% B in 20 min); ESIMS$^+$ (*m*/*z*): [M + H]$^+$ calcd for $C_{106}H_{180}N_{18}O_{48}S_6$, 2666.1; found, 2666.1.

Heteroglycocluster 13. Heteroglycocluster **13** was obtained from **9** (15 mg, 0.0097 mmol), **2** (11.0 mg, 0.0466 mmol) and **1** (11.4 mg, 0.058 mmol) as described for **5**. Yield: 54% (14.4 mg); analytical RP-HPLC: t_R = 8.06 min (gradient: 5 to 100% B in 20 min); ESIMS$^+$ (*m*/*z*): [M + H]$^+$ calcd for $C_{110}H_{184}N_{20}O_{48}S_6$, 2747.1; found, 2747.2.

Supporting Information

Supporting Information File 1

HPLC chromatograms and mass spectra of all compounds.
[http://www.beilstein-journals.org/bjoc/content/supplementary/1860-5397-10-160-S1.pdf]

Acknowledgments

This work was supported by the "Communauté d'agglomération Grenoble-Alpes Métropole" (Nanobio program), the "Cluster de Recherche Chimie de la Région Rhône-Alpes" (BT), the Ligue contre le cancer (MF), the Agence Nationale de la Recherche Grant ANR-12-JS07-0001-01 "VacSyn" (GCD), the COST action CM1102 and the Labex ARCANE (ANR-11-LABX-0003-01).

References

1. Varki, A.; Cummings, R. D.; Esko, J. D.; Freeze, H. H.; Stanley, P.; Bertozzi, C. R.; Hart, G. W.; Etzler, M. E. *Essentials of Glycobiology,* 2nd ed.; Cold Spring Harbour: New York, 2009.
2. Kiessling, L. L.; Gestwicki, J. E.; Strong, L. E. *Angew. Chem., Int. Ed.* **2006,** *45,* 2348. doi:10.1002/anie.200502794
3. Chabre, Y. M.; Roy, R. *Adv. Carbohydr. Chem. Biochem.* **2010,** *63,* 165. doi:10.1016/S0065-2318(10)63006-5
4. Renaudet, O.; Roy, R. *Chem. Soc. Rev.* **2013,** *42,* 4515. doi:10.1039/C3CS90029K
5. Jiménez Blanco, J. L.; Ortiz Mellet, C.; Garcia Fernández, J. M. *Chem. Soc. Rev.* **2013,** *42,* 4518. doi:10.1039/c2cs35219b
6. Patel, A.; Lindhorst, T. K. *Eur. J. Org. Chem.* **2002,** 79. doi:10.1002/1099-0690(20021)2002:1<79::AID-EJOC79>3.0.CO;2-1
7. Ortega-Muñoz, M.; Perez-Balderas, F.; Morales-Sanfrutos, J.; Hernandez-Mateo, F.; Isac-García, J.; Santoyo-Gonzalez, F. *Eur. J. Org. Chem.* **2009,** 2454. doi:10.1002/ejoc.200801169
8. Katajisto, J.; Karskela, T.; Heinonen, P.; Lönnberg, H. *J. Org. Chem.* **2002,** *67,* 7995. doi:10.1021/jo026053b
9. Lindhorst, T. K.; Bruegge, K.; Fuchs, A.; Sperling, O. *Beilstein J. Org. Chem.* **2010,** *6,* 801. doi:10.3762/bjoc.6.90
10. Keding, S. J.; Danishefsky, S. J. *Proc. Natl. Acad. Sci. U. S. A.* **2004,** *101,* 11937. doi:10.1073/pnas.0401894101
11. Deguise, I.; Lagnoux, D.; Roy, R. *New J. Chem.* **2007,** *31,* 1321. doi:10.1039/b701237c

12. Wolfenden, M. L.; Cloninger, M. J. *Bioconjugate Chem.* **2006,** *17,* 958. doi:10.1021/bc060107x
13. Gómez-García, M.; Benito, J. M.; Rodríguez-Lucena, D.; Yu, J.-X.; Chmurski, K.; Ortiz Mellet, C.; Gutiérrez Gallego, R.; Maestre, A.; Defaye, J.; Garcìa Fernàndez, J. M. *J. Am. Chem. Soc.* **2005,** *127,* 7970. doi:10.1021/ja050934t
14. Gómez-García, M.; Benito, J. M.; Gutiérrez-Gallego, R.; Maestre, A.; Ortiz Mellet, C.; García Fernández, J. M.; Jiménez Blanco, J. L. *Org. Biomol. Chem.* **2010,** *8,* 1849. doi:10.1039/b920048g
15. Gómez-Garcia, M.; Benito, J. M.; Butera, A. P.; Ortiz-Mellet, C.; Garcia Fernàndez, J. M.; Jiménez Blanco, J. L. *J. Org. Chem.* **2012,** *77,* 1273. doi:10.1021/jo201797b
16. Geng, J.; Mantovani, G.; Tao, L.; Nicolas, J.; Chen, G.; Wallis, R.; Mitchell, D. A.; Johnson, B. R. G.; Evans, S. D.; Haddleton, D. M. *J. Am. Chem. Soc.* **2007,** *129,* 15156. doi:10.1021/ja072999x
17. Dondoni, A. *Angew. Chem., Int. Ed.* **2008,** *47,* 8995. doi:10.1002/anie.200802516
18. Rostovtsev, V. V.; Green, L. G.; Fokin, V. V.; Sharpless, K. B. *Angew. Chem., Int. Ed.* **2002,** *41,* 2596. doi:10.1002/1521-3773(20020715)41:14<2596::AID-ANIE2596>3.0.CO;2-4
19. Elsner, K.; Boysen, M. M. K.; Lindhorst, T. K. *Carbohydr. Res.* **2007,** *342,* 1715. doi:10.1016/j.carres.2007.05.005
20. Thomas, B.; Fiore, M.; Bossu, I.; Dumy, P.; Renaudet, O. *Beilstein J. Org. Chem.* **2012,** *8,* 421. doi:10.3762/bjoc.8.47
21. Fiore, M.; Chambery, A.; Marra, A.; Dondoni, A. *Org. Biomol. Chem.* **2009,** *7,* 3910. doi:10.1039/b912686d
22. Kottari, N.; Chabre, Y. M.; Shiao, T. C.; Roy, R. *Chem. Commun.* **2014,** *50,* 1983. doi:10.1039/C3CC46633G
23. MacDougall, J. M.; Zhang, X.-D.; Polgar, W. E.; Kharoyan, T. V.; Toll, L.; Cashman, J. R. *J. Med. Chem.* **2004,** *47,* 5809. doi:10.1021/jm049554t
24. Bernardes, G. J. L.; Gamblin, D. P.; Davis, B. G. *Angew. Chem., Int. Ed.* **2006,** *45,* 4007. doi:10.1002/anie.200600685
25. Gingras, M.; Chabre, Y. M.; Roy, M.; Roy, R. *Chem. Soc. Rev.* **2013,** *42,* 4823. doi:10.1039/c3cs60090d
26. Fiore, M.; Berthet, N.; Marra, A.; Gillon, E.; Dumy, P.; Dondoni, A.; Imberty, A.; Renaudet, O. *Org. Biomol. Chem.* **2013,** *11,* 7113. doi:10.1039/c3ob41203b
27. Eggimann, G. A.; Buschor, S.; Darbre, T.; Reymond, J.-L. *Org. Biomol. Chem.* **2013,** *11,* 6717. doi:10.1039/C3OB41023D

License and Terms

BEILSTEIN JOURNAL OF ORGANIC CHEMISTRY

Multivalent scaffolds induce galectin-3 aggregation into nanoparticles

Candace K. Goodman[1], Mark L. Wolfenden[1], Pratima Nangia-Makker[1,2], Anna K. Michel[1], Avraham Raz[1,2] and Mary J. Cloninger[*1]

Full Research Paper

Open Access

Address:
[1]Department of Chemistry and Biochemistry, Montana State University, Bozeman, Montana 59717, USA and [2]The Departments of Oncology and Pathology, School of Medicine, Wayne State University, 110 East Warren Avenue, Detroit, Michigan 48201, USA

Email:
Mary J. Cloninger[*] - mcloninger@chemistry.montana.edu

* Corresponding author

Keywords:
dendrimers; galectin-3; glycodendrimers; multivalency; multivalent glycosylation; protein aggregation

Beilstein J. Org. Chem. **2014,** *10,* 1570–1577.
doi:10.3762/bjoc.10.162

Received: 03 March 2014
Accepted: 18 June 2014
Published: 10 July 2014

This article is part of the Thematic Series "Multivalent glycosystems for nanoscience".

Guest Editor: J.-L. Reymond

Abstract

Galectin-3 meditates cell surface glycoprotein clustering, cross linking, and lattice formation. In cancer biology, galectin-3 has been reported to play a role in aggregation processes that lead to tumor embolization and survival. Here, we show that lactose-functionalized dendrimers interact with galectin-3 in a multivalent fashion to form aggregates. The glycodendrimer–galectin aggregates were characterized by dynamic light scattering and fluorescence microscopy methodologies and were found to be discrete particles that increased in size as the dendrimer generation was increased. These results show that nucleated aggregation of galectin-3 can be regulated by the nucleating polymer and provide insights that improve the general understanding of the binding and function of sugar-binding proteins.

Introduction

The role of multivalency in biology is well established, and examples of this phenomenon abound [1]. The ability of multivalency to enhance weak interactions has been shown in a variety of protein:carbohydrate systems using a wide assortment of scaffolds and carbohydrates [2]. As research with multivalent glycosystems advances, one important target for potential therapy and understanding is the galectin family of proteins [3]. Members of the galectin family share a common conserved sequence carbohydrate recognition domain (CRD) made of ~130 amino acids that are arranged in a folded beta-sheet structure and have an affinity for β-galactosides [4-7]. Galectin-3, one of the most studied members, is commonly up or down regulated in different cancers and is implicated in tumor formation and proliferation, apoptosis, angiogenesis, and B cell activation [8-10]. Galectin-3 has been reported to be involved in mechanisms that cluster cell surface glycoproteins [10,11], cross-link receptors [12], and form lattices and larger aggregates [13]. Structurally, galectin-3 is composed of one

carbohydrate recognition domain and a collagen-like N-terminus tail [14].

The native quaternary structure of this unique galectin is a current topic of debate. Brewer et al. found that galectin-3 pentamers can be formed at high concentrations of protein [15], a noncovalent dimer and a monomer form of galectin-3 have also been reported [16,17]. Recent anisotropy binding measurements support two types of galectin-3 oligomerization, dominated by either N- or C-terminal interactions [18], and both N- and C-terminal domains are reported to be required for binding to targets such as lipopolysaccharide [19,20]. Galectin-3 can serve as a cellular docking site or a crosslinker for microorganisms binding to pathogens directly [20,21], and galectin-3 can act as a scaffold for the presentation of ligands such as lipopolysaccharides into an aggregate that stimulates cellular responses [19].

Binding affinities have been reported for a series of carbohydrate-based ligands to galectin-3, which binds to lactose significantly better than to galactose or to *N*-acetylgalactosamine but does not bind to mannose [22-24]. Both the glycan ligand and the topological display on the cell surface are required for high affinity, selective binding of galectins, as demonstrated in galectin binding studies with neuroblastoma cells [25].

Here, we demonstrate that glycodendrimers bearing lactose can be used to form large, discrete aggregates of galectin-3. Since, as noted above, glycan clustering and galectin-3-mediated aggregations have been demonstrated to be important for biological interactions ranging from bacterial invasion to cancer cellular responses, the development of systems such as glycodendrimers that can aggregate galectin-3 into nanoparticles in a highly controlled fashion is an important area of research. The study of galectin-3 binding and cluster formation by a series of glycodendrimers is a central step in the development of a synthetic multivalent antagonist that can intercept and influence galectin-3-mediated cellular processes and may be of clinical value as a non-cytotoxic drug and/or be developed for cancer imaging.

Results and Discussion

Synthesis and characterization of glycodendrimers

Poly(amidoamine) (PAMAM) dendrimers are well-defined, water-soluble, symmetric scaffolds that contain a controlled and tuneable number of end groups. The number of end groups is specified by the dendrimer generation and approximately doubles for each subsequent generation [26]. These dendrimers are commercially available for generations zero, denoted G(0), to generation 10, denoted G(10). The amine termini can be functionalized with a variety of molecules, making these scaffolds an excellent choice for systematic studies of chemical and biological phenomena [27,28]. In this investigation, PAMAM dendrimers were functionalized using a methodology similar to previous literature [29]. Synthesis of β-lactoside derivative **1** was performed as shown in Scheme 1. Lewis acid facilitated glycosylation, which was directed by neighboring group participation of the 2-*O*-acetyl protecting group, afforded the desired anomers in good yields. The trichloroacetimidate intermediate was formed to enhance coupling.

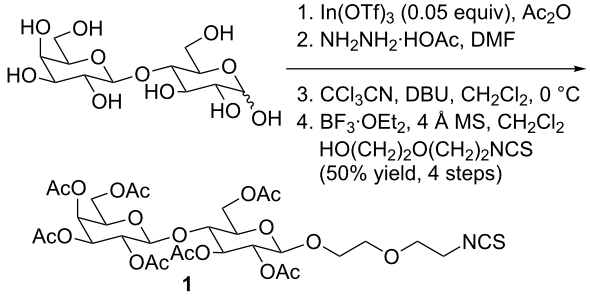

Scheme 1: Synthesis of isothiocyanato-functionalized lactoside **1**.

Syntheses of the carbohydrate-functionalized dendrimers were performed by addition of compound **1** as shown in Scheme 2. The functionalized dendrimers were characterized by MALDI–TOF–MS (matrix-assisted laser desorption time of flight mass spectrometry). The average numbers of sugars that were incorporated are shown in Scheme 2. The loadings were determined by both the changes in weight average molecular weight (M_w) upon addition of **1** and the changes in M_w upon deacetylation, enabling characterization of the average number of sugars per dendrimer [30]. Additional characterization details (including ^{1}H NMR spectra) are provided in Supporting Information File 1.

Characterization of dendrimer/galectin-3 aggregates

Dynamic light scattering (DLS) was used to characterize the size and polydispersity of aggregate formation between lactose-functionalized dendrimers **2**, **3**, **4**, and **5**, with galectin-3. Three concentrations of glycodendrimers (11.5, 3.3 and 0.14 μM) were added to a constant concentration of galectin-3 (31 μM in PBS) to obtain a ratio of galectin-3 to glycodendrimer of 220:1, 9:1, or 3:1. These ratios were chosen so that results obtained from experiments using a large excess, a significant excess, and a slight excess of galectin-3 could be compared.

Regardless of the amount of excess galectin-3 that was used, the size and polydispersity of the aggregates was shown to increase

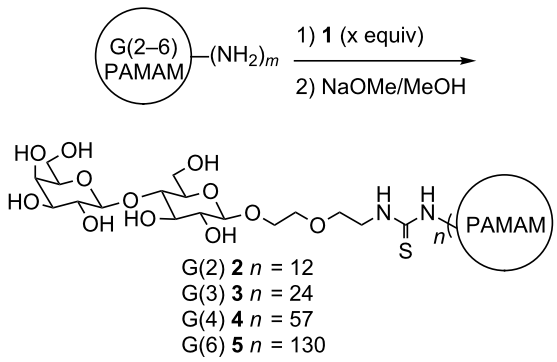

Scheme 2: Synthesis of carbohydrate-functionalized PAMAM dendrimers. (Values for *m* and for x equivalents added are given in Supporting Information File 1.)

with increasing dendrimer generation (Figure 1 and Table 1). The largest aggregates were observed for the 9:1 ratio of galectin-3 to glycodendrimer, and smaller aggregates were formed when a large excess or a very small excess of galectin-3 was used. This trend is logical if the glycodendrimer is serving as the nucleating agent for galectin-3 aggregation. For example, when the concentration of galectin-3 is comparable to the concentration of glycodendrimer, then galectin-3 is presented with many different nucleating scaffolds, and smaller particles are formed. On the other hand, when galectin-3 is present in large excess, not as many nucleating sites can be incorporated into each aggregate, which causes the aggregates to be smaller. A schematic representation of glycodendrimer-mediated galectin-3 aggregation is shown in Figure 2. This trend was also observed in other systems. Ottaviani, et al. reported enhanced aggregation of amyloid peptides at low concentrations of maltose and maltotriose-functionalized poly(propylene imine) dendrimers and inhibition at high glycodendrimer concentrations [31]. Previous studies of asialofetuin/galectin-3 aggregation indicated that the glycoprotein ligand could serve to initiate aggregation, but carbohydrate binding was not required for all of the galectin-3 lectins that were involved in the interaction. Some galectin-3/galectin-3 interactions, in addition to carbohydrate/galectin-3 interactions, were proposed [18].

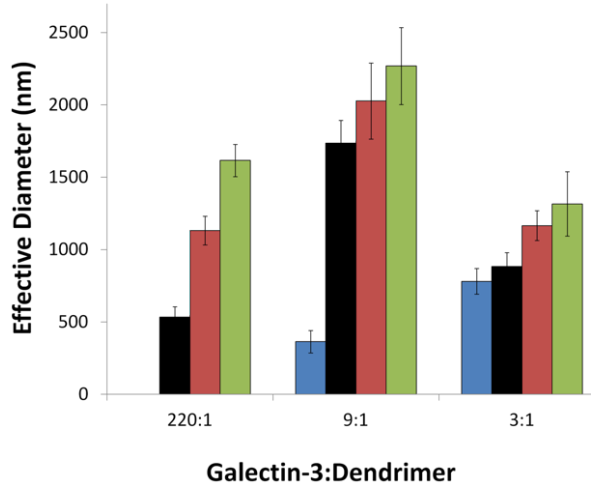

Figure 1: Effective diameter of galectin-3/glycodendrimer aggregates (DLS). Final concentration of galectin-3 31 μM; final concentration of glycodendrimers 0.14, 3.3, 11.5 μM for 220:1, 9:1, 3:1, respectively. **2** (blue), **3** (black), **4** (red) and **5** (green). Aggregate size was below the detection limit for **2** at 0.14 μM.

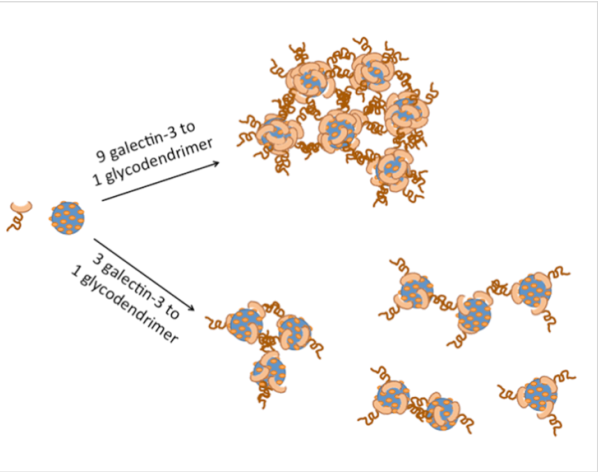

Figure 2: Schematic representation of galectin-3/glycodendrimer aggregates at varying stoichiometries.

A series of control experiments indicate that aggregation is induced by the binding of galectin-3 to lactose on the dendrimers. No observable particles were detected upon addition of a mannose-functionalized G(4) dendrimer (Table S3 in Supporting Information File 1). Pre-incubation of galectin-3

Table 1: Summary of aggregate characterization.

Compound	No. of particles	Mean diameter (FM, nm)	Avg. effective diameter (DLS, nm)
2	59	240 ± 50	not detectable
3	221	700 ± 290	560 ± 40
4	137	1070 ± 350	1180 ± 80
5	146	1790 ± 650	1620 ± 110

with 1 mM lactose solution completely inhibited aggregate formation in the presence of glycodendrimers **3**, **4**, and **5** (Table S3 in Supporting Information File 1). Titration of a lactose solution into the solution of preformed aggregates did result in disassembly, but titration of an equivalent volume of PBS also resulted in disassembly (Table S3, Supporting Information File 1). Analysis of concentration effects and kinetics of aggregation and disaggregation are beyond the scope of this report but are under investigation. Experiments using **5** and truncated galectin-3, which has only the carbohydrate recognition domain without the N-terminal domain, did not result in aggregate formation (see Table S3, Supporting Information File 1). No aggregates were observed for dendrimers **2**–**5** in solution without addition of galectin-3, and no aggregates were observed for galectin-3 when glycodendrimers were absent from the solution. Taken together, these data support aggregate initiation as a response to specific carbohydrate binding interactions between lectin and glycodendrimer. They also reveal the significance of the N-terminal domain in formation of higher order aggregates.

The presence of these aggregates was confirmed by epifluorescence microscopy using galectin-3 fluorescently labelled with AlexaFluor 488 (A488gal-3, Figure 3). Following conjugation, the labelled galectin-3 was dialyzed against PBS to maintain identical conditions to DLS experiments. Size quantification using image analysis software (Pixcavator 6.0) and fluorescent microsphere standards (Dragon Green, Bangs Laboratories, Inc.) provided similar diameters as those obtained in DLS experiments (Figure 3, Table 1). The polydispersity calculated from the micrographs (Figure 4) was higher than that calculated by DLS, but this is likely due to sampling bias of DLS measurements as a result of attenuating the incident light (smaller particles that remain undetected in DLS were observed in microscopy images). For both methods, the trend of increasing size and polydispersity with increasing dendrimer generation was observed.

The aggregate size is remarkably large compared to galectin-3 and the dendrimers. The largest dendrimer used (generation 6) has a reported unfunctionalized diameter of 6.8 nm [32,33], and addition of the sugar adds about 4 nm to the overall diameter according to our DLS results with **5** (Table S3, Supporting Information File 1). The measured diameter of the CRD domain from the crystal structure of galectin-3 is roughly 3 nm [34]. The N-terminal domain consists of slightly fewer amino acids but is unstructured. Assuming the unstructured portion contributes about the same size or slightly more to the diameter of the protein as the CRD, the glycodendrimer complex would be expected to have a much smaller diameter than the observed values. Considering the large number of copies of dendrimer and protein that are required to form nanoparticle aggregates of the observed sizes, the aggregates are highly monodisperse. Although it has been previously determined using turbidity and precipitation assays that carbohydrate-functionalized dendrimers induce lectin aggregation, the consistent formation of large nanoparticles has to our knowledge not been previously identified and characterized.

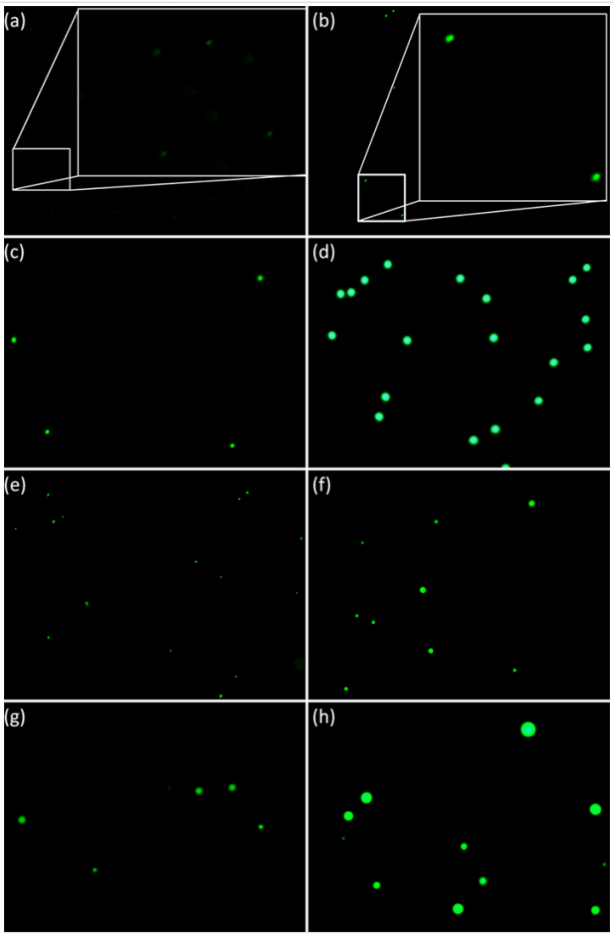

Figure 3: Fluorescence microscopy images of labelled particles. Microbead standards at similar exposure times are shown in (a)–(d); (a) 190 nm, inset is a 4× enlargement of selected area, (b) 520 nm, inset is a 4× enlargement of selected area, (c) 1020 nm and (d) 1900 nm. Aggregates formed after ca. 60 min incubation of Alexa 488 labelled galectin-3 (A488gal-3) with lactose-functionalized dendrimers are shown in (e)–(h); (e) A488gal-3 and **2**; (f) A488gal-3 and **3**; (g) A488gal-3 and **4**; (h) A488gal-3 and **5**. Exposure times of lectin–glycodendrimer aggregates are provided in Table S6, Supporting Information File 1.

The most likely explanation for the formation of large, monodisperse nanoparticle aggregates from galectin-3/glycodendrimer solutions is as follows. The glycodendrimer serves to nucleate the aggregation process through the specific binding of lactose into the carbohydrate binding site on galectin-3. Binding of the carbohydrate into the galectin-3 binding site must then be enabling protein–protein interactions. Some of these

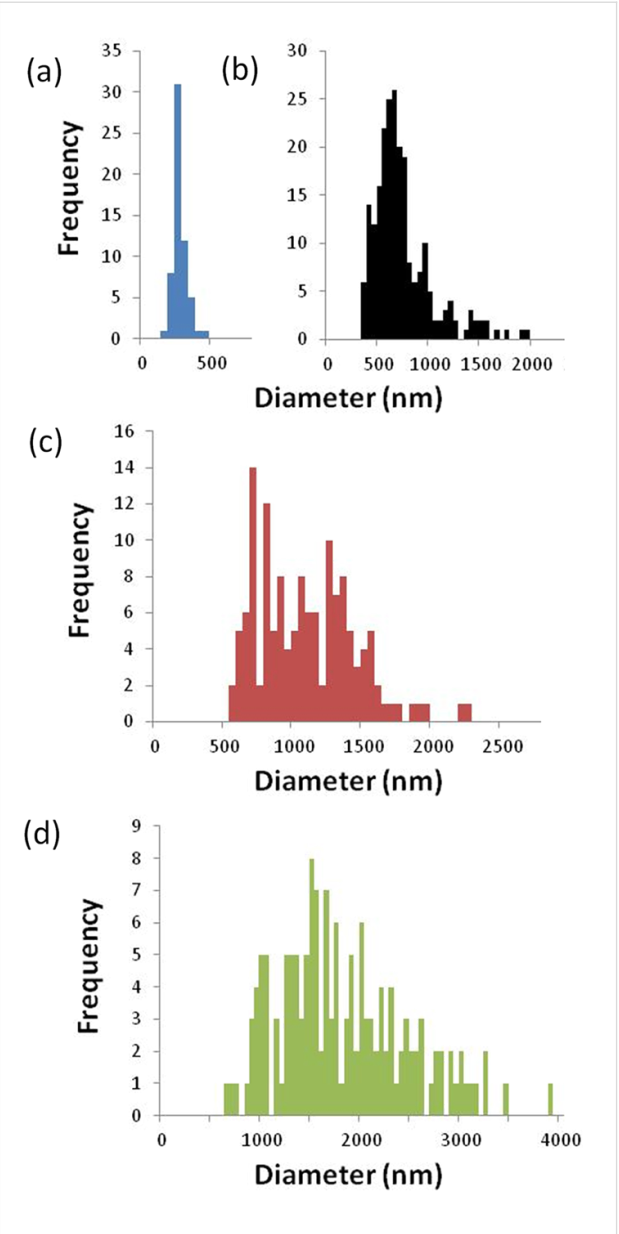

Figure 4: Aggregate diameter distribution of fluorescence microscopy images; 31 μM galectin-3 and 0.14 μM (a) **2**, (b) **3**, (c) **4** and (d) **5**.

protein–protein interactions may occur because of intertwining of the N-terminal domains that are now in close proximity. However, protein–protein interactions using the carbohydrate recognition domains of galectin-3 after an initial carbohydrate binding event is entirely consistent with a recently proposed binding mechanism [18], and is also consistent with proposed models for scaffold-mediated nucleation of protein signalling complexes [35].

Conclusion

In summary, β-lactoside functionalized PAMAM dendrimers **2**–**5** were synthesized and characterized. The presence of complex multivalent interactions between galectin-3 and lactose-functionalized dendrimers is indicated by the observation of large aggregates in DLS and epifluorescence experiments.

The large and relatively monodisperse nature of the glycodendrimer/galectin-3 aggregates that were formed (as determined by DLS and fluorescence microscopy) was dependent on both the dendrimer concentration and the generation. Third and fourth generation glycodendrimers formed smaller, more monodisperse aggregates, than sixth generation glycodendrimers. Aggregates formed at molar ratios of 9:1 galectin:glycodendrimer were largest while 220:1 and 3:1 ratios produced smaller complexes. The difference in aggregate sizes may relate to the size and shape complementarity between dendrimer and lectin or to the interplay of enthalpic and entropic contributions to aggregate formation as previously postulated [18,31,36]. Ongoing studies on the aggregate stoichiometry should provide valuable insight on this matter.

Overall, the results presented here indicate that clustering and aggregation events should be considered in addition to carbohydrate binding affinity for galectin-3, and also for other biological processes that are mediated by multivalent carbohydrate–protein interactions.

Experimental

General experimental methods

General reagents were purchased from Acros and Aldrich Chemical Companies. PAMAM dendrimers were purchased from Dendritech. Fluorescent microbead standards were purchased from Bangs Laboratories, Inc.. Dichloromethane was purified on basic alumina; other solvents were used as received. Silica gel (32–63 μm “40 micron flash”) for flash column chromatography purification was purchased from Scientific Adsorbants Incorporated.

5-Isothiocyanato-3-oxapentyl 2,3,4,6-tetra-*O*-acetyl-β-D-galactopyranosyl-[1→4]-2,3,6-tri-*O*-acetyl-β-D-glucopyranoside (**1**)

2,3,4,6-Tetra-*O*-acetyl-β-D-galactopyranose-[1→4]-1,2,3,6-tetra-*O*-acetyl-β-D-glucopyranose (4.4 g, 6.4 mmol) was dissolved in dry DMF (20 mL). Hydrazine acetate (0.77 g, 8.4 mmol) was added and the reaction mixture was heated to 55 °C for 1 h. The mixture was diluted into CH_2Cl_2 (20 mL) and washed with brine (2 × 10 mL) and water (2 × 10 mL), dried over $MgSO_4$, filtered and the solvent was removed in vacuo. The residual product was added to a solution of trichloroacetonitrile (3.34 g, 23.1 mmol) in CH_2Cl_2 (20 mL). After cooling the mixture in an ice bath, DBU (60 mg, 0.32 mmol) was added drop-wise and the mixture was stirred for 3 h. The reaction mixture was dissolved in CH_2Cl_2 (30 mL),

and the organic layer was washed with brine (2 × 10 mL) and water (2 × 10 mL), dried over $MgSO_4$, filtered and the solvent was removed in vacuo. The residual product was taken up in CH_2Cl_2 (50 mL) with 2-(2-isothiocyantoethoxy)ethanol (0.6 g, 4 mmol) and 4 Å molecular sieves. BF_3OEt_2 (0.6 g, 4 mmol) was added to the mixture over 30 min at 0 °C, and the reaction mixture was let stir and warmed to room temperature over 2 h. The solvent was removed and the residue was taken up in ethyl acetate (50 mL), washed with saturated aqueous $NaHCO_3$ solution (2 × 20 mL), brine (2 × 20 mL), and water (1 × 20 mL), dried over $MgSO_4$, filtered and the solvent was removed in vacuo. The oily residue was purified by silica gel column chromatography with a 60:40 ethyl acetate/hexanes eluent, followed by a 20:1 ethyl acetate/MeOH eluent to yield 2.6 g of product. ^{1}H NMR (300 MHz, $CDCl_3$) δ 5.33 (d, J = 3.1 Hz, 1H, H4'), 5.20 (app t, J = 9.3 Hz, 1H, H3), 5.09 (dd, J = 8.1 and 10.1 Hz, 1H, H2'), 4.93 (m, 2H, H2 and H3'), 4.50 (m, 3H, H1, H1' and H6), 4.06 (m, 4H), 3.89 (m, 6H), 3.78 (m, 3H), 3.63 (m, 6H), 2.13 (s, 3H), 2.10 (s, 3H), 2.04 (s, 3H), 2.02 (m, 9H), 1.95 (s, 3H). As reported [37].

General procedure for the synthesis of acetyl-protected lactose-functionalized dendrimers

An aqueous solution of amine terminated G(4)-PAMAM dendrimer (2.48 g of a 17% w/w solution in water, 421 mg, 31.2 μmol) was lyophilized to leave a foamy residue. 7.02 mL of DMSO was added to this residue to give a 60 mg/mL solution of the dendrimer. 0.47 mL of a 300 mM solution of **1** (184 mg, 141 μmol) was added to 0.5 mL of the 60 mg/mL G(4) PAMAM dendrimer (30 mg, 2.20 μmol) solution. The mixture was stirred for 8 h at which point a 75 μL aliquot was collected and lyophilized for MALDI–TOF and NMR analysis. The remainder of the reaction mixture was lyophilized and subjected to the deacetylation procedure. This procedure for carbohydrate functionalization of dendrimers was performed in a manner similar to our previously described procedure [29]. Amounts used in the syntheses of **2–5** are provided in Table S1, Supporting Information File 1. Characterization data for acetylated precursors of **2–5** are provided in Supporting Information File 1.

General procedure for deacetylation to afford lactose-functionalized dendrimers

To the lyophilized solid per-*O*-acetylated dendrimers, 1 mL of 1:1 water/methanol was added, at which point the dendrimer became a white precipitate. To this mixture was added 0.2 equiv of NaOMe (0.8 M in MeOH) for each peripheral carbohydrate, and let stir for 3 h. If, at this time, the mixture had not become a clear solution a further 0.2 equiv of NaOMe (0.8 M in MeOH) was added and this step was repeated until the mixture became a clear and colourless solution. Aqueous HCl (0.1 M) was then added slowly until the pH was ~7. This neutralized solution was placed in a dialysis membrane (MW cutoff 3500 Da) and dialyzed in 1 L of deionized water for 8 h. The water was changed and let stand for a further 8 h twice more. The remaining liquid in the membrane was frozen and lyophilized to give a white fluffy solid. This procedure for deacetylation was performed in a manner similar to our previously described procedure [29]. Characterization data for dendrimers is provided in Supporting Information File 1.

NMR spectroscopy

^{1}H NMR spectra were recorded on Bruker DPX 300 (300 MHz) and Bruker DPX-500 (500 MHz) spectrometers. Chemical shifts are reported in ppm from tetramethylsilane with the residual protic solvent resonance as the internal standard (chloroform: δ 7.25 ppm; dimethyl sulfoxide: δ 2.50 ppm). Data are reported as follows: chemical shift, multiplicity (s = singlet, bs = broad singlet, d = doublet, t = triplet, q = quartet, p = pentet, m = multiplet, app = apparent), integration, coupling constants (in Hz) and assignments. Sample NMR spectra are provided in Figures S2 through S6, Supporting Information File 1.

MALDI–TOF mass spectrometry

MALDI mass spectra were acquired using a Bruker Biflex-III time-of-flight mass spectrometer. Spectra of all-functionalized dendrimers were obtained using a *trans*-3-indolacrylic acid matrix with a matrix:analyte ratio of 3000:1 or 1000:1. Bovine serum albumin (M_w 66,431 g/mol), cytochrome C (M_w 12,361 g/mol), and trypsinogen (M_w 23,982 g/mol) were used as external standards. An aliquot corresponding to 12–15 pmol of the analyte was deposited on the laser target. Positive ion mass spectra were acquired in linear mode and the ions were generated by using a nitrogen laser (337 nm) pulsed at 3 Hz with a pulse width of 3 nanoseconds. Ions were accelerated at 19,000–20,000 volts and amplified using a discrete dynode multiplier. Spectra (100 to 200) were summed into a LeCroy LSA1000 high-speed signal digitizer. All data processing was performed using Bruker XMass/XTOF V 5.0.2. Molecular mass data and polydispersities (PDI) of the broad peaks were calculated by using the Polymer Module included in the software package. The peaks were analysed using the continuous mode. M_w values for **2–5** are provided in Table S2, Supporting Information File 1.

Dynamic light scattering (DLS)

DLS measurements were acquired with the Brookhaven 90Plus Particle Size Analyzer equipped with a 15 mW solid state, 633 nm laser and upgraded APD detector. Scattered light was detected at 90° incidence and optimized to a count rate of 200–400 kilocounts per second (kcps) through adjustment of a neutral density filter prior to the sample chamber. The intensity

was maximized for samples producing less than 200 kcps. Temperature control was stabilized at 25 °C, and each sample was scanned for 5 min (3 min for control samples). Autocorrelation curves were analyzed via the provided software using the method of cumulants (quadratic fit) unless otherwise noted. This provided the effective diameter and relative variance reported below. For dust-free, relatively monodispersed samples, this analysis provided results similar to NNLS and CONTIN algorithms. Protocols for preparation of solutions and a brief discussion of the theory for DLS are provided in Supporting Information File 1. Representative fitted data is shown in Supporting Information Fle 1, Figure S7 for **4** and **5**.

Fluorescence microscopy

Fluorescence images were captured on either a Nikon Eclipse TE2000-U with a 60× oil immersion objective lens (**2**, **3**, **4**) or Olympus BX-61 with a 100× oil immersion objective (**3**, **4**, **5**). Exposure time was optimized for each sample and 20–30 images were taken. These images were combined using Gimp 2 image manipulation software. Fluorescent microsphere standards (190, 520, 1020, and 1900 nm, Bangs Laboratories, Inc.) were used to calibrate the measured particle perimeter (pixels) to particle diameter (nm) for each exposure setting (Supporting Information File 1, Figure S8, equations in Table S4). Diameters of standards were verified with DLS (Table S5, Supporting Information File 1). The imaged particle perimeters were determined through Pixcavator Image Analysis software (Intelligent Perception). The y-intercept of each calibration curve represents the lower detection limit for the given exposure time. Protocols for preparation of samples for fluorescence microscopy are provided in Supporting Information File 1.

Supporting Information

Supporting Information File 1

Amounts of reagents used in glycodendrimer syntheses; characterization data for glycodendrimers; sample calculations; detailed protocols for galectin-3 isolation and solution and sample preparations; sample NMR spectra; characterization data for glycodendrimer aggregates.
[http://www.beilstein-journals.org/bjoc/content/supplementary/1860-5397-10-162-S1.pdf]

Acknowledgements

This research was supported by NIH GM62444 and NSF 1214134. We thank Dr. Sandra Halonen and Dr. Trevor Douglas for making their instruments available for use, Anna Michel for synthesis work and assistance with Pixcavator, Jenni Monaco for help preparing the Alexa488 galectin-3 conjugate, and Julie Sprenger, Julianna Weiel, and Kylene Compton for producing galectin-3. This paper is dedicated to the memory of Chris Wolfenden, who courageously battled cancer.

References

1. Mammen, M.; Choi, S.-K.; Whitesides, G. M. *Angew. Chem., Int. Ed.* **1998,** *37,* 2754–2794. doi:10.1002/(SICI)1521-3773(19981102)37:20<2754::AID-ANIE2754>3.0.CO;2-3
2. Choi, S.-K. *Synthetic multivalent molecules;* Wiley: New York, 2004. doi:10.1002/0471578908
3. Klyosov, A. A.; Zbigniew, D. P.; Witczak, J.; Platt, D. *Galectins;* John Wiley and Sons, 2008. doi:10.1002/9780470378076
4. Barondes, S. H.; Castronovo, V.; Cooper, D. N. W.; Cummings, R. D.; Drickamer, K.; Feizi, T.; Gitt, M. A.; Hirabayashi, J.; Hughes, C.; Kasai, K.; Leffler, H.; Liu, F.-T.; Lotan, R.; Mercurio, A. M.; Monsigny, M.; Pillai, S.; Poirer, F.; Raz, A.; Rigby, P. W. J.; Rini, J. M.; Wang, J. L. *Cell* **1994,** *76,* 597–598. doi:10.1016/0092-8674(94)90498-7
5. Barondes, S. H.; Cooper, D. N. W.; Gitt, M. A.; Leffler, H. *J. Biol. Chem.* **1994,** *269,* 20807–20810.
6. Gray, C. A.; Adelson, D. L.; Bazer, F. W.; Burghardt, R. C.; Meeusen, E. N. T.; Spencer, T. E. *Proc. Natl. Acad. Sci. U. S. A.* **2004,** *101,* 7982–7987. doi:10.1073/pnas.0402669101
7. Kasai, K.; Hirabayashi, J. *J. Biochem.* **1996,** *119,* 1–8. doi:10.1093/oxfordjournals.jbchem.a021192
8. Ochieng, J.; Furtak, V.; Lukyanov, P. *Glycoconjugate J.* **2002,** *19,* 527–535. doi:10.1023/B:GLYC.0000014082.99675.2f
9. Califice, S.; Castronovo, V.; Van Den Brule, F. *Int. J. Oncol.* **2004,** *25,* 983–992.
10. Stillman, B. N.; Hsu, D. K.; Pang, M.; Brewer, C. F.; Johnson, P.; Liu, F.-T.; Baum, L. G. *J. Immunol.* **2006,** *176,* 778–789. doi:10.4049/jimmunol.176.2.778
11. Friedrichs, J.; Manninen, A.; Muller, D. J.; Helenius, J. *J. Biol. Chem.* **2008,** *283,* 32264–32272. doi:10.1074/jbc.M803634200
12. Delacour, D.; Greb, C.; Koch, A.; Salomonsson, E.; Leffler, H.; Le Bivic, A.; Jacob, R. *Traffic* **2007,** *8,* 379–388. doi:10.1111/j.1600-0854.2007.00539.x
13. Nieminen, J.; Kuno, A.; Hirabayashi, J.; Sato, S. *J. Biol. Chem.* **2007,** *282,* 1374–1383. doi:10.1074/jbc.M604506200
14. Nangia-Makker, P.; Raz, T.; Tait, L.; Hogan, V.; Fridman, R.; Raz, A. *Cancer Res.* **2007,** *67,* 11760–11768. doi:10.1158/0008-5472.CAN-07-3233
15. Ahmad, N.; Gabius, H.-J.; André, S.; Kaltner, H.; Sabesan, S.; Roy, R.; Liu, B.; Macaluso, F.; Brewer, C. F. *J. Biol. Chem.* **2004,** *279,* 10841–10847. doi:10.1074/jbc.M312834200
16. Ochieng, J.; Platt, D.; Tait, L.; Hogan, V.; Raz, T.; Carmi, P.; Raz, A. *Biochemistry* **1993,** *32,* 4455–4460. doi:10.1021/bi00067a038
17. Kuklinski, S.; Probstmeier, R. *J. Neurochem.* **1998,** *70,* 814–823. doi:10.1046/j.1471-4159.1998.70020814.x
18. Lepur, A.; Salomonsson, E.; Nilsson, U. J.; Leffler, H. *J. Biol. Chem.* **2012,** *287,* 21751–21756. doi:10.1074/jbc.C112.358002
19. Fermino, M. L.; Polli, C. D.; Toledo, K. A.; Liu, F.-T.; Hsu, D. K.; Roque-Barreira, M. C.; Pereira-da-Silva, G.; Bernardes, E. S.; Halbwachs-Mecarelli, L. *PLoS One* **2011,** *6,* e26004. doi:10.1371/journal.pone.0026004
20. Quattroni, P.; Li, Y.; Lucchesi, D.; Lucas, S.; Hood, D. W.; Herrmann, M.; Gabius, H.-J.; Tang, C. M.; Exley, R. M. *Cell. Microbiol.* **2012,** *14,* 1657–1675. doi:10.1111/j.1462-5822.2012.01838.x

21. Kavanaugh, D.; Kane, M.; Joshi, L.; Hickey, R. M. *Appl. Environ. Microbiol.* **2013,** *79,* 3507–3510. doi:10.1128/AEM.03694-12
22. Sörme, P.; Arnoux, P.; Kahl-Knutsson, B.; Leffler, H.; Rini, J. M.; Nilsson, U. J. *J. Am. Chem. Soc.* **2005,** *127,* 1737–1743. doi:10.1021/ja043475p
23. Ahmad, N.; Gabius, H.-J.; Sabesan, S.; Oscarson, S.; Brewer, C. F. *Glycobiology* **2004,** *14,* 817–825. doi:10.1093/glycob/cwh095
24. Tellez-Sanz, R.; Garcia-Fuentes, L.; Vargas-Berenguel, A. *Curr. Med. Chem.* **2013,** *20,* 2979–2990. doi:10.2174/09298673113209990163
25. Kopitz, J.; Bergmann, M.; Gabius, H.-J. *IUBMB Life* **2010,** *62,* 624–628. doi:10.1002/iub.358
26. Newkome, G. R.; Moorefield, C. N.; Vögtle, F. *Dendrimers and Dendrons: Concepts, Syntheses, Applications;* Wiley-VCH: Weinheim, 2001. doi:10.1002/3527600612
27. Labieniec, M.; Watala, C. *Cent. Eur. J. Biol.* **2009,** *4,* 434–451. doi:10.2478/s11535-009-0056-7
28. Pourianazar, N. T.; Mutlu, P.; Gunduz, U. *J. Nanopart. Res.* **2014,** *16,* No. 2342. doi:10.1007/s11051-014-2342-1
29. Wolfenden, M. L.; Cloninger, M. J. *Bioconjugate Chem.* **2006,** *17,* 958–966. doi:10.1021/bc060107x
30. Walter, E. D.; Sebby, K. B.; Usselman, R. J.; Singel, D. J.; Cloninger, M. J. *J. Phys. Chem. B* **2005,** *109,* 21532–21538. doi:10.1021/jp0515683
31. Ottaviani, M. F.; Cangiotti, M.; Fiorani, L.; Fattori, A.; Wasiak, T.; Appelhans, D.; Klajnert, B. *Curr. Med. Chem.* **2012,** *19,* 5907–5921. doi:10.2174/092986712804143259
32. Jackson, C. L.; Chanzy, H. D.; Booy, F. P.; Drake, B. J.; Tomalia, D. A.; Bauer, B. J.; Amis, E. J. *Macromolecules* **1998,** *31,* 6259–6265. doi:10.1021/ma9806155
33. Tomalia, D. A.; Naylor, A. M.; Goddard, W. A., III. *Angew. Chem., Int. Ed. Engl.* **1990,** *29,* 138–175. doi:10.1002/anie.199001381
34. Seetharaman, J.; Kanigsberg, A.; Slaaby, R.; Leffler, H.; Barondes, S. H.; Rini, J. M. *J. Biol. Chem.* **1998,** *273,* 13047–13052. doi:10.1074/jbc.273.21.13047
35. Yang, J.; Hlavacek, W. S. *Math. Biosci.* **2011,** *232,* 164–173. doi:10.1016/j.mbs.2011.06.003
36. Schlick, K. H.; Lange, C. K.; Gillispie, G. D.; Cloninger, M. J. *J. Am. Chem. Soc.* **2009,** *131,* 16608–16609. doi:10.1021/ja904073p
37. Seah, N.; Santacroce, P. V.; Basu, A. *Org. Lett.* **2009,** *11,* 559–562. doi:10.1021/ol802613r

License and Terms

BEILSTEIN JOURNAL OF ORGANIC CHEMISTRY

Photoswitchable precision glycooligomers and their lectin binding

Daniela Ponader[1], Sinaida Igde[1], Marko Wehle[2], Katharina Märker[1], Mark Santer[2], David Bléger[*3] and Laura Hartmann[*1]

Full Research Paper

Open Access

Address:
[1]Max Planck Institute of Colloids and Interfaces, Department of Biomolecular Systems, Research Campus Golm, 14424 Potsdam, Germany, [2]Max Planck Institute of Colloids and Interfaces, Department of Theory & Bio-Systems, Research Campus Golm, 14424 Potsdam, Germany and [3]Humboldt University, Department of Chemistry, Brook-Taylor-Str. 2, 12489 Berlin, Germany

Email:
David Bléger[*] - david.bleger@chemie.hu-berlin.de; Laura Hartmann[*] - laura.hartmann@mpikg.mpg.de

* Corresponding author

Keywords:
azobenzene; glycopolymer; lectin binding; multivalency; multivalent glycosystems; photoswitch; precision polymer

Beilstein J. Org. Chem. **2014,** *10,* 1603–1612.
doi:10.3762/bjoc.10.166

Received: 28 February 2014
Accepted: 17 June 2014
Published: 15 July 2014

This article is part of the Thematic Series "Multivalent glycosystems for nanoscience".

Guest Editor: B. Turnbull

Abstract

The synthesis of photoswitchable glycooligomers is presented by applying solid-phase polymer synthesis and functional building blocks. The obtained glycoligands are monodisperse and present azobenzene moieties as well as sugar ligands at defined positions within the oligomeric backbone and side chains, respectively. We show that the combination of molecular precision together with the photoswitchable properties of the azobenzene unit allows for the photosensitive control of glycoligand binding to protein receptors. These stimuli-sensitive glycoligands promote the understanding of multivalent binding and will be further developed as novel biosensors.

Introduction

Carbohydrate ligand–receptor interactions underpin many important processes in biology, for example in host-pathogen interactions [1,2]. Although monosaccharides usually exhibit only low binding affinities, nature is able to obtain high affinity carbohydrate ligands by displaying several monosaccharides/oligosaccharides on a protein scaffold or through a patch of lipids. This is known as the glycocluster effect or the multivalent presentation of sugar ligands [3,4]. This strategy can also be employed for the synthesis of carbohydrate mimetics, where several sugar ligands are attached to a non-natural scaffold. Glycopolymers where natural sugar ligands are presented along a synthetic polymer chain are an emerging class of carbohydrate mimetics [5]. Such glycopolymers offer great potential for various biotechnological and biomedical applications, for

antiviral and antibacterial treatments [6]. However, most of these systems are optimized empirically and very little is known about the underlying structure–property relations of glycopolymers. Due to their inherent polydisperse nature and the limitation in controlling precise positioning of functionalities along the backbone, polymer scaffolds make it particularly difficult to correlate their chemical structure with the resulting binding properties.

Recently, we introduced a novel synthetic approach towards monodisperse, sequence-defined glycooligomers, so-called precision glycomacromolecules, via the combination of solid phase polymer synthesis and tailor-made building blocks [7-9]. Through a stepwise assembly of our functional building blocks, we can now control the kind, number, and spacing of sugar ligands along a monodisperse scaffold. Thus, our precision glycomacromolecules allow for direct structure–property correlations and a deeper insight into the multivalent binding of glycomimetics. Through this knowledge we can predict the resulting affinity of a glycomacromolecule based on the number and spacing of sugar ligands attached to the scaffold [7,10,11]. Furthermore, it would be highly interesting to also modulate the binding affinity of a single molecule through a structural change as a response to an external stimulus, for example light.

In order to gain such control over the binding affinity of glycooligomers towards specific lectins, a few studies have recently been dedicated to the construction of photoactive glycoligand incorporating a light-sensitive unit [12-15]. The possibility to photomodulate the complexation of a ligand could lead to a deeper understanding of the typically multivalent binding processes of carbohydrates to proteins, in addition to offer potential perspectives for the sensing and adhesion of bacteriological targets on various substrates. The examples reported so far make use of azobenzene [16], a well-known photochromic compound offering robustness and straightforward preparation. It is able to reversibly isomerize between an extended and planar form (*E*-isomer, thermodynamically favored) and a more compact and twisted state (*Z*-isomer). Monovalent [15] and divalent [16] photoswitchable glycoconjugates described in the literature showed a different binding behavior depending on the configuration of the azobenzene (*E* or *Z*), although the effect was rather modest.

We anticipated that the photomodulation of the binding activity could be enhanced within more complex architectures, i.e., divalent and trivalent glycooligomers incorporating one or two photoswicthes in the backbone, as a result of a large photoinduced geometrical change in the oligomer shape and concomitantly in the sugar ligands accessibility. Indeed, dramatic shrinking of rigid-rod polymers for example, occurs upon photoirradiation when several azobenzenes are introduced in the main-chain, the embedded photoswitches acting as hinges [17,18].

In the present study, an azobenzene functionalized with an Fmoc-protected aminomethyl group and a carboxylic acid both *para* to the N=N bond was used as one building block during solid-phase polymer synthesis of precision glycomacromolecules (see AZO, Figure 1) [19-22]. The benzylamine fragment was favored over the phenylamine one for two reasons: first, its higher nucleophilicity allows for a smoother synthesis and

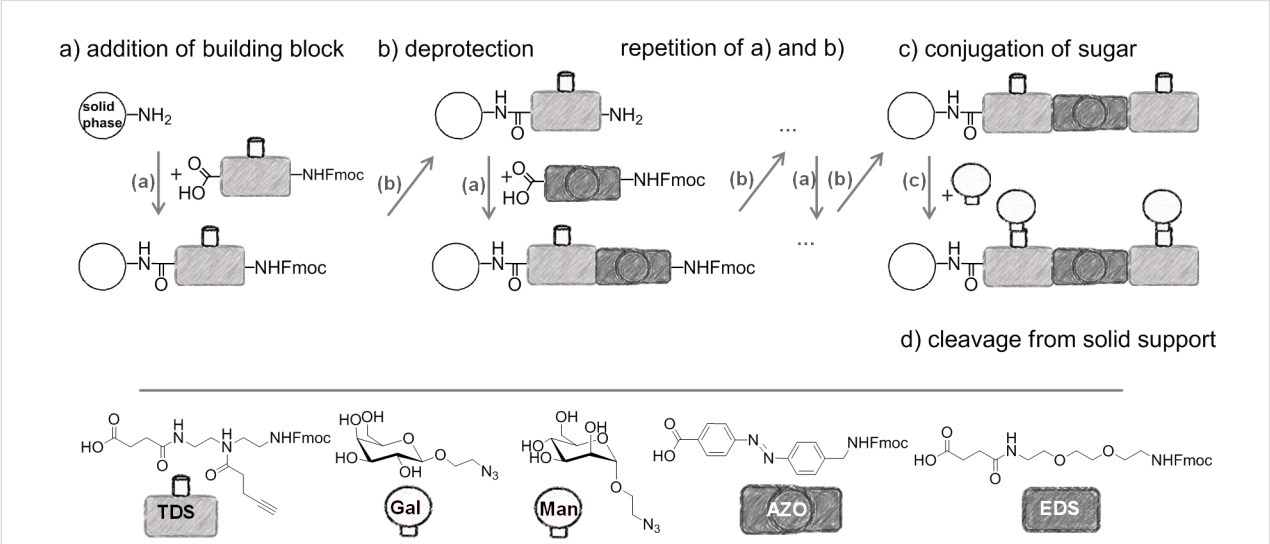

Figure 1: Synthesis of photoswitchable precision glycooligomers via stepwise addition of building blocks on solid support followed by on-resin functionalization of alkyne side chains with sugar azide ligands and final cleavage from the support.

second, the resulting *Z*-azobenzene exhibits a high thermal stability as compared to the fully conjugated push-pull azobenzene based on the phenylamine fragment. In total, five precision glycooligomers were synthesized containing up to two azobenzene units in the oligomeric backbone and presenting galactose residues in the side chains. As control structures, glycooligomers containing either a hydrophilic flexible linker unit instead of the azobenzene moiety, or mannose instead of galactose ligands were synthesized. The photoswitchable behavior of all azobenzene-containing glycooligomers was evaluated along with their photoswitchable binding affinities towards PA-IL (also called LecA) as targeted lectin receptor [23].

Results and Discussion

Synthesis of photoswitchable precision glycooligomers

The synthesis of photoswitchable precision glycooligomers is based on the previously developed solid-phase assembly of functional dimer building blocks [7,24,25]. The term dimer building block refers to the coupling of diacid and diamine building blocks in solution prior to solid phase coupling. The obtained building blocks contain a free carboxy- and an Fmoc-protected amino group and thus can be coupled via standard peptide coupling protocols giving a polyamide backbone. Additionally, dimer building blocks can carry functional groups as side groups or in the main chain, thereby allowing for the conjugation of sugar ligands and the control of the backbone properties. Three different dimer building blocks were employed for the synthesis of the photoswitchable glycooligomers: the triple bond-functionalized building block TDS [7], an ethylene glycol spacer building block EDS [7], and the photoswitchable building block AZO. TDS allows for the conjugation of sugar azide ligands via the copper-catalyzed azide–alkyne cycloaddition (CuAAC). The synthesis and coupling on solid support of TDS and EDS has been previously described [7,10]. AZO was synthesized via Mills coupling adapting literature protocols [20-22].

Five glycooligomers were synthesized – three photoswitchable glycooligomers containing the AZO building-block and two non-switchable control structures containing EDS instead of AZO (Table 1). The synthesis proceeded following standard peptide coupling protocols followed by introduction of the sugar ligands (Figure 1): Starting from an ethylenediamine functionalized trityl resin (0.0125 mmol), the first building block, i.e., TDS (8 equiv) was attached via activation with PyBOP/HOBt (8 equiv/4 equiv) and DIPEA (16 equiv) in DMF and subsequent coupling for 1 hour. After a washing step, the terminal Fmoc protecting group was cleaved by treatment with 25% piperidine in DMF three times for 5, 10 and 15 minutes. After complete removal of the Fmoc protecting group, the second building block (AZO or EDS) was coupled following the same reaction conditions. After repetition of the coupling/deprotection steps, the oligomeric backbone was formed on the solid support. In the next step, the sugar ligands were introduced to the oligomeric backbone via CuAAC. To this end, two sugar azides (2-azidoethyl galactoside and 2-azidoethyl mannoside) were previously synthesized following literature protocols [26]. 8 equiv of sugar azide, 20 mol % sodium ascorbate and 20 mol % $CuSO_4$ per alkyne group were dissolved in DMF/H_2O, added to the resin and shaken for 4 hours. Excess reagents as well as the copper catalyst were removed by washing with a 23 mM solution of sodium diethyl dithiocarbamate in DMF as well as water and DCM. The final precision glycooligomers were obtained after cleavage from the resin using 30 vol % TFA in DCM and isolated after precipitation from cold Et_2O. Crude products containing AZO building blocks were obtained with ~80% purity as determined by RP-HPLC (see Supporting Information File 1) and further purified by preparative RP-HPLC. Glycooligomers containing EDS building blocks were obtained in high purity (>95%) directly after cleavage. After purification, all final products were obtained in ~60% yield and >90% purity as confirmed by ESIMS, HPLC and NMR (see Supporting Information File 1).

Characterization of the photoswitchable properties

The photochromic behavior of the newly synthesized AZO-glycooligomers was investigated by UV–vis absorption spectroscopy and ultraperformance liquid chromatography (UPLC). Aqueous solutions of **Azo-Gal(1,3)-3** and **Azo-Gal(1,3,5)-5** (the compounds were dissolved in the buffer used for the SPR measurements, see Supporting Information File 1 for the details) were irradiated at λ = 360 nm to induce the $E \rightarrow Z$ isomerization. The typical decrease of the $\pi \rightarrow \pi^*$ band at 330 nm and increase of the $n \rightarrow \pi^*$ band centered at 440 nm was observed in the UV–vis absorbance spectra of both photoswitchable glycooligomers (see Figure 2 for the spectrum of **Azo-Gal(1,3,5)-5**). The presence of well-defined isosbestic points at 290 nm and 395 nm indicates a clean photoisomerization process. The composition at the photostationary state (PSS) was analyzed by UPLC using integration of the UV signal at the wavelengths of the isosbestic points. Starting from an **Azo-Gal(1,3,5)-5** aqueous solution containing mainly the *E,E*-isomer, irradiation in the UV-region led to a majority of *Z,Z*-isomer (70%), together with significant quantities of mixed isomers (10% of *E,Z* and 10% of *Z,E*), whereas 10% of *E,E*-isomer did not isomerize (see Supporting Information File 1 for more details). This values correspond to a total amount of 80% of *Z*-azobenzenes in the PSS mixture, in accordance to the 78% of *Z*-azobenzene found in the PSS solution of **Azo-Gal(1,3)-3**

Table 1: List of photoswitchable precision glycooligomers obtained via solid phase polymer synthesis.

Entry	Sample name	Chemical structure
1	 Azo-Gal(1,3)-3	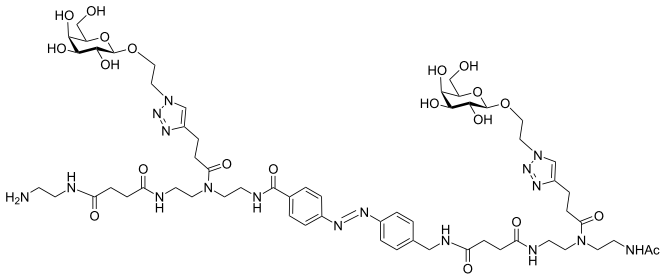
2	 Azo-Gal(1,3,5)-5	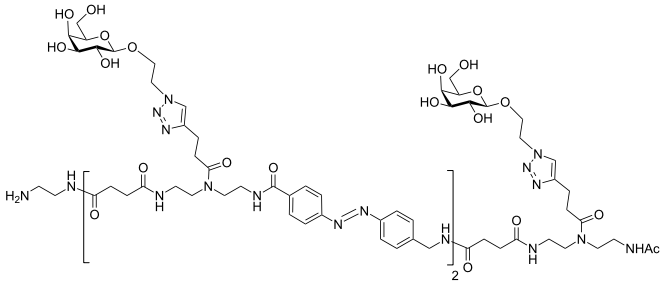
3	 Azo-Man(1,3,5)-5	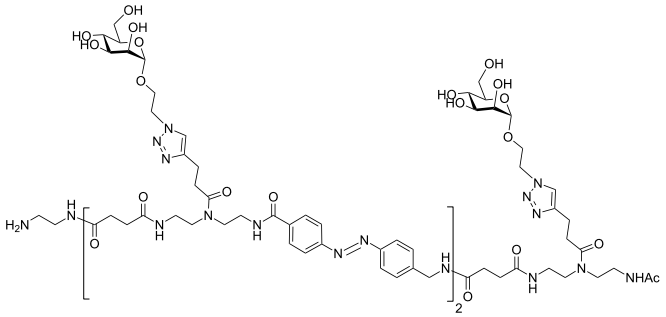
4	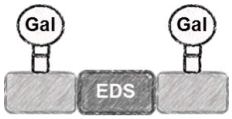 EDS-Gal(1,3)-3	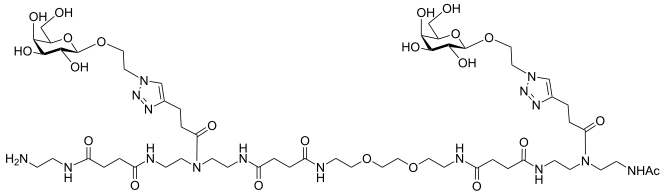
5	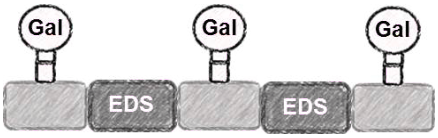 EDS-Gal(1,3,5)-5	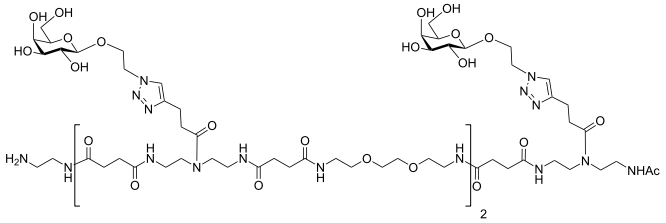

upon irradiation at 360 nm, indicating that the two photochromic units of **Azo-Gal(1,3,5)-5** operate independently. The $Z \rightarrow E$ back-isomerization was triggered upon illumination at λ > 400 nm, leading to solutions containing 92% of *E*-isomers. Further *Z*/*E* isomerization cycles could be performed similarly without affecting the PSS ratio, demonstrating the reversibility of the systems. Finally, the thermal stability of *Z*-**Azo-Gal(1,3)-3** in the buffer solution is quite high. Indeed, after 48 h at 25 °C only 12% of the *Z*-isomers converted back to the *E*-isomer (see Supporting Information File 1). The thermal stability of the trivalent **Azo-Gal(1,3,5)-5** *Z*-isomers is anticipated to be very similar since their two azo units were found to operate indepen-

dently. The long-lived *Z*-forms of these glycoconjugates allows for a convenient handling of the PSS mixtures and a precise measurement of their binding affinities.

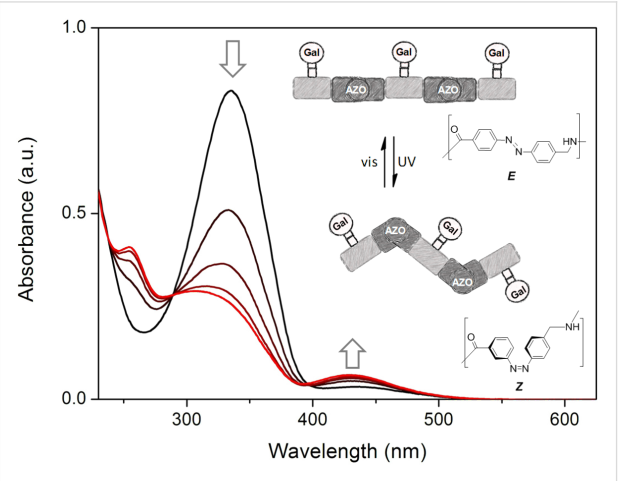

Figure 2: Characterization of the *E* → *Z* photoisomerization (λ = 360 nm) of **Azo-Gal(1,3,5)-5** in buffer solution at 25 °C via UV–vis absorption spectroscopy measurements.

Lectin binding studies

Competition binding assay

After the photophysical characterization of the new glycooligomers containing photoswitchable azobenzene moieties in the backbone, their ability to bind to a protein receptor via their sugar ligands was investigated. Depending on the properties of the backbone (EDS vs AZO moieties and *E*- vs *Z*-configuration), we can expect differences in the glycooligomer-receptor binding mode and thus in the resulting glycooligomer ligand affinity.

As targeted receptor, we chose PA-IL, a tetrameric, calcium dependent lectin specifically binding to α-galactoside and β-galactoside structures [27]. It is composed of 121 amino acids (51 kDa) associated as homotetramers [28]. The crystal structure reveals a tetrameric arrangement with a general rectangular shape with the smaller distance of binding sites being 2.6 nm and the longer one being 7.9 nm [27]. Thus, in the *E*-configuration, the distance between two neighboring sugar ligands on the di- and trivalent glycooligomers can span the distance of two neighboring binding sites and potentially allow for chelate binding (see Figure 3). Upon switching to the *Z*-configuration this distance will decrease and therefore can be expected to strongly impact the ligand–receptor binding and thus the resulting binding affinity.

In order to determine the binding affinity of the precision glycooligomers to PA-IL, surface plasmon resonance (SPR) experiments were performed. At first, an inhibition/competition assay was carried out. The SPR chip was modified with a β-D-galactose-polymer and α-D-mannose-polymer as negative control (see Supporting Information File 1). In a first experiment, binding of PA-IL (1 μM) to the chip was determined and set as 100%. In a second set of experiments, binding of preincubated mixtures of PA-IL (1 μM) and glycooligomers at serial dilutions (400 μM to 0.1 μM) were measured. Binding of glycooligomer to PA-IL resulted in a decrease of PA-IL binding on the chip. Plotting this concentration dependent decrease in binding against time, sigmoidal curves were obtained and fitted with the Hill equation. The inhibitory concentration at 50% binding (IC_{50}) was derived for the different glycooligomers (Table 2).

Table 2: IC_{50} values obtained by SPR inhibition/competition assays of the photoswitchable glycooligomers and control structures.

#	Compound name		IC_{50} [μM]
1	**AZO-Gal(1,3)-3**	*E*	5.7 ± 1.7
		PSS[a]	9.4 ± 0.1
2	**AZO-Gal(1,3,5)-5**	*E*	3.4 ± 0.4
		PSS[a]	4.1 ± 1.3
3	**AZO-Man(1,3,5)-5**		n.b.[b]
4	**EDS-Gal(1,3)-3**		3.2 ± 0.2
5	**EDS-Gal(1,3,5)-5**		2.0 ± 0.6
6	**β-Me-Gal**		55 ± 6

[a]PSS: photostationary state @ 360 nm; [b]n.b.: no binding.

All galactose-containing glycooligomers can bind to PA-IL. The mannose-containing control oligomer does not show any binding. This confirms that the backbone itself does not undergo non-specific interactions with the receptor, as we could previously also show for glycooligomers binding to Concanavalin A (Con A) lectin receptor [7,10,11]. All multivalent glycooligomers show a decrease in IC_{50}, i.e., an increase in binding affinity in comparison to the monovalent β-methyl galactoside. Overall, IC_{50} values are in the μM range, with the EDS based di- and trivalent glycooligomers giving the highest binding affinity with IC_{50} values of 2.0 and 3.2 μM, respectively. The corresponding di- and trivalent oligomers containing the AZO spacer instead of the EDS unit show higher IC_{50} values for both *E*- and *Z*-isomers, i.e., a slightly less favorable binding to the receptor.

Comparing the binding behavior of the *E*-glycooligomers vs their corresponding PSS mixtures, we see that the IC_{50} values for the divalent glycooligomer **Azo-Gal(1,3)-3** shows a significant decrease in binding affinity upon switching (entry 1 Table 2), whereas the trivalent glycooligomer **Azo-Gal(1,3,5)-5** binds with the same affinity before and after switching (entry 2

Table 2). In order to gain a first insight into the possible conformations of the glycooligomers and thus their potential binding modes, we performed molecular modeling as outlined in the caption of Figure 3. This data suggests that the trivalent **Azo-Gal(1,3,5)-5** can bind with two sugar ligands to the PA-IL receptor in both *E* and *Z*-configurations. In the all-*E* configuration two neighboring sugar ligands can span the distance of two neighboring binding sites (Figure 3a). Through the change in conformation for the all-*Z* configuration, the overall distance between the sugar ligands decreases, now presenting the two terminal sugar ligands with the same distance as the neighboring sugar ligands in the *E*-configuration (Figure 3b), and thus again allowing for a bivalent binding to the receptor. This model is supported by the experimental finding that there is no change in binding affinity from the *E*- to the *Z*-glycooligomer.

In contrast to this, the divalent glycooligomer (**Azo-Gal(1,3)-3**) shows a significant decrease in binding affinity from an IC_{50} value of 5.7 ± 1.7 μM for the *E*-form to 9.4 ± 0.1 μM in the PSS. This indicates a change in the accessibility of the sugar ligands for receptor binding, with the *Z*-oligomer having a less accessible conformation. Following the same model as for the trivalent ligand, the divalent ligand has the opportunity to bind in a bivalent fashion in its *E*-form (Figure 3a) while the *Z*-form only allows for a monovalent binding of one of the sugars to the protein receptor (Figure 3b). Such a change in binding mode is expected to lead to the observed decrease in binding affinity. It is important to note that additional binding modes might contribute to the multivalent binding of the glycooligomer ligands as well. Further studies will evaluate in more detail different potential binding modes such as chelate binding, intermolecular crosslinking, and rebinding effects.

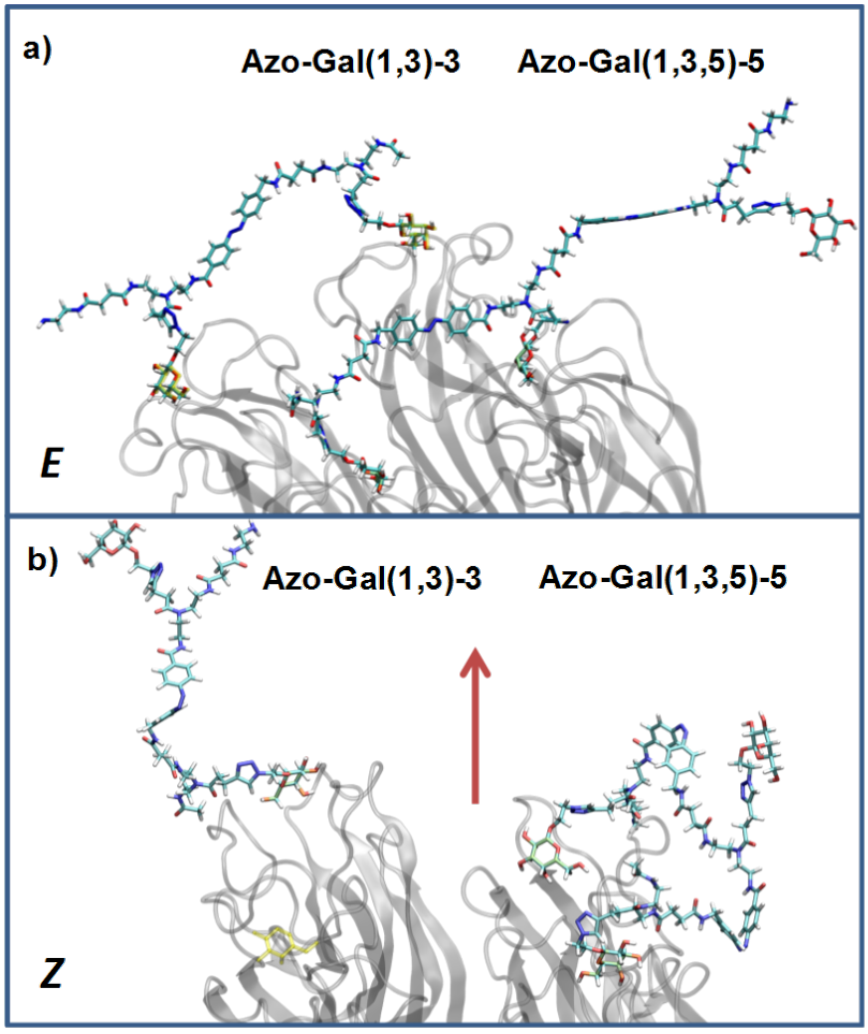

Figure 3: Structural models of **Azo-Gal(1,3)-3** and **Azo-Gal(1,3,5)-5** in (a) *E*- and (b) all-*Z*-configurations of the connecting azobenzene groups. The dimer is shown to the left, the trimer to the right. To facilitate the representation in (b), the whole complex has been rotated around the indicated in-plane axis (arrow). The PA-IL protein structure has been inferred from the Protein Data Bank (PDB code 4ljh).

In order to approach practical applications of a photoswitchable device that could modulate its binding affinity towards PA-IL lectins on demand, we were intrigued in the ability of our light-responsive systems to work when immobilized on a surface. To this end we attached the photoswitchable precision glycooligomers directly to the SPR chip and performed a second set of lectin binding experiments using SPR and measuring PA-IL binding on the chip. The glycooligomers were covalently linked to the chip via their terminal amine group and the simultaneous activation of the carboxyl-functionalized chip surface as *N*-hydroxysuccinimide (NHS) ester (see Supporting Information File 1). Successful functionalization was monitored by SPR. Photoswitching of the glycooligomers was realized either ex situ prior to surface functionalization or in situ by direct irradiation of the functionalized chip. The equilibrium constant K_D was obtained by fitting the obtained binding values at the turning point between binding- and dissociation-curve with a steady-state affinity model (Biacore T100 Evaluation Software 2.0.3). In agreement with the previously determined IC_{50} values, all K_D values are in the μM range.

We observed a significant difference for the ex situ irradiated samples in comparison to irradiation of the glycooligomers directly on the chip. The K_D values showed no difference in binding affinity between *E*- and *Z*-isomers when the chip was irradiated directly. This indicates that either the light could not penetrate efficiently through the organic layer of the chip, or more likely that photoswitching was prohibited due to a lack of conformational freedom, as often observed in the solid state. However, for the ex situ irradiated glycooligomers, we observed a significant decrease in binding affinity for **Azo-Gal(1,3,5)-5** from K_D = 3.3 ± 0.3 for the *E*-form to K_D = 7.4 ± 0.9 in the PSS, whereas **Azo-Gal-(1,3)-3** shows a small difference in lectin binding before and after photoswitching (entry 1, Table 3). This is in contrast to the previous finding of the inhibition/competition assay, where after photoswitching the **Azo-Gal(1,3,5)-5** was unaffected while **Azo-Gal-(1,3)-3** showed a significant difference in binding.

In contrast to the inhibition/competition assay where both components were in solution, now the glycooligomer is attached via one chain end to the chip surface. Thus, the degree of functionalization of the surface as well as the surface-oligomer linker has to be taken into consideration. From the values of refractive index determined via SPR on the glycooligomer functionalized chip, we can assume a similar degree of surface functionalization for all switched and non-switched glycooligomers (see Supporting Information File 1). Since all glycooligomers were attached directly via their free *N*-terminus (see Table 1) without any additional linker moieties, we believe that the first sugar ligand, i.e., the closest to the NHS-connection, might not be accessible for interactions with the receptor. Thus the divalent **Azo-Gal(1,3)-3** is reduced to an effective monovalent ligand. Independent of their *E*- or *Z*-configurations, the divalent glycooligomers can only bind in a monovalent fashion explaining that no difference in binding affinity was observed upon photoswitching. Following this hypothesis, trivalent **Azo-Gal(1,3,5)-5** would be reduced to an effective divalent ligand upon attachment to the SPR chip. Therefore **Azo-Gal(1,3,5)-5** should now show similar changes in binding behavior as were previously measured for divalent **Azo-Gal(1,3)-3** in solution**.** Indeed, we observe a similar decrease in binding affinity from K_D = 3.3 ± 0.3 for the *E*-form to K_D = 7.4 ± 0.9 in the PSS.

Conclusion

We have presented the straightforward synthesis of a series of photoswitchable glycooligomers by combination of solid phase polymer synthesis and functional building blocks. We could show that the azobenzene moieties introduced into the oligomeric backbone retain their photoswitchable behavior and thus allow for a light-induced change in the geometry of the glycooligomers. Binding studies of the galactose-functionalized glycooligomers showed specific binding to PA-IL and a controlled reduction in binding affinity upon $E \rightarrow Z$ photoisomerization. We proposed a first model to explain our findings based on molecular modelling for ligand binding. Ongoing studies further investigate ligand binding by additional techniques such as isothermal titration calorimetry and fluorescence spectroscopy. Overall, we have successfully developed photoswitchable glycomimetics that allow for a stimulus-induced change in binding affinity. Therefore we will further explore our photoswitchable glycooligomers as tunable glycomimetic ligands and their potential for a variety of biotechnological and biomedical applications such as the sensing and isolation of bacteria as well as the development of antibacterial treatments.

Table 3: K_D values obtained by SPR direct binding assay of the photoswitchable glycooligomers (PSS: photostationary state @ 360 nm).

Azo-Gal(1,3)-3	K_D [μM]	**Azo-Gal(1,3,5)-5**	K_D [μM]
E	1.7 ± 0.1	*E*	3.3 ± 0.3
PSS (ex situ irradiation)	2.4 ± 0.1	PSS (ex situ irradiation)	7.4 ± 0.9
PSS (irradiation on chip)	1.8 ± 0.1	PSS (irradiation on chip)	3.2 ± 0.9

Experimental

AZO building block synthesis: *N*-Fmoc-*para*-(aminomethyl)phenylazobenzoic acid was prepared adapting literature procedures [19,23] (see Supporting Information File 1).

General solid phase coupling protocols

General coupling protocol: Commercially available trityl-tentagel-OH resin was modified with an ethylenediamine linker and used as resin for solid phase synthesis. 0.0125 mmol of resin were swollen in DCM for 15 min. The initial coupling to the ethylenediamine linker was performed with a 0.1 mmol building block solution (8 equiv, TDS, EDS or AZO) in DMF (0.5 mL), followed by the addition of a 0.1 mmol PyBOP solution (8 equiv) together with 0.05 mmol HOBt (4 equiv) and 0.2 mmol (16 equiv) DIPEA in DMF (0.1 mL). This solution was added to the resin. After shaking for one hour the resin was washed from excessive reagent with DMF.

General CuAAC protocol: 0.1 mmol (8 equiv) of 2-azidoethyl pyranoside per alkyne group, dissolved in 1 mL DMF was added to 0.0125 mmol of resin loaded with EDS/AZO and TDS building blocks. 20 mol % sodium ascorbate per alkyne group and 20 mol % $CuSO_4$ per alkyne group were dissolved in 0.5 mL of water and also added to the resin. The resulting mixture was shaken for at least four hours. After that, the resin was washed with a 23 mM solution of sodium diethyl dithiocarbamate in DMF, water, DMF and DCM.

Fmoc cleavage: The Fmoc protecting group was cleaved by the addition of a solution of 25% piperidine in DMF three times for 5, 10 and 15 minutes, respectively. This was followed by carefully washing the resin with DMF.

Capping of N-teminal site: The free primary amine, obtained after final Fmoc cleavage, was capped with an acetyl group by the addition of 2.5 mL acetic anhydride. After shaking the mixture for 15 min, the resin was washed with DMF and DCM.

Cleavage from solid phase: 30% TFA in DCM was added to the resin and the mixture was shaken for one hour. The filtrate was added to cold diethyl ether (40 mL) resulting in white precipitate. This was centrifuged and the ether decanted. The crude product was dried in N_2 stream, dissolved in water (1 mL) and lyophilized.

Azo-Gal(1,3)-3: This structure was synthesized by applying the general coupling protocol three times with building blocks in the sequence TDS, AZO, TDS. After capping the primary amine, two galactose units were conjugated to the scaffold according to the general CuAAC protocol. The product was cleaved from the resin as final step giving 13 mg (yield: 75%). ^{1}H NMR (400 MHz, D_2O) δ 7.84–7.73 (m, 12H), 7.54–7.48 (m, 2H), 4.50–4.42 (m, 9H), 4.29–4.07 (m, 4H), 4.07 (br. s, 2H), 3.78 (s, 4H), 3.67–2.48 (m, 50 H), 1.85 (d, J = 21.0 Hz, 3H) ppm; RP-HPLC (5%/95% MeCN/H_2O → 30%/70% MeCN/H_2O in 30 min): t_R = 14.8 min;. ESIMS $[M + H]^+$: calcd for $C_{60}H_{89}N_{17}O_{20}$, 1368.6; found, 1368.4; $[M + 2H]^{2+}$ 684.8; found, 684.8, $[M + 3H]^{3+}$ 456.9; found, 457.0.

AZO-Gal(1,3,5)-5: This structure was synthesized by applying the general coupling protocol five times with building blocks in the sequence TDS, AZO, TDS, AZO, TDS. After capping the primary amine, three galactose units were conjugated to the scaffold according to the general CuAAC protocol. The product was cleaved from the resin as final step giving 18 mg (yield: 68%). ^{1}H NMR (400 MHz, D_2O) δ 7.73–7.45 (m, 12H), 7.34 (br. s, 3H), 4.48–4.31 (m, 9H), 4.25–4.08 (m, 8H), 3.78–3.66 (m, 8H), 3.66–3.30 (m, 32H), 3.18 (br. s, 4H), 2.98 (br. s, 3H), 2.98–2.35 (m, 25H), 1.82 (d, J = 10.6 Hz, 3H) ppm; RP-HPLC (5%/95% MeCN/H_2O → 30%/705% MeCN/H_2O in 30 min): t_R = 21.7 min; ESIMS $[M + 2H]^{2+}$ calcd for $C_{95}H_{134}N_{26}O_{30}$, 1060.5; found, 1060.4; $[M + H + Na]^{2+}$ 1082.9; found, 1082.6; $[M + 3H]^{3+}$ 707.4; found, 707.5, $[M + 4H]^{4+}$ 530.7; found, 530.8.

AZO-Man(1,3,5)-5: This structure was synthesized by applying the general coupling protocol five times with building blocks in the sequence TDS, AZO, TDS, AZO, TDS. After capping the primary amine, three mannose units were conjugated to the scaffold according to the general CuAAC protocol. The product was cleaved from the resin as final step giving 17 mg (yield: 64%). ^{1}H NMR (400 MHz, D_2O) δ 7.68–7.48 (m, 12H), 7.32 (br. s, 3H), 4.69–4.58 (m, 3H), 4.41–4.30 (m, 8H), 3.90 (br. s, 2 H), 3.75–3.70 (m, 6H), 3.62–3.08 (m, 48H), 2.86–2.45 (m, 32H), 1.82 (d, J = 8.5 Hz, 3H) ppm; RP-HPLC (5%/95% MeCN/H_2O → 30%/705% MeCN/H_2O in 30 min): t_R = 21.7 min; ESIMS $[M + H + Na]^{2+}$calcd for $C_{95}H_{134}N_{26}O_{30}$, 1082.9; found, 1082.8; $[M + 3H]^{3+}$ 707.4; found, 707.5; $[M + 4H]^{4+}$ 530.7; found, 530.8.

EDS-Gal(1,3)-3: This structure was synthesized by applying the general coupling protocol three times with building blocks in the sequence TDS, EDS, TDS. After capping the primary amine, two galactose units were conjugated to the scaffold according to the general CuAAC protocol. The product was cleaved from the resin as final step giving 21 mg (yield: quant). ^{1}H NMR (400 MHz, D_2O) δ 8.00 (s, 2H), 4.44 (d, J = 7.8 Hz, 2H), 4.40–4.32 (m, 2H), 4.21–4.12 (m, 2H), 3.99–3.96 (m, 2H), 3.83–3.79 (m, 4H), 3.78–3.64 (m, 16H), 3.59–3.50 (m, 12H), 3.43 (t, J = 10.1 Hz, 12H), 3.21 (t, J = 5.8 Hz, 2H), 3.08 (t, J = 7.0 Hz, 4H), 2.86 (t, J = 6.9 Hz, 4H), 2.62–2.52 (m, 12H), 2.00 (d, J = 6.0 Hz, 3H) ppm; RP-HPLC (5%/95% MeCN/H_2O →

30%/70% MeCN/H_2O in 60 min): t_R = 12.9 min; ESIMS [M + 2H]$^{2+}$ calcd for $C_{56}H_{96}N_{16}O_{23}$, 681.3; found, 681.3; [M + 3H]$^{3+}$ 454.6; found, 454.6.

EDS-Gal(1,3,5)-5 [9]: This structure was synthesized by applying the general coupling protocol five times with building blocks in the sequence TDS, EDS, TDS, EDS, TDS. After capping the primary amine, three galactose units were conjugated to the scaffold according to the general CuAAC protocol. The product was cleaved from the resin. ^{1}H NMR (400 MHz, D_2O) δ 8.04 (d, *J* = 7 Hz, 3H), 4.74 (br. s, 6H), 4.43 (d, *J* = 8 Hz, 3H), 4.38–4.33 (m, 3H), 4.19–4.14 (m, 3H), 3.97 (s, 3H), 3.81–3.79 (m, 7H), 3.72 (s, 10H), 3.65 (m, 10H), 3.56–3.51 (m, 16H), 3.44–3.39 (m, 18H), 3.20 (t, *J* = 6 Hz, 2H), 3.08 (t, *J* = 6 Hz, 6H), 2.85 (t, *J* = 7 Hz, 6H), 2.58–2.50 (m, 20H), 1.99 (d, *J* = 5 Hz, 3H) ppm; RP-HPLC (5%/95% MeCN/H_2O → 30%/70% MeCN/H_2O in 60 min) t_R = 14.1 min; ESIMS [M + 2H]^2 calcd for $C_{87}H_{148}N_{24}O_{36}$, 1053.5; found, 1053.8, [M + 3H]$^{3+}$ 702.7; found, 702.8, [M + 4H]$^{4+}$ 527.3; found, 527.4, [M + 5H]$^{5+}$ 422.0; found, 422.2.

Supporting Information

Supporting Information File 1

Further experimental procedures, characterization data and spectra.
[http://www.beilstein-journals.org/bjoc/content/supplementary/1860-5397-10-166-S1.pdf]

Acknowledgements

The authors thank the Max Planck Society as well as the German Research Foundation (DFG, Emmy Noether program HA5950/1-1 and research grant BL1269/1-1) and the Collaborative Research Center (SFB) 765 for financial support.

References

1. Gabius, H.-J.; Siebert, H.-C.; André, S.; Jiménez-Barbero, J.; Rüdiger, H. *ChemBioChem* **2004,** *5,* 740–764. doi:10.1002/cbic.200300753
2. Lepenies, B.; Yin, J.; Seeberger, P. H. *Curr. Opin. Chem. Biol.* **2010,** *14,* 404–411. doi:10.1016/j.cbpa.2010.02.016
3. Lindhorst, T. K. *Essentials of Carbohydrate Chemistry and Biochemistry;* Wiley-VCH: Weinheim, Germany, 2007.
4. Lundquist, J. J.; Toone, E. J. *Chem. Rev.* **2002,** *102,* 555–578. doi:10.1021/cr000418f
5. Becer, C. R. *Macromol. Rapid Commun.* **2012,** *33,* 742–752. doi:10.1002/marc.201200055
6. Bernardi, A.; Jiménez-Barbero, J.; Casnati, A.; De Castro, C.; Darbre, T.; Fieschi, F.; Finne, J.; Funken, H.; Jaeger, K.-E.; Lahmann, M.; Lindhorst, T. K.; Marradi, M.; Messner, P.; Molinaro, A.; Murphy, P. V.; Nativi, C.; Oscarson, S.; Penadés, S.; Peri, F.; Pieters, R. J.; Renaudet, O.; Reymond, J.-L.; Richichi, B.; Rojo, J.; Sansone, F.; Schäffer, C.; Turnbull, W. B.; Velasco-Torrijos, T.; Vidal, S.; Vincent, S.; Wennekes, T.; Zuilhof, H.; Imberty, A. *Chem. Soc. Rev.* **2013,** *42,* 4709–4727. doi:10.1039/c2cs35408j
7. Ponader, D.; Wojcik, F.; Beceren-Braun, F.; Dernedde, J.; Hartmann, L. *Biomacromolecules* **2012,** *13,* 1845–1852. doi:10.1021/bm300331z
8. Wojcik, F.; O'Brien, A. G.; Götze, S.; Seeberger, P. H.; Hartmann, L. *Chem.–Eur. J.* **2013,** *19,* 3090–3098. doi:10.1002/chem.201203927
9. Wojcik, F.; Lel, S.; O'Brien, A. G.; Seeberger, P. H.; Hartmann, L. *Beilstein J. Org. Chem.* **2013,** *9,* 2395–2403. doi:10.3762/bjoc.9.276
10. Ponader, D.; Maffre, P.; Aretz, J.; Pussak, D.; Ninnemann, N. M.; Schmidt, S.; Seeberger, P. H.; Rademacher, C.; Nienhaus, G. U.; Hartmann, L. *J. Am. Chem. Soc.* **2014,** *136,* 2008–2016. doi:10.1021/ja411582t
11. Pussak, D.; Ponader, D.; Mosca, S.; Vargas Ruiz, S.; Hartmann, L.; Schmidt, S. *Angew. Chem., Int. Ed.* **2013,** *52,* 6084–6087. doi:10.1002/anie.201300469
12. Srinivas, O.; Mitra, N.; Surolia, A.; Jayaraman, N. *J. Am. Chem. Soc.* **2002,** *124,* 2124–2125. doi:10.1021/ja0173066
13. Chandrasekaran, V.; Lindhorst, T. K. *Chem. Commun.* **2012,** *48,* 7519–7521. doi:10.1039/c2cc33542e
14. Ogawa, Y.; Yoshiyama, C.; Kitaoka, T. *Langmuir* **2012,** *28,* 4404–4412. doi:10.1021/la300098q
15. Chandrasekaran, V.; Kolbe, K.; Beiroth, F.; Lindhorst, T. K. *Beilstein J. Org. Chem.* **2013,** *9,* 223–233. doi:10.3762/bjoc.9.26
16. Beharry, A. A.; Woolley, G. A. *Chem. Soc. Rev.* **2011,** *40,* 4422–4437. doi:10.1039/c1cs15023e
17. Bléger, D.; Yu, Z.; Hecht, S. *Chem. Commun.* **2011,** *47,* 12260–12266. doi:10.1039/c1cc15180k
18. Bléger, C.; Liebig, T.; Thiermann, R.; Maskos, M.; Rabe, J. P.; Hecht, S. *Angew. Chem., Int. Ed.* **2011,** *123,* 12767–12771. doi:10.1002/ange.201106879
19. Ulysse, L.; Chmielewski, J. *Bioorg. Med. Chem. Lett.* **1994,** *4,* 2145–2146. doi:10.1016/S0960-894X(01)80118-9
20. Behrendt, R.; Schenk, M.; Musiol, H.-J.; Moroder, L. *J. Pept. Sci.* **1999,** *5,* 519–529. doi:10.1002/(SICI)1099-1387(199911)5:11<519::AID-PSC223>3.0.CO;2-3
21. Rück-Braun, K.; Kempa, S.; Priewisch, B.; Richter, A.; Seedorff, S.; Wallach, L. *Synthesis* **2009,** 4256–4267. doi:10.1055/s-0029-1217074
22. Priewisch, B.; Rück-Braun, K. *J. Org. Chem.* **2005,** *70,* 2350–2352. doi:10.1021/jo048544x
23. Stover, C. K.; Pham, X. Q.; Erwin, A. L.; Mizoguchi, S. D.; Warrener, P.; Hickey, M. J.; Brinkman, F. S. L.; Hufnagle, W. O.; Kowalik, D. J.; Lagrou, M.; Garber, R. L.; Goltry, L.; Tolentino, E.; Westbrock-Wadman, S.; Yuan, Y.; Brody, L. L.; Coulter, S. N.; Folger, K. R.; Kas, A.; Larbig, K.; Lim, R.; Smith, K.; Spencer, D.; Wong, G. K.-S.; Wu, Z.; Paulsen, I. T.; Reizer, J.; Saier, M. H.; Hancock, R. E. W.; Lory, S.; Olson, M. V. *Nature* **2000,** *406,* 959–964. doi:10.1038/35023079
24. Mosca, S.; Dannehl, C.; Möqinger, U.; Brezesinski, G.; Hartmann, L. *Org. Biomol. Chem.* **2013,** *11,* 5399–5403. doi:10.1039/c3ob41135d
25. Wojcik, F.; Mosca, S.; Hartmann, L. *J. Org. Chem.* **2012,** *77,* 4226–4234. doi:10.1021/jo202561k

26. Ladmiral, V.; Mantovani, G.; Clarkson, G. J.; Cauet, S.; Irwin, J. L.; Haddleton, D. M. *J. Am. Chem. Soc.* **2006,** *128,* 4823–4830. doi:10.1021/ja058364k
27. Cecioni, S.; Faure, S.; Darbost, U.; Bonnamour, I.; Parrot-Lopez, H.; Roy, O.; Taillefumier, C.; Wimmerová, M.; Praly, J.-P.; Imberty, A.; Vidal, S. *Chem.–Eur. J.* **2011,** *17,* 2146–2159. doi:10.1002/chem.201002635
28. Avichezer, D.; Katcoff, D. J.; Garber, N. C.; Gilboa-Garber, N. *J. Biol. Chem.* **1992,** *267,* 23023–23027.

License and Terms

BEILSTEIN JOURNAL OF ORGANIC CHEMISTRY

Clicked and long spaced galactosyl- and lactosylcalix[4]arenes: new multivalent galectin-3 ligands

Silvia Bernardi[1], Paola Fezzardi[1], Gabriele Rispoli[1], Stefania E. Sestito[2], Francesco Peri[*2], Francesco Sansone[1] and Alessandro Casnati[*1]

Full Research Paper

Open Access

Address:
[1]Dipartimento di Chimica, Università degli Studi di Parma, Parco Area delle Scienze 17/a, 43124 Parma, Italy and [2]Dipartimento di Biotecnologie e Bioscienze, Università degli Studi di Milano-Bicocca, Piazza della Scienza 2, 20126 Milano, Italy

Email:
Francesco Peri[*] - francesco.peri@unimib.it; Alessandro Casnati[*] - casnati@unipr.it

* Corresponding author

Keywords:
glycocalixarenes; cluster glycoside effect; multivalency; click chemistry; surface plasmon resonance

Beilstein J. Org. Chem. **2014,** *10,* 1672–1680.
doi:10.3762/bjoc.10.175

Received: 05 March 2014
Accepted: 23 June 2014
Published: 23 July 2014

This article is part of the Thematic Series "Multivalent glycosystems for nanoscience".

Guest Editor: B. Turnbull

Abstract

Four novel calix[4]arene-based glycoclusters were synthesized by conjugating the saccharide units to the macrocyclic scaffold using the CuAAC reaction and using long and hydrophilic ethylene glycol spacers. Initially, two galactosylcalix[4]arenes were prepared starting from saccharide units and calixarene cores which differ in the relative dispositions of the alkyne and azido groups. Once the most convenient synthetic pathway was selected, two further lactosylcalix[4]arenes were obtained, one in the cone, the other one in the 1,3-alternate structure. Preliminary studies of the interactions of these novel glycocalixarenes with galectin-3 were carried out by using a lectin-functionalized chip and surface plasmon resonance. These studies indicate a higher affinity of lactosyl- over galactosylcalixarenes. Furthermore, we confirmed that in case of this specific lectin binding the presentation of lactose units on a cone calixarene is highly preferred with respect to its isomeric form in the 1,3-alternate structure.

Introduction

Lectins are carbohydrate-binding proteins (CBP) [1-3] without any catalytic or immunogenic activity. In the latest decades, they attracted an increasing interest due to their involvement in a series of fundamental biological processes such as cell adhesion, cell activation, cell growth, differentiation and apoptosis. Among different families of lectins, the ones showing a selectivity for β-D-galactoside and β-D-galactose-terminating oligosaccharides are called galectins and play important roles in a series of pathological events such as inflammation, fibrosis, heart diseases and cancer [4,5]. The role of one member of this family in particular, namely galectin-3 (Gal-3), has been intensively investigated lately and it was shown that it is deeply involved in cancer metastasis and migration. Based on these findings and with the aim to inhibit its activity and to target it

for therapeutic or diagnostic purposes, Gal-3 became a rather important target in medicine. Remarkably interesting is the intra-family selectivity and, especially, the ability to block Gal-3 but not Gal-1. Gal-1, in fact, can act as anti-inflammatory agent, while Gal-3 has a pro-inflammatory activity [6]. Furthermore, Gal-3 can act as a competitive inhibitor against Gal-1 which, on the other side, induces anoikis of tumor cells [7,8]. Glycocalixarenes [9-12], calixarenes [13-15] adorned with carbohydrates at the upper and/or at the lower rims, have been demonstrated to be efficient multivalent ligands for a series of pathological lectins. For instance, cholera toxin is bound rather efficiently by calix[4]arene [16] and calix[5]arene [17] derivatives, while examples of *Pseudomonas aeruginosa* LecB binding were reported with galactosylcalixarenes blocked in different conformations [18,19]. A few years ago we [20,21] reported about the synthesis and inhibitory properties of a small library of lactosylthioureidocalixarenes and found that the cone derivatives **I** and **III** (Figure 1) were able to efficiently inhibit the adhesion of Gal-3 to tumor cells in vitro, but not that of galectin-1 [22].

The opposite behavior was observed for the 1,3-alternate derivative **II**, able to inhibit Gal-1 but not Gal-3. On the basis of these findings, we herein report the synthesis of a new subfamily of galactosyl- and lactosylcalix[4]arenes **1**–**4** (Figure 2) which are characterized by long hydrophilic spacers between the glycosyl units and the multivalent calixarene scaffold. We also report on preliminary studies of the interaction of the novel subfamily of galactosyl- and lactosylcalix[4]arenes with Gal-3 by surface plasmon resonance (SPR).

Results and Discussion

Synthesis of the glycocalixarenes

"Click Chemistry" [23] reactions are extensively used to conjugate (oligo)saccharides to macrocyclic structures due to the mild conditions and the high yields [24]. For the synthesis of glycocalixarenes the amino–isothiocyanate condensation [25-30] or the 1,3-dipolar cycloaddition have been widely studied in their scope and limitations [10,31]. In particular, the Huisgen cycloaddition reaction was first applied to a calixarene in 2000 by Santoyo-González [32]. Later on, Marra et al. [33] demonstrated that the copper-catalyzed azide–alkyne cycloaddition (CuAAC) [34,35] at room temperature could afford divalent and tetravalent glycocalixarenes in very high yields and regioselectivity. Following these studies, a wide series of other examples appeared in the literature [18,36-39] also exploiting the use of microwaves, ionic liquids and protected or even deprotected [17] saccharides. Usually, either the strategy of reacting an alkynylated-saccharide with a polyazide calixarene (dipolarophile-on-the-sugar) or an azido-sugar and a polyalkynocalixarene (dipolarophile-on-the-calix) work smoothly [33]. However, a sort of autocatalytic effect was evidenced in the case of the reaction between a 1-ethynyl-C-glycoside with a tetraazidocalix[4]arene (dipolarophile-on-the sugar strategy). It was suggested by the authors that the first intermolecular reaction, leading to a Cu-triazolide adduct, allows the copper ion to coordinate an ethynyl glycoside, thus entailing an intramolecular CuAAC reaction with an adjacent azido-arm [37].

Firstly, we decided to evaluate the effectiveness of the two approaches dipolarophile-on-the-calix and dipolarophile-on-the-

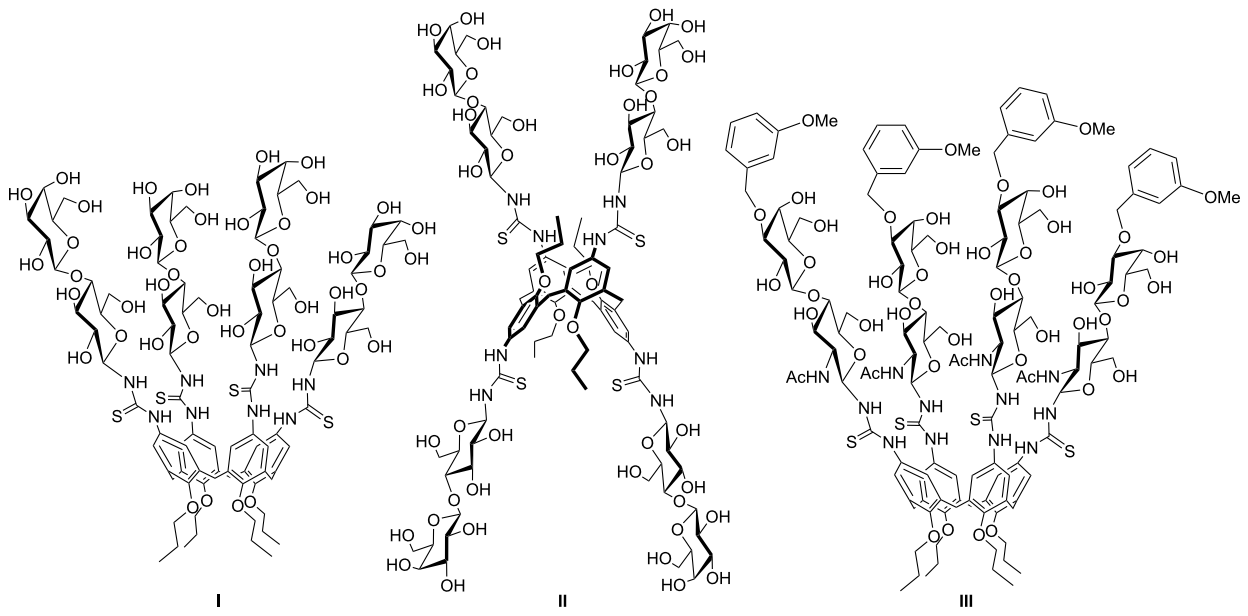

Figure 1: Lactosylthioureidocalix[4]arenes **I–III** used to inhibit Gal-3 [20,21].

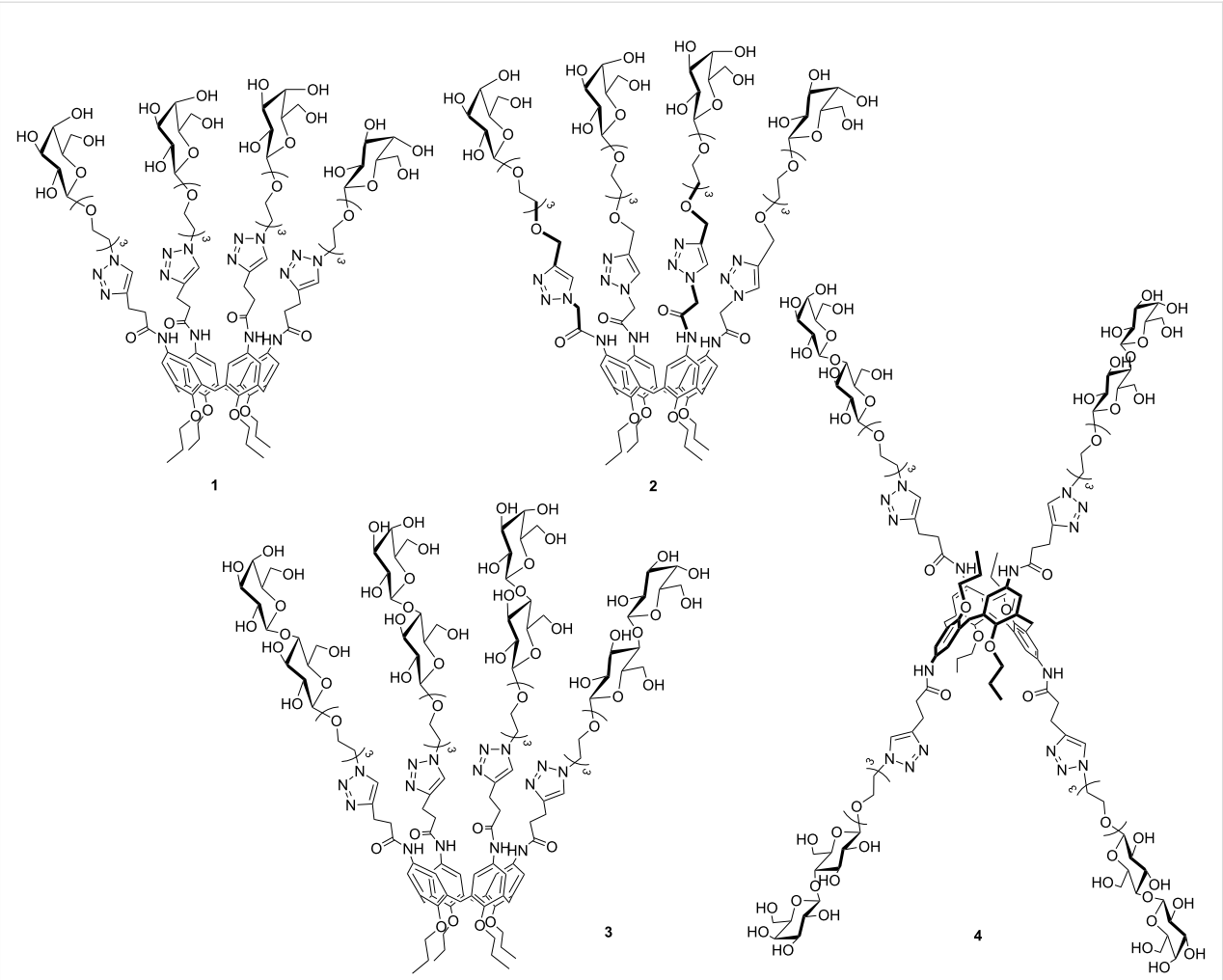

Figure 2: The new glycocalix[4]arenes **1–4** synthesized in this study.

sugar by using a galactose and cone calixarene scaffolds. This investigation was carried out with the idea to extend the study to stronger ligating units for galectins such as lactose and different calixarene structures, also including the 1,3-alternate isomer. The first route explored (dipolarophile-on-the-calix) was applied to the preparation of the multivalent compound **1**, which could be synthesized by exploiting a convergent synthetic approach. This approach was based on the connection, by CuAAC reaction, of the azido-terminating tetraacetylgalactose **5** [40,41] to calix[4]arene **8** decorated at the upper rim with alkyne terminating chains (Scheme 1).

In order to introduce the alkyne units at the upper rim of the macrocycle, we decided to exploit the easily available and highly versatile *p*-aminocalixarene **6** prepared according to literature procedures [25]. The coupling reaction between amino-calix[4]arene **6** and 4-pentynoic acid (**7**) in the presence of dicyclohexylcarbodiimide (DCC) led to compound **8** in 44% yield. Due to the concurrent formation of dicyclohexylurea (DCU), several purification steps were necessary to obtain pure calix[4]arene **8**. The use of 1-ethyl-3-(3-dimethylaminopropyl)-carbodiimide (EDC) as an alternative coupling agent allowed us to isolate pure compound **8** in a more straightforward way and higher yield (66%). Any attempts to connect the alkyne functionality in closer proximity to the calixarene core by decreasing the number of carbon atoms between the carboxylic group and the triple bond did not give fruitful results. Reactions between amino-calix[4]arene **6** and propiolic acid were carried out with a variety of coupling agents. In the presence of DCC the tetra-condensation product was only obtained in very low yields. Furthermore, it was not possible to purely isolate it from the crude reaction mixture due to the high amount of byproducts formed during the reaction. The CuAAC reaction between the tetraalkyne calix[4]arene **8** and azido-galactoside **5** to give glycocluster **9** (83% yield) was carried out in DMF and H_2O with $CuSO_4$ and sodium ascorbate following a microwave-

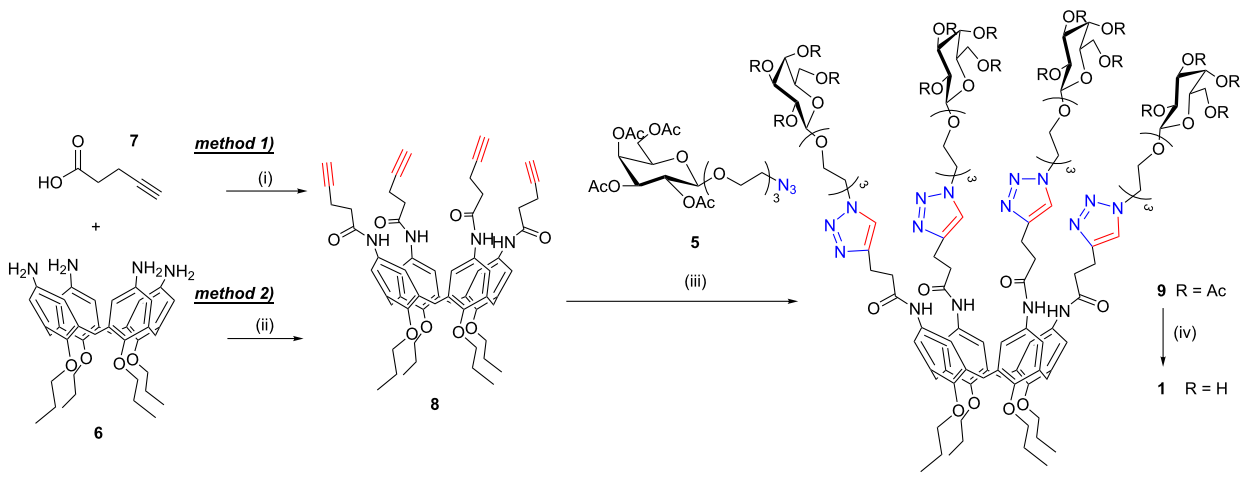

Scheme 1: Synthesis of the cone galactosylcalix[4]arenes **1**. Reaction conditions: (i) DCC, DMAP, CH_2Cl_2, under reflux, 5 h, 44%; (ii) EDC, CH_2Cl_2/py (7:3), rt, 18 h, 66%; (iii) $CuSO_4{\cdot}5H_2O$, Na-ascorbate, DMF/H_2O, μW (150 W), 80 °C, 20 min, 83%; (iv) CH_3ONa, CH_3OH, rt, 1 h – IR120/H^+, rt, 30 min, quantitative.

assisted procedure (20 min, 150 W, 80 °C). No partially functionalized compounds or other byproducts were detected in the crude mixtures.

The second strategy studied (dipolarophile-on-the-sugar) also exploits a convergent approach, but in this case an alkyne-functionalized galactose **10** was prepared according to literature [42], so that it reacts with calixarene **12**, which was previously functionalized with azido terminating arms (Scheme 2). This latter compound was synthesized in two steps starting again from tetraamino derivative **6**. In the first step compound **6** was treated with chloroacetyl chloride to give the α-choloroacetamido compound **11** [43]. Subsequent substitution of the chlorine ions with azide groups led to the formation of the tetraazidocalixarene derivative **12** (1 h, 75% yield).

The CuAAC conjugation reaction was carried out following exactly the same procedure as for compound **9** and allowed the isolation of **13** in very high yields (81%). Glycoconjugates **9** and **13** were fully characterized by ^1H and ^{13}C NMR spectroscopy, which displayed the disappearance of the alkyne protons and the appearance of the typical broad signal of 1,4-disubstituted triazole protons at 7.75–7.85 ppm (CD_3OD/$CDCl_3$). ESIMS (+) analyses showed peaks for the $[M + 2Na]^{2+}$

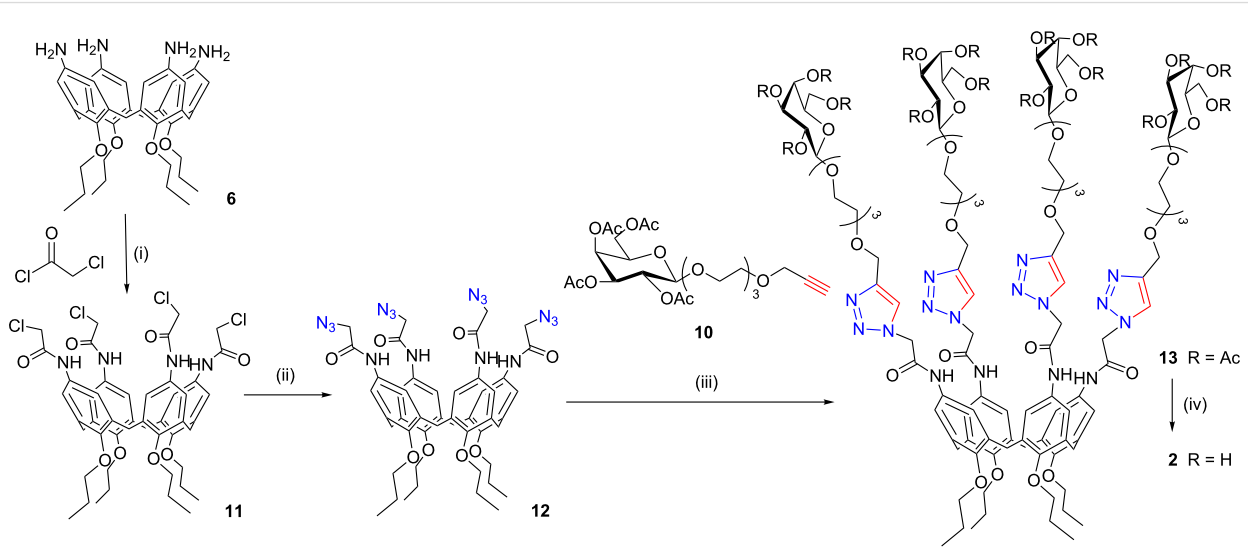

Scheme 2: Synthesis of the cone galactosylcalix[4]arenes **2**. Reaction conditions: (i) DIPEA, CH_2Cl_2, rt, 6 h, 55%; (ii) NaN_3, CH_3OH/DMF, reflux, 1 h, 75%; (iii) $CuSO_4{\cdot}5H_2O$, Na-ascorbate, DMF/H_2O, μW (150 W), 80 °C, 20 min, 81%; (iv) CH_3ONa, CH_3OH, rt, 1 h – IR120/H^+, rt, 30 min, quantitative.

and $[M + 3Na]^{3+}$ adducts, which indicates the conjugation of all four macrocycle arms to the saccharide units. On the basis of the comparison between the efficiency of the conjugation steps bringing to glycoconjugates **9** and **13** (yields >80% in both cases) and contrary to the observation by Marra et al. [37], we could not collect any evidence for an autocatalytic effect in the dipolarophile-on-the-sugar approach [44]. The deprotection of compounds **9** and **13** from the acetyl groups was carried out by a transesterification reaction in the presence of CH_3ONa in CH_3OH at room temperature according to the standard Zemplén procedure. Complete deacetylation was achieved in 1 hour, as confirmed by NMR and ESIMS(+) spectra of compounds **1** and **2**. It is noteworthy that while compound **1** exhibited a high stability under Zemplén conditions even if the reaction was continued overnight, compound **2** started to decompose after 18 hours. ESIMS profiles showed the presence of products originating from a cleavage at the amide bond with a loss of the entire glycosylated chain and the formation of an amine group at the upper rim of the calixarene. For this reason and on the basis of the synthetic availability of intermediates, we decided to privilege the dipolarophile-on-the-calix route to synthesize the triazole-containing lactosylcalixarenes **3** and **4**.

We first attempted to prepare the lactoside derivative **14** by reacting peracetylated-lactose with 2-(2-(2-chloroethoxy)ethoxy)ethanol in the presence of $BF_3{\cdot}Et_2O$ [45]. However, we could only obtain a mixture of α and β-anomers (α/β ratio 2:3), which is very difficult to separate by flash chromatographic methods. On the other hand, the recently reported glycosylation reactions of lactose peracetate exploiting $SnCl_4$ and CF_3CO_2Ag as promoters [46] gave compound **14** mainly as a β-anomer (α/β ratio 1:4) in 74% isolated yield.

The subsequent substitution reaction of chloride with NaN_3 (Scheme 3) led to the corresponding azido derivative **15**, which was used to "click" both the cone (**8**) and 1,3-alternate (**18**) pentynoic amides. Compound **18** was obtained from the corresponding 1,3-alternate *p*-aminocalix[4]arene **17** [47] by a reaction with EDC in CH_2Cl_2 and pyridine 7:3 as previously described for compound **8**. The CuAAC "click" reaction was carried out as previously described for the galacto-clusters **9** and **13** and afforded the cone calix[4]arene **16** (Scheme 3) and 1,3-alternate calix[4]arene **19** (Scheme 4) in 46% isolated yield. Microwave irradiation (150 W, 80 °C) facilitated the complete tetra-functionalization in only 40 minutes. Subsequent deacetylation with the Zemplén method led to target compounds **3** and **4**, both of which were characterized by 1D and 2D NMR techniques and ESIMS analyses.

Gal-3/glycocalixarenes interaction studies by SPR

His_6-tagged full-length Gal-3 was expressed in *E. coli* BL21 and purified on IMAC (immobilized metal ion affinity chromatography) columns. Purified protein was characterized by SDS-

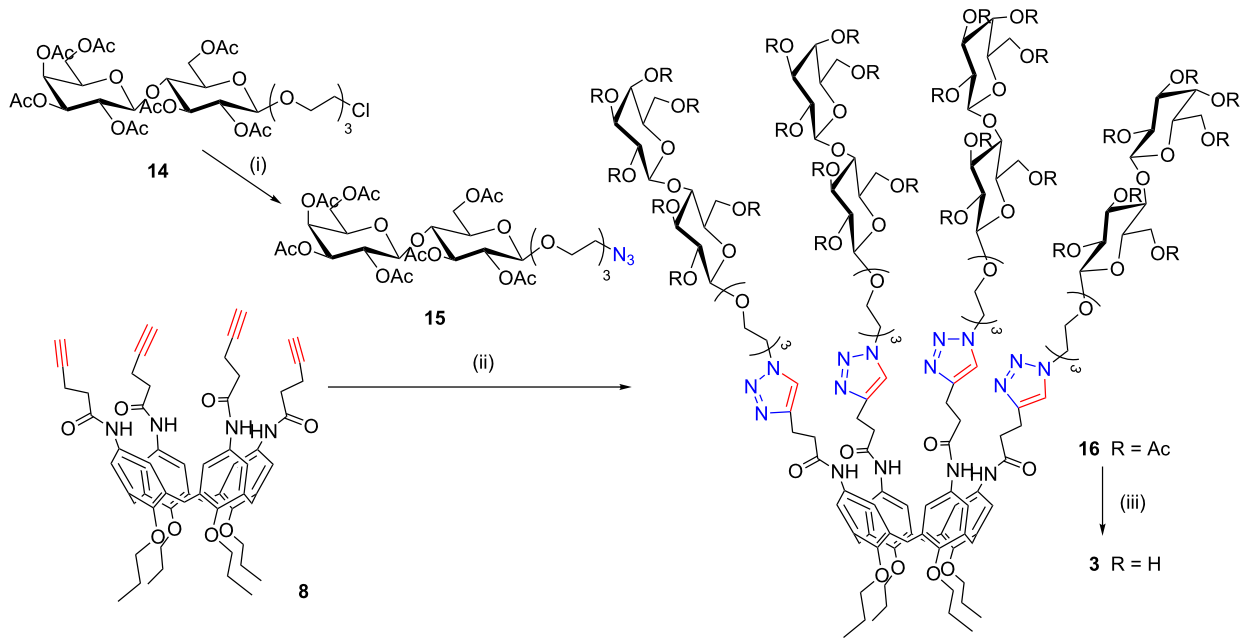

Scheme 3: Synthesis of the cone lactosylcalix[4]arenes **3**. Reaction conditions: (i) NaN_3, *n*-Bu_4NI, DMF, 90 °C, 24 h, 60%; (ii) $CuSO_4{\cdot}5H_2O$, Na-ascorbate, DMF/H_2O, μW (150 W), 80 °C, 40 min, 46%; (iii) CH_3ONa, CH_3OH, rt, 2 h – IR120/H^+, rt, 30 min, 73%.

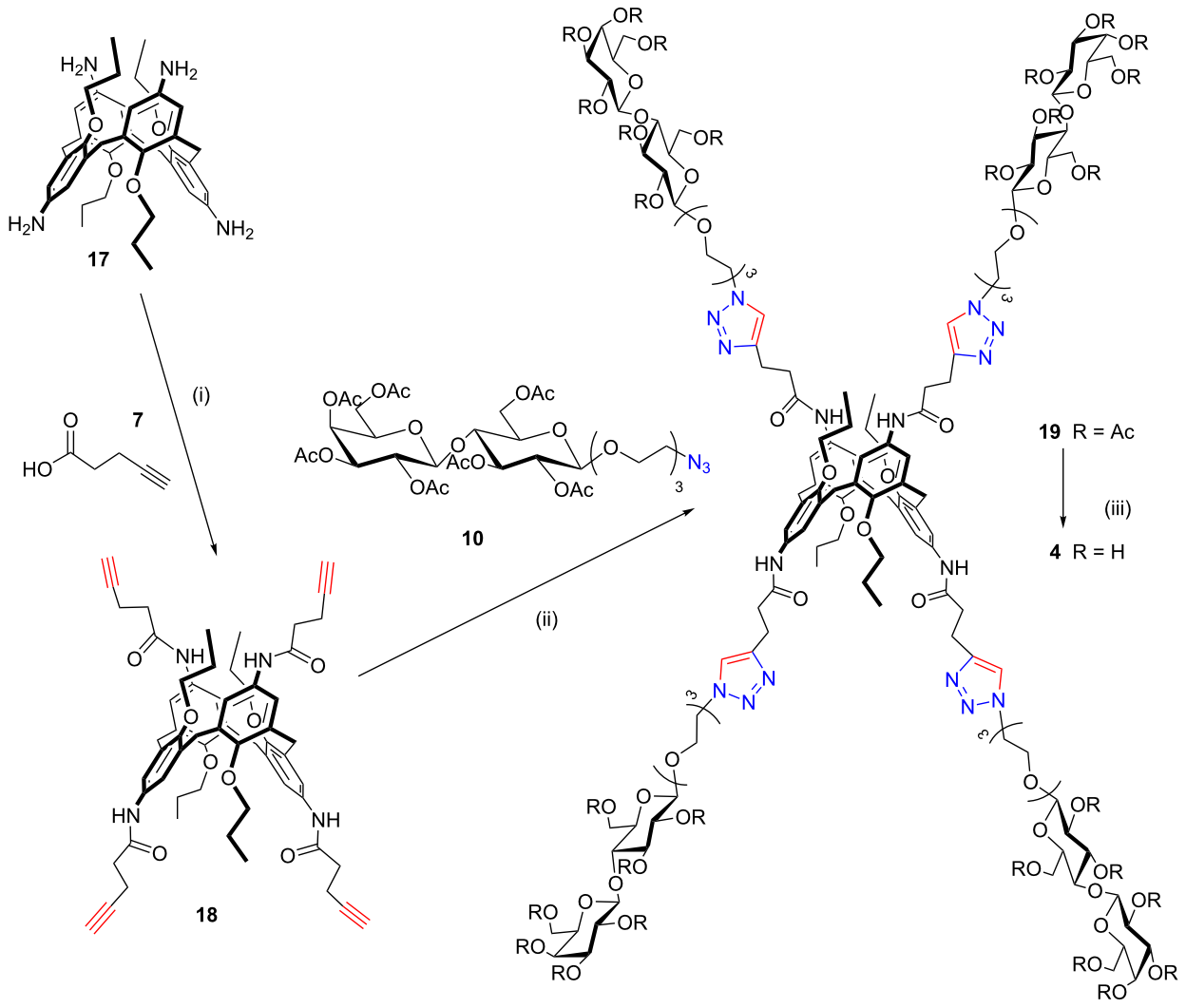

Scheme 4: Synthesis of the 1,3-alternate lactosylcalix[4]arenes **4**. Reaction conditions: (i) EDC, CH_2Cl_2/py (7:3), rt, 18 h, 65%; (ii) $CuSO_4{\cdot}5H_2O$, Na-ascorbate, DMF/H_2O, μW (150 W), 80 °C, 40 min, 46%; (iii) CH_3ONa, CH_3OH, rt, 2 h – IR120/H^+, rt, 30 min, 71%.

PAGE electrophoresis, circular dichroism (CD), and MS/MS analysis upon digestion on trypsin gel (see Figure S15, Supporting Information File 1). A preliminary evaluation of the interaction between the glycocalixarenes **1**, **3**, **4** and Gal-3 was obtained by SPR analysis by using a His-tagged Gal-3 immobilized on a Ni-NTA chip and the glycocalixarenes in solution. This approach differs from other SPR studies of the calixarene–galectin interaction with the protein in solution [38] and is tailored to have the immobilized protein properly oriented for the interaction with ligands. The sensorgrams shown in Figure 3 were obtained by fluxing an 1 mM solution of calixarenes over the protein-coated chip.

The small increases of resonance units in the sensograms (Figure 3) showed a weak affinity of all calixarenes for Gal-3. However, the three synthetic molecules showed a very similar trend of Gal-3 binding affinity in three independent measurements (experiments A, B and C in Figure 4a). In particular, glycocalixarene **3** (cone structure, four lactosides) exhibited the highest affinity for Gal-3 in all experiments, while **4**, (1,3-alternate structure, four lactosides) displayed a lower affinity and **1** (cone structure, four galactosides) showed no interaction at all. The more efficient ligand, compound **3**, showed a dose-dependent affinity for the protein.

The higher affinities of lactose-containing compounds **3** and **4** for Gal-3 compared to galactose-containing compound **1** reflect the higher affinity of lactose over galactose for Gal-3. The lactosylcalixarene with the cone structure appears to bind better to Gal-3 than the corresponding isomer in the 1,3-alternate

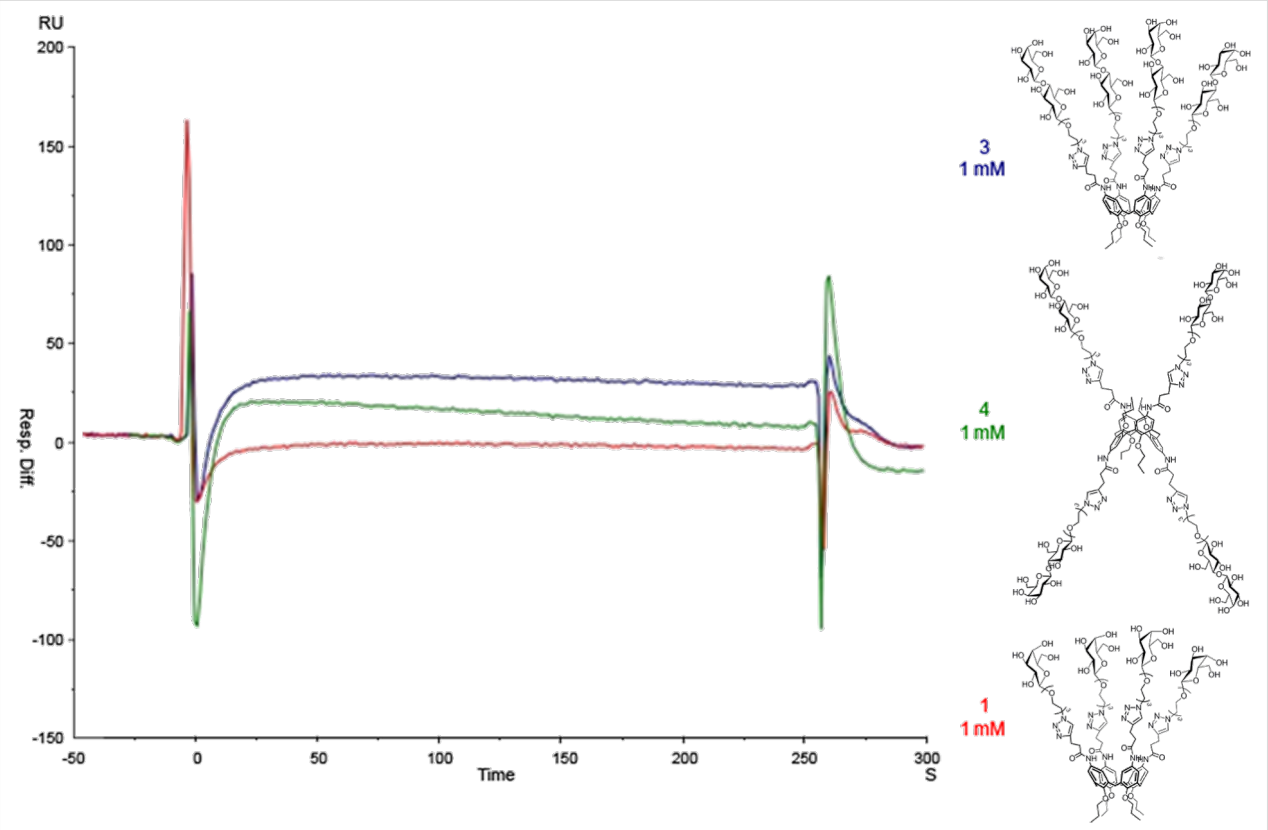

Figure 3: SPR sensorgrams of binding experiment between immobilized Gal-3 and glycocalixarenes **1**, **3** and **4**.

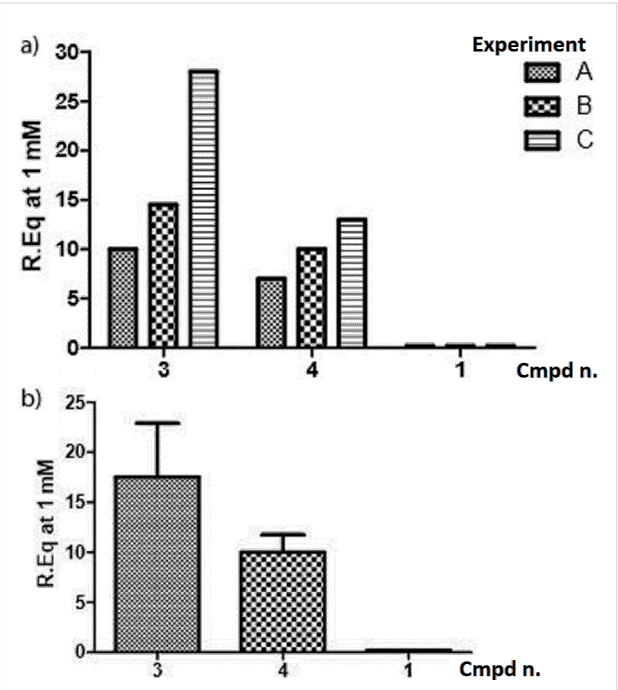

Figure 4: a) Relative affinities of glycocalixarene **1**, **3**, **4** (1 mM) towards Gal-3, expressed in terms of the increase of the resonance unit (RU) in three independent (A, B, C) SPR experiments. b) average affinities of glycocalixarenes with standard deviations.

structure. This confirms the data previously obtained in a series of inhibition experiments of the same lectin in surface-immobilized asialofetuin and on cells with the lactosylthioureidocalixarenes (**I–III**) [20,21]. A direct comparison with ligands (**I–III**) was, however, not feasible since the lactosylthioreido derivatives tend to aggregate and precipitate under the conditions used for SPR experiments.

Conclusion

Four glycocalixarenes **1–4** characterized by long hydrophilic spacers between the glycosyl units and the macrocyclic scaffold were synthesized by the copper(I)-catalyzed azido–alkyne cycloaddition (CuAAC). The homogeneous series of ligands **1**, **3** and **4** were subsequently studied in the binding to surface-immobilized His-tagged Gal-3 by SPR experiments. In spite of the weak intensity of the signals, an affinity order for the interaction of ligands **1**, **3** and **4** with the immobilized Gal-3 was obtained. A preference for the lactosyl clusters over the galactose functionalized ones (**3** > **4** >> **1**) and a higher efficiency in the binding of Gal-3 shown by the cone derivative compared to its isomeric 1,3-alternate counterpart (**3** > **4**) were observed. Work is in progress to study by SPR experiments the interaction between lactosylcalixarenes covalently immobilized on the chip and Gal-3 samples in solution.

Supporting Information

Detailed experimental procedures (general information, synthetic procedures, expression and purification of Gal-3, Gal-3/glycocalixarene binding experiments), ^{1}H NMR spectra of selected intermediates, and final glycocalixarenes **1**–**4** together with electrophoresis gel, circular dichroism spectrum and thermal unfolding of purified Gal-3.

Supporting Information File 1

Experimental part.
[http://www.beilstein-journals.org/bjoc/content/supplementary/1860-5397-10-175-S1.pdf]

Acknowledgements

The authors gratefully acknowledge financial support from the Italian Ministry of Instruction, University and Research (MIUR, PRIN2010JMAZML MultiNanoIta) and EU-COST Action CM1102 'MultiGlycoNano'. The Centro Interdipartimentale di Misure (CIM) of the Parma University 'G. Casnati' is acknowledged for the use of the NMR and Mass facilities.

References

1. Lis, H.; Sharon, N. *Chem. Rev.* **1998,** *98,* 637–674. doi:10.1021/cr940413g
2. Gabius, H.-J. *Eur. J. Biochem.* **1997,** *243,* 543–576. doi:10.1111/j.1432-1033.1997.t01-1-00543.x
3. Gabius, H.-J.; Siebert, H.-C.; André, S.; Jiménez-Barbero, J.; Rüdiger, H. *ChemBioChem* **2004,** *5,* 740–764. doi:10.1002/cbic.200300753
4. Gabius, H.-J.; André, S.; Jiménez-Barbero, J.; Romero, A.; Solis, D. *Trends Biochem. Sci.* **2011,** *36,* 298–313. doi:10.1016/j.tibs.2011.01.005
5. Ingrassia, L.; Camby, I.; Lefranc, F.; Mathieu, V.; Nshimyumukiza, P.; Darro, F.; Kiss, R. *Curr. Med. Chem.* **2006,** *13,* 3513–3527. doi:10.2174/092986706779026219
6. Rubinstein, N.; Ilarregui, J. M.; Toscano, M. A.; Rabinovich, G. A. *Tissue Antigens* **2004,** *64,* 1–12. doi:10.1111/j.0001-2815.2004.00278.x
7. Sanchez-Ruderisch, H.; Fischer, C.; Detjen, K. M.; Welzel, M.; Wimmel, A.; Manning, J. C.; André, S.; Gabius, H.-J. *FEBS J.* **2010,** *277,* 3552–3563. doi:10.1111/j.1742-4658.2010.07764.x
8. André, S.; Sanchez-Ruderisch, H.; Nakagawa, H.; Buchholz, M.; Kopitz, J.; Forberich, P.; Kemmner, W.; Böck, C.; Deguchi, K.; Detjen, K. M.; Wiedenmann, B.; von Knebel Doeberitz, M.; Gress, T. M.; Nishimura, S.-I.; Rosewicz, S.; Gabius, H.-J. *FEBS J.* **2007,** *274,* 3233–3256. doi:10.1111/j.1742-4658.2007.05851.x
9. Baldini, L.; Casnati, A.; Sansone, F.; Ungaro, R. *Chem. Soc. Rev.* **2007,** *36,* 254–266. doi:10.1039/b603082n
10. Dondoni, A.; Marra, A. *Chem. Rev.* **2010,** *110,* 4949–4977. doi:10.1021/cr100027b
11. Sansone, F.; Rispoli, G.; Casnati, A.; Ungaro, R. Multivalent Glycocalixarenes. In *Synthesis and Biological Applications of Multivalent Glycoconjugates;* Renaudet, O.; Spinelli, N., Eds.; Bentham Science Publishers: Dordrecht, 2011; pp 36–63. doi:10.2174/978160805277611101010036
12. Sansone, F.; Casnati, A. *Chem. Soc. Rev.* **2013,** *42,* 4623–4639. doi:10.1039/c2cs35437c
13. Gutsche, C. D. *Calixarenes: An Introduction,* 2nd ed.; Royal Society of Chemistry: Cambridge, 2008. doi:10.1039/9781847558190
14. Baldini, L.; Sansone, F.; Casnati, A.; Ungaro, R. Calixarenes in molecular recognition. In *Supramolecular Chemistry: from Molecules to Nanomaterials;* Steed, J. W.; Gale, P. A., Eds.; John Wiley & Sons: Chichester, 2012; pp 863–894. doi:10.1002/9780470661345.smc052
15. Casnati, A. *Gazz. Chim. Ital.* **1997,** *127,* 637–649.
16. Arosio, D.; Fontanella, M.; Baldini, L.; Mauri, L.; Bernardi, A.; Casnati, A.; Sansone, F.; Ungaro, R. *J. Am. Chem. Soc.* **2005,** *127,* 3660–3661. doi:10.1021/ja0444029
17. Garcia-Hartjes, J.; Bernardi, S.; Weijers, C. A. G. M.; Wennekes, T.; Gilbert, M.; Sansone, F.; Casnati, A.; Zuilhof, H. *Org. Biomol. Chem.* **2013,** *11,* 4340–4349. doi:10.1039/c3ob40515j
18. Cecioni, S.; Lalor, R.; Blanchard, B.; Praly, J.-P.; Imberty, A.; Matthews, S. E.; Vidal, S. *Chem.–Eur. J.* **2009,** *15,* 13232–13240. doi:10.1002/chem.200901799
19. Moni, L.; Pourceau, G.; Zhang, J.; Meyer, A.; Vidal, S.; Souteyrand, E.; Dondoni, A.; Morvan, F.; Chevolot, Y.; Vasseur, J.-J.; Marra, A. *ChemBioChem* **2009,** *10,* 1369–1378. doi:10.1002/cbic.200900024
20. André, S.; Grandjean, C.; Gautier, F.-M.; Bernardi, S.; Sansone, F.; Gabius, H.-J.; Ungaro, R. *Chem. Commun.* **2011,** *47,* 6126–6128. doi:10.1039/c1cc11163a
21. André, S.; Sansone, F.; Kaltner, H.; Casnati, A.; Kopitz, J.; Gabius, H.-J.; Ungaro, R. *ChemBioChem* **2008,** *9,* 1649–1661. doi:10.1002/cbic.200800035
22. Dings, R. P. M.; Miller, M. C.; Nesmelova, I.; Astorgues-Xerri, L.; Kumar, N.; Serova, M.; Chen, X.; Raymond, E.; Hoye, T. R.; Mayo, K. H. *J. Med. Chem.* **2012,** *55,* 5121–5129. doi:10.1021/jm300014q
    An aglyconocalixarene was also shown to be able to inhibit galectin binding to the cell surface, but it was demonstrated that its action is caused by an allosteric inhibition of the glycan/carbohydrate recognition at a site away from the CRD.
23. Kolb, H. C.; Finn, M. G.; Sharpless, K. B. *Angew. Chem., Int. Ed.* **2001,** *40,* 2004–2021. doi:10.1002/1521-3773(20010601)40:11<2004::AID-ANIE2004>3.0.CO;2-5
24. Renauldet, O.; Roy, R., Eds. Thematic issue: Multivalent scaffolds in glycosciences. *Chem. Soc. Rev.* **2014,** *42,* 4515.
25. Sansone, F.; Chierici, E.; Casnati, A.; Ungaro, R. *Org. Biomol. Chem.* **2003,** *1,* 1802–1809. doi:10.1039/b301595e
26. Sansone, F.; Baldini, L.; Casnati, A.; Ungaro, R. *Supramol. Chem.* **2008,** *20,* 161–168. doi:10.1080/10610270701777344
27. Torvinen, M.; Neitola, R.; Sansone, F.; Baldini, L.; Ungaro, R.; Casnati, A.; Vainiotalo, P.; Kalenius, E. *Org. Biomol. Chem.* **2010,** *8,* 906–915. doi:10.1039/b916268b
28. Consoli, G. M. L.; Cunsolo, F.; Geraci, C.; Mecca, T.; Neri, P. *Tetrahedron Lett.* **2003,** *44,* 7467–7470. doi:10.1016/j.tetlet.2003.08.039
29. Viola, S.; Consoli, G. M. L.; Merlo, S.; Drago, F.; Sortino, M. A.; Geraci, C. *J. Neurochem.* **2008,** *107,* 1047–1055. doi:10.1111/j.1471-4159.2008.05656.x

30. Consoli, G. M. L.; Cunsolo, F.; Geraci, C.; Sgarlata, V. *Org. Lett.* **2004,** *6,* 4163–4166. doi:10.1021/ol0485767
31. Cardona, F.; Isoldi, G.; Sansone, F.; Casnati, A.; Goti, A. *J. Org. Chem.* **2012,** *77,* 6980–6988. doi:10.1021/jo301155p
32. Calvo-Flores, F. G.; Isac-Garcia, J.; Hernandez-Mateo, F.; Pérez-Balderas, F.; Calvo-Asin, J. A.; Sanchéz-Vaquero, E.; Santoyo-González, F. *Org. Lett.* **2000,** *2,* 2499–2502. doi:10.1021/ol006175v
33. Dondoni, A.; Marra, A. *J. Org. Chem.* **2006,** *71,* 7546–7557. doi:10.1021/jo0607156
34. Rostovtsev, V. V.; Green, L. G.; Fokin, V. V.; Sharpless, K. B. *Angew. Chem., Int. Ed.* **2002,** *41,* 2596–2599. doi:10.1002/1521-3773(20020715)41:14<2596::AID-ANIE2596>3.0.CO;2-4
35. Tornoe, C. W.; Christensen, C.; Meldal, M. *J. Org. Chem.* **2002,** *67,* 3057–3064. doi:10.1021/jo011148j
36. Bew, S. P.; Brimage, R. A.; L'Hermite, N.; Sharma, S. V. *Org. Lett.* **2007,** *9,* 3713–3716. doi:10.1021/ol071047t
37. Vecchi, A.; Melai, B.; Marra, A.; Chiappe, C.; Dondoni, A. *J. Org. Chem.* **2008,** *73,* 6437–6440. doi:10.1021/jo800954z
38. Cecioni, S.; Matthews, S. E.; Blanchard, H.; Praly, J.-P.; Imberty, A.; Vidal, S. *Carbohydr. Res.* **2012,** *356,* 132–141. doi:10.1016/j.carres.2012.02.006
39. Aleandri, S.; Casnati, A.; Fantuzzi, L.; Mancini, G.; Rispoli, G.; Sansone, F. *Org. Biomol. Chem.* **2013,** *11,* 4811–4817. doi:10.1039/c3ob40732b
40. Bouillon, C.; Meyer, A.; Vidal, S.; Jochum, A.; Chevolot, Y.; Cloarec, J.-P.; Praly, J.-P.; Vasseur, J.-J.; Morvan, F. *J. Org. Chem.* **2006,** *71,* 4700–4702. doi:10.1021/jo060572n
41. Sasaki, A.; Murahashi, N.; Yamada, H.; Morikawa, A. *Biol. Pharm. Bull.* **1994,** *17,* 680–685. doi:10.1248/bpb.17.680
42. Michel, O.; Ravoo, B. J. *Langmuir* **2008,** *24,* 12116–12118. doi:10.1021/la802304w
43. Alyapyshev, M. Yu.; Babain, V. A.; Boyko, V. I.; Eliseev, I. I.; Kirsanov, D. O.; Klimchuk, O. V.; Legin, A. V.; Mikhailina, E. S.; Rodik, R. V.; Smirnov, I. V. *J. Inclusion Phenom. Macrocyclic Chem.* **2010,** *67,* 117–126. doi:10.1007/s10847-009-9685-8
44. No autocatalytic effect was observed even if the distance between the triazole unit and the macrocycle (3 atoms) is exactly the same.
45. Kato, H.; Uzawa, H.; Nagatsuka, T.; Kondo, S.; Sato, K.; Ohsawa, I.; Kanamori-Kataoka, M.; Takei, Y.; Ota, S.; Furuno, M.; Dohi, H.; Nishida, Y.; Seto, Y. *Carbohydr. Res.* **2011,** *346,* 1820–1826. doi:10.1016/j.carres.2011.06.025
46. Xue, J. L.; Cecioni, S.; He, L.; Vidal, S.; Praly, J.-P. *Carbohydr. Res.* **2009,** *344,* 1646–1653. doi:10.1016/j.carres.2009.06.004
47. Sansone, F.; Dudič, M.; Donofrio, G.; Rivetti, C.; Baldini, L.; Casnati, A.; Cellai, S.; Ungaro, R. *J. Am. Chem. Soc.* **2006,** *128,* 14528–14536. doi:10.1021/ja0634425

License and Terms

BEILSTEIN JOURNAL OF ORGANIC CHEMISTRY

Bifunctional dendrons for multiple carbohydrate presentation via carbonyl chemistry

Davide Bini, Francesco Nicotra and Laura Cipolla*

Letter

Open Access

Address:
Department of Biotechnology and Biosciences, University of Milano-Bicocca, Piazza della Scienza 2, 20126 Milano, Italy

Email:
Laura Cipolla* - laura.cipolla@unimib.it

* Corresponding author

Keywords:
bis-MPA; carbohydrates; dendrons; levulinic acid; multivalency; multivalent glycosystems

Beilstein J. Org. Chem. **2014,** *10,* 1686–1691.
doi:10.3762/bjoc.10.177

Received: 28 February 2014
Accepted: 27 June 2014
Published: 25 July 2014

This article is part of the Thematic Series "Multivalent glycosystems for nanoscience".

Guest Editor: B. Turnbull

Abstract

The synthesis of new dendrons of the generations 0, 1 and 2 with a double bond at the focal point and a carbonyl group at the termini has been carried out. The carbonyl group has been exploited for the multivalent conjugation to a sample saccharide by reductive amination and alkoxyamine conjugation.

Introduction

Recognition processes between glycans and their receptors are of paramount relevance in several biological phenomena, both in physiological [1,2] and in pathological [3-5] conditions. These processes can be exploited in diagnostic tools [6,7], in nanobiotechnology applications [8], and in the development of smart biomaterials for regenerative medicine [9-12]. Beside the variation of carbohydrate residues in glycoconjugates, a key issue in the recognition process is their spatial topographical presentation eliciting high affinity recognition events. In order to better understand these phenomena, dendrimers and dendrons have been developed to provide multivalent glycoconjugates [13,14]. Here, we propose the synthesis of novel dendron structures which allow for the multivalent conjugation of carbohydrates via carbonyl chemistry.

Results and Discussion

The heterobifunctional dendrons were designed in order to have bio-orthogonal functional groups at the focal point and at their termini. More specifically, a double bond was placed at the desired matrix as the focal point for further conjugation by thiol–ene chemistry, and carbonyl groups were added at the termini. The carbonyl groups can be exploited for carbohydrate functionalization [15,16] by reductive amination, oxime or hydrazone formation to yield suitably functionalized saccha-

rides (Figure 1). Given the relevance of L-fucose in mammal oligosaccharides, α-L-(2-aminoethyl) fucoside [17] and α-*O*-L-fucopyranosyloxyamine [18] were used as sample monosaccharides for the conjugation of the dendron (Scheme 1).

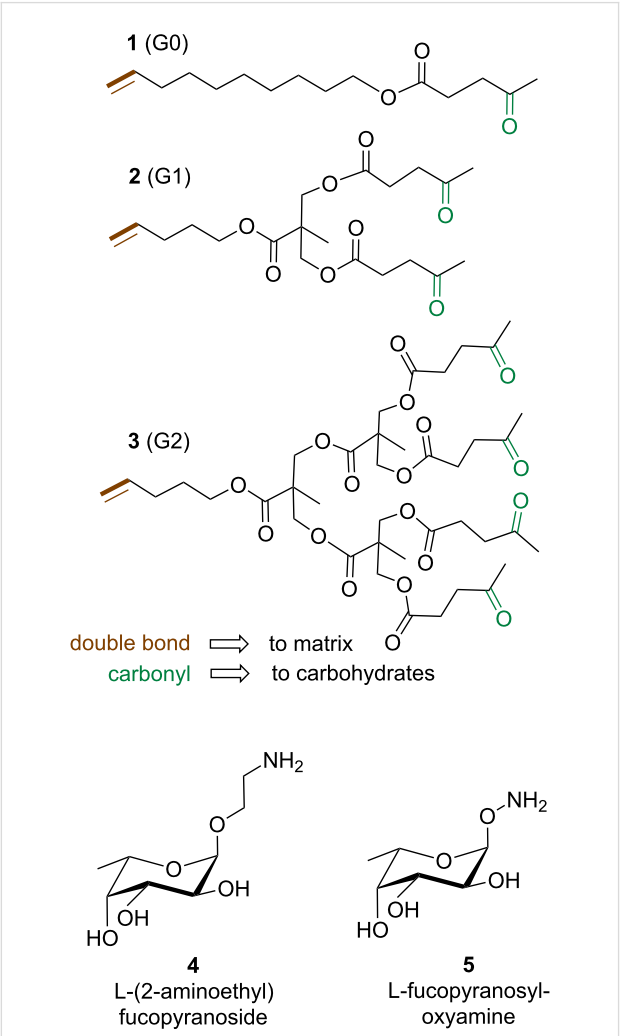

Figure 1: Synthesized G0, G1 and G2 dendrons and functionalized saccharides used for carbonyl conjugation.

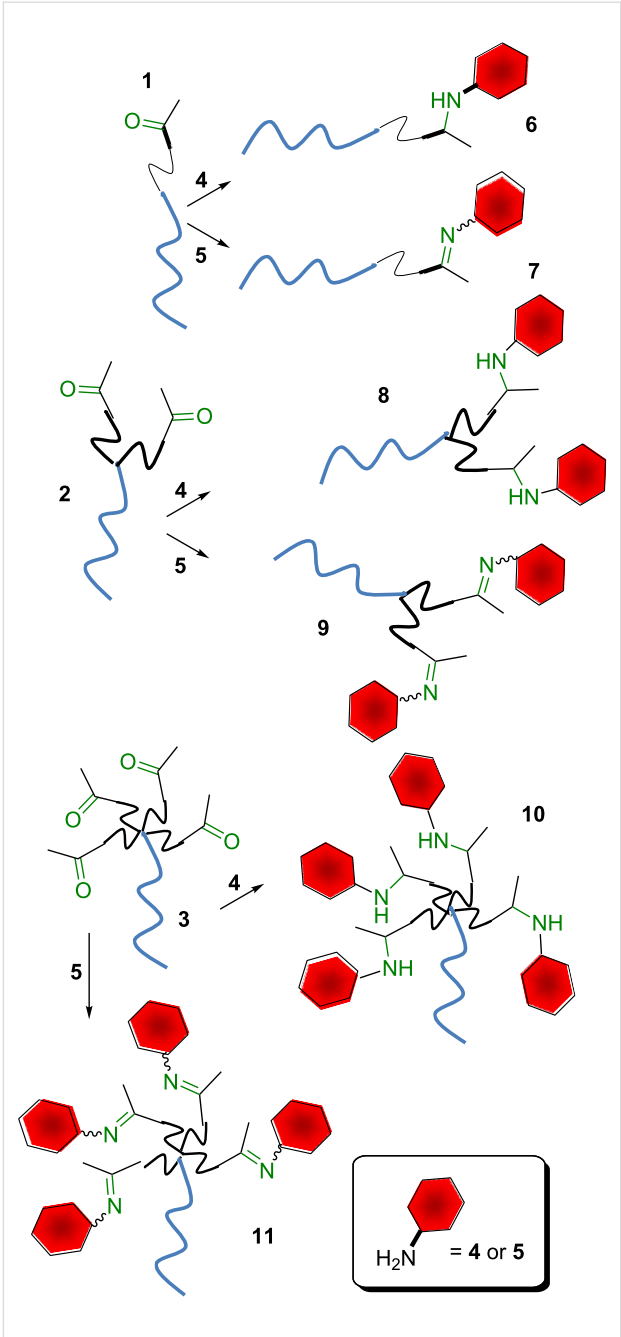

Scheme 1: Schematic depiction of dendron conjugation to saccharides by carbonyl chemistry.

Synthesis of dendrons

Zero, first and second generation heterobifunctional dendrons **1–3** were synthesized starting from 9-decen-1-ol (**12**) or selected building blocks **13** and **14** (Scheme 2) [11] by esterification reactions with levulinic acid (**15**). Building blocks **13** and **14** were synthesized starting from bis-(hydroxymethyl)propionic acid (bis-MPA) and bromo-1-pentene [11] in one and four steps, respectively.

L-Fucose derivatives synthesis

α-L-(2-Aminoethyl) fucopyranoside (**4**) and α-O-L-fucopyranosyloxyamine (**5**) were synthesized from commercial L-fucopyranose in 4 and 5 steps, respectively, as already reported by Flitsch and co-workers [17] and Dumy and co-workers [18].

Dendron conjugation to L-fucose by reductive amination

α-L-(2-Aminoethyl) fucopyranoside (**4**) was conjugated first to G0 dendron **1** by reductive amination in the presence of $NaCNBH_3$ (Scheme 3). The reaction afforded the desired glyco-

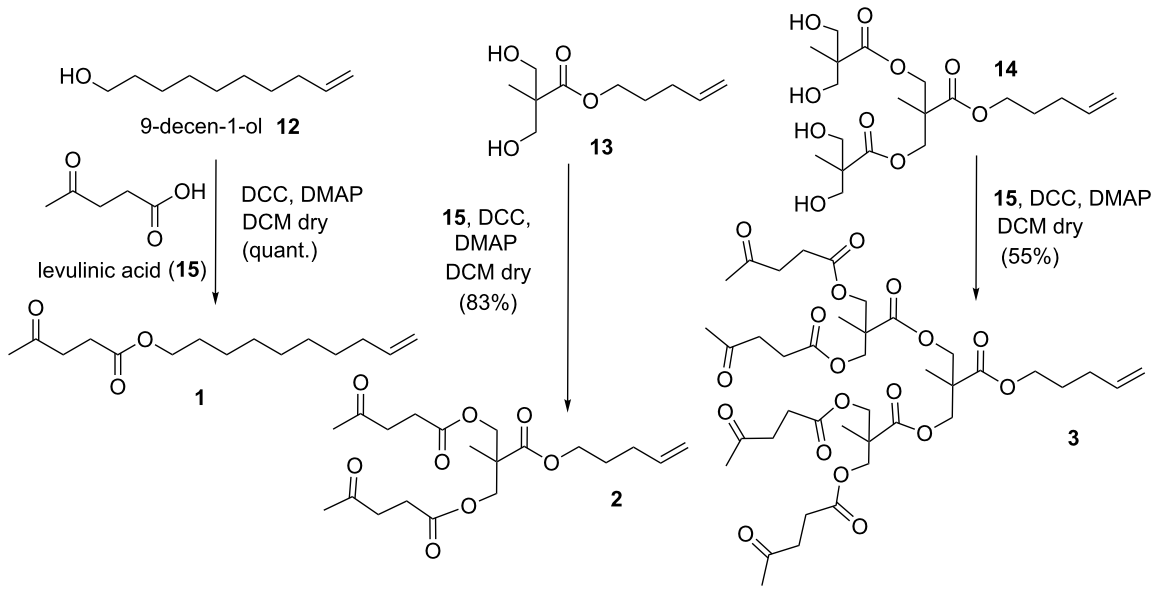

Scheme 2: Synthesis of the dendrons.

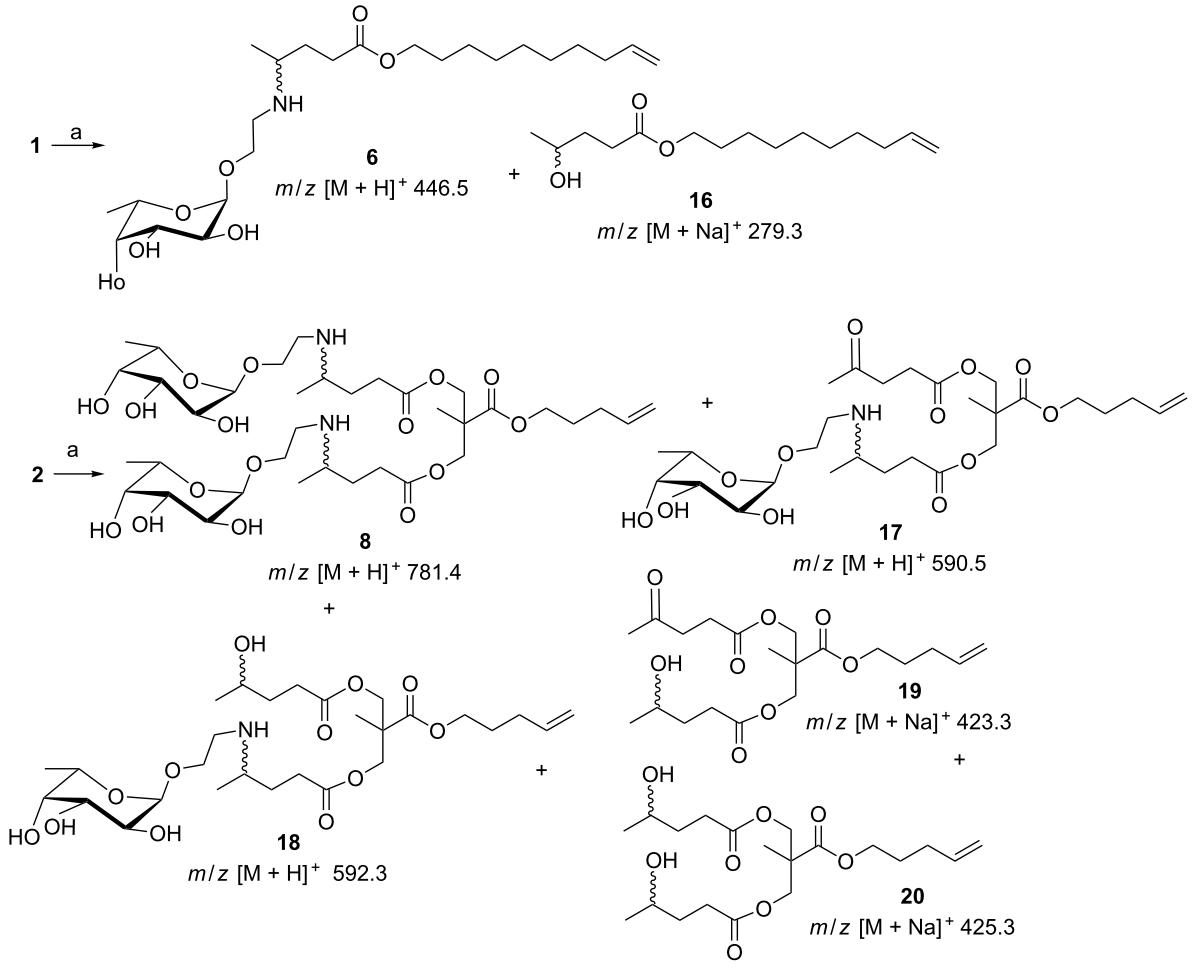

Scheme 3: Dendron conjugation to fucose moieties by reductive amination. Reagents and conditions: a) **4**, 3 M Na_2SO_4, AcOH, $NaCNBH_3$, EtOH, 80 °C, 6 h.

sylated dendron **6** in 27% yield. The very low yield was ascribed to the competing carbonyl reduction to the corresponding alcohol **16** as a byproduct.

The same reaction on the G1 dendron **2** gave an even more complex mixture of products, identified by mass spectrometry (System Applied Biosystems MDS SCIEX instruments: Q TRAP, LC/MS/MS, turbo ion spray and Q STAR elite nano spray) performed directly on the TLC spots following literature procedures [19]. By mass values, the mixture was composed of the desired fucosylated dendron **8** as the minor product together with the monoglycosylated derivatives **17** and **18** and the alcohols **19** and **20**. In order to reduce the formation of alcohol byproducts, a "milder" reducing agent such as $Na(AcO)_3BH$ was tried, but without any success.

Given the high extent of byproducts and the low efficiency of the glycoconjugation to the G0 dendron and G1 dendron by reductive amination, we decided to evaluate the possibility to obtain better conjugation yields by oxime ligation. Thus, G0, G1 and G2 dendrons **1**–**3** were reacted with α-O-L-fucopyranosyloxyamine (**5**) in citrate buffer at pH 3.5 [20] (Scheme 4). Due to the partial hydrophobic nature of the dendrons **1**–**3** they do not fully dissolve in the buffer, and the solution is not completely clear.

The dendrons **1**–**3** were reacted overnight at room temperature with α-O-L-fucopyranosyloxyamine (**5**) affording the desired glycoconjugate structures **7**, **9** and **11** in quantitative yields.

Conclusion

In conclusion, novel G0, G1 and G2 dendrons suitable for glycoconjugation by carbonyl chemistry were synthesized. The conjugation of the saccharide by reductive amination was characterized by a low efficiency. On the other hand, the oxime ligation afforded the glycoconjugated dendrons in quantitative

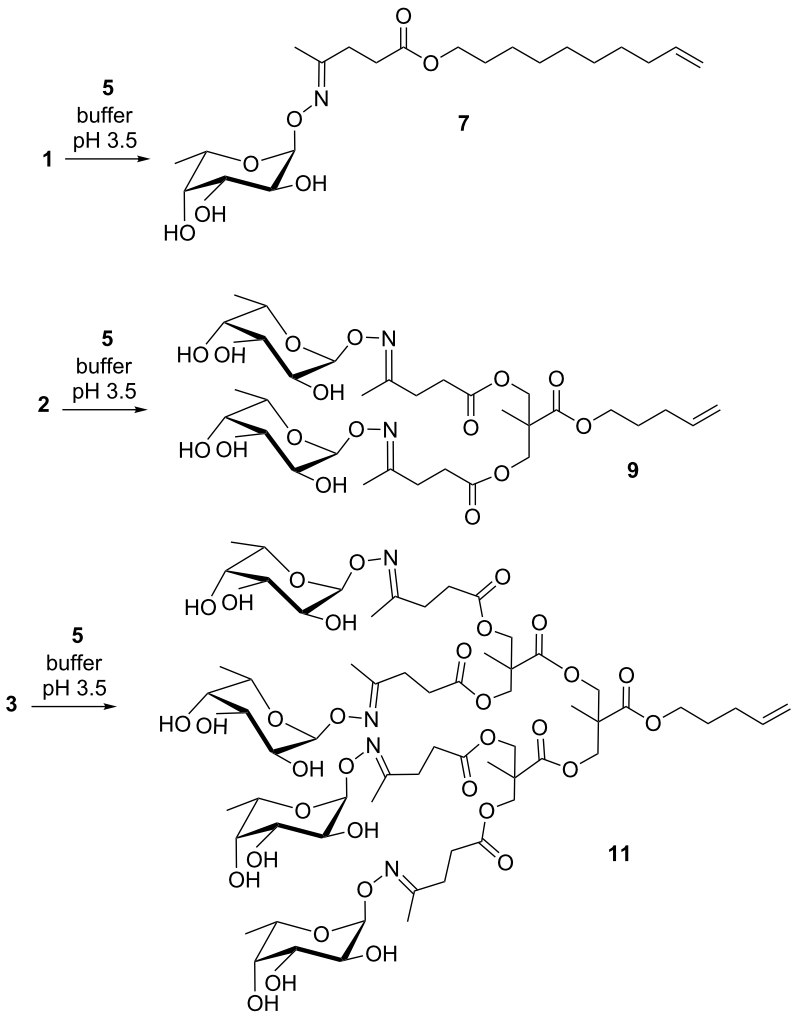

Scheme 4: Dendron conjugation to fucose via oxime ligation (buffer = citrate buffer).

yields. The glycosylated dendrons can be exploited for further chemoselctive thiol–ene reactions with matrices suitably functionalized with thiol groups, i.e., cysteine residues in proteins.

Experimental

General methods

All chemicals were purchased from Sigma-Aldrich and used without further purification. All solvents were dried over molecular sieves, for at least 24 h prior to use, when required. When dry conditions were required, the reaction was performed under an Ar atmosphere. Thin-layer chromatography (TLC) was performed on silica gel 60 F254 coated glass plates (Merck) with UV detection when possible, or spots were visualized by charring with a conc. H_2SO_4/EtOH/H_2O solution (10:45:45 v/v/v), or with a solution of $(NH_4)_6Mo_7O_{24}$ (21 g), $Ce(SO_4)_2$ (1 g), conc. H_2SO_4 (31 mL) in water (500 mL) and then by heating to 110 °C for 5 min. Flash column chromatography was performed on silica gel 230–400 mesh (Merck). Routine ^1H and ^{13}C NMR spectra were recorded on a Varian Mercury instrument at 400 MHz (^1H) and 100.57 MHz (^{13}C). Chemical shifts are reported in parts per million downfield from TMS as an internal standard, *J* values are given in Hz. Mass spectra were recorded on System Applied Biosystems MDS SCIEX instruments: Q TRAP, LC/MS/MS, turbo ion spray and Q STAR elite nanospray.

General procedure for levulinic acid condensation (compounds 1–3): To a 0.1 M solution of the appropriate compound dissolved in dry DCM, levulinic acid (1.2 equiv), DMAP (0.2 equiv) and DCC (1.5 equiv) were added, and the reaction mixture was stirred at room temperature (for 1 to 24 h, depending on the substrate). The precipitates were filtered off and washed with CH_2Cl_2. The solvent was evaporated, and the residue was purified by column chromatography on a silica gel column with a suitable eluent. See Supporting Information File 1 for full experimental data.

General procedure for reductive amination reaction (compounds 6, 8):The appropriate dendron (1 equiv) and α-L-(2-aminoethyl) fucoside (**4**, 1 equiv) were dissolved in EtOH (0.1 M in respect to **4**). AcOH (1 equiv) and 3 M Na_2SO_4 (1% of solvent volume) were added, and the mixture was heated under reflux for 2 h. $NaCNBH_3$ (1.5 equiv) was then added, and the reaction was heated under reflux for further 4 h. See Supporting Information File 1 for full experimental data.

General procedure for dendron/ alkoxyamine conjugation (compounds 7, 9, 11): The appropriate dendron (1 equiv) and α-O-L-fucopyranosyloxyamine (**5**, 1 equiv) were dissolved in citrate buffer (pH 3.5, 0.1 M in respect to **5**) and stirred at room temperature overnight. The mixture was concentrated and the product isolated. See Supporting Information File 1 for full experimental data.

Supporting Information

Supporting Information File 1

Experimental part.
[http://www.beilstein-journals.org/bjoc/content/supplementary/1860-5397-10-177-S1.pdf]

Acknowledgements

This research was financially supported by the Cariplo Fundation under the grant numbers 2010-0378, 2011-0270 and PRIN 2010L9SH3K.

References

1. Johnson, J. L.; Jones, M. B.; Ryan, S. O.; Cobb, B. A. *Trends Immunol.* **2013,** *34,* 290–298. doi:10.1016/j.it.2013.01.006
2. Moremen, K. W.; Tiemeyer, M.; Nairn, A. V. *Nat. Rev. Mol. Cell Biol.* **2012,** *13,* 448–462. doi:10.1038/nrm3383
3. Schedin-Weiss, S.; Winblad, B.; Tjernberg, L. O. *FEBS J.* **2014,** *281,* 46–62. doi:10.1111/febs.12590
4. Kleene, R.; Schachner, M. *Nat. Rev. Neurosci.* **2004,** *5,* 195–208. doi:10.1038/nrn1349
5. Ohtsubo, K.; Marth, J. D. *Cell* **2006,** *126,* 855–867. doi:10.1016/j.cell.2006.08.019
6. Morais, G. R.; Falconer, R. A.; Santos, I. *Eur. J. Org. Chem.* **2013,** 1401–1410. doi:10.1002/ejoc.201201457
7. Cipolla, L.; Gregori, M.; So, P.-W. *Curr. Med. Chem.* **2011,** *18,* 1002–1018. doi:10.2174/092986711794940851
8. Sapsford, K. E.; Algar, W. R.; Berti, L.; Boeneman Gemmill, K.; Casey, B. J.; Oh, E.; Stewart, M. H.; Medintz, I. L. *Chem. Rev.* **2013,** *113,* 1904–2074. doi:10.1021/cr300143v
9. Cipolla, L.; Russo, L.; Taraballi, F.; Lupo, C.; Bini, D.; Gabrielli, L.; Capitoli, A.; Nicotra, F. Smart biomaterials: the contribution of glycoscience**.** In *Specialist Periodical Reports, SPR Carbohydrate Chemistry*; 2012, Vol. 38, pp. 416–445 .
10. Russo, L.; Battocchio, C.; Secchi, V.; Magnano, E.; Nappini, S.; Taraballi, F.; Gabrielli, L.; Comelli, F.; Papagni, A.; Costa, B.; Polzonetti, G.; Nicotra, F.; Natalello, A.; Doglia, S. M.; Cipolla, L. *Langmuir* **2014,** *30,* 1336–1342. doi:10.1021/la404310p
11. Bini, D.; Russo, L.; Battocchio, C.; Natalello, A.; Polzonetti, G.; Doglia, S. M.; Nicotra, F.; Cipolla, L. *Org. Lett.* **2014,** *16,* 1298–1301. doi:10.1021/ol403476z
12. Du, J.; Yarema, K. J. *Adv. Drug Delivery Rev.* **2010,** *62,* 671–682. doi:10.1016/j.addr.2010.01.003
13. Bernardi, A.; Jimenez-Barbero, J.; Casnati, A.; De Castro, C.; Darbre, T.; Fieschi, F.; Finne, J.; Funken, H.; Jaeger, K.-E.; Lahmann, M.; Lindhorst, T. K.; et al. *Chem. Soc. Rev.* **2013,** *42,* 4709–4727. doi:10.1039/c2cs35408j
14. Sanchez-Navarro, M.; Rojo, J. *Drug News Perspect.* **2010,** *23,* 557–572. doi:10.1358/dnp.2010.23.9.1437246
15. Paez, J. I.; Martinelli, M.; Brunetti, V.; Strumia, M. C. *Polymers* **2012,** *4,* 355–395. doi:10.3390/polym4010355
16. Röglin, L.; Lempens, E. H. M.; Meijer, E. W. *Angew. Chem., Int. Ed.* **2011,** *50,* 102–112. doi:10.1002/anie.201003968

17. Šardzík, R.; Noble, G. T.; Weissenborn, M. J.; Martin, A.; Webb, S. J.; Flitsch, S. L. *Beilstein J. Org. Chem.* **2010,** *6,* 699–703. doi:10.3762/bjoc.6.81
18. Duléry, V.; Renaudet, O.; Philouze, C.; Dumy, P. *Carbohydr. Res.* **2007,** *342,* 894–900. doi:10.1016/j.carres.2007.02.003
19. St. Hilaire, P. M.; Cipolla, L.; Tedebark, U.; Meldal, M. *Rapid Commun. Mass Spectrom.* **1998,** *12,* 1475–1484. doi:10.1002/(SICI)1097-0231(19981030)12:20<1475::AID-RCM365>3.0.CO;2-F
20. Hudak, J. E.; Yu, H. H.; Bertozzi, C. R. *J. Am. Chem. Soc.* **2011,** *133,* 16127–16135. doi:10.1021/ja206023e

License and Terms

BEILSTEIN JOURNAL OF ORGANIC CHEMISTRY

Convergent synthetic methodology for the construction of self-adjuvanting lipopeptide vaccines using a novel carbohydrate scaffold

Vincent Fagan[1], Istvan Toth[1,2] and Pavla Simerska[*1]

Full Research Paper

Open Access

Address:
[1]The University of Queensland, School of Chemistry and Molecular Biosciences, Cooper Road, St. Lucia QLD 4072, Australia and [2]The University of Queensland, School of Pharmacy, Pharmacy Australia Centre of Excellence, Cornwall Street, Woolloongabba, QLD 4072, Australia

Email:
Pavla Simerska[*] - p.simerska@uq.edu.au

* Corresponding author

Keywords:
amino acid lipidation; cycloadditon reaction; multivalent glycosystems; peptide vaccine; tetrapropargyl glucopyranose

Beilstein J. Org. Chem. **2014,** *10,* 1741–1748.
doi:10.3762/bjoc.10.181

Received: 03 April 2014
Accepted: 03 July 2014
Published: 30 July 2014

This article is part of the Thematic Series "Multivalent glycosystems for nanoscience".

Guest Editor: V. Křen

Abstract

A novel convergent synthetic strategy for the construction of multicomponent self-adjuvanting lipopeptide vaccines was developed. A tetraalkyne-functionalized glucose derivative and lipidated Fmoc-lysine were prepared by novel efficient and convenient syntheses. The carbohydrate building block was coupled to the self-adjuvanting lipidic moiety (three lipidated Fmoc-lysines) on solid support. Four copies of a group A streptococcal B cell epitope (J8) were then conjugated to the glyco-lipopeptide using a copper-catalyzed cycloaddition reaction. The approach was elaborated by the preparation of a second vaccine candidate which incorporated an additional promiscuous T-helper epitope.

Introduction

Vaccination is often the most effective and economic long-term way to prevent disease [1]. Through vaccination, successful outcomes have been achieved for diseases such as smallpox, polio and diphtheria, thus providing motivation for the development of superior vaccines for other diseases. Traditionally, vaccines consisted of killed or live attenuated pathogens, or their purified components. While these approaches have proved highly beneficial, in some instances they have shown associated risks, such as cross-reactivity with self-tissue (leading to autoimmune conditions), and the possibility of infection, particularly with immuno-compromized patients [2,3]. To overcome such issues, subunit vaccines, which contain only the minimum B and T cell peptide epitopes, were developed. However, when such peptide epitopes are administered alone, they are poorly immunogenic. This is due to their instability in the presence of proteases, and due to the absence of other important immuno-

stimulatory components, known as adjuvants [4]. Adjuvant development has advanced slowly and for many decades, aluminium salts were the only adjuvants approved for clinical use [5]. Recently, research efforts have focused on the development of adjuvants which activate specific pattern recognition receptors (PRRs) found on immune cells. PRRs recognize conserved pathogen-associated molecular patterns. This leads to activation of cells of the innate and adaptive immune system, resulting in significantly enhanced immune responses [6]. By preparing agonists for a particular type of PRR (e.g., Toll Like Receptor (TLR)), an appropriate immune response can be induced for each type of pathogen [7]. The TLR2 is a receptor present on cells of the innate and adaptive immune system. It recognizes lipidic structural components of bacteria, fungi and viruses, and plays a key role in the body's defences, particularly against Gram positive bacteria [8]. Research efforts within our group have shown that a short sequence of synthetic lipoamino acids (Lipid Core Peptide (LCP)), can bind to the TLR2, which results in increased immune responses to otherwise poorly immunogenic peptide antigens [9-12].

The model pathogen chosen for this study was *Streptococcus pyogenes*, a Gram positive bacteria that affects the skin and upper respiratory tract, and causes a range of health issues that are collectively referred to as group A streptococcal (GAS) infections [13]. The most severe GAS related problems are post-streptococcal rheumatic fever and rheumatic heart disease, which are responsible for over half a million deaths annually [14]. Previously, we developed methodologies for the synthesis of carbohydrate building blocks as scaffold carriers of multiple B cell epitopes derived from GAS. The vaccine constructs consisted of the LCP adjuvanting moiety, and a carbohydrate core bearing four copies of a GAS B cell epitope [11,15-18]. When administered to B10.BR (H-2^k) mice, the carbohydrate-based LCP vaccines elicited high serum IgG antibody titres [11]. One of the B cell epitopes used was the J8-peptide antigen. This epitope was identified from the conserved C-terminal region of the M protein (a cell surface protein and a major virulence factor) of *S. pyogenes* [19]. For comparison purposes, the J8 epitope was also employed in the current studies.

The previously reported carbohydrate-based vaccine constructs [11] were prepared by a divergent approach, where the carbohydrate core was coupled to the resin-bound LCP adjuvanting moiety, followed by stepwise synthesis of the B cell epitopes using solid-phase peptide synthesis (SPPS). Using this divergent approach, purification could not be performed until the end of the synthesis and crude samples of final vaccine candidates often required multiple purification steps. The current study outlines a new convergent synthetic methodology for the synthesis of novel carbohydrate-based GAS vaccine delivery systems, where each building block can be synthesized and purified prior to final assembly of the vaccine candidates. The building blocks may be assembled in different ways so that libraries of vaccine candidates can be prepared faster and more efficiently compared to the previous divergent approach.

Results and Discussion

As part of the new convergent approach, here, we report an efficient and convenient synthesis of a versatile alkyne-functionalized carbohydrate building block **1**, which can be conveniently incorporated into peptide sequences using SPPS (Scheme 1). The copper-catalyzed alkyne–azide cycloaddition 'click' reaction [20] was employed to couple multiple copies of purified B cell peptide antigens onto the carbohydrate core and lipidic adjuvanting moiety.

This type of convergent approach has a number of advantages over the previously described divergent route. Since each component is synthesized separately and purified before final assembly, purification of the vaccine candidates is less demanding. As a result, additional components can be incorporated, giving vaccine candidates of greater complexity. Taking advantage of this, we synthesized a second vaccine candidate containing a known promiscuous T-helper epitope [21], the lipidic adjuvanting moiety and four copies of the GAS B cell epitope coupled to the carbohydrate carrier. Although B cells may be activated via a number of T cell-independent routes, the T cell-dependent activation of B cells can lead to stronger and more long-term immune responses [6].

Synthesis of carbohydrate carrier

Tetra-*O*-acetyl-α-D-glucopyranosyl bromide (**2**) was prepared according to a literature procedure [22] and immediately used in the proceeding Koenigs–Knorr glycosylation of methyl 6-hydroxyhexanoate (**3**). Hydroxy ester **3** was synthesized in high yield (81%) by addition of a catalytic amount of H_2SO_4 to ε-caprolactone in methanol, according to Duffy et al. [23]. However, the procedure was optimized by decreasing the reaction time from 48 h to 30 minutes and purification by distillation was not required. The glycosylation was carried out by addition of silver(I) oxide to a solution of glycosyl bromide **2** and hydroxy ester **3**, which yielded a mixture of orthoester byproduct **4** and desired glycosylation product **5** (Scheme 2). A catalytic amount of trimethylsilyl trifluoromethanesulfonate (TMSOTf) was added to the mixture, which resulted in ring-opening of orthoester **4** and conversion to the desired glycosylation product **5**. The presence of unreacted hydroxy ester **3** made purification of glycosylation product **5** difficult. Therefore, the crude reaction mixture was subjected to Zemplén deacetylation [24] to give intermediate **6**, and the unreacted

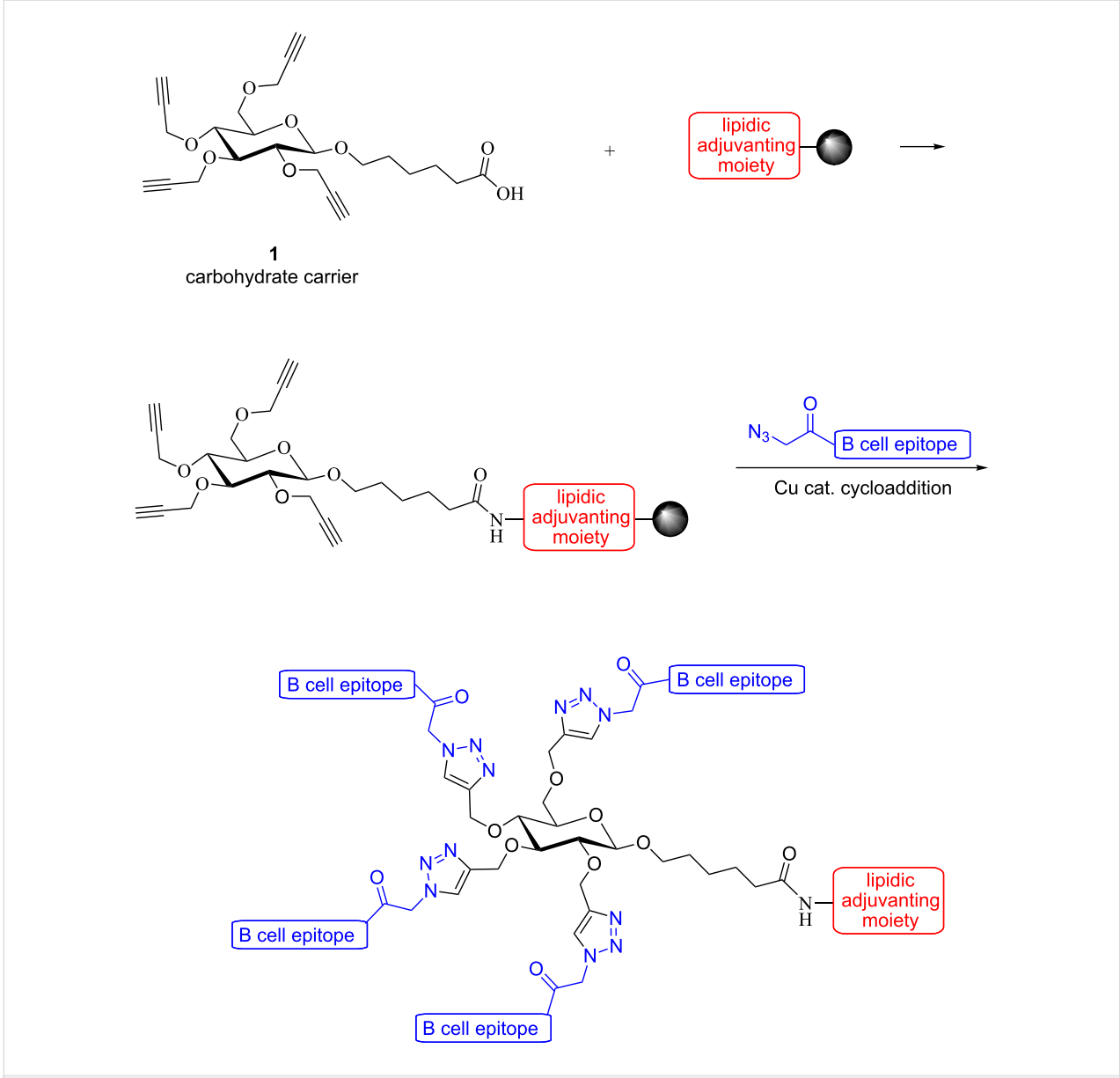

Scheme 1: Convergent construction of self-adjuvanting vaccines bearing multiple copies of a B cell epitope.

hydroxy ester **3** was removed during work-up. The residue was alkylated with sodium hydride and propargyl bromide in dry tetrahydrofuran (THF) to give intermediate **7**, which was not isolated. The methoxy ester was hydrolyzed in situ by addition of sodium hydroxide. Acid–base extraction and purification by flash chromatography gave the novel carbohydrate building block **1** in 31% overall yield (Scheme 2). Similar carbohydrates have been used for the preparation of glycoclusters for lectin binding [25-28] and as scaffold carriers of multiple peptide antigens [17,29]. However, the synthesis of the new carbohydrate building block **1** reported here is concise and efficient, involving only one chromatographic step and takes advantage of the highly efficient "click" reaction.

Synthesis of lipo-amino acid

Lipidation of peptides is important as it is often used to improve stability and permeability of potential therapeutics [30]. The lipo-amino acids used previously for synthesis of the LCP system [31] were prepared by a multistep synthesis which resulted in a racemic mixture. In the current study, enantiomerically pure lipidated Fmoc-lysine (**8**) was synthesized and used to prepare the lipidic adjuvanting moiety. Treatment of commercially available Fmoc-Lys-OH with lauroyl chloride, in the presence of diisopropylethylamine (DIPEA), gave lipidated Fmoc-lysine (**8**) in 35% yield after flash chromatography (Scheme 3A). The low yield could be attributed to the formation of a significant amount of a dimeric lysine byproduct,

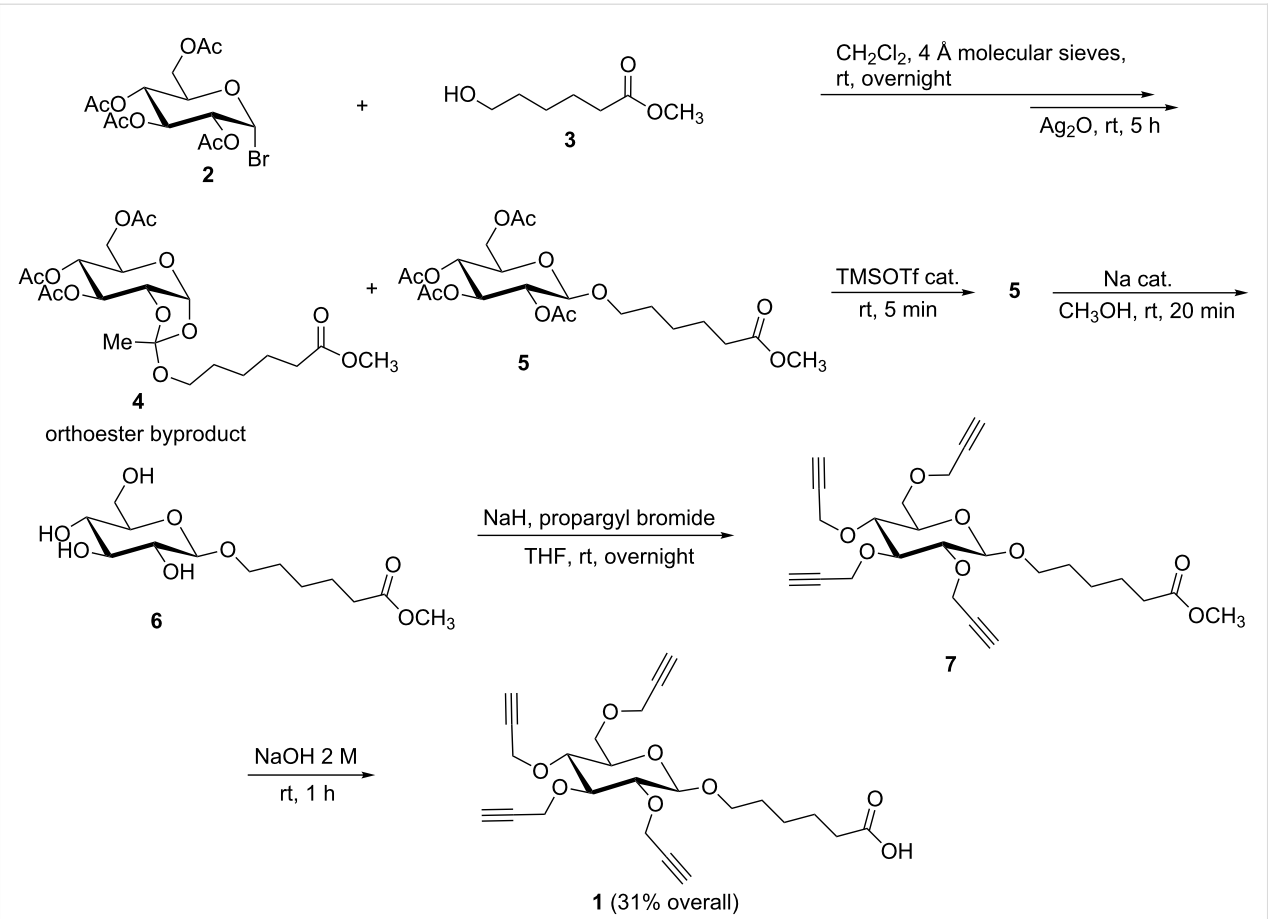

Scheme 2: Synthesis of carbohydrate building block **1**.

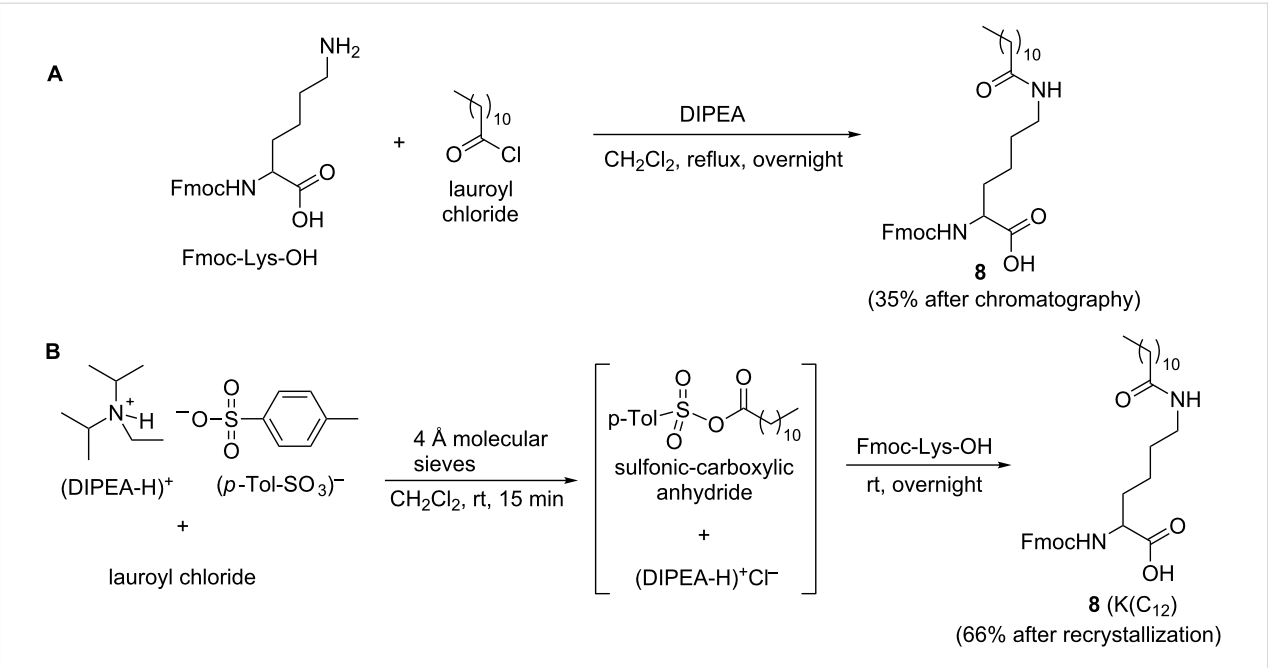

Scheme 3: (A) Lipidation of Fmoc-Lys-OH with lauroyl chloride: (B) Lipidation of Fmoc-Lys-OH with sulfonic-carboxylic anhydride.

which was not characterized. A number of different conditions were explored in order to inhibit the formation of the byproduct. By utilizing a sulfonic-carboxylic anhydride as the acylating agent, lipidated product **8** (K(C_{12})) could be synthesized smoothly and formation of the byproduct was avoided. The sulfonic-carboxylic anhydride was prepared in situ by the addition of lauroyl chloride to a solution containing DIPEA and *p*-toluenesulfonic acid, and Fmoc-Lys-OH was subsequently added to this mixture (Scheme 3B).

Because of this optimization, chromatography was not necessary and the lipidated product **8** could be purified by recrystallization (66% yield) (Scheme 3B). Compound **8** has been synthesized previously by Zhang et al. [32] using a procedure which required chromatography. The simple modification reported here significantly increased the efficiency of the procedure and may have wider application for the convenient acylation of Fmoc-lysine.

Synthesis of azide functionalized J8 B cell epitope (N_3-J8)

The conserved C-terminal region of the M protein adopts an α-helical secondary structure [13]. In order to maintain this native secondary structure, the J8 epitope (QAEDKVKQ-**SREAKKQVEKAL**-KQLEDKVQ) consists of a short C-terminal peptide from the M protein (in bold), placed within a sequence derived from the GCN4 leucine zipper DNA binding protein of yeast, which is known to promote an α-helical structure [33]. This chimeric peptide has been shown to elicit systemic IgG antibodies, which were capable of opsonizing the GAS pathogen and inducing protective immunity against GAS [19]. In the current study, the J8 epitope was synthesized using standard Fmoc SPPS. Azidoacetic acid was synthesized according to Brabez et al. [34] and was coupled to the N-terminus of the J8 epitope. The peptide was cleaved from the resin and purified by preparative RP (reversed phase)-HPLC.

Construction of vaccine candidates

The lipidic adjuvanting moiety was synthesized by standard Fmoc SPPS using the lipidated lysine amino acid **8** (K(C_{12})). This lipidic sequence, lysine lipid core peptide (LLCP; K(C_{12})-G-K(C_{12})-K(C_{12})-G), is enantiomerically pure and analogous to the LCP sequence (C_{12}-G-(C_{12})-(C_{12})-G) which has been shown to be an effective adjuvanting moiety [11]. The new carbohydrate carrier **1** was coupled to the LLCP sequence, the intermediate was cleaved from the resin using standard Fmoc SPPS cleavage conditions and the product, glyco-lipopeptide **9**, was used in the final reaction step without purification. Four copies of the N_3-J8 epitope were then coupled to glyco-lipopeptide **9** using the copper-catalyzed alkyne–azide cycloaddition reaction (Scheme 4), which was performed according to Urbani et al. [35,36]. The progress of the reaction was monitored by

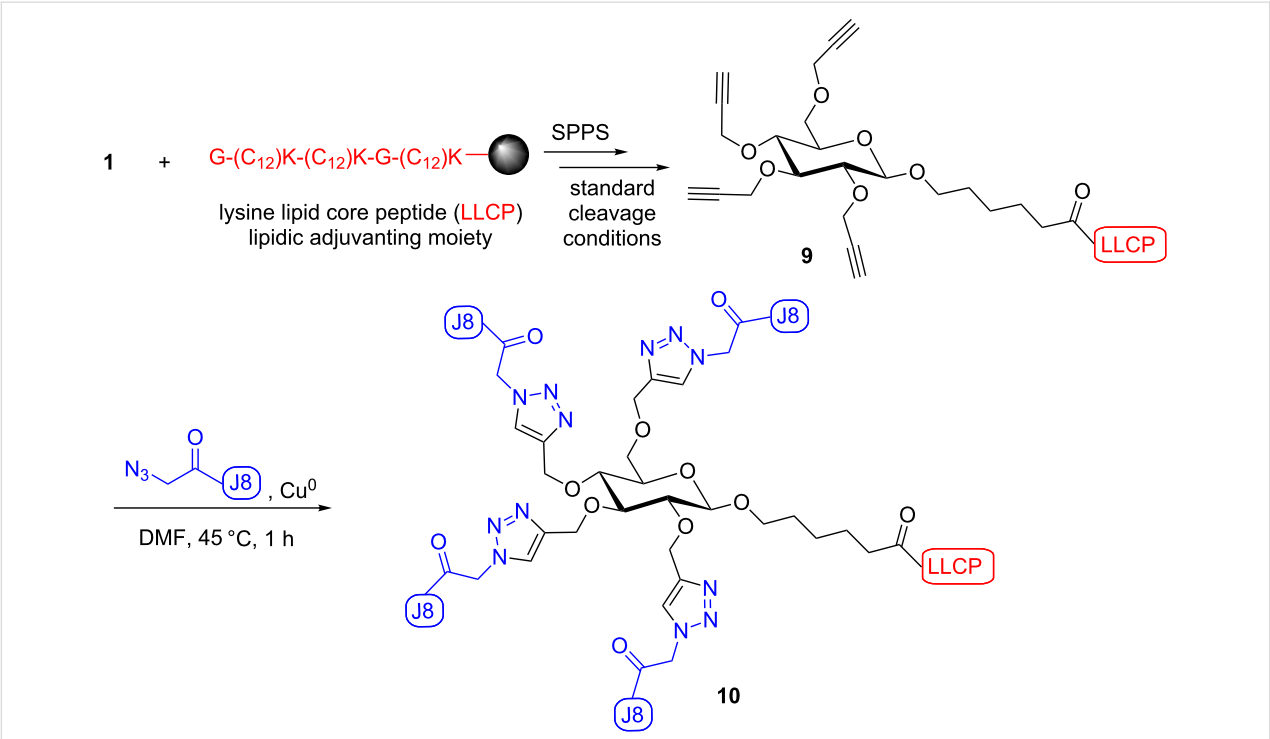

Scheme 4: Convergent synthesis of self-adjuvanting vaccine candidate **10** consisting of lipidic adjuvanting moiety LLCP, carbohydrate carrier and four copies of J8 peptide epitope.

analytical RP-HPLC (C4 column, 0–100% solvent B (CH_3CN/10% H_2O/0.1% TFA)) and was complete in approximately 1 h (Figure 1). After purification by RP-HPLC vaccine candidate **10** was obtained in 32% yield and characterized by mass spectrometry and RP-HPLC (Supporting Information File 1).

After the successful synthesis of vaccine candidate **10**, further complexity was introduced into this system. In this case, following the synthesis of LLCP, stepwise SPPS was continued in order to incorporate a T-helper epitope (Pan DR Epitope; PADRE; KFVAAWTLKAA), resulting in a linear peptide containing the T-helper epitope and the LLCP (Scheme 5). The PADRE T-helper epitope has been shown to be recognized by a high percentage of the human population, and is thus referred to as a promiscuous T-helper epitope [21]. Incorporation of this epitope should allow for T cell-dependent activation of B cells, and lead to a stronger and longer lasting immune response. The carbohydrate carrier **1** was coupled to the N-terminus of the linear T-helper-LLCP peptide, the intermediate was cleaved from the resin using standard Fmoc SPPS cleavage conditions and the product, glyco-lipopeptide **11**, was used in the final step without purification (Scheme 5). The copper-catalyzed cycloaddition reaction was performed as described before and gave the desired self-adjuvanting vaccine candidate **12**, the identity and purity of which was confirmed by mass spectrometry and analytical HPLC (Supporting Information File 1).

Conclusion

A concise and convenient synthesis of a versatile carbohydrate building block was devised. A very efficient procedure for the lipidation of Fmoc-lysine is reported, which may find widespread application for the preparation of lipopeptides. Using these building blocks, a new synthetic methodology was developed, and complex structures were prepared that contain all the necessary components of a self-adjuvanting vaccine in one pure compound. Purification of glyco-lipopeptide **9** and **11** would have significantly improved the yields of the final step, however, this was not required, making the overall synthesis far more efficient. Purification of the final vaccine candidate **10** was achieved in one chromatographic step without difficulty and thus, was less demanding compared to vaccine candidates prepared previously. As a result, the more complex vaccine candidate **12** was synthesized, which contained multiple copies of a B cell epitope coupled to the carbohydrate core, a lipidic adjuvanting moiety, as well as, a promiscuous T-helper epitope to enhance the immune response. Using this synthetic approach a library of GAS vaccine candidates will be synthesized for in vivo evaluation using immunological assays.

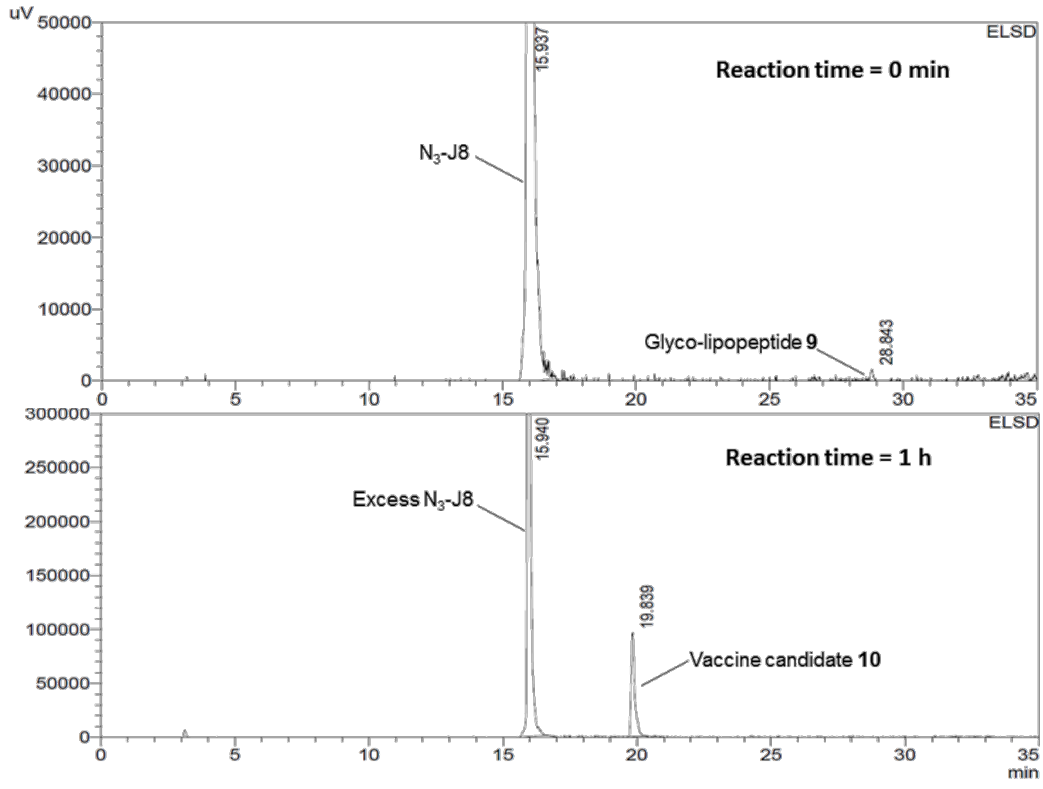

Figure 1: Analytical HPLCs of copper-catalyzed alkyne–azide cycloaddition reaction at the start (top) and after 1 h (bottom) (gradient; 0–100% solvent B over 30 min).

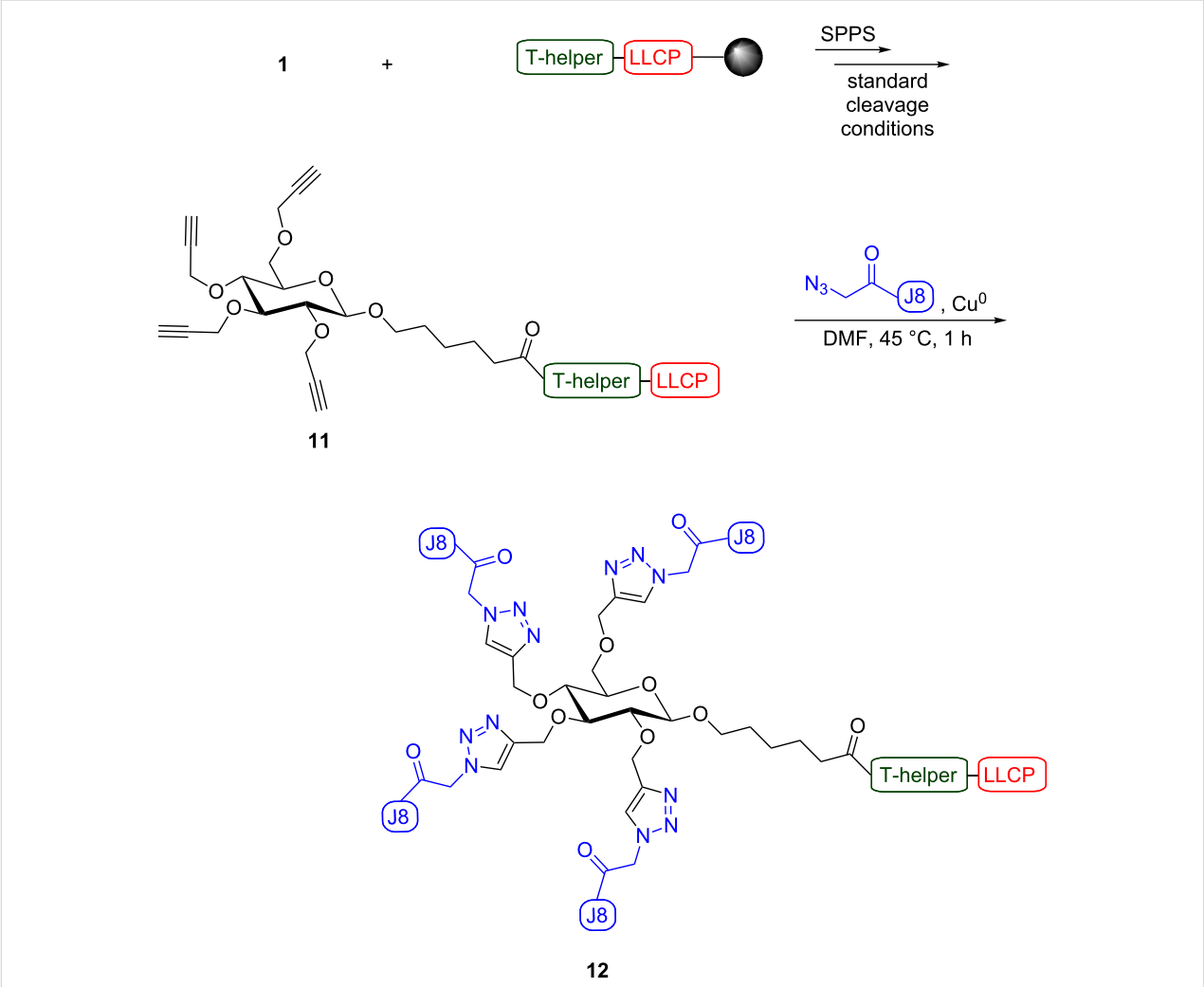

Scheme 5: Convergent synthesis of self-adjuvanting vaccine candidate **12** consisting of lipidic adjuvanting moiety LLCP, T-helper epitope, carbohydrate carrier and four copies of J8 B cell epitope.

Supporting Information

All experimental procedures are given. ^{1}H, ^{13}C, DEPT, COSY, HSQC NMR spectra are provided for compounds **4**, **5** and **1**, as well as, analytical RP-HPLC chromatograms and ESIMS spectra for N_3-J8 peptide, and vaccine candidates **10** and **12**.

Supporting Information File 1

Experimental part.
[http://www.beilstein-journals.org/bjoc/content/supplementary/1860-5397-10-181-S1.pdf]

Acknowledgements

This work was supported by the Australian National Health and Medical Research Council (NHMRC) with the NHMRC Project Grant (APP1026488) and it is gratefully acknowledged. We would also like to acknowledge the Australian Research Council for their support of this work with the Professorial Research Fellowship to I.T. (DP110100212); and The University of Queensland for the Deputy Vice-Chancellor Fellowship to P.S. (606431). We thank Mr. Alun Jones for the HRMS analysis.

References

1. Ozawa, S.; Mirelman, A.; Stack, M. L.; Walker, D. G.; Levine, O. S. *Vaccine* **2012,** *31,* 96–108. doi:10.1016/j.vaccine.2012.10.103
2. Purcell, A. W.; McCluskey, J.; Rossjohn, J. *Nat. Rev. Drug Discovery* **2007,** *6,* 404–414. doi:10.1038/nrd2224
3. Dale, J. B.; Beachey, E. H. *J. Exp. Med.* **1985,** *162,* 583–591. doi:10.1084/jem.162.2.583
4. Burdin, N.; Guy, B.; Moingeon, P. *BioDrugs* **2004,** *18,* 79–93. doi:10.2165/00063030-200418020-00002

5. Leroux-Roels, G. *Vaccine* **2010,** *28* (Suppl. 3), C25–C36. doi:10.1016/j.vaccine.2010.07.021
6. Chorny, A.; Puga, I.; Cerutti, A. *Immunol. Res.* **2012,** *54,* 4–13. doi:10.1007/s12026-012-8307-5
7. Boog, C. J. P. *Immunol. Lett.* **2009,** *122,* 104–107. doi:10.1016/j.imlet.2008.11.009
8. Kawai, T.; Akira, S. *Curr. Opin. Immunol.* **2005,** *17,* 338–344. doi:10.1016/j.coi.2005.02.007
9. Abdel-Aal, A.-B. M.; Al-Isae, K.; Zaman, M.; Toth, I. *Bioorg. Med. Chem. Lett.* **2011,** *21,* 5863–5865. doi:10.1016/j.bmcl.2011.07.102
10. Simerska, P.; Moyle, P. M.; Toth, I. *Med. Res. Rev.* **2011,** *31,* 520–547. doi:10.1002/med.20191
11. Simerska, P.; Abdel-Aal, A.-B. M.; Fujita, Y.; Moyle, P. M.; McGeary, R. P.; Batzloff, M. R.; Olive, C.; Good, M. F.; Toth, I. *J. Med. Chem.* **2008,** *51,* 1447–1452. doi:10.1021/jm701410p
12. Abdel-Aal, A.-B. M.; Batzloff, M. R.; Fujita, Y.; Barozzi, N.; Faria, A.; Simerska, P.; Moyle, P. M.; Good, M. F.; Toth, I. *J. Med. Chem.* **2008,** *51,* 167–172. doi:10.1021/jm701091d
13. Smeesters, P. R.; McMillan, D. J.; Sriprakash, K. S.; Georgousakis, M. M. *Expert Rev. Vaccines* **2009,** *8,* 1705–1720. doi:10.1586/erv.09.133
14. Carapetis, J. R.; Steer, A. C.; Mulholland, E. K.; Weber, M. *Lancet Infect. Dis.* **2005,** *5,* 685–694. doi:10.1016/S1473-3099(05)70267-X
15. Simerska, P.; Abdel-Aal, A.-B. M.; Fujita, Y.; Batzloff, M. R.; Good, M. F.; Toth, I. *Biopolymers* **2008,** *90,* 611–616. doi:10.1002/bip.20992
16. Simerska, P.; Lu, H.; Toth, I. *Bioorg. Med. Chem. Lett.* **2009,** *19,* 821–824. doi:10.1016/j.bmcl.2008.12.013
17. Zhong, W.; Skwarczynski, M.; Fujita, Y.; Simerska, P.; Good, M. F.; Toth, I. *Aust. J. Chem.* **2009,** *62,* 993–999. doi:10.1071/CH09065
18. Zhong, W.; Skwarczynski, M.; Simerska, P.; Good, M. F.; Toth, I. *Tetrahedron* **2009,** *65,* 3459–3464. doi:10.1016/j.tet.2009.02.060
19. Hayman, W. A.; Brandt, E. R.; Relf, W. A.; Cooper, J.; Saul, A.; Good, M. F. *Int. Immunol.* **1997,** *9,* 1723–1733. doi:10.1093/intimm/9.11.1723
20. Tornøe, C. W.; Christensen, C.; Meldal, M. *J. Org. Chem.* **2002,** *67,* 3057–3064. doi:10.1021/jo011148j
21. Alexander, J.; Sidney, J.; Southwood, S.; Ruppert, J.; Oseroff, C.; Maewal, A.; Snoke, K.; Serra, H. M.; Kubo, R. T.; Sette, A.; Grey, H. M. *Immunity* **1994,** *1,* 751–761. doi:10.1016/S1074-7613(94)80017-0
22. Osborn, H. M. I., Ed. *Carbohydrates,* 1st ed.; Academic Press, 2003; pp 77–78.
23. Duffy, M. G.; Grayson, D. H. *J. Chem. Soc., Perkin Trans. 1* **2002,** 1555–1563. doi:10.1039/b203389p
24. Zemplén, G.; Pacsu, E. *Ber. Dtsch. Chem. Ges. B* **1929,** *62,* 1613–1614. doi:10.1002/cber.19290620640
25. Lee, D. J.; Yang, S.-H.; Williams, G. M.; Brimble, M. A. *J. Org. Chem.* **2012,** *77,* 7564–7571. doi:10.1021/jo3013435
26. Dubber, M.; Lindhorst, T. K. *J. Org. Chem.* **2000,** *65,* 5275–5281. doi:10.1021/jo000432s
27. Kulkarni, A. A.; Weiss, A. A.; Iyer, S. S. *Anal. Chem.* **2010,** *82,* 7430–7435. doi:10.1021/ac101579m
28. Gao, Y.; Eguchi, A.; Kakehi, K.; Lee, Y. C. *Bioorg. Med. Chem.* **2005,** *13,* 6151–6157. doi:10.1016/j.bmc.2005.06.036
29. Wang, L.-X.; Ni, J.; Singh, S. *Bioorg. Med. Chem.* **2003,** *11,* 159–166. doi:10.1016/S0968-0896(02)00339-5
30. Avadisian, M.; Gunning, P. T. *Mol. BioSyst.* **2013,** *9,* 2179–2188. doi:10.1039/c3mb70147f
31. Skwarczynski, M.; Toth, I. Lipid-core-peptide system for self-adjuvanting synthetic vaccine delivery. In *Bioconjugation Protocols: Strategies and Methods,* 2nd ed.; Mark, S. S., Ed.; Methods in Molecular Biology, Vol. 751; Springer: New York, NY, United States; pp 297–308. doi:10.1007/978-1-61779-151-2_18
32. Zhang, L.; Robertson, C. R.; Green, B. R.; Pruess, T. H.; White, H. S.; Bulaj, G. *J. Med. Chem.* **2009,** *52,* 1310–1316. doi:10.1021/jm801397w
33. Relf, W. A.; Cooper, J.; Brandt, E. R.; Hayman, W. A.; Anders, R. F.; Pruksakorn, S.; Currie, B.; Saul, A.; Good, M. F. *Pept. Res.* **1996,** *9,* 12–20.
34. Brabez, N.; Lynch, R. M.; Xu, L.; Gillies, R. J.; Chassaing, G.; Lavielle, S.; Hruby, V. J. *J. Med. Chem.* **2011,** *54,* 7375–7384. doi:10.1021/jm2009937
35. Urbani, C. N.; Bell, C. A.; Whittaker, M. R.; Monteiro, M. J. *Macromolecules* **2008,** *41,* 1057–1060. doi:10.1021/ma702707e
36. Skwarczynski, M.; Zaman, M.; Urbani, C. N.; Lin, I.-C.; Jia, Z.; Batzloff, M. R.; Good, M. F.; Monteiro, M. J.; Toth, I. *Angew. Chem., Int. Ed.* **2010,** *49,* 5742–5745. doi:10.1002/anie.201002221

License and Terms

BEILSTEIN JOURNAL OF ORGANIC CHEMISTRY

Synthesis of rigid *p*-terphenyl-linked carbohydrate mimetics

Maja Kandziora and Hans-Ulrich Reissig*

Full Research Paper

Open Access

Address:
Freie Universität Berlin, Institut für Chemie und Biochemie, Takustraße 3, D-14195 Berlin, Germany

Email:
Hans-Ulrich Reissig* - hans.reissig@chemie.fu-berlin.de

* Corresponding author

Keywords:
carbohydrate mimetics; hydrogenolysis; multivalent glycosystems; 1,2-oxazines; samarium diiodide; Suzuki cross-coupling

Beilstein J. Org. Chem. **2014,** *10,* 1749–1758.
doi:10.3762/bjoc.10.182

Received: 19 March 2014
Accepted: 23 June 2014
Published: 30 July 2014

This article is part of the Thematic Series "Multivalent glycosystems for nanoscience".

Guest Editor: B. Turnbull

Abstract

An approach to β-D-2-aminotalose- and β-D-2-aminoidose-configured carbohydrate mimetics bearing a phenyl substituent is described. Unnatural divalent rigid *p*-terphenyl-linked *C*-aryl glycosides with 2.0 nm dimension are available using Suzuki cross-couplings. The key compound, a *p*-bromophenyl-substituted 1,2-oxazine, was prepared by a stereoselective [3 + 3]-cyclization of a D-isoascorbic acid-derived (*Z*)-nitrone and lithiated TMSE-allene. The Lewis acid-induced rearrangement of this heterocycle provided the corresponding bicyclic 1,2-oxazine derivative that may be regarded as internally protected amino sugar analogue. After subsequent reduction of the carbonyl group, the resulting bicyclic compound was used for Suzuki cross-couplings to form biphenyl aminopyran or *p*-terphenyl-linked dimers. Hydrogenolysis afforded new unnatural aminosugar mimetics. Zinc in the presence of acid or samarium diiodide were examined for the N–O bond cleavage in order to obtain the rigid *p*-terphenyl-linked *C*-glycosyl dimers.

Introduction

Carbohydrates are the class of biomolecules with the highest structural diversity [1,2]. Specific carbohydrates are responsible for cell-type specific interactions [3] and they are involved in different diseases such as cancer [4], inflammation [5], and infections [6]. However, the use of carbohydrates as drugs has been strongly limited due to the hydrolytic lability of the glycosidic bond [7] and the weak binding affinities of single molecules. With the development of artificial *C*-glycosides which possess structural and functional aspects of the corresponding carbohydrates, these disadvantages can be overcome, resulting in an improved bioavailability, higher affinities and improved selectivities [8-13]. Recent results indicate that divalent rigid carbohydrate conjugates may have even higher binding affinities and specificities than their flexible multivalent equivalents [14,15]. The rigidity of the system is supposed to improve the overall activity of the ligands by over-

coming the entropic penalty of flexible multivalent scaffolds [16].

Cross-coupling reactions are among the best methods to prepare *C*-arylglycosides, *C*-nucleosides and *C*-glycosidic oligomers when new artificial pharmacophores are approached [17]. With Suzuki cross-couplings *C*-glycoside analogues of phloriain with antidiabetic properties [18] or aryl-scaffolded dimers and trimers were successfully prepared [19]. The Suzuki cross-coupling is particularly suitable for carbohydrate chemistry due to the mild reaction conditions and its tolerance to a variety of functional groups [20]. In addition, the reactions are easy to perform and the required boronic acids exhibit exceptional stabilities to heat, air and moisture compared to other organometallic reagents [21]. Up to now there are not many examples of nanorod-like carbohydrate dimers with aryl-linked divalent glycosides. A mannopyranoside dimer was generated by a palladium-catalyzed Ullmann-type reductive homocoupling [22] and biphenyl-linked dimers were prepared by Lewis acid-catalyzed glycosidations [23]. All these examples possess an acid-labile *O*-glycosidic bond and are labile to hydrolysis and enzymes. Therefore, new approaches to the synthesis of rigid multivalent *C*-arylglycosides should be a valuable extension of compounds with potential biological activity. In order to achieve this goal we investigated the synthesis of divalent compounds of general structure **1** and their monovalent analogues **2** (Scheme 1). Structurally similar aminopyrans without aryl groups have intensively been studied as carbohydrate mimetics in our group [24,25]. When they are coupled by amide bonds to gold nanoparticle and O-sulfated these conjugates gave extremely high binding affinities towards L- and P-selectin in sub-nanomolar concentrations. These results were achieved by a multivalent presentation (ca. 1000–1200 ligands per nanoparticle) of the sulfated pyrans [26,27]. We were therefore interested to prepare inhibitors offering only a small number of ligands to get better information about structure–activity relationships and to study the influence of the flexible and rigid spacer units.

In this report we present methods for the synthesis of divalent compounds **1** with *p*-terphenyl spacers and of β-D-2-aminotalose- or β-D-2-aminoidose-configured carbohydrate mimetics **2** (Scheme 1). These novel carbohydrate mimetics represent unique structures, combining the features of *C*-aryl-glycosides and aminosugars. The *p*-bromophenyl-substituted bicyclic 1,2-oxazine derivative **3** was used as key building block for the Suzuki cross-coupling reaction to synthesize *p*-terphenyl-linked derivatives **1**. The key intermediate **3** was prepared by a Lewis acid-induced rearrangement of 3,6-dihydro-2*H*-oxazine **4**, that origins from a stereoselective [3 + 3]-cyclization of D-isoascorbic acid-derived (*Z*)-nitrone **6** and lithiated TMSE-allene **5**.

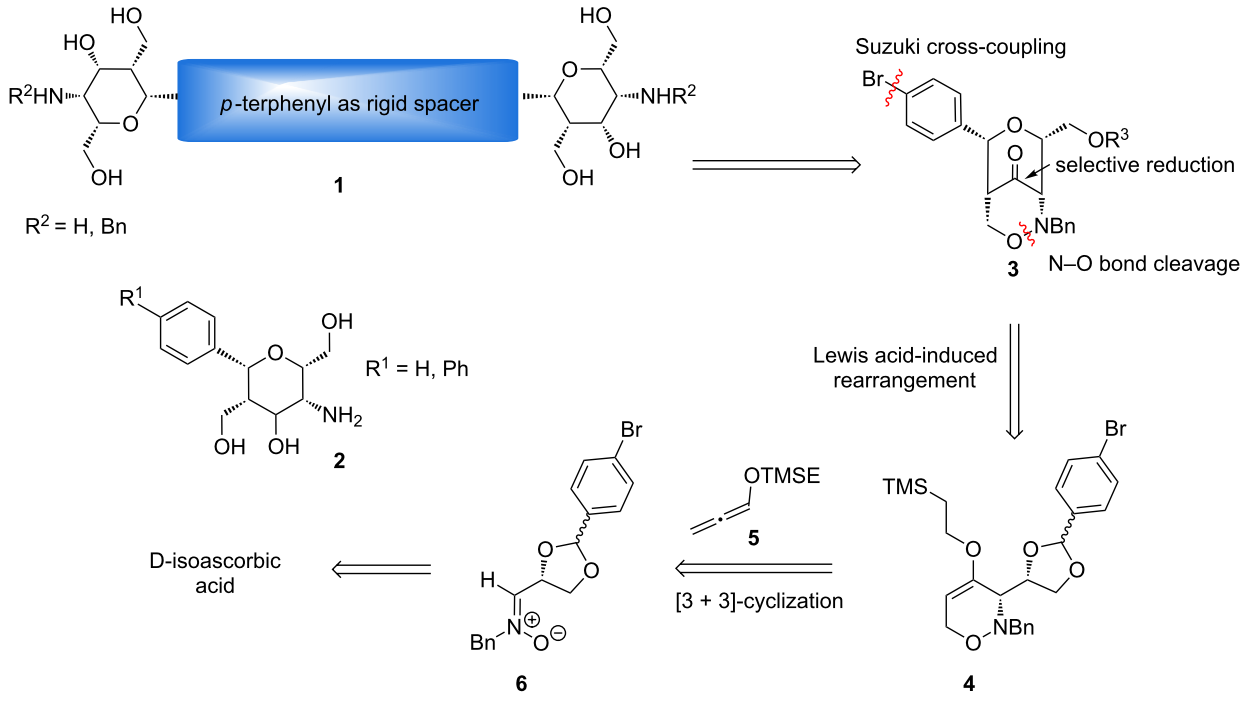

Scheme 1: Approach to divalent carbohydrate mimetics **1** with rigid spacer and monovalent analogues **2**.

Results and Discussion

For our synthesis of new divalent carbohydrate mimetics we required 1,2-oxazine derivatives derived from (*Z*)-nitrone **6** and lithiated alkoxyallenes. The 4-bromophenyl group should allow transition metal-promoted coupling reactions to a variety of new compounds. For this purpose the D-erythrose-configured ester **7**, easily available from D-isoascorbic acid [28], was converted into nitrone **6** in a three step procedure (Scheme 2). Its reduction with lithium aluminum hydride was performed under standard conditions providing diol **8** in excellent yield in multigram scale (up to 20 g). Attention should be paid to a possible reductive removal of the bromine substituent that can occur at higher temperature or longer reaction times as the resulting debrominated product is hard to remove from diol **8** by column chromatography. According to the protocol of Dondoni et al. [29] glycol cleavage of diol **8** afforded the corresponding aldehyde that was directly treated with *N*-benzylhydroxylamine to furnish the desired (*Z*)-nitrone **6**. All compounds in this sequence of reactions are mixtures of the two diastereomers at the dioxolane C-2 (ratios close to 1:1).

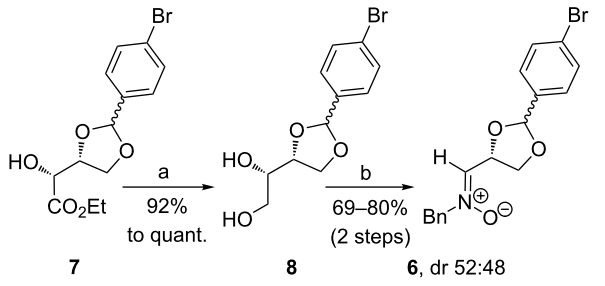

Scheme 2: Synthesis of (*Z*)-nitrone **6**. Conditions: a) $LiAlH_4$, THF, 1 h, rt; b) 1. $NaIO_4$, CH_3CN/H_2O, 1 h, rt; 2. *N*-benzylhydroxylamine, $MgSO_4$, CH_2Cl_2, 18 h, rt.

The preparation of *syn*-1,2-oxazine **4** was achieved in good yields ranging from 67–77% by stereocontrolled addition of lithiated (trimethylsilyl)ethoxyallene **9** to (*Z*)-nitrone **6** at −78 °C (Scheme 3). Although the formation of four stereoisomers is possible only two were observed. Due to the complexation of lithiated allene **9** to the nitrone **6** an exclusive formation of the two *syn*-1,2-oxazines **4** was observed. This result suggests that the configuration at C-2 of the dioxolane moiety has no influence on the stereochemical outcome of the reaction. The model suggested by Dondoni et al. [30] can also be employed for this process to rationalize the observed diastereoselectivity of the addition step. The subsequent [3 + 3]-cyclization to 3,6-dihydro-2*H*-1,2-oxazine **4** follows the previously reported mechanism [31]. In the presented sequence *syn*-1,2-oxazine **4** was successfully prepared in six steps with an overall yield of 46%. The diastereomers can easily be separated by column chromatography, but this turned out not to be mandatory. The next step of our anticipated sequence, the Lewis acid-induced rearrangement, converts the dioxolane C-2 carbon into an sp^2-hybridized carbon and hence the configuration of the precursor does not play a role for this reaction.

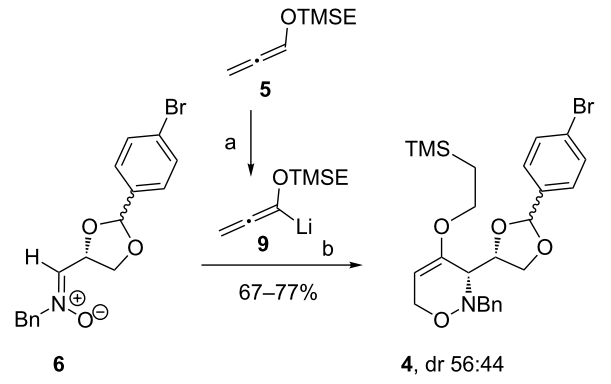

Scheme 3: [3 + 3]-Cyclization of (*Z*)-nitrone **6** with lithiated allene **9**. Conditions: a) *n*-BuLi, THF, 15 min, −40 °C; b) 1. THF, 2 h, −78 °C; 2. H_2O, 1 h, −78 °C → rt.

An alternative route to prepare 1,2-oxazine **4** is depicted in Scheme 4. The preparation of the 4-bromophenyl-1,3-dioxolane moiety started from diol **10** that has successfully been used earlier for the preparation of phenylthio-substituted 1,2-oxazine derivatives [32]. Compound **10** is easily accessible by a mild cleavage of the corresponding acetonide by an indium trichloride-mediated hydrolysis [33]. By using cerium ammonium nitrate as Lewis acid [34] in high concentration (13 mmol/mL) as well as an excess of 1-bromo-4-(dimethoxymethyl)benzene enabled the synthesis of *syn*-1,2-oxazine **4**. The conversion of this reaction was high (>80%) giving the two diastereomers of **4** (ca. 1:1), but only one diastereomer was isolated in pure form. The second diastereomer could hardly be separated from the excess of 1-bromo-4-(dimethoxymethyl)-benzene by column chromatography or distillation. Besides, Brønsted acids like trifluoroacetic acid, *p*-toluenesulfonic acid,

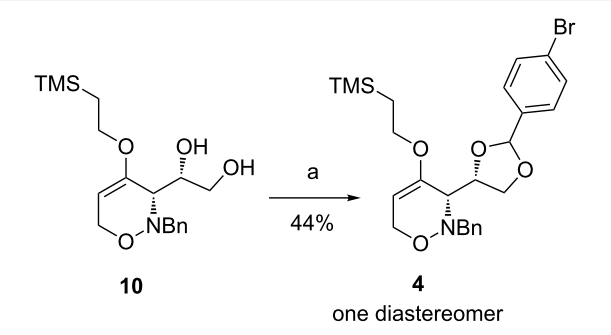

Scheme 4: Synthesis of 1,2-oxazine **4** by acetal formation from **10**. Conditions: a) 1-bromo-4-(dimethoxymethyl)benzene (10 equiv.), CAN, CH_2Cl_2, 3 d, rt.

that are usually used to generate ketals, or weaker acids like pyridine/hydrogen fluoride led to a side product [35].

The Lewis acid-promoted rearrangement of 1,3-dioxolanyl-substituted 1,2-oxazines to bicyclic ketones has been described in many examples [24]. Gratifyingly, starting from 1,2-oxazine **4** with tin(IV) chloride as Lewis acidic promoter the corresponding ketone was obtained in excellent stereoselectivity. The subsequent protection of the primary hydroxy group as TBS ether under standard conditions provided **11** in very good yields of up to 82% (Scheme 5). In order to perform the Lewis acid-promoted rearrangement and the protection in one step, we also employed TBSOTf as Lewis acid for the rearrangement step [24], however, no product formation could be observed in this case. The mechanism of the rearrangement **4** → **11** can be described as an aldol-type cyclization process. The Lewis acid coordinates to the sterically less hindered oxygen atom of the dioxolane ring of **4** opening this ring and forming a carbenium ion that intramolecularly attacks the enol ether moiety. A six-membered chair-like transition state with the bulky 4-bromophenyl group in an equatorial position for this crucial step rationalizes the product configuration as shown.

TBS-protected bicyclic ketone **11** was subsequently reduced with sodium borohydride at −40 °C to form alcohols **12a** and **12b** as 81:19 mixture of diastereomers in 72% yield (Scheme 5). In contrast, the reduction with L-selectride at −10 °C selectively furnished pure diastereomer **12a** in 73% yield. In accordance with previous observations of reductions of related phenylthio-substituted bicyclic compounds [25], a hydride attack from the side of the pyran moiety is assumed since the 1,2-oxazine side is more hindered by the bulky *N*-benzyl moiety. The secondary hydroxy group of **12a** was protected employing *t*-butyldimethylsilyl trifluoromethanesulfonate and 2,6-lutidine in quantitative yield.

The Lewis acid-promoted rearrangement of 1,2-oxazine derivative **4** and the direct reduction of the unpurified ketone **14** furnished bicyclic diol **15** in good overall yield of 58% (Scheme 6). The reduction of unprotected ketone **14** with L-selectride was less stereoselective and provided a 72:28 mixture of **15**. The higher selectivity of the TBS-protected compound **11** may be explained by an indirect effect of the bulky TBS-group, possibly pushing the *N*-benzyl moiety to the top of the ring shielding the 1,2-oxazine side more efficiently. Separation of the two diastereomers and protection of the primary hydroxy group of **15a** with trityl chloride provided compound **16** in 83% yield. This protecting group should allow its removal together with the benzyl group during hydrogenolysis. Surprisingly, a benzyl protection under the same conditions was not possible.

Before approaching divalent compounds such as **1** we wanted to convert our building blocks into simple monocyclic carbohydrate mimetics. To prepare phenyl-substituted aminopyrans the N–O bond of bicyclic compounds **15a** and **15b** was cleaved by

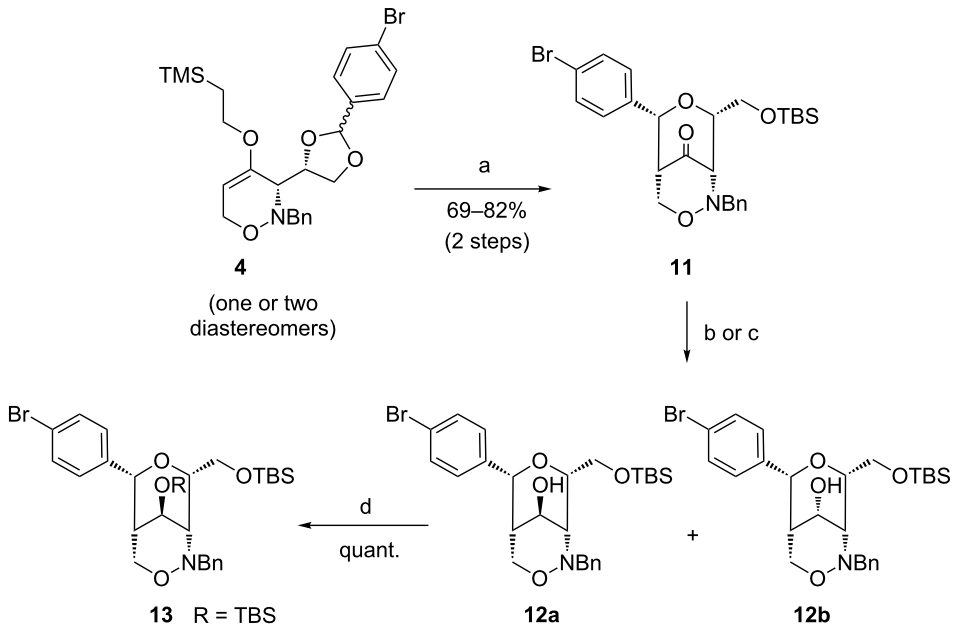

Scheme 5: Synthesis of bicyclic ketone **11** by Lewis acid-induced rearrangement and reduction to alcohols **12a** and **12b** and protection of **12a** to 1,2-oxazine derivative **13**. Conditions: a) 1. $SnCl_4$, CH_3CN, 4 h, −30 °C → rt; 2. TBSCl, imidazole, THF, 4 h, rt; b) $NaBH_4$, EtOH, 4 h, −40 °C, 72%, dr 81:19; c) L-selectride, THF, 2 h, −10 °C, 73%, only **12a**; d) TBSOTf, 2,6-lutidine, THF, 2 h, 0 °C.

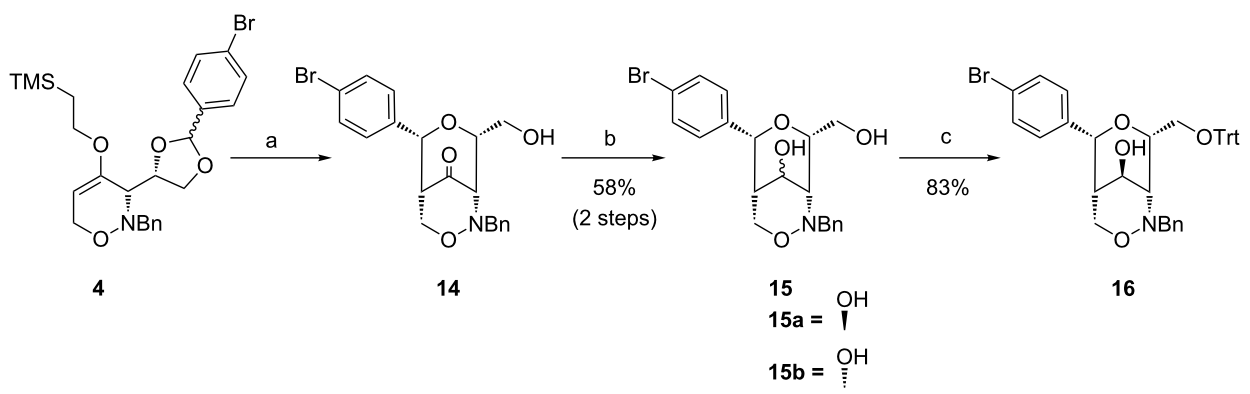

Scheme 6: Synthesis of bicyclic diols **15** and of trityl-protected bicyclic 1,2-oxazine **16**. Conditions: a) $SnCl_4$, CH_3CN, 18 h, −30 °C → rt, b) 1) L-selectride, THF, 4 h, −15 °C, dr 72:28; 2) separation by column chromatography (silica gel, hexanes/EtOAc 1:1 → 1:2); c) TrtCl, DMAP, pyridine, 3 d, rt.

hydrogenolysis. These reactions are challenging because the resulting aminopyrans are apparently poisoning the catalyst and hence large amounts of palladium on charcoal are required for full conversion. We did not add acid to diminish catalyst poisoning since we were afraid of other side reactions of the complex product. In addition, the resulting products are very polar and difficult to purify. In our recent report [28] related compounds were reduced in methanol as solvent providing several side products and the yield of the reactions were not fully reproducible. Nevertheless, 1,2-oxazine **15a** was converted into aminopyran **17a** (Scheme 7) by hydrogenolysis under standard conditions in methanol in a yield of 78%, but this yield was not fully reproducible and the conditions were optimized. We found that isopropanol as solvent and addition of one equivalent triethylamine were more reliable and the yield of **17a** could be slightly improved. Triethylamine was added to neutralize the formed acid [36] that is generated in the first step by a very fast debromination. The debenzylation and the N–O bond cleavage occur as next steps. Under these improved conditions the isomeric bicyclic 1,2-oxazine **15b** was converted into aminopyran **17b** in a good yield of 77%. The formed aminopyrans **17a** and **17b** can be regarded as amino *C*-glycosides. Compound **17a** is related to compounds with β-D-talose configuration that are rarely found in nature, an exception being the antibiotic amino glycoside hygromycin B [37]. Aminopyran **17b** correlates to β-D-idopyranose; iduronic acid is a component of sulfated glycosamine glycans such as chrondroitin sulfate and heparan sulfate [38].

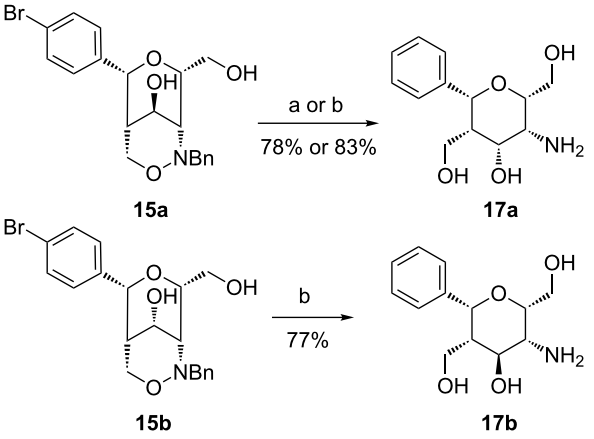

Scheme 7: Hydrogenolyses of bicyclic 1,2-oxazine derivatives **15a** and **15b**. Conditions: a) H_2, Pd/C, MeOH, EtOAc, 20 h, rt; b) H_2, Pd/C, iPrOH, EtOAc, NEt_3, 18 h, rt.

The prepared *p*-bromophenyl-substituted bicyclic 1,2-oxazine derivatives **12**, **13**, **15** and **16** provide options to perform cross-coupling reactions such as Buchwald/Hartwig, Heck, Hiyama, Kumada, Sonogashira or Stille couplings. In order to examine the conditions for Suzuki cross-couplings we subjected bicyclic compound **15a** to phenylboronic acid under standard conditions of this reaction. The desired product **18** was obtained in 81% yield (Scheme 8) and the subsequent hydrogenolysis furnished carbohydrate mimetic **19** bearing a biphenyl substituent.

The smooth transformation of bicyclic compound **15a** into a biphenyl compound by Suzuki cross-coupling encouraged us to aim the synthesis of divalent compound **21**. 1,4-Phenylenediboronic acid (**20**) was used as precursor and coupled to two equivalents of **12a** to afford the desired *p*-terphenyl compound **21** in excellent 84% yield (Scheme 9). Unfortunately, the subsequent hydrogenolysis of this compound under conditions as above led to a complex product mixture and no product could be observed. An alternative method for N–O cleavage employs elemental zinc in the presence of acid [39], conditions that should simultaneously cleave the TBS protective groups. For the conversion of **21** into **22** long reaction times were required and the high acidity led to the formation of side products.

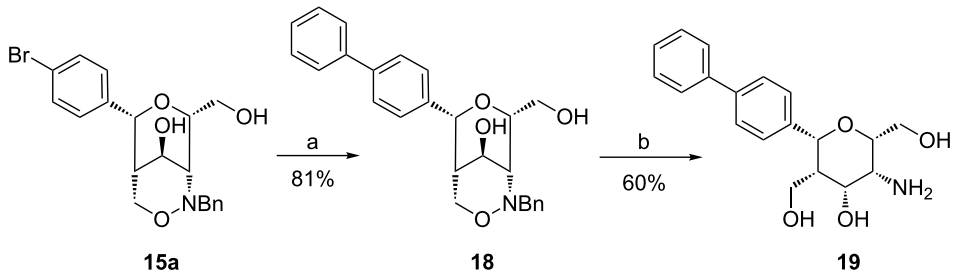

Scheme 8: Suzuki cross-coupling of **15a** leading to biphenyl derivative **18** and hydrogenolysis to **19**. Conditions: a) phenylboronic acid, $Pd(PPh_3)_4$, 2 M Na_2CO_3 aq, THF, 70 °C, 48 h; b) H_2, Pd/C, iPrOH, THF, rt, 24 h.

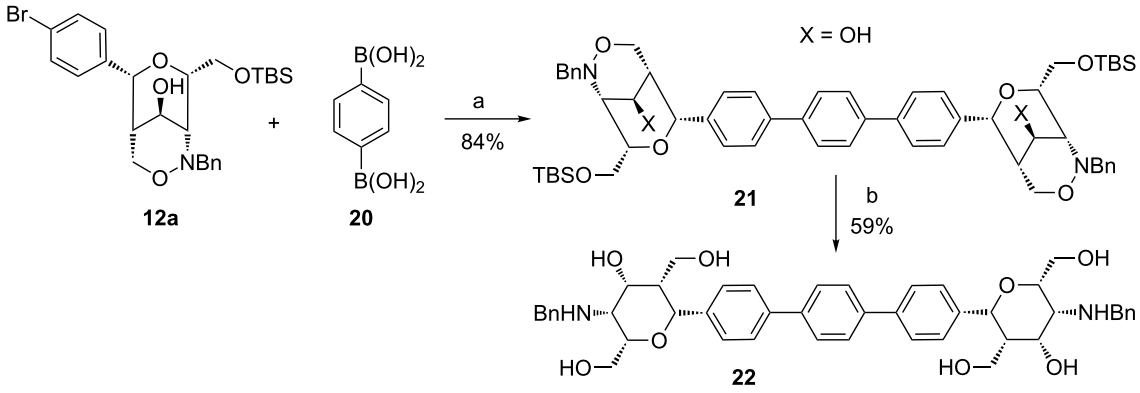

Scheme 9: Synthesis of *N*-benzylated *p*-terphenyl derivative **21** by Suzuki cross-coupling of **12a** with **20** and subsequent reduction with zinc. Conditions: a) $Pd(PPh_3)_4$, 2 M Na_2CO_3 aq, THF/DMF (8:2), 70 °C, 48 h; b) Zn, AcOH, THF, 60 °C, 18 h.

Nevertheless, the target compound **22** was isolated in a moderate yield of 59%.

As a milder alternative, samarium diiodide was examined for the N–O bond cleavage [40-45]. With this selective reagent a TBS protected aminopyran dimer **23** was expected that should be well soluble in organic solvents and therefore more suitable for subsequent transformations (Scheme 10). Disappointingly, a samarium diiodide solution converted compound **21** in a complex reaction mixture. For a better understanding of this unexpected result the reductive cleavage was examined with the simpler bicyclic 1,2-oxazine derivative **12a**. Here the unexpected bicyclic compound **24** was isolated as major product in 79% yield together with the desired aminopyran derivative **25** in 14% yield. It was observed by ^{1}H NMR spectroscopy that aminopyran **25** is not stable and slowly cyclizes to **24**; after two days in $CDCl_3$ solution approximately 20% of aminopyran **25** were converted into **24**. This result indicates that the N–O bond cleavage of **12a** preceded as expected, but that the produced amino group of the pyran ring seems to be in close proximity to the C-5 hydroxy group and leads to a nucleophilic substitution under formation of the pyrrolidine moiety. This process is possibly promoted by samarium(III) which can act as Lewis acid and by the steric demanding TBS group which decreases the distance between the two functional groups. This unexpected side reaction leading to **24** indicates that in the above mentioned unclean reaction of samarium diiodide with dimer **21** similar complications may lead to the observed mixture.

To overcome these difficulties dimer **21** was deprotected with tetra-*n*-butylammonium fluoride giving the poorly soluble polyhydroxylated compound **26** (Scheme 11). Due to the amphiphilic character this compound was only soluble in pyridine that makes purification and subsequent reactions fairly difficult. The conversion of the deprotection step was high but the yield after purification was only 30%. The reduction with samarium diiodide was then performed in a methanol/tetrahydrofuran mixture in which compound **26** was scarcely soluble. Gratifyingly, after one hour reaction time and purification by column chromatography aminopyran **22** was isolated in 30% yield. Interestingly, no cyclization product similar to **24** was detected in this case.

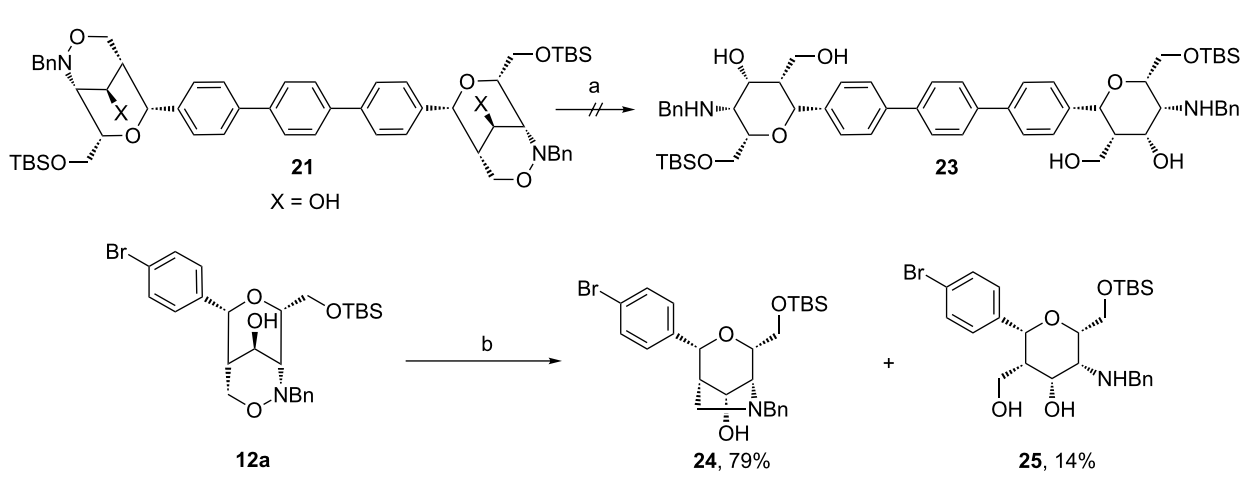

Scheme 10: Attempted reductive cleavage of the N–O bond of compound **21** by samarium diiodide and reaction of **12a**. Conditions: a) SmI_2 (0.09 M in THF), MeOH, rt, 60 min; b) SmI_2 (0.1 M in THF), THF, rt, 45 min.

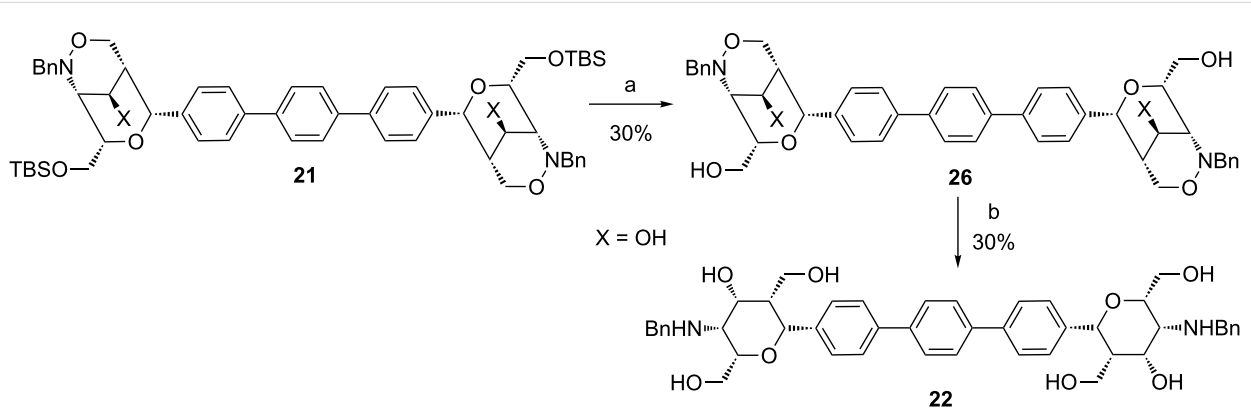

Scheme 11: Deprotection of compound **21** and samarium diiodide-mediated reaction of **26**. Conditions: a) TBAF, THF, rt, 2 d; b) SmI_2 (0.09 M in THF), MeOH, rt, 60 min.

We also investigated the Suzuki cross-coupling of bicyclic compound **16** with 1,4-phenylenediboronic acid (**20**) (Scheme 12). Although the trityl group is quite far away from the reacting bromo substituent it led to longer reaction times and slightly lower yields, but the expected product **27** was obtained in 51% yield as a well soluble compound.

The trityl protective groups enabled the deprotection of dimer **27** in one step. The *O*-trityl and *N*-benzyl groups were removed by hydrogenolysis under acidic conditions to obtain a mixture of compounds **28** and **29** (Scheme 13). As solvent a 3:2 mixture of isopropanol/hexafluoro-2-propanol was used in order to combine high polarity with product solubility and to avoid side

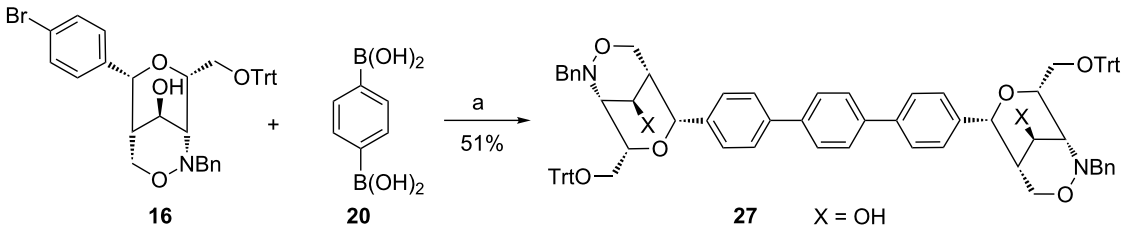

Scheme 12: Suzuki cross-coupling of compound **16**. Conditions: $Pd(PPh_3)_2Cl_2$, 2 M Na_2CO_3, DMF, 80 °C, 3 d.

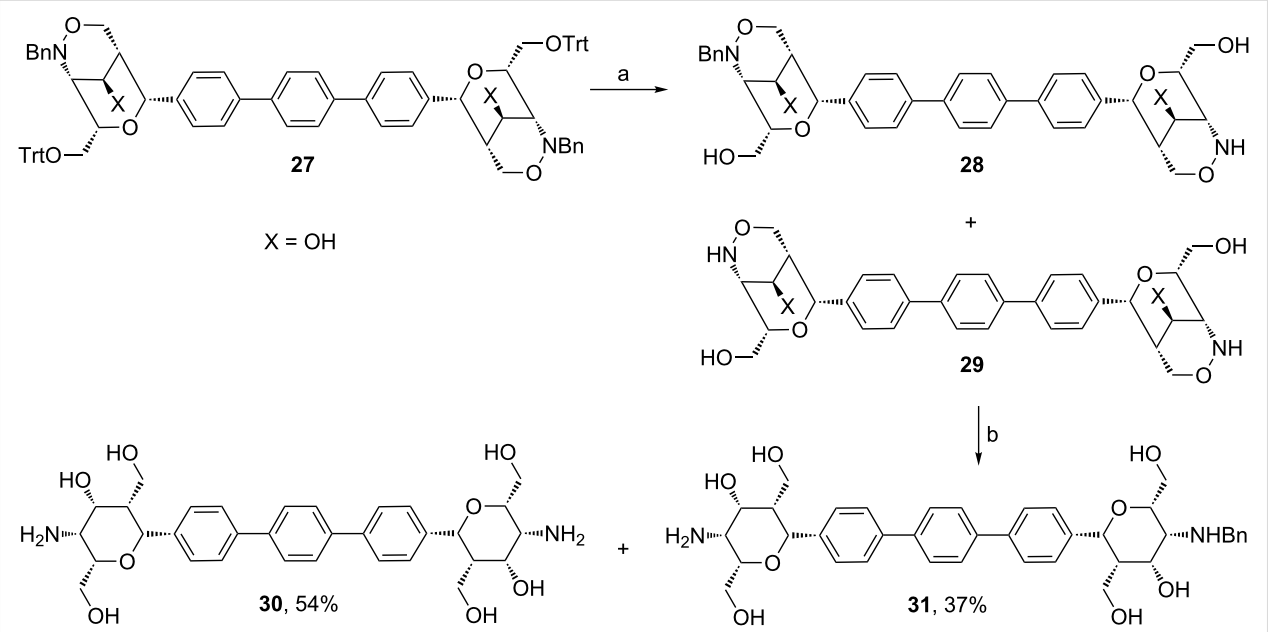

Scheme 13: Hydrogenolysis of compound **27** and samarium diiodide-mediated reaction leading to compounds **30** and **31**. Conditions: a) H_2, Pd/C, TFA, HFIP, iPrOH, 8 h, rt; b) SmI_2 (0.1 M in THF), MeOH, 30 min, rt. HFIP = hexafluoro-2-propanol.

product formation [26]. The ratio of mono-benzylated **28** and fully deprotected *p*-terphenyl derivative **29** was 59:41 as confirmed by ^{1}H NMR spectroscopy of the crude product. The reaction mixture was directly filtered through a pad of Celite® and the solvents were removed in vacuo to provide a crude product that was used for the subsequent samarium diiodide-mediated reduction without any purification. This reaction proceeded smoothly and furnished the very polar compounds **30** and **31**. Removal of the formed samarium salts by size exclusion chromatography provided the two divalent carbohydrate mimetics in very good overall yield. The considerably better yield in this samarium diiodide-mediated reaction is probably due to the good solubility of compounds **28** and **29** in methanol/THF.

In summary, by optimizing the protective group strategy and the reductive cleavage methods we were able to prepare the desired rigid *p*-terphenyl-linked carbohydrate mimetic **30** in twelve steps starting from D-isoascorbic acid, but in only six steps with respect to crucial intermediate **4**. The overall yields of 6% or 13% are quite respectable. The distance between the two terminal amino groups is in the range of 2.0 nm (according to optimized molecular geometry obtained by MM2 calculations performed by ChemBio3D Ultra 11.0 from ChemBioOffice 2008).

Conclusion

We successfully established methods for the efficient preparation of phenyl-substituted aminopyrans and rigid divalent *p*-terphenyl-linked *C*-aryl glycoside using Suzuki cross-couplings as key method. Starting from the D-isoascorbic acid-derived diol **8**, which was converted into the corresponding *p*-bromophenyl-substituted (*Z*)-nitrone, a stereoselective [3 + 3]-cyclization with lithiated TMSE-allene provided the required 1,2-oxazine **4** in six steps with an overall yield of 46%. Alternatively, this 1,2-oxazine could be obtained under the formation of a 4-bromophenyl-1',3'-dioxolane moiety from diol **10** (actually derived from D-mannitol) which is a promising route to differently substituted 1,2-oxazines, introducing the dioxolane substituent at a late stage. The Lewis acid-induced rearrangement of the 1,2-oxazine **4** afforded the bicyclic ketone **11** which can be regarded as an internally protected amino sugar. After subsequent reduction of the carbonyl group the resulting bicyclic compound **12** was used as substrate for Suzuki cross-couplings to form a biphenyl-substituted aminopyran or rigid *C*-aryl dimers in good yields. These *p*-terphenyl-linked aminopyran derivatives **22**, **30** and **31** have a dimension of approximately 2.0 nm.

p-Bromophenyl-substituted intermediates such as **15** or **16** are also useful precursors for the synthesis of other *C*-aryl glycosides with potential biological activity. By simple hydrogenolysis of the bicyclic compounds, three new aminopyrans could be synthesized. Different methods for N–O bond cleavage like palladium-catalyzed hydrogenolysis, zinc/acid or samarium diiodide were tested. For each of the substrates the suitable method has to be found. By the N–O bond cleavage of compound **12a** with samarium diiodide an unexpected bicyclic

pyrrolidine derivative **24** was isolated. The prepared unnatural *C*-aryl glycosides could find applications in medicinal chemistry, e.g., as selectin inhibitors. After O-sulfation the biological activity of these divalent compounds will be studied together with that of related carbohydrate mimetics.

Experimental

For general methods: See Supporting Information File 1

Supporting Information

Supporting Information File 1

Experimental procedures.
[http://www.beilstein-journals.org/bjoc/content/supplementary/1860-5397-10-182-S1.pdf]

Supporting Information File 2

Characterization data ^{1}H NMR and ^{13}C NMR spectra of synthesized compounds.
[http://www.beilstein-journals.org/bjoc/content/supplementary/1860-5397-10-182-S2.pdf]

Acknowledgements

This work was generously supported by the Deutsche Forschungsgemeinschaft (SFB 765) and by Bayer HealthCare. We acknowledge valuable discussions and help during preparation of the manuscript by Dr. R. Zimmer and Dr. L. Bouché.

References

1. Werz, D. B.; Ranzinger, R.; Herget, S.; Adibekian, A.; von der Lieth, C.-W.; Seeberger, P. H. *ACS Chem. Biol.* **2007,** *2,* 685–691. doi:10.1021/cb700178s
2. Adibekian, A.; Stallforth, P.; Hecht, M.-L.; Werz, D. B.; Gagneux, P.; Seeberger, P. H. *Chem. Sci.* **2011,** *2,* 337–344. doi:10.1039/c0sc00322k
3. Hakomori, S.-i. *Pure Appl. Chem.* **1991,** *63,* 473–482. doi:10.1351/pac199163040473
4. Kannagi, R.; Izawa, M.; Koike, T.; Miyazaki, K.; Kimura, N. *Cancer Sci.* **2004,** *95,* 377–384. doi:10.1111/j.1349-7006.2004.tb03219.x
5. Lasky, L. A. *Annu. Rev. Biochem.* **1995,** *64,* 113–140. doi:10.1146/annurev.bi.64.070195.000553
6. Sharon, N. *FEBS Lett.* **1987,** *217,* 145–157. doi:10.1016/0014-5793(87)80654-3
7. Levy, D. E.; Tang, C. *The Chemistry of C-glycosides;* Elsevier Science Ltd.: Oxford, 1995.
8. Sears, P.; Wong, C.-H. *Angew. Chem.* **1999,** *111,* 2446–2471. doi:10.1002/(SICI)1521-3757(19990816)111:16<2446::AID-ANGE2446>3.0.CO;2-4
Angew. Chem., Int. Ed. **1999**, *38*, 2300-2324. doi:10.1002/(sici)1521-3773(19990816)38:16<2300::aid-anie2300>3.0.co;2-6
9. Koester, D. C.; Holkenbrink, A.; Werz, D. B. *Synthesis* **2010,** 3217–3242. doi:10.1055/s-0030-1258228
10. Koester, D. C.; Werz, D. B. *Beilstein J. Org. Chem.* **2012,** *8,* 675–682. doi:10.3762/bjoc.8.75
11. Koester, D. C.; Leibeling, M.; Neufeld, R.; Werz, D. B. *Org. Lett.* **2010,** *12,* 3934–3937. doi:10.1021/ol101625p
12. Ernst, B.; Magnani, J. L. *Nat. Rev. Drug Discovery* **2009,** *8,* 661–677. doi:10.1038/nrd2852
13. Koester, D. C.; Kriemen, E.; Werz, D. B. *Angew. Chem.* **2013,** *125,* 3059–3063. doi:10.1002/ange.201209697
Angew. Chem., Int. Ed. **2013**, *52*, 2985-2989. doi:10.1002/anie.201209697
14. Mackeviča, J.; Ostrovskis, P.; Leffler, H.; Nilsson, U. J.; Rudovica, V.; Viksna, A.; Belyakov, S.; Turksa, M. *ARKIVOC* **2014,** No. (iii), 90–112. doi:10.3998/ark.5550190.p008.402
15. Pertici, F.; de Mol, N. J.; Kemmink, J.; Pieters, R. J. *Chem.–Eur. J.* **2013,** *19,* 16923–16927. doi:10.1002/chem.201303463
16. Pertici, F.; Varga, N.; van Duijn, A.; Rey-Carrizo, M.; Bernardi, A.; Pieters, R. J. *Beilstein J. Org. Chem.* **2013,** *9,* 215–222. doi:10.3762/bjoc.9.25
17. Merino, P.; Tejero, T.; Marca, E.; Gomollón-Bel, F.; Delso, I.; Matute, R. *Heterocycles* **2012,** *86,* 791–820. doi:10.3987/REV-12-SR(N)3
18. Link, J. T.; Sorensen, B. K. *Tetrahedron Lett.* **2000,** *41,* 9213–9217. doi:10.1016/S0040-4039(00)01709-3
19. Johnson, C. R.; Johns, B. A. *Synlett* **1997,** 1406–1408.
20. Kotha, S.; Lahiri, K.; Kashinath, D. *Tetrahedron* **2002,** *58,* 9633–9695. doi:10.1016/S0040-4020(02)01188-2
21. Kotha, S.; Lahiri, K. *Eur. J. Org. Chem.* **2007,** 1221–1236. doi:10.1002/ejoc.200600519
22. Bergeron-Brlek, M.; Giguère, D.; Shiao, T. C.; Saucier, C.; Roy, R. *J. Org. Chem.* **2012,** *77,* 2971–2977. doi:10.1021/jo2025652
23. Bergeron-Brlek, M.; Shiao, T. C.; Trono, M. C.; Roy, R. *Carbohydr. Res.* **2011,** *346,* 1479–1489. doi:10.1016/j.carres.2011.03.041
24. Al-Harrasi, A.; Pfrengle, F.; Prisyazhnyuk, V.; Yekta, S.; Kóóš, P.; Reissig, H.-U. *Chem.–Eur. J.* **2009,** *15,* 11632–11641. doi:10.1002/chem.200900996
25. Pfrengle, F.; Reissig, H.-U. *Chem.–Eur. J.* **2010,** *16,* 11915–11925. doi:10.1002/chem.201001060
26. Dernedde, J.; Enders, S.; Reissig, H.-U.; Roskamp, M.; Schlecht, S.; Yekta, S. *Chem. Commun.* **2009,** 932–934. doi:10.1039/b818263a
27. Roskamp, M.; Enders, S.; Pfrengle, F.; Yekta, S.; Dekaris, V.; Dernedde, J.; Reissig, H.-U.; Schlecht, S. *Org. Biomol. Chem.* **2011,** *9,* 7448–7456. doi:10.1039/c1ob05583f
28. Bouché, L.; Kandziora, M.; Reissig, H.-U. *Beilstein J. Org. Chem.* **2014,** *10,* 213–223. doi:10.3762/bjoc.10.17
29. Dondoni, A.; Franco, S.; Junquera, F.; Merchán, F. L.; Merino, P.; Tejero, T. *Synth. Commun.* **1994,** *24,* 2537–2550. doi:10.1080/00397919408010565
30. Dondoni, A.; Franco, S.; Junquera, F.; Merchán, F. L.; Merino, P.; Tejero, T.; Bertolasi, V. *Chem.–Eur. J.* **1995,** *1,* 505–520. doi:10.1002/chem.19950010804
31. Helms, M.; Schade, W.; Pulz, R.; Watanabe, T.; Al-Harrasi, A.; Fišera, L.; Hlobilová, I.; Zahn, G.; Reissig, H.-U. *Eur. J. Org. Chem.* **2005,** 1003–1019. doi:10.1002/ejoc.200400627
32. Pfrengle, F.; Lentz, D.; Reissig, H.-U. *Angew. Chem.* **2009,** *121,* 3211–3215. doi:10.1002/ange.200805724
Angew. Chem., Int. Ed. **2009**, *48*, 3165-3169. doi:10.1002/anie.200805724
33. Pfrengle, F.; Dekaris, V.; Schefzig, L.; Zimmer, R.; Reissig, H.-U. *Synlett* **2008,** 2965–2968. doi:10.1055/s-0028-1083628

34. Manzo, E.; Barone, G.; Parrilli, M. *Synlett* **2000,** 887–889. doi:10.1055/s-2000-6700
35. Bressel, B.; Egart, B.; Al-Harrasi, A.; Pulz, R.; Reissig, H.-U.; Brüdgam, I. *Eur. J. Org. Chem.* **2008,** 467–474. doi:10.1002/ejoc.200700792
36. Boerner, A.; Krause, H. *J. Prakt. Chem.* **1990,** *332,* 307–312. doi:10.1002/prac.19903320305
37. Neuss, N.; Koch, K. F.; Molloy, B. B.; Day, W.; Huckstep, L. L.; Dorman, D. E.; Roberts, J. D. *Helv. Chim. Acta* **1970,** *53,* 2314–2319. doi:10.1002/hlca.19700530846
38. Pellissier, H. *Org. Prep. Proced. Int.* **2002,** *34,* 441–465. doi:10.1080/00304940209355764
39. Wuts, P. G. M.; Jung, Y. W. *J. Org. Chem.* **1988,** *53,* 1957–1965. doi:10.1021/jo00244a021
40. Keck, G. E.; McHardy, S. F.; Wager, T. T. *Tetrahedron Lett.* **1995,** *36,* 7419–7422. doi:10.1016/0040-4039(95)01557-4
41. Chiara, J. L.; Destabel, C.; Gallego, P.; Marco-Contelles, J. *J. Org. Chem.* **1996,** *61,* 359–360. doi:10.1021/jo951571q
42. Jung, S. H.; Lee, J. E.; Koh, H. Y. *Bull. Korean Chem. Soc.* **1998,** *19,* 33–35.
43. Pulz, R.; Al-Harrasi, A.; Reissig, H.-U. *Org. Lett.* **2002,** *4,* 2353–2355. doi:10.1021/ol0260573
44. Revuelta, J.; Cicchi, S.; Brandi, A. *Tetrahedron Lett.* **2004,** *45,* 8375–8377. doi:10.1016/j.tetlet.2004.09.050
45. Jasiński, M.; Watanabe, T.; Reissig, H.-U. *Eur. J. Org. Chem.* **2013,** 605–610. doi:10.1002/ejoc.201201210

License and Terms

BEILSTEIN JOURNAL OF ORGANIC CHEMISTRY

Expeditive synthesis of trithiotriazine-cored glycoclusters and inhibition of *Pseudomonas aeruginosa* biofilm formation

Meriem Smadhi[1,2], Sophie de Bentzmann[*3], Anne Imberty[*4], Marc Gingras[5], Raoudha Abderrahim[2] and Peter G. Goekjian[*1]

Full Research Paper

Open Access

Address:
[1]Laboratoire Chimie Organique 2 Glycochimie, Université de Lyon, ICBMS, UMR 5246 – CNRS, Université Claude Bernard Lyon 1, Bat. 308 –CPE Lyon, 43 Bd. du 11 Novembre 1918, 69622 Villeurbanne, France. Fax: +33-4-72448109; Tel: +33-4-72448183, [2]Université de Carthage, Faculté des sciences Bizerte, Tunisie, [3]Laboratoire d'Ingénierie des Systèmes Macromoléculaires, Institut de Biologie Structurale et Microbiologie, CNRS-Aix Marseille University, UMR7255, 31 Chemin Joseph Aiguier, 13402 Marseille Cedex 20, France, [4]Centre de Recherches sur les Macromolécules Végétales (CERMAV), UPR 5301 CNRS et Université Grenoble Alpes, BP53, 38041 Grenoble, France and [5]Aix-Marseille Université, CNRS, CINaM UMR 7325, 163 Avenue de Luminy 13288 Marseille, France

Email:
Sophie de Bentzmann* - bentzman@imm.cnrs.fr; Anne Imberty* - imberty@cermav.cnrs.fr; Peter G. Goekjian* - goekjian@univ-lyon1.fr

* Corresponding author

Keywords:
antibiotic; biofilm; glycocluster; lectin; multivalency effect; multivalent glycosystems

Beilstein J. Org. Chem. **2014,** *10,* 1981–1990.
doi:10.3762/bjoc.10.206

Received: 14 February 2014
Accepted: 30 July 2014
Published: 25 August 2014

This article is part of the Thematic Series "Multivalent glycosystems for nanoscience".

Guest Editor: B. Turnbull

Abstract

Readily accessible, low-valency glycoclusters based on a triazine core bearing D-galactose and L-fucose epitopes are able to inhibit biofilm formation by *Pseudomonas aeruginosa*. These multivalent ligands are simple to synthesize, are highly soluble, and can be either homofunctional or heterofunctional. The galactose-decorated cluster shows good affinity for *Pseudomonas aeruginosa* lectin lecA. They are convenient biological probes for investigating the roles of lecA and lecB in biofilm formation.

Introduction

Pseudomonas aeruginosa (PA) is an opportunistic human pathogen known to cause a variety of hospital-borne infections. It poses a severe threat to immunocompromised patients, as well as to those suffering from cystic fibrosis or cancer [1-3]. Its virulence is largely associated with multi-resistance to antibiotics, in particular due to the physical barrier created by surface-attached biofilms, thus limiting antibiotic penetration [4-6]. A challenging and useful task is therefore to develop novel strategies against PA colonies at this late stage of virulence. Among recent approaches, targeting biofilm formation or

promoting its dissolution is thus particularly appealing. Because the formation of PA biofilm is a complex process partly mediated by the D-galactose-specific lectin lecA (PA-IL) [7-10] and the L-fucose-specific lectin lecB (PA-IIL) [11-13], lectin-carbohydrate interactions can provide a new target for pharmacological intervention. Further investigations of the specific functions played by these lectins in PA biofilm formation will provide useful understanding, and ultimately a means of prevention of PA virulence. The creative design of glycomimetics that can interfere or can modulate the bioactivity of these lectins in host recognition and adhesion in biofilm formation represents an attractive antibacterial strategy, as multivalent carbohydrate motifs on cell surfaces are known to mediate a broad range of cellular and tissue adhesion processes.

Carbohydrate recognition in biological systems is often based on the recognition of multiple epitopes through a synergistic and cooperative effect, called the ‘’glycocluster effect” [14-16]. It has been shown in a number of systems that multivalency effects can be exploited to obtain high-avidity synthetic ligands against various types of lectins in the form of glycoclusters [17], poly(glycomer)s [18-21], and glycodendrimers [22-24]. In regards to PA, *C*-fucosylpeptide dendrimers were shown to inhibit biofilm formation and to efficiently disperse established biofilms in both reference and hospital strains of PA [25-27]. Recently, galactosylated peptide dendrimers have shown a strong affinity for lecA while inhibiting or dispersing biofilms [28,29]. This anti-biofilm effect mediated by glycodendrimers validates a new approach to the control PA propagation and infection.

In this work and following those lines, we had in mind to develop simpler, lower molecular weight, and hydrosoluble multivalent ligands against lecA and lecB, able to exert useful biofilm inhibition and to provide useful tools for investigating the roles of lecA and lecB in the colonization process. Our investigations further aimed at concentrating a high density of proximate carbohydrate epitopes with limited degrees of freedom onto a sulfurated heteroaromatic scaffold as novel glycosylated asterisk ligands [30]. We have thus designed a simple, yet effective new family of multivalent glycosylated architectures built around a trithiotriazine core. Both homo- and heterobifunctional ligands are obtained by a straightforward preparative route, as an innovative approach. Additionally, isothermal titration calorimetry (ITC) and dynamic light scattering (DLS) helped to better understand lectin–ligand interactions between lecA or lecB and these trithiotriazine-based ligands.

Results and Discussion

Design of ligands

A previous study from our laboratories [30] has shown that low-valent glycoasterisk ligands based on a persulfurated benzene core [31,32] could have a dual role as a probe and as a ligand, due to their phosphorescence [33] and electrochemical properties [34] (Figure 1). They were also highly potent lectin

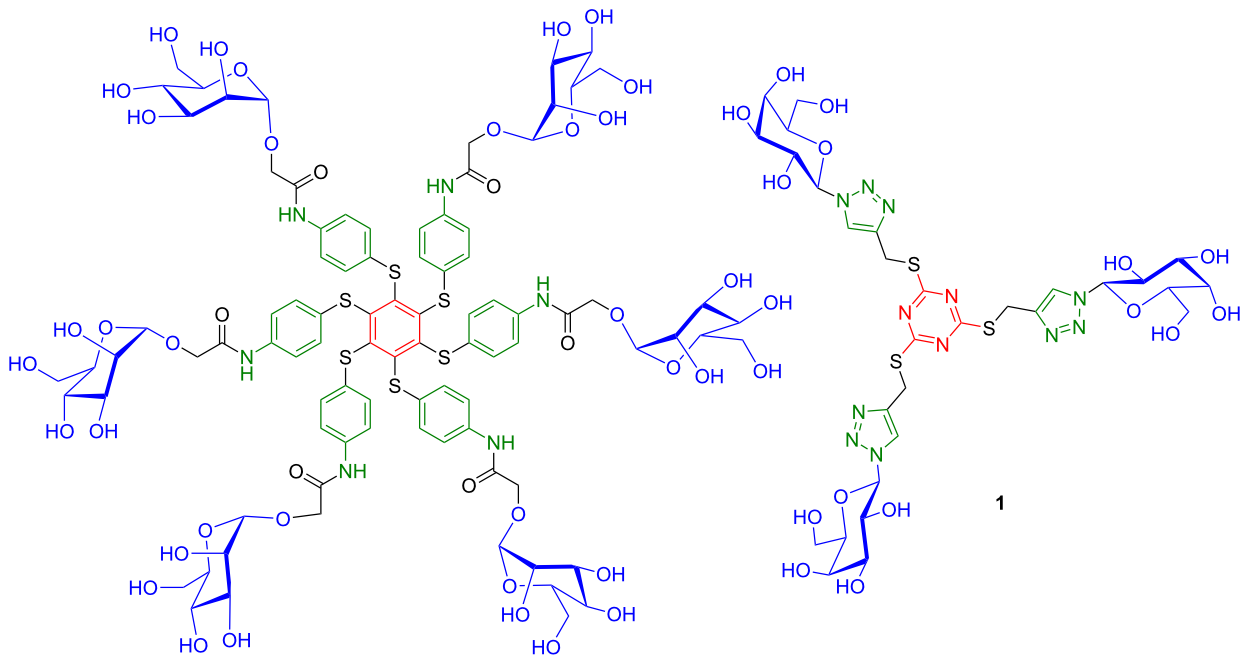

Figure 1: Previously reported low-valent glycoasterisk α-D-Man ligand based on a persulfurated benzene core [30] and currenly reported β-D-Gal compound **1**.

aggregators. Among other aromatic glycoasterisks, Roy et al. described the synthesis of densely substituted hexaphenylbenzene glycoclusters [35].

In this work, we have designed a new family of low-valent glycoclusters based on a heteroaromatic core with the benefit of sulfur chemistry [36]. Sulfur facilitates the synthesis by providing a strong nucleophile and access to a thioether linkage under mild conditions, but it also enhances a number of potentially useful physical properties. For instance, polysulfuration of an aromatic core is known to significantly modify the HOMO–LUMO orbital energies, and thus change the redox potentials [31-34]. It also shifts the spectroscopic absorption and emission wavelengths and can lead to a phosphosrescence emission [33]. Additionally, an aza-aromatic core would improve water solubility by modifying π–π-interactions and by favoring hydrogen-bonding to water. These compounds also lack the hydrophobic peripheral benzene units of the previous glycoasterisk ligands. They were replaced with a methylene-triazole linker in order to increase water solubility and to modulate the degree of flexibility.

Synthesis of ligands

The glycoclusters were prepared from the inexpensive trithiocyanuric acid (1,3-5-triazine-2,4,6-trithiol) as the heteroaromatic core (Scheme 1). Trisubstitution of the commercial trisodium salt with propargyl bromide ensured the facile preparation of 2,4,6-tris(propargylthio)-1,3,5-triazine (**2**) as a key

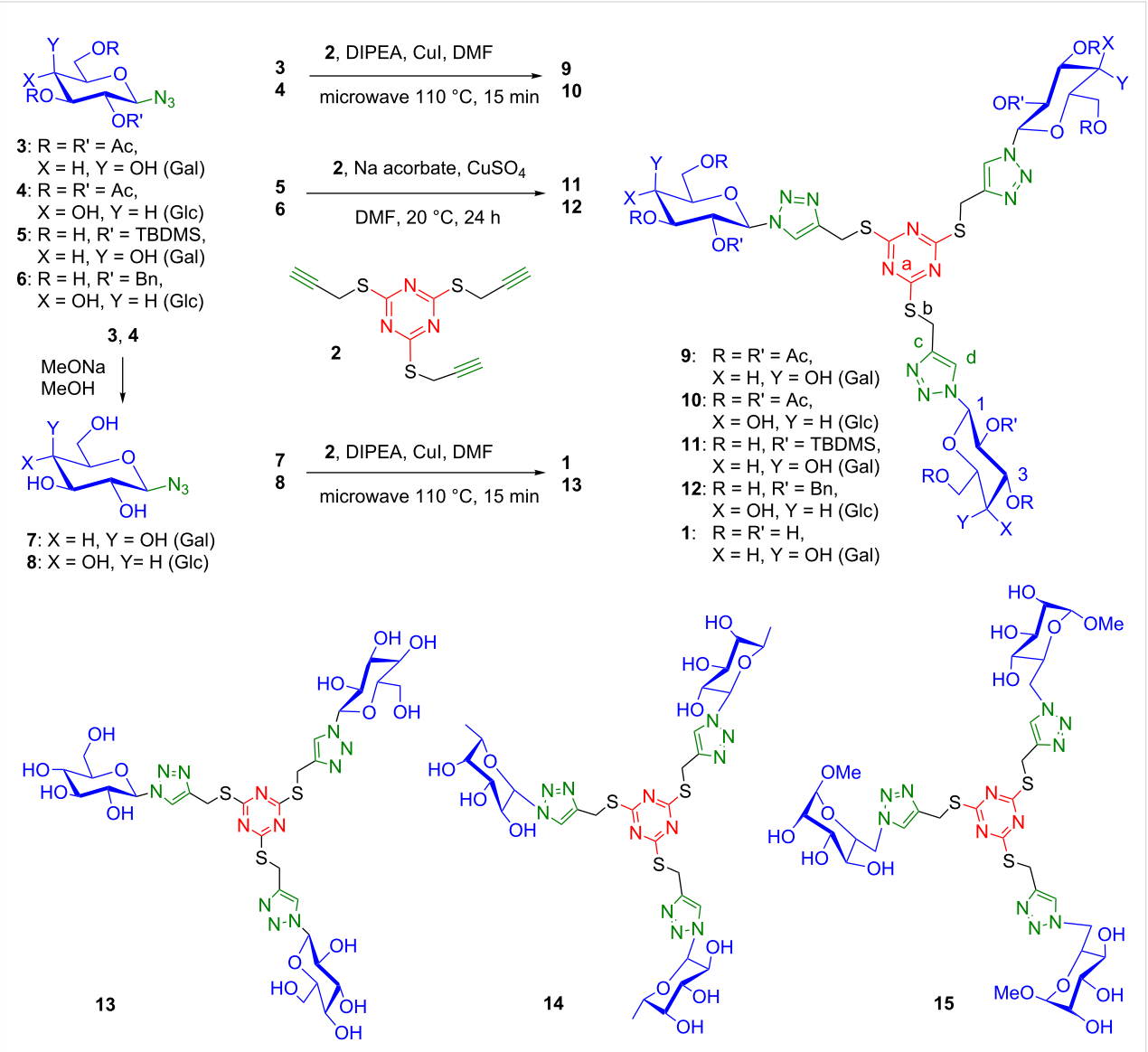

Scheme 1: Synthesis of trivalent trithiotriazine-based glycoclusters.

precursor [37]. The glycosyl units were incorporated via Cu(I)-catalyzed Huisgen cycloaddition with protected or unprotected glycosyl azides.

We first investigated the Cu-catalyzed azide–alkyne cycloaddition (CuAAC) of acetyl protected β-D-galactopyranosyl azide **3** [38], to tris(propargylthio)triazine **2**, using CuI and diisopropylethylamine (DIPEA) in DMF under microwave irradiation at 110 °C for 15 min. It provided the peracetylated D-galactopyanosyl cluster **9** in 73% yield. The peracetyl D-glucopyranosyl cluster **10** was similarly obtained in 92% yield.

The deacetylation of the carbohydrate units proved to be problematic, as a result of the instability of the triazine system under either forcing or mild Zemplén deprotection conditions. The *tert*-butyldimethylsilyl-protected galactopyranosyl azide **5** was therefore prepared via the epoxidation of silylated D-galactal with dimethyldioxirane (DMDO) generated in situ in the presence of a phase-transfer catalyst, followed by treatment with NaN_3 [39]. This afforded the silyl-protected D-galactose trithiotriazine–triazole glycocluster **11** under $CuSO_4$/sodium ascorbate-catalyzed cycloaddition conditions [40] (20 °C, 24 h), in a satisfactory 87% yield. The benzyl protected D-glucose glycocluster **12** was similarly prepared from tri-*O*-benzyl-β-D-glucopyranosyl azide **6** [39] in 92% yield. The removal of the silyl groups with TBAF led to complete degradation of the scaffold. Ammonium fluoride in THF or trifluoroacetic acid also led to the fragmentation of the cluster core, which preceded complete deprotection of the carbohydrate groups. We were unable to obtain the deprotected glycoclusters by this route.

We therefore investigated a direct route to the glycoasterisks using unprotected azidosugars, thus avoiding the final deprotection step. The unprotected azidosugars were obtained by straightforward deprotection of the corresponding acetyl-protected azides [38]. The trivalent glycoclusters decorated with D-galactose, **1**, D-glucose, **13**, and L-fucose, **14**, epitopes were thus obtained directly in 53%, 50%, and 44% yields, respectively, after reversed-phase chromatography. Methyl 6-azido-6-deoxy-α-D-mannoside was similarly coupled as a less expensive isostere of L-fucose [41]. The tris 6-*C*-(6-deoxy-D-mannosyl) cluster **15** was thus obtained in 47% yield. The cycloaddition conditions were optimized using 3.3 equiv of glycosyl azide [39] and one equivalent of tris(propargylthio)-triazine **2** in DMF, catalyzed by CuI and DIPEA under microwave irradiation. The incorporation of three carbohydrate residues was established unambiguously by ESIMS, ^{1}H NMR, ^{13}C NMR, and HMBC analysis, in particular based on the symmetry of the molecule, and on the lack of signals corresponding to the residual alkynes in the NMR and MS. The connectivity was established thanks to HMBC ^3J proton–carbon correlations between the anomeric proton of the sugar and the triazole methine carbon (H-1–C-d), between the trizaole methine carbon and the thiomethylene protons (C-d–H-b), and between the thiomethylene protons and the triazine carbon (H-b–C-a). Despite the moderate yields, these products are readily accessible, being easy to purify, simple to characterize, and able to be produced on a relatively large scale.

The current process also offers the possibility of synthesizing mixed glycoclusters. Reducing the number of equivalents of glycosyl azide **7** to 2 equiv in the presence of CuI and DIPEA in DMF at 110 °C under microwave irradiation provided a statistical mixture with the bivalent cluster as the major product. The bis-D-galactosyl cluster **16** was thus isolated in 34% yield. A second [3 + 2] cycloaddition with a different glycoside, such as D-glycopyranosyl azide **8**, under the same conditions, provided for example the mixed Gal_2-Glc triazine cluster **17** (Scheme 2).

The efficient conjugation of unprotected glycosyl azides to trithiotriazine **2** thus provides convenient access to low valency mono- or heterobifunctional glycoclusters. As expected, they display excellent aqueous solubility due of the combination of a dendritic polyheterocyclic architecture and carbohydrate epitopes.

Biophysical studies

Dynamic light scattering experiments (DLS) were performed on the trivalent and divalent galactose-substituted clusters **1**, **16** and **17**, as well as the glucose-substituted cluster **13** as a negative control. The results show that of the four clusters, only the divalent bis-D-Gal propargyl cluster **16** induces rapid aggregation of lecA (Figure 2 and Supporting Information File 1). Although such results should not be over-interpreted, they confirm that two epitopes are sufficient for aggregation, and suggest that additional hydrophobic and hydrophilic interactions play a role. The inability of these systems to efficiently aggregate lectins is in stark contrast to the hexavalent benzene cluster [30], which may be attributed to differences in rigidity and hydrophobicity between the two systems [25]. It thus appears that the direct diaryl sulfide bridge presents a more optimal degree of semi-rigidity.

The affinities of the designed glycoconjugates with lecA and lecB were determined by isothermal titration calorimetry (ITC) by addition of the ligands to a solution of lectin (Figure 3). Dissociation constants (K_d) and thermodynamic parameters (ΔG, ΔH, $-T\Delta S$) are listed in Table 1, together with the experimental binding stoichiometry (n), defined as the number of glycocluster ligands per monomer of lectin.

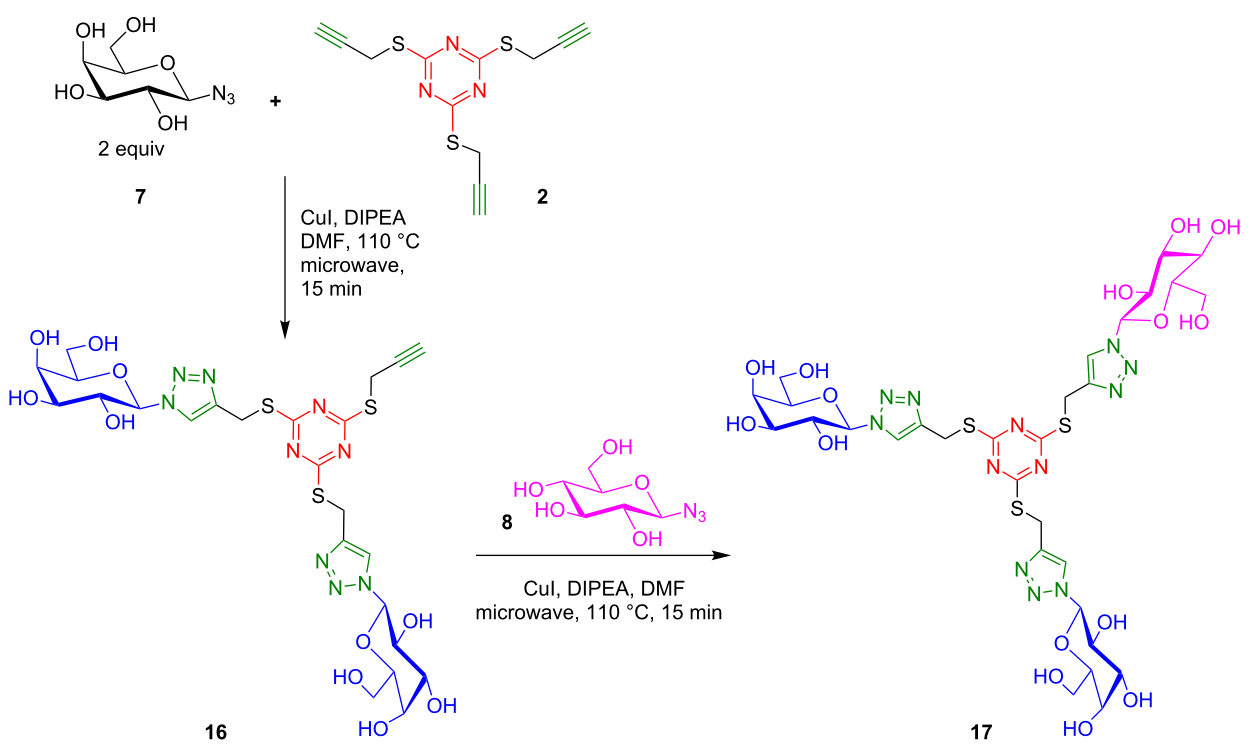

Scheme 2: Synthesis of mixed triazine-based glycoclusters.

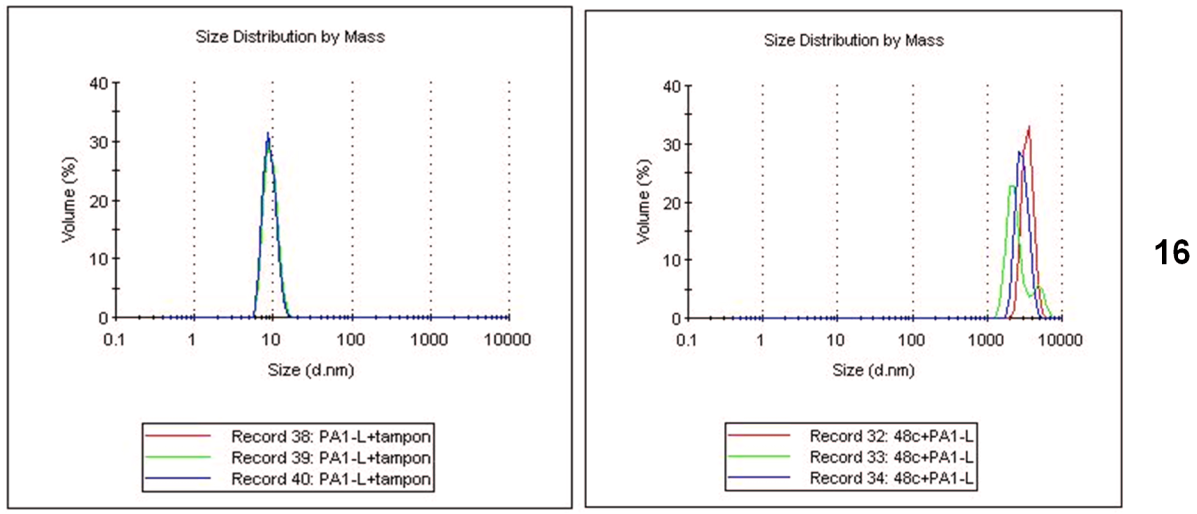

Figure 2: Dynamic light scattering experiments of bis-D-galactosyl proparyl cluster **16** with lecA. Distribution by mass for lecA + buffer (left) and lecA + **16** (200 μM, right) at 3 minute intervals. Additional experiments can be found in Supporting Information File 1.

The trivalent tris-galacosylated glycoconjugate **1** displays a good affinity and a K_d value of 1.09 μM, compared to 94 μM for the monovalent reference, methyl β-D-galactoside (Table 1). The stoichiometry indicates that each cluster binds to three lecA sites. The tris-glucosylated cluster **13** was used as a negative control with nearly identical physical properties, and showed no affinity for the lectin, confirming that the recognition is epitope-specific. The bivalent clusters containing two galactose residues **16** and **17** have similar binding constants, although the mixed cluster **17** containing two D-galactose and one D-glucose residues provided better ITC titration curves and more rational *n* values than the bis D-galactosyl monopropargyl cluster **16**,

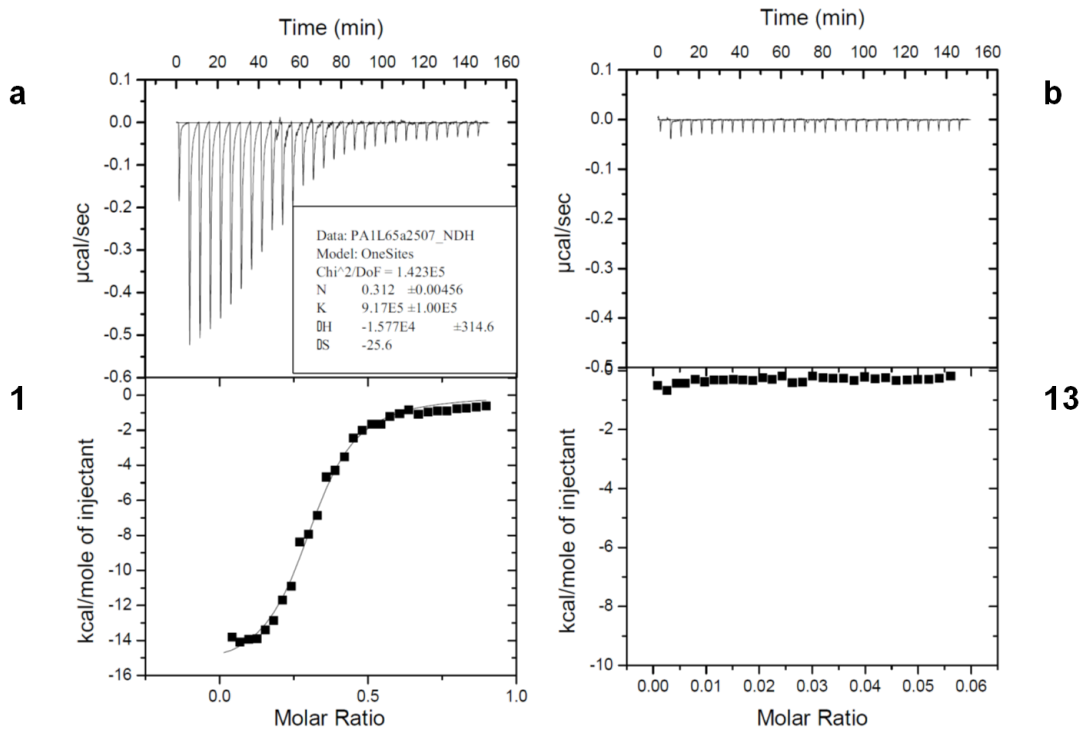

Figure 3: Typical ITC measurements representing the raw ITC data (top) and integrated titration curves (bottom) for the binding to lecA of a) tris-D-galactosyl triazine cluster **1**, and b) tris D-glucosyl glycocluster **13** (negative control).

Table 1: Thermodynamic parameters of glycoclusters upon binding to lecA by ITC[a].

cmpd	val.	n[b]	ΔH kJ/mol	−TΔS kJ/mol	ΔG kJ/mol	K_d µM	β/N[c]
β-D-GalOMe[d]	1	0.8	−42.8	19.8	−23.0	94	1
Gal_3-tzn, **1**	3	0.31	−66.0	31.9	−34.1	1.09	29
Gal_2Glc-tzn, **17**	2	0.54	−51.0	19.7	−31.3	3.4	14
Gal_2Pg-tzn, **16**	2	0.79	−47.6	17.2	−30.5	4.4	11
Glc_3-tzn, **13**	3				<0		

[a]T = 298 K. [b]Stoichiometry. [c]Improvement in affinity relative to the methyl glycoside, divided by the valency. [d]Data from reference [50]. Pg = propargyl; tzn = tris(triazolylmehylthio)triazine.

which may reflect precipitation of the lectin-cluster complex during the ITC experiment in the latter case, based on the DLS results above.

The observed β/N values in Table 1, which reflect the relative affinity per unit sugar, are 29 for the trivalent cluster and in the range of 12 for the bivalent clusters. These values most likely reflect sub-site binding by the heterocyclic rings. Indeed, the divalent clusters **16** and **17** show a relatively less unfavorable entropy contribution, compared to methyl β-D-galactopyranoside, which is consistent with the contribution of additional hydrophobic interactions. No chelate binding is expected in this first generation cluster, as the arm length is well below the 29 Å distance between sugar binding sites [7]. Not unexpectedly, several reported multivalent clusters have achieved higher affinities, yet the values observed here fall within the range obtained with far more complex multivalent systems [28,42-50]. The β-fucoside-containing trivalent cluster **14** was also tested by ITC and a K_d of 50 µM was obtained, which is significantly higher than the K_d for α-MeFuc (0.43 µM) [41] (data not shown). This confirms that lecB has lower affinity for β-fucosides than for the α-anomers, but the trimeric β-fucoside cluster **14** still demonstrated reasonable binding. The 6-deoxymannose isostere **15** was not tested, in view of the low affinity of the

β-fucose epitopes. These clusters thus represent a readily accessible, highly soluble, and convenient tool for the investigation of the role of lecA and lecB in the formation of biofilms by *Pseudomonas aeruginosa*.

Inhibition of biofilm formation

While the expectation that glycoclusters with high affinity to lecA and lecB should inhibit biofilm formation is now a common design hypothesis, it is nonetheless important to show whether individual synthetic clusters do so in fact. This has only been done in a limited number of examples [9,10], perhaps due to lack of solubility, lack of availability, or other reasons. The response of PA biofilms to different clusters is not necessarily directly correlated to their affinity, as many other factors may intervene, and the accumulation of biofilm data will therefore be an important factor in our understanding of this complex process.

The *P. aeruginosa* adherence assay was performed in 24 well microplates. Biofilms were obtained after 24 h of incubation at 30 °C in LB medium alone or in the presence or galactose, fucose, or glucose (control)-substituted trivalent clusters and stained with crystal violet (CV).

A statistically significant reduction in biofilm formation was observed at 5 mM concentration of either the galactose- or the fucose-bearing cluster, **1** and **14**, respectively, as compared to the glucose-bearing cluster, **13**, or absence of cluster (Figure 4). To check that differences observed were not due to bacterial growth defect in the presence of clusters, a growth inhibition control experiment was performed (Figure 4C). No growth defect was observed, further confirming that observed reduction of biofilm formation in the presence of the galactose or the fucose-bearing clusters is due to potential effects on *P. aeruginosa* lectins.

Conclusion

We have developed a convenient synthesis of simple, low-valency glycoclusters. These compounds have good solubility, are readily accessible, and are easy to purify and to characterize. The presence of the sulfur provides beneficial structural and synthetic elements, and the heterocyclic systems improve solu-

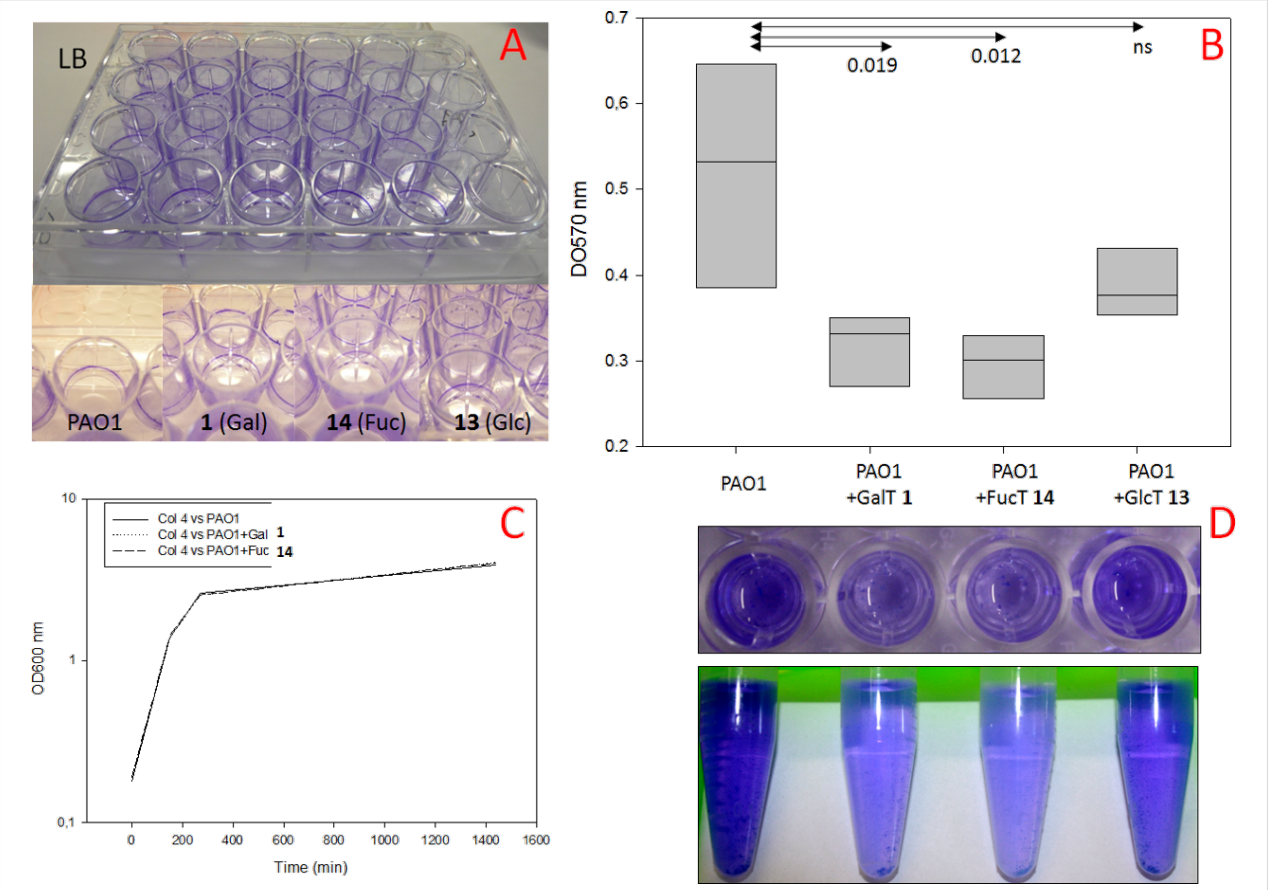

Figure 4: Inhibition of PAO1 biofilm formation by D-galactose cluster **1**, L-fucose cluster **14**, and D-glucose cluster **13** (negative control). A) Biofilm growth assay in LB medium. B) Statistical analysis (above, n = 5, duplicate UV measurements) of ethanol-solubilized biofilm recovered from each well (below). C) PAO1 growth inhibition control test.

bility and may potentially lead to better pharmacodynamic properties for eventual biological applications. They show good affinities for the lectins, comparable to more complex multivalent systems. The recognition is sugar-specific, as the corresponding D-glucose glycocluster shows no affinity for the lectin, and can thus be used as a negative control. Both the D-galactose and L-fucose clusters are able to inhibit biofilm formation. These compounds therefore provide convenient tools for further investigation of lectin-mediated processes in *P. aeruginosa* biofilm formation.

Experimental

2,4,6-tris(1-(β-D-galactopyranosyl)triazol-4-ylmethylthio)-1,3,5-triazine (1). A solution of compound **2** (22 mg, 0.073 mmol, 1 equiv), β-D-galactopyranosyl azide (59.7 mg, 0.294 mmol, 4 equiv), CuI (0.022 mmol, 4.2 mg, 0.3 equiv) and DIPEA (0.2 mL, 15 equiv) in DMF (2 mL) was heated under microwave irradiation for 15 minutes at 110 °C. The reaction mixture was concentrated in vacuo and the residue was purified by C18 chromatography (Combiflash, Grace Reveleris C18 RP 4g Cartridge, H_2O/MeOH gradient). Yield = 53%. TLC (C18; MeOH/H_2O 1:1). R_f = 0.42. $[\alpha]_D$ +14.5 (*c* 1, H_2O); IR (neat) υ = 3287.6 cm^{-1} (OH) 1474.3 (triazole); ^1H NMR (400 MHz, DMSO-d_6) δ 8.20 ppm (s, 3H, H-d), 5.45 (d, *J* = 9.2 Hz, 3H, H-1), 5.22 (d, *J* = 6.0 Hz, 3H, OH-2), 5.01 (d, *J* = 5.7 Hz, 3H, OH-3), 4.69 (t, 3H, OH-6), 4.64 (d, *J* = 5.4 Hz, 3H, OH-4), 4.52 (s, 6H, H-b), 4.01 (ddd, *J* = 9.3 Hz, *J* = 9.2 Hz, *J* = 6.0 Hz, 3H, H-2), 3.76 (br dd, *J* = 5.7, 3.4 Hz, 3H, H-4), 3.69 (br dd, *J* = 6.1, *J* = 6.1 Hz, 3H, H-5), 3.55–3.44 (m, 9H, H-3, H-6, H-6'); ^{13}C NMR (100 MHz, DMSO-d_6) δ 178.5 ppm (C-a), 142.4 (C-c), 122.5 (C-d), 88.1 (C-1), 78.4 (C-5), 73.6(C-3), 69.2 (C-2), 68.4 (C-4), 60.4 (C-6), 24.6 (C-b); HRMS–ESI (*m*/*z*): [M + H]$^+$ calcd for $C_{30}H_{43}N_{12}O_{15}S_3$, 907.2170; found, 907.2127; (*m*/*z*): [M + Na]$^+$ calcd for $C_{30}H_{43}N_{12}NaO_{15}S_3$, 929.1980; found, 929.1947.

2,4,6-tris(1-(β-D-glucopyranosyl)triazol-4-ylmethylthio)-1,3,5-triazine (13). A solution of compound **2** (18.1 mg, 0.062 mmol, 1 equiv), β-D-glucopyranosyl azide (51 mg, 0.25 mmol, 4 equiv), CuI (3.5 mg, 0.3 equiv) and DIPEA (0.74 mmol, 0.16 mL, 15 equiv) in DMF (1 mL) was heated under microwave irradiation for 15 minutes at 110 °C. The reaction mixture was concentrated in vacuo and the residue was purified by C18 chromatography (Combiflash, Grace Reveleris C18 RP 4g Cartridge, H_2O/MeOH gradient). Yield = 50%. TLC (C18; MeOH/H_2O 1:1). R_f = 0.47. $[\alpha]_D$ −2.0 (*c* 0.46, H_2O); ^1H NMR (300 MHz, DMSO-d_6) δ 8.25 ppm (s, 3H, H-d), 5.51 (d, *J* = 9.3Hz, 3H, H-1), 5.38 (d, *J* = 6.0Hz, 3H, OH-2), 5.27 (d, *J* = 4.9, 3H, OH-3), 5.14 (d, *J* = 5.5, 3H, OH-4), 4.63 (t, *J* = 5.6, 3H, OH-6), 4.52 (s, 6H, H-b), 3.77–3.66 (m, 6H, H-2, H-6), 3.46–3.32 (m, 6H, H-3, H-5, H-6'), 3.25–3.15 (m, 3H, H-4); ^{13}C NMR (75 MHz, DMSO-d_6) δ 178.6ppm (C-a), 142.4 (C-c), 122.9 (C-d), 87.5 (C-1), 79.9 (C-3), 76.9 (C-5), 72.0 (C-2), 69.5 (C-4), 60.7 (C-6), 24.6 (C-b); HRMS–ESI (*m*/*z*): [M + H]$^+$ calcd for $C_{30}H_{43}N_{12}O_{15}S_3$, 907.2132; found, 907.2127; (*m*/*z*): [M + Na]$^+$ calcd for $C_{30}H_{43}N_{12}NaO_{15}S_3$. 929.1943; found, 929.1947.

2,4,6-tris(1-(β-L-fucopyranosyl)triazol-4-ylmethylthio)-1,3,5-triazine (14). Compound **2** (132.9 mg, 0.458 mmol, 1 equiv), β-L-fucopyranosyl azide (345.6 mg, 1.82 mmol, 4 equiv), CuI (26 mg, 0.13 mmol, 0.3 equiv) and DIPEA (1.13 mL, 16.8 mmol, 5 equiv) in DMF (2 mL) was heated under microwave irradiation for 15 minutes at 110 °C. The reaction mixture was concentrated in vacuo and the residue was purified by C18 chromatography (Combiflash, Grace Reveleris C18 RP 4g Cartridge, H_2O/MeOH gradient). Yield = 44%. TLC (C18; MeOH/H_2O 1:1) R_f = 0.5. $[\alpha]_D$ +5.2 (*c* 0.17; H_2O); ^1H NMR (400 MHz, DMSO-d_6) δ 8.18 ppm (s, 3H, H-d), 5.44 (d, *J* = 9.2 Hz, 3H, H-1), 5.22 (d, *J* = 6.0 Hz, 3H, OH-2), 5.00 (d, *J* = 5.5 Hz, 3H, OH-3), 4.70 (d, *J* = 5.4 Hz, 3H, OH-4), 4.52 (s, 6H, H-b), 4.03–3.94 (m, 3H, H-2), 3.88 (br. q, *J* = 6.3 Hz, 3H, H-5), 3.57–3.51 (m, 6H, H-4, H-3), 1.13 (d, *J* = 6.4 Hz, 9H, CH_3); ^{13}C NMR (100 MHz, DMSO-d_6) δ 178.1ppm (C-a), 142.0 (C-c), 122.0 (C-d), 87.6 (C-1), 73.6 (C-3), 73.0 (C-5), 71.0 (C-4), 68.5 (C-2), 24.3 (C-b), 16.3 (CH_3); HRMS–ESI (*m*/*z*): [M + H]$^+$ calcd for $C_{30}H_{43}N_{12}O_{12}S_3$, 859.2299; found, 859.2280 ; (*m*/*z*): [M + Na]$^+$ calcd for $C_{30}H_{42}N_{12}NaO_{12}S_3$, 881.2096; found, 881.2099.

2,4-bis(1-(β-D-galactopyranosyl)triazol-4-ylmethylthio)-6-(prop-2-ynylthio)-1,3,5-triazine (16). A solution of compound **2** (35.9 mg, 0.123 mmol, 1 equiv), β-D-galactopyranosyl azide (50.6 mg, 0.240 mmol, 2 equiv), CuI (0.036 mmol, 7 mg, 0.3 equiv) and DIPEA (1.84 mmol, 0.32 mL, 15 equiv) in DMF (2 mL) was heated under microwave irradiation for 15 minutes at 110 °C. The reaction mixture was concentrated in vacuo and the residue was purified by C18 chromatography (Combiflash, Grace Reveleris C18 RP 4g Cartridge, H_2O/MeOH gradient). Yield = 34%. $[\alpha]_D$ +4.3 (c 0.36, H_2O); ^1H NMR (400 MHz, DMSO-d_6) δ 8.18 ppm (s, 2H, H-d), 5.44 (d, *J* = 9.2 Hz, 2H, H-1), 5.23 (d, *J* = 6.0 Hz, 2H, OH-2), 5.02 (d, *J* = 5.6 Hz, 2H, OH-3), 4.70 (t, *J* = 5.6 Hz, 2H, OH-6), 4.67 (d, *J* = 5.3 Hz, 2H, OH-4), 4.58–4.50 (AB, *J* ~ 15.0 Hz, 4H, H-b), 4.05–4.03 (m, 2H, H-e), 4.0 (ddd, *J* = 9.3 Hz, *J* = 9.2 Hz, *J* = 6.0 Hz, 2H, H-2), 3.76 (br dd, *J* = 5.3 Hz, *J* = 3.5 Hz, 2H, H-4), 3.69 (br t, *J* = 6.0 Hz, 2H, H-5), 3.54–3.46 (m, 6H, H-3, H-6, H-6'), 3.23 (t, *J* = 2.5 Hz, 1H, H-g);^{13}C NMR (100 MHz, DMSO-d_6) δ 178.4 ppm (C-a), 177.8 (C-a'), 142.4 (C-c), 122.3 (C-d), 87.9 (C-1), 79.5 (C-f), 78.2 (C-5), 73.8 (C-g), 73.4 (C-3), 69.1 (C-2), 68.3 (C-4), 60.2 (C-6), 24.4 (C-b), 18.4 (C-e); HRMS–ESI (*m*/*z*): [M + H]$^+$ calcd for $C_{24}H_{32}N_9O_{10}S_3$, 702.1461; found, 702.1429;

(m/z): $[M + Na]^+$ calcd for $C_{24}H_{31}N_9NaO_{10}S_3$, 724.1277; found, 724.1248.

2,4-bis(1-(β-D-galactopyranosyl)triazol-4-ylmethylthio)-6-(1-(β-D-glucopyranosyl)triazol-4-ylmethylthio)-1,3,5-triazine (17). A solution of the bis-Gal triazine cluster **16** (12.2 mg, 0.017 mmol, 1 equiv), β-D-glucopyranosyl azide (5.3 mg, 0.026 mmol, 1.5 equiv), CuI (1 mg, 0.3 equiv) and DIPEA (0.043 mL, 15 equiv) in DMF (1mL) was heated under microwave irradiation for 15 minutes at 110 °C. The reaction mixture was concentrated in vacuo and the residue was purified by C18 chromatography (Combiflash, Grace Reveleris C18 RP 4g Cartridge, H_2O/MeOH gradient). Yield = 30%. $[\alpha]_D$ −1.2 (*c* 0.1, H_2O); ^{1}H NMR (500 MHz, D_2O) δ 8.20 ppm (s, 2H, Gal H-d), 8.16 (s, 1H, Glc H-d), 5.70 (d, J = 9.2 Hz, 1H, Glc H-1), 5.65 (d, 2H, J = 9.2 Hz, Gal H-1), 4.40 (s, 6H, H-b), 4.19 (t, J = 9.5 Hz, 2H, Gal H-2), 4.09 (d, J = 3.2 Hz, 2H, Gal H-5), 4.01–3.94 (m, 3H, Gal H-4,Glc H-2), 3.88 (dd, J = 9.3 Hz, J = 3.2 Hz, 2H, Gal H-3), 3.77 (d, J = 12.1 Hz, 2H, Gal H-6), 3.76 (d, J = 12.1 Hz, 2H, Gal H-6'), 3.74 (d, J = 11.6 Hz, 1H, Glc H-6), 3.73 (d, J = 11.6 Hz, 1H, Glc H-6'), 3.71–3.67 (m, 2H, Glc H-3, Glc H-4), 3.62 (t, J = 9.4 Hz, 1H, Glc H-5); ^{13}C NMR (125 MHz, D_2O) δ 178.7 ppm (C-a), 144.4 (C-c), 123.4 (C-d), 87.1 (Gal C-1), 87.4 (Glc C-1), 78.9 (Glc C-4), 78.3 (Gal C-4), 75.9 (Glc C-3), 73.0 (Gal C-3), 72.3 (Glc C-2), 69.8 (Glc C-5), 68.6 (Gal C-5), 62.5 (Glc C-6), 60.8 (Gal C-6), 24.4 (Cb); HRMS–ESI (m/z): $[M + Na]^+$ calcd for $C_{30}H_{42}N_{12}NaO_{15}S_3$, 929.1916; found, 929.1947.

Supporting Information

Full 1D and 2D NMR spectra of compounds **1**, **2**, and **9**–**17**; experimental procedures for ITC and biofilm inhibition studies, and for the synthesis of tris propargyl precursor **2**, protected clusters **9**–**12,** and 6-*C*-mannose cluster **15**; additional DLS and ITC spectra, additional biofilm quantification information.

Supporting Information File 1

Experimental procedures, characterization checklist and NMR, DLS and ITC data.
[http://www.beilstein-journals.org/bjoc/content/supplementary/1860-5397-10-206-S1.pdf]

Acknowledgements

Funding was provided by the French National Research Agency [ANR PCV08_322689 Glycoasterix], the COST actions CM1102 and BM1003, the Labex ARCANE (ANR-11-LABX-003), the French Ministry of Higher Education and Research (MENSR), and the National Center for Scientific Research (CNRS). MS gratefully acknowledges a PhD scholarship from the Faculy of Sciences, Carthage University. Emilie Gilloon and David Redelberger are thanked for outstanding technical assistance. All of the experimental work was performed by MS. The remaining authors contributed equally to this work.

References

1. Ramos, J.-L., Ed. *Pseudomonas;* Springer Science: New York, U.S.A., 2004; Vol. 1–3.
2. Bodey, G. P.; Elting, L. S.; Narro, J.; Koller, C.; O'Brien, S.; Estey, E.; Benjamin, R. *J. Antimicrob. Chemother.* **1993,** *32,* 141–152. doi:10.1093/jac/32.1.141
3. Mendelson, M. H.; Gurtman, A.; Szabo, S.; Neibart, E.; Meyers, B. R.; Policar, M.; Cheung, T. W.; Lillienfeld, D.; Hammer, G.; Reddy, S.; Choi, K.; Hirschman, S. Z. *Clin. Infect. Dis.* **1994,** *18,* 886–895. doi:10.1093/clinids/18.6.886
4. Wagner, V. E.; Iglewski, B. H. *Clin. Rev. Allergy Immunol.* **2008,** *35,* 124–134. doi:10.1007/s12016-008-8079-9
5. Lister, P. D.; Wolter, D. J.; Hanson, N. D. *Clin. Microbiol. Rev.* **2009,** *22,* 582–610. doi:10.1128/CMR.00040-09
6. Penha Escudeiro, B. M.; Baracho Marques, E. C., Eds. *Pseudomonas Aeruginosa: Symptoms of Infection, Antibiotic Resistance and Treatment;* Nova Science Publishers, 2012.
7. Imberty, A.; Wimmerová, M.; Mitchell, E. P.; Gilboa-Garber, N. *Microbes Infect.* **2004,** *6,* 221–228. doi:10.1016/j.micinf.2003.10.016
8. Cioci, G.; Mitchell, E. P.; Gautier, C.; Wimmerová, M.; Sudakevitz, D.; Pérez, S.; Gilboa-Garber, N.; Imberty, A. *FEBS Lett.* **2003,** *555,* 297–301. doi:10.1016/S0014-5793(03)01249-3
9. Garber, N.; Guempel, U.; Belz, A.; Gilboa-Garber, N.; Doyle, R. J. *Biochim. Biophys. Acta* **1992,** *1116,* 331–333. doi:10.1016/0304-4165(92)90048-Y
10. Diggle, S. P.; Stacey, R. E.; Dodd, C.; Cámara, M.; Williams, P.; Winzer, K. *Environ. Microbiol.* **2006,** *8,* 1095–1104. doi:10.1111/j.1462-2920.2006.001001.x
11. Mitchell, E.; Houles, C.; Sudakevitz, D.; Wimmerová, M.; Gautier, C.; Pérez, S.; Wu, M. A.; Gilboa-Garber, N.; Imberty, A. *Nat. Struct. Mol. Biol.* **2002,** *9,* 918–921. doi:10.1038/nsb865
12. Loris, R.; Tielker, D.; Jaeger, K.-E.; Wyns, L. *J. Mol. Biol.* **2003,** *331,* 861–870. doi:10.1016/S0022-2836(03)00754-X
13. Tielker, D.; Hacker, S.; Loris, R.; Strathmann, M.; Wingender, J.; Wilhelm, S.; Rosenau, F.; Jaeger, K.-E. *Microbiology* **2005,** *151,* 1313–1323. doi:10.1099/mic.0.27701-0
14. Mammen, M.; Choi, S. K.; Whitesides, G. M. *Angew. Chem., Int. Ed.* **1998,** *37,* 2754–2794. doi:10.1002/(SICI)1521-3773(19981102)37:20<2754::AID-ANIE2754>3.0.CO;2-3
15. Lee, Y. C.; Lee, R. T. *Acc. Chem. Res.* **1995,** *28,* 321–327. doi:10.1021/ar00056a001
16. Lundquist, J. J.; Toone, E. J. *Chem. Rev.* **2002,** *102,* 555–578. doi:10.1021/cr000418f
17. Renaudet, O.; Roy, R., Eds. Multivalent Scaffolds in Glycoscience. *Chem. Soc. Rev.* **2013,** *42,* 4507–4844.
18. Roy, R. *Curr. Opin. Struct. Biol.* **1996,** *6,* 692–702. doi:10.1016/S0959-440X(96)80037-6
19. Mortell, K. H.; Gingras, M.; Kiessling, L. L. *J. Am. Chem. Soc.* **1994,** *116,* 12053–12054. doi:10.1021/ja00105a056
20. Roy, R.; Laferrière, C. *J. Chem. Soc., Chem. Commun.* **1990,** 1709–1711. doi:10.1039/c39900001709

21. Spaltenstein, A.; Whitesides, G. M. *J. Am. Chem. Soc.* **1991,** *113,* 686–687. doi:10.1021/ja00002a053
22. Chabre, Y. M.; Roy, R. *Chem. Soc. Rev.* **2013,** *42,* 4657–4708. doi:10.1039/c3cs35483k
23. Chabre, Y. M.; Roy, R. *Adv. Carbohydr. Chem. Biochem.* **2010,** *63,* 165–393. doi:10.1016/S0065-2318(10)63006-5
24. Turnbull, W. B.; Stoddart, J. F. *J. Biotechnol.* **2002,** *90,* 231–255.
25. Johansson, E. M. V.; Kadam, R. U.; Rispoli, G.; Crusz, S. A.; Bartels, K.-M.; Diggle, S. P.; Cámara, M.; Williams, P.; Jaeger, K.-E.; Darbre, T.; Reymond, J.-L. *Med. Chem. Commun.* **2011,** *2,* 418–420. doi:10.1039/c0md00270d
26. Johansson, E. M. V.; Crusz, S. A.; Kolomiets, E.; Buts, L.; Kadam, R. U.; Cacciarini, M.; Bartels, K.-M.; Diggle, S. P.; Cámara, M.; Williams, P.; Loris, R.; Nativi, C.; Rosenau, F.; Jaeger, K.-E.; Darbre, T.; Reymond, J.-L. *Chem. Biol.* **2008,** *15,* 1249–1257. doi:10.1016/j.chembiol.2008.10.009
27. Consoli, G. M. L.; Granata, G.; Cafiso, V.; Stefani, S.; Geraci, C. *Tetrahedron Lett.* **2011,** *52,* 5831–5834. doi:10.1016/j.tetlet.2011.08.142
28. Kadam, R. U.; Bergmann, M.; Hurley, M.; Garg, D.; Cacciarini, M.; Swiderska, M. A.; Nativi, C.; Sattler, M.; Smyth, A. R.; Williams, P.; Cámara, M.; Stocker, A.; Darbre, T.; Reymond, J.-L. *Angew. Chem., Int. Ed.* **2011,** *50,* 10631–10635. doi:10.1002/anie.201104342
29. Reymond, J.-L.; Bergmann, M.; Darbre, T. *Chem. Soc. Rev.* **2013,** *42,* 4814–4822. doi:10.1039/c3cs35504g
30. Sleiman, M.; Varrot, A.; Raimundo, J.-M.; Gingras, M.; Goekjian, P. G. *Chem. Commun.* **2008,** 6507–6509. doi:10.1039/b814816c
31. Gingras, M.; Raimundo, J.-M.; Chabre, Y. M. *Angew. Chem., Int. Ed.* **2006,** *45,* 1686–1712. doi:10.1002/anie.200500032
32. Gingras, M.; Pinchart, A.; Dallaire, C. *Angew. Chem., Int. Ed.* **1998,** *37,* 3149–3151. doi:10.1002/(SICI)1521-3773(19981204)37:22<3149::AID-ANIE3149>3.0.CO;2-4
33. Bergamini, G.; Fermi, A.; Botta, C.; Giovanella, U.; Di Motta, S.; Negri, F.; Peresutti, R.; Gingras, M.; Ceroni, P. *J. Mater. Chem. C* **2013,** *1,* 2717–2724. doi:10.1039/C3TC00878A
34. Tucker, J. H. R.; Gingras, M.; Brand, H.; Lehn, J.-M. *J. Chem. Soc., Perkin Trans. 2* **1997,** 1303–1308. doi:10.1039/a608455i
35. Chabre, Y. M.; Brisebois, P. P.; Abbassi, L.; Kerr, S. C.; Fahy, J. V.; Marcotte, I.; Roy, R. *J. Org. Chem.* **2011,** *76,* 724–727. doi:10.1021/jo102215y
36. Gingras, M.; Chabre, Y. M.; Roy, M.; Roy, R. *Chem. Soc. Rev.* **2013,** *42,* 4823–4841. doi:10.1039/C3CS60090D
    See for a review of sulfur-containing glycodendrimers.
37. Azev, Y. A.; Dülcks, T.; Gabel, D. *Tetrahedron Lett.* **2003,** *44,* 8689–8691. doi:10.1016/j.tetlet.2003.09.153
38. Tropper, F. D.; Andersson, F. O.; Braun, S.; Roy, R. *Synthesis* **1992,** 618–620. doi:10.1055/s-1992-26175
39. Lafont, D.; D'Attoma, J.; Gomez, R.; Goekjian, P. G. *Tetrahedron: Asymmetry* **2011,** *22,* 1197–1204. doi:10.1016/j.tetasy.2011.06.027
40. Lee, B.-Y.; Park, S. R.; Jeon, H. B.; Kim, K. S. *Tetrahedron Lett.* **2006,** *47,* 5105–5109. doi:10.1016/j.tetlet.2006.05.079
41. Sabin, C.; Mitchell, E. P.; Pokorná, M.; Gautier, C.; Utille, J.-P.; Wimmerová, M.; Imberty, A. *FEBS Lett.* **2006,** *580,* 982–987. doi:10.1016/j.febslet.2006.01.030
42. Bernardi, A.; Jiménez-Barbero, J.; Casnati, A.; De Castro, C.; Darbre, T.; Fieschi, F.; Finne, J.; Funken, H.; Jaeger, K.-E.; Lahmann, M.; Lindhorst, T. K.; Marradi, M.; Messner, P.; Molinaro, A.; Murphy, P. V.; Nativi, C.; Oscarson, S.; Penadés, S.; Peri, F.; Pieters, R. J.; Renaudet, O.; Reymond, J.-L.; Richichi, B.; Rojo, J.; Sansone, F.; Schäfer, C.; Turnbull, W. B.; Velasco-Torrijos, T.; Vidal, S.; Vincent, S.; Wennekes, T.; Zuilhof, H.; Imberty, A. *Chem. Soc. Rev.* **2013,** *42,* 4709–4727. doi:10.1039/c2cs35408j
43. Soomro, Z. H.; Cecioni, S.; Blanchard, H.; Praly, J.-P.; Imberty, A.; Vidal, S.; Matthews, S. E. *Org. Biomol. Chem.* **2011,** *9,* 6587–6597. doi:10.1039/c1ob05676j
44. Cecioni, S.; Oerthel, V.; Iehl, J.; Holler, M.; Goyard, D.; Praly, J.-P.; Imberty, A.; Nierengarten, J.-F.; Vidal, S. *Chem. – Eur. J.* **2011,** *17,* 3252–3261. doi:10.1002/chem.201003258
45. Cecioni, S.; Faure, S.; Darbost, U.; Bonnamour, I.; Parrot-Lopez, H.; Roy, O.; Taillefumier, C.; Wimmerová, M.; Praly, J.-P.; Imberty, A.; Vidal, S. *Chem. – Eur. J.* **2011,** *17,* 2146–2159. doi:10.1002/chem.201002635
46. Cecioni, S.; Lalor, R.; Blanchard, B.; Praly, J.-P.; Imberty, A.; Matthews, S. E.; Vidal, S. *Chem. – Eur. J.* **2009,** *15,* 13232–13240. doi:10.1002/chem.200901799
47. Otsuka, I.; Blanchard, B.; Borsali, R.; Imberty, A.; Kakuchi, T. *ChemBioChem* **2010,** *11,* 2399–2408. doi:10.1002/cbic.201000447
48. Pertici, F.; Pieters, R. J. *Chem. Commun.* **2012,** *48,* 4008–4010. doi:10.1039/c2cc30234a
49. Reynolds, M.; Marradi, M.; Imberty, A.; Penadés, S.; Pérez, S. *Chem. – Eur. J.* **2012,** *18,* 4264–4273. doi:10.1002/chem.201102034
50. Chabre, Y. M.; Giguère, D.; Blanchard, B.; Rodrigue, J.; Rocheleau, S.; Neault, M.; Rauthu, S.; Papadopoulos, A.; Arnold, A. A.; Imberty, A.; Roy, R. *Chem. – Eur. J.* **2011,** *17,* 6545–6562. doi:10.1002/chem.201003402

License and Terms

BEILSTEIN JOURNAL OF ORGANIC CHEMISTRY

Indium-mediated allylation in carbohydrate synthesis: A short and efficient approach towards higher 2-acetamido-2-deoxy sugars

Christopher Albler, Ralph Hollaus, Hanspeter Kählig and Walther Schmid*

Full Research Paper

Open Access

Address:
Department of Organic Chemistry, University of Vienna, Währingerstrasse 38, 1090 Vienna, Austria

Email:
Walther Schmid* - walther.schmid@univie.ac.at

* Corresponding author

Keywords:
allylation; carbohydrates; epoxidation; indium; multivalent glycosystems; organocatalysis

Beilstein J. Org. Chem. **2014,** *10,* 2230–2234.
doi:10.3762/bjoc.10.231

Received: 02 June 2014
Accepted: 11 September 2014
Published: 19 September 2014

This article is part of the Thematic Series "Multivalent glycosystems for nanoscience".

Guest Editor: B. Turnbull

Abstract

Higher aminosugars are interesting targets in carbohydrate synthesis since these compounds play important roles in biological systems. However, their availability from natural sources is limited. Thus, in order to investigate their biological function, the development of facile and adaptable routes to this class of compounds is of fundamental importance. Our synthetic route towards these target molecules makes use of readily accessible pentoses and hexoses, which are subjected to indium-mediated two-carbon chain elongation. Subsequent ozonolysis and treatment with base yields α,β-unsaturated aldehydes, which are stereoselectively epoxidized using Jørgenson's protocol. After Wittig chain elongation the obtained allylic epoxides were regio- and stereoselectively opened with trimethylsilyl azide under palladium catalysis. Finally, a suitable deprotection protocol, starting with acidic acetate cleavage and ozonolysis was established. Peracetylation of the products simplifies purification and subsequent azide reduction followed by final deacetylation using methanolic sodium methoxide furnishes the title compounds.

Introduction

The indium-mediated allylation of carbonyl compounds has proven to be a valuable tool for carbon chain elongation [1-3] in order to access rare, biologically active carbohydrates [4-8]. Herein we report the extension of this method towards the field of higher aminosugars by additionally applying a stereoselective epoxidation–azide opening strategy. The resulting compounds, aminoheptoses and octoses, have been scarcely investigated yet. However, they comprise interesting synthetic targets. Aminoheptoses function as constituents of the cell wall lipopolysaccharides of certain bacteria [9] whereas their ^{99m}Tc complexes find practical applications in medicinal chemistry as tracers for tumor detection, myocardial ischemia or infarct diagnostics [10]. The group of Perez et al has taken a particular interest in the chemistry of 2-aminoheptoses [11-14] which they

prepared via an amino-nitrile synthesis [15]. This method, first described by Kuhn and Kirschenlohr [16] for the synthesis of aminohexoses, proved to be straightforward, albeit the reproducibility and yield usually suffered from the formation of multiple side products [17]. Another interesting approach for the synthesis of higher aminosugars, published by Kunz and Deloisy, consists of an aza-Cope rearrangement of *N*-galactosyl-*N*-homoallylamines [18]. Aminooctoses, on the other hand, are present in the aminoglycoside antibiotic apramycin [19], in the form of an aminooctodiose derivative. However, only few syntheses of this dipyranoid aminosugar [20,21] were reported so far. Thus, we were interested in developing a general route towards the synthesis of these higher aminosugars. Since the preparation of new potent aminoglycoside antibiotics remains an important topic in medicinal chemistry [22], our precursors used should be flexible in terms of stereochemical variety, thus potentially allowing for an evaluation of structure–activity relationships.

Results and Discussion

We started our reaction sequence with an indium-mediated allylation of unprotected carbohydrates using D-arabinose (**1a**), D-galactose (**1b**) and D-glucose (**1c**) as starting materials. The Barbier-type chain elongation reaction furnished olefins **2a** and **2b** after acetylation in quantitative yield (Scheme 1). In the gluco-case a yield of 70% for **2c** was obtained owing to incomplete consumption of the starting material **1c**. Ozonolysis of the olefins **2** was performed using thiourea as reducing agent. Subsequently the generated 2-deoxyaldoses were treated with triethylamine (TEA) to yield α,β-unsaturated aldehydes **3a–c** quantitatively.

The aldehydes **3a–c** were stereoselectively epoxidized by applying the conditions developed by Jørgenson et al [23-25]. The required amine catalyst was synthesized starting from L-proline following a literature procedure [26]. In general the desired epoxyaldehydes were obtained with high diastereoselectivity at low temperatures (Table 1). The stereochemistry of compounds **3a–c** is in accordance with the proposed reaction mechanism [24] and was proven by applying various NMR methods on the final products (vide infra), which adopt rigid pyranoid conformations.

Table 1: Epoxidation of aldehydes **3a–c**.

entry	aldehyde	dr[a]	yield[b] [%]
1	**3a**	9:1	64
2	**3b**	99:1	77
3	**3c**	9:1	61

[a]Determined either by comparison of integrals of representative ^{1}H NMR signals of crude reaction products or after conventional column chromatographic separation of diastereomers; [b]isolated yields of corresponding 2,3-epoxyaldehydes.

Unfortunately, we were not able to directly achieve the opening of the obtained 2,3-epoxyaldehydes with azide nucleophiles. A variety of different Lewis acids, solvent systems and azide sources were screened but all attempts led to the decomposition of these labile compounds. Conversion of the carbonyl moiety to an acetal group followed by treatment with azide nucleophiles also failed to yield any desired products. Therefore we decided to mask the aldehyde as an olefin. A Wittig

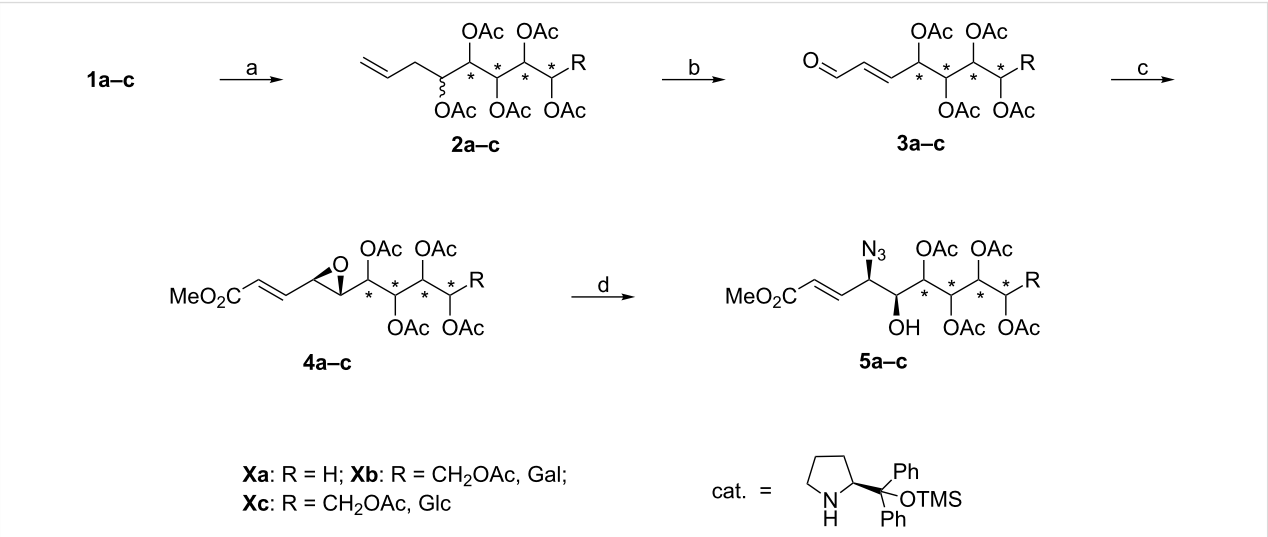

Scheme 1: Functionalization of carbohydrates; reagents and conditions: (a) In, allyl bromide, EtOH/H_2O, ultrasound, 2.5–7 h, then Ac_2O/pyridine, DMAP, rt, 16 h, quant.; (b) O_3, CH_2Cl_2, −78 °C then thiourea, rt, 16 h, then TEA, rt, 30–50 min, quant.; (c) H_2O_2, cat., CH_2Cl_2, −20 °C, 16 h, then $Ph_3P(CHCO_2Me)$, CH_2Cl_2, rt, 1 h, 72–75%, 2 steps; (d) $TMSN_3$, $Pd(PPh_3)_4$, THF, rt, 1 h, 76–85%.

reaction with methyl (triphenylphosphoranylidene)acetate ($Ph_3P(CHCO_2Me)$) generated allylic epoxides **4a–c**, which in turn permitted the application of reliable palladium chemistry for the epoxide opening [27-29]. Thus, compounds **4a–c** were regio- and stereoselectively opened with trimethylsilyl azide and $Pd(PPh_3)_4$ as a catalyst [30], furnishing *syn*-azido alcohols **5a–c**.

In the case of allylic azide **5a** we observed an acetate migration which resulted in a complex mixture of products bearing a free hydroxy moiety (mixture of free C5-OH/C6-OH/C7-OH = 2/1/1; Scheme 1). We reasoned that this migration was limited to the inherent *syn* relationship between C5-OH and C6-OAc in compound **5a**, since this behavior was not observed with compounds **5b** and **5c** which feature an *anti* alignment of the hydroxy groups. Next, we investigated the reduction of the azide moiety which should be followed by cleavage of the acetate protecting groups and ozonolysis in order to generate the target compounds. However, we found that compounds **5a–c** easily underwent 1,4-additions in the presence of nucleophiles or were decomposed under basic conditions. In this respect, DL-dithiothreitol/diisopropylamine (DTT/DIPA), DIBALH and $NaBH_4$/MeOH failed to furnish the desired reduction products. Treatment with Pd/H_2, PPh_3, $P(OMe)_3$ or $SnCl_2$ on the other hand resulted in no or only very low conversion. Thus, we decided to change the reaction sequence. Consequently, we performed the acetate cleavage as the first step, since direct ozonolysis of compounds **5a** and **5c** again resulted in decomposition. Deacetylation in a methanolic HCl solution proved to be most efficient and the subsequent ozonolysis generated sugar azides **6a–c** (Scheme 2).

It turned out to be essential to perform the acidic acetate cleavage of compounds **5a–c** under strictly dry conditions, since even small amounts of water promoted an intramolecular Michael addition, leading to the formation of highly substituted tetrahydrofuran derivatives of the C-glycoside type [31].

Next, we investigated the azide reduction of compounds **6a–c** under different reaction conditions. Unfortunately DTT/DIPA, thioacetic acid, tributylphosphine/H_2O and H_2/Pd followed by *N*-acetylation with *N*-acetoxyphthalimide did not afford products **8a–c** in acceptable yields and/or purity. Since compounds **8a–c** could not be purified by conventional silica gel chromatography we decided to perform an additional acetylation step in order to avoid reversed-phase HPLC and to maintain our procedure as simple as possible. Hence, compounds **6a–c** were acetylated under standard conditions, subsequently reduced with DTT/DIPA and *N*-acetylated to yield compounds **7a–c** which could be easily purified. Final treatment with sodium methoxide in dry methanol then furnished the neat title compounds **8a–c**.

The configurations of compounds **6**, **7** and **8** were determined by applying various NMR methods. Since the stereochemistry at C-4 is given by the starting material, configurations of C-2

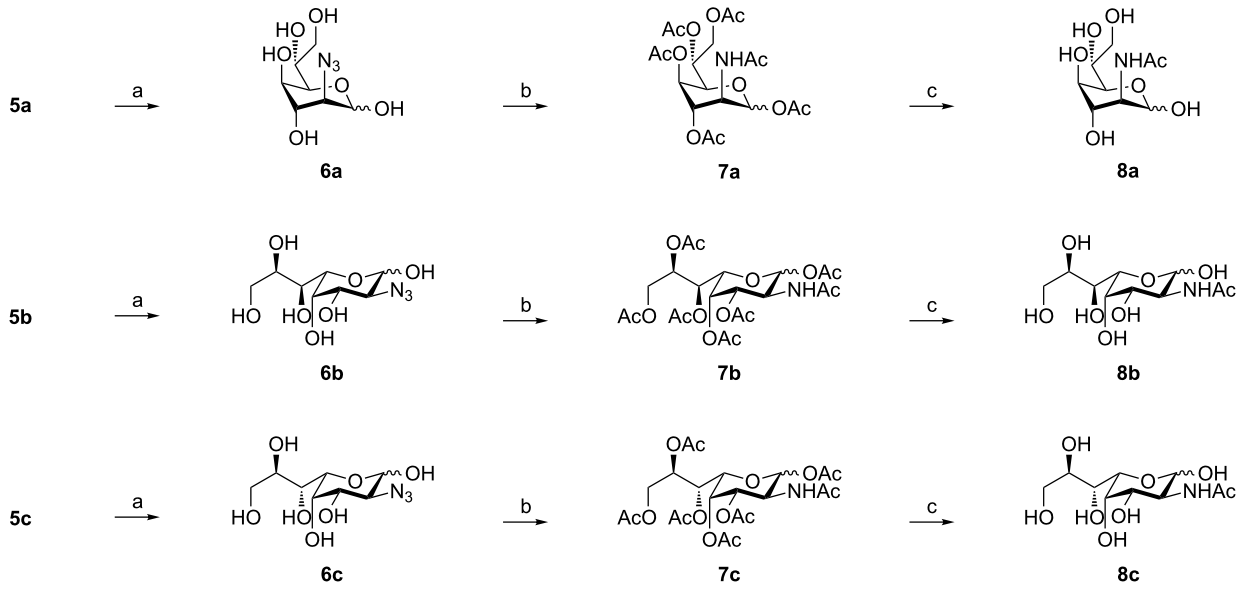

Scheme 2: Deprotection sequence; reagents and conditions: (a): HCl/MeOH, rt, 16–24 h, then MeOH, CH_2Cl_2, O_3, −78 °C then PPh_3, rt, 16 h, 71–82%, 2 steps; (b): Ac_2O/pyridine, DMAP, rt, 16 h then CH_3CN, DTT, DIPA, rt, 2 h, then Ac_2O/pyridine, DMAP, rt, 16 h, 59–66%, 3 steps; (c): NaOMe/MeOH, rt, 2–3 h, quant.

and C-3 can be easily deduced from the magnitude of the respective $^3J_{H,H}$ coupling constants which reflect the torsion angles between these groups (Table 2).

Table 2: Characteristic coupling constants of compounds **7a–c**.

Compound	$^3J_{1,2}$ [Hz]	$^3J_{2,3}$ [Hz]	$^3J_{3,4}$ [Hz]	$^3J_{4,5}$ [Hz]
7a-α[a]	1.8	3.1	3.1	1.9
7a-β[a]	2.1	2.9	2.9	1.8
7b-α	3.7	11.5	3.3	0.9
7b-β	9.0	11.3	3.5	1.1
7c-α	3.7	11.6	3.3	1.0
7c-β	8.8	11.1	3.3	0.5

[a] $^4C_1$-pyranoid form.

Therefore, the anticipated configuration of the final products could be verified. Since compounds **6a** and **8a** were found to exist as complex mixtures of conformers, only anomeric signals were assigned. This finding is in agreement with the fact that *ido*-configurated pyranose derivatives are known to adopt multiple conformations [32-34]. We were able to isolate and fully assign four distinct forms of the acetylated monosaccharide derivative **7a** (β-furanoid, $^4C_1$ α/β-pyranoid and $^1C_4$ α-pyranoid). Although **7a** is a known compound [15], the published NMR data are scarce. Herein, we provide the complete NMR data sets of 2-acetamido-1,3,4,6,7-penta-*O*-acetyl-2-deoxy-D-glycero-D-*ido*-heptose (**7a**). In the cases of compounds **6b**, **6c**, **7b**, **7c** and **8b** only α,β-pyranoid forms were detected (see copies of NMR spectra provided in Supporting Information File 1). However, NMR spectra of **8c** showed minor amounts of a compound which we considered to be its corresponding furanoid form. Unfortunately, we were not able to confirm this hypothesis owing to the very low concentration of this compound.

Conclusion

In summary, we developed a simple, highly versatile route for the synthesis of rare, 2-amino-functionalized heptoses and octoses. The indium-mediated allylation strategy again revealed to be a useful tool for the preparation of two-carbon chain elongated carbohydrates. Two new stereocenters were formed with high diastereoselectivity in the course of the synthesis owing to the use of a chiral L-proline derived epoxidation catalyst. The introduction of nitrogen was achieved via a Tsuji–Trost-like azide opening of allylic epoxides. Although global deprotection proved to be cumbersome, we were able to develop a versatile reaction sequence to overcome this problem. The desired higher aminosugars were obtained in an overall yield of 21–29% over 7 steps. Additionally, these compounds should now be available in all stereochemical combinations by means of varying the starting materials, the epoxidation catalysts, or the mode of azide opening, respectively [35]. Furthermore, biologically active octodioses are now accessible from compounds **7b** and **7c**, which is subject of ongoing research.

Supporting Information

Supporting Information File 1

Experimental section, spectral data and copies of ^1H and ^{13}C NMR spectra of compounds **2**–**8**.
[http://www.beilstein-journals.org/bjoc/content/supplementary/1860-5397-10-231-S1.pdf]

References

1. Li, C.-J.; Chan, T.-H. *Tetrahedron* **1999,** *55,* 11149–11176. doi:10.1016/S0040-4020(99)00641-9
2. Araki, S.; Hirashita, T. *Indium in Organic Synthesis*. In *Main Group Metals in Organic Synthesis;* Yamamoto, H.; Oshima, K., Eds.; Wiley-VCH Verlag GmbH & Co. KGaA: Weinheim, Germany, 2005.
3. Augé, J.; Lubin-Germain, N.; Uziel, J. *Synthesis* **2007,** 1739–1764. doi:10.1055/s-2007-983703
4. Chan, T.-H.; Li, C.-J. *J. Chem. Soc., Chem. Commun.* **1992,** 747–748. doi:10.1039/c39920000747
5. Gao, J.; Härter, R.; Gordon, D. M.; Whitesides, G. M. *J. Org. Chem.* **1994,** *59,* 3714–3715. doi:10.1021/jo00092a040
6. Prenner, R. H.; Binder, W. H.; Schmid, W. *Liebigs Ann. Chem.* **1994,** 73–78. doi:10.1002/jlac.199419940113
7. Schmölzer, C.; Fischer, M.; Schmid, W. *Eur. J. Org. Chem.* **2010,** 4886–4892. doi:10.1002/ejoc.201000623
8. Lee, Y. J.; Kubota, A.; Ishiwata, A.; Ito, Y. *Tetrahedron Lett.* **2011,** *52,* 418–421. doi:10.1016/j.tetlet.2010.11.078
9. Weise, G.; Drews, G.; Jann, B.; Jann, K. *Arch. Microbiol.* **1970,** *71,* 89–98.
10. Steinmetz, H. J.; Schwochau, K. Technetium complexes, processes for the preparation thereof and application kits for the formation of technetium complexes. Ger. Patent 4,128,181, Feb 29, 1996.
11. Gonzáles, F. G.; Guillen, M. G.; Pérez, J. A. G.; Galán, E. R. *Carbohydr. Res.* **1980,** *78,* 17–23. doi:10.1016/S0008-6215(00)83656-3
12. Pérez, J. A. G.; Albarrán, J. C. P.; Galán, E. R. *Carbohydr. Res.* **1983,** *114,* 158–163. doi:10.1016/0008-6215(83)88182-8
13. Perez, J. A. G.; Caballero, R. B.; Ventula, A. C. *Carbohydr. Res.* **1985,** *143,* 129–141. doi:10.1016/S0008-6215(00)90702-X
14. Avalos, M.; Babiano, R.; Cintas, P.; Jiménez, J. L.; Palacios, J. C.; Valencia, C. *Tetrahedron* **1993,** *49,* 2676–2690. doi:10.1016/S0040-4020(01)86345-6
15. Perez, J. A. G.; Corraliza, R. M. P.; Galan, E. R.; Guillen, M. G. *An. Quim. (1968–1979)* **1979,** *75,* 387–391.
16. Kuhn, R.; Kirschenlohr, W. *Angew. Chem.* **1955,** *67,* 786. doi:10.1002/ange.19550672405
17. Albarran, J. C. P.; Galan, E. R.; Perez, J. A. G. *Carbohydr. Res.* **1985,** *143,* 117–128. doi:10.1016/S0008-6215(00)90701-8
18. Deloisy, S.; Kunz, H. *Tetrahedron Lett.* **1998,** *39,* 791–794. doi:10.1016/S0040-4039(97)10720-1

19. Matt, T.; Ng, C. L.; Lang, K.; Sha, S.-H.; Akbergenov, R.; Shcherbakov, D.; Meyer, M.; Duscha, S.; Xie, J.; Dubbaka, S. R.; Perez-Fernandez, D.; Vasella, A.; Ramakrishnan, V.; Schacht, J.; Böttger, E. C. *Proc. Natl. Acad. Sci. U. S. A.* **2012,** *109,* 10984–10989. doi:10.1073/pnas.1204073109
20. Tatsuta, K.; Akimoto, K.; Takahashi, H.; Hamatsu, T.; Annaka, M.; Kinoshita, M. *Tetrahedron Lett.* **1983,** *24,* 4867–4870. doi:10.1016/S0040-4039(00)94028-0
21. Martin, O. R.; Szarek, W. A. *Carbohydr. Res.* **1984,** *130,* 195–219. doi:10.1016/0008-6215(84)85280-5
22. Fair, R. J.; Hensler, M. E.; Thienphrapa, W.; Dam, Q. N.; Nizet, V.; Tor, Y. *ChemMedChem* **2012,** *7,* 1237–1244. doi:10.1002/cmdc.201200150
23. Marigo, M.; Franzén, J.; Poulsen, T. B.; Zhuang, W.; Jørgensen, K. A. *J. Am. Chem. Soc.* **2005,** *127,* 6964–6965. doi:10.1021/ja051808s
24. Zhao, G.-L.; Ibrahem, I.; Sundén, H.; Córdova, A. *Adv. Synth. Catal.* **2007,** *349,* 1210–1224. doi:10.1002/adsc.200600529
25. Jensen, K. L.; Dickmeiss, G.; Jiang, H.; Albrecht, L.; Jørgensen, K. A. *Acc. Chem. Res.* **2012,** *45,* 248–264. doi:10.1021/ar200149w
26. Kanth, J. V. B.; Periasamy, M. *Tetrahedron* **1993,** *49,* 5127–5132. doi:10.1016/S0040-4020(01)81877-9
27. Trost, B. M.; Bunt, R. C.; Lemoine, R. C.; Calkins, T. L. *J. Am. Chem. Soc.* **2000,** *122,* 5968–5976. doi:10.1021/ja000547d
28. Trost, B. M.; Jiang, C.; Hammer, K. *Synthesis* **2005,** 3335–3345. doi:10.1055/s-2005-918443
29. Trost, B. M.; Horne, D. B.; Woltering, M. J. *Chem. – Eur. J.* **2006,** *12,* 6607–6620. doi:10.1002/chem.200600202
30. Miyashita, M.; Mizutani, T.; Tadano, G.; Iwata, Y.; Miyazawa, M.; Tanino, K. *Angew. Chem., Int. Ed.* **2005,** *44,* 5094–5097. doi:10.1002/anie.200500838
31. The structure of prepared C-glycosides was determined by NMR, mass and IR spectroscopy although the final proof for the stereochemistry of these compounds is a matter of ongoing research.
32. Bhacca, N. S.; Horton, D.; Paulsen, H. *J. Org. Chem.* **1968,** *33,* 2484–2487. doi:10.1021/jo01270a068
33. Horita, D. A.; Hajduk, P. J.; Lerner, L. E. *Glycoconjugate J.* **1997,** *14,* 691–696. doi:10.1023/A:1018561215401
34. Kräutler, V.; Müller, M.; Hünenberger, P. H. *Carbohydr. Res.* **2007,** *342,* 2097–2124. doi:10.1016/j.carres.2007.05.011
35. Righi, G.; Manni, L. S.; Bovicelli, P.; Pelagalli, R. *Tetrahedron Lett.* **2011,** *52,* 3895–3896. doi:10.1016/j.tetlet.2011.05.085

License and Terms

The definitive version of this article is the electronic one which can be found at:
doi:10.3762/bjoc.10.231

BEILSTEIN JOURNAL OF ORGANIC CHEMISTRY

Expanding the scope of cyclopropene reporters for the detection of metabolically engineered glycoproteins by Diels–Alder reactions

Anne-Katrin Späte[1], Verena F. Schart[1], Julia Häfner[2], Andrea Niederwieser[1], Thomas U. Mayer[2] and Valentin Wittmann[*1,§]

Full Research Paper

Open Access

Address:
[1]University of Konstanz, Department of Chemistry and Konstanz Research School Chemical Biology (KoRS-CB), Universitätsstraße 10, 78457 Konstanz, Germany and [2]University of Konstanz, Department of Biology and Konstanz Research School Chemical Biology (KoRS-CB), Universitätsstraße 10, 78457 Konstanz, Germany

Email:
Valentin Wittmann[*] - mail@valentin-wittmann.de

* Corresponding author
§ Phone: +49-7531-884572, Fax: +49-7531-884573

Keywords:
bioorthogonal chemistry; carbohydrates; cyclopropenes; inverse-electron-demand Diels-Alder reactions; metabolic oligosaccharide engineering

Beilstein J. Org. Chem. **2014,** *10,* 2235–2242.
doi:10.3762/bjoc.10.232

Received: 20 May 2014
Accepted: 01 September 2014
Published: 22 September 2014

This article is part of the Thematic Series "Multivalent glycosystems for nanoscience".

Guest Editor: A. Casnati

Abstract

Monitoring glycoconjugates has been tremendously facilitated by the development of metabolic oligosaccharide engineering. Recently, the inverse-electron-demand Diels–Alder reaction between methylcyclopropene tags and tetrazines has become a popular ligation reaction due to the small size and high reactivity of cyclopropene tags. Attaching the cyclopropene tag to mannosamine via a carbamate linkage has made the reaction even more efficient. Here, we expand the application of cyclopropene tags to *N*-acyl-galactosamine and *N*-acylglucosamine derivatives enabling the visualization of mucin-type O-glycoproteins and O-GlcNAcylated proteins through Diels–Alder chemistry. Whereas the previously reported cyclopropene-labeled *N*-acylmannosamine derivative leads to significantly higher fluorescence staining of cell-surface glycoconjugates, the glucosamine derivative gave higher labeling efficiency with protein preparations containing also intracellular proteins.

Introduction

The glycan chains of glycoproteins and lipids have been shown to be involved in numerous biological recognition and regulation events [1]. Glycan research, especially the visualization of glycoconjugates in vitro and in vivo, has significantly profited from the recent developments in the area of metabolic oligosaccharide engineering (MOE) and the chemical reporter strategy [2-4]. In this approach, functional groups with a unique reactivity are incorporated into glycoconjugates via the cell's

biosynthetic machinery and are subsequently reacted in bioorthogonal labeling reactions that allow visualization [5,6]. Whereas in the first report on glycan labeling by this approach the ketone–hydrazide ligation was employed [7], later investigations mainly relied on the Staudinger ligation [8] and azide–alkyne [3 + 2] cycloaddition (copper-catalyzed [9,10] or strain-promoted [11,12]). Since the initial reports from 2008 [13-15], more and more laboratories successfully employ the inverse-electron-demand Diels–Alder (DAinv) reaction as a bioorthogonal ligation reaction for different applications [16-18]. In the meantime, the DAinv reaction has also found application in MOE, and several dienophiles, such as terminal alkenes [19], isonitriles [20,21], and cyclopropenes [22-24], have been incorporated in carbohydrate derivatives and detected by reaction with 1,2,4,5-tetrazines [25] (Scheme 1). An important advantage of the DAinv reaction is the fact that it can be orthogonal to the azide–alkyne cycloaddition [22,26,27] which allows dual labeling of two different sugars within one experiment [19,21,23,24].

Among the dienophiles mentioned above, strained cyclopropenes have the highest reaction rates for DAinv reactions with tetrazines and are small enough to be accepted by cellular enzymes during MOE [22-24]. Also, they are stable in aqueous solution in the presence of biological nucleophiles [22,28]. Consequently, cyclopropene tags were attached by an amide linkage to sialic acid [22] and ManNAc derivatives including Ac_4ManNCyc (**4**) [23] (Figure 1) to label sialic acid residues on the surface of living cells via MOE. Since carbamate-linked methylcyclopropenes have significantly higher reaction rates in DAinv reactions with tetrazines [22,28], we recently introduced Ac_4ManNCyoc (**3**) as a derivative for rapid labeling of metabolically engineered cell-surface sialic acids [24]. The application of **3** was prompted by the previous observation that carbamate-modified ManNAc derivatives are also accepted in the biosynthetic pathway [19,29]. Derivative **3** in combination with a sulfo-Cy3-tetrazine conjugate enabled dual sugar labeling by simultaneous DAinv reaction and strain-promoted azide–alkyne cycloaddition in a single step [24]. The potential of Ac_4ManNCyoc (**3**) for labeling of sialoglycoconjugates was also recognized by others [30]. Sialic acids are prominently positioned at the outer end of membrane glycoproteins which makes them well-accessible for labeling reactions [31]. However it has become of increasing interest to also investigate intracellular glycoproteins. We, thus, developed the glucosamine and galactosamine derivatives Ac_4GlcNCyoc (**1**) and Ac_4GalNCyoc (**2**) which are expected to be incorporated into O-GlcNAcylated proteins and mucin-type *O*-glycans [30]. Here, we show that **1** and **2** can be employed for both labeling of cell-

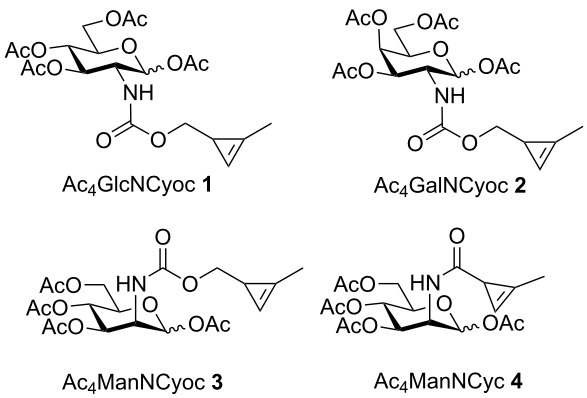

Figure 1: Hexosamine derivatives with cyclopropene tags. Cyoc = (2-methylcycloprop-2-en-1-yl)methoxycarbonyl, Cyc = 2-methylcycloprop-2-ene-1-carbonyl.

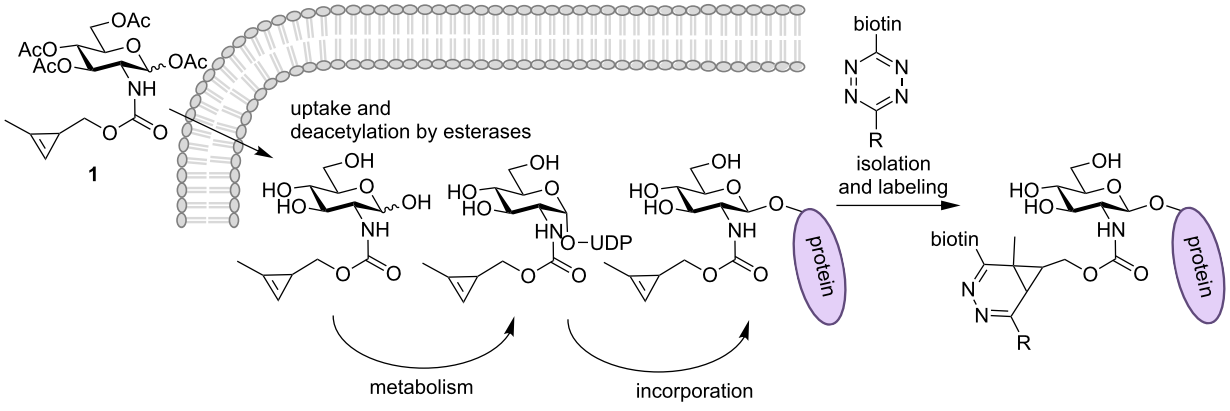

Scheme 1: Principle of MOE with Ac_4GlcNCyoc (**1**) and subsequent ligation by a DAinv reaction: The chemically modified sugar is fed to cells, taken up by the cells and deacetylated by non-specific esterases. The monosaccharide is metabolized and incorporated into glycoproteins (i.e., O-GlcNAcylated proteins). Subsequently, a ligation reaction is performed to visualize the glycan.

surface glycoconjugates (detected by confocal fluorescence microscopy) and isolated glycoproteins (detected by Western blot).

Results and Discussion

For the synthesis of the cyclopropene-tagged sugars **1** and **2** we neutralized the corresponding hexosamine hydrochlorides **5** and **6** with sodium methoxide and coupled them to the activated cyclopropene **7** (Scheme 2), the synthesis of which we reported previously [24]. Subsequent acetylation of the carbamates **8** and **9** gave Ac_4GlcNCyoc (**1**) and Ac_4GalNCyoc (**2**).

With the cyclopropene-modified hexosamines in hand we first investigated their metabolic incorporation into cell-surface glycoconjugates of HEK 293T cells. The cells were incubated for 48 h with **1**, **2**, **3**, or solvent control (phosphate buffered saline, PBS) and then reacted with Tz–biotin **10** [19], followed by labeling with streptavidin–AlexaFluor647 (streptavidin–AF647) (Scheme 3). With all three sugars staining of the plasma membrane was detected by confocal laser scanning microscopy of living cells (Figure 2A, B, C). Only the solvent control did not show any membrane staining (Figure 2D, for additional experiments see Figure S1, Supporting Information File 1). Brightfield images were recorded to check the cell morphology. These experiments show that all three cyclopropene derivatives **1**, **2**, and **3** are accepted by the cell's biosynthetic machinery. However, membrane staining resulting from metabolized Ac_4ManNCyoc (**3**) was significantly more intense than staining after cultivation with Ac_4GlcNCyoc (**1**) or Ac_4GalNCyoc (**2**). Similar experiments were carried out with HeLa S3 cells (Figure S2, Supporting Information File 1). Again, Ac_4ManNCyoc (**3**) gave the most intensive and Ac_4GlcNCyoc (**1**) only weak staining. The staining intensity resulting from the galactosamine derivative **2** was in between. Previous work from Bertozzi and coworkers suggests that GlcNAc derivatives such as *N*-azidoacetylglucosamine (GlcNAz) can only enter cell-surface glycans via less efficient conversion of GlcNAz to *N*-azidoacetylmannosamine (ManNAz) and subsequently to the corresponding sialic acid [32,33] following a metabolic pathway known also for the natural sugars [34]. Also, the efficiency by which non-natural GlcNAc and GalNAc derivatives are metabolized is dependent on the type of modification and the cell line. These findings might provide an explanation for the reduced staining intensities obtained with sugars **1** and **2**.

We also performed a Western blot analysis of proteins isolated from HeLa S3 cells that had been cultured in the presence of cyclopropene-labeled hexosamines **1**, **2**, or **3**, or with PBS (solvent control). Cells were harvested, lysed and the lysate was cleared by centrifugation resulting in a mixture of intracellular and membrane proteins. In the cleared lysate we performed a DAinv reaction with Tz–biotin **10**. Visualization of glycoproteins was achieved by immunoblotting for biotin, and equal protein loading was verified by blotting against tubulin (Figure 3). All three investigated sugars resulted in labeled protein bands. In this case, samples from cells treated with Ac_4GlcNCyoc (**1**) produced a significantly higher signal compared to cells treated with Ac_4GalNCyoc (**2**) or Ac_4ManNCyoc (**3**). Similar trends were also observed with Jurkat cells by Prescher and coworkers [30]. Since O-GlcNAcylation is a modification primarily found for cytosolic and nuclear proteins [35] and the sample preparation includes the fraction of intracellular proteins, these results suggest that Ac_4GlcNCyoc (**1**) is suitable to target O-GlcNAcylated proteins.

Conclusion

In summary, we have shown that cyclopropene-labeled hexosamine derivatives Ac_4GlcNCyoc (**1**) and Ac_4GalNCyoc (**2**) can be used to monitor glycosylation of both cell-surface glycoconjugates and isolated, soluble glycoproteins. Whereas Ac_4ManNCyoc (**3**) leads to significantly higher fluorescence staining of cell-surface glycoconjugates, Ac_4GlcNCyoc (**1**) gave higher labeling efficiency with protein preparations containing also intracellular proteins, possibly by targeting

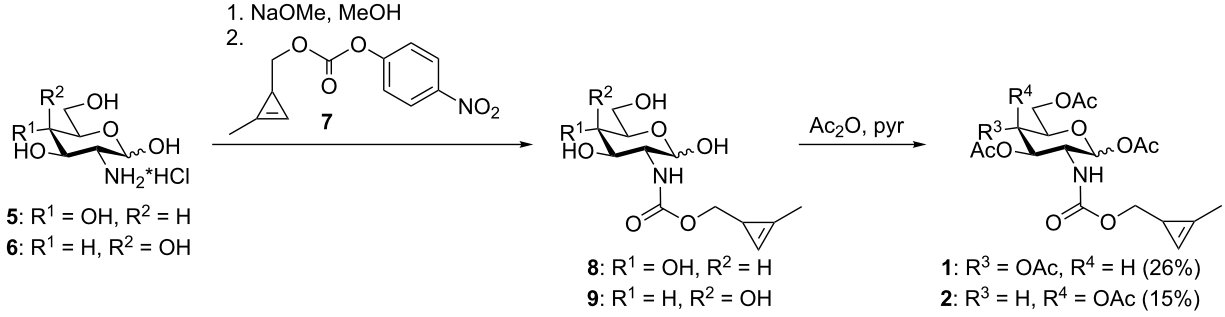

Scheme 2: Synthesis of the cyclopropene-modified hexosamine derivatives **1** and **2**.

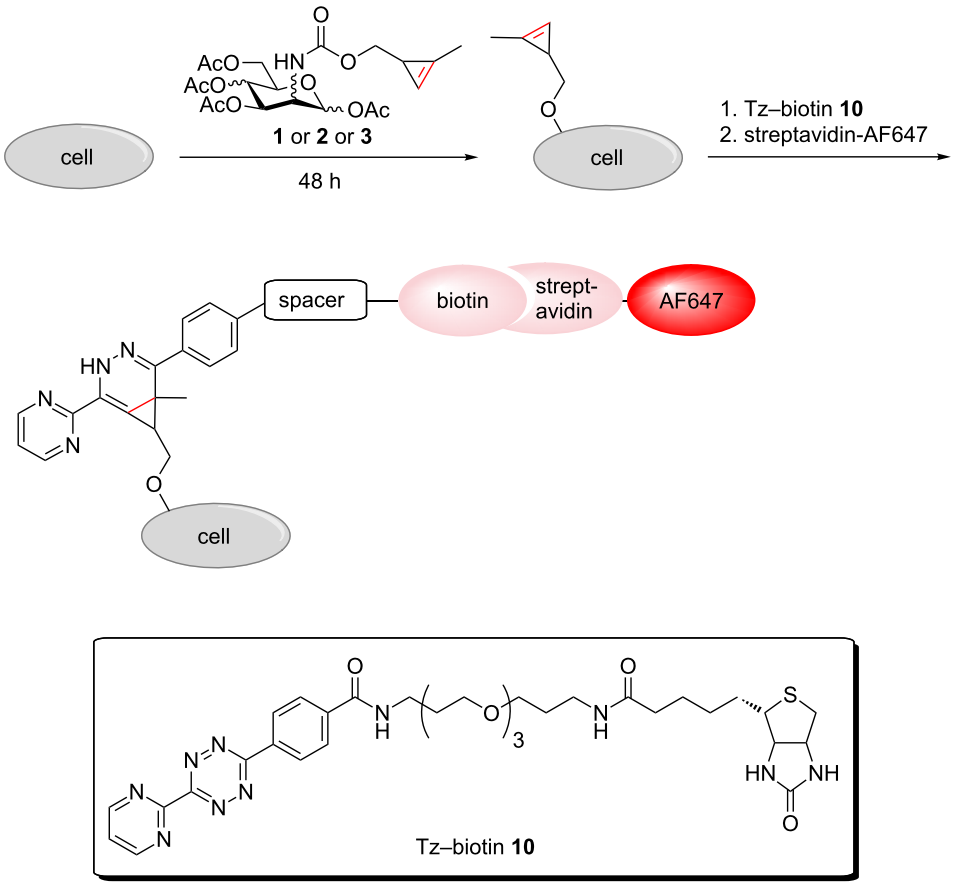

Scheme 3: Labeling strategy for metabolically incorporated monosaccharides.

O-GlcN-acylated proteins. Since O-GlcN-acylation of proteins is associated with numerous crucial biological events, **1** represents a promising probe for future glycomics studies. Of special interest is the fact that cyclopropene tags can be combined with azide–alkyne cycloaddition to achieve dual labeling of two different (sugar) moieties as was shown earlier [19,21,23,24,30].

Experimental

General methods. All chemicals were purchased from Aldrich, Fluka, Dextra, and Carbosynth and used without further purification. AlexaFluor-labeled streptavidin and Hoechst33342 were purchased from Invitrogen. Technical solvents were distilled prior to use. All reactions were carried out in dry solvents. Reactions were monitored by TLC on silica gel 60 F254 (Merck) with detection by UV light ($\lambda = 254$ nm). Additionally, acidic ethanolic *p*-anisaldehyde solution or basic $KMnO_4$ solution followed by gentle heating was used for visualization. Preparative flash column chromatography (FC) was performed with an MPLC-Reveleris system from Grace. Nuclear magnetic resonance (NMR) spectra were recorded at room temperature on Avance III 400 and Avance III 600 instruments from Bruker. Chemical shifts are reported relative to solvent signals ($CDCl_3$: $\delta_H = 7.26$ ppm, $\delta_C = 77.16$ ppm). Signals were assigned by first-order analysis and, when feasible, assignments were supported by two-dimensional $^1H,^1H$ and $^1H,^{13}C$ correlation spectroscopy (COSY, HMBC and HSQC). HRMS mass spectra were obtained with a micrOTOF II instrument from Bruker Daltonics. Semi-preparative high performance liquid chromatography (HPLC) was conducted on a LC-20A prominence system (pumps LC-20AT, auto sampler SIL-20A, column oven CTO-20AC, diode array detector SPD-M20A, ELSD-LT II detector, controller CBM-20A and software LC-solution) from Shimadzu under the following conditions. Column: Kinetex 5U C18 100A Axia from Phenomenex (250 × 21.2 mm); flow: 9 mL min^{-1}; mobile phase: gradient of acetonitrile with 0.1% formic acid (solvent A) in water with 0.1% formic acid (solvent B). Microscopy was performed using a point laser scanning

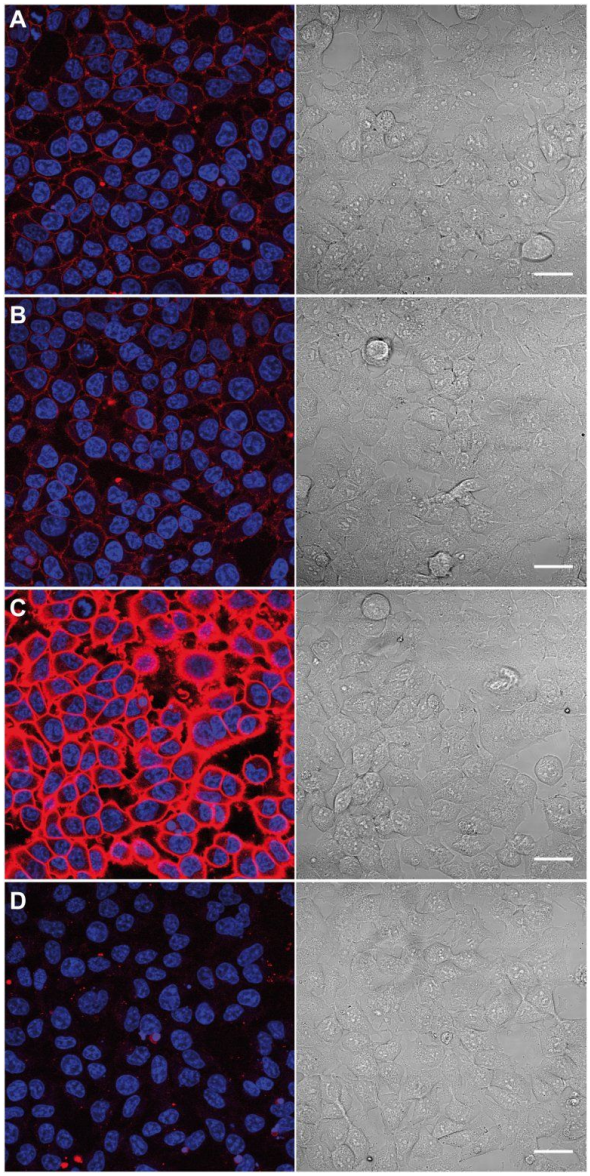

Figure 2: Labeling of metabolically engineered cell-surface glycoconjugates. HEK 293T cells were grown for 48 h with 50 μM Ac_4GlcNCyoc (**1**, A), 50 μM Ac_4GalNCyoc (**2**, B), 50 μM Ac_4ManNCyoc (**3**, C), or with PBS (solvent control, D) and subsequently incubated with Tz–biotin **10** (1 mM, 1 h, 37 °C) followed by incubation with streptavidin–AF647. Nuclei were stained with Hoechst33342. Scale bar: 30 μm.

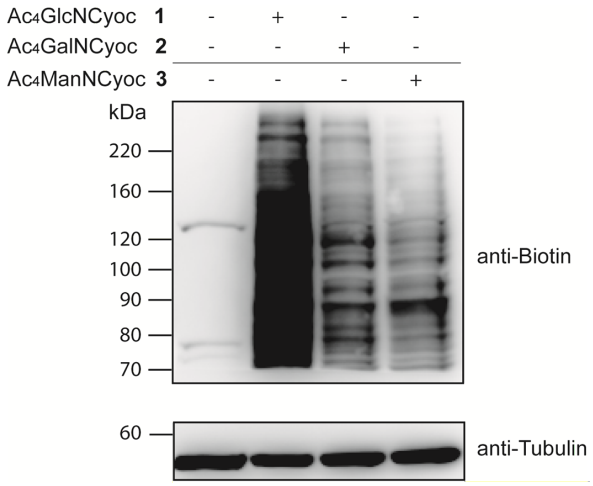

Figure 3: Western blot analysis of soluble glycoproteins. HeLa S3 cells were grown for 48 h with 100 μM cyclopropene-labeled sugar (Ac_4GlcNCyoc (**1**), Ac_4GalNCyoc (**2**), or Ac_4ManNCyoc (**3**)) or with PBS (solvent control), lysed, and the cleared lysate was reacted with Tz–biotin **10** (150 μM, 90 min, rt). Proteins were immunoblotted for biotin and tubulin (loading control). Protein bands visible in the first lane can be explained either by non-specific binding of the anti-biotin antibody or by the occurrence of naturally biotinylated proteins.

confocal microscope Zeiss LSM 510 Meta equipped with a Meta detector for spectral imaging.

The synthesis of **1** and **2** was carried out as described for the synthesis of Ac_4ManNCyoc (**3**) [24].

1,3,4,6-Tetra-*O*-acetyl-2-deoxy-2-((2-methylcycloprop-2-en-1-yl)methoxycarbonylamino)-D-glucopyranose (Ac_4GlcNCyoc, 1). To a solution of glucosamine hydrochloride (**5,** 2 g, 9.2 mmol) in MeOH (20 mL) NaOMe (18 mL of a 0.5 M solution in MeOH, 9.2 mmol) was added under nitrogen. After stirring for 90 min at room temperature, the solution was added to activated cyclopropene **7** (2 g, 9.7 mmol). After stirring for 48 h at room temperature the solvent was evaporated under reduced pressure. The residue was dissolved in pyridine (20 mL) and acetic anhydride (10 mL) was added. After stirring for 24 h at room temperature additional 5 mL acetic anhydride were added to complete the acetylation. After additional 24 h the solvents were evaporated under reduced pressure. The residue was dissolved in CH_2Cl_2 (250 mL), washed with 10 % aq $KHSO_4$ (200 mL), satd aq $NaHCO_3$ (200 mL) and brine (200 mL). The organic layer was dried ($MgSO_4$) and the solvent was evaporated under reduced pressure. The residue was purified by FC (silica, petroleum ether/ethyl acetate 10:1) to afford Ac_4GlcNCyoc (**1**) as a mixture of anomers (1.08 g, 2.36 mmol, 26%). R_f = 0.36 (petroleum ether/ethyl acetate 1:1); HRMS *m/z*: [M + Na]$^+$ calcd for $C_{20}H_{27}NO_{11}$, 480.14763; found, 480.14511.

Further purification by semi-preparative HPLC (45% A for 10 min, then 45–70% A for 15 min) allowed separation of the anomers. Retention time β-anomer: 15 min, α-anomer: 17.2 min.

α-Anomer: ^{1}H NMR (400 MHz, $CDCl_3$) δ 6.53 (s, 1H, =CH), 6.19 (d, *J* = 3.5 Hz, 1H, H-1), 5.31–5.12 (m, 2H, H-3, H-4),

4.75 (d, J = 9.1 Hz, 1H, NH), 4.25 (dd, J = 12.3, 3.1 Hz, 1H, H-6a), 4.18 (td, J = 10.2, 3.3 Hz, 1H, H-2), 4.05 (dd, J = 12.5, 2.0 Hz, 1H, H-6b), 4.02–3.96 (m, 1H, H-5), 3.96–3.85 (m, 2H, CH_2), 2.18 (s, 3H, OAc), 2.10 (s, 3H, CH_3), 2.07 (s, 3H, OAc), 2.04 (s, 3H, OAc), 2.03 (s, 3H, OAc), 1.59 (s, 1H, C*H*CH_2) ppm; ^{13}C NMR (101 MHz, $CDCl_3$) δ 171.4 (C=O), 170.8 (C=O), 169.3 (C=O), 168.8 (C=O), 156.1 (HNC=O), 120.5, 102.1, 102.0, 91.0 (C-1), 73.1, 73.0, 70.8 (C-3 or C-5), 69.8 (C-3 or C-5), 67.8 (C-4), 61.7 (C-6), 52.9(C-2), 21.0 (OAc), 20.8 (OAc), 20.7 (OAc), 17.22 (CH_2*C*H), 17.18 (CH_2*C*H), 11.70 (=C*C*H_3) ppm.

β-Anomer: ^{1}H NMR (400 MHz, $CDCl_3$) δ 6.53 (s, 1H, =CH), 5.70 (dd, J = 8.7, 1H, H-1), 5.22–5.15 (m, 1H, H-3), 5.11 (t, J = 9.5, 9.5 Hz, 1H, H-4), 4.73 (d, J = 8.1 Hz, 1H, NH), 4.28 (dd, J = 12.4, 4.6 Hz, 1H, H-6a), 4.11 (dd, J = 12.4, 2.1 Hz, 1H, H-6b), 3.97–3.87 (m, 3H, H-2, CH_2), 3.81 (ddd, J = 9.8, 4.6, 2.2 Hz, 1H, H-5), 2.12 (s, 6H, CH_3, OAc), 2.08 (s, 3H, OAc), 2.04 (s, 3H, OAc), 2.03 (s, 3H, OAc), 1.61 (s, 1H, C*H*CH_2) ppm; ^{13}C NMR (101 MHz, $CDCl_3$) δ 170.8 (C=O), 169.5 (C=O), 156.3 (HNC=O), 120.64, 120.58, 102.10, 102.07, 92.8 (C-1), 76.8 (C-3 or C-5 or CH_2), 73.0 (C-3 or C-5 or CH_2), 72.5 (C-3 or C-5 or CH_2), 68.1 (C-4), 61.8 (C-6), 55.0 (C-2), 21.0 (OAc), 20.9 (OAc), 20.8 (OAc), 20.7 (OAc), 17.2 (CH_2*C*H), 11.74 (=C*C*H_3), 11.73 (=C*C*H_3) ppm.

1,3,4,6-Tetra-*O*-acetyl-2-deoxy-2-((2-methylcycloprop-2-en-1-yl)methoxycarbonylamino)-D-galactopyranose (Ac_4GalNCyoc 2). To a solution of galactosamine hydrochloride (**6**, 1.75 g, 8.11 mmol) in MeOH (18 mL) NaOMe (16 mL of a 0.5 M solution in MeOH, 8.06 mmol) was added under nitrogen. After stirring for 90 min at room temperature, the solution was added to activated cyclopropene **7** (1.75 g, 8.4 mmol). After stirring at room temperature overnight the solvent was evaporated under reduced pressure. The residue was dissolved in pyridine (18 mL) and acetic anhydride (9 mL) was added. After stirring for 40 h at room temperature the solvents were evaporated under reduced pressure. The residue was dissolved in CH_2Cl_2 (230 mL), washed with 10% aq $KHSO_4$ (100 mL), satd aq $NaHCO_3$ (180 mL) and brine (180 mL). The organic layer was dried ($MgSO_4$) and the solvent was evaporated under reduced pressure. The residue was purified by FC (silica, petroleum ether/ethyl acetate 1:1 –> 1:2) to afford Ac_4GalNCyoc (**2**) as a mixture of anomers (551 mg, 1.2 mmol, 15%). R_f = 0.33 (petroleum ether/ethyl acetate 1:1); HRMS *m/z*: $[M + Na]^+$ calcd for $C_{20}H_{27}NO_{11}$, 480.14763; found, 480.14551.

Further purification by HPLC (45% A for 10 min, then 45–70% A for 15 min) allowed purification of the β-anomer. Retention time β-anomer: 15 min, α-anomer: 16.5 min.

β-Anomer: ^{1}H NMR (400 MHz, $CDCl_3$) δ 6.54 (s, 1H, =CH), 5.72 (d, J = 8.7 Hz, 1H, H-1), 5.39 (dd, J = 3.6, 1.1 Hz, 1H, H-4), 5.10 (ddq, J = 11.4, 3.4, 1.4 Hz, 1H, H-3), 4.61–4.48 (m, 1H, NH), 4.14 (qd, J = 11.3, 6.6 Hz, 3H, H-2, H-6), 4.02 (td, J = 6.5, 1.0 Hz, 1H, H-5), 3.93 (d, J = 5.2 Hz, 2H, CH_2), 2.16 (s, 3H, OAc), 2.14 (s, 3H, OAc), 2.12 (s, 3H, CH_3), 2.04 (s, 3H, OAc), 2.02 (s, 3H, OAc), 1.61 (d, J = 5.6 Hz, 1H, C*H*CH_2) ppm; ^{13}C NMR (151 MHz, $CDCl_3$) δ (ppm) 170.5 (2 C=O), 170.3 (C=O), 169.5 (C=O), 156.4 (HNC=O), 120.64, 120.55, 102.14, 102.07, 93.1 (C-1), 73.0 (CH_2), 71.9 (C-5), 70.4 (C-3), 66.6 (C-4), 61.4 (C-6), 51.5 (C-2), 21.0 (OAc), 20.9 (OAc), 20.8 (OAc), 20.8 (OAc), 17.21 (CH_2*C*H), 17.23 (CH_2*C*H), 11.8 (=C*C*H_3) ppm.

Cell growth conditions. As described in [24] HEK 293T and HeLa S3 cells were grown in Dulbecco's Modified Eagle's Medium (DMEM) supplemented with 5% FBS, 100 units mL^{-1} penicillin and 100 μg mL^{-1} streptomycin. All cells were incubated in a 5% carbon dioxide, water saturated incubator at 37 °C.

Fluorescence microscopy with Tz–biotin 10. HEK 293T cells (22,000 cells/cm^2) were seeded in 4-well ibiTreat μ-Slides (ibidi) coated with fibronectin (25 μg mL^{-1}) and poly-L-lysine (0.01%, 1 h, 37 °C). After 12 h cells were incubated for 48 h with 50 μM cyclopropene-labeled sugar (Ac_4GlcNCyoc (**1**), Ac_4GalNCyoc (**2**), or Ac_4ManNCyoc (**3**)). The sugars were prepared as stock solutions (0.36 mM) in PBS and diluted into media. Only PBS was added as solvent control. Cells were washed two times with PBS and then treated with Tz–biotin **10** [19] (1 mM) for 1–3 h at 37 °C. After two washes with PBS, cells were incubated with Streptavidin–AF647 (6.6 μg mL^{-1}) and Hoechst33342 (10 μg mL^{-1}) for 20 minutes at room temperature in the dark. Cells were washed twice with PBS, and DMEM was added for microscopy. A Zeiss LSM 510 Meta equipped with a 40 × 1.3 NA Plan-Neofluar oil DIC immersion objective was employed for imaging. Analysis of the obtained data was performed using Image J software version 1.45 S.2.

Western blot analysis. HeLa S3 cells were seeded (900,000 cells/10 cm dish) and after 16 h the media were exchanged with media containing 100 μM of cyclopropene-labeled sugar (Ac_4GlcNCyoc (**1**), Ac_4GalNCyoc (**2**), or Ac_4ManNCyoc (**3**)). Sugars were diluted from a 0.36 mM stock solution in PBS. As a solvent control PBS was added instead of the sugar stock solution. The cells were cultured for 48 h with or without the additional sugar. Cells were trypsinated and re-suspended in PBS (10 mL) and pelleted by centrifugation (5 min, 400*g*). The supernatant was discarded and the pellet re-suspended in PBS (1 mL) and pelleted by centrifugation (5 min, 400*g*). The cells were lysed in lysis buffer (400 μL)

containing Triton X-100 (0.5%) (for permeabilization of membranes and solubilization of proteins and to prevent aggregate formation), DNase (30 μg mL^{-1}), RNase (30 μg mL^{-1}), β-glycerophosphate (20 mM) (Ser/Thr phosphatase inhibitor), sodium fluoride (20 mM) (Ser/Thr phosphatase inhibitor), sodium orthovandadate (0.3 mM) (inhibitor for ATPase, tyrosine and alkaline phosphatases), complete X protease inhibitor (Roche) (1X), NaCl (300 mM), TrisHCl pH 7.4 (25 mM), EDTA (5 mM) (to chelate metal ions and reduce oxidation damage), *O*-(2-acetamido-2-deoxy-D-glucopyranosylidenamino) *N*-phenylcarbamate (PUGNAc) (Sigma-Aldrich) (100 μM) (O-GlcNAc-β-*N*-acetylglucosaminidase inhibitor to maintain O-GlcNAcylation during lysis) and incubated at 4 °C for 30 min. The lysate was cleared by centrifugation (22,000*g*, 30 min, rt). Tz–biotin **10** was added to the cleared supernatant to a final concentration of 150 μM. The samples were incubated for 90 min at rt, 3× SDS-sample buffer was added, and the sample was boiled at 90 °C for 15 min. Proteins were separated by SDS-polyacrylamide gel electrophoresis using 10% polyacrylamide gels and transferred to nitrocellulose membranes (BioRad). Transfer efficiency was analyzed with Ponceau S staining. The membranes were blocked in milk (5% in PBS-T) for 1 h at rt, followed by incubation with anti-biotin antibody (Abnova, Anti-Biotin mAb clone SB58c, 1:2000 dilution in milk) at 4 °C overnight or anti-alpha-tubulin antibody (AA4.3, hypridoma supernatant in 1% FCS, 1:200 dilution in milk) for 1 h at rt. The membranes were washed (3 times, 10–15 min, PBS-T), incubated with secondary horseradish-peroxidase-conjugated anti-mouse antibody (Dianova, goat anti-mouse IgG (H+L)-HRP, 1:50000 dilution in milk, 1 h, rt), and washed again (3 times, 10–15 min, PBS-T). Blots were developed by an ECL detection system (clarity Western ECL substrate, BioRad) and visualised with a CCD camera (Raytest-1000, Fujifilm).

Supporting Information

Additional MOE experiments and ^{1}H and ^{13}C NMR spectra of Ac_4GlcNCyoc (**1**) and Ac_4GalNCyoc (**2**).

Supporting Information File 1

Additional MOE experiments and NMR spectra.
[http://www.beilstein-journals.org/bjoc/content/supplementary/1860-5397-10-232-S1.pdf]

Acknowledgements

This work was supported by the Deutsche Forschungsgemeinschaft (SFB 969), the University of Konstanz, and the Konstanz Research School Chemical Biology. We thank Rebecca Faißt, Jessica Pfotzer, and Verena Goldbach for synthesis of cyclopropene derivatives and the Bioimaging Center of the University of Konstanz for providing the fluorescence microscopy instrumentation.

References

1. Varki, A.; Cummings, R. D.; Esko, J. D.; Freeze, H. H.; Stanley, P.; Bertozzi, C. R.; Hart, G. W.; Etzler, M. E., Eds. *Essentials of Glycobiology,* 2nd ed.; Cold Spring Harbor Laboratory Press: Cold Spring Harbor, NY, 2009.
2. Keppler, O. T.; Horstkorte, R.; Pawlita, M.; Schmidt, C.; Reutter, W. *Glycobiology* **2001,** *11,* 11R–18R. doi:10.1093/glycob/11.2.11R
3. Dube, D. H.; Bertozzi, C. R. *Curr. Opin. Chem. Biol.* **2003,** *7,* 616–625. doi:10.1016/j.cbpa.2003.08.006
4. Prescher, J. A.; Bertozzi, C. R. *Cell* **2006,** *126,* 851–854. doi:10.1016/j.cell.2006.08.017
5. Sletten, E. M.; Bertozzi, C. R. *Angew. Chem., Int. Ed.* **2009,** *48,* 6974–6998. doi:10.1002/anie.200900942
6. Hackenberger, C. P. R.; Schwarzer, D. *Angew. Chem., Int. Ed.* **2008,** *47,* 10030–10074. doi:10.1002/anie.200801313
7. Mahal, L. K.; Yarema, K. J.; Bertozzi, C. R. *Science* **1997,** *276,* 1125–1128. doi:10.1126/science.276.5315.1125
8. Saxon, E.; Bertozzi, C. R. *Science* **2000,** *287,* 2007–2010. doi:10.1126/science.287.5460.2007
9. Tornøe, C. W.; Christensen, C.; Meldal, M. *J. Org. Chem.* **2002,** *67,* 3057–3064. doi:10.1021/jo011148j
10. Rostovtsev, V. V.; Green, L. G.; Fokin, V. V.; Sharpless, K. B. *Angew. Chem., Int. Ed.* **2002,** *41,* 2596–2599. doi:10.1002/1521-3773(20020715)41:14<2596::AID-ANIE2596>3.0.CO;2-4
11. Agard, N. J.; Prescher, J. A.; Bertozzi, C. R. *J. Am. Chem. Soc.* **2004,** *126,* 15046–15047. doi:10.1021/ja044996f
12. Ning, X.; Guo, J.; Wolfert, M. A.; Boons, G.-J. *Angew. Chem., Int. Ed.* **2008,** *47,* 2253–2255. doi:10.1002/anie.200705456
13. Braun, K.; Wiessler, M.; Ehemann, V.; Pipkorn, R.; Spring, H.; Debus, J.; Didinger, B.; Koch, M.; Muller, G.; Waldeck, W. *Drug Des., Dev. Ther.* **2008,** *2,* 289–301. doi:10.2147/DDDT.S3572
14. Blackman, M. L.; Royzen, M.; Fox, J. M. *J. Am. Chem. Soc.* **2008,** *130,* 13518–13519. doi:10.1021/ja8053805
15. Devaraj, N. K.; Weissleder, R.; Hilderbrand, S. A. *Bioconjugate Chem.* **2008,** *19,* 2297–2299. doi:10.1021/bc8004446
16. Knall, A.-C.; Slugovc, C. *Chem. Soc. Rev.* **2013,** *42,* 5131–5142. doi:10.1039/c3cs60049a
17. Šečkutė, J.; Devaraj, N. K. *Curr. Opin. Chem. Biol.* **2013,** *17,* 761–767. doi:10.1016/j.cbpa.2013.08.004
18. Beckmann, H. S. G.; Niederwieser, A.; Wiessler, M.; Wittmann, V. *Chem. – Eur. J.* **2012,** *18,* 6548–6554. doi:10.1002/chem.201200382
19. Niederwieser, A.; Späte, A.-K.; Nguyen, L. D.; Jüngst, C.; Reutter, W.; Wittmann, V. *Angew. Chem., Int. Ed.* **2013,** *52,* 4265–4268. doi:10.1002/anie.201208991
20. Stairs, S.; Neves, A. A.; Stöckmann, H.; Wainman, Y. A.; Ireland-Zecchini, H.; Brindle, K. M.; Leeper, F. J. *ChemBioChem* **2013,** *14,* 1063–1067. doi:10.1002/cbic.201300130
21. Wainman, Y. A.; Neves, A. A.; Stairs, S.; Stöckmann, H.; Ireland-Zecchini, H.; Brindle, K. M.; Leeper, F. J. *Org. Biomol. Chem.* **2013,** *11,* 7297–7300. doi:10.1039/c3ob41805g
22. Patterson, D. M.; Nazarova, L. A.; Xie, B.; Kamber, D. N.; Prescher, J. A. *J. Am. Chem. Soc.* **2012,** *134,* 18638–18643. doi:10.1021/ja3060436

23. Cole, C. M.; Yang, J.; Šečkutė, J.; Devaraj, N. K. *ChemBioChem* **2013,** *14,* 205–208. doi:10.1002/cbic.201200719
24. Späte, A.-K.; Bußkamp, H.; Niederwieser, A.; Schart, V. F.; Marx, A.; Wittmann, V. *Bioconjugate Chem.* **2014,** *25,* 147–154. doi:10.1021/bc4004487
25. Sauer, J.; Heldmann, D. K.; Hetzenegger, J.; Krauthan, J.; Sichert, H.; Schuster, J. *Eur. J. Org. Chem.* **1998,** 2885–2896. doi:10.1002/(SICI)1099-0690(199812)1998:12<2885::AID-EJOC2885>3.0.CO;2-L
26. Karver, M. R.; Weissleder, R.; Hilderbrand, S. A. *Angew. Chem., Int. Ed.* **2012,** *51,* 920–922. doi:10.1002/anie.201104389
27. Willems, L. I.; Li, N.; Florea, B. I.; Ruben, M.; van der Marel, G. A.; Overkleeft, H. S. *Angew. Chem., Int. Ed.* **2012,** *51,* 4431–4434. doi:10.1002/anie.201200923
28. Yang, J.; Šečkutė, J.; Cole, C. M.; Devaraj, N. K. *Angew. Chem., Int. Ed.* **2012,** *51,* 7476–7479. doi:10.1002/anie.201202122
29. Bateman, L. A.; Zaro, B. W.; Chuh, K. N.; Pratt, M. R. *Chem. Commun.* **2013,** *49,* 4328–4330. doi:10.1039/c2cc37963e
30. Patterson, D. M.; Jones, K. A.; Prescher, J. A. *Mol. BioSyst.* **2014,** *10,* 1693–1697. doi:10.1039/C4MB00092G
This report was published during the preparation of the current manuscript.
31. Du, J.; Meledeo, M. A.; Wang, Z.; Khanna, H. S.; Paruchuri, V. D. P.; Yarema, K. J. *Glycobiology* **2009,** *19,* 1382–1401. doi:10.1093/glycob/cwp115
32. Saxon, E.; Luchansky, S. J.; Hang, H. C.; Yu, C.; Lee, S. C.; Bertozzi, C. R. *J. Am. Chem. Soc.* **2002,** *124,* 14893–14902. doi:10.1021/ja027748x
33. Vocadlo, D. J.; Hang, H. C.; Kim, E.-J.; Hanover, J. A.; Bertozzi, C. R. *Proc. Natl. Acad. Sci. U. S. A.* **2003,** *100,* 9116–9121. doi:10.1073/pnas.1632821100
34. Hinderlich, S.; Stäsche, R.; Zeitler, R.; Reutter, W. *J. Biol. Chem.* **1997,** *272,* 24313–24318. doi:10.1074/jbc.272.39.24313
35. Hart, G. W.; Housley, M. P.; Slawson, C. *Nature* **2007,** *446,* 1017–1022. doi:10.1038/nature05815

License and Terms

BEILSTEIN JOURNAL OF ORGANIC CHEMISTRY

Synthesis and immunological evaluation of protein conjugates of *Neisseria meningitidis* X capsular polysaccharide fragments

Laura Morelli[1], Damiano Cancogni[1], Marta Tontini[2], Alberto Nilo[2], Sara Filippini[2], Paolo Costantino[2], Maria Rosaria Romano[2], Francesco Berti[2], Roberto Adamo[*2] and Luigi Lay[*1]

Full Research Paper

Open Access

Address:
[1]Dipartimento di Chimica and ISTM-CNR, Universita degli Studi di Milano, via Golgi 19, I-20133 Milano, Italy and [2]Novartis Vaccines, Via Fiorentina 1, 53100 Siena, Italy

Email:
Roberto Adamo[*] - roberto.adamo@novartis.com; Luigi Lay[*] - luigi.lay@unimi.it

* Corresponding author

Keywords:
carbohydrates; glycoconjugates; immunology; multivalent glycosystems *Neisseria meningitidis*; vaccines

Beilstein J. Org. Chem. **2014,** *10,* 2367–2376.
doi:10.3762/bjoc.10.247

Received: 09 May 2014
Accepted: 18 September 2014
Published: 13 October 2014

This article is part of the Thematic Series "Multivalent glycosystems for nanoscience".

Guest Editor: R. Pieters

Abstract

A vaccine to prevent infections from the emerging *Neisseria meningitidis* X (MenX) is becoming an urgent issue. Recently MenX capsular polysaccharide (CPS) fragments conjugated to CRM_{197} as carrier protein have been confirmed at preclinical stage as promising candidates for vaccine development. However, more insights about the minimal epitope required for the immunological activity of MenX CPS are needed. We report herein the chemical conjugation of fully synthetic MenX CPS oligomers (monomer, dimer, and trimer) to CRM_{197}. Moreover, improvements in some crucial steps leading to the synthesis of MenX CPS fragments are described. Following immunization with the obtained neoglycoconjugates, the conjugated trimer was demonstrated as the minimal fragment possessing immunogenic activity, even though significantly lower than a pentadecamer obtained from the native polymer and conjugated to the same protein. This finding suggests that oligomers longer than three repeating units are possibly needed to mimic the activity of the native polysaccharide.

Introduction

Neisseria meningitidis is an encapsulated, aerobic gram-negative diplococcus which causes significant morbidity and mortality in newborns, children and young adults worldwide through meningitis and/or septicemia. Although sporadic cases occur in Europe and North America, major meningitis epidemics have been recorded in Africa, in an area termed “the meningitis belt”, extending from Senegal to Ethiopia and including 21 countries with a population of over 300 million

people. According to the chemical composition of the bacterial capsular polysaccharide (CPS) [1], 13 serogroups of *N. meningitidis* have been so far defined. Until recently only five of them (A, B, C, Y, W135) were associated with significant pathogenic potential [2,3]. In particular serogroup A (MenA), that caused significant meningitis outbreaks in industrialised countries until the 1970s [4], is currently a major responsible for epidemics in the African meningitis belt. Additionally, since 2002 serogroup W135 has also been considered a major threat. In the past 20 years sporadic cases or clusters of meningitis due to other *N. meningitidis* serogroups have emerged. While the impact of infections caused by serogroup X of *N. meningitidis* (MenX) was initially considered negligible, in the last decade incidence rates and disease characteristics very similar to other virulent meningococcal isolates have been reported. As a matter of fact, the meningitis cases ascribed to MenX do not present any clinical or epidemiological differences to those due to serogroup A. Most cases (93%) were recorded during the dry season, with a mean age of the patients of 9.2 years and a fatality rate of 11.9% [5]. MenX was first described in the 1960s [6], when it was found to cause a few cases of invasive disease across North America, Europe, Asia and Africa [7]. The first case of MenX disease in Africa was documented in 1974 and, since then, several sporadic cases have been observed in other African countries [8]. In 2006, the occurrence in Niger of MenX related meningitis infections with unprecedented incidence led the World Health Organization (WHO) to consider MenX as a substantial threat [9]. However, it was only in 2010 that, following a very large MenX outbreak in Burkina Faso, the WHO-Inter-country Support Team (WHO-IST) weekly bulletins on meningitis started to specifically document MenX epidemics [10]. Interestingly, while MenA incidence decreased in most meningitis belt countries following the introduction in 2010 of a monovalent MenA conjugate vaccine (MenAfriVac) [11,12], an increase in MenX cases has been observed. Recently a study revealed that in Burkina Faso the levels of MenX carriage after the introduction of the MenA conjugate vaccine are significantly higher than they were before the vaccine introduction [13]. This could suggest a serotype replacement due to mass vaccination with MenAfriVac, although this event should be considered unlikely on the basis of previous experiences with the introduction of the MenC conjugate vaccine [14]. Undoubtedly the recent increase of MenX infections has led to take in consideration this emerging serogroup for the development of new meningococcal vaccines [15,16]. Recently it has been reported that coupling long chain oligosaccharides from MenX CPS to the nontoxic mutant of diphtheria toxin Cross-Reacting Material 197 (CRM_{197}), a protein widely used in manufactured vaccines,[17] provides a potent candidate for the development of a glycoconjugate vaccine against this serogroup [18].

MenX CPS is a homopolymer of (1→4)-linked 2-acetamido-2-deoxy-α-D-glucopyranosyl phosphate residues (Figure 1). The synthesis of the repeating unit was first reported in 1974 [19], and more recently an improved protocol for larger scale preparation of the monomer as analytical tool has been also described [20]. Notably, the minimal CPS portion which can confer protection against meningococcal infections is still unknown.

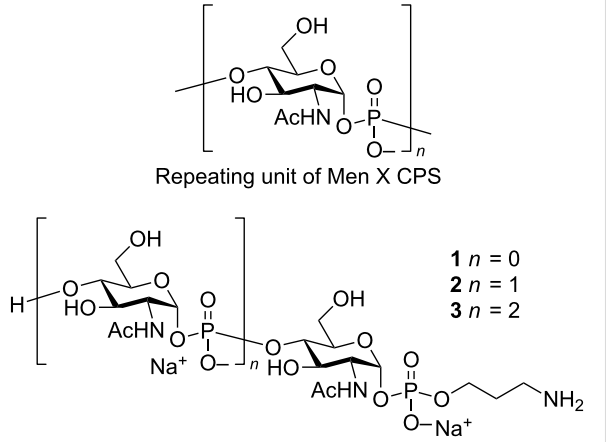

Figure 1: Structures of the repeating unit of MenX CPS and synthetic oligomers **1–3**.

Over the recent years, advances in the synthesis of complex glycans are rendering accessible a variety of carbohydrate antigens with well-defined chemical structure and devoid of bacterial contaminations which could derive from purification of biological materials [21-24]. This could be a crucial feature to improve batch-to-batch consistency in vaccine manufacturing and to confer a better safety profile.

Some of us have recently achieved the first synthesis of short-chain MenX CPS oligomers (compounds **1**–**3**, Figure 1) provided with a phosphodiester-linked aminopropyl spacer suitable for their conjugation to a carrier protein [25].

These synthetic molecules are valuable tools to obtain information on the minimal structural requirements for the immunological activity of MenX CPS and for evaluation as vaccine candidates. In the present work we report the preparation and in vivo immunological evaluation of neo-glycoconjugates from the fragments **1**–**3.** In this context, we describe the significant improvements recently achieved in some crucial steps of our previously reported synthesis [25] that will render more expeditious the preparation of this type of oligomers.

The synthetic oligomers **1**–**3** were conjugated to the surface abundant lysine residues of the carrier protein CRM_{197} by

means of the di(*N*-succinimidyl) adipate (SIDEA) linker. We have already shown that this spacer, which is used in commercial anti-meningococcal vaccines for the feature of being immuno-silent, can be efficiently utilized for the conjugation of short synthetic antigens bearing an amino spacer [26,27]. The synthesized CRM_{197} glycoconjugates were first tested for their capability of eliciting anti MenX CPS antibodies in mice. The functional activity of the generated antibodies was then assessed by the in vitro bactericidal assay recently developed for the evaluation of MenX CPS conjugates [18].

Results and Discussion

Improvements in α-H-phosphonate synthesis

Our previous synthesis of oligomers **1**–**3** featured the use of 2-azido-2-deoxy glucopyranosyl building blocks and their corresponding glycosyl hydrogenphosphonates (H-phosphonates) intermediates for the installation of the phosphodiester linkages [28].

We were confident that the use of the non-participating and electron-withdrawing azido group could strongly enhance the stability of the anomeric phosphodiester linkages. However, we experienced a dramatic drop of the overall yield during the conversion of the azido groups in acetamides on protected glycosyl phosphosaccharide intermediates [25].

We therefore sought to design a different strategy based on GlcNAc instead of azido glucose building blocks, where the azide reduction is rather performed at an early stage of the synthetic route than on valuable advanced intermediates. Accordingly, the azide reduction with $NiCl_2/NaBH_4$ protocol [29] occurred smoothly on the previously described [25] silyl glycoside **4**, and after standard N-acetylation furnished acetamide **5** in high yield (Scheme 1).

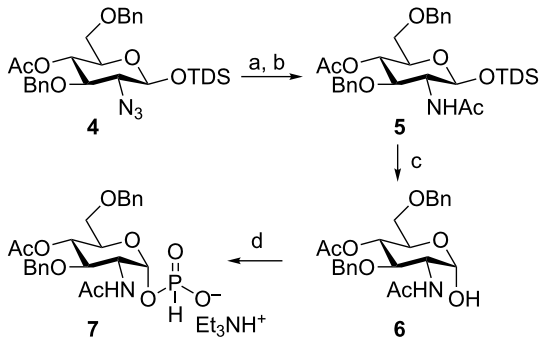

Scheme 1: Reagents and conditions: a) $NiCl_2/NaBH_4$, MeOH; b) Ac_2O, 86% over 2 steps; c) TBAF, THF, −40 °C to rt, 81%; d) salicylchlorophosphite, pyridine, then 1M triethylammonium hydrogencarbonate buffer solution (TEAB): Batch 62% yield; MRT 76% yield. TDS: Thexyldimethylsilyl.

On the other hand, the same reaction carried out on protected glycosyl phosphosaccharides afforded the corresponding acetamides in 25–35% yield [25]. Interestingly, when compound **5** was subjected to 1-O-desilylation with tetrabutylammonium fluoride in THF at –40 °C, we obtained exclusively the α-hemiacetal **6** in 81% yield (Scheme 1). The formation of the α anomer was confirmed by the doublet of H-1 at 5.23 ppm in the ^1H NMR spectrum with the typical value of $^1J_{1,2}$ = 3.5 Hz, and the appearance of the C-1 signal at 92.0 ppm in the ^{13}C NMR spectrum (see Supporting Information File 1).

Most importantly, when the hemiacetal **6** was treated with salicylchlorophosphite in pyridine at room temperature the α-H-phosphonate **7** was obtained as a single anomer in only 2 h in 62% yield. We reasoned that the occurrence of an intramolecular hydrogen bond involving the acetamido group could be the main responsible for the high selectivity observed in the formation of compound **6** and, consequently, for the attainment of the pure α-H-phosphonate **7**. Indeed, the desilylation of the 2-azido counterpart of intermediate **5** provided a mixture of anomers. On the other hand, the same reaction carried out on a 2-acetamido derivative very similar to **5** but protected as a 4,6-*O*-benzylidene acetal also led to an anomeric mixture, suggesting that conformational factors might be also involved. In addition, the treatment of this mixture with salicylchlorophosphite produced a mixture of anomeric H-phosphonates, indicating that no equilibration of the anomers occurs during this reaction. We, therefore, ascribed the high stereoselectivity observed in the formation of compound **7** to the stability of compound **6**, whose configuration is preserved during the reaction with salicylchlorophosphite. This finding introduced a great improvement in our reported synthesis of MenX CPS oligomers, since in the previous protocol extremely long reaction times (6–7 days) were needed for the exclusive formation of the most thermodynamically stable α-H-phosphonate by equilibration in the presence of H_3PO_3 of the initially formed mixture of anomeric H-phosphonates [25]. An additional improvement in α-H-phosphonate **7** formation was achieved by carrying out the reaction under microfluidic conditions. The Micro Reactor Technology (MRT) is gaining increasing attention for drug discovery. Some of its various possible advantages when compared to more conventional approaches are improved safety characteristics, enhanced rates of heat and mass transfer, simplicity and robustness in scale-up and easiness in handling the instrumentation [30-33]. For the synthesis of compound **7**, two distinct solutions containing the hemiacetal **6** in pyridine and salicylchlorophosphite in CH_3CN, respectively, were pumped in a 100 μL glass microreactor. The device was completed by a reservoir connected to the outlet of the microreactor, refilled with a solution of triethylammonium bicarbonate buffer (TEAB) 1.0 M to stabilize the H-phosphonate product.

Setting the residence time to 3 min, 46 mg of the α-H-phosphonate **7** were obtained in 0.5 h at higher isolated yield (76%) and purity than batch reaction. Based on the maximum volume of the syringes employed in our continuous-flow system (5 mL, see Supporting Information File 1), we can estimate that a production rate of 2.2 g/day would be achievable. To the best of our knowledge, this is the first example of the synthesis of glycosyl H-phosphonates using the continuous-flow MRT [30-33].

The occurrence of the H-phosphonate **7** was ascertained by a signal at 1.87 ppm in the ^{31}P NMR, and the presence in the ^{1}H NMR of the diagnostic doublet at 6.93 ppm with the characteristic value of $^{1}J_{H,P}$ = 631.8 Hz, typical of this class of compounds [34]. The α-configuration of the anomeric carbon was confirmed by a doublet of doublet at 5.53 ppm, with $^{1}J_{1,2}$ = 3.2 Hz, $^{1}J_{1,P}$ = 8.4 Hz (see Supporting Information File 1).

The benefit of the easy availability of the α-hemiacetal **6** was illustrated by the improved synthesis of the spacer-linked MenX monomer **1** (Scheme 2). The PivCl-mediated coupling of **6** with compound **8** [35,36] provided the glycosylphosphodiester **9** as a pure α-anomer, demonstrating the configurational stability of the hemiacetal under these reaction conditions. Compound **9** was subjected to Zemplén transesterification with NaOMe in methanol to afford alcohol **10**, and the hydrogenolytic removal of the remaining protective groups furnished the spacer-linked monomer **1** in excellent yield (Scheme 2).

Chemical synthesis of neo-glycoconjugates

Fragments **1**–**3**, obtained as previously reported [25], were employed as follows for the synthesis of the corresponding CRM_{197} conjugates. First the oligomers **1**–**3** were activated by reaction with an excess of SIDEA in the presence of triethylamine in DMSO (Scheme 3). The products were purified by precipitation from ethyl acetate, and after freeze-drying the half esters **11**–**13** were obtained at 49–65% yield. Of note, while we have utilized a similar procedure for fast and efficient insertion of the monoester of the immunosilent adipate linker onto a number of different length glycans [26,27], lower yields were attained in the present case. This can be explained with the higher solubility in organic solvents of the short structures **11**–**13** employed in the present study in comparison to other reported oligosaccharides [26,27], which did not allow complete precipitation of the activated oligomers. To increase the yield of this step, compounds **11**–**13** were recovered from the dimethylsulfoxide–ethyl acetate mixture by evaporation of ethyl acetate and addition of fresh ethyl acetate at 0 °C. The newly precipitated activated carbohydrates were freeze-dried and coupled to the protein. In this way, almost quantitative recovery of the activated sugars **11**–**13** was achieved.

Active esters **11**–**13** were then coupled with the amino groups of the protein in sodium phosphate buffer (100 mM NaPi, pH 7.2) at room temperature for 24 h (Scheme 3).

The glycoconjugates **14**–**16** were purified from the excess of unconjugated carbohydrate by precipitation with ammonium sulfate and reconstitution in 10 mM NaP_i pH 7.2. The occurrence of conjugation was assessed by SDS-PAGE (sodium dodecyl sulfate polyacrylamide gel electrophoresis) and MALDI–TOF mass spectrometry (see Supporting Information File 1). The latter analytical technique enabled determination of the saccharide/protein molar ratio (saccharide loading). The characteristics of the prepared glycoconjugates are summarized in Table 1.

A moderate loading (5–7 sugars/protein) was obtained in compounds **14**–**16** in respect to conjugates prepared by the same conjugation chemistry and different carbohydrate structures [26,27]. However, it needs to be taken in consideration that this loading is comparable to that achieved in the preparation of anti-meningococcal vaccines commercially available [37]. Furthermore, a number of 2.5 and 1.7–4.1 sugar moieties were incorporated in our positive control **17** and in the MenX CPS glycoconjugates recently reported to induce protective anti-

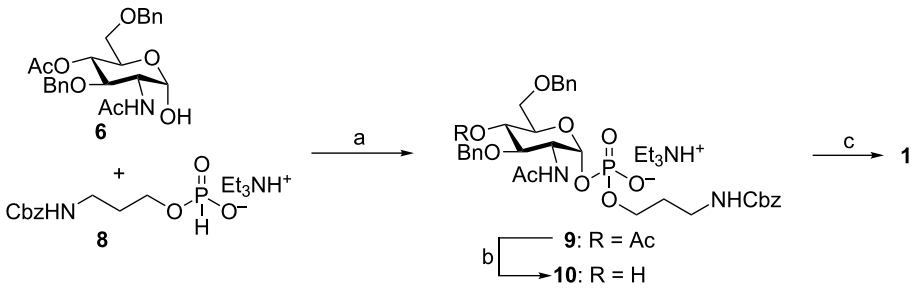

Scheme 2: Reagents and conditions: a) PivCl in pyridine, then I_2 in 19:1 pyridine/H_2O, then 1 M TEAB (45%); b) NaOMe, MeOH; c) H_2, Pd/C, MeOH/H_2O, then H_2O, Dowex 50W X8 resin (H^+ form), then Dowex 50W X8 resin (Na^+ form) (96% over two steps).

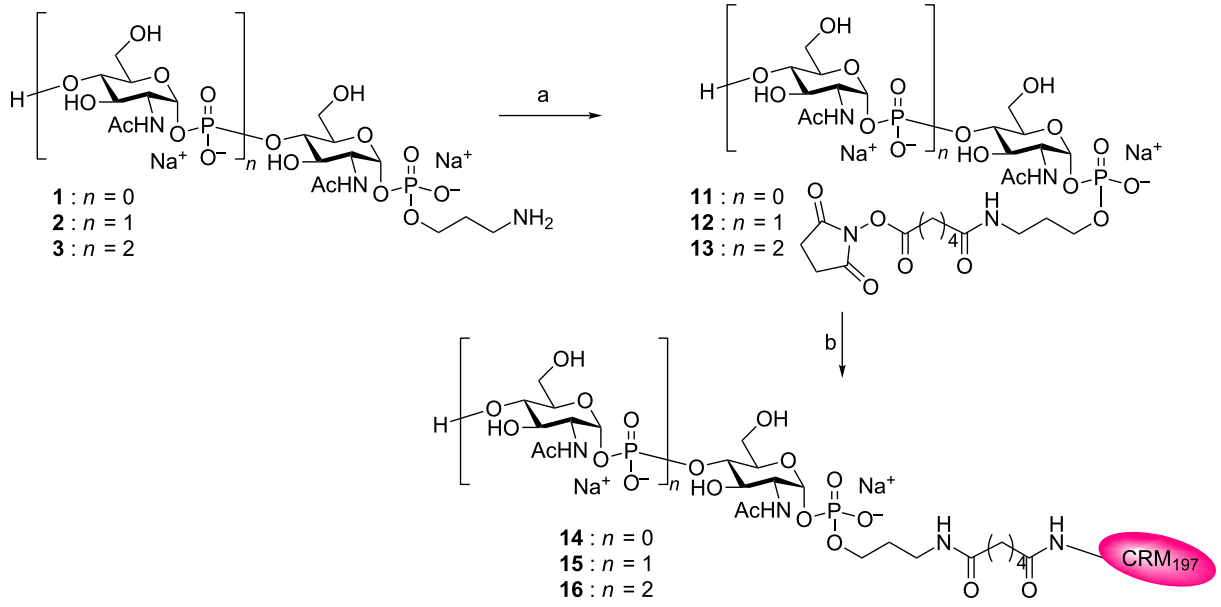

Scheme 3: Reagents and conditions: a) SIDEA, Et_3N, DMSO: **11** (64%), **12** (49%), **13** (51%); b) CRM_{197}, 100 mM NaP_i pH 7.2.

Table 1: Characteristics of the synthesized glycoconjugates.

Glyco conjugate	Activated ester/protein (mol/mol)[a]	Saccharide conjugation (mol/mol)[b]	MW (Da)	Loading efficiency %[a]
14	75:1	7	61523	9
15	75:1	4.5	61731	6
16	75:1	4.7	63256	6
MenXDP15CRM_{197} **17**	13:1	2.5	n.d.	19

[a]Mol of activated glycan: mol of protein used in the conjugation reaction. [b]Sugar:protein molar ratio determined by MALDI–TOF MS for **14**–**16**, and by HPAEC-PAD analysis for MenXDP15-CRM_{197} conjugate **17**.

bodies, respectively [18]. Thus, we deemed the loading of glycoconjugates **14**–**16** sufficient to determine in vivo their capability of eliciting anti-MenX CPS antibodies.

Immunological evaluation of CRM_{197} conjugates

To evaluate the immunogenicity of the synthesized glycoconjugates, groups of 8 BALB/c mice were immunized with three doses (two weeks apart) of 0.3 μg on saccharide base of the neo-glycoconjugates. The conjugated trimer **16** was also injected at 1 μg carbohydrate base dose to evaluate the effect of dose variation. The conjugates were formulated with aluminum phosphate, an adjuvant commonly used for vaccines in the market or in preclinical development [38]. As a control, the CRM_{197} conjugate with MenX fragments having an average degree of polymerization (avDP) of 15 (MenXDP15-CRM conjugate, compound **17**) was used at the saccharide base doses of 0.3 and 1 μg, respectively.

As shown in Figure 2, while the CRM_{197} conjugates of the monomer **1** and the dimer **2** did not induce polysaccharide specific IgG titers, the conjugated trimer **3** elicited anti-MenX CPS IgG titers, with no statistical difference (p 0.05) at the doses of 0.3 and 1 μg, respectively.

The MenXDP15 conjugate **17** also induced anti-MenX CPS antibodies that were comparable each other at the two different doses (p 0.05). However, the IgG levels induced by the trimer conjugate **16** at both 0.3 and 1 μg dose were significantly lower than those elicited by the conjugate **17** administered at the corresponding doses (p 0.0009 and 0.039 for 0.3 and 1 μg dose, respectively). Importantly, all the conjugates induced very low anti-MenX IgM titers, but the trimer **3** and the MenXDP15 antigens conjugated to the carrier enabled switching from IgM to IgG, which is characteristic of the T cell dependent response (for IgM levels see Supporting Information File 1).

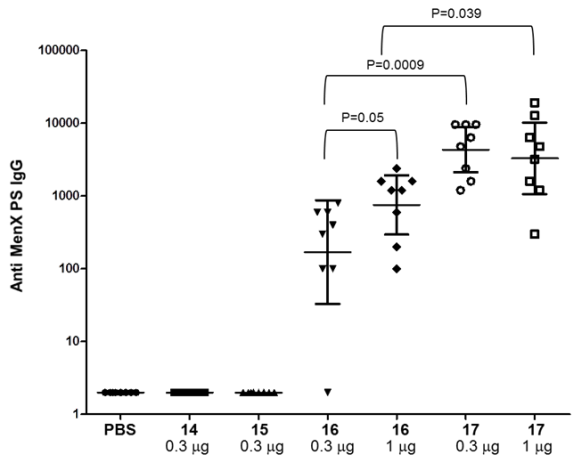

Figure 2: IgG levels detected at OD = 1 in individual post 3 sera (sera collected two weeks after the third immunization) of BALB/c mice immunization at 0.3 or 1 µg saccharide dose of antigen against MenX CPS as coating plate. Each dot represents individual mouse sera; horizontal bars indicate geometric mean titers (GMT) of each group with 95% statistical confidence intervals indicated by upper and lower bars.

Since the trimer **3**, among the set of conjugated synthetic oligomers, was the only structure capable of inducing IgG antibodies against the MenX CPS, we interrogated whether the sera from the three conjugated synthetic fragments were capable to recognize their own structures. To answer this question, conjugates with HSA were prepared with a similar protocol to that used for the formation of the CRM_{197} conjugates, except that a bis-succinimidyl ester penta-ethylene glycol ($BS(PEG)_5$) linker was used to rule out the interference of the spacer (details are reported in Supporting Information File 1). ELISA analysis using HSA conjugates as coating reagent demonstrated that the conjugated monomer **1** and the dimer **2** at the present dose elicited extremely low levels of antibodies against themselves and were, therefore, scarcely antigenic. By contrast, the trimer **3** was the only fragment which evoked a robust antibody production against its own structure (Figure 3A).

Surprisingly, when the trimer-HSA conjugate was used as coating reagent for the ELISA analysis (Figure 3B), sera elicited by the monomer **1** exhibited low anti-trimer antibodies, whereas sera induced by the conjugated dimer **2** and the trimer **3** possessed comparable levels of antibodies against the trisaccharide structure. The IgG levels raised by the trimer-CRM_{197} conjugate **16** were in turn significantly lower (p 0.0005) than those elicited by the MenXDP15-CRM_{197} conjugate **17**, where the trisaccharide is repeated multiple times. We hypothesize that the improved binding of antibodies induced by **14** and, primarily, by **15** to the coated trisaccharide conjugate rather than to **1**- and **2**-HSA conjugates, respectively, might be the result of a better exposition of monosaccharide and disaccharide MenX units in the context of the trimer-HSA

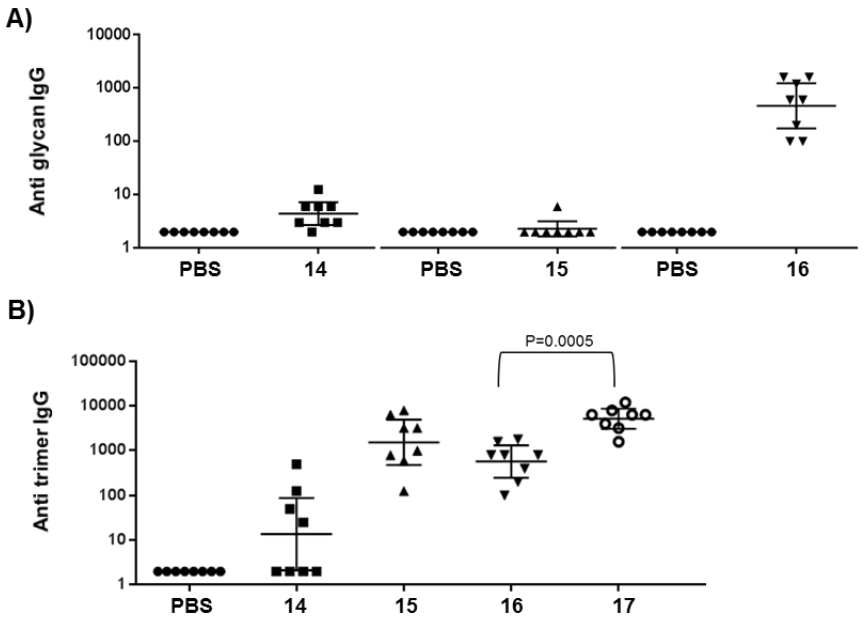

Figure 3: A) IgG levels detected at OD = 1 in individual post 3 sera of BALB/c mice immunization at 0.3 µg saccharide dose of antigen. A) Sera from conjugates **14**, **15** and **16** were tested against the monomer-, dimer- and trimer-HSA conjugate, respectively, presenting different linker and protein (see Supporting Information File 1). B) Comparison of anti trimer-HSA antibody levels in sera from conjugates **14**–**17**. Each point represents individual mouse sera; horizontal bars indicate geometric mean titers (GMT) of each group with 95% statistical confidence intervals indicated by upper and lower bars.

molecule, due presumably to conformational or spatial factors. However, this peculiar recognition was not observed when the native MenX CPS, which is the structure that best resembles the bacterial sugar surface and consequently of major interest for vaccine development, was used as coating reagent (Figure 2). Together, these evidences indicated that the trimer is the minimal antigenic portion of the polymer which is also capable of inducing antibodies recognizing epitopes of MenX CPS.

Next, the functionality of the induced antibodies was assessed by measuring the rabbit complement-mediated lysis of *N. meningitidis* [39]. This in vitro bactericidal assay is typically used to predict the effectiveness of anti-meningococcal vaccines [40,41]. Rabbit complement serum bactericidal assay (rSBA) titers were determined using pooled sera from mice immunized with the conjugated monomer **14**, dimer **15**, trimer **16** and MenXDP15 **17**. As it can be seen from Table 2, rSBA titers showed a trend similar to the measured ELISA IgG levels.

Table 2: rSBA titers of sera from immunized mice.

Sample	Antigen dose	Adjuvant	rSBA titer
PBS	-	Al phosphate	<16
14	0.3 μg	Al phosphate	<16
15	0.3 μg	Al phosphate	<16
16	0.3 μg	Al phosphate	512
16	1 μg	Al phosphate	512
MenXDP15-CRM_{197} **17**	0.3 μg	Al phosphate	8192
MenXDP15-CRM_{197} **17**	1 μg	Al phosphate	8192

Only pooled sera from mice immunized with the conjugated trimer **16** demonstrated to be functional, whereas compounds **14** and **15** did not exhibit any bactericidal activity. However, the rSBA titers of the trimer at 0.3 and 1 μg saccharide base doses were significantly lower (<10 fold in terms of titer) than MenXDP15-CRM_{197} conjugate **17** at the corresponding doses (512 and 8192, respectively).

To sum up, following conjugation to the carrier protein the chain of three repeating units constitutes the minimal antigenic structure of MenX polysaccharide, but its immunogenicity towards the native polysaccharide is lower than a medium size MenX CPS fragment (avDP 15) both in terms of IgG levels and functionality of the induced antibodies.

Conclusion

Serogroup X *N. meningitidis* is dramatically emerging among the causative agents of meningitis, particularly in Africa. Similarly to other serogroups, polysaccharide-based conjugates have been recently proposed as target molecules for the development of a vaccine with a broader coverage. We have undertaken the preparation of neo-glycoconjugates from fully synthetic MenX fragments in order to gain structural insights about minimal epitopes of this polysaccharide, and investigate the possibility of using synthetic pure and well-defined carbohydrates for the development of a glycoconjugate vaccine.

While, at the present dose and carbohydrate loading, conjugates of the synthetic MenX PS monomer and dimer with CRM_{197} were poorly antigenic, the conjugated trimer resulted in the minimal structure eliciting antibodies that can recognize both itself and epitopes of the native polysaccharide. Furthermore, these antibodies possess anti-meningococcal bactericidal activity towards serogroup X, although in less extent than a medium size native MenX CPS fragment (avDP 15).

This finding suggests that oligomers longer than three repeating units might be required to fully mimic the polysaccharide activity, and paves the ground for a deeper understanding of the structural requirements needed to develop a conjugate vaccine based on well-defined oligosaccharides attained by chemical synthesis. The preparation of these longer chain MenX fragments, based on the synthetic improvements and also the benefits of the continuous-flow microreactor technology herein described, is currently ongoing in our laboratory and it will be reported in due course. Besides the length of the carbohydrate haptens, the saccharide loading onto the protein is another key parameter which has been shown to deeply affect the immunogenicity of glycoconjugate vaccines [42,43]. In the present preliminary study, glycoconjugates with moderate loading were compared. It has been reported for other bacterial systems that the immunogenicity of short oligosaccharides can be enhanced by increasing the number of glycan antigens incorporated onto the carrier protein. The utilization of other conjugation chemistries enabling the achievement of higher carbohydrate loadings and the study of the effect of different glycan–protein ratios on glycoconjugates prepared from these short synthetic MenX fragments also deserve further exploration.

Experimental

General procedure for conjugation of fragments 1–3. This procedure is similar to that reported in reference [27]. The glycan (10 μmol) dissolved in DMSO (250 μL) containing triethylamine (25 equiv), was slowly dropped into a mixture of bis(*N*-succinimidyl) adipate (10 equiv) in DMSO (250 μL). After 3 hours under vigorous stirring, the activated oligosaccharide was purified by precipitation of the reaction mixture in nine volumes (9 mL) of ethyl acetate. The pellet obtained by subsequent centrifugation was washed with ethyl acetate (10 times × 3 mL), and freeze dried. After spectrophotometric

determination of active ester groups, the pellet was incubated overnight with the protein in 100 mM NaP_i pH 7.2.

The glycoconjugate was washed on a 30 kDa Amicon centrifugal filter with 10 mM NaP_i pH 7 (8 × 100 µL), and subsequently reconstituted with 10 mM NaP_i pH 7. Yields (recovered glycoprotein as determined by microBCA, Pierce Thermo): 85–95%. Loading of glycoconjugate was determined by matrix-assisted laser desorption ionization time-of-flight mass spectrometry (MALDI–TOF MS; UltraFlex III MALDI–TOF/TOF instrument, Bruker Daltonics) in linear mode and with positive ion detection. The samples for analysis were prepared by mixing 2.5 µL of product and 2.5 µL of sinapinic acid matrix (Bruker Daltonics); 2.5 µL of each mixture was deposited on a samples plate, dried at room temperature for 10 min, and subjected to the spectrometer.

For SDS page analysis, the samples (5 µg) were electrophoresed on a 7% TrisAcetate gel or 4–12% Bis-Tris gel (NuPage, Invitrogen) and stained with Coomassie blue.

Immunization of mice. Animal experimental guidelines set forth by the Novartis Animal Care Department were followed in the conduct of all animal studies. For the formulation of the vaccines, to a volume of glycoconjugate corresponding to 0.3 µg or 1 µg/dose) aluminium phosphate (100 µl of a solution 1.2 mg/mL, 120 µg/dose) was added. The final volume of the formulation was diluted to 200 µL/dose by addition of PBS pH 7.2 buffer. An injection volume of 200 µL per mouse was used. MenX vaccines were administered to mice in 0.3 or 1 µg per dose based on saccharide content. As in [27] mice were immunized subcutaneously at day 1, 14 and 28. Bleedings were performed at day 0 (pre immune), day 28 (post 2) and day 42 (post 3). Control groups received PBS with adjuvant.

ELISA analysis. The antibody response induced by the glycoconjugates against the MenX polysaccharide and the HSA conjugates (see Supporting Information File 1) were measured by ELISA. Similarly as described in [27], plates were coated with the polysaccharide by adding 100 µL/well of a 5 µg/mL polysaccharide solution in pH 8.2 PBS buffer, and with the HSA conjugates adding 100 µL/well of a 2 µg/mL in term of protein solution in pH 7.2 PBS buffer, followed by incubation overnight at 4 °C. Coating solutions were removed from the plates by washing each well three times with PBS buffer containing 0.05% of Tween 20 (Sigma) (TPBS). A blocking step was performed by adding 100 µL of BSA solution at 3% in TPBS and incubating the plates 1 h at 37 °C. Blocking solution was removed from the plates by washing three times per well with TPBS. 200 µL of pre-diluted serum (1:25 for pre immune, 1:200 for a reference serum, 1:50–1:100 for test sera) was added to the first well of each column of the plate, while 100 µL of TPBS was dispensed into the remaining wells. Eight two-fold serial dilutions along each column were then performed by transferring from well to well 100 µL of sera solutions. After primary Abs dilution, plates were incubated for 2 h at 37 °C. After three washings with TPBS, 100 µL TPBS solutions of secondary antibody alkaline phosphatases conjugates (anti-mouse IgG 1:10000, anti-mouse IgM 1:5000 Sigma-Aldrich) were added and the plates incubated 1 h at 37 °C. Three more washes with TPBS were performed, when 100 µL/well of a 1 mg/mL of p-NPP (Sigma) in a 0.5 M diethanolamine buffer pH 9.6 were added. After 30 min of incubation at room temperature, plates were read at 405 nm using a Biorad plate reader. Raw data acquisition was performed by Microplate Manager Software (Biorad). Sera titers were expressed as the reciprocal of sera dilution corresponding to a cut-off OD = 1. Each immunization group is represented as the geometrical mean (GMT) of the single mouse titers. The statistical and graphical analysis was performed by GraphPad 5.0 software.

Rabbit serum bactericidal assay (rSBA). The functionality of antibodies induced by vaccine immunization was assessed by measuring the complement-mediated lysis of *N. meningitidis* with an in vitro bactericidal assay as described in the literature [15,26]. Titers were expressed as the reciprocal serum dilution resulting in 50% of bactericidal killing. Z9615 (MenX) was used as reference strain.

Supporting Information

Supporting Information File 1

Experimental procedures for the synthesis of compounds **1**, **5**, **6**, **7**, **9**, **19**, copies of ^{1}H NMR and ^{13}C NMR spectra of compounds **5–6** and ^{1}H NMR, ^{13}C NMR and ^{31}P NMR spectra of compounds **1**, **7**, **9**.
[http://www.beilstein-journals.org/bjoc/content/supplementary/1860-5397-10-247-S1.pdf]

Acknowledgements

We gratefully acknowledge MIUR-Italy (PRIN 2010-2011: contract 2010JMAZML_003) for financial support. We are grateful to Stefano Crotti for contributing to the MALDI TOF analysis of glycoconjugates.

References

1. Yogev, R.; Tan, T. *Hum. Vaccines* **2011,** *7,* 828–837. doi:10.4161/hv.7.8.16270
2. Morley, S. L.; Pollard, A. J. *Vaccine* **2001,** *20,* 666–687.

3. Nicolas, P.; Norheim, G.; Garnotel, E.; Djibo, S.; Caugant, D. A. *J. Clin. Microbiol.* **2005,** *43,* 5129–5135. doi:10.1128/JCM.43.10.5129-5135.2005
4. Stephens, D. S.; Greenwood, B.; Brandtzaeg, P. *Lancet* **2007,** *369,* 2196–2210. doi:10.1016/S0140-6736(07)61016-2
5. Djibo, S.; Nicolas, P.; Alonso, J.-M.; Djibo, A.; Couret, D.; Riou, J.-Y.; Chippaux, J.-P. *Trop. Med. Int. Health* **2003,** *8,* 1118–1123. doi:10.1046/j.1360-2276.2003.01126.x
6. Devine, L. F.; Rhode, S. L., III; Hagerman, C. R. *Infect. Immun.* **1972,** *5,* 48–54. http://iai.asm.org/content/5/1/48
7. Gagneux, S.; Wirth, T.; Hodgson, A.; Ehrhard, I.; Morelli, G.; Kriz, P.; Genton, B.; Smith, T.; Binka, F.; Pluschke, G.; Achtman, M. *Emerging Infect. Dis.* **2002,** *8,* 462–466. doi:10.3201/eid0805.010227
8. Xie, O.; Pollard, A. J.; Mueller, J. E.; Norheim, G. *Vaccine* **2013,** *31,* 2852–2861. doi:10.1016/j.vaccine.2013.04.036
9. Boisier, P.; Nicolas, P.; Djibo, S.; Taha, M.-K.; Jeanne, I.; Mainassara, H. B.; Tenebray, B.; Kairo, K. K.; Giorgini, D.; Chanteau, S. *Clin. Infect. Dis.* **2007,** *44,* 657–663. doi:10.1086/511646
10. Delrieu, I.; Yaro, S.; Tamekloé, T. A.; Njanpop-Lafourcade, B.-M.; Tall, H.; Jaillard, P.; Ouedraogo, M. S.; Badziklou, K.; Sanou, O.; Drabo, A.; Gessner, B. D.; Kambou, J. L.; Mueller, J. E. *PLoS One* **2011,** *6,* e19513. doi:10.1371/journal.pone.0019513
11. Roberts, L. *Science* **2010,** *330,* 1466–1467. doi:10.1126/science.330.6010.1466
12. Sow, S. O.; Okoko, B. J.; Diallo, A.; Viviani, S.; Borrow, R.; Carlone, G.; Tapia, M.; Akinsola, A. K.; Arduin, P.; Findlow, H.; Elie, C.; Haidara, F. C.; Adegbola, R. A.; Diop, D.; Parulekar, V.; Chaumont, J.; Martellet, L.; Diallo, F.; Idoko, O. T.; Tang, Y.; Plikaytis, B. D.; Kulkarni, P. S.; Marchetti, E.; LaForce, F. M.; Preziosi, M.-P. *N. Engl. J. Med.* **2011,** *364,* 2293–2304. doi:10.1056/NEJMoa1003812
13. Kristiansen, P. A.; Diomandé, F.; Ba, A. K.; Sanou, I.; Ouédraogo, A.-S.; Ouédraogo, R.; Sangaré, L.; Kandolo, D.; Eké, F.; Saga, I. M.; Iark, T. A.; Misegades, L.; Martin, S. W.; Thomas, J. D.; Tiendrebeogo, S. R.; Hassan-King, M.; Djingarey, M. H.; Messonnier, N. E.; Préziosi, M.-P.; LaForce, F. M.; Caugant, D. A. *Clin. Infect. Dis.* **2013,** *56,* 354–363. doi:10.1093/cid/cis892
14. Trotter, C. L.; Ramsay, M. E.; Gray, S.; Fox, A.; Kaczmarski, E. *Lancet Infect. Dis.* **2006,** *6,* 616–617. doi:10.1016/S1473-3099(06)70584-9
15. http://www.who.int/nuvi/meningitis/en/index.html
16. Hong, E.; Giuliani, M. M.; Deghmane, A.-E.; Comanducci, M.; Brunelli, B.; Dull, P.; Pizza, M.; Taha, M.-K. *Vaccine* **2013,** *31,* 1113–1116. doi:10.1016/j.vaccine.2012.12.022
17. Bröker, M.; Costantino, P.; DeTora, L.; McIntosh, E. D.; Rappuoli, R. *Biologicals* **2011,** *39,* 195–204. doi:10.1016/j.biologicals.2011.05.004
18. Micoli, F.; Romano, M. R.; Tontini, M.; Cappelletti, E.; Gavini, M.; Proietti, D.; Rondini, S.; Swennen, E.; Santini, L.; Filippini, S.; Balocchi, C.; Adamo, R.; Pluschke, G.; Norheim, G.; Pollard, A. J.; Saul, A.; Rappuoli, R.; MacLennan, C. A.; Berti, F.; Costantino, P. *Proc. Natl. Acad. Sci. U. S. A.* **2013,** *110,* 19077–19082. doi:10.1073/pnas.1314476110
19. Bundle, D. R.; Jennings, H. R. *Can. J. Biochem.* **1974,** *52,* 723–725. doi:10.1139/o74-102
20. Adamo, R.; Micoli, F.; Proietti, D.; Berti, F. *Synth. Commun.* **2014,** *44,* 1266–1273. doi:10.1080/00397911.2013.853189
21. Morelli, L.; Poletti, L.; Lay, L. *Eur. J. Org. Chem.* **2011,** 5723–5777. doi:10.1002/ejoc.201100296
22. Costantino, P.; Rappuoli, R.; Berti, F. *Expert Opin. Drug Discovery* **2011,** *6,* 1045–1067. doi:10.1517/17460441.2011.609554
23. Hsu, C.-H.; Hung, S.-C.; Wu, C.-Y.; Wong, C.-H. *Angew. Chem., Int. Ed.* **2011,** *50,* 11872–11923. doi:10.1002/anie.201100125
24. Hecht, M.-L.; Stallforth, P.; Varón Silva, D.; Adibekian, A.; Seeberger, P. H. *Curr. Opin. Chem. Biol.* **2009,** *13,* 354–359. doi:10.1016/j.cbpa.2009.05.127
25. Morelli, L.; Lay, L. *ARKIVOC* **2013,** *Part (ii),* 166–184. doi:10.3998/ark.5550190.0014.214
26. Adamo, R.; Romano, M. R.; Berti, F.; Leuzzi, R.; Tontini, M.; Danieli, E.; Cappelletti, E.; Cakici, O. S.; Swennen, E.; Pinto, V.; Brogioni, B.; Proietti, D.; Galeotti, C. L.; Lay, L.; Monteiro, M. A.; Scarselli, M.; Costantino, P. *ACS Chem. Biol.* **2012,** *7,* 1420–1428. doi:10.1021/cb300221f
27. Gao, Q.; Tontini, M.; Brogioni, G.; Nilo, A.; Filippini, S.; Harfouche, C.; Polito, L.; Romano, M. R.; Costantino, P.; Berti, F.; Adamo, R.; Lay, L. *ACS Chem. Biol.* **2013,** *8,* 2561–2567. doi:10.1021/cb400463u
28. Nikolaev, A. V.; Botvinko, I. V.; Ross, A. J. *Carbohydr. Res.* **2007,** *342,* 297–344. doi:10.1016/j.carres.2006.10.006
29. Guilano, R. M.; Deisenroth, T. W. *J. Carbohydr. Chem.* **1987,** *6,* 295–299. doi:10.1080/07328308708058878
30. Mason, B. P.; Price, K. E.; Steinbacher, J. L.; Bogdan, A. R.; McQuade, D. T. *Chem. Rev.* **2007,** *107,* 2300–2318. doi:10.1021/cr050944c
31. Geyer, K.; Gustafsson, T.; Seeberger, P. H. *Synlett* **2009,** 2382–2391. doi:10.1055/s-0029-1217828
32. Hartman, R. L.; McMullen, J. P.; Jensen, K. F. *Angew. Chem., Int. Ed.* **2011,** *50,* 7502–7519. doi:10.1002/anie.201004637
33. McQuade, D. T.; Seeberger, P. H. *J. Org. Chem.* **2013,** *78,* 6384–6389. doi:10.1021/jo400583m
34. Nikolaev, A. V.; Rutherford, T. J.; Ferguson, M. A. J.; Brimacombe, J. S. *J. Chem. Soc., Perkin Trans. 1* **1995,** 1977–1987. doi:10.1039/P19950001977
35. Thijssen, M.-J. L.; Hales, K. M.; Kamerling, J. P.; Vliegenthart, J. F. G. *Bioorg. Med. Chem.* **1994,** *2,* 1309–1317. doi:10.1016/S0968-0896(00)82081-7
36. Gao, Q.; Zaccaria, C.; Tontini, M.; Poletti, L.; Costantino, P.; Lay, L. *Org. Biomol. Chem.* **2012,** *10,* 6673–6681. doi:10.1039/c2ob25222h
37. Bardotti, A.; Averani, G.; Berti, F.; Berti, S.; Carinci, V.; D'Ascenzi, S.; Fabbri, B.; Giannini, S.; Giannozzi, A.; Magagnoli, C.; Proietti, D.; Norelli, F.; Rappuoli, R.; Ricci, S.; Costantino, P. *Vaccine* **2008,** *26,* 2284–2296. doi:10.1016/j.vaccine.2008.01.022
38. Vecchi, S.; Bufali, S.; Skibinski, D. A. G.; O'Hagan, D. T.; Singh, M. *J. Pharm. Sci.* **2012,** *101,* 17–20. doi:10.1002/jps.22759
39. Giuliani, M. M.; Santini, L.; Brunelli, B.; Biolchi, A.; Arico, B.; Di Marcello, F.; Cartocci, E.; Comanducci, M.; Masignani, V.; Lozzi, L.; Savino, S.; Scarselli, M.; Rappuoli, R.; Pizza, M. *Infect. Immun.* **2005,** *73,* 1151–1160. doi:10.1128/IAI.73.2.1151-1160.2005
40. Andrews, N.; Borrow, R.; Miller, E. *Clin. Diagn. Lab. Immunol.* **2003,** *10,* 780–786. doi:10.1128/CDLI.10.5.780-786.2003
41. Hirve, S.; Bavdekar, A.; Pandit, A.; Juvekar, S.; Patil, M.; Preziosi, M.-P.; Tang, Y.; Marchetti, E.; Martellet, L.; Findlow, H.; Elie, C.; Parulekar, V.; Plikaytis, B.; Borrow, R.; Carlone, G.; Kulkarni, P. S.; Goel, A.; Suresh, K.; Beri, S.; Kapre, S.; Jadhav, S.; Preaud, J.-M.; Viviani, S.; LaForce, F. M. *Vaccine* **2012,** *30,* 6456–6460. doi:10.1016/j.vaccine.2012.08.004
42. Poszgay, V.; Chu, C.; Pannell, L.; Wolfe, J.; Robbins, J. B.; Schneerson, R. *Proc. Natl. Acad. Sci. U. S. A.* **1999,** *96,* 5194–5197. doi:10.1073/pnas.96.9.5194

43. Mawas, F.; Niggemann, J.; Jones, C.; Corbel, M. J.; Kamerling, J. P.; Vliegenthart, J. F. G. *Infect. Immun.* **2002,** 5107–5114. doi:10.1128/IAI.70.9.5107-5114.2002